frontiers | Research Topics

Exploring the influence of gut microbiome on human health: mechanistic insights from pig models

Edited by
Lifeng Zhu, Wen-Chao Liu, Congying Chen,
François J. M. A. Meurens, Wei Liu and Shimeng Huang

Published in
Frontiers in Microbiology

ISSN 1664-8714
ISBN 978-2-8325-5902-4
DOI 10.3389/978-2-8325-5902-4

About Frontiers

Frontiers is more than just an open access publisher of scholarly articles: it is a pioneering approach to the world of academia, radically improving the way scholarly research is managed. The grand vision of Frontiers is a world where all people have an equal opportunity to seek, share and generate knowledge. Frontiers provides immediate and permanent online open access to all its publications, but this alone is not enough to realize our grand goals.

Frontiers journal series

The Frontiers journal series is a multi-tier and interdisciplinary set of open-access, online journals, promising a paradigm shift from the current review, selection and dissemination processes in academic publishing. All Frontiers journals are driven by researchers for researchers; therefore, they constitute a service to the scholarly community. At the same time, the *Frontiers journal series* operates on a revolutionary invention, the tiered publishing system, initially addressing specific communities of scholars, and gradually climbing up to broader public understanding, thus serving the interests of the lay society, too.

Dedication to quality

Each Frontiers article is a landmark of the highest quality, thanks to genuinely collaborative interactions between authors and review editors, who include some of the world's best academicians. Research must be certified by peers before entering a stream of knowledge that may eventually reach the public - and shape society; therefore, Frontiers only applies the most rigorous and unbiased reviews. Frontiers revolutionizes research publishing by freely delivering the most outstanding research, evaluated with no bias from both the academic and social point of view. By applying the most advanced information technologies, Frontiers is catapulting scholarly publishing into a new generation.

What are Frontiers Research Topics?

Frontiers Research Topics are very popular trademarks of the *Frontiers journals series*: they are collections of at least ten articles, all centered on a particular subject. With their unique mix of varied contributions from Original Research to Review Articles, Frontiers Research Topics unify the most influential researchers, the latest key findings and historical advances in a hot research area.

Find out more on how to host your own Frontiers Research Topic or contribute to one as an author by contacting the Frontiers editorial office: frontiersin.org/about/contact

Exploring the influence of gut microbiome on human health: mechanistic insights from pig models

Topic editors

Lifeng Zhu — Nanjing University of Chinese Medicine, China
Wen-Chao Liu — Guangdong Ocean University, China
Congying Chen — Jiangxi Agricultural University, China
François J. M. A. Meurens — Montreal University, Canada
Wei Liu — Zhejiang Academy of Agricultural Sciences, China
Shimeng Huang — China Agricultural University, China

Citation

Zhu, L., Liu, W.-C., Chen, C., Meurens, F. J. M. A., Liu, W., Huang, S., eds. (2025). *Exploring the influence of gut microbiome on human health: mechanistic insights from pig models*. Lausanne: Frontiers Media SA. doi: 10.3389/978-2-8325-5902-4

Table of contents

frontiers | Frontiers in Microbiology

TYPE Editorial
PUBLISHED 28 March 2025
DOI 10.3389/fmicb.2025.1570451

OPEN ACCESS

EDITED AND REVIEWED BY
Jing Liu,
Agricultural Research Service (USDA),
United States

*CORRESPONDENCE
François Meurens
✉ francois.meurens@umontreal.ca

RECEIVED 03 February 2025
ACCEPTED 14 March 2025
PUBLISHED 28 March 2025

CITATION
Meurens F, Huan S, Liu W-C, Zhu L and Liu W (2025) Editorial: Exploring the influence of gut microbiome on human health: mechanistic insights from pig models.
Front. Microbiol. 16:1570451.
doi: 10.3389/fmicb.2025.1570451

Editorial: Exploring the influence of gut microbiome on human health: mechanistic insights from pig models

François Meurens[1,2]*, Shimeng Huan[3], Wen-Chao Liu[4], Lifeng Zhu[5] and Wei Liu[6]

[1]Research Group on Infectious Diseases in Production Animals (GREMIP) & Swine and Poultry Infectious Diseases Research Center (CRIPA), Faculty of Veterinary Medicine, University of Montreal, St-Hyacinthe, QC, Canada, [2]Department of Veterinary Microbiology and Immunology, Western College of Veterinary Medicine, University of Saskatchewan, Saskatoon, SK, Canada, [3]State Key Laboratory of Animal Nutrition, China Agricultural University, Beijing, China, [4]Department of Animal Science, College of Coastal Agricultural Sciences, Guangdong Ocean University, Zhanjiang, China, [5]School of Medicine & Holistic Integrative Medicine, Nanjing University of Chinese Medicine, Nanjing, China, [6]Plant Protection and Microbiology Research Institute, Zhejiang Academy of Agricultural Sciences, Hangzhou, Zhejiang, China

KEYWORDS

pig, microbiota, gut, health, human health

Editorial on the Research Topic
Exploring the influence of gut microbiome on human health: mechanistic insights from pig models

The exploration of gut health in swine (Hu et al., 2024; Upadhaya and Kim, 2022), in humans (Hou et al., 2022) and in various species has gained considerable attention lastly, with multiple studies elucidating the intricate interplay between the gut microbiome, host genetics, and health outcomes. This editorial synthesizes findings from recent research in Frontiers in Microbiology that highlights the potential for dietary interventions and genetic considerations in enhancing swine health and productivity. It also presents two recent studies, in humans, where the gut microbiota has been shown as having a major impact.

In their study, Han et al. presented critical findings regarding the adverse effects of artificial piglet rearing on the intestinal microbiota and overall gut health. Through their study, they nicely demonstrated that artificially reared piglets experienced increased diarrhea incidence and detrimental alterations in gut microbiota composition. These outcomes raise essential questions about current management practices in pig production, underlining the necessity for strategies that mitigate the negative impacts of artificial rearing methods. Complementing that study, Jiang et al. examined an interesting relationship between testosterone levels and fecal microbiota in developing Meishan male pigs. Their research revealed dynamic interactions indicating that testosterone influences the composition of gut microbiota, while the microbiome may also play a role in testosterone metabolism. Understanding these relationships could serve as a foundation for developing breeding strategies aimed at optimizing hormonal health in pigs. Then, in an interesting and recent study, Liu W. et al. explored the effects of a multispecies probiotic complex on bile acid metabolism and gut microbiota using an *in vitro* fermentation model. They demonstrated significant alterations in bile acid profiles and modifications to gut microbiota composition following probiotic treatment. This indicates a promising therapeutic application of probiotic interventions for managing metabolic disorders and enhancing gut health in swine. Complementing the research on probiotics, Zhu et al.

investigated the effects of maternal diets supplemented with probiotics and synbiotics on the colonic microbiome and metabolome of offspring. Their findings illustrated that maternal supplementation significantly shapes the gut microbiota composition in piglets, thereby emphasizing the critical role of maternal nutrition on progeny health. This study advocates for strategic maternal dietary interventions not only to enhance immediate gut health in offspring but also to promote long-term benefits for growth and disease resistance in swine. Zhu et al. argue for the implementation of probiotics during gestation and lactation as a means to promote a favorable microbiome in neonates, which could result in better health outcomes and productivity throughout the life of the pig. More specifically, Liu X. et al. focused on the probiotic bacterium *Clostridium butyricum* CBX 2021 strain, assessing its mechanisms in improving pig health through *in vivo* and *in vitro* approaches. Their study reported that strain CBX 2021 enhanced growth indicators and reduced diarrhea rates in weaned piglets. The probiotic also exhibited beneficial effects on immune response and gut microbiota composition, highlighting its potential role in developing new probiotic products to improve swine health. Still about the effect of one bacterium, Yuan et al. examined *Bacillus amyloliquefaciens* SC06's effects on weaned piglets experiencing endoplasmic reticulum (ER) and oxidative stress. The study demonstrated that SC06 supplementation significantly improved growth performance while decreasing markers of oxidative and ER stress. Through transcriptomic and metagenomic analyses, SC06 was shown to positively influence gene expression linked to antioxidant activity and to alter gut microbiome composition, thus contributing to better intestinal health in stressed piglets.

Regarding the use of amino acids, Liu G. et al. investigated the effects of tryptophan (Trp) supplementation in lipopolysaccharide (LPS)-stimulated piglets. Their findings revealed that Trp enhances the abundance of beneficial gut bacteria and short-chain fatty acids (SCFAs) while reducing inflammation and improving intestinal barrier function. This suggests that dietary Trp supplementation could serve as an effective strategy for mitigating the adverse effects of inflammatory challenges in piglets. On their side, Yu et al. investigated the effects of dietary galacto-oligosaccharides (GOS) and hyocholic acids (HCA) on sow reproductive performance, particularly during late gestation and lactation. Their study, involving 60 multiparous sows divided into four dietary groups, revealed that GOS and HCA supplementation significantly contributed to shorter labor times and increased piglet birth weights. Furthermore, they observed improvements in serum triglyceride levels and total antioxidant capacity among sows on supplemented diets. Notably, GOS and HCA also induced changes in gut microbiota composition, suggesting that dietary interventions could augment reproductive performance and enhance milk quality. These findings advocate for the strategic use of dietary nutrients in optimizing both sow health and offspring vitality, illustrating the cascading benefits of microbial modulation on reproductive success.

Focusing on the impact of the microbiota on distant organs, Qi et al. advanced our understanding of how gut microbiota influences hypothalamic function and overall health. Their whole transcriptome analysis illustrated significant alterations in gene expression related to energy metabolism and cell signaling in the presence or absence of gut microbiota. This interplay marks a crucial step in unraveling the microbiota-gut-brain axis, with important implications for metabolic and neurodegenerative diseases, emphasizing potential therapeutic interventions. Still in the field of microbio-endocrinology, Zheng et al. explored the interplay between intestinal melatonin levels and gut microbiota, focusing on how melatonin's synthesis occurs locally in the gut independent of the pineal gland's influence. Their research utilized a pig model with pinealectomy to investigate these effects. They found that while the removal of the pineal gland did not alter gastrointestinal melatonin levels or overall gut microbiota composition, supplementing melatonin led to significant changes in the gut microbiota structure. This indicates that melatonin synthesized in the intestinal tract may play a crucial role in regulating gut microbiota, reinforcing its importance in maintaining gut health and homeostasis. The findings underscore that melatonin might serve as a modifiable dietary component that can support gut health through its regulatory effects, presenting further opportunities for dietary supplementation in livestock management. To gain a better understanding of the causes of obesity, Zeng et al. studied fluctuations in the fecal microbiota of Bama minipigs during periods of weight gain and loss, highlighting the crucial role of gut microbiota in managing obesity. Their research demonstrated significant correlations between microbial diversity and variations in body weight, indicating that specific microbial communities may be associated with weight gain or loss. Zeng et al.'s findings suggest that targeted dietary or microbial interventions could serve as effective strategies for managing obesity not only in swine but potentially in human models as well. This study highlights the intricate relationships between diet, microbiota, and body weight regulation, paving the way for innovative approaches to tackle obesity through microbiome manipulation.

In elderly pigs, Qiao et al. investigated the relationship between the oral-gut microbiome and inflamm-aging employing a multi-omics approach. Their findings demonstrated age-dependent shifts in microbial composition correlating with systemic inflammation markers. These results underscore the relevance of gut health in aging, suggesting that targeted interventions could help manage gut microbiota and potentially extend healthy lifespan. Then, Wang et al. contributed to our understanding of the relationship between host genetics and gut microbiome composition regarding fat deposition traits. By analyzing a resource population of pigs, they identified specific microbial candidates correlated with the percentage of leaf fat and intramuscular fat content. This research emphasizes the significance of microbiome interactions in optimizing meat quality and refining selection criteria for future pig breeding strategies.

In a review article, Yang et al. examined the role of gut archaea within the swine microbiome. They highlighted the previously understudied diversity of gut archaea and their potential links to economically important traits, such as weight gain and feed efficiency in pigs. While bacteria have traditionally received most of research attention, Yang et al. advocated for a more inclusive approach that investigates archaeal species. The mini-review discusses how these microorganisms could act as potential

probiotics, enhancing pig growth and overall health. They suggest that further research into the metabolic functions of gut archaea could uncover unique contributions to the gut environment that support digestion, nutrient absorption, and immune function in swine. Thus, integrating archaeal research into swine breeding and health management could lead to innovative strategies for improving livestock productivity and resilience.

In their study in humans, Chen et al. investigated the causal relationship between gut microbiota and leukemia using a two-sample Mendelian randomization method. They identified ten gut microbial taxa associated with leukemia risk. Notably, *Blautia* and *Lactococcus* were recognized as risk factors for acute lymphoblastic leukemia, while several *Ruminococcaceae* taxa were associated with chronic myeloid leukemia. This study highlights the potential of gut microbiota as biomarkers for leukemia, suggesting that microbiome modulation could offer new avenues for early detection and targeted treatment strategies. Still in the human species, Fu and Hao explored the causal relationships between gut microbiota (GM) and non-Hodgkin lymphoma (NHL) using bidirectional Mendelian randomization analysis. Their findings identified 27 specific gut microbial species linked to NHL, with 20 showing a negative association and seven a positive one. This research emphasizes the complex role of gut microbiota in cancer development, indicating that understanding these relationships could lead to innovative preventive and therapeutic strategies for NHL.

Collectively, these studies, in pigs, pig biomedical model, and humans, offer profound insights into the multifaceted relationships between dietary interventions, microbiota composition, and overall health. They inform future strategies aimed at enhancing animal welfare and productivity through targeted microbiome management, dietary enrichment, and innovative breeding practices. The findings across these diverse studies illustrate the importance of integrating gut health considerations into all aspects of swine production, from gestation through to market readiness.

Author contributions

FM: Writing – original draft, Writing – review & editing. SH: Writing – original draft, Writing – review & editing. W-CL: Writing – original draft, Writing – review & editing. LZ: Writing – original draft, Writing – review & editing. WL: Writing – original draft, Writing – review & editing.

Acknowledgments

The editors thank the Frontiers administrative team for their wonderful support with the Research Topic as well as the numerous peer reviewers.

Conflict of interest

The authors declare that the research was conducted in the absence of any commercial or financial relationships that could be construed as a potential conflict of interest.

The author(s) declared that they were an editorial board member of Frontiers, at the time of submission. This had no impact on the peer review process and the final decision.

Publisher's note

References

Hou, K., Wu, Z.-X., Chen, X.-Y., Wang, J.-Q., Zhang, D., Xiao, C., et al. (2022). Microbiota in health and diseases. *Signal Transd. Targ. Ther.* 7, 1–28. doi: 10.1038/s41392-022-00974-4

Hu, J., Chen, J., Ma, L., Hou, Q., Zhang, Y., Kong, X., et al. (2024). Characterizing core microbiota and regulatory functions of the pig gut microbiome. *ISME J.* 18:wrad037. doi: 10.1093/ismejo/wrad037

Upadhaya, S. D., and Kim, I. H. (2022). Maintenance of gut microbiome stability for optimum intestinal health in pigs – a review. *J. Animal Sci. Biotechnol.* 13:140. doi: 10.1186/s40104-022-00790-4

frontiers | Frontiers in Microbiology

ORIGINAL RESEARCH
published: 04 July 2022
doi: 10.3389/fmicb.2022.919431

Tryptophan Supplementation Enhances Intestinal Health by Improving Gut Barrier Function, Alleviating Inflammation, and Modulating Intestinal Microbiome in Lipopolysaccharide-Challenged Piglets

Guangmang Liu[1], Jiajia Lu[1], Weixiao Sun[1], Gang Jia[1], Hua Zhao[1], Xiaoling Chen[1], In Ho Kim[2], Ruinan Zhang[1]* and Jing Wang[3]*

[1] Key Laboratory for Animal Disease-Resistance Nutrition, Ministry of Education, Ministry of Agriculture and Rural Affairs, Key Laboratory of Sichuan Province, Institute of Animal Nutrition, Sichuan Agricultural University, Chengdu, China, [2] Department of Animal Resource and Science, Dankook University, Cheonan, South Korea, [3] Maize Research Institute, Sichuan Agricultural University, Chengdu, China

OPEN ACCESS

Edited by:
Xiangfeng Kong, Institute of Subtropical Agriculture (CAS), China

Reviewed by:
Ruqing Zhong, Institute of Animal Sciences (CAAS), China
Hongbo Yi, Guangdong Academy of Agricultural Sciences (GDAAS), China
Matteo Dell'Anno, University of Milan, Italy

***Correspondence:**
Guangmang Liu
liugm@sicau.edu.cn
Ruinan Zhang
scu06zrn@foxmail.com

Specialty section:
This article was submitted to Microorganisms in Vertebrate Digestive Systems, a section of the journal Frontiers in Microbiology

Received: *13 April 2022*
Accepted: *08 June 2022*
Published: *04 July 2022*

Citation:
Liu G, Lu J, Sun W, Jia G, Zhao H, Chen X, Kim IH, Zhang R and Wang J (2022) Tryptophan Supplementation Enhances Intestinal Health by Improving Gut Barrier Function, Alleviating Inflammation, and Modulating Intestinal Microbiome in Lipopolysaccharide-Challenged Piglets. Front. Microbiol. 13:919431. doi: 10.3389/fmicb.2022.919431

Tryptophan (Trp) can modify the gut microbiota. However, there is no information about the effect of Trp on intestinal microbiota after lipopolysaccharide (LPS) challenge. This study aimed to investigate the effect of Trp on intestinal barrier function, inflammation, antioxidant status, and microbiota in LPS-challenged piglets. A total of 18 weaned castrated piglets were randomly divided into three treatments with 6 replicate per treatment, namely, (i) non-challenged control (CON); (ii) LPS-challenged control (LPS-CON); and (iii) LPS + 0.2% Trp (LPS-Trp). After feeding with control or 0.2% tryptophan-supplemented diets for 35 days, pigs were intraperitoneally injected with LPS (100 μg/kg body weight) or saline. At 4 h post-challenge, all pigs were slaughtered, and colonic samples were collected. The samples were analyzed for gut microbiota, fatty acids, antioxidant parameters, and the expression of mRNA and protein. The community bar chart showed that Trp supplementation to LPS-challenged pigs increased the relative abundance of *Anaerostipes* ($P < 0.05$) and tended to increase the relative abundance of *V9D2013_group* ($P = 0.09$), while decreased the relative abundance of *Corynebacterium* ($P < 0.05$) and *unclassified_c__Bacteroidia* ($P < 0.01$). Gas chromatography showed that Trp increased the concentrations of acetate, propionate, butyrate, and isovalerate in the colonic digesta ($P < 0.05$). Trp reduced the mRNA level of pro-inflammatory cytokines ($P < 0.01$), and increased mRNA level of aryl hydrocarbon receptor, cytochrome P450 (*CYP*) *1A1* and *CYP1B1* ($P < 0.05$). Correlation analysis results showed that acetate, propionate, and butyrate concentrations were positively correlated with mRNA level of *occludin* and *CYP1B1* ($P < 0.05$), and were negatively correlated with pro-inflammatory cytokines gene expression ($P < 0.05$). Isovalerate

concentration was positively correlated with catalase activity ($P < 0.05$), and was negatively correlated with pro-inflammatory cytokines gene expression ($P < 0.05$). Furthermore, Trp enhanced the antioxidant activities ($P < 0.01$), and increased mRNA and protein expressions of claudin-1, occludin, and zonula occludens-1 ($P < 0.01$) after LPS challenge. These results suggest that Trp enhanced intestinal health by a modulated intestinal microbiota composition, improved the short chain fatty acids synthesis, reduced inflammation, increased antioxidant capacity, and improved intestinal barrier function.

Keywords: tryptophan, intestinal barrier function, microbiota, inflammation, piglets

INTRODUCTION

Weaning is a critical period for the piglets' growth. The physiological, nutritional, and environmental stress caused by problems such as intestinal barrier and inflammation leads to intestinal infections and performance reduction (Chen et al., 2018; Gao et al., 2019). Gut microbial dysbiosis is a major cause of intestinal infection and post-weaning diarrhea. There is a complex interaction between the intestinal flora and the host. Intestinal microorganisms produce a variety of metabolites (short-chain fatty acids [SCFAs], synthetic amino acids and vitamins), which not only affect digestion, absorption, and metabolism of nutrients, but also affect the growth of intestinal mucosa and the health growth of the host (Schwiertz et al., 2010; Ang and Ding, 2016; Ohira et al., 2017; Wang et al., 2018). The imbalance of gut microbiota structure leads to the disturbance of the body's physiological function balance, colon cancer (Garrett, 2019), inflammatory bowel disease (Matsuoka and Kanai, 2015), intestinal stress syndrome (Lee and Bak, 2011), and other intestinal diseases. Gut microbial colonization has a significant effect on the development of innate and adaptive immune responses, and the homeostasis of intestinal barrier function (Nicholson et al., 2012). Dietary nutrients have a positive effect on intestinal homeostasis, host digestion, absorption, and immunity. In addition, it is necessary to use nutritional strategies in maintaining the health of the intestine. Amino acids are crucial for maintaining gut tissue integrity and the growth of microbiota (Liao, 2021).

The tryptophan (Trp) is regarded as the second-limiting amino acid in most corn–soybean diets of piglets (Mao et al., 2014), which must be supplied from the feed (Bravo et al., 2013). Previous studies have demonstrated that Trp supplementation increases feed intake (Trevisi et al., 2009), growth (Shen et al., 2012), gut integrity (Koopmans et al., 2006), and antioxidant status (Jacobitz et al., 2021; Liu et al., 2022). In addition, dietary Trp enhances intestinal cell protein turnover, tight junction protein expression (Tossou et al., 2016), and microbiota diversity (Dai et al., 2015), thereby improving intestinal barrier function. Moreover, Trp supplementation attenuates intestinal inflammation-induced increases of intestinal permeability, and the pro-inflammatory cytokine gene expression in pigs (Kim et al., 2010; Liu et al., 2022). Furthermore, being used for protein synthesis *in vivo*, Trp can also be catabolized through various pathways, such as kynurenine, serotonin, and gut microbiota metabolic pathways (Saraf et al., 2017; Agus et al., 2018). A growing number of studies showed that the metabolism of Trp involved in many diseases, such as inflammatory bowel disease, neurodegenerative diseases, and psychiatric disorders (Bosi et al., 2020). Trp can be directly catabolized by bacteria in the intestinal, forming indole, and its derivatives, which are involved in intestinal permeability, inflammation regulation, and host immunity (Lamas et al., 2016; Gao et al., 2018). Some Trp metabolites are regarded as ligands for aryl hydrocarbon receptor (AhR), improve local interleukin production and immunity. In addition, AhR is crucial for the renewal of intestinal epithelial cells and the integrity of the intestinal mucosal barrier (Nikolaus et al., 2017). Moreover, cytochrome P450 (CYP)1A1 acts as a direct transcriptional target of AhR constituting a feedback loop of AhR signaling (Schiering et al., 2017). 0.5% Trp supplementation inhibits colitis symptoms and the secretion of pro-inflammatory cytokines in mice by activating AhR (Islam et al., 2017). Trp metabolites increase the protein expression of zonula occluden (ZO)-1 and occludin (Liang et al., 2018b). However, there is no information about the effect of Trp on intestinal microbiota after lipopolysaccharide (LPS) challenge. LPS irritates the intestine, causing mucosal injury, metabolic disorder, and bacterial translocation, it has been used to mimic features of endotoxin-induced acute intestinal injury (Xu et al., 2018). In this study, LPS was injected to establish an intestinal inflammation model, and our objective was to test the hypothesis of whether Trp can improve gut barrier function, alleviate inflammation, and modulate intestinal microbiome in LPS-challenged piglets.

MATERIALS AND METHODS

Experimental Design and Animals

The experimental protocol used in this study was approved by Sichuan Agricultural University Animal Care and Use Committee (SICAU-2021-08). A total of 18 castrated piglets (Duroc × Yorkshire × Landrace; weaned at 24 ± 1 days of age) were randomly distributed to three treatments. Each group has six replicates (one pig per replicate and one pen per pig). According to a previous study (Liu et al., 2016), the room temperature and relative humidity were adjusted to 30°C and 50–60%, respectively. The piglets were allowed to access clean water during the whole experiment. The basal diet (**Table 1**) was

TABLE 1 | Ingredient composition of experimental diets (%, as-fed basis).

Ingredient	Content (%)	
	7–11 kg	11–25 kg
Corn meal	27.37	30.6
Extruded corn	30.84	32.00
Soybean oil	2.50	1.40
Glucose	2.00	2.00
Whey powder	5.00	5.00
Dehulled Soybean meal (46% CP)	13.24	13.04
Soybean protein concentrate	5.00	5.00
Extruded soybean	7.00	5.00
Fish meal (67% CP)	3.00	2.50
L-Lysine-HCl (78.8%)	0.52	0.44
DL-Methionine (99%)	0.11	0.08
L-Threonine (98.5%)	0.20	0.15
L-Tryptophan (98%)	0.03	0.01
L-Alanine (99%)	0.46	0.32
Choline chloride (50%)	0.15	0.15
Limestone	0.68	0.41
Monocalcium phosphate	1.35	1.35
NaCl	0.25	0.25
Vitamin premix[1]	0.05	0.05
Mineral premix[2]	0.25	0.25
Total	100.00	100.00
Nutrient level[3]	**Content (%)**	
Digestible energy, Mcal/kg	3.55	3.49
Crude protein, %	19.72	18.65
Calcium, %	0.80	0.68
Total phosphorus, %	0.66	0.64
Available phosphorus, %	0.48	0.46
SID-Lysine, %	1.36	1.24
SID-Methionine, %	0.40	0.36
SID-Threonine, %	0.80	0.73
SID-Tryptophan, %	0.23	0.20

[1]The vitamin premix provides the following per kilogram of diet: VA 15000 IU; VD_3 5000 IU; VE 40 IU; VK_3 5 mg; VB_1 5 mg; VB_2 12.5 mg; VB_6 6 mg; VB_{12} 600 μg; D-pantothenic acid 25 mg; nicotinic acid 50 mg; folic acid 2.5 mg; biotin 2.5 mg.
[2]The mineral premix provides the following per kilogram of diet: copper ($CuSO_4 \cdot 5H_2O$) 6 mg; iron ($FeSO_4 \cdot H_2O$) 100 mg; zinc ($ZnSO_4 \cdot H_2O$) 100 mg; manganese ($MnSO_4 \cdot H_2O$) 4 mg; iodine (KI) 0.14 mg; selenium (Na_2SeO_3) 0.3 mg.
[3]Nutrient levels are calculated values.

formulated based on the National Research Council (Southern and Adeola, 2012) requirements for all nutrients.

The experiment was carried out for a total of 35 days, and the experiment was divided into two stages according to the feeding weight: (1) 7–11 kg; (2) 11–25 kg. The experiment included three treatments: (1) non-challenged treatment (CON, the pigs were administered a control diet and received a 0.9% NaCl injection); (2) LPS-challenged treatment (LPS-CON, the pigs were given the same diet as the control group and were treated with *Escherichia coli* [*E. coli*] LPS); and (3) LPS-challenged + 0.2% tryptophan (Trp) treatment (LPS-Trp, the pigs were given with 0.2% Trp [CJ International Trading Co., Ltd.] diet and were treated with *E. coli* LPS [*E. coli* serotype 055: B5; Sigma Chemical Inc., St. Louis, MO, United States]). The Trp concentration was selected according to the previous research (Liang et al., 2018a). On the 35th day of the treatment, the challenged groups were intraperitoneally injected with *E. coli* LPS at 100 μg/kg body weight, and the unchallenged group was injected with the same amount of 0.9% saline. The LPS dose was selected in accordance with the previous research (Pi et al., 2014). At the end of the experimental trial, corresponding to day 35, all piglets fasted for 4 h before being slaughtered to avoid the potential effects of changes in feed intake in the intestine.

Intestinal Sample Collection

On the 35th day of the treatment, 4 h after all pigs were intraperitoneally injected with *E. coli* LPS solution or sterile saline, 6 piglets from each treatment (one pig per pen) were electrocuted. After all pigs were sacrificed, each intestinal segment was ligated and separated, the colon was washed with saline, and a 2 cm middle segment of the colon was cut, each sample was collected at the same location. The colonic mucosa was scraped with glass slides for the determination of some immune indexes, some colon tissue samples were taken into sterilized EP tubes, quick-frozen in liquid nitrogen, and stored at −80°C for determination of antioxidants and genes. Colon contents were collected and aliquoted into sterile EP tubes for gut microbiome and volatile fatty acid determination.

Short-Chain Fatty Acids Analysis

In each digesta sample, the main concentrations of SCFAs was separated and quantified by using a gas chromatograph (CP3800, Varian) with capillary column 30 m × 0.53 mm × 1 μm film thickness (HP-FFAP) and flame ionization detector, 250°C according to previous study (Zamora-Gasga et al., 2014). Standard samples (e.g., acetate, propionate, butyrate, isovalerate, isobutyrate, and valerate, Supelco, Sigma-Aldrich Trading Co., Ltd., Shanghai, China) were used. Briefly, 0.7 g of sample was collected in a centrifuge tube, and was mixed with ultrapure water (1.5 ml) for 30 min and centrifuged (1,000 g, 15 min). The supernatant (1 ml) was added 0.2 mL of 25% (w/v) metaphosphate solution (Tianjin Kemiu Chemical Reagent Co., Ltd., Tianjing, China) and 23.3 μl of 210 mmol/l crotonic acid solution (Sigma-Aldrich Trading Co., Ltd., Shanghai, China), and the mixture was incubated for 30 min and then centrifuged at 8,000 g for 10 min. The supernatant (0.3 ml) was mixed with 0.9 ml of chromatographic methanol (Thermo Fisher Scientic Inc., Waltham, MA, United States) at 8,000 g for 5 min. One milliliter of the supernatant was subjected to capillary gas chromatography (CP3800, Varian).

16S rRNA Analysis of Colonic Digesta-Associated Microbiota

The method to extract the genomic DNA using FastDNA® Spin Kit (MP Biomedicals, Irvine, CA, United States) was according to previous study (Layton et al., 2006). Briefly, 0.5 g sample was added with 978 μl sodium phosphate buffer and 122 μl MT buffer, and homogenized for 40 s (FastPrep-24 5G, MP Biomedicals, United States) and centrifuged (14,000 g, 5–10 min). 250 μl of PPS was added to the supernatant mixed

and centrifuged (14,000 g, 5 min). About 600 μl of the mixture was placed in a SPIN^{TM} filter and centrifuged (14,000 x g, 1 min). Finally, 500 μl of prepared SEWS-M was added, centrifuged at room temperature (14,000 rpm, 2 min), discarded the SPIN^{TM} Filter. Total DNA was obtained. After genomic DNA extraction, the extracted genomic DNA was determined by 1% agarose gel electrophoresis. The ABI Gene Amp 9700 PCR Thermocycle Instrument (Applied Biosystems, Inc., Carlsbad, CA, United States) was applied to amplify DNA. Next, all samples were carried out according to formal experimental conditions. Each sample was repeated 3 times. PCR products from the same sample were blended and identified on a 2% agarose gel, then recovered by gel cutting with an AxyPrepDNA Gel Recovery kit (Axygen, Union City, CA, United States) and detected using a QuantiFluor-ST Handheld Fluorometer with UV/Blue Channels (Promega, Madison, WI, United States). The PCR products were sequenced on Miseq after concentration normalization (Illumina Inc., San Diego, CA, United States).

Bioinformatics Analysis

The Paired-end reads generated by Miseq sequencing were first stitched together according to overlap relationships, and the sequence quality was checked and filtered. Usearch (version 7.0.1090[1]) was used to accomplish operational taxonomic units (OTU) clustering analysis (similarity cutoff rate of 97%). For classification analysis (confidence threshold 70%), each 16S rRNA gene sequence was compared to the Silva 16S rRNA database (version 138[2]) using the ribosomal database project classifier (version 11.5[3]). Alpha diversity index analysis on account of OTU clustering data from Mothur (version 1.30.2[4]). Qiime (version 1.9.1[5]) was used to conduct principal coordinate analysis (PCoA) on account of bray-curtis distance, and subsequently ANOSIM analysis on account of bray-curtis distance to evaluate clear differences among samples.

Measurement of the Antioxidant Parameters

Antioxidant-related parameters were evaluated employing commecial kits (Jiancheng Bioengineering Institute, Nanjing, China) to determine the antioxidant activity of the colonic mucosa. Briefly, the catalase (CAT) activity, the malondialdehyde (MDA) content, the total superoxide dismutase (T-SOD), and the glutathione peroxidase (GSH-Px) activities were evaluated in conformity with earlier studies (Cao et al., 2016).

Real-Time PCR Analysis

The real-time PCR analysis methods were in accordance with a previous experiment (Cao et al., 2017). Briefly, samples were extracted with Trizol (Takara, Dalian, China), and total RNA was dissolved in diethyl pyrocarbonate (Beyotime Biotechnology, Shanghai, China). The concentration and purity of total RNA were spectrophotometrically measured at OD260 and OD280 according to a previous study (Fang et al., 2017). Subsequently, the total RNA from each colon sample was utilized to transcribe into cDNA with the Prime Script^{TM} RT reagent kit, as well as gDNA Eraser (Takara, Dalian, China). Our study utilized Primer Express Software (version 3.0; Applied Biosystems, Foster City, CA, United States) to design gene-specific primers, which were produced by Takara Biotechnology Company (Takara, Dalian, China). The forward and reverse primers of the genes were shown in **Supplementary Table 1**. The reaction system and PCR procedure was in conformity to our previous study (Fang et al., 2017). Samples was carried out on Real-Time PCR System (ABI 7900HT, Applied Biosystems), and the total volume of system is ten microliters [2 μl of cDNA, 2 μl of ddH_2O water, 0.5 μl each of both reverse and forward primer and 5 μl SYBR® Premix Ex Taq _II (TaKaRa, Dalian, China)]. The reaction condition was as follows: 41 cycles of 95°C for 30 s, followed by 95°C for 10 s and 58°C for 35 s. A housekeeping gene β-actin (ACTB) was utilized for data normalization. Relative mRNA expression was calculated in conformity to the $2^{-\Delta\Delta ct}$ method.

Western Blot

The Western blotting analysis was tested on the basis of the steps by Chen et al. (2016). In brief, 0.1 g of colonic mucosal tissue in 900 μL RIPA lysis buffer with 1% phenylmethanesulfonyl fluoride and 2% phosphatase inhibitor cocktail A, 50X (Beyotime, Shanghai, China) was homogenized at 4°C. The pulverized tissues were centrifuged (13,000 g, 15 min) at 4°C, and the supernatant was collected for western blot analysis. The protein concentration of sample was tested by using the Enhanced BCA Protein Assay kit (Beyotime, Shanghai, China) to normalize. After normalization, 5 × loading buffer in a ratio of 1:4 was added and the proteins were boiled for 10 min to denature. The total proteins in the colonic mucosa were isolated and transferred to polyvinylidene fluoride membranes using sodium dodecyl sulfate polyacrylamide gel electrophoresis (Millipore, Eschborn, Germany). The running buffer is prepared by dissolving 3.03 g Tris base, 14.4 g glycine and 1 g SDS in double-distilled water to 1,000 mL. The electrophoresis process was 80 V constant pressure (30 min), and then changed to 120 V constant pressure (90 min), until the bromophenol blue moved to about 1 cm from the bottom of the gel and stopped. The total proteins in the colonic mucosa were isolated and transferred to polyvinylidene fluoride membranes using sodium dodecyl sulfate polyacrylamide gel electrophoresis (Millipore, Eschborn, Germany). The transfer buffer was prepared by dissolving 3.03 g Tris base, 14.4 g glycine and 200 mL methanol in double-distilled water to 1,000 mL. The transfer process was performed at a constant voltage of 100 V. Depending on protein molecular weight, claudin-1 was transferred for 32 min, occludin were transferred for 67 min and ZO-1 was transferred for 225 min, and β-actin was transferred for 52 min. After transfer, the membrane was washed twice with 1 × TBST for 5 min each at room temperature, pourd out 1 × TBST, and then dried it. The membrane was blocked with 5 ml 1 × TBST buffer containing 0.25 g fat-free milk at room temperature for 1 h. The blocking solution was discarded after

[1]http://www.drive5.com/uparse/

[2]https://www.arb-silva.de

[3]https://rdp.cme.msu.edu/

[4]https://www.mothur.org/wiki/Download_mothur

[5]http://qiime.org/install/index.html

blocking. The membrane was washed three times with 1 × TBST for 5 min each at room temperature, pourd out with 1 × TBST, and then dried it. The membrane was incubated with the primary antibody at room temperature for 60 min and overnight at 4°C. After overnight, the membrane was washed three times with 1 × TBST for 10 min each. The antibodies were used including ZO-1, occludin, and claudin-1 (1:1,000, Proteintech Group, Inc., Wuhan, China). Finally, the membrane was incubated with the rabbit second antibody at room temperature for 90 min. The target bands were visualized through a high-sensitivity multi-function imaging system (ChemiDoc^{TM}, Bio-Rad). Enhanced chemiluminescence was utilized to display the clarity western signals (Beyotime, Shanghai, China). Afterward, the intensity of the bands was determined using Image Lab software (version 6.1, Bio-Rad, Berkeley, CA, United States).

STATISTICAL ANALYSIS

All data were evaluated with the independent-samples *t*-test using the SPSS (version 26, IBM, Chicago, IL, United States). A Shapiro–Wilk test was used as a test of normality. Levene's test was employed to examine homogeneity of variances. All results were expressed as the mean ± standard error. In addition, we normalized the data to equalize the OTU sequence. Species were selected for correlation network graph analysis based on pearson correlation coefficient (Majorbio Bio-pharm Technology Co., Ltd, Shanghai, China). $P < 0.05$ was deemed statistically significant. *P*-values between 0.05 and 0.10 were used to identify the trends.

RESULTS

Diversity of the Microbiome

In our experiment, we obtained a total of 1159521477743542 bases optimized sequences, with an average of 412 bases per sample. The OTUs were clustered with 97% similarity. The CON group, LPS-CON group, and LPS-Trp group each comprised 837, 850, and 807 core OTUs, respectively, whereas 707 core OTUs were common among all the three groups (**Figure 1A**). The three groups did not differ significantly in terms of PCoA diversity on the basis of bray-curtis distance (**Figure 1B**). The α diversity of gut microbiota was shown in **Figures 1C–F**. The Trp did not affect the shannon, simpson, ace, and chao indexes.

Bacterial Abundance in the Colon

The digesta microbiota composition was shown in **Figure 2**. At the phylum level, we identified two predominant phyla (e.g., Firmicutes and Bacteroidetes). Firmicutes accounted for 81.99, 83.67, and 79.40% in the CON, LPS-CON, and LPS-Trp treatments, respectively. Bacteroidetes accounted for 11.59, 10.04, and 13.16% in the CON group, LPS-CON group, and LPS-Trp group, respectively (**Figure 2A**). The abundances of Firmicutes and Bacteroidetes were shown in **Figures 2B,C**.

At the genus level, the genera (at least one treatment group) with relative abundances greater than 0.1% were shown in **Figure 3**. *Terrisporobacter* (CON group: 11.35%, LPS-CON group: 11.38%, LPS-Trp group: 6%), *Clostridium_sensu_stricto_1* (CON group: 8.74%, LPS-CON group: 8.96%, LPS-Trp group: 5.99%), *Blautia*, *Lactobacillus*, and *Prevotella* were the dominant genera (**Figure 3A**).

According to statistical analysis, compared with the LPS-CON group, the relative abundances of *Corynebacterium* ($P < 0.05$, **Figure 3B**) and *unclassified_c__Bacteroidia* ($P < 0.01$, **Figure 3C**) in the LPS-Trp group were significantly decreased. Moreover, the relative abundances of *Anaerostipes* was significantly increased ($P < 0.05$, **Figure 3D**), and the relative abundance of *V9D2013_group* tended to increase ($P = 0.09$, **Figure 3E**) in the LPS-Trp group.

Short-Chain Fatty Acids Concentrations in Colonic Digesta

The SCFAs concentrations are shown in **Figure 4**. Relative to the CON group, the LPS challenge significantly decreased the concentrations of acetate, valerate ($P < 0.05$), butyrate, propionate ($P < 0.01$), and the concentrations of isovalerate ($P = 0.069$) and isobutyrate ($P = 0.061$) tended to decrease. Compared with the LPS-CON group, the LPS-Trp group had higher acetate, propionate, butyrate, and isovalerate concentrations ($P < 0.05$) in colonic digesta, and no significant change was observed in the concentrations of valerate and isobutyrate.

mRNA Expression of Colonic Mucosa

The mRNA expressions of colonic pro-inflammatory cytokines were shown in **Figure 5A**. Relative to the CON group, the LPS-CON group had significantly higher mRNA expressions of *IL-1*β, *IL-6*, *IL-8*, and *TNF*-α ($P < 0.01$). The LPS-Trp group had significantly lower mRNA expressions of *IL-1*β, *IL-6*, *IL-8*, and *TNF*-α ($P < 0.01$) than the LPS-CON group. The mRNA expressions of colonic mucosa were shown in **Figure 5B**. Relative to CON group, the LPS-CON group had significantly lower *AhR*, *CYP1A1*, and *CYP1B1* ($P < 0.01$) mRNA expressions. Compared with the LPS-CON group, the LPS-Trp group had significantly higher *AhR*, *CYP1A1*, and *CYP1B1* ($P < 0.01$) mRNA expressions.

Antioxidant Indicators in the Colon

The antioxidant indicators were shown in **Figure 6**. Relative to the CON group, the LPS challenge significantly decreased the activities of GSH-Px, T-SOD ($P < 0.01$) and CAT ($P < 0.05$), and significantly increased the content of MDA ($P < 0.01$). In addition, compared with the LPS-CON group, Trp supplementation significantly increased the activities of GSH-Px, T-SOD, and CAT ($P < 0.01$), and significantly declined the content of MDA ($P < 0.01$).

Tight Junction Gene and Protein Expression Levels in Colonic Mucosa

The effect of Trp supplementation on the mRNA expression of tight junction protein was shown in **Figure 7**. Relative to

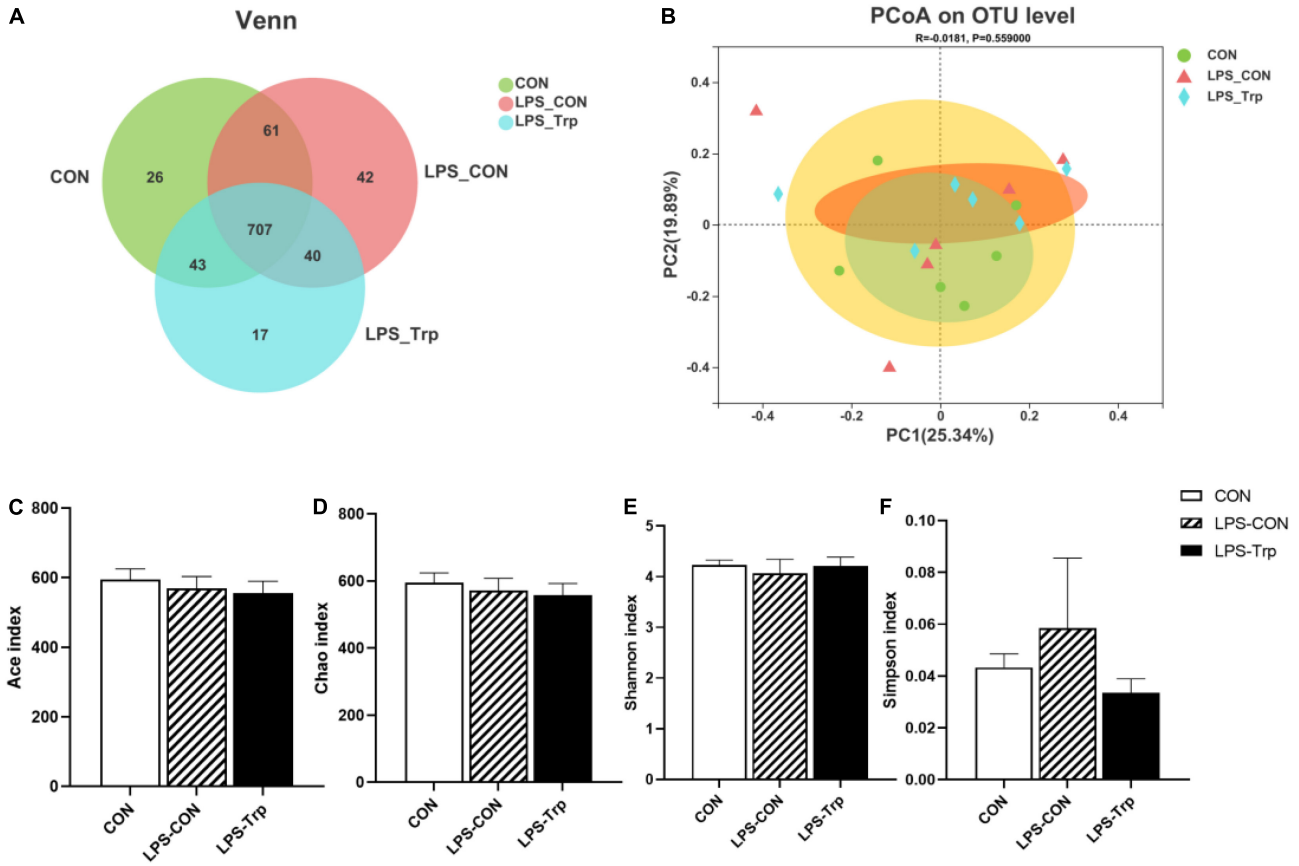

FIGURE 1 | The effects of tryptophan supplementation on the diversity of colonic digesta in lipopolysaccharide-challenged piglets. CON, control group; LPS-CON, piglets challenged with lipopolysaccharide; LPS-Trp, piglets fed with tryptophan and challenged with lipopolysaccharide. **(A)** Venn diagram of core operational taxonomic units. **(B)** Principal coordinate analysis on colonic microbiota, significant differences were determined using ANOSIM analysis. **(C)** Ace index of colonic mucosa microbiota. **(D)** Chao index of colonic mucosa microbiota. **(E)** Shannon index of colonic mucosa microbiota. **(F)** Simpson index of colonic mucosa microbiota. Values are shown as mean ± standard error (n = 6).

CON group, the LPS-CON group had significantly lower *claudin-1* ($P < 0.01$), *occludin* ($P < 0.05$), and *ZO-1* ($P < 0.01$) mRNA expression. Compared with the LPS-CON group, the LPS-Trp group had significantly higher *claudin-1*, *occludin*, and *ZO-1* ($P < 0.01$) mRNA expression. The effect of Trp supplementation on the expressions of tight junction protein was shown in **Figure 8**. Relative to CON pigs, the LPS-CON pigs had lower ratios of claudin-1/β-actin ($P < 0.05$), occludin/β-actin ($P = 0.087$), and ZO-1/β-actin ($P < 0.01$). Relative to LPS-CON pigs, the LPS-Trp pigs had higher ratios of claudin-1/β-actin, occludin/β-actin ($P < 0.05$), and ZO-1/β-actin ($P < 0.01$).

Correlation Analysis Between the Gut Microbiota Metabolites and Inflammation, Antioxidant, Barrier-Relative Parameters in Piglets

The heat maps of the Pearson correlation coefficient between the gut microbial metabolite SCFAs and antioxidant capacity and the expressions of colonic mucosa-related genes were shown in **Figure 9**. Acetate concentration was positively correlated with mRNA level of *occludin* ($r = +0.054$, $P = 0.033$) and *CYP1B1* ($r = +0.669$, $P = 0.002$), and was negatively correlated with MDA content ($r = -0.716$, $P = 0.001$) and *TNF*-α gene expression ($r = -0.475$, $P = 0.047$). Propionate concentration was positively correlated with mRNA level of *occludin* ($r = +0.502$, $P = 0.034$) and *CYP1B1* ($r = +0.682$, $P = 0.002$), and was negatively correlated with MDA content ($r = -0.805$, $P = 0.000$), and with mRNA level of *IL-1*β ($r = -0.500$, $P = 0.035$), *IL-6* ($r = -0.566$, $P = 0.014$), *IL-8* ($r = -0.494$, $P = 0.037$), and *TNF*-α ($r = -0.522$, $P = 0.026$). Butyrate concentration was positively correlated with mRNA level of *occludin* ($r = +0.593$, $P = 0.010$) and *CYP1B1* ($r = +0.554$, $P = 0.020$), and with T-SOD activity ($r = +0.499$, $P = 0.035$), and was negatively correlated with MDA content ($r = -0.880$, $P = 0.000$), and with mRNA level of *IL-1*β ($r = -0.567$, $P = 0.014$), *IL-6* ($r = -0.569$, $P = 0.014$), and *TNF*-α ($r = -0.583$, $P = 0.011$). Isovalerate concentration was positively correlated with CAT activity ($r = +0.469$, $P = 0.050$), and was negatively correlated with MDA content ($r = -0.620$, $P = 0.006$), and with mRNA level of *TNF*-α ($r = -0.627$, $P = 0.005$), *IL-1*β ($r = -0.502$, $P = 0.034$), *IL-6* ($r = -0.486$, $P = 0.041$), and *IL-8* ($r = -0.504$, $P = 0.033$).

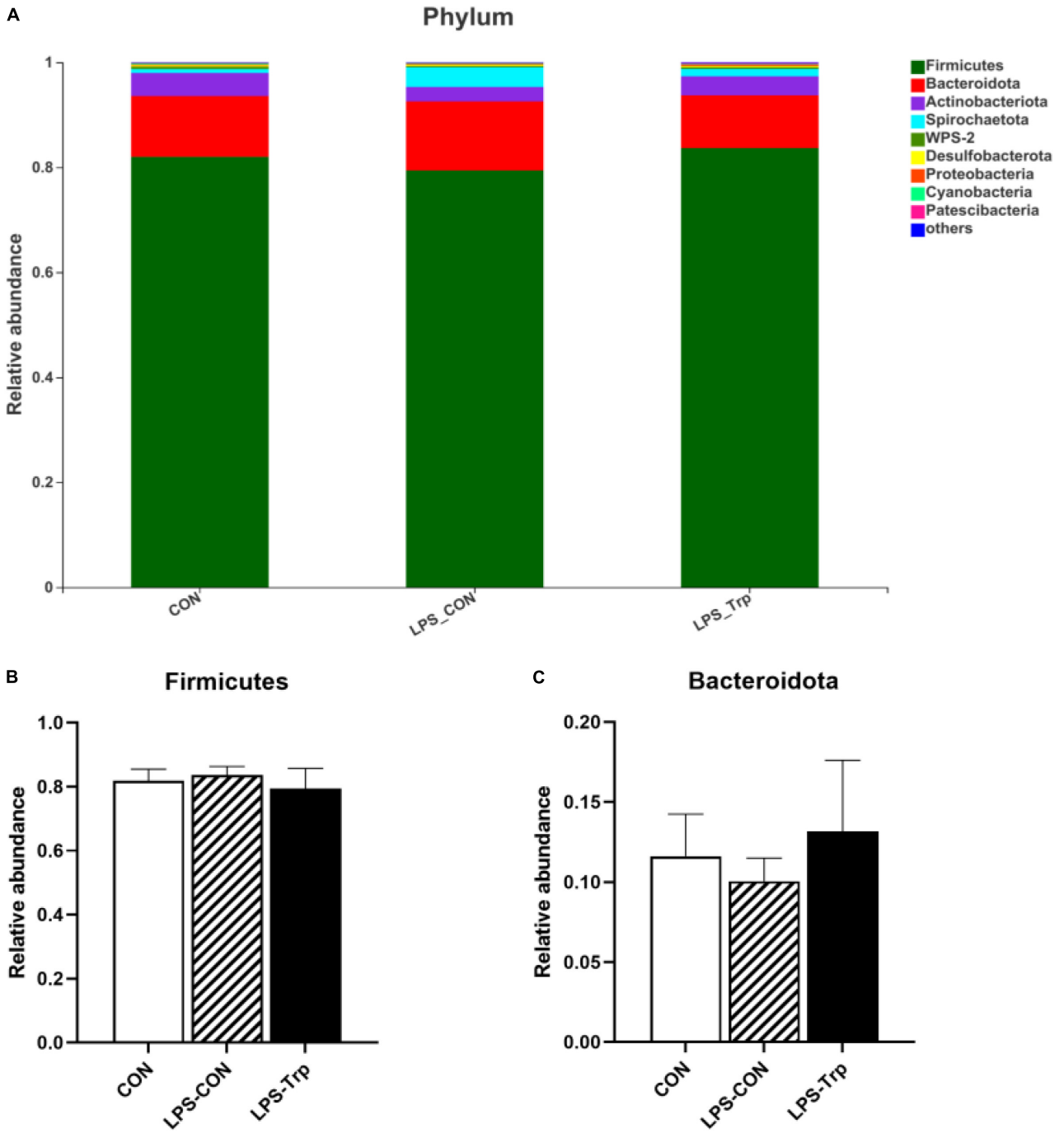

FIGURE 2 | At the phylum level, the effects of tryptophan supplementation on the relative abundance of colonic digesta. CON, control group; LPS-CON, piglets challenged with lipopolysaccharide; LPS-Trp, piglets fed with tryptophan and challenged with lipopolysaccharide. **(A)** The graph showed the level composition of phylum. **(B)** The change of Firmicutes. **(C)** The change of Bacteroidota. Values are shown as mean ± standard error (n = 6).

DISCUSSION

Complex and various microbial community colonization is crucial in maintaining innate and adaptive immune responses and intestinal health (Nicholson et al., 2012; Gardiner et al., 2020). Diets regulate the microbial composition and diversity (Zhang et al., 2018). Trp regulates the composition and diversity of cecal microbia (Liang et al., 2018b). However, how the intestinal microbiota is regulated by Trp after LPS challenge remains unknown. The colon is the intestinal segment with the most active microbial metabolic activity (Sommer and Bäckhed, 2016). Thus, selecting the colon was emphasized in this study.

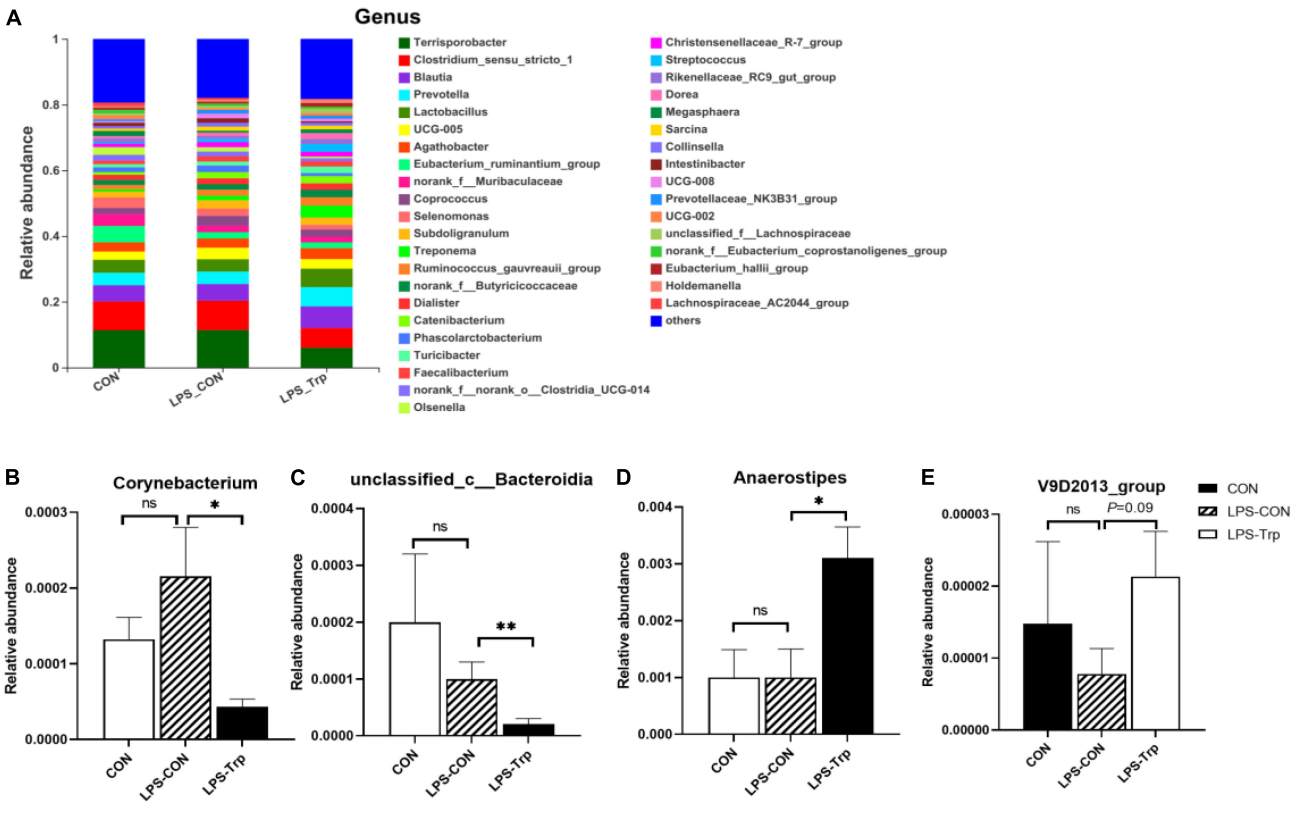

FIGURE 3 | At the genus level, the effects of tryptophan supplementation on the relative abundance of colonic digesta. CON, control group; LPS-CON, piglets challenged with lipopolysaccharide; LPS-Trp, piglets fed with tryptophan and challenged with lipopolysaccharide. **(A)** The graph showed the level composition of genus. **(B)** The change of Corynebacterium. **(C)** The change of unclassified_c__Bacteroidia. **(D)** The change of Anaerostipes. **(E)** The change of V9D2013_group. Values are shown as mean ± standard error ($n = 6$). $0.05 \leq P < 0.10$ was considered as a tendency. $^{*}P < 0.05$; $^{**}P < 0.01$. "ns" was considered as not significant.

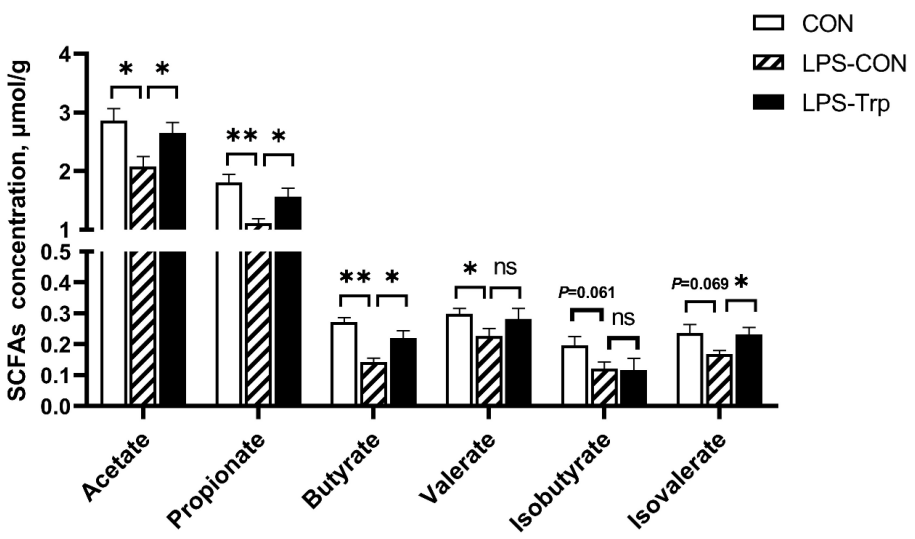

FIGURE 4 | The effects of tryptophan supplementation on SCFAs concentrations in colon of lipopolysaccharide-challenged piglets. SCFAs, short-chain fatty acids; CON, control group; LPS-CON, piglets challenged with lipopolysaccharide; LPS-Trp, piglets fed with tryptophan and challenged with lipopolysaccharide. Values are shown as mean ± standard error ($n = 6$). $0.05 \leq P < 0.10$ was considered as a tendency. $^{*}P < 0.05$; $^{**}P < 0.01$. "ns" was considered as not significant.

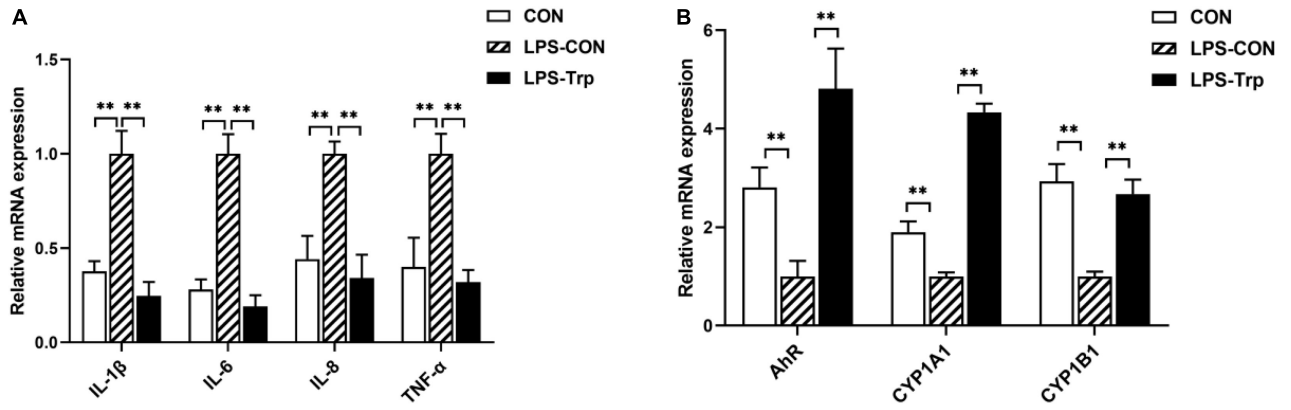

FIGURE 5 | (A) The effects of tryptophan supplementation on the expression of colonic pro-inflammatory cytokines in the piglets. **(B)** The effects of tryptophan supplementation on the expression of colonic mucosa-related genes in the piglets. IL-1β, interleukin-1β; IL-6, interleukin-6; IL-8, interleukin-8; TNF-α, tumor necrosis factor-α; AhR, aryl hydrocarbon receptor; CYP1A1, cytochrome P4501A1; CYP1B1, cytochrome P4501B1; CON, control group; LPS-CON, piglets challenged with lipopolysaccharide; LPS-Trp, piglets fed with tryptophan and challenged with lipopolysaccharide. Values are shown as mean ± standard error ($n = 6$). $^{**}P < 0.01$.

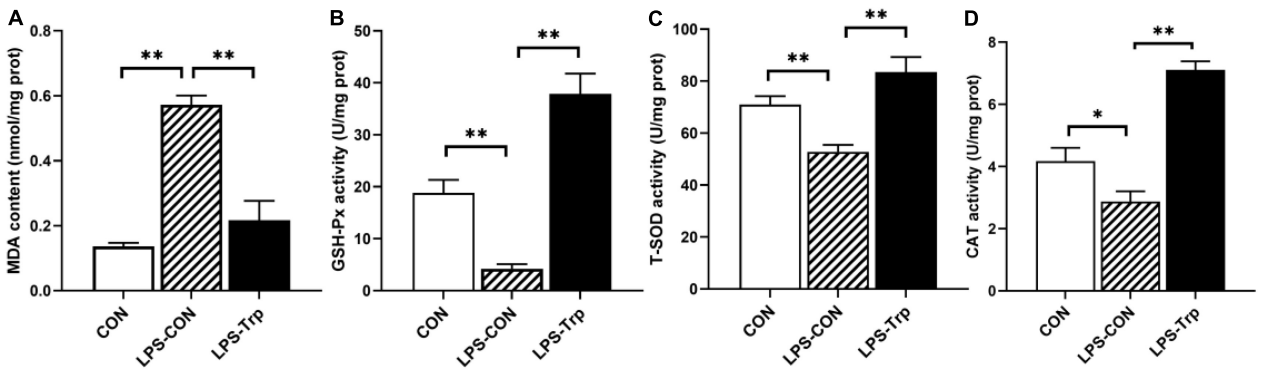

FIGURE 6 | The effects of tryptophan supplementation on antioxidant capacity in colonic mucosa of piglets. MDA, malondialdehyde; GSH-Px, glutathione peroxidase; T-SOD, total superoxide dismutase; CAT, catalase; CON, control group; LPS-CON, piglets challenged with lipopolysaccharide; LPS-Trp, piglets fed with tryptophan and challenged with lipopolysaccharide. **(A)** The content of MDA. **(B)** The activity of GSH-Px. **(C)** The activity of T-SOD. **(D)** The activity of CAT. Values are shown as mean ± standard error ($n = 6$). $0.05 \leq P < 0.10$ was considered as a tendency. $^{*}P < 0.05$; $^{**}P < 0.01$.

Colon microbiota was extracted to investigate the role of Trp on intestinal microbiota. At the phylum level in this study, we found that the majority of the microbiota composition was Firmicutes and Bacteroidota. Firmicutes produce SCFAs modulating intestinal homeostasis (Ellekilde et al., 2014; Louis and Flint, 2017). At the genus level, we found that the majority of the microbiota composition was *Terrisporobacter*, followed by *Clostridium_sensu_stricto_1*, *Blautia*, *Prevotella*, and *Lactobacillus*. Compared with the LPS-CON group, Trp supplementation decreased the proportion of *Terrisporobacter* and *Clostridium_sensu_stricto_1* abundance, as well as increased the proportion of *Blautia*, *Prevotella* and *Lactobacillus* abundances. *Terrisporobacter* is regarded as a member of the *Peptostreptococcaceae* family. The increased abundance of *Terrisporobacter* can induce oxidative stress and inflammation in the host (Cai et al., 2019). This is in agreement with our study that Trp supplementation to the LPS-challenged pigs decreased the proportion of *Terrisporobacter* abundance. *Blautia* occurs widely in the feces and intestines of mammals, as a genus of the *Lachnospiraceae* family, which modulates inflammation, metabolic disorders, and against specific microorganisms (Liu et al., 2021). Consistent with our finding, Trp supplementation to the LPS-challenged pigs increased the proportion of *Blautia* abundance. *Prevotella* belongs to *Bacteroidetes*, which produce SCFAs regulating intestinal homeostasis (Atarashi et al., 2011; Ramakrishna, 2013; Gonçalves et al., 2018). In addition, this is in agreement with our study that Trp supplementation to the LPS-challenged pigs increased the proportion of *Prevotella* abundance. *Lactobacillus* is crucial for regulating LPS-induced intestinal damage in piglets (Sugawara et al., 2020). The experiment showed that in the LPS-induced colitis assay, the cell wall content of *Lactobacillus* reduces immune inflammation and enhances antioxidant defense to prevent induced colitis in mice (Chorawala et al., 2021). Moreover, Trp supplementation to the LPS-challenged pigs increased the proportion of *Lactobacillus* abundance. Trp

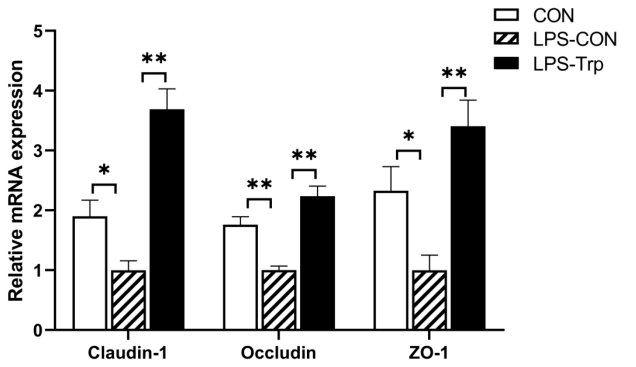

FIGURE 7 | The effects of tryptophan supplementation on the mRNA expression of tight junction protein. ZO-1, zonula occludens-1; CON, control group; LPS-CON, piglets challenged with lipopolysaccharide; LPS-Trp, piglets fed with tryptophan and challenged with lipopolysaccharide. Values are shown as mean ± standard error (n = 6). *P < 0.05; **P < 0.01.

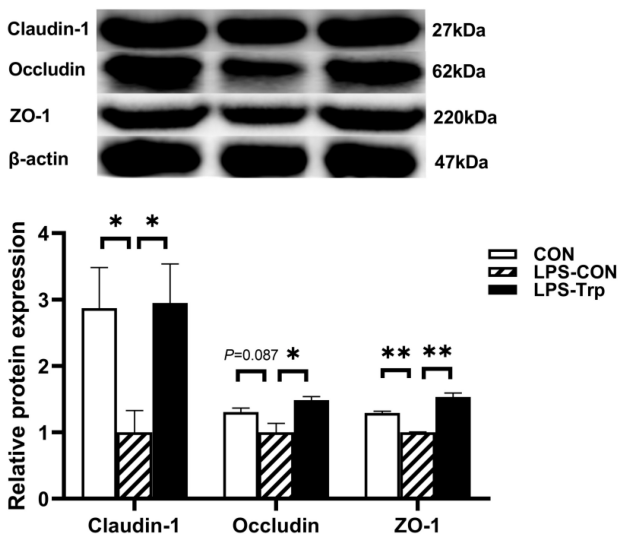

FIGURE 8 | The effects of tryptophan supplementation on the ratios of claudin-1/β-actin, occludin/β-actin, and ZO-1/β-actin of weaning piglets after lipopolysaccharide challenge. ZO-1, zonula occludens-1; CON, control group; LPS-CON, piglets challenged with lipopolysaccharide; LPS-Trp, piglets fed with tryptophan and challenged with lipopolysaccharide. The bands shown are the representative western blot images of claudin-1 and occludin. Values are shown as mean ± standard error (n = 4). 0.05 ≤ P < 0.10 was considered as a tendency. *P < 0.05; **P < 0.01.

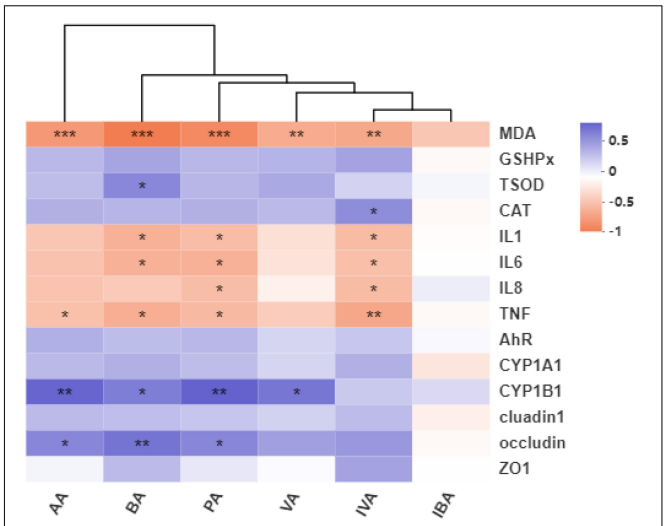

FIGURE 9 | Heat maps of the pearson correlation coefficient and significant tests between the gut microbial metabolite SCFAs and antioxidant capacity, expressions of colonic mucosa-related genes. AA, acetate; BA, butyrate; PA, propionate; VA, valerate; IVA, isovalerate; IBA, isobutyrate; MDA, malondialdehyde; GSHPx, glutathione peroxidase; TSOD, total superoxide dismutase; CAT, catalase; IL1, interleukin-1β; IL6, interleukin-6; IL8, interleukin-8; TNF-α, tumor necrosis factor-α; AhR, aryl hydrocarbon receptor; CYP1A1, cytochrome P4501A1; CYP1B1, cytochrome P4501B1; ZO1, zonula occludens-1; CON, control group; LPS-CON, piglets challenged with lipopolysaccharide; LPS-Trp, piglets fed with tryptophan and challenged with lipopolysaccharide. R values were shown in different colors in the figure. The color range of different R values was shown in the legend on the right. Values are shown as mean ± standard error (n = 6). *P < 0.05; **P < 0.01; ***P < 0.001.

promotes the beneficial bacteria in the intestinal flora and inhibits the pathogenic bacteria (Krishnan et al., 2018; Liang et al., 2018b). This is crucial for the host's intestinal health and systemic homeostasis (Yao et al., 2011; Kaur et al., 2019; Comai et al., 2020).

The gut microbiota was a factor in intestinal inflammation of inflammatory bowel disease (Shim, 2013; Imhann et al., 2018), and the characteristics of the gut microbiota changed when intestinal inflammation occurred. In our study, Trp changed the relative abundance of four genera in LPS challenge. For example, Trp supplementation to the LPS-challenged pigs increased the abundance of *Anaerostipes*, and decreased the abundances of *Corynebacterium* and *unclassified_c__Bacteroidia* at the genus level. *Anaerostipes* converse the anaerobic inositol stereoisomers to propionate and acetate, which is crucial for adapting the change of gut nutritional supplementation (Bui et al., 2021). This is in agreement with our results that Trp supplementation to the LPS-challenged pigs increased the relative abundance of *Anaerostipes*. SCFAs have anti-inflammatory effects on the intestine (Gonçalves et al., 2018). In this study, LPS-challenge increased the concentrations of inflammatory cytokines, and Trp supplementation to the LPS-challenged pigs inhibited the increase in the concentrations of inflammatory cytokines caused by LPS. As a result, our data implied that Trp helped in maintaining the colonic mucosal microbiota homeostasis in LPS-challenged piglets by supporting beneficial bacteria colonization.

Trp metabolite acts as an endogenous ligand of AhR activation. Kynurenine and indole, the metabolites of Trp, bind and activate the AhR and its downstream effector molecules (*CYP1A1* and *CYP1B1*) in regulating intestinal immunity (Marsland, 2016). In this study, Trp supplementation to the LPS-challenged pigs increased the gene expression of *AhR*, *CYP1A1*, and *CYP1B1*. This result is consistent with a previous study finding that bacterial metabolites of Trp activated *AhR* and the downstream *CYP1A1* and *CYP1B1* gene to achieve the effect of regulating intestinal immunity and homeostasis

(Zelante et al., 2013). Moreover, the activation of the AhR signaling is crucial for anti-inflammatory responses (Wenzel et al., 2020). This is in agreement with this study that the intestinal mRNA levels of *IL-1*β, *IL-6*, *IL-8*, and *TNF*-α were decreased in LPS-Trp piglets compared with the CON-LPS group. This is also consistent with this study that propionate, butyrate, and isovalerate concentrations were negatively correlated with the mRNA expression of *IL-1*β, *IL-6*, and *TNF*-α. Moreover, this result is in agreement with the previous report that SCFAs regulates cytokine and immune cell functions, which is crucial in alleviating inflammation (Louis et al., 2014; Parada Venegas et al., 2019).

Inflammation causes oxidative stress. In this study, LPS increased the oxidative stress of the colon by inhibiting the activities of antioxidant enzymes T-SOD, GSH-Px, and CAT in the gut; this finding is in agreement with the previous result (Tian et al., 2018). We found that 0.2% of Trp reduced the oxidative stresses caused by LPS in weaned pigs, which was consistent with the previous finding that Trp had antioxidant capacity (Oxenkrug, 2011). In addition, acetate, propionate, butyrate, and isovalerate concentrations were negatively correlated with MDA content; this result is also in agreement with a previous report that SCFAs, especially acetate and butyrate, reduce oxidative stress caused by high glucose and LPS in mesangial cells (Huang et al., 2017). Therefore, these results suggested that Trp alleviates oxidative stress of LPS-challenged piglets.

Inflammatory cytokines disrupts intestinal barrier function by rearranging tight junction proteins (Vancamelbeke and Vermeire, 2017). The intestinal tight junction is the major component of the intestinal epithelium's physical barrier and governs the intestinal epithelium's selective permeability (Pearce et al., 2018). External stressors make intestinal tight junctions vulnerable, thereby resulting in local or systemic inflammation (Gao et al., 2021). In our study, relative to the LPS-CON pigs, Trp supplementation had higher protein expression of claudin-1, occludin, and ZO-1. This study showed that concentration of acetate, propionate, and butyrate concentrations were positively correlated with *occludin* gene expression. This is also consistent with the study that SCFAs affects the gut barrier function (Li et al., 2020). Therefore, Trp contributes to the colonic epithelial barrier function in LPS-challenged piglets.

CONCLUSION

These results suggest that Trp enhances intestinal health, in part, by modulating intestinal microbiota composition, improving the SCFAs, reducing inflammation, increasing antioxidant capacity, and improving intestinal barrier function.

DATA AVAILABILITY STATEMENT

The datasets presented in this study can be found in online repositories. The names of the repository/repositories and accession number(s) can be found below: https://www.ncbi.nlm.nih.gov/, SRP321842.

ETHICS STATEMENT

The animal study was reviewed and approved by Sichuan Agricultural University Animal Care and Use Committee (SICAU-2021-0830). Written informed consent was obtained from the owners for the participation of their animals in this study.

AUTHOR CONTRIBUTIONS

GL, JL, and WS performed the research and analyzed the data. GJ, HZ, XC, IK, RZ, and JW contributed to the analysis and manuscript preparation. All authors contributed to the article and approved the submitted version.

FUNDING

This work was supported by the Specific Research Supporting Program for Discipline Construction in Sichuan Agricultural University (number 03570126).

ACKNOWLEDGMENTS

The authors would like to thank the members of our team and the laboratory for their industrious assistance in this experiment.

SUPPLEMENTARY MATERIAL

The Supplementary Material for this article can be found online at: https://www.frontiersin.org/articles/10.3389/fmicb.2022.919431/full#supplementary-material

REFERENCES

Agus, A., Planchais, J., and Sokol, H. (2018). Gut microbiota regulation of tryptophan metabolism in health and disease. *Cell Host Microbe* 23, 716–724. doi: 10.1016/j.chom.2018.05.003

Ang, Z., and Ding, J. L. (2016). GPR41 and GPR43 in obesity and inflammation-protective or causative? *Front. Immunol.* 7:28. doi: 10.3389/fimmu.2016.00028

Atarashi, K., Tanoue, T., Shima, T., Imaoka, A., Kuwahara, T., Momose, Y., et al. (2011). Induction of colonic regulatory t cells by indigenous *Clostridium* species. *Science* 331, 337–341. doi: 10.1126/science.1198469

Bosi, A., Banfi, D., Bistoletti, M., Giaroni, C., and Baj, A. (2020). Tryptophan metabolites along the microbiota-gut-brain axis: an interkingdom communication system influencing the gut in health and disease. *Int. J. Tryptophan Res.* 13:1178646920928984. doi: 10.1177/1178646920928984

Bravo, R., Matito, S., Cubero, J., Paredes, S. D., Franco, L., Rivero, M., et al. (2013). Tryptophan-enriched cereal intake improves nocturnal sleep, melatonin,

serotonin, and total antioxidant capacity levels and mood in elderly humans. *Age* 35, 1277–1285. doi: 10.1007/s11357-012-9419-5

Bui, T. P. N., Mannerås-Holm, L., Puschmann, R., Wu, H., Troise, A. D., Nijsse, B., et al. (2021). Conversion of dietary inositol into propionate and acetate by commensal *Anaerostipes* associates with host health. *Nat. Commun.* 12:4798. doi: 10.1038/s41467-021-25081-w

Cai, C. X., Zhang, Z. X., Morales, M., Wang, Y. N., Khafipour, E., and Friel, J. (2019). Feeding practice influences gut microbiome composition in very low birth weight preterm infants and the association with oxidative stress: a prospective cohort study. *Free Radic. Biol. Med.* 142, 146–154. doi: 10.1016/j.freeradbiomed.2019.02.032

Cao, W., Wu, X. J., Jia, G., Zhao, H., Chen, X. L., Wu, C. M., et al. (2017). New insights into the role of dietary spermine on inflammation, immune function and related-signalling molecules in the thymus and spleen of piglets. *Arch. Anim. Nutr.* 71, 175–191. doi: 10.1080/1745039X.2017.1314610

Cao, W., Xiao, L., Liu, G. M., Fang, T. T., Wu, X. J., Jia, G., et al. (2016). Dietary arginine and N-carbamylglutamate supplementation enhances the antioxidant statuses of the liver and plasma against oxidative stress in rats. *Food Funct.* 7, 2303–2311. doi: 10.1039/C5FO01194A

Chen, L., Li, S., Zheng, J., Li, W. T., Jiang, X. M., Zhao, X. L., et al. (2018). Effects of dietary *Clostridium butyricum* supplementation on growth performance, intestinal development, and immune response of weaned piglets challenged with lipopolysaccharide. *J. Anim. Sci. Biotechnol.* 9, 1–14. doi: 10.1186/s40104-018-0275-8

Chen, X. L., Zhou, B., Luo, Y. L., Huang, Z. Q., Jia, G., Liu, G. M., et al. (2016). Tissue distribution of porcine FTO and its effect on porcine intramuscular preadipocytes proliferation and differentiation. *PLoS One* 11:e0151056. doi: 10.1371/journal.pone.0151056

Chorawala, M. R., Chauhan, S., Patel, R., and Shah, G. (2021). Cell wall contents of probiotics (*Lactobacillus* species) protect against lipopolysaccharide (LPS)-induced murine colitis by limiting immuno-inflammation and oxidative stress. *Probiotics Antimicrob. Proteins* 13, 1005–1017. doi: 10.1007/s12602-020-09738-4

Comai, S., Bertazzo, A., Brughera, M., and Crottid, C. (2020). Tryptophan in health and disease. *Adv. Clin. Chem.* 95, 165–218. doi: 10.1016/bs.acc.2019.08.005

Dai, Z. L., Wu, Z. L., Hang, S. Q., Zhu, W. Y., and Wu, G. Y. (2015). Amino acid metabolism in intestinal bacteria and its potential implications for mammalian reproduction. *MHR Basic Sci. Reprod. Med.* 21, 389–409. doi: 10.1093/molehr/gav003

Ellekilde, M., Selfjord, E., Larsen, C. S., Jakesevic, M., Rune, I., Tranberg, B., et al. (2014). Transfer of gut microbiota from lean and obese mice to antibiotic treated mice. *Sci. Rep.* 4:5922. doi: 10.1038/srep05922

Fang, T. T., Wu, X. J., Cao, W., Jia, G., Zhao, H., Chen, X. L., et al. (2017). Effects of dietary fiber on the antioxidant capacity, immune status, and antioxidant-relative signaling molecular gene expression in rat organs. *RSC Adv.* 7, 19611–19620. doi: 10.1039/C7RA02464A

Gao, J., Xu, K., Liu, H. N., Bai, M. M., Peng, C., Li, T. J., et al. (2018). Impact of the gut microbiota on intestinal immunity mediated by tryptophan metabolism. *Front. Cell. Infect. Microbiol.* 8:13. doi: 10.3389/fcimb.2018.00013

Gao, J., Yin, J., Xu, K., Li, T. J., and Yin, Y. L. (2019). What is the impact of diet on nutritional diarrhea associated with gut microbiota in weaning piglets: a system review. *Biomed Res. Int.* 2019:6916189. doi: 10.1155/2019/6916189

Gao, R., Tian, S., Wang, J., and Zhu, W. Y. (2021). Galacto-oligosaccharides improve barrier function and relieve colonic inflammation via modulating mucosa-associated microbiota composition in lipopolysaccharides-challenged piglets. *J. Anim. Sci. Biotechnol.* 12, 1–16. doi: 10.1186/s40104-021-00612-z

Gardiner, G. E., Metzler-Zebeli, B. U., and Lawlor, P. G. (2020). Impact of intestinal microbiota on growth and feed efficiency in pigs: a review. *Microorganisms* 8:1886. doi: 10.3390/microorganisms8121886

Garrett, W. S. (2019). The gut microbiota and colon cancer. *Science* 364, 1133–1135. doi: 10.1126/science.aaw2367

Gonçalves, P., Araújo, J. R., and Di Santo, J. P. (2018). A cross-talk between microbiota-derived short-chain fatty acids and the host mucosal immune system regulates intestinal homeostasis and inflammatory bowel disease. *Inflamm. Bowel Dis.* 24, 558–572. doi: 10.1093/ibd/izx029

Huang, W., Guo, H. L., Deng, X., Zhu, T. T., Xiong, J. F., Xu, Y. H., et al. (2017). Short-chain fatty acids inhibit oxidative stress and inflammation in mesangial cells induced by high glucose and lipopolysaccharide. *Exp. Clin. Endocrinol. Diabetes* 125, 98–105. doi: 10.1055/s-0042-121493

Imhann, F., Vila, A. V., Bonder, M. J., Fu, Y. J., Gevers, D., Visschedijk, M. C., et al. (2018). Interplay of host genetics and gut microbiota underlying the onset and clinical presentation of inflammatory bowel disease. *Gut* 67, 108–119. doi: 10.1136/gutjnl-2016-312135

Islam, J., Sato, S., Watanabe, K., Watanabe, T., Ardiansyah, Hirahara, K., et al. (2017). Dietary tryptophan alleviates dextran sodium sulfate-induced colitis through aryl hydrocarbon receptor in mice. *J. Nutr. Biochem.* 42, 43–50. doi: 10.1016/j.jnutbio.2016.12.019

Jacobitz, A. W., Liu, Q., Suravajjala, S., and Agrawal, N. J. (2021). Tryptophan oxidation of a monoclonal antibody under diverse oxidative stress conditions: distinct oxidative pathways favor specific tryptophan residues. *J. Pharm. Sci.* 110, 719–726. doi: 10.1016/j.xphs.2020.10.039

Kaur, H., Bose, C., and Mande, S. S. (2019). Tryptophan metabolism by gut microbiome and gut-brain-axis: an in silico analysis. *Front. Neurosci.* 2019:1365. doi: 10.3389/fnins.2019.01365

Kim, C. J., Kovacs-Nolan, J. A., Yang, C. B., Archbold, T., Fan, M. Z., and Mine, Y. (2010). L-tryptophan exhibits therapeutic function in a porcine model of dextran sodium sulfate (DSS)-induced colitis. *J. Nutr. Biochem.* 21, 468–475. doi: 10.1016/j.jnutbio.2009.01.019

Koopmans, S. J., Guzik, A. C., Van Der Meulen, J., Dekker, R., Kogut, J., Kerr, B. J., et al. (2006). Effects of supplemental L-tryptophan on serotonin, cortisol, intestinal integrity, and behavior in weanling piglets. *J. Anim. Sci.* 84, 963–971. doi: 10.2527/2006.844963x

Krishnan, S., Ding, Y., Saedi, N., Choi, M., Sridharan, G. V., Sherr, D. H., et al. (2018). Gut microbiota-derived tryptophan metabolites modulate inflammatory response in hepatocytes and macrophages. *Cell Rep.* 23, 1099–1111. doi: 10.1016/j.celrep.2018.03.109

Lamas, B., Richard, M. L., Leducq, V., Pham, H. P., Michel, M. L., Da Costa, G., et al. (2016). CARD9 impacts colitis by altering gut microbiota metabolism of tryptophan into aryl hydrocarbon receptor ligands. *Nat. Med.* 22, 598–605. doi: 10.1038/nm.4102

Layton, A., McKay, L., Williams, D., Garrett, V., Gentry, R., Sayler, G., et al. (2006). Development of *Bacteroides* 16S rRNA gene TaqMan-based real-time PCR assays for estimation of total, human, and bovine fecal pollution in water. *Appl. Environ. Microbiol.* 72, 4214–4224. doi: 10.1128/AEM.01036-05

Lee, B. J., and Bak, Y. T. (2011). Irritable bowel syndrome, gut microbiota and probiotics. *J. Neurogastroenterol. Motil.* 17, 252–266. doi: 10.5056/jnm.2011.17.3.252

Li, X. Y., He, C., Zhu, Y., and Lu, N. H. (2020). Role of gut microbiota on intestinal barrier function in acute pancreatitis. *World J. Gastroenterol.* 26, 2187–2193. doi: 10.3748/wjg.v26.i18.2187

Liang, H. W., Dai, Z. L., Kou, J., Su, K. J., Chen, J. Q., Yang, Y., et al. (2018a). Dietary L-tryptophan supplementation enhances the intestinal mucosal barrier function in weaned piglets: implication of tryptophan-metabolizing microbiota. *Int. J. Mol. Sci.* 20:20. doi: 10.3390/ijms20010020

Liang, H. W., Dai, Z. L., Liu, N., Ji, Y., Chen, J. Q., Zhang, Y. C., et al. (2018b). Dietary L-tryptophan modulates the structural and functional composition of the intestinal microbiome in weaned piglets. *Front. Microbiol.* 9:1736. doi: 10.3389/fmicb.2018.01736

Liao, S. F. (2021). Invited review: maintain or improve piglet gut health around weanling: the fundamental effects of dietary amino acids. *Animals* 11:1110. doi: 10.3390/ani11041110

Liu, G. M., Cao, W., Jia, G., Zhao, H., Chen, X. L., Wang, J., et al. (2016). Effect of spermine on liver and spleen antioxidant status in weaned rats. *J. Anim. Feed Sci.* 25, 335–342. doi: 10.22358/jafs/67668/2016

Liu, G. M., Tao, J. Y., Lu, J. J., Jia, G., Zhao, H., Chen, X. L., et al. (2022). Dietary tryptophan supplementation improves antioxidant status and alleviates inflammation, endoplasmic reticulum stress, apoptosis, and pyroptosis in the intestine of piglets after lipopolysaccharide challenge. *Antioxidants* 11:872. doi: 10.3390/antiox11050872

Liu, X. M., Mao, B. Y., Gu, J. Y., Wu, J. Y., Cui, S. M., Wang, G., et al. (2021). Blautia-a new functional genus with potential probiotic properties? *Gut Microbes* 13, 1–21. doi: 10.1080/19490976.2021.1875796

Louis, P., and Flint, H. J. (2017). Formation of propionate and butyrate by the human colonic microbiota. *Environ. Microbiol.* 19, 29–41. doi: 10.1111/1462-2920.13589

Louis, P., Hold, G. L., and Flint, H. J. (2014). The gut microbiota, bacterial metabolites and colorectal cancer. *Nat. Rev. Microbiol.* 12, 661–672. doi: 10.1038/nrmicro3344

Mao, X. B., Lv, M., Yu, B., He, J., Zheng, P., Yu, J., et al. (2014). The effect of dietary tryptophan levels on oxidative stress of liver induced by diquat in weaned piglet. *J. Anim. Sci. Biotechnol.* 5, 1–7. doi: 10.1186/2049-1891-5-49

Marsland, B. J. (2016). Regulating inflammation with microbial metabolites. *Nat. Med.* 22, 581–583. doi: 10.1038/nm.4117

Matsuoka, K., and Kanai, T. (2015). The gut microbiota and inflammatory bowel disease. *Semin. Immunopathol.* 37, 47–55. doi: 10.1007/s00281-014-0454-4

Nicholson, J. K., Holmes, E., Kinross, J., Burcelin, R., Gibson, G., Jia, W., et al. (2012). Host-gut microbiota metabolic interactions. *Science* 336, 1262–1267. doi: 10.1126/science.1223813

Nikolaus, S., Schulte, B., Al-Massad, N., Thieme, F., Schulte, D. M., Bethge, J., et al. (2017). Increased tryptophan metabolism is associated with activity of inflammatory bowel diseases. *Gastroenterology* 153, 1504–1516. doi: 10.1053/j.gastro.2017.08.028

Ohira, H., Tsutsui, W., and Fujioka, Y. (2017). Are short chain fatty acids in gut microbiota defensive players for inflammation and atherosclerosis? *J. Atheroscler. Thromb.* 24, 660–672. doi: 10.5551/jat.RV17006

Oxenkrug, G. F. (2011). Interferon-gamma-inducible kynurenines/pteridines inflammation cascade: implications for aging and aging-associated psychiatric and medical disorders. *J. Neural Transm.* 118, 75–85. doi: 10.1007/s00702-010-0475-7

Parada Venegas, D., De la Fuente, M. K., Landskron, G., González, M. J., Quera, R., Dijkstra, G., et al. (2019). Short chain fatty acids (SCFAs)-mediated gut epithelial and immune regulation and its relevance for inflammatory bowel diseases. *Front. Immunol.* 10:277. doi: 10.3389/fimmu.2019.00277

Pearce, S. C., Al-Jawadi, A., Kishida, K., Yu, S. Y., Hu, M., Fritzky, L. F., et al. (2018). Marked differences in tight junction composition and macromolecular permeability among different intestinal cell types. *BMC Biol.* 16:19. doi: 10.1186/s12915-018-0481-z

Pi, D., Liu, Y., Shi, H., Li, S., Odle, J., Lin, X., et al. (2014). Dietary supplementation of aspartate enhances intestinal integrity and energy status in weanling piglets after lipopolysaccharide challenge. *J. Nutr. Biochem.* 25, 456–462. doi: 10.1016/j.jnutbio.2013.12.006

Ramakrishna, B. S. (2013). Role of the gut microbiota in human nutrition and metabolism. *Gastroenterol. Hepatol. (N. Y.)* 28, 9–17. doi: 10.1111/jgh.12294

Saraf, M. K., Piccolo, B. D., Bowlin, A. K., Mercer, K. E., LeRoith, T., Chintapalli, S. V., et al. (2017). Formula diet driven microbiota shifts tryptophan metabolism from serotonin to tryptamine in neonatal porcine colon. *Microbiome* 5, 1–13. doi: 10.1186/s40168-017-0297-z

Schiering, C., Wincent, E., Metidji, A., Iseppon, A., Li, Y., Potocnik, A. J., et al. (2017). Feedback control of AHR signalling regulates intestinal immunity. *Nature* 542, 242–245. doi: 10.1038/nature21080

Schwiertz, A., Taras, D., Schäfer, K., Beijer, S., Bos, N. A., Donus, C., et al. (2010). Microbiota and SCFA in lean and overweight healthy subjects. *Obesity* 18, 190–195. doi: 10.1038/oby.2009.167

Shen, Y. B., Voilqué, G., Kim, J. D., Odle, J., and Kim, S. W. (2012). Effects of increasing tryptophan intake on growth and physiological changes in nursery pigs. *J. Anim. Sci.* 90, 2264–2275. doi: 10.2527/jas.2011-4203

Shim, J. O. (2013). Gut microbiota in inflammatory bowel disease. *Pediatr. Gastroenterol. J. Hepatol.* 16, 17–21. doi: 10.5223/pghn.2013.16.1.17

Sommer, F., and Bäckhed, F. (2016). Know your neighbor: microbiota and host epithelial cells interact locally to control intestinal function and physiology. *BioEssays* 38, 455–464. doi: 10.1002/bies.201500151

Sugawara, T., Sawada, D., Yanagihara, S., Aoki, Y., Takehara, I., Sugahara, H., et al. (2020). Daily intake of paraprobiotic *Lactobacillus amylovorus* CP1563 improves pre-obese conditions and affects the gut microbial community in healthy pre-obese subjects: a double-blind, randomized, placebo-controlled study. *Microorganisms* 8:304. doi: 10.3390/microorganisms8020304

Southern, L. L., and Adeola, O. (2012). *Nutrient Requirements of Swine*, 11th revised Edn. Washington, DC: The National Academies Press. doi: 10.17226/13298

Tian, Y., Xu, Q., Sun, L. Q., Ye, Y., and Ji, G. Z. (2018). Short-chain fatty acids administration is protective in colitis-associated colorectal cancer development. *J. Nutr. Biochem.* 57, 103–109. doi: 10.1016/j.jnutbio.2018.03.007

Tossou, M. C. B., Liu, H. N., Bai, M. M., Chen, S., Cai, Y. H., Duraipandiyan, V., et al. (2016). Effect of high dietary tryptophan on intestinal morphology and tight junction protein of weaned pig. *Biomed Res. Int.* 2016:2912418. doi: 10.1155/2016/2912418

Trevisi, P., Melchior, D., Mazzoni, M., Casini, L., De Filippi, S., Minieri, L., et al. (2009). A tryptophan-enriched diet improves feed intake and growth performance of susceptible weanling pigs orally challenged with *Escherichia coli* K88. *J. Anim. Sci.* 87, 148–156. doi: 10.2527/jas.2007-0732

Vancamelbeke, M., and Vermeire, S. (2017). The intestinal barrier: a fundamental role in health and disease. *Expert Rev. Gastroenterol. Hepatol.* 11, 821–834. doi: 10.1080/17474124.2017.1343143

Wang, H., Ji, Y., Yin, C., Deng, M., Tang, T., Deng, B., et al. (2018). Differential analysis of gut microbiota correlated with oxidative stress in sows with high or low litter performance during lactation. *Front. Microbiol.* 9:1665. doi: 10.3389/fmicb.2018.01665

Wenzel, T. J., Gates, E. J., Ranger, A. L., and Klegeris, A. (2020). Short-chain fatty acids (SCFAs) alone or in combination regulate select immune functions of microglia-like cells. *Mol. Cell. Neurosci.* 105:103493. doi: 10.1016/j.mcn.2020.103493

Xu, X., Chen, S. K., Wang, H. B., Tu, Z. X., Wang, S. H., Wang, X. Y., et al. (2018). Medium-chain TAG improve intestinal integrity by suppressing toll-like receptor 4, nucleotide-binding oligomerisation domain proteins and necroptosis signalling in weanling piglets challenged with lipopolysaccharide. *Br. J. Nutr.* 119, 1019–1028. doi: 10.1017/S000711451800003X

Yao, K., Fang, J., Yin, Y. L., Feng, Z. M., Tang, Z. R., and Wu, G. Y. (2011). Tryptophan metabolism in animals: important roles in nutrition and health. *Front. Biosci. (Schol. Ed.)* 3:286–297. doi: 10.2741/s152

Zamora-Gasga, V. M., Loarca-Piña, G., Vázquez-Landaverde, P. A., Ortiz-Basurto, R. I., Tovar, J., and Sáyago-Ayerdi, S. G. (2014). *In vitro* colonic fermentation of food ingredients isolated from *Agave tequilana* Weber var. *azul* applied on granola bars. *LWT Food Sci. Technol.* 60, 766–772. doi: 10.1016/j.lwt.2014.10.032

Zelante, T., Iannitti, R. G., Cunha, C., Luca, A. D., Giovannini, G., Pieraccini, G., et al. (2013). Tryptophan catabolites from microbiota engage aryl hydrocarbon receptor and balance mucosal reactivity via interleukin-22. *Immunity* 39, 372–385. doi: 10.1016/j.immuni.2013.08.003

Zhang, N., Ju, Z., and Zuo, T. (2018). Time for food: the impact of diet on gut microbiota and human health. *Nutrition* 51, 80–85. doi: 10.1016/j.nut.2017.12.005

Conflict of Interest: The authors declare that the research was conducted in the absence of any commercial or financial relationships that could be construed as a potential conflict of interest.

frontiers | Frontiers in Microbiology

TYPE Original Research
PUBLISHED 17 August 2022
DOI 10.3389/fmicb.2022.934890

OPEN ACCESS

EDITED BY
Zhi Liu,
Huazhong University of Science and Technology, China

REVIEWED BY
Yong Su,
Nanjing Agricultural University, China
Xianghua Yan,
Huazhong Agricultural University, China
Zhigang Zhou,
Feed Research Institute (CAAS), China

*CORRESPONDENCE
Xiangfeng Kong
nnkxf@isa.ac.cn

SPECIALTY SECTION
This article was submitted to Microorganisms in Vertebrate Digestive Systems, a section of the journal Frontiers in Microbiology

RECEIVED 03 May 2022
ACCEPTED 11 July 2022
PUBLISHED 17 August 2022

CITATION
Zhu Q, Song MT, Azad MAK, Cheng YT, Liu YT, Liu Y, Blachier F, Yin YL and Kong XF (2022) Probiotics or synbiotics addition to sows' diets alters colonic microbiome composition and metabolome profiles of offspring pigs.
Front. Microbiol. 13:934890.
doi: 10.3389/fmicb.2022.934890

Probiotics or synbiotics addition to sows' diets alters colonic microbiome composition and metabolome profiles of offspring pigs

Qian Zhu[1,2], Mingtong Song[1], Md. Abul Kalam Azad[1], Yating Cheng[1,2], Yating Liu[1,2], Yang Liu[1], François Blachier[3], Yulong Yin[1,2] and Xiangfeng Kong[1,2,4]*

[1]Hunan Provincial Key Laboratory of Animal Nutritional Physiology and Metabolic Process, Key Laboratory of Agro-Ecological Processes in Subtropical Region, National Engineering Laboratory for Pollution Control and Waste Utilization in Livestock and Poultry Production, Institute of Subtropical Agriculture, Chinese Academy of Sciences, Changsha, China, [2]College of Advanced Agricultural Sciences, University of Chinese Academy of Sciences, Beijing, China, [3]Université Paris-Saclay, AgroParisTech, INRAE, UMR PNCA, Paris, France, [4]Research Center of Mini-Pig, Huanjiang Observation and Research Station for Karst Ecosystems, Chinese Academy of Sciences, Huanjiang, China

Little information exists about the effects of maternal probiotics and synbiotics addition on the gut microbiome and metabolome of offspring. The present study evaluated the effects of probiotics or synbiotics addition to sows' diets on colonic microbiota and their metabolites in offspring using 16S rRNA gene sequencing and metabolome strategy. A total of 64 pregnant Bama mini-pigs were randomly divided into control, antibiotic, probiotics, and synbiotics groups and fed the corresponding experimental diets during pregnancy and lactation. After weaning, two piglets per litter and eight piglets per group were selected and fed a basal diet. The β-diversity analysis showed that the colonic microbiota of offspring had a clear distinction among the four groups at 65 days of age. Maternal probiotics addition increased the Actinobacteria abundance at 65 days of age and Tenericutes and Firmicutes abundances at 95 days of age of offspring compared with the other three groups, whereas maternal antibiotic addition increased Spirochaetes and Proteobacteria abundances at 95 days of age of offspring compared with the other three groups. Metabolomic analysis showed that colonic metabolites were different between the groups, regardless of the days of age. Furthermore, both PICRUSt2 and enrichment analysis of metabolic pathways showed that maternal probiotics and synbiotics addition affected metabolism of carbohydrate, amino acid, cofactors and vitamins in the colonic microbiota. Compared with the control group, the colonic concentration of indole decreased and skatole increased in the probiotics group, whereas indole increased and skatole decreased in the synbiotics group. Maternal probiotics addition increased the colonic concentrations of acetate and butyrate at 65 and 125 days of age, whereas probiotics and synbiotics addition decreased short-chain fatty acids concentrations at 95 days of age. In addition, the

colonic concentrations of putrescine, cadaverine, 1,7-heptanediamine, and spermidine were increased in the antibiotic, probiotics, and synbiotics groups compared with the control group at 95 days of age. The correlation analysis showed that *Gemmiger*, *Roseburia*, and *Faecalibacterium* abundances were positively correlated with acetate, propionate, and butyrate concentrations; *Gemmiger*, *Blautia*, and *Faecalibacterium* were positively correlated with putrescine and spermidine; and *Faecalibacterium*, *Blautia*, *Clostridium*, and *Streptococcus* were positively correlated with (R)-3-hydroxybutyric acid. Collectively, these findings suggest that probiotics and synbiotics addition to sows' diets exerts effects on offspring pigs by altering gut microbiota composition and their metabolites. The potential beneficial effect on gut health is discussed.

KEYWORDS

bacterial metabolites, Bama mini-pigs, microbiome, probiotics, synbiotics

Introduction

Microbiota harbored in the mammalian gut not only have the major function of harvesting undigested or not fully digested dietary compounds, but also influence a range of metabolic, developmental, and physiological processes of the host (Xiao et al., 2020). The gut microbiota exert their effects notably by fermenting dietary ingredients to produce various bioactive compounds (Schroeder and Bäckhed, 2016). These metabolites signal to the intestinal mucosa, and after absorption, distant organs in the body, thus enabling enteric bacteria to connect to host metabolism by regulating several metabolic pathways and impacting the physiological and pathological status of the host (Koh et al., 2016; Blachier et al., 2017). Gut microbiota live in a symbiotic interaction with the host and co-exist in dynamic equilibrium when contributing to host physiology (Monteagudo-Mera et al., 2016). In recent years, more attention has been paid to the colonization, composition, and function of intestinal microbes. Microbial colonization in the mammalian gut occurs at the very first life stage and undergoes drastic changes during early childhood (Wang et al., 2016), which represents an important driver for the development and maturation of the gut and likely contributes significantly to the long-term health of the host (Korpela et al., 2018). In addition, bacteria transmission from the mother to the neonate through direct contact with maternal microbiota during birth and breast milk during lactation also seems to influence the gut colonization of the infant, with potential health consequences (Sanz, 2011). Considering that the gut microbiota of piglets is mainly derived from the sows' intestinal strains (Ferretti et al., 2018), the study of the regulation of the maternal intestinal microecology deserves attention.

It has been documented that probiotics and synbiotics may represent an effective strategy to improve the gut microbiota in animals and humans. The health-promoting potentials of probiotics include maintenance of gut homeostasis, alienating pathogens, enhancing the nutrient bioavailability, and stimulating and modulating host immune system (Xavier-Santos et al., 2019). A balanced microbiota is an indispensable constituent of a healthy gut, and probiotics can correct the microbiota imbalance in the gut on some occasions, and improve the overall health of the host (Patil et al., 2019). Probiotics and synbiotics also have gained considerable attention concerning their beneficial effects on livestock performance and health. Dietary probiotics supplementation can improve gut health and nutrient digestibility and thus benefit nutrient utilization and growth performance of pigs. Previous studies have demonstrated that probiotics improved the reproductive performance of sows and the growth performance of neonatal piglets by improving intestinal microbiota (Hayakawa et al., 2016). Moreover, synbiotics may stimulate the growth of beneficial microbiota, and enhance the production of beneficial bacterial metabolites like short-chain fatty acids (SCFAs) in sows, while decreasing the production of deleterious metabolites, such effects being possibly associated with improved growth performance and gut microbiota balance in piglets (Śliżewska and Chlebicz, 2019; Girard et al., 2021). Furthermore, the effects of dietary probiotics and synbiotics may mainly target the cecum and colon of pigs, where an abundant and diverse microbial population is harbored (Liao and Nyachoti, 2017). For example, probiotics and prebiotics are conducive to the increase of beneficial microbiota through the growth and production of their metabolites in the host (Sanders et al., 2019). Prebiotics has beneficial effects on the ecological and genetic stability of gut microbiota (Ma et al., 2020a). Moreover, synbiotics may play beneficial roles in the gut microbiota of pigs (Chlebicz-Wojcik and Slizewska, 2020).

Our previous studies showed that dietary synbiotics supplementation could alter the composition of gut microbiota in pregnant and lactating sows and improve colonic microbiota

composition and metabolic activity in suckling piglets (Ma et al., 2020b,c). Moreover, maternal probiotics and synbiotics supplementation may improve the antioxidant capacity, mitochondrial function, and immune response of weaned piglets by modifying the gut microbiota (Wang et al., 2021a,b). Furthermore, it can be hypothesized that maternal probiotics and synbiotics addition can improve feed intake and meat quality by altering the metabolism and gene expression related to the meat quality of offspring. However, the long-term effects of probiotics and synbiotics addition to sows' diets on the colonic microbiota and metabolites in offspring pigs are poorly known. Based on the foregoing, the present study hypothesized that the long-term effects of maternal probiotics and synbiotics addition might regulate the colonic microbiota and metabolome of offspring pigs. Bama mini-pigs are a famous local miniature pig breed in China, and different meat processing methods for this pig breed have different slaughter weight requirements. A previous study has reported that 7.5–10 kg mini-pigs are generally used for roasting pork, whereas pigs with heavier body weights are used for processing bacon (Cai et al., 2021). This study was conducted using Bama mini-pigs to determine the effects of probiotics and synbiotics addition to sows' diets on colonic microbiome and metabolome of offspring pigs during different time points (65, 95, and 125 days of age) after weaning and explored the correlation between microbiota and their metabolites. These findings will provide a basis for the application of probiotics and synbiotics in mother-offspring integration.

Materials and methods

Animals, diets, and treatments

This study was conducted at the mini-pig experimental base of Goat Chong, Shimen Town, Changde City, Hunan Province, China. A total of 64 pregnant Bama mini-pigs with parities of 3–5 and initial body weight (BW) of 92.60 ± 11.76 kg were selected and randomly divided into four groups with 16 sows (pens) per group. The treatment groups included the control group (fed antibiotic-free basal diet), antibiotic group (SA, 50 g/t virginiamycin with the basal diet), probiotics group (SP, 200 mL/d probiotics mixture per animal with the basal diet), and synbiotics group [SS, 500 g xylo-oligosaccharides (XOS) per ton diet + 200 mL/d probiotics mixture per animal with the basal diet]. The probiotics mixture was provided by Hunan Lifeng Biotechnology Co., Ltd. (Changsha, Hunan, China), and contained *Lactobacillus plantarum* B90 (CGMCC1.12934) $\geq 1 \times 10^8$ CFU/mL and *Saccharomyces cerevisiae* P11 (CGMCC2.3854) $\geq 0.2 \times 10^8$ CFU/mL. The XOS (≥ 35%) was provided by Shandong Longlive Biotechnology Co., Ltd. (Shandong, China) and contained xylobiose (55%), xylotriose (25%), xylotetraose (10%), xylopentose (5%), xylohexaose (3%), and xyloheptaose (2%), which met the feed additive of XOS recommended requirements (GB/T23747-2009). The supplemented probiotics mixture was mixed with the feed before feeding the sows, and XOS was added during feed production. The doses of the probiotics and synbiotics were as recommended by the manufacturers and referred to the previous studies (Tan et al., 2016; Ma et al., 2020c).

The sows were housed individually in gestation crates (2.2 × 0.6 m) from day 1 to day 105 of pregnancy, transferred to farrowing crates (2.2 × 1.8 m) on day 106 of pregnancy, and housed until weaning. Creep feed was provided to the suckling piglets from 7 to 28 days of age. After weaning, at 28 days of age, two piglets close to the average BW per litter were selected and transferred to the nursery house for the subsequent feeding trial. After one week of adaption, four piglets from two litters in the same group were merged into one pen. There were eight pens (replicates) and 32 piglets per group. A total of 128 piglets were fed the basal diet for the remaining days of the trial. The composition and nutrient levels of basal diets for sows and piglets are presented in **Supplementary Tables 1, 2**, respectively. Feeding and management were performed according to the standard operations of commercial pig farms.

Sample collection

At 65, 95, and 125 days of age, the offspring pigs from each group were fasted for 12 h and weighed, and then one pig per pen (a total of eight pigs per group) was selected and euthanized under commercial conditions using electrical stunning (120 V, 200 HZ) and exsanguination. Then the pigs were dissected and the head, legs, tail, and viscera were removed. The colonic contents were sampled into sterile centrifuge tubes and immediately stored at −20°C until further analysis for indole, skatole, SCFAs, and bioamines, and stored at −80°C until further analysis for microbiota and metabolites.

Deoxyribonucleic acid extraction, Illumina MiSeq sequencing, data processing, and analysis

Total genomic deoxyribonucleic acid (DNA) from the individual samples of colonic contents was extracted using the Fast DNA SPIN extraction kits (MP Biomedicals, Santa Ana, CA, United States) according to the manufacturer's instructions. The DNA concentration of each sample was quantified using the NanoDrop ND-1000 spectrophotometer (Thermo Fisher Scientific, Waltham, MA, United States), and the resulting polymerase chain reaction (PCR) products were separated using agarose gel electrophoresis. The genes of all microbial 16S rRNA in the hypervariable regions of V3−V4

were amplified by PCR using a universal forward primer F (5′-ACTCCTACGGGAGGCAGCA-3′) and a reverse primer R (5′-GGACTACHVGGGTWTCTAAT-3′). The PCR thermal cycle conditions were as below: 2 min initial denaturation at 98°C, 25 cycles of 15 s at 98°C, 30 s annealing at 55°C, and 30 s elongation at 72°C, and a final extension at 72°C for 5 min. The PCR components include: 5 μL of Q5 reaction buffer (5×), 5 μL of Q5 High-Fidelity GC buffer (5×), 0.25 μL of Q5 High-Fidelity DNA Polymerase (5 U/μL), 2 μL (2.5 mM) of dNTPs, 1 μL (10 μM) each of forward and reverse primers, 2 μL of DNA template, and 8.75 μL of ddH_2O. The PCR amplicons were purified using the Agencourt AMPure Beads (Beckman Coulter, Indianapolis, IN, United States) and quantified with the PicoGreen dsDNA Assay Kit (Invitrogen, Carlsbad, CA, United States), according to the manufacturer's instructions. The purified amplicons were pooled in equimolar from each sample and paired-end sequenced (2 × 300) using the NovaSeq 6000 SP Reagent Kit (500 cycles) on an Illumina MiSeq platform (Illumina, San Diego, CA, United States), according to the standard protocols by Shanghai Personal Biotechnology Co., Ltd. (Shanghai, China).

The raw sequence data generated from 16S rRNA NovaSeq sequencing were demultiplexed and quality-filtered using quantitative insights into microbial ecology (QIIME2; version 2019.4) with slight modification according to the official tutorials.[1] Sequences were quality filtered, denoised, merged, and chimera removed using the DADA2 plugin (Callahan et al., 2016). After quality control and filtering chimeras, non-singleton amplicon sequence variants (ASVs) were aligned with mafft (Katoh et al., 2002) and used to construct a phylogeny with fasttree2 (Price et al., 2010). Taxonomy was assigned to ASVs in the Greengenes database using a classify-sklearn naïve Bayes taxonomy classifier in the feature-classifier plugin against the Greengenes 13_8 99% operational taxonomic units (OTUs) reference sequences (Bokulich et al., 2018). The α-diversity indices, including rarefaction analysis, Chao1, Observed species, Shannon, Simpson, and Pielou's evenness, were estimated using the diversity plugin. Non-metric multidimensional scaling (NMDS) plots based on the Bray-Curtis distance metric were used to visualize differences in microbial community composition among the groups. Analysis of similarity (ANOSIM) for multivariate data was performed using the "vegan" package in R.[2] The partial least square discriminant analysis (PLS-DA) was also performed using the R package to visualize the differences in microbial community composition. The Kruskal-Wallis test was used to identify statistically different microbial taxa at phylum and genus levels among the four groups. The abundance of different microbiota and the Kyoto Encyclopedia of Genes and Genomes (KEGG) pathways were classified using the linear discriminant analysis (LDA) effect size algorithm if the logarithmic LDA values of bacteria exceeded 2.0 using the online procedure of Galaxy.[3] The 16S rRNA sequencing data obtained in this study are deposited in the NCBI Sequence Read Archive (SRA) with under the accession number PRJNA825463[4].

Colonic metabolome and data analysis

The colonic contents were put into the 2-mL EP tube with two steel balls and homogenized by the tissue grinder. The homogenized samples (100 mg) were vortexed for 30 s with 0.6 mL methanol (including internal standard), then grinded, and centrifuged at 12,000 × *g* for 10 min at 4°C to obtain the supernatant. The supernatant was filtered through 0.22 μM membrane to obtain the prepared samples for liquid chromatography-tandem mass spectrometry (LC-MS). The details were as previously described (Chen et al., 2017). The quality control samples were obtained by mixing a small and equal volume of each experimental sample and injected at regular intervals to monitor the stability of the analysis. The LC-MS analysis was performed on Vanquish Ultrahigh-performance LC System (Thermo Fisher Scientific, Waltham, MA, United States) coupled with an Orbitrap Q Exactive series mass spectrometer (Thermo Fisher Scientific). The raw data files were converted into mzXML format by Proteowizard software (v3.0.8789) and then processed by the XCMS software[5] for peaks identification, filtration, and alignment. The metabolites were identified by comparison with the internal library using the mass-to-charge ratio (m/z), retention time, and chromatographic data. The internal standard was used for data QC (reproducibility), and metabolic features in which the relative standard deviation (RSD) of QC > 30% was discarded. The metabolite annotation was performed with the Compound Discoverer program and referenced to the mzCloud database,[6] as well as MetDNA, BioDeepDB, and MoNA.[7]

Principal components analysis (PCA) using an unsupervised method was applied to obtain an overview of the metabolic data, general clustering, and trends. Orthogonal projections to latent structures discriminate analysis (OPLS-DA) was used for statistical analysis to determine the global metabolic changes among the four groups. Variable importance in projection (VIP) was calculated in the OPLS-DA model. The fitting validity and projective ability of the selected OPLS-DA model were assessed by the parameters R^2Y and Q^2Y, respectively. Discriminating metabolites among the four groups were identified using a statistically significant VIP threshold

1 https://docs.qiime2.org/2019.4/tutorials/
2 https://www.r-project.org/
3 http://huttenhower.sph.harvard.edu/galaxy/
4 https://www.ncbi.nlm.nih.gov/sra/PRJNA825463/
5 www.bioconductor.org
6 http://www.mzcloud.org/
7 mona.fiehnlab.ucdavis.edu

of value (VIP $\geq$ 1) and further validated by univariate analysis of variance (ANOVA) analysis ($P \leq 0.05$). The significantly different abundant metabolites screened from untargeted metabolomics were imported into the MetaboAnalyst 5.0 and KEGG databases[8] to perform pathway analysis. Heatmaps were constructed using Euclidian distances and complete linkage grouping with the pheatmap package in R (see text footnote 2). The correlation between the different metabolites was evaluated with the Spearman's rank correlation test using the R package.

Colonic short-chain fatty acids, indole, skatole, and bioamines analysis

The SCFAs concentrations in colonic contents were determined by gas chromatography (Agilent 7890A, Agilent Inc., Palo Alto, CA, United States) according to the method described in previous studies (Ji et al., 2018). Indole, skatole, and bioamines concentrations in colonic contents were measured using high-performance liquid chromatography (Agilent 1290, Agilent Inc., Palo Alto, CA, United States) as described previously (Hu et al., 2019).

Statistical analysis

One-way ANOVA (SPSS 25.0; IBM Inc., Chicago, IL, United States) and Tukey *post-hoc* test were used to analyze the data of colonic metabolites and visualized using GraphPad Prism version 8.0 (GraphPad Software, San Diego, CA, United States). The level of significance was set at *P*-value < 0.05. The analysis of the correlation between metabolites and microbiota abundance at the genus level was determined with the Spearman's rank correlation test using the R package (see text footnote 2).

Results

Microbial diversity in colonic contents of the offspring pigs

The rarefaction curves show that the sampling in each group provided sufficient OTU coverage (**Supplementary Figure 1**). The statistical estimates of α-diversity from each sample at a genetic distance of 3% are presented in **Supplementary Table 3**. No effects were observed on any indices due to probiotics and synbiotics addition to sows' diets (**Supplementary Table 3**), including OTUs, richness estimators (Chao1 and Observed species), diversity indices (Shannon and Simpson), and evenness index (Pielou's). Then the β-diversity analysis was conducted to measure the dissimilarity of the microbial communities. The NMDS ordination plot based on the Bray-Curtis distance metric showed that the microbial communities in colonic contents were clearly separated at 65 days of age (**Figure 1A**; ANOSIM, $P = 0.003$). However, there were not clearly separated among the four groups at 95 and 125 days of age (**Figures 1B,C**; ANOSIM, $P > 0.05$). Furthermore, the PLS-DA indicated that the microbial communities in colonic contents at 65, 95, and 125 days of age of offspring pigs were clearly separated and clustered into distinct groups (**Figures 1D–F**).

Microbiota structure in colonic contents of the offspring pigs

At the phylum level, the dominant microbiota were Firmicutes, Bacteroidetes, Spirochaetes, and Cyanobacteria at 65, 95, and 125 days of age (**Figures 2A–C**), while other phyla were present at very low relative abundances. At 65 days of age, these four phyla accounted for 97.84, 94.56, 95.95, and 97.87% of the reads for offspring pigs from the four groups, respectively (**Figure 2A**). At 95 days of age, these four phyla accounted for 97.81, 97.41, 96.84, and 97.98% of the reads for offspring pigs from the four groups, respectively (**Figure 2B**). At 125 days of age, these four phyla accounted for 97.03, 97.82, 97.92, and 97.85% of the reads for offspring pigs from the four groups, respectively (**Figure 2C**). At the genus level, the ten most dominant genera were *Lactobacillus*, *Gemmiger*, *unclassified_Clostridiales*, *Ruminococcus*, *Streptococcus*, *Treponema*, *Oscillospira*, *SMB53*, *Prevotella,* and *Blautia* at 65 days of age (**Figure 2F**); *Lactobacillus*, *unclassified_Clostridiales*, *Treponema*, *Oscillospira*, *SMB53*, *Ruminococcus*, *Prevotella*, *Clostridium*, *unclassified_Lachnospiraceae*, and *Gemmiger* at 95 days of age (**Figure 2G**); and *Lactobacillus*, *unclassified_Clostridiales*, *Oscillospira*, *SMB53*, *Prevotella*, *Treponema*, *Turicibacter*, *Ruminococcus*, *Clostridium,* *unclassified_Lachnospiraceae*, and *Gemmiger* at 125 days of age (**Figure 2H**). These results indicated that *Lactobacillus* was the most dominant genus in different treatment groups and at different growth stages. *Lactobacillus*, *Gemmiger*, *unclassified_Clostridiales*, *Ruminococcus*, *Treponema*, *Oscillospira*, *SMB53*, and *Prevotella* were the common genera at 65, 95, and 125 days of age.

Significant differences of microbiota at phylum and genus levels in colonic contents among the four groups at different stages were further identified using Kruskal-Wallis analysis. At 65 days of age, the relative abundance of Actinobacteria was increased ($P < 0.05$) in offspring pigs from the SP group compared with the SS group (**Figure 2D**). At 95 days of age, the relative abundances of Spirochaetes from the SP group and Proteobacteria from the SS group in offspring pigs were

8 www.kegg.jp

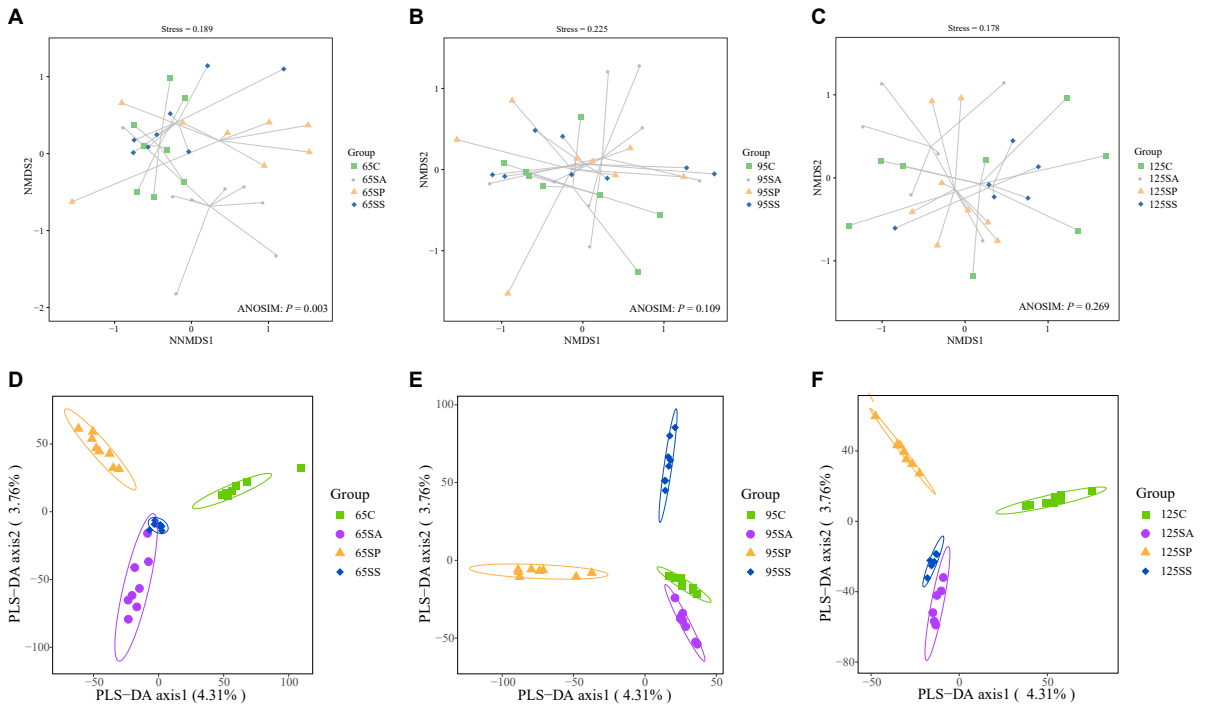

FIGURE 1
Non-metric multidimensional scaling (NMDS) ordination plots based on the Bray-Curtis distance metric **(A–C)** and partial least square discriminant analysis (PLS-DA) plots **(D–F)** of the colonic microbiota community of offspring pigs at 65, 95, and 125 days of age. 65C, 95C, and 125C, sow fed with basal diet; 65SA, 95SA, and 125SA, sow fed with antibiotic; 65SP, 95SP, and 125SP, sow fed with probiotics; 65SS, 95SS, and 125SS, sow fed with synbiotics.

decreased ($P < 0.05$) compared with the SA group (Figure 2E); the relative abundance of Tenericutes was increased ($P < 0.05$) in offspring pigs from the SP group (Figure 2E) compared with the control group. At the genus level, there was an increasing trend in the relative abundances of *Blautia* ($P = 0.068$) and *Dorea* ($P = 0.041$) in the SA and SP groups at 65 days of age, however, *unclassified_Clostridiales* ($P = 0.037$) and *SMB53* ($P = 0.041$) were decreased (Figure 2I) compared with the control and SS groups. The relative abundance of *Catenibacterium* in the SP group was increased ($P < 0.05$) compared with the SS group at 65 days of age (Figure 2I). At 95 days of age, the relative abundance of *Treponema* in the SP group was decreased ($P < 0.05$), whereas that of *Clostridium* was increased ($P < 0.05$) compared with the SA group. Compared with the SA group, the relative abundance of *02d06* was increased ($P < 0.05$) in the SS group. There was a remarkable increase ($P < 0.05$) in the relative abundance of *Gemmiger* in the SP group compared with the control group. The relative abundances of *Roseburia* ($P = 0.051$) and *Blautia* ($P = 0.054$) in the SP group had an increasing trend compared with the other three groups (Figure 2J). At 125 days of age, there was an increasing trend in the relative abundance of *unclassified_Clostridiales* ($P = 0.067$) in the SS group compared with the other three groups, as well as *SMB53* ($P = 0.076$) and *Streptococcus* ($P = 0.080$) in the SA group (Figure 2K).

The linear discriminant analysis effect size analysis of different microbiota in colonic contents of the offspring pigs

The clustering heat map with the abundance of the genus with the top 50 average abundance was drawn to analyze the trend of species abundance distribution in each treatment group. The results indicated that there were different enriched genera among the four groups at 65, 95, and 125 days of age (Supplementary Figure 2).

At the phylum level, the LEfSe analysis revealed that Actinobacteria was enriched in the SP group at 65 days of age (Figure 3A). In addition, there were relatively higher Spirochaetes and [Thermi] abundances in the control group, Acidobacteria, Gemmatimonadetes, and Chloroflexi in the SA group, and Tenericutes and Firmicutes in the SP group at 95 days of age (Figure 3B). At the genus level, the LEfSe analysis indicated that *Allobaculum* and *Desulfovibrio* were enriched in the control group, *Streptomyces* and *Dorea* were enriched in the SA group, *Sphingomonas*, *Catenibactrium*, and *RFN20*

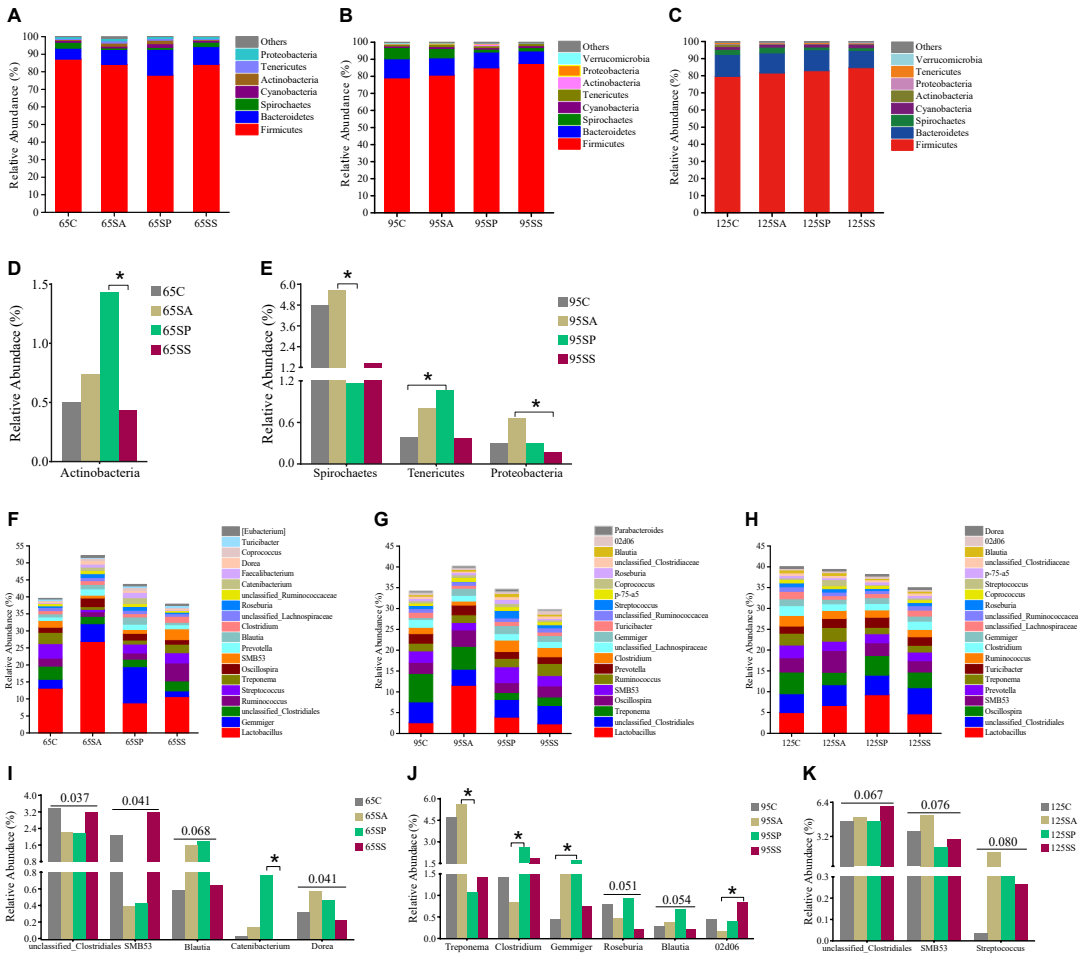

FIGURE 2
Relative abundance of colonic microbiota at phylum level (relative abundance > 0.1%) **(A–C)** and genus level (the top 20 genera) **(F–H)** of offspring pigs. The significant changes of phyla at 65 **(D)** and 95 **(E)** days of age and genera at 65 **(I)**, 95 **(J)**, and 125 **(K)** days of age are presented. The values are expressed as the median. Statistical differences are calculated by the Kruskal-Wallis test: Significance is considered at a *P*-value < 0.05 and the tendency is considered at a *P*-value between 0.05 and 0.1. Asterisk represents $P < 0.05$. 65C, 95C, and 125C, sow fed with basal diet; 65SA, 95SA, and 125SA, sow fed with antibiotic; 65SP, 95SP, and 125SP, sow fed with probiotics; 65SS, 95SS, and 125SS, sow fed with synbiotics.

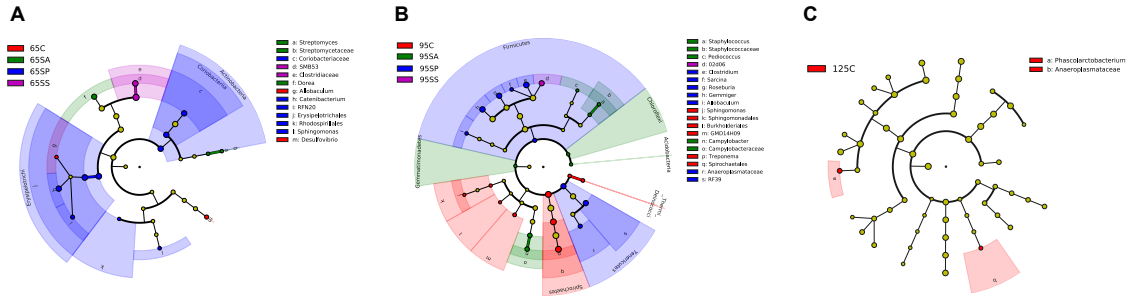

FIGURE 3
Different enrichment of microbiota in colonic contents of offspring pigs. Analysis of taxonomic abundance using linear discriminant analysis effect size (LEfSe analysis) (LDA score ≥ 2, $P < 0.05$) in colonic contents of offspring pigs at 65 **(A)**, 95 **(B)**, and 125 **(C)** days of age. The cladogram shows the microbial species with a significant difference between the experimental groups and the control group. 65C, 95C, and 125C, sow fed with basal diet; 65SA, 95SA, and 125SA, sow fed with antibiotic; 65SP, 95SP, and 125SP, sow fed with probiotics; 65SS, 95SS, and 125SS, sow fed with synbiotics.

were enriched in the SP group, and *SMB53* was enriched in the SS group at 65 days of age (**Figure 3A**). Moreover, *Treponema* and *Sphingomonas* were enriched in the control group, *Pediococcus*, *Campylobacter*, and *Staphylococcus* were enriched in the SA group, *Clostridium*, *Gemmiger*, *Roseburia*, *Allobaculum*, and *Sarcina* were enriched in the SP group, and *02d06* was enriched in the SS group at 95 days of age (**Figure 3B**). The relative abundance of *Phascolatobacterium* was enriched in the control group than in the other three groups at 125 days of age (**Figure 3C**).

Predicted microbiota functions in colonic contents of the offspring pigs

To understand the microbial metabolic function of the colonic contents, a PICRUSt2 approach was used to predict the KEGG pathway composition of the microbial communities. As shown in **Supplementary Figure 3**, at level 1, approximately 76.43, 75.68, and 75.89% of the pathways were affiliated with metabolism; 14.80, 14.73, and 14.78% of pathways were involved with genetic information processing; and 2.84, 2.70, and 2.75% of pathways belonged to environmental information processing at 65, 95, and 125 days of age, respectively. At level 2, a total of 31, 32, and 32 KEGG pathways were identified in the microbiota of colonic contents at 65, 95, and 125 days of age, respectively. The majority of these pathways were associated with carbohydrate metabolism, amino acid metabolism, metabolism of cofactors and vitamins, metabolism of terpenoids and polyketides, metabolism of other amino acids, replication and repair, as well as lipid and energy metabolism (**Supplementary Figure 3**). Then, the differences in functional pathways between different groups were analyzed at level 2 (**Figures 4A–C**). At 65 days of age, the relative abundances of several pathways were higher in the SA group, including immune disease, cardiovascular disease, energy metabolism, and xenobiotics biodegradation and metabolism, while cellular community-prokaryotes displayed lower relative abundance in the SA group (**Figure 4A**). There was no significant difference in the functional pathways at 95 and 125 days of age (**Figures 4B,C**). In addition, the composition of pathways was further analyzed at level 3, identifying 16, 2, and 2 significantly enriched pathways at 65, 95, and 125 days of age, respectively (**Figures 4D–F**). At 65 days of age, a total of eight pathways (including bisphenol degradation, toluene degradation, homologous recombination, aminoacyl-tRNA biosynthesis, terpenoid backbone biosynthesis, selenocompound metabolism, chlorocyclohexane and chlorobenzene degradation, and RNA degradation) were significantly enriched in the SA group, two pathways (including drug metabolism-other enzymes and chloroalkane and chloroalkene degradation) were significantly enriched in the SP group, and six pathways (including biosynthesis of ansamycins, nitrotoluene degradation, pantothenate and CoA biosynthesis, ascorbate and aldarate metabolism, phosphonate and phosphinate metabolism, and *Vibrio cholerae* pathogenic cycle) were significantly enriched in the SS group (**Figure 4D**). At 95 days of age, bisphenol degradation was significantly enriched in the control group and toluene degradation was significantly enriched in the SA group (**Figure 4E**). At 125 days of age, glyoxylate and dicarboxylate metabolism was significantly enriched in the control group and the pathway involved in photosynthesis was significantly enriched in the SS group (**Figure 4F**).

Metabolome analysis in the colonic contents of the offspring pigs

The PCA was conducted to visualize the differences in colonic metabolite composition of the offspring pigs in the four groups at different days of age (**Supplementary Figure 4**). At 65, 95, and 125 days of age, the metabolite composition in offspring pigs was more different among the four groups in the negative model than that in the positive model. To investigate the specific metabolites associated with maternal probiotics and synbiotics addition, the OPLS-DA was carried out, and this analysis was able to appropriately categorize all samples among different groups (**Figure 5**). The best-fitted OPLS-DA model was selected and validated by a cross-validation of all candidate models using a 200-cycle permutation test (**Supplementary Figure 5**). These results suggest that the changes occurred in the colonic metabolome of offspring pigs due to maternal probiotics and synbiotics addition.

A total of 182 metabolites were identified. Moreover, 39, 49, and 27 metabolites were significantly altered among the four groups at 65, 95, and 125 days of age, respectively (**Figure 6**). These different metabolites were mainly related to amino acids, carbohydrate, and lipid metabolism. The proportions of these three metabolites were 35.90, 15.38, and 28.21% at 65 days of age (**Supplementary Figure 6A**), 26.53, 20.41, and 32.65% at 95 days of age (**Supplementary Figure 6B**), and 18.52, 18.52, and 40.74% at 125 days of age (**Supplementary Figure 6C**), respectively. The different metabolic patterns in the different experimental groups are shown in **Figure 6**. When the VIP $\geq$ 2, there were five (including beta-sitosterol, trioxilin A3, D-glucuronic acid, 9,10–12,13-diepoxyoctadecanoate, and dimethyl sulfone), two (including phytosphingosine and N6,N6,N6-trimethyl-L-lysine), and eight (including tetracosanoic acid, N-acetylhistamine, palmitic acid, dimethyl sulfone, fructose 6-phosphate, putrescine, chenodeoxycholic acid, and 4-hydroxycinnamic acid) different metabolites at 65, 95, and 125 days of age, respectively.

To further identify the pivotal metabolites, a pairwise comparison between different treatment groups was conducted. There were 18 common metabolites at three different days of age (**Supplementary Figures 6D–F**). Combining the results

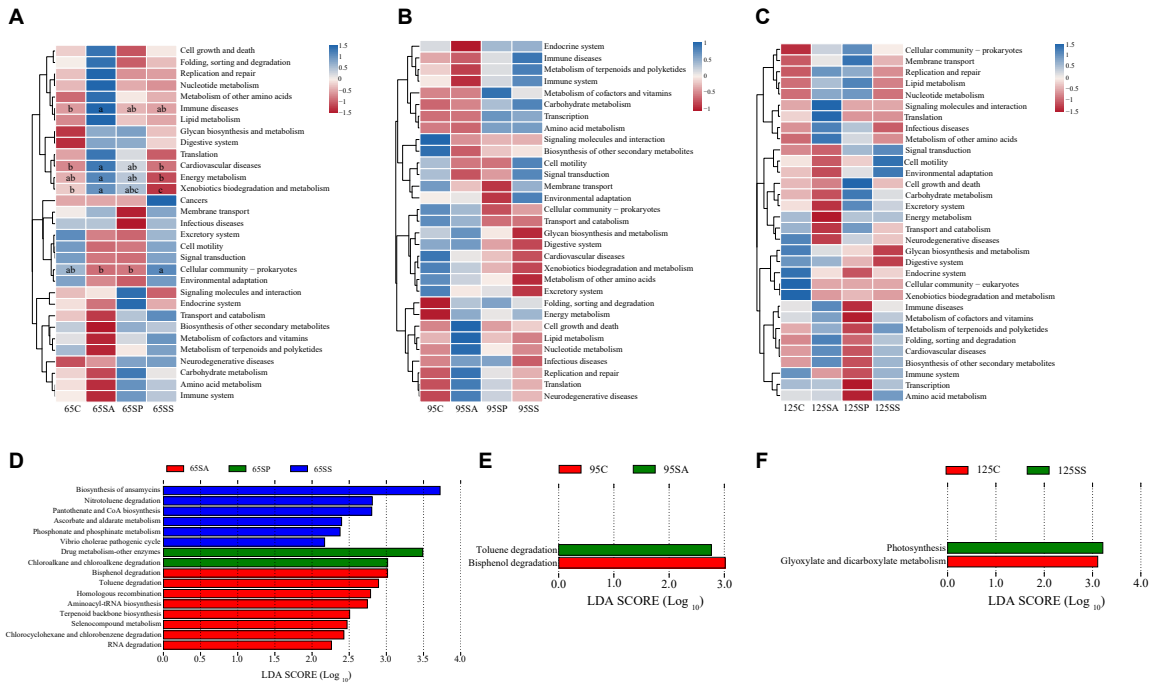

FIGURE 4
Predicted function of colonic microbiota of offspring pigs between the experimental groups and the control group. The heatmap showed that the comparisons of microbiota pathways among different treatment groups at 65 **(A)**, 95 **(B)**, and 125 **(C)** days of age at level 2 using Kruskal-Wallis test. The LEfSe histogram showed that the different metabolic pathways among different groups at 65 **(D)**, 95 **(E)**, and 125 **(F)** days of age at level 3. Different lowercase letters in the same row were significantly different ($P < 0.05$). 65C, 95C, and 125C, sow fed with basal diet; 65SA, 95SA, and 125SA, sow fed with antibiotic; 65SP, 95SP, and 125SP, sow fed with probiotics; 65SS, 95SS, and 125SS, sow fed with synbiotics.

of the pairwise comparison and ANOVA analysis, there were 11 (Figure 7), 9 (Figure 8), and 5 (Figure 9) metabolites were identified at 65, 95, and 125 days of age, respectively. At 65 days of age, the normalized intensity of (+)-7-isojasmonic acid, (R)-3-hydroxybutyric acid, 8(R)-hydroperoxylinoleic acid, 9,10-12,13-diepoxyoctadecanoate, and D-glucuronic acid was increased ($P < 0.05$) in the SA, SP and SS groups, whereas that of 9-oxoODE, beta-sitosterol, maleic acid, trioxilin A3, and niacinamide was decreased ($P < 0.05$) compared with the control group (Figure 7). The normalized intensity of N6,N6,N6-trimethyl-L-lysine in the SP group was higher ($P < 0.05$) than in the SA group, as well as that in the SS group than in the control and SA groups (Figure 7). At 95 days of age, the normalized intensity of 8(R)-hydroperoxylinoleic acid, (R)-3-hydroxybutyric acid, 9,10-12,13-diepoxyoctadecanoate, and D-glucuronic acid was increased ($P < 0.05$) in the SP and SS groups, while that of maleic acid and N6,N6,N6-trimethyl-L-lysine was decreased ($P < 0.05$) compared with the control group (Figure 8). The normalized intensity of 1-aminocyclopropanecarboxylic acid in the control group was higher ($P < 0.05$) among the four groups (Figure 8). In addition, the normalized intensity of 9-oxoODE and (+)-7-isojasmonic acid in the SS group was decreased ($P < 0.05$) compared with the other three groups (Figure 8). At 125 days of age, the normalized intensity of 1-aminocyclopropanecarboxylic acid and 1-naphthylamine was increased ($P < 0.05$), whereas N-acetylhistamine and tetracosanoic acid was decreased ($P < 0.05$) in the SA, SP, and SS groups compared with the control group (Figure 9). Furthermore, the normalized intensity of D-glucuronic acid in the SS group was lower ($P < 0.05$) than in the control group (Figure 9). In addition, the correlations between the metabolites at 65, 95, and 125 days of age were consistent with the variation trend of the normalized intensity of these metabolites in Figures 7–9, as well as Supplementary Figure 7.

To further investigate metabolic pathways involved in these different metabolites, a differential metabolite pathway analysis was conducted. As shown in Figure 10, several metabolic pathways were affected by maternal probiotics and synbiotics addition. At 65 days of age, the different metabolic pathways were lysine degradation, non-alcoholic fatty liver disease, insulin signaling pathway, nicotinate and nicotinamide metabolism, and pentose phosphate pathway (Figure 10A). At 95 days of age, the primary metabolic pathways were ABC transporters, non-alcoholic fatty liver disease, rheumatoid arthritis, human papillomavirus infection, biotin metabolism, AMPK signaling pathway, lysine degradation, central carbon metabolism in cancer, and linoleic acid metabolism (Figure 10B), and those at

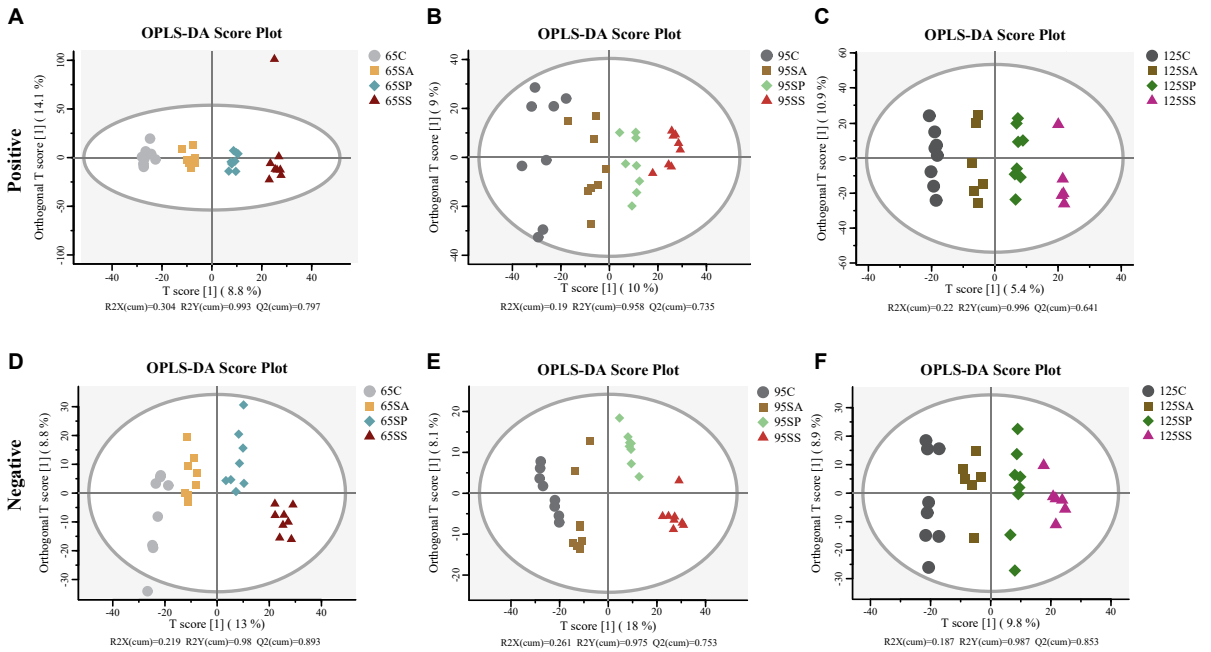

FIGURE 5
Orthogonal partial least squares discriminant analysis (OPLS-DA) plots based on the metabolites in colonic contents of offspring pigs. The OPLS-DA plots of the metabolites in colonic contents in positive **(A–C)** and negative **(D–F)** modes at 65, 95, and 125 days of age among the four groups. 65C, 95C, and 125C, sow fed with basal diet; 65SA, 95SA, and 125SA, sow fed with antibiotic; 65SP, 95SP, and 125SP, sow fed with probiotics; 65SS, 95SS, and 125SS, sow fed with synbiotics.

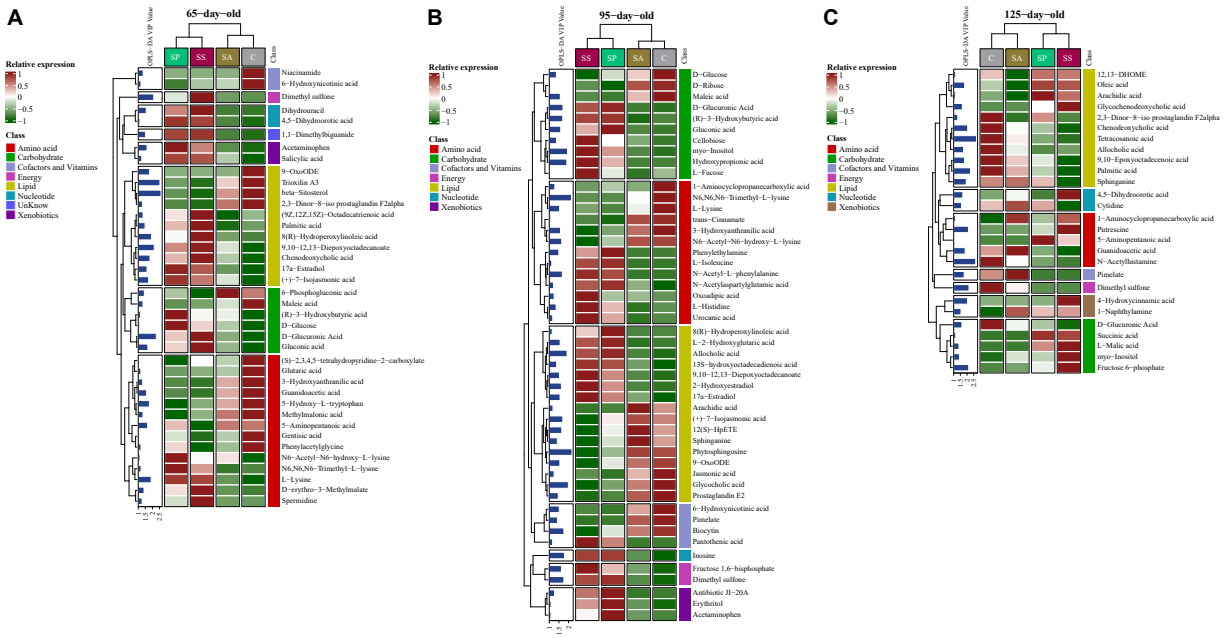

FIGURE 6
Analysis of different metabolites in colonic contents of offspring pigs. The heatmap of different metabolites at 65 **(A)**, 95 **(B)**, and 125 **(C)** days of age. 65C, 95C, and 125C, sow fed with basal diet; 65SA, 95SA, and 125SA, sow fed with antibiotic; 65SP, 95SP, and 125SP, sow fed with probiotics; 65SS, 95SS, and 125SS, sow fed with synbiotics.

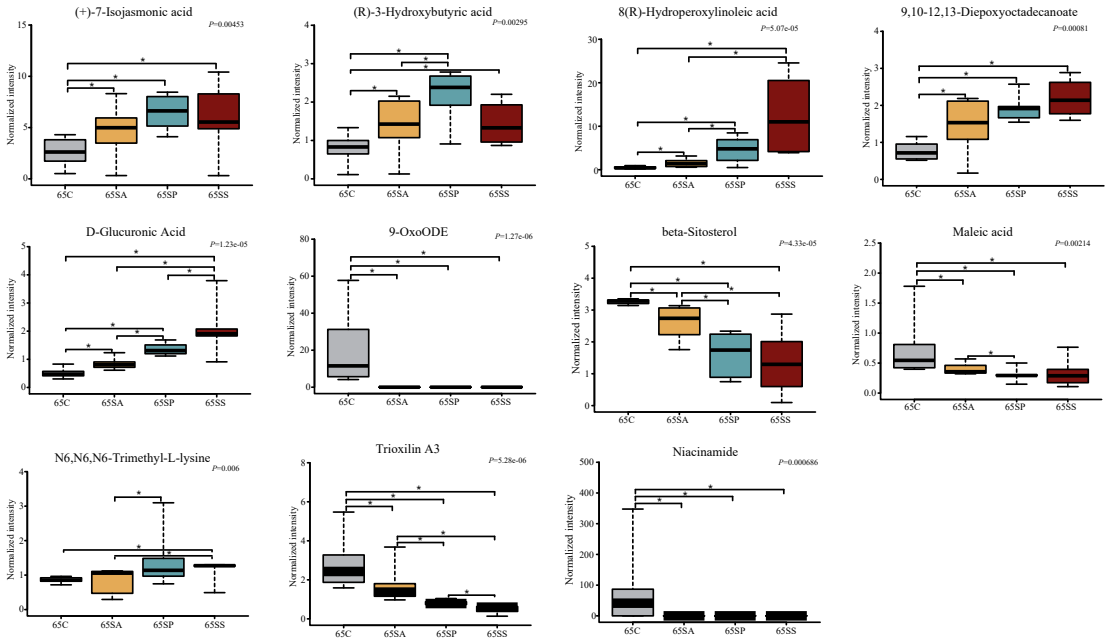

FIGURE 7
The box plots of different metabolites at 65 days of age. Asterisk represents $P < 0.05$. 65C, sow fed with basal diet; 65SA, sow fed with antibiotic; 65SP, sow fed with probiotics; 65SS, sow fed with synbiotics.

125 days of age were renal cell carcinoma, arginine and proline metabolism, and glucagon signaling pathway (Figure 10C).

The concentrations of indole, skatole, short-chain fatty acids, and bioamines in colonic contents of the offspring pigs

As shown in Figure 11A, the indole concentration was lower ($P < 0.05$) in the SP group at 65 and 95 days of age, whereas that was higher ($P < 0.05$) in the SS group at 65 days of age, as well as that in the SA group at 125 days of age, compared with the other groups. The skatole concentration was higher ($P < 0.05$) in the SA group at 95 days of age, as well as that in the SP group at 125 days of age, whereas that was lower ($P < 0.05$) in the SS group, compared with the other groups.

As shown in Figure 11B, at 65 days of age, the butyrate concentration was higher and isovalerate concentration was lower in the SP group compared with the other groups, whereas isobutyrate concentration was lower in the SP group compared with the control and SS groups ($P < 0.05$). In addition, the valerate concentration in the SA, SP, and SS groups was decreased ($P < 0.05$) compared with the control group. As shown in Figure 11C, at 95 days of age, the concentrations of propionate, butyrate, and total SCFA were lower ($P < 0.05$) in the SS group compared with the other groups; the concentration of acetate was lower ($P < 0.05$) in the SS group than in the control group, whereas isobutyrate in the SP and SS groups and isovalerate in the SP group were lower ($P < 0.05$) compared with the control and SA groups. As shown in Figure 11D, at 125 days of age, the acetate concentration was increased ($P < 0.05$) in the SP group compared with the control group; isovalerate concentration was increased ($P < 0.05$) in the SP group compared with the SS group. As shown in Figure 11E, at 65 days of age, the putrescine concentration was higher ($P < 0.05$) in the SS group, as well as spermidine and spermine in the SP group, compared with the other groups. In addition, the phenylethylamine concentration was increased ($P < 0.05$) in the SP and SS groups compared with the control and SA groups. As shown in Figure 11F, at 95 days of age, the concentrations of putrescine, cadaverine, spermidine, spermine, and 1,7-heptanediamine were increased ($P < 0.05$) in the SA, SP, and SS groups compared with the control group. The phenylethylamine concentration was increased ($P < 0.05$) in the SP and SS groups compared with the control and SA groups. Furthermore, the tryptamine concentration was increased ($P < 0.05$) in the SA and SP groups compared with the control and SS groups. As shown in Figure 11G, at 125 days of age, the concentrations of putrescine, cadaverine spermidine, tryptamine, and phenylethylamine were higher ($P < 0.05$) in the SA group than the other three groups, whereas the spermine concentration was higher ($P < 0.05$) in the SA group compared than the control and SS groups. The

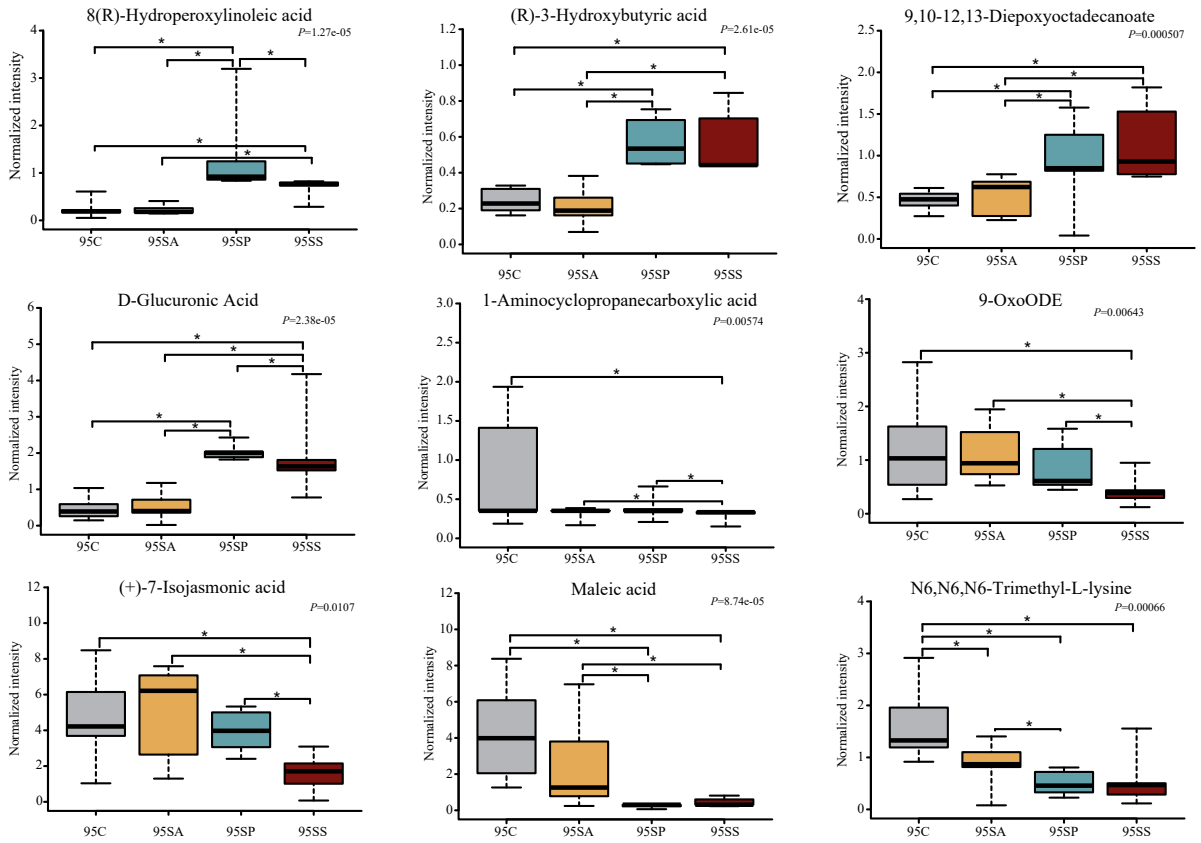

FIGURE 8
The box plots of different metabolites at 95 days of age. Asterisk represents $P < 0.05$. 95C, sow fed with basal diet; 95SA, sow fed with antibiotic; 95SP, sow fed with probiotics; 95SS, sow fed with synbiotics.

1,7-heptanediamine concentration was decreased ($P < 0.05$) in the SP and SS groups compared with the control and SA groups.

Correlation between metabolites and microbiota in colonic contents of the offspring pigs

To explore the functional correlation between changes in the colonic microbiota and metabolites, Spearman's correlation analysis was generated by calculating Spearman's correlation coefficient among the microbial composition affected by the dietary treatments (at the genus level, adjusted $P < 0.05$) and metabolites (Figure 12). A clear significant correlation ($P < 0.05$) was identified between the changes in the colonic microbiome and metabolome. The correlation analysis revealed that fewer metabolites from the metabolome were correlated with the colonic microbiota, whereas more metabolites (including indole, skatole, SCFAs, and bioamines) were correlated with the colonic microbiota (Figure 12).

As shown in Figure 12A, at 65 days of age, the positive correlation ($P < 0.05$) included between (R)-3-hydroxybutyric acid with *Blautia*; (R)-3-hydroxybutyric acid and (+)-7-isojasmonic acid with *Faecalibacterium*; 9-OxoODE with *02d06*; (R)-3-hydroxybutyric acid with *Collinsella* and *Sphingomonas*; N6,N6,N6-trimethyl-L-lysine, (R)-3-hydroxybutyric acid, D-glucuronic acid, 8(R)-hydroperoxylinoleic acid, and 9,10-12,13-diepoxyoctadecanoate with *RFN20*; maleic acid, beta-sitosterol, and trioxilin A3 with *Allobaculum*; maleic acid and 9-OxoODE with *Desulfovibrio*. In addition, the negative correlation ($P < 0.05$) included between 9-OxoODE with *Sphingomonas*; 9-OxoODE, beta-sitosterol, and trioxilin A3 with *RFN20*; N6,N6,N6-trimethyl-L-lysine, (R)-3-hydroxybutyric acid, D-glucuronic acid, (+)-7-isojasmonic acid, 8(R)-hydroperoxylinoleic acid, and 9,10-12,13-diepoxyoctadecanoate with *Allobaculum*; (R)-3-hydroxybutyric acid and D-glucuronic acid with *Desulfovibrio*. As shown in Figure 12B, at 95 days of age, the positive correlation ($P < 0.05$) included between 1-aminocyclopropanecarboxylic acid with *Sphaerochaeta*; (R)-3-hydroxybutyric acid with *Clostridium*, *Streptococcus*, *02d06*, *Allobaculum*, and *Sarcina*; D-glucuronic acid with *Clostridium*, *Streptococcus*, *02d06*, *Allobaculum*, and *Sarcina*; maleic acid with *Treponema*; (+)-7-isojasmonic acid with *Lachnospira*;

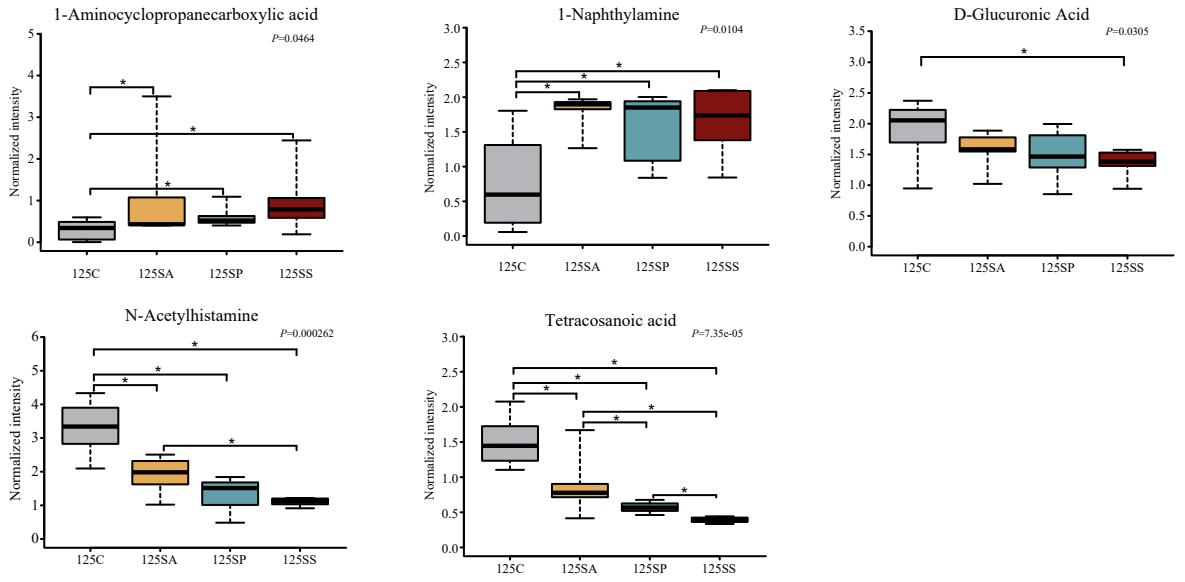

FIGURE 9
The box plots of different metabolites at 125 days of age. Asterisk represents $P < 0.05$. 125C, sow fed with basal diet; 125SA, sow fed with antibiotic; 125SP, sow fed with probiotics; 125SS, sow fed with synbiotics.

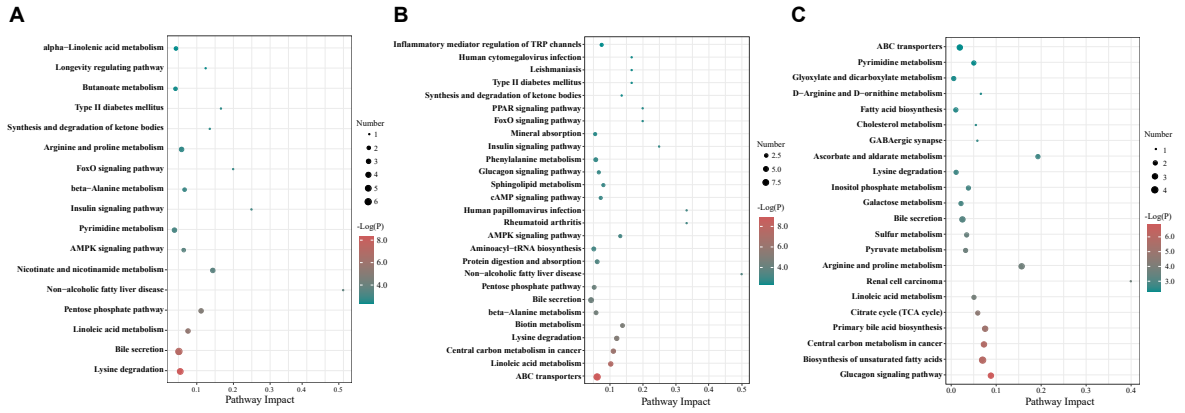

FIGURE 10
The bubble chart of enrichment analysis for metabolic pathways in colonic contents of offspring pigs at 65 **(A)**, 95 **(B)**, and 125 **(C)** days of age. The manipulated metabolic pathways are based on the analysis of different metabolites in colonic contents of offspring pigs among different groups following the KEGG pathway database. The metabolome view shows all matched pathways according to the *P*-values from the pathway enrichment analysis and impact values from the topology analysis. The node colors varied from green to red, indicating that the metabolites have different levels of significance.

8(R)-hydroperoxylinoleic acid with *Clostridium*, *Allobaculum*, and *Sarcina*; 9,10-12,13-diepoxyoctadecanoate with *L7A_E11*, *Allobaculum*, and *Sarcina*; In addition, the negative correlation ($P < 0.05$) included between N6,N6,N6-trimethyl-L-lysine with *Gemmiger*, *Allobaculum*, *Sarcina*, and *Campylobacter*; (R)-3-hydroxybutyric acid with *Treponema*; D-glucuronic acid with *Treponema* and *Pediococcus*; maleic acid with *Clostridium*, *Gemmiger*, *Blautia*, *Allobaculum*, and *Sarcina*; maleic acid with *L7A_E11* and *02d06*; 8(R)-hydroperoxylinoleic acid with *Treponema* and *Pediococcus*; 9,10-12,13-diepoxyoctadecanoate with *Treponema* and *Sphingomonas*. As shown in **Figure 12C**, at 125 days of age, the positive correlation ($P < 0.05$) included between N-acetylhistamine with *Phascolarctobacterium*. In addition, the negative correlation ($P < 0.05$) included between 1-aminocyclopropanecarboxylic acid with *Prevotella*; D-glucuronic acid with *Lactobacillus* and *Dorea*; 1-naphthylamine with *Parabacterioides*.

As shown in **Figure 12D**, at 65 days of age, the positive correlation ($P < 0.05$) included between skatole with *SMB53*, *Faecalibacterium*, and *02d06*; tryptamine with

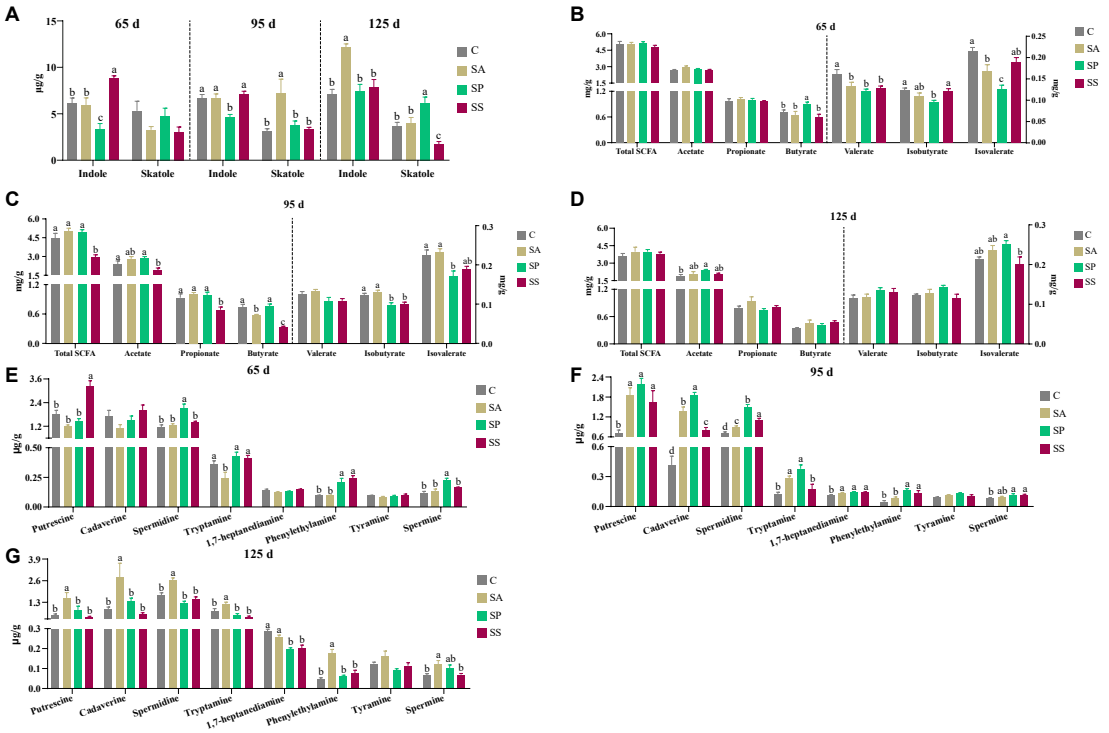

FIGURE 11
Concentrations of indole, skatole, short-chain fatty acids (SCFAs), and bioamines in colonic contents of offspring pigs at 65, 95, and 125 days of age. Concentrations of indole and skatole in colonic contents at 65, 95, and 125 days of age **(A)**; concentrations of SCFAs in colonic contents at 65, 95, and 125 days of age **(B–D)**, respectively; and concentrations of bioamines in colonic contents at 65, 95, and 125 days of age **(E–G)**, respectively. Different superscript letters mean a significant difference ($P < 0.05$). 65 d, 65 days of age; 95 d, 95 days of age; 125 d, 125 days of age; C, sow fed with basal diet; SA, sow fed with antibiotic; SP, sow fed with probiotics; SS, sow fed with synbiotics.

Sphingomonas; phenylethyamine with *RFN20*; spermidine and spermine with *Blautia*, *Faecalibacterium*, *Collinsella*, *Catenibacterium*, and *Sphingomonas*; acetate and propionate with *Gemmiger*, *Roseburia*, and *Faecalibacterium*; butyrate with *Gemmiger*, *Blautia*, *Roseburia*, *Faecalibacterium*, *Coprococcus*, *Collinsella*, and *Bulleidia*; valerate with *SMB53*; isobutyrate and isovalerate with *SMB53*, *Clostridium*, *Turicibacter*, *02d06*, and *unclassified_Erysipelotriichaceae*; total SCFA with *Gemmiger*, *Roseburia*, *Faecalibacterium*, *Coprococcus*, and *Bulleidia*. In addition, the negative correlation ($P < 0.05$) included between indole with *Roseburia* and *Corprococcus*; skatole with *Dorea*; tryptamine with *SMB53*, *Turicibacter*, *02d06*, *unclassified_Erysipelotriichaceae*, and *Phascolarctobacterium*; cadaverine with *Turicibacter* and *02d06*; 1,7-heptanediamine with *02d06* and *unclassified_Erysipelotriichaceae*; tyramine with *Clostridium* and *Turicibacter*; spermidine and spermine with *Treponema*, *02d06*, and *Parabacteroides*; butyrate with *Treponema*; valerate with *Sphaerochaeta*; isobutyrate and isovalerate with *Dorea*.

As shown in Figure 12E, at 95 days of age, the positive correlation ($P < 0.05$) included between indole with *Anaerovibrio*; skatole with *Lachnospira* and *Anaerovibrio*; tryptamine with *Clostridium*, *Gemmiger*, *Blautia*, and *Bulleidia*; phenythylamine with *Ruminococcus*, *Clostridium*, *Gemmiger*, *Allobaculum*, and *Sarcina*; putrescine with *Ruminococcus*, *Gemmiger*, and *Bulleidia*; cadaverine with *Bacteroides* and *Sphaerochaeta*; 1,7-heptanediamine with *Gemmiger*, *Allobaculum*, and *Campylobacter*; tyramine with *Gemmiger* and *Bacteroides*; spermidine with *Clostridium*, *Gemmiger*, *Blautia*, *Allobaculum*, and *Sarcina*; spermine with *Lactobacillus* and *Gemmiger*; acetate, propionate, butyrate, and total SCFA with *Roseburia*, *Lachnospira*, and *Faecalibacterium*; butyrate with *Clostridium*; valerate and isobutyrate with *Lachnospira*; isovalerate with *Lachnospira*, *Phascolarctobacterium*, and *Anaerovibrio*. In addition, the negative correlation ($P < 0.05$) included between skatole with *Ruminococcus*; tryptamine and phenythylamine with *Phascolarctobacterium*; putrescine with *L7A_E11* and *Phascolarctobacterium*; cadaverine with *Bacteroides*, *Sphaerochaeta*, and *L7A_E11*; 1,7-heptanediamine with *Trepnema*; tyramine with *L7A_E11* and *Phascolarctobacterium*; butyrate with *Streptococcus*; isobutyrate and valerate with *Akkermansia*.

As shown in Figure 12F, at 125 days of age, the positive correlation ($P < 0.05$) included between indole with *Lactobacillus* and *Streptococcus*; tryptamine with *SMB53*, *Gemmiger*, *Blautia*, and *Faecalibacterium*; phenylethylamine

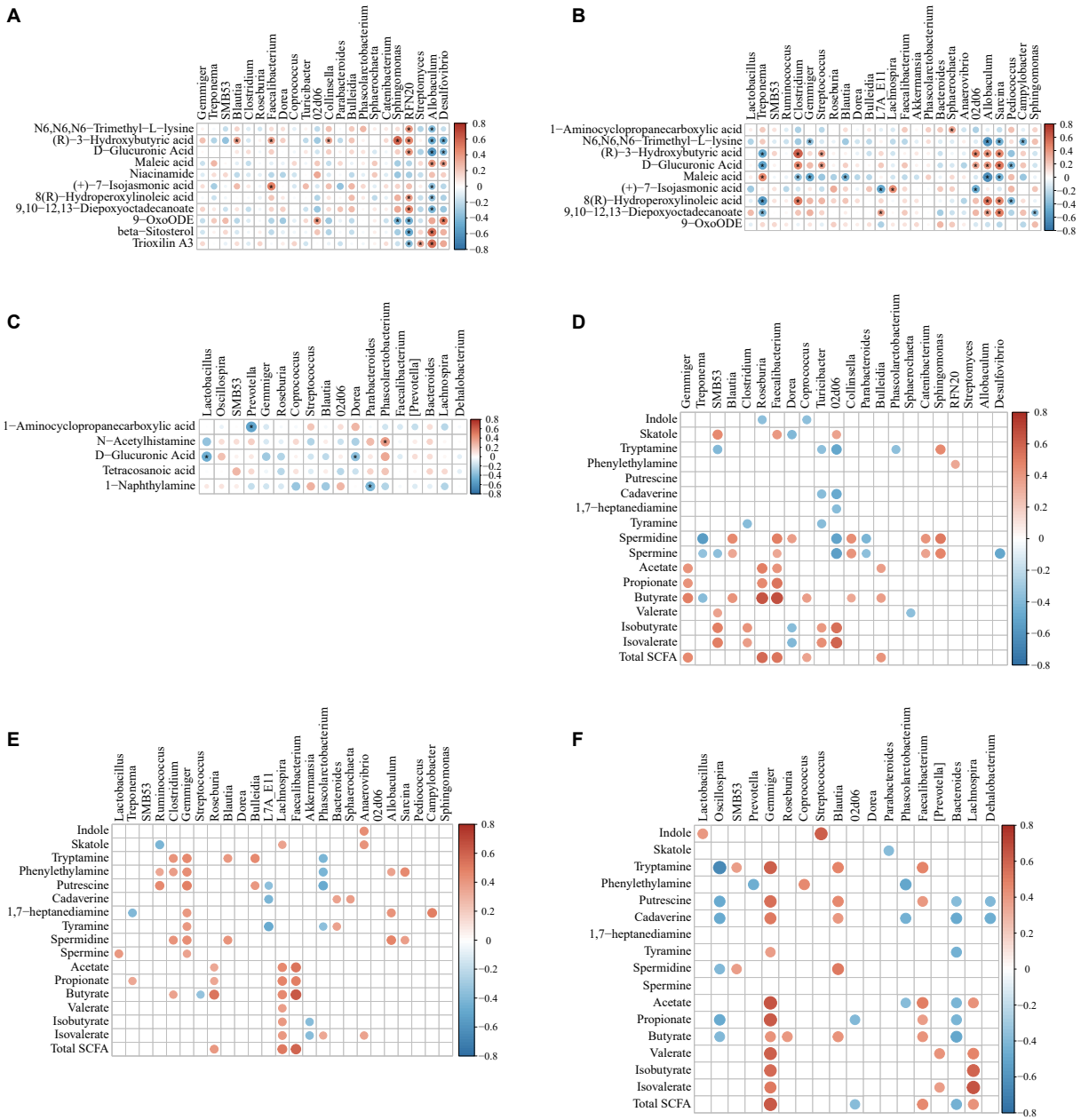

FIGURE 12
Spearman correlation analysis of different microbiota and metabolites [from metabolomic analysis, **(A–C)** indole, skatole, SCFAs, and bioamine, **(D–F)**] in colonic contents of offspring pigs at 65, 95, and 125 days of age, respectively. The red represents positive correlation while the blue represents negative correlation. Asterisk **(A–C)** and red or blue circle **(D–F)** represents *P*-value < 0.05.

with *Coprococcus*; putrescine with *Gemmiger*, *Blautia*, and *Faecalibacterium*; cadaverine with *Gemmiger* and *Blautia*; tyramine with *Gemmiger*; spermidine with *SMB53* and *Blautia*; acetate with *Gemmiger*, *Faecalibacterium*, and *Lachnospira*; propionate with *Gemmiger* and *Faecalibacterium*; butyrate with *Gemmiger*, *Roseburia*, *Blautia*, and *Faecalibacterium*; valerate with *Gemmiger*, *[Prevotella]*, and *Lachnospira*; isobutyrate and isovalerate with *Gemmiger* and *Lachnospira*; total SCFA with *Gemmiger*, *Faecalibacterium*, and *Lachnospira*. In addition, the negative correlation ($P < 0.05$) included between skatole with *Parabacteroides*; tryptamine with *Oscillospira*; phenylethylamine with *Prevotella* and *Phascolarctobacterium*; putrescine with *Oscillospira*, *Bacteroides*, and *Dehalobacterium*; cadaverine with *Oscillospira*, *Phascolarctobacterium*, *Bacteroides*, and *Dehalobacterium*; tyramine with *Bacteroides*; spermidine with *Oscillospira*; acetate with *Phascolarctobacterium*

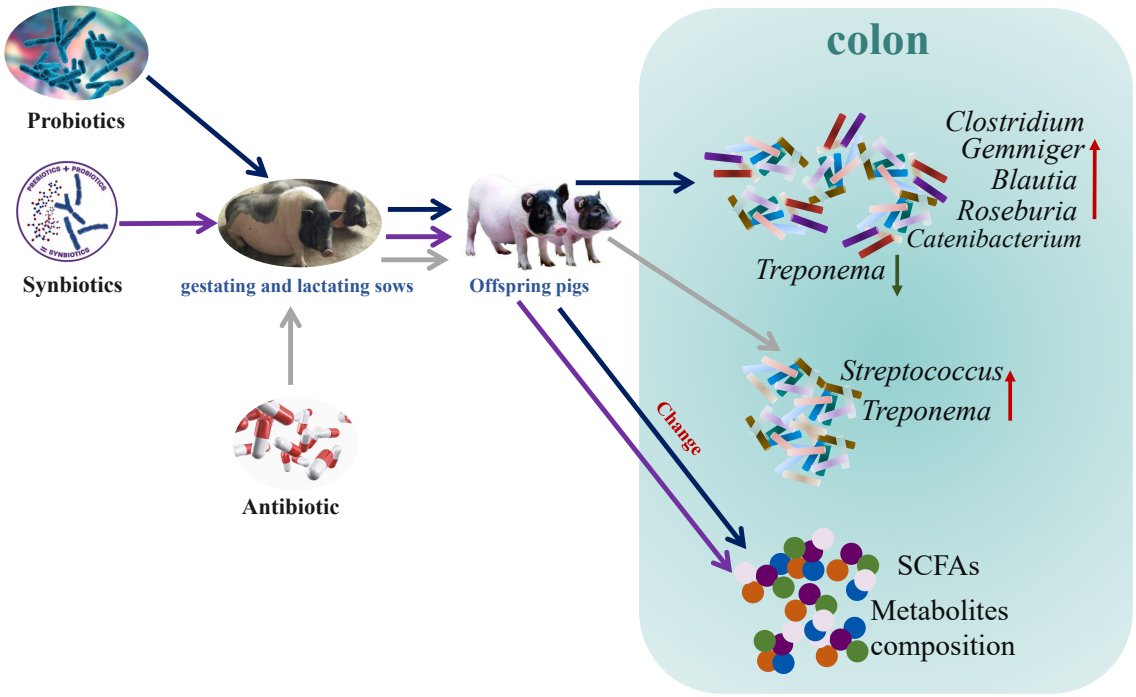

FIGURE 13
Schematic presentation of the effects of maternal probiotics and synbiotics addition to sows' diets on colonic microbiome and metabolome of offspring pigs.

and *Bacteroides*; propionate with *Oscillospira*, *02d06*, and *Bacteroides*; butyrate with *Oscillospira* and *Bacteroides*; total SCFA with *02d06* and *Bacteroides*.

Discussion

The importance of gut microbiota is widely acknowledged because of their pivotal role in the health of animals, whose diversity provides the host with beneficial functions (Kim and Isaacson, 2015). Probiotics and synbiotics play prodigious roles in regulating the gut microbiota and the metabolites of the host. Moreover, probiotics and synbiotics addition to sows' diets may be envisaged as beneficial for sows and their progeny. The results of the present study clearly show that probiotics and synbiotics supplementation in sows' diets results in a marked difference in the composition and metabolic capacity of the colonic microbiota in the offspring. These findings provide a theoretical basis for the application of probiotics and synbiotics to the "integration of mother-offspring" regulation.

The colon is the main site of microbial colonization, which plays a key role in animal health (Luo et al., 2013). In general, high microbial diversity is favorable for the overall health and productivity of animals (Hildebrand et al., 2013). In the present study, maternal probiotics and synbiotics addition did not affect the richness and diversity of colonic microbiota in the offspring pigs. This is consistent with the results of Zhang et al. (2016), who reported that oral administration of *Lactobacillus* did not change the α-diversity of cecal and colonic microbiota. In addition, the β-diversity analysis indicated that the four groups had discrete microbiota structures at 65 days of age, as evidenced by the Bray-Curtis distance. The PLS-DA also showed that the colonic microbiota structure of different groups at 65, 95, and 125 days of age were distinct, suggesting that the offspring pigs showed different microbiota compositions due to probiotics and synbiotics addition to sows' diets.

Bacteria belonging to Firmicutes, Bacteroidetes, and Proteobacteria phyla constitute the dominant microbiota in porcine intestines (McCormack et al., 2017). In the present study, the most predominant phyla identified in colonic contents were Firmicutes and Bacteroidetes at 65, 95, and 125 days of age, which accounted for more than 90% of microbiota. This is in accordance with previous studies showing that Firmicutes and Bacteroidetes are the most dominant phyla in pigs (Niu et al., 2015; Chae et al., 2016).

Probiotics and synbiotics are commonly used as feed additives to regulate the gut microbiota community. In the present study, maternal probiotics and synbiotics addition altered the colonic microbiota community of offspring pigs. Our analysis showed that the Actinobacteria abundance in the SP group was higher at 65 days of age. Previous studies

demonstrated that yeast supplementation resulted in the increased abundance of Actinobacteria, which is associated with its beneficial effects of maintaining the homeostasis of intestinal microbiota (Kiros et al., 2018). In addition, the abundances of *Blautia* and *Catenibacterium* were increased and the ratio of feed/gain was decreased with no significance in the SP group at 65 days of age (Zhu et al., 2022). These findings are consistent with a previous study that reported that *Blautia* and *Catenibacterium* had a positive association with feed efficiency (Bergamaschi et al., 2020). Furthermore, at 95 days of age, maternal probiotics addition increased the abundances of several beneficial bacteria, such as Tenericutes, *Clostridium*, *Gemmiger*, *Blautia*, and *Roseburia*. These are consistent with the results of LEfSe analysis, which showed that *Clostridum*, *Gemmiger*, *Roseburia*, *Allobaculum*, and *Sarcina* were more abundant in the SP group in the present study. Previous studies reported that *Blautia* and *Roseburia* play an important regulatory role in lipid metabolism and fat deposition (Kasahara et al., 2018; Ozato et al., 2019). *Clostridium* spp. contributes to complex carbohydrate breakdown in the gut and produces SCFAs, which are beneficial to intestinal epithelial cells (El Kaoutari et al., 2013). *Gemmiger*, *Faecalibacterium*, *Bulleidia*, and *Prevotella* were the core functional genera after *Lactobacillus* supplementation (Zhang et al., 2021). Moreover, the supplementation with probiotics increased the abundances of beneficial bacteria in the colonic mucosa, including *Prevotella*, *Faecalibacterium*, *Gemmiger*, and *Coprococcus* (Qian et al., 2020). Therefore, these findings demonstrate that maternal probiotics addition may improve the lipid metabolism of offspring and maintain the homeostasis of intestinal microbiota by increasing beneficial microbiota.

Previous studies demonstrated that the health-associated lactic acid bacteria, such as *Lactobacillus* spp., play important roles in preventing disease (Gresse et al., 2017). Therefore, it is commonly used as probiotics to maintain the homeostasis of gut microbiota. In addition, some species of *Lactobacillus* help to shape the composition of the gut microbiota by producing antimicrobial bacteriocins (Zhang et al., 2016). At the genus level, *Lactobacillus* was dominant at 65, 95, and 125 days of age in the present study. Previous studies demonstrated that *Treponema* could cause colon inflammation and swine blood dysentery (Mølbak et al., 2006). Maternal probiotics addition decreased the relative abundance of *Treponema* at 95 days of age in the present study, suggesting that probiotics inhibited the growth of harmful bacteria. Moreover, a previous study also demonstrated that *Lactobacillus* could decrease the abundance of *Treponema* (Kim and Isaacson, 2015). These findings suggest that maternal probiotics addition inhibited several potentially harmful bacteria.

Spirochaetes include several pathogens, such as *Treponema* (Nakamura, 2020). Proteobacteria also contain opportunistic pathogens, such as *Campylobacter*, *Escherichia*, *Shigella*, *Salmonella*, and *Helicobacter* (Khan and Chousalkar, 2021), and the proliferation of multiple anaerobic bacteria in Proteobacteria can lead to gut dysbiosis and inflammation in the host (Bäumler and Sperandio, 2016). In addition, *Streptococcus* is a potentially pathogenic bacteria, being presumably involved in colon carcinogenesis (Goyette-Desjardins et al., 2014). In the present study, the abundances of these harmful bacteria, including Spirochaetes, Proteobacteria, *Treponema*, *Streptococcus*, *Campylobacter*, *Staphylococcus*, Acidobacteria, Gemmatimonadetes, and Chloroflexi were increased in the SA group. These findings suggest that maternal antibiotic addition exerted detrimental effects on the gut of offspring pigs through an increase of potentially deleterious bacterial species. Moreover, a previous study also demonstrated that antibiotic alters the nutritional landscape of the gut and leads to the expansion of pathogenic populations (Bäumler and Sperandio, 2016).

The gut microbiota is a vital regulator of host metabolism (Schoeler and Caesar, 2019). PICRUSt2 was used to predict putative metagenomes based on 16S rRNA gene profiles and to determine the metabolic functional changes. In the present study, the majority of pathways were carbohydrate metabolism, amino acid metabolism, metabolism of cofactors and vitamins, and metabolism of terpenoids and polyketides. The gut microbiota not only participates in the metabolism of carbohydrate and amino acid but also in the production of vitamin (Bik, 2009). In the present study, pathways related to pantothenate and CoA biosynthesis, ascorbate and aldarate metabolism, as well as phosphonate and phosphinate metabolism were enriched in the SS group, suggesting that maternal synbiotics addition increased the metabolism of cofactors and vitamins, carbohydrate metabolism, and metabolism of other amino acids. Consistent with these results, pathway enrichment analysis in metabolomics confirmed the effects of dietary probiotics and synbiotics addition on the metabolism.

In addition, our results showed that the pathways belonging to the xenobiotics biodegradation and metabolism were enriched in the SA group at 65 and 95 days of age, suggesting that maternal antibiotic addition promotes the metabolism of xenobiotics of offspring pigs. The study on germ-free animals and conventional animals in which the intestinal microbiota composition is affected by treatment with antibiotics or dietary modification indicated that the gut microbiota is involved in xenobiotic metabolism (Koppel et al., 2017). This may be related to the negative effects of maternal antibiotic addition on the offspring. Several studies demonstrated that maternal antibiotic exposure during pregnancy increases the risk of childhood allergic diseases and results in the dysbiosis of gut microbiota (Zhong et al., 2020). However, the underlying mechanisms require further investigation.

Gut microbiota and its metabolites impact physiology function and modulate metabolic activities of the host (Schroeder and Bäckhed, 2016). Furthermore, these metabolites

are key intermediates in host-microbiota interactions and influence a wide variety of physiological functions (Koh and Bäckhed, 2020). Colonic metabolites can reflect the results of nutrient metabolism by both the gut bacteria and the host. In the present study, PCA and OPLS-DA analyses showed a clear separation of colonic metabolites profiles of offspring pigs due to maternal probiotics and synbiotics addition. Moreover, the heatmap of different metabolites were also distinct at different stages. These findings suggest that maternal probiotics and synbiotics addition has a significant effect on the metabolic profiles of offspring. Our results also showed that the different metabolites mainly belong to amino acid, carbohydrate, and lipid. These may result from the fact that gut microbiota may affect the metabolism of these compounds (Wang et al., 2020). When VIP > 2, the different metabolites were beta-sitosterol, trioxilin A3, D-glucuronic acid, and 9,10–12,13-diepoxyoctadecanoate at 65 days of age, as well as phytosphingosin and N6,N6,N6-trimethyl-L-lysine at 95 days of age, and tetracosanoic acid, N-acetylhistamine, palmitic acid, fructose 6-phosphate, putrescine, and chenodeoxycholic acid at 125 days of age. These changes may have beneficial effects on the offspring. For example, beta-sitosterol exhibits anti-inflammatory activity in intestinal endothelial cells (Loizou et al., 2010), putrescine is essential for the proliferation of intestinal epithelial cells (Mouillé et al., 2003), and hydroxycinnamic acids could inhibit intestinal pathogens (Lee et al., 2006).

Regarding the specific case of the putrescine, spermidine, and spermine, of which colonic concentrations were increased in the offspring obtained from sows supplemented with either probiotics or synbiotics, it is worth noting that polyamines are known to play important roles in the intestinal epithelium, and more largely on the intestinal mucosa physiology. Indeed, these polyamines are involved in fluid secretion by colonic crypts (Cheng et al., 2004), and in post-prandial colonic motility (Fioramonti et al., 1994). Dietary supplementation with spermidine reinforces the intestinal barrier function in mice (Ma et al., 2020d), and putrescine stimulates DNA synthesis in intestinal epithelial cells (Ginty and Seidel, 1989). In addition, polyamines appear required for intestinal epithelium renewal (McCormack et al., 1993; Wang, 2007; Rao et al., 2020). Of note, a mixture of putrescine, spermidine, and spermine has been found to be necessary for normal postnatal development of the small intestine and colon mucosa (Löser et al., 1999). Microbial putrescine represents a stimulant for the proliferation of colonic epithelial cells (Nakamura et al., 2021). Lastly, putrescine, spermine, and spermidine improve the integrity of the gut by increasing tight junction protein expression and mucus secretion (Oliphant and Allen-Vercoe, 2019).

The gut microbiota is able to produce putrescine, cadaverine, tyramine, and histamine from their respective amino acid precursors that are ornithine/arginine, lysine, tyrosine, and histidine, respectively (Davila et al., 2013). Tryptamine plays a role in regulating intestinal motility and immune function (Gao et al., 2018). Since the present study showed that the concentrations of putrescine, spermine, and spermidine increased in the SA, SP, and SS groups, as well as the tryptamine in the SP and SS groups, these results suggest that maternal addition with these additives could enhance the metabolism of amino acids and have beneficial effects of gut integrity. In addition, the correlation analysis showed that colonic putrescine, spermine, and spermidine concentrations were positively correlated with the abundance of several beneficial bacteria, such as *Gemmiger*, *Blautia*, and *Faecalibacterium*. This could explain the increase in colonic polyamine concentration because dietary probiotics can increase the polyamine concentration in the intestinal lumen. Therefore, there is an increasing interest in the use of gut commensal bacteria as potential probiotics, such as *Bacteroides*, *Clostridium*, *Bifidobacterium*, and *Faecalibacterium* (Tofalo et al., 2019).

Palmitic acid was reported to damage gut epithelium integrity (Carta et al., 2017) and initiate inflammatory cytokine production (Ghezzal et al., 2020). In the present study, the normalized intensity of palmitic acid was decreased by maternal probiotics and synbiotics addition, which may be beneficial to the gut health of the host. (R)-3-hydroxybutyric acid is a key metabolite of butanoate metabolism, which plays an important role in regulating intestinal immune tolerance to antigens (Zou et al., 2021). In the present study, (R)-3-hydroxybutyric acid was increased in the SP and SS groups, suggesting the beneficial effects of maternal probiotics and synbiotics addition on the gut health of offspring. These may be related to the changes in gut microbiota. (R)-3-hydroxybutyric acid is synthesized *via* the metabolism of butyrate and acetate (Murugesan et al., 2018). In the present study, the correlation analysis between the metabolites and microbiota showed that (R)-3-hydroxybutyric acid was positively associated with several SCFAs-producing bacteria, including *Faecalibacterium*, *Blautia*, *Clostridium*, and *Streptococcus*. A previous study also reported that *Bacteroides*, *Bifidobacterium*, *Prevotella*, *Ruminococcus*, *Blautia*, *Clostridium*, and *Streptococcus* can produce acetate, and *Coprococcus*, *Faecalibacterium*, and *Roseburia* can produce butyrate (Murugesan et al., 2018). These findings suggest that the addition of probiotics and synbiotics could alter the metabolite profiles by affecting the composition of gut microbiota.

Indole and skatole are the main end-products of tryptophan metabolism by gut microbiota (Lu et al., 2021). Indole can improve the integrity of colon barrier function, while skatole can cause gut epithelial cell dysfunction (Gao et al., 2018). Indeed, skatole in excess can induce cell death in colonocytes (Kurata et al., 2019). In the present study, the colonic indole concentration increased and skatole decreased in the SS group, suggesting that sow dietary synbiotics addition has a beneficial effect on the gut barrier function and gut epithelial cell function.

However, maternal probiotics addition results in the changes of colonic indole and skatole concentrations that need to be further studied since gut health can be affected by several bacterial metabolites present in the colonic fluid. Antibiotic use is an important factor influencing skatole level (Gao et al., 2018). Our findings showed that the colonic concentrations of indole and skatole were increased in the SA group. However, the underlying mechanisms require further investigation.

The SCFAs, especially acetate, propionate, and butyrate, have been shown to prevent intestinal oxidative stress and inflammation and to protect the intestinal barrier (Liu et al., 2021). The butyrate is a major energy source for the colonocytes and exerts antimicrobial and anti-inflammatory activities by several mechanisms (Waldecker et al., 2008). The present study observed a significant increase in the colonic acetate and butyrate concentrations in the SP group at 65 and 125 days of age, suggesting the beneficial effects of maternal probiotics addition on gut health. Previous studies demonstrated that probiotics could accelerate the degradation of polysaccharides, thereby increasing the butyric acid concentration in the colon (Liu et al., 2014). In addition, maternal probiotics and synbiotics addition decreased the colonic SCFAs concentration at 95 days of age, which may result from the rapid absorption through the colonic epithelium by the host or utilization by other members of the gut microbiota (Loh et al., 2006). This decrease may be also related to the fact that the amount and relative proportion of each SCFA depends on the diet, microbiota composition, and expression of dedicated transporters (Macfarlane and Macfarlane, 2003). *Roseburia* produces acetate and butyrate, and *Faecalibacterium* produces butyrate (Oliphant and Allen-Vercoe, 2019). The correlation analysis showed that the colonic acetate, propionate, and butyrate concentrations were positively correlated with *Gemmiger*, *Roseburia*, and *Faecalibacterium* abundances in the present study. Moreover, the abundances of *Roseburia* and *Faecalibacterium* were increased in the SP group at 65 days of age, whereas decreased in the SS group at 95 days of age. This may be the reason why maternal probiotics addition increased the colonic butyrate concentration, whereas synbiotics addition decreased the acetate and butyrate concentrations, such a decrease being presumably deleterious given notably the role of these metabolites for energy supply in colonocytes (Leschelle et al., 2000).

Conclusion

Maternal probiotics addition increased *Catenibacterium*, *Clostridium*, *Gemmiger*, *Blautia*, and *Roseburia* abundances and decreased *Treponema* abundance, whereas antibiotic addition increased *Treponema* and *Streptococcus* abundances in the colon of offspring pigs. In addition, maternal probiotics and synbiotics addition affected the metabolism pathways, including carbohydrate and amino acid metabolism, as well as cofactors and vitamins metabolism. These findings suggest that maternal probiotics and synbiotics addition present beneficial effects on gut health by altering the gut microbiota composition, their metabolites, and metabolic functions of the gut microbiota (**Figure 13**). Our results provide insights into the consequences of an intervention on the maternal gut microbiota for the offspring microbiota composition and metabolic activity.

Data availability statement

The datasets presented in this study can be found in online repositories. The names of the repository/repositories and accession number(s) can be found in the article/**Supplementary material**.

Ethics statement

The animal study was reviewed and approved by the Animal Care and Use Committee of Institute of Subtropical Agriculture, Chinese Academy of Sciences.

Author contributions

XK and YY conceived and designed the experiments and revised the manuscript. QZ analyzed the data and wrote the manuscript. QZ and MS completed the feeding experiments and analyses. QZ, MS, YC, YTL, and YL assisted in the completion of part of the feeding experiments and sample collection. QZ, FB, and MA amended the manuscript. All authors read and approved the final manuscript.

Funding

This study was jointly supported by the Key Project of Regional Innovation and Development Joint Fund of National Natural Science Foundation of China (U20A2056), the Special Funds for Construction of Innovative Provinces in Hunan Province (2019RS3022), and the Industry and Research Talent Support Project from Wang Kuancheng of the Chinese Academy of Sciences.

Acknowledgments

We thank the staff and postgraduate students of Hunan Provincial Key Laboratory of Animal Nutritional Physiology and Metabolic Process for collecting samples, and technicians from the Key Laboratory of Agro-ecological Processes in Subtropical Region for providing technical assistance. We acknowledge Suzhou Bionovogene for metabolome measurement service.

Conflict of interest

The authors declare that the research was conducted in the absence of any commercial or financial relationships that could be construed as a potential conflict of interest.

Publisher's note

All claims expressed in this article are solely those of the authors and do not necessarily represent those of their affiliated organizations, or those of the publisher, the editors and the reviewers. Any product that may be evaluated in this article, or claim that may be made by its manufacturer, is not guaranteed or endorsed by the publisher.

Supplementary material

The Supplementary Material for this article can be found online at: https://www.frontiersin.org/articles/10.3389/fmicb.2022.934890/full#supplementary-material

References

Bäumler, A. J., and Sperandio, V. (2016). Interactions between the microbiota and pathogenic bacteria in the gut. *Nature* 535, 85–93. doi: 10.1038/nature18849

Bergamaschi, M., Tiezzi, F., Howard, J., Huang, Y. J., Gray, K. A., Schillebeeckx, C., et al. (2020). Gut microbiome composition differences among breeds impact feed efficiency in swine. *Microbiome* 8:110. doi: 10.1186/s40168-020-00888-9

Bik, E. M. (2009). Composition and function of the human-associated microbiota. *Nutr. Rev.* 67, S164–S171. doi: 10.1111/j.1753-4887.2009.00237.x

Blachier, F., Beaumont, M., Andriamihaja, M., Davila, A. M., Lan, A., Grauso, M., et al. (2017). Changes in the luminal environment of the colonic epithelial cells and physiopathological consequences. *Am. J. Pathol.* 187, 476–486. doi: 10.1016/j.ajpath.2016.11.015

Bokulich, N. A., Kaehler, B. D., Rideout, J. R., Dillon, M., Bolyen, E., Knight, R., et al. (2018). Optimizing taxonomic classification of marker-gene amplicon sequences with QIIME 2 ' s q2-feature-classifier plugin. *Microbiome* 6:90. doi: 10.1186/s40168-018-0470-z

Cai, Q., Hu, C., Tang, W., Jiang, H., Geng, M., Huang, X., et al. (2021). Dietary addition with and xylo-oligosaccharides improves carcass trait and meat quality of Huanjiang mini-pigs. *Front. Nutr.* 8:748647. doi: 10.3389/fnut.2021.748647

Callahan, B. J., McMurdie, P. J., Rosen, M. J., Han, A. W., Johnson, A. J. A., and Holmes, S. P. (2016). DADA2: high-resolution sample inference from Illumina amplicon data. *Nat. Methods* 13, 581–583. doi: 10.1038/nmeth.3869

Carta, G., Murru, E., Banni, S., and Manca, C. (2017). Palmitic acid: physiological role, metabolism and nutritional implications. *Front. Physiol.* 8:902. doi: 10.3389/fphys.2017.00902

Chae, J. P., Pajarillo, E. A., Oh, J. K., Kim, H., and Kang, D. K. (2016). Revealing the combined effects of lactulose and probiotic enterococci on the swine faecal microbiota using 454 pyrosequencing. *Microb. Biotechnol.* 9, 486–495. doi: 10.1111/1751-7915.12370

Chen, Y., Zhou, Z., Yang, W., Bi, N., Xu, J., He, J., et al. (2017). Development of a data-independent targeted metabolomics method for relative quantification using liquid chromatography coupled with tandem mass spectrometry. *Anal. Chem.* 89, 6954–6962. doi: 10.1021/acs.analchem.6b04727

Cheng, S. X., Geibel, J. P., and Hebert, S. C. (2004). Extracellular polyamines regulate fluid secretion in rat colonic crypts *via* the extracellular calcium-sensing receptor. *Gastroenterology* 126, 148–158. doi: 10.1053/j.gastro.2003.10.064

Chlebicz-Wojcik, A., and Slizewska, K. (2020). The effect of recently developed synbiotic preparations on dominant fecal microbiota and organic acids concentrations in feces of piglets from nursing to fattening. *Animals* 10:1999. doi: 10.3390/ani10111999

Davila, A. M., Blachier, F., Gotteland, M., Andriamihaja, M., Benetti, P. H., Sanz, Y., et al. (2013). Intestinal luminal nitrogen metabolism: role of the gut microbiota and consequences for the host. *Pharmacol. Res.* 68, 95–107. doi: 10.1016/j.phrs.2012.11.005

El Kaoutari, A., Armougom, F., Gordon, J. I., Raoult, D., and Henrissat, B. (2013). The abundance and variety of carbohydrate-active enzymes in the human gut microbiota. *Nat. Rev. Microbiol.* 11, 497–504. doi: 10.1038/nrmicro3050

Ferretti, P., Pasolli, E., Tett, A., Asnicar, F., Gorfer, V., Fedi, S., et al. (2018). Mother-to-infant microbial transmission from different body sites shapes the developing infant gut microbiome. *Cell Host Microbe* 24, 133–145. doi: 10.1016/j.chom.2018.06.005

Fioramonti, J., Fargeas, M. J., Bertrand, V., Pradayrol, L., and Buéno, L. (1994). Induction of postprandial intestinal motility and release of cholecystokinin by polyamines in rats. *Am. J. Physiol.* 267, G960–G965. doi: 10.1152/ajpgi.1994.267.6.G960

Gao, J., Xu, K., Liu, H., Liu, G., Bai, M., Peng, C., et al. (2018). Impact of the gut microbiota on intestinal immunity mediated by tryptophan metabolism. *Front. Cell. Infect. Microbiol.* 8:13. doi: 10.3389/fcimb.2018.00013

Ghezzal, S., Postal, B. G., Quevrain, E., Brot, L., Seksik, P., Leturque, A., et al. (2020). Palmitic acid damages gut epithelium integrity and initiates inflammatory cytokine production. *Biochim. Biophys. Acta Mol. Cell. Biol. Lipids* 1865:158530. doi: 10.1016/j.bbalip.2019.158530

Ginty, D. D., and Seidel, E. R. (1989). Polyamine-dependent growth and calmodulin-regulated induction of ornithine decarboxylase. *Am. J. Physiol.* 256, G342–G348. doi: 10.1152/ajpgi.1989.256.2.G342

Girard, M., Tretola, M., and Bee, G. (2021). A single dose of synbiotics and vitamins at birth affects piglet microbiota before weaning and modifies post-weaning pperformance. *Animals* 11:84. doi: 10.3390/ani11010084

Goyette-Desjardins, G., Auger, J. P., Xu, J., Segura, M., and Gottschalk, M. (2014). *Streptococcus suis*, an important pig pathogen and emerging zoonotic agent-an update on the worldwide distribution based on serotyping and sequence typing. *Emerg. Microbes Infect.* 3:e45. doi: 10.1038/emi.2014.45

Gresse, R., Chaucheyras-Durand, F., Fleury, M. A., Van de Wiele, T., Forano, E., and Blanquet Diot, S. (2017). Gut microbiota dysbiosis in postweaning piglets: understanding the keys to health. *Trends Microbiol.* 25, 851–873. doi: 10.1016/j.tim.2017.05.004

Hayakawa, T., Masuda, T., Kurosawa, D., and Tsukahara, T. (2016). Dietary administration of probiotics to sows and/or their neonates improves the reproductive performance, incidence of post-weaning diarrhea and histopathological parameters in the intestine of weaned piglets. *Anim. Sci. J.* 87, 1501–1510. doi: 10.1111/asj.12565

Hildebrand, F., Nguyen, T. L. A., Brinkman, B., Yunta, R. G., Cauwe, B., Vandenabeele, P., et al. (2013). Inflammation-associated enterotypes, host genotype, cage and inter-individual effects drive gut microbiota variation in common laboratory mice. *Genome Biol.* 14:R4. doi: 10.1186/gb-2013-14-1-r4

Hu, C. J., Li, F. N., Duan, Y. H., Yin, Y. L., and Kong, X. F. (2019). Glutamic acid supplementation reduces body fat weight in finishing pigs when provided solely or in combination with arginine and it is associated with colonic propionate and butyrate concentrations. *Food Funct.* 10, 4693–4704. doi: 10.1039/c9fo00520j

Ji, Y. J., Guo, Q. P., Yin, Y. L., Blachier, F., and Kong, X. F. (2018). Dietary proline supplementation alters colonic luminal microbiota and bacterial metabolite composition between days 45 and 70 of pregnancy in Huanjiang mini-pigs. *J. Anim. Sci. Biotechnol.* 9:18. doi: 10.1186/s40104-018-0233-5

Kasahara, K., Krautkramer, K. A., Org, E., Romano, K. A., Kerby, R. L., Vivas, E. I., et al. (2018). Interactions between *Roseburia intestinalis* and diet modulate atherogenesis in a murine model. *Nat. Microbiol.* 3, 1461–1471. doi: 10.1038/s41564-018-0272-x

Katoh, K., Misawa, K., Kuma, K., and Miyata, T. (2002). MAFFT: a novel method for rapid multiple sequence alignment based on fast Fourier transform. *Nucleic Acids Res.* 30, 3059–3066. doi: 10.1093/nar/gkf436

Khan, S., and Chousalkar, K. K. (2021). Functional enrichment of gut microbiome by early supplementation of *Bacillus* based probiotic in cage free hens: a field study. *Anim. Microb.* 3:50. doi: 10.1186/s42523-021-00112-5

Kim, H. B., and Isaacson, R. E. (2015). The pig gut microbial diversity: understanding the pig gut microbial ecology through the next generation high throughput sequencing. *Vet. Microbiol.* 177, 242–251. doi: 10.1016/j.vetmic.2015.03.014

Kiros, T. G., Derakhshani, H., Pinloche, E., D'Inca, R., Marshall, J., Auclair, E., et al. (2018). Effect of live yeast *Saccharomyces cerevisiae* (Actisaf Sc 47) supplementation on the performance and hindgut microbiota composition of weanling pigs. *Sci. Rep.* 8:5315. doi: 10.1038/s41598-018-23373-8

Koh, A., and Bäckhed, F. (2020). From association to causality: the role of the gut microbiota and its functional products on host metabolism. *Mol. Cell* 78, 584–596. doi: 10.1016/j.molcel.2020.03.005

Koh, A., De Vadder, F., Kovatcheva-Datchary, P., and Bäckhed, F. (2016). From dietary fiber to host physiology: short-chain fatty acids as key bacterial metabolites. *Cell* 165, 1332–1345. doi: 10.1016/j.cell.2016.05.041

Koppel, N., Maini Rekdal, V., and Balskus, E. P. (2017). Chemical transformation of xenobiotics by the human gut microbiota. *Science* 356:eaag2770. doi: 10.1126/science.aag2770

Korpela, K., Salonen, A., Vepsäläinen, O., Suomalainen, M., Kolmeder, C., Varjosalo, M., et al. (2018). Probiotic supplementation restores normal microbiota composition and function in antibiotic-treated and in caesarean-born infants. *Microbiome* 6:182. doi: 10.1186/s40168-018-0567-4

Kurata, K., Kawahara, H., Nishimura, K., Jisaka, M., Yokota, K., and Shimizu, H. (2019). Skatole regulates intestinal epithelial cellular functions through activating aryl hydrocarbon receptors and p38. *Biochem. Biophys. Res. Commun.* 510, 649–655. doi: 10.1016/j.bbrc.2019.01.122

Lee, H. C., Jenner, A. M., Low, C. S., and Lee, Y. K. (2006). Effect of tea phenolics and their aromatic fecal bacterial metabolites on intestinal microbiota. *Res. Microbiol.* 157, 876–884. doi: 10.1016/j.resmic.2006.07.004

Leschelle, X., Delpal, S., Goubern, M., Blottière, H. M., and Blachier, F. (2000). Butyrate metabolism upstream and downstream acetyl-CoA synthesis and growth control of human colon carcinoma cells. *Eur. J. Biochem.* 267, 6435–6442. doi: 10.1046/j.1432-1327.2000.01731.x

Liao, S. F. F., and Nyachoti, M. (2017). Using probiotics to improve swine gut health and nutrient utilization. *Anim. Nutr.* 3, 331–343. doi: 10.1016/j.aninu.2017.06.007

Liu, H., Zhang, J., Zhang, S. H., Yang, F. J., Thacker, P. A., Zhang, G. L., et al. (2014). Oral administration of *Lactobacillus fermentum* I5007 favors intestinal development and alters the intestinal microbiota in formula-fed piglets. *J. Agric. Food Chem.* 62, 860–866. doi: 10.1021/jf403288r

Liu, P., Wang, Y., Yang, G., Zhang, Q., Meng, L., Xin, Y., et al. (2021). The role of short-chain fatty acids in intestinal barrier function, inflammation, oxidative stress, and colonic carcinogenesis. *Pharmacol. Res.* 165:105420. doi: 10.1016/j.phrs.2021.105420

Loh, G., Eberhard, M., Brunner, R. M., Hennig, U., Kuhla, S., Kleessen, B., et al. (2006). Inulin alters the intestinal microbiota and short-chain fatty acid concentrations in growing pigs regardless of their basal diet. *J. Nutr.* 136, 1198–1202. doi: 10.1093/jn/136.5.1198

Loizou, S., Lekakis, I., Chrousos, G. P., and Moutsatsou, P. (2010). Beta-sitosterol exhibits anti-inflammatory activity in human aortic endothelial cells. *Mol. Nutr. Food Res.* 54, 551–558. doi: 10.1002/mnfr.200900012

Löser, C., Eisel, A., Harms, D., and Fölsch, U. R. (1999). Dietary polyamines are essential luminal growth factors for small intestinal and colonic mucosal growth and development. *Gut* 44, 12–16. doi: 10.1136/gut.44.1.12

Lu, Y., Chong, J., Shen, S., Chammas, J. B., Chalifour, L., and Xia, J. (2021). TrpNet: understanding tryptophan metabolism across gut microbiome. *Metabolites* 12:10. doi: 10.3390/metabo12010010

Luo, J., Zheng, A., Meng, K., Chang, W., Bai, Y., Li, K., et al. (2013). Proteome changes in the intestinal mucosa of broiler (*Gallus gallus*) activated by probiotic *Enterococcus faecium*. *J. Proteomics* 91, 226–241. doi: 10.1016/j.jprot.2013.07.017

Ma, C. C., Wasti, S., Huang, S., Zhang, Z., Mishra, R., Jiang, S. M., et al. (2020a). The gut microbiome stability is altered by probiotic ingestion and improved by the continuous supplementation of galactooligosaccharide. *Gut Microbes* 12:1785252. doi: 10.1080/19490976.2020.1785252

Ma, C., Gao, Q. K., Zhang, W. H., Zhu, Q., Tang, W., Blachier, F., et al. (2020b). Supplementing synbiotic in sows' diets modifies beneficially blood parameters and colonic microbiota composition and metabolic activity in suckling piglets. *Front. Vet. Sci.* 7:575685. doi: 10.3389/fvets.2020.575685

Ma, C., Zhang, W. H., Gao, Q. K., Zhu, Q., Song, M. T., Ding, H., et al. (2020c). Dietary synbiotic alters plasma biochemical parameters and fecal microbiota and metabolites in sows. *J. Funct. Foods* 75:104221. doi: 10.1016/j.jff.2020.104221

Ma, L., Ni, Y., Wang, Z., Tu, W., Ni, L., Zhuge, F., et al. (2020d). Spermidine improves gut barrier integrity and gut microbiota function in diet-induced obese mice. *Gut Microbes* 12, 1–19. doi: 10.1080/19490976.2020.1832857

Macfarlane, S., and Macfarlane, G. T. (2003). Regulation of short-chain fatty acid production. *Proc. Nutr. Soc.* 62, 67–72. doi: 10.1079/PNS2002207

McCormack, S. A., Viar, M. J., and Johnson, L. R. (1993). Polyamines are necessary for cell migration by a small intestinal crypt cell line. *Am. J. Physiol.* 264, G367–G374. doi: 10.1152/ajpgi.1993.264.2.G367

McCormack, U. M., Curião, T., Buzoianu, S. G., Prieto, M. L., Ryan, T., Varley, P., et al. (2017). Exploring a possible link between the intestinal microbiota and feed efficiency in pigs. *Appl. Environ. Microbiol.* 83:e00380–17. doi: 10.1128/AEM.00380-17

Mølbak, L., Klitgaard, K., Jensen, T. K., Fossi, M., and Boye, M. (2006). Identification of a novel, invasive, not-yet-cultivated *Treponema* sp. in the large intestine of pigs by PCR amplification of the 16S rRNA gene. *J. Clin. Microbiol.* 44, 4537–4540. doi: 10.1128/JCM.01537-06

Monteagudo-Mera, A., Arthur, J. C., Jobin, C., Keku, T., Bruno-Barcena, J. M., and Azcarate-Peril, M. A. (2016). High purity galacto-oligosaccharides enhance specific *Bifidobacterium* species and their metabolic activity in the mouse gut microbiome. *Benef. Microbes* 7, 247–264. doi: 10.3920/BM2015.0114

Mouillé, B., Delpal, S., Mayeur, C., and Blachier, F. (2003). Inhibition of human colon carcinoma cell growth by ammonia: a non-cytotoxic process associated with polyamine synthesis reduction. *Biochim. Biophys. Acta* 1624, 88–97. doi: 10.1016/j.bbagen.2003.09.014

Murugesan, S., Nirmalkar, K., Hoyo-Vadillo, C., García-Espitia, M., Ramírez-Sánchez, D., and García-Mena, J. (2018). Gut microbiome production of short-chain fatty acids and obesity in children. *Eur. J. Clin. Microbiol. Infect. Dis.* 37, 621–625. doi: 10.1007/s10096-017-3143-0

Nakamura, K., Kojima, R., Uchino, E., Ono, K., Yanagita, M., Murashita, K., et al. (2021). Health improvement framework for actionable treatment planning using a surrogate Bayesian model. *Nat. Commun.* 12:3088. doi: 10.1038/s41467-021-23319-1

Nakamura, S. (2020). Spirochete flagella and motility. *Biomolecules* 10:550. doi: 10.3390/biom10040550

Niu, Q., Li, P. H., Hao, S. S., Zhang, Y. Q., Kim, S. W., Li, H. Z., et al. (2015). Dynamic distribution of the gut microbiota and the relationship with apparent crude fiber digestibility and growth stages in pigs. *Sci. Rep.* 5:7. doi: 10.1038/srep09938

Oliphant, K., and Allen-Vercoe, E. (2019). Macronutrient metabolism by the human gut microbiome: major fermentation by-products and their impact on host health. *Microbiome* 7:91. doi: 10.1186/s40168-019-0704-8

Ozato, N., Saito, S., Yamaguchi, T., Katashima, M., Tokuda, I., Sawada, K., et al. (2019). *Blautia* genus associated with visceral fat accumulation in adults 20-76 years of age. *NPJ Biofilms Microbiomes* 5:28. doi: 10.1038/s41522-019-0101-x

Patil, Y., Gooneratne, R., and Ju, X. H. (2019). Interactions between host and gut microbiota in domestic pigs: a review. *Gut Microbes* 11, 310–334. doi: 10.1080/19490976.2019.1690363

Price, M. N., Dehal, P. S., and Arkin, A. P. (2010). FastTree 2-approximately maximum-likelihood trees for large alignments. *PLoS One* 5:e9490. doi: 10.1371/journal.pone.0009490

Qian, L. M., Huang, J. M., and Qin, H. L. (2020). Probiotics and dietary intervention modulate the colonic mucosa-associated microbiota in high-fat diet populations. *Turk. J. Gastroenterol.* 31, 295–304. doi: 10.5152/tjg.2020.19013

Rao, J. N., Xiao, L., and Wang, J. Y. (2020). Polyamines in gut epithelial renewal and barrier function. *Physiology* 35, 328–337. doi: 10.1152/physiol.00011.2020

Sanders, M. E., Merenstein, D. J., Reid, G., Gibson, G. R., and Rastall, R. A. (2019). Probiotics and prebiotics in intestinal health and disease: from biology to the clinic. *Nat. Rev. Gastroenterol. Hepatol.* 16, 605–616. doi: 10.1038/s41575-019-0173-3

Sanz, Y. (2011). Gut microbiota and probiotics in maternal and infant health. *Am. J. Clin. Nutr.* 94, 2000S–2005S. doi: 10.3945/ajcn.110.001172

Schoeler, M., and Caesar, R. (2019). Dietary lipids, gut microbiota and lipid metabolism. *Rev. Endocr. Metab. Disord.* 20, 461–472. doi: 10.1007/s11154-019-09512-0

Schroeder, B. O., and Bäckhed, F. (2016). Signals from the gut microbiota to distant organs in physiology and disease. *Nat. Med.* 22, 1079–1089. doi: 10.1038/nm.4185

Śliżewska, K., and Chlebicz, A. (2019). Synbiotics impact on dominant faecal microbiota and short-chain fatty acids production in sows. *FEMS Microbiol. Lett.* 366:fnz157. doi: 10.1093/femsle/fnz157

Tan, B., Ji, Y. J., Ding, H., Li, F. W., Zhou, Q. H., and Kong, X. F. (2016). Effects of xylo-oligosaccharide on growth performance, diarrhea rate and plasma biochemical parameters of weaned piglets. *Chin. J. Anim. Nutr.* 28, 2556–2563. doi: 10.3969/j.issn.1006-267x.2016.08.028

Tofalo, R., Cocchi, S., and Suzzi, G. (2019). Polyamines and gut microbiota. *Front. Nutr.* 6:16. doi: 10.3389/fnut.2019.00016

Waldecker, M., Kautenburger, T., Daumann, H., Busch, C., and Schrenk, D. (2008). Inhibition of histone-deacetylase activity by short-chain fatty acids and some polyphenol metabolites formed in the colon. *J. Nutr. Biochem.* 19, 587–593. doi: 10.1016/j.jnutbio.2007.08.002

Wang, H., Xu, R., Zhang, H., Su, Y., and Zhu, W. (2020). Swine gut microbiota and its interaction with host nutrient metabolism. *Anim. Nutr.* 6, 410–420. doi: 10.1016/j.aninu.2020.10.002

Wang, J. Y. (2007). Polyamines and mRNA stability in regulation of intestinal mucosal growth. *Amino Acids* 33, 241–252. doi: 10.1007/s00726-007-0518-z

Wang, K., Hu, C. J., Tang, W., Azad, M. A. K., Zhu, Q., He, Q. H., et al. (2021a). The enhancement of intestinal immunity in offspring piglets by maternal probiotic or synbiotic supplementation is associated with the alteration of gut microbiota. *Front. Nutr.* 8:686053. doi: 10.3389/fnut.2021.686053

Wang, K., Kong, X. F., Azad, M. A. K., Zhu, Q., Xiong, L., Zheng, Y. Z., et al. (2021b). Maternal probiotic or synbiotic supplementation modulates jejunal and colonic antioxidant capacity, mitochondrial function, and microbial abundance in Bama mini-piglets. *Oxid. Med. Cell. Longev.* 2021:6618874. doi: 10.1155/2021/6618874

Wang, Y. B., Du, W., Fu, A. K., Zhang, X. P., Huang, Y., Lee, K. H., et al. (2016). Intestinal microbiota and oral administration of *Enterococcus faecium* associated with the growth performance of new-born piglets. *Benef. Microbes* 7, 529–538. doi: 10.3920/BM2015.0099

Xavier-Santos, D., Bedani, R., Lima, E. D., and Saad, S. (2019). Impact of probiotics and prebiotics targeting metabolic syndrome. *J. Funct. Foods* 64:103666. doi: 10.1016/j.jff.2019.103666

Xiao, H. W., Cui, M., Li, Y., Dong, J. L., Zhang, S. Q., Zhu, C. C., et al. (2020). Gut microbiota-derived indole 3-propionic acid protects against radiation toxicity *via* retaining acyl-CoA-binding protein. *Microbiome* 8:69. doi: 10.1186/s40168-020-00845-6

Zhang, D., Ji, H., Liu, H., Wang, S., Wang, J., and Wang, Y. (2016). Changes in the diversity and composition of gut microbiota of weaned piglets after oral administration of *Lactobacillus* or an antibiotic. *Appl. Microbiol. Biotechnol.* 100, 10081–10093. doi: 10.1007/s00253-016-7845-5

Zhang, D., Liu, H., Wang, S., Zhang, W., Wang, S., Wang, Y., et al. (2021). Sex-dependent changes in the microbiota profile, serum metabolism, and hormone levels of growing pigs after dietary supplementation with *Lactobacillus*. *Appl. Microbiol. Biotechnol.* 105, 4775–4789. doi: 10.1007/s00253-021-11310-1

Zhong, Y. J., Zhang, Y. H., Wang, Y., and Huang, R. J. (2020). Maternal antibiotic exposure during pregnancy and the risk of allergic diseases in childhood: a meta-analysis. *Pediatr. Allergy Immunol.* 32, 445–456. doi: 10.1111/pai.13411

Zhu, Q., Song, M., Azad, M. A. K., Ma, C., Yin, Y., and Kong, X. (2022). Probiotics and synbiotics addition in Bama mini-pigs' diets improve carcass traits and meat quality by altering plasma metabolites and related gene expression of offspring. *Front. Vet. Sci.* 9:779745. doi: 10.3389/fvets.2022.779745

Zou, Y., Zhou, J., Wu, C., Zhang, W., Shen, H., Xu, J., et al. (2021). Protective effects of *Poria cocos* and its components against cisplatin-induced intestinal injury. *J. Ethnopharmacol.* 269:113722. doi: 10.1016/j.jep.2020.113722

frontiers | Frontiers in Microbiology

TYPE Original Research
PUBLISHED 20 September 2022
DOI 10.3389/fmicb.2022.925200

OPEN ACCESS

EDITED BY
Franck Carbonero,
Washington State University Health Sciences Spokane, United States

REVIEWED BY
Huan Li,
Lanzhou University, China
Ruihua Huang,
Nanjing Agricultural University, China

*CORRESPONDENCE
Bang Liu
liubang@mail.hzau.edu.cn

†These authors have contributed equally to this work and share first authorship

SPECIALTY SECTION
This article was submitted to Microorganisms in Vertebrate Digestive Systems, a section of the journal Frontiers in Microbiology

RECEIVED 21 April 2022
ACCEPTED 24 August 2022
PUBLISHED 20 September 2022

CITATION
Wang Y, Zhou P, Zhou X, Fu M, Wang T, Liu Z, Liu X, Wang Z and Liu B (2022) Effect of host genetics and gut microbiome on fat deposition traits in pigs.
Front. Microbiol. 13:925200.
doi: 10.3389/fmicb.2022.925200

Effect of host genetics and gut microbiome on fat deposition traits in pigs

Yuan Wang[1†], Ping Zhou[1†], Xiang Zhou[1,2,3,4], Ming Fu[1], Tengfei Wang[1], Zuhong Liu[1], Xiaolei Liu[1,2,3,4], Zhiquan Wang[5] and Bang Liu[1,2,3,4*]

[1]Key Laboratory of Agricultural Animal Genetics, Breeding, and Reproduction of Ministry of Education, and Key Laboratory of Swine Genetics and Breeding of Ministry of Agriculture, Huazhong Agricultural University, Wuhan, China, [2]The Cooperative Innovation Center for Sustainable Pig Production, Wuhan, China, [3]The Engineering Technology Research Center of Hubei Province Local Pig Breed Improvement, Wuhan, China, [4]Hubei Hongshan Laboratory, Wuhan, China, [5]Livestock Gentec, Department of Agricultural, Food and Nutritional Science, University of Alberta, Edmonton, AB, Canada

Fat deposition affects meat quality, flavor, and production in pigs. Fat deposition is influenced by both genetics and environment. Symbiotic microbe with the host is an important environmental factor to influence fat deposition. In this study, the fat deposition traits were measured in 239 individuals obtained from Tongcheng pigs × Large White pigs resource population. The interactions between genetics and gut microbiome in fat deposition traits were investigated through whole-genome sequencing and cecum microbial 16S ribosomal RNA sequencing. The results showed that the percentage of leaf fat (PL) and intramuscular fat content (IMF) were significantly influenced by host genetics–gut microbiome interaction. The effects of interactions between host genetics and gut microbiome on PL and IMF were 0.13 and 0.29, respectively. The heritability of PL and IMF was estimated as 0.71 and 0.89, respectively. The microbiability of PL and IMF was 0.20 and 0.26, respectively. Microbiome-wide association analysis (MWAS) revealed *Anaeroplasma*, *Paraprevotella*, *Pasteurella*, and *Streptococcus* were significantly associated with PL, and *Sharpea* and *Helicobacter* exhibited significant association with IMF ($p < 0.05$). Furthermore, *Paraprevotella* was also identified as a critical microbe affecting PL based on the divergent Wilcoxon rank-sum test. Overall, this study reveals the effect of host genetics and gut microbiome on pig fat deposition traits and provides a new perspective on the genetic improvement of pig fat deposition traits.

KEYWORDS

percentage of leaf fat, intramuscular fat content, heritability, microbiability, microbe

Introduction

Fat deposition is closely related to carcass and meat quality traits in pigs. Fat deposition in different parts of the body has different effects. Subcutaneous backfat thickness is an important target trait in pig breeding. There is a negative correlation between backfat thickness and carcass lean percentage. In the viscera, fat could support and protect organs, and it affects dressing percentage and feed consumption in pigs. In addition, intramuscular fat content (IMF) is an important factor determining the tenderness, juiciness, flavor, meat quality characteristics, and consumer acceptance (Gao and Zhao, 2009). IMF is positively correlated with juiciness and flavor of meat (Fortin et al., 2005). Thus, fat deposition is an important economic trait of pigs, which affects meat quality and production in pig. Furthermore, the physiological traits and biochemical indices of pigs are similar to humans, thus, pig can be used as a model animal for studying human obesity (Hishikawa et al., 2005).

Fat deposition traits are a type of quantitative traits with moderate-to-high heritability. This quantitative trait is influenced by heredity and environment. The gut microbiota that are symbiotic with the host are irreplaceable environmental factors. The gut microbiome is known as the second genome of humans (Zhu et al., 2010), which inhabits 10 times more gut microbial cells than human cells (Savage, 1977). Pig has richer gut microbes and is considered to be the main model animal of human obesity and disease research (Hishikawa et al., 2005; Merlotti et al., 2017). A reference gene catalog of pig gut microbiome with a total of 7.69 million genes has been established by metagenome sequencing of 278 pig fecal microbiome (Xiao et al., 2016).

The influence of gut microbe on host phenotype, the ratio of microbial relative abundance variance to the phenotype variance, is defined as "microbiability" (Difford et al., 2018). Microbiability has been used for the studies in pigs (Camarinha-Silva et al., 2017; Tang et al., 2020), cattle (Difford et al., 2018), and chicken (Wen et al., 2019b). According to the microbiability of traits, cecal microbiota has a greater contribution to fat deposition than other large intestine microorganisms (Wen et al., 2019b; Tang et al., 2020). Moreover, the *Treponema* in cecum has been reported to be associated with feed conversion (Quan et al., 2018). The *Prevotellaceae ucg-001* in cecum is positively correlated with backfat thickness and IMF (Tang et al., 2020). Besides, the cecum exhibits high capabilities of degradation and digestion, whose metabolites can provide energy for the host (Yang et al., 2016). Therefore, the cecum could be considered as the representative of gut segments for fat deposition research.

However, the effect of interactions between host genetics and gut microbiome on fat deposition traits remains largely unclear. In our study, the resource population was obtained by crossing a Chinese local breed (Tongcheng pigs) and a commercial breed (Large White pigs). We measured fat deposition traits (backfat thickness at shoulder (SBFT), loin (LBFT), rump (RBFT), average backfat thickness (ABFT), percentage of leaf and caul fat (PL, PC, and PLC), and intramuscular fat content (IMF)). We performed whole-genome sequencing and cecal microbial 16S ribosomal RNA sequencing of 239 pigs to determine whether there are any interactions between the host genetics and gut microbiome. Then, we estimated heritability and microbiability for the detected interactions between host genetic–gut microbiomes and further screened candidate microbes influencing traits. This study provides a new perspective and opportunity for the genetic improvement of pig fat deposition traits.

Materials and methods

Resource population, fat deposition traits measured, and sample collection

The resource population is an advanced generation intercross population. F1 was obtained by crossing 36 Tongcheng sows (a Chinese local breed) with 11 Large White boars (a commercial breed). The F1 sows and boars were subsequently intercrossed to produce F2. Then, intercross was performed in each generation until F9 population was produced. In this study, a total of 239 individuals from 9 to 10 intercross generations including 119 castrated boars and 120 castrated sows were used for further analysis. All the pigs were provided by Yunzhi Farm (Tongcheng Country, Hubei province, China) with coincident feeding and management conditions. All individuals were healthy, and they were not administered any antibiotics before being slaughtered.

The phenotypes of 239 pigs were collected, including live body weight (BW) before slaughter, carcass weight (CW), backfat thickness at the thickest shoulder (SBFT), loin (LBFT), rump (RBFT), weight of leaf fat, weight of caul fat, and intramuscular fat content (IMF). Backfat thickness was measured using Vernier caliper. The average backfat thickness (ABFT) was an average of three measurements of backfat thickness at the shoulder, loin, and rump. The weight of leaf and caul fat was measured using a scale with an accuracy of 0.01 kg. The percentage of leaf fat (PL) was calculated as the weight of leaf fat divided by CW. Similarly, percentage of caul fat (PC) was calculated as the weight of caul fat divided by CW. The percentage of leaf and caul fat (PLC) was sum of PL and PC. A near-infrared spectroscopy analyzer was used to measure the IMF of the longissimus dorsi samples. The longissimus dorsi samples were collected from the penultimate 3rd to 4th thoracic vertebrae, about 20–30 cm long. The gut contents of 239 individuals were sampled from cecum after pigs were slaughtered, snap-frozen in liquid nitrogen, and stored at −80°C until sequencing. Spleen tissues were collected into

50 ml centrifuge tubes containing 75% alcohol by volume and stored at −20°C.

All the animal experiments in this study were approved by the Animal Care and Use Committee of Huazhong Agricultural University.

Whole-genome sequencing and analysis

Genomic DNA samples were extracted from spleen of 239 pigs to construct the whole-genome sequencing libraries. Each library was sequenced using 150 bp paired-end reads with a HiSeq X5 instrument (Illumina). To minimize mapping error, low-quality reads were removed using FastQC software. The clean reads from each pig were aligned to the porcine reference genome using the Burrows-Wheeler Alignment tool (BWA ver 0.7.15) with default parameters. We subsequently used the Picard toolkit to sort the alignment results and remove potential PCR duplicate reads. The resultant alignments were indexed using SAMtools (ver 1.6) and processed with the Genome Analysis Toolkit (GATK, ver 3.7). To call variants, we set a minimum quality score as 20 based on the bases and mapped reads. The single nucleotide polymorphisms (SNPs) of each pig were combined to obtain a common dataset of single nucleotide polymorphism (SNP) data, and the dataset was processed by GATK. Finally, the software PLINK (ver 1.90) was used for quality control of the obtained dataset with the following filtering criteria: SNP call rate >80%, minor allele frequency >1%, and Hardy–Weinberg equilibrium p-value $<10^{-6}$.

16S ribosomal ribonucleic acid sequencing and analysis

First, the total DNA of cecal contents was extracted to construct sequencing library, and 30 ng genomic DNA samples and their corresponding fusion primers were used to prepare PCR reaction system. PCR reaction was performed to amplify V3-V4 region of 16S ribosomal RNA (rRNA) with the primers of 338R (ACTCCTACGGGAGGCAGCAG) and 806R (GGACTACHVGGGGTWTCTAAT). A 468 bp segment was amplified by PCR with the number of tags of 50,000. The PCR products were purified by using Agencourt AMPure XP magnetic beads and dissolved in the Elution Buffer. Agilent 2100 Bioanalyzer was used to detect the fragment range and concentration of the library. According to the size of the inserted fragment, HiSeq platform was selected for pair-end sequencing. FLASH (Fast Length Adjustment of Short reads, ver 1.2.11) was used to splice the sequences. Based on the sequence overlapping relationship, the paired reads obtained from pair-end sequencing were assembled into tags. The assembled tags were clustered into operational taxonomic units (OTUs) using software USEARCH (ver 7.0.1090). Clustering analysis was performed by using UPARSE under 97% similarity to obtain representative sequence of each OTU. Afterward, OTU representative sequences were aligned against the Greengene database by ribosomal database project (RDP) classifier (ver 2.2) software to obtain the annotation at the levels of phylum, class, order, family, and genus.

Analysis of interactions between host genetics and gut microbiome

Construction of genomic relationship matrix

A total of 14,139,625 filtered SNPs were used to estimate the genomic relationship matrix (GRM) using the HIBLUP software[1] according to the following equation:

$$G = MM'/2\sum_{i=1}^{n} p_i(1-p_i)$$

In which M indicates m (the number of individuals) × n (the number of loci) matrix, and p_i is the frequency of the coded allele.

Construction of microbial relationship matrix

All the OTUs were used to construct the microbial relationship matrix (MRM) by R script (Wen et al., 2019b) based on the following equation:

$$m_{ij} = \frac{1}{N}\sum_{o=1}^{N}\frac{(X_{io}-X_o)(X_{jo}-X_o)}{\sigma_o^2}$$

In which m_{ij} is the estimation of microbial similarity in cecum of individual i and individual j; X_{io} and X_{jo} indicate the relative abundance of OTU o in the cecum of individual i and individual j; X_o represents the average relative abundance of OTU o in cecum of the whole population; σ_o^2 is the variance of OTU o relative abundance; and N is the total OTU count in cecum.

Interactions between host genetics and gut microbiome

The following multiple random effects model was established to estimate variance components of the target traits using HIBLUP software (see text footnote 1).

$$y = 1\mu + Z_1 g + Z_2 m + Z_3 a + e$$

In which y is the n × 1 vector of the fat deposition traits; μ is the overall mean; $g \sim N(0, G\sigma_g^2)$ is the q × 1 vector of host genetic random effect, where G and σ_g^2 are the GRM and host genetic variance; $m \sim N(0, M\sigma_m^2)$ is the q × 1 vector of gut

1 https://www.hiblup.com/

microbiome random effect, where M and σ_m^2 are the MRM and gut microbiome variance; $a \sim N\ (0, A\sigma_a^2)$ is the q × 1 vector of interactions between host genetics and gut microbiome random effect, where A and σ_a^2 are the GRM × MRM and variance of interactions between host genetics and gut microbiome; $e \sim N\ (0, \sigma_e^2)$is an n × 1 vector of residual effect, where σ_e^2 is the residual variance; Z_1, Z_2, and Z_3 are, respectively, the corresponding incidence matrices of g, m, and a.

Estimation of heritability of fat deposition traits

A total of 14,139,625 filtered SNPs were used to estimate the principal components and heritability based on GRM using genome-wide complex trait analysis (GCTA) software [ver 1.93.1; (Yang et al., 2011)] according to the following equation:

$$y = Kc + g_1 + \varepsilon$$

where y is a vector of the phenotype; c is a vector of fixed covariates, including sex effect and body weight (BW); K is the matrix corresponding to c; and g_1 is a vector of the total effects of all SNPs following $g_1 \sim N\ (0, G^{'}\sigma_{g_1}^2)$ where $G^{'}$ and $\sigma_{g_1}^2$ are the GRM and genetic variance, respectively; and ε is the residual effect. The $G^{'}$ estimation equation is as follows:

$$g_{jk} = \frac{1}{N}\sum_{i=1}^{N}\frac{(X_{ij} - 2p_i)(X_{ik} - 2p_i)}{2p_i(1-p_i)}$$

In which g_{jk} is the genetic similarity between individual j and individual k; X_{ij} and X_{ik} represent the number of reference alleles in individual j and individual k; p_i is the reference allele frequency; and N is the SNP number.

Estimation of microbiability of fat deposition traits

The microbiability is referred to the ratio of cecum microbial variance to phenotypic variance, and it was calculated by the following equation:

$$y = Kc + m_1 + \varepsilon$$

where y and ε are phenotype and residual effect vectors, respectively. m_1 is the gut microbiota effect following the $m_1 \sim N\ (0, M\sigma_{m_1}^2)$. The microbiability was estimated by GCTA software with the MRM substituted for GRM. In our study, $\boldsymbol{c}$ contained six covariates, namely, covariates 1–6. Covariate 1 included BW and the first five host genetic principal components (PCs); covariate 2 included BW and the first two PCs generated at SNPs which were significantly associated with PL and IMF; covariate 3 consisted of BW, the first five host genetic PCs, and the first two PCs generated at SNPs which were significantly associated with PL and IMF; covariate 4 included BW, sex, and the first five host genetic PCs; covariate 5 included BW, sex, and the first two PCs generated at SNPs which were significantly associated with PL and IMF; covariate 6 consisted of BW, sex, the first five host genetic PCs, and the first two PCs generated at SNPs which were significantly associated with PL and IMF. The first five PCs were generated by the genome relationship matrix to account for population structure.

The Bayesian information criterion (BIC) was calculated to select the model with optimal covariates. The smaller the BIC value was, the higher the model's fitting level was. The BIC was calculated according to the following formula:

$$BIC = kIn(n) - 2In(L)$$

where k is the number of model parameters, n is the number of samples, and L is the likelihood value.

Identification of candidate microbes with fat deposition traits

The divergent Wilcoxon rank-sum test and microbiome-wide association analysis (MWAS) were used to identify the candidate microbes for target traits.

Differences in genera, percentage of leaf fat, and intramuscular fat content between divergent groups

According to the distribution of fat deposition traits of the 239 individuals, the highest 20% (n = 48) and lowest 20% (n = 48) were formed into two extreme divergent groups. The Wilcoxon rank-sum test was used to test the significance in 56 genera with average relative abundance greater than 0.01% between the two groups. By the same method, microbes were grouped in terms of the relative abundance of the genus, and the significance in individual traits between the two divergent groups was tested by the Wilcoxon rank-sum test with the $P < 0.05$ as the chosen significant test criteria.

Microbiome-wide association analysis of percentage of leaf fat and intramuscular fat content

The MWAS between the fat deposition traits of 239 individuals and 56 genera whose average relative abundance was more than 0.01% was conducted using Gaston package[2] in R software with the following equation:

$$y = X\beta + u + \varepsilon$$

y is the vector of fat deposition traits; β is a fixed effect vector, including 56 genera with average relative abundance

2 https://cran.r-project.org/web/packages/gaston

value >0.01%; u is a random effect vector. At the same time, sex and BW are considered as covariates. F-test is used to determine the significance of the regression coefficients.

Results

Characterization of fat deposition traits and sequencing outcomes

Host fat deposition phenotype characteristics are presented in Table 1. There are three categories of fat depositions including subcutaneous fat (SBFT, RBFT, LBFT, and ABFT), viscera fat (PL, PC, and PLC), and intramuscular fat (IMF). All measured traits displayed a high coefficient of variation (15.39 to 42.69%) (Table 1). The distribution of each trait is shown in the Supplementary Figure 1. The host genetics was analyzed by the whole-genome sequencing, and the whole-genome sequencing information of the 239 individuals was analyzed subsequently. The SNPs were quality-controlled by Plink software. After quality control, a total of 14,139,625 SNPs was obtained for subsequent analysis.

TABLE 1 Summary of fat deposition traits in the resource population.

Trait	Sex	N	Mean	SD	CV (%)
SBFT (mm)	♂	119	52.09	8.01	15.39
	♀	120	52.57	8.54	16.24
	Total	239	52.33	8.27	15.8
LBFT (mm)	♂	119	27.88	6.83	24.49
	♀	120	29.19	7.16	24.54
	Total	239	28.54	7.01	24.58
RBFT (mm)	♂	119	29.06	6.49	22.32
	♀	120	32	7.51	23.46
	Total	239	30.53	7.16	23.44
ABFT (mm)	♂	119	36.34	6.4	17.61
	♀	120	37.92	7.01	18.49
	Total	239	37.13	6.75	18.16
PL (%)	♂	119	6.57	1.37	20.79
	♀	120	6.52	1.32	20.31
	Total	239	6.54	1.34	20.52
PC (%)	♂	119	3.52	0.94	26.66
	♀	120	3.64	0.97	26.58
	Total	239	3.58	0.95	26.62
PLC (%)	♂	119	10.08	2.05	20.37
	♀	120	10.16	1.98	19.52
	Total	239	10.12	2.02	19.91
IMF (%)	♂	119	2.13	0.91	42.69
	♀	120	1.89	0.64	34.12
	Total	239	2.01	0.8	39.6

SBFT, backfat thickness at shoulder; LBFT, backfat thickness at loin; RBFT, backfat thickness at rump; ABFT, average backfat thickness; PL, percentage of leaf fat; PC, percentage of caul fat; PLC, percentage of leaf fat and caul; IMF, intramuscular fat content; SD, standard deviation; CV, coefficient of variation.

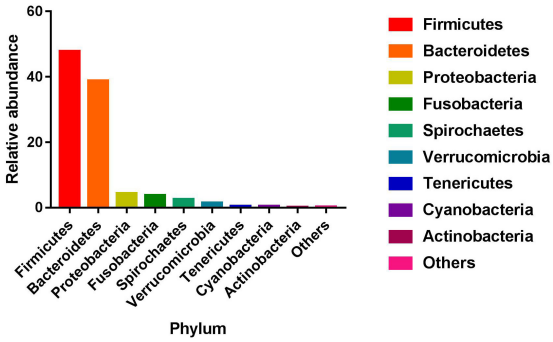

FIGURE 1
Phylum of relative abundance.

The gut microbiome was analyzed by the cecal 16S rRNA sequencing. The 16S rRNA sequencing analysis produced a total of 31,801,522 reads from the 239 samples with an average of 133,061 reads, and 2,324 OTUs were then clustered with 97% sequencing identity. Subsequently, these 2,324 OTUs were clustered into 19 phyla, 33 classes, 56 orders, 87 families, and 144 genera (Supplementary Table 1). At the phylum level, the phyla with relative abundance at the top five were *Firmicutes*, *Bacteroidetes*, *Proteobacteria*, *Fusobacteria*, and *Spirochaetes* (Figure 1). At the genus level, the average relative abundance of 56 genera was greater than 0.01% (Supplementary Table 2). The average Sobs index, Chao index, Ace index, Shannon index, and Simpson index of the microbiota are 782.92, 970.75, 962.85, 4.63, and 0.04, respectively (Supplementary Table 3).

Influence of host genetic–gut microbiome interactions on percentage of leaf fat and intramuscular fat content

The effects of host genetics and gut microbiome on all traits were different (Table 2). The results indicated that host genetics ($\boldsymbol{g}$) and gut microbiome ($\boldsymbol{m}$) exhibited 0.62 and 0.20 independent effect on SBFT, 0.68 and 0.18 independent effect on LBFT, and 0.86 and 0.11 independent effect on RBFT, respectively. In addition, ABFT displayed 0.75 $\boldsymbol{g}$ effect and 0.18 $\boldsymbol{m}$ effect. Generally, the $\boldsymbol{g}$ effect was higher than the $\boldsymbol{m}$ effect in the presence of other environmental factors. RBFT exhibited the highest $\boldsymbol{g}$ effect among backfat thickness at three positions. The PC exhibited 0.40 $\boldsymbol{g}$ effect and 0.24 $\boldsymbol{m}$ effect. However, PL displayed 0.77 $\boldsymbol{g}$ effect, 0.10 $\boldsymbol{m}$ effect, and 0.13 effect of interactions between host genetics and gut microbiome ($\boldsymbol{a}$). The multiple variance components completely explained the phenotypic variation of PL and IMF. The IMF showed 0.71

TABLE 2 Host genetics and gut microbiome effects for fat deposition traits.

Trait	*g*			*m*			*a*		
	σ_g^2	σ_g^2/σ_p^2	*P-value*	σ_m^2	σ_m^2/σ_p^2	*P-value*	σ_a^2	σ_a^2/σ_p^2	*P-value*
SBFT	65.92	0.62	0.23	20.92	0.20	0.14	0.00	0.00	0.25
LBFT	39.45	0.68	0.20	10.74	0.18	0.12	0.00	0.00	0.19
RBFT	66.19	0.86	0.22	8.07	0.11	0.10	0.00	0.00	0.25
ABFT	52.40	0.75	0.23	12.30	0.18	0.13	0.00	0.00	0.24
PL	1.54	0.77	0.18	0.19	0.10	0.09	0.26	0.13	0.18
PC	0.34	0.40	0.15	0.20	0.24	0.14	0.00	0.00	0.27
PLC	3.44	0.89	0.16	0.45	0.11	0.09	0.00	0.00	0.16
IMF	0.98	0.71	0.23	0.00	0.00	0.09	0.34	0.29	0.26

g, the effect of host genetics; ***m***, the effect of gut microbiome; ***a***, the effect of interactions between host genetics and gut microbiome; SBFT, backfat thickness at shoulder; LBFT, backfat thickness at loin; RBFT, backfat thickness at rump; ABFT, average backfat thickness; PL, percentage of leaf fat; PC, percentage of caul fat; PLC, percentage of leaf fat and caul; IMF, intramuscular fat content. The significant *P*-value bounds are $P < 0.05$.

independent ***g*** effect and 0.29 ***a*** effect, but no independent ***m*** effect. The ***a*** effect of PL and IMF was estimated as 0.13 and 0.29, indicating that host genetic–gut microbiome interactions affected the formation of PL and IMF.

Heritability and microbiability of percentage of leaf fat and intramuscular fat content

The heritability of PL was estimated as 0.71 and that of IMF as 0.89. PL and IMF were mainly affected by host genetics in the resource population (Table 3). To estimate microbiability of PL and IMF, six models were established based on host genetics, population structure, sex, and BW (Supplementary Table 4). The BIC value was used to select optimal model fitting PL and IMF. The optimal model to calculate PL microbiability contained three covariates including BW, the first five host genetic principal components (PCs), and the first two PCs generated at SNPs significantly associated with PL. The microbiability of PL was estimated as 0.20 (Table 3). The optimal model to calculate IMF microbiability contained two covariates including BW and the first two PCs generated at SNPs significantly associated with IMF. The microbiability of IMF was estimated to be 0.26 (Table 3).

The genera that are significant association with percentage of leaf fat and intramuscular fat content

To identify the candidate microbiome from the resource population, we tested the significance in traits or relative abundance between the highest 20% and lowest 20% microbial abundance or trait groups by Wilcoxon rank-sum test. We chose the microbes with significant difference in trait and genus relative abundance between divergent groups as candidate microbes (Figure 2) in the subsequently association analysis. PL and IMF had different candidate microbes. *Campylobacter* and *Paraprevotella* exhibited significant difference between divergent groups of PL, while PL also showed significant difference between divergent groups of *Campylobacter* and *Paraprevotella* ($P < 0.05$, Table 4). PL was 6.18% in the highest 20% group of *Campylobacter* relative abundance, while PL was 7.08% in the lowest 20% group ($P < 0.05$, Table 4). Then, PL was 6.25% in the highest 20% group of *Paraprevotella* relative abundance, while it was 6.95% in the lowest 20% group ($P < 0.05$, Table 4). For divergent Wilcoxon rank-sum test of IMF, *Actinobacillus*, *Dialister*, and *YRC22* exhibited significant differences in relative abundance between highest 20% and lowest 20% groups ($P < 0.05$, Table 4). For divergent Wilcoxon rank-sum test of genus relative abundance, *Anaeroplasma*, *Megasphaera*, and *Succinivibrio* exhibited significant differences between highest 20% and lowest 20% IMF ($P < 0.05$, Table 4). However, there were no overlapping genera between divergent groups of traits and genus relative abundance (Table 4).

Microbiome-wide association analysis of percentage of leaf fat and intramuscular fat content

The MWAS was used to investigate whether there were significant associations between genus relative abundance and traits (PL and IMF). The MWAS results are shown in Supplementary Table 5. The number of microbes

TABLE 3 Heritability and microbiability of PL and IMF in the resource population.

Trait	h^2	SE	*P-value*	m^2	SE	*P-value*
PL	0.71	0.17	<0.01	0.20	0.12	0.02
IMF	0.89	0.16	<0.01	0.26	0.12	0.02

h^2, heritability; m^2, microbiability. The significant *P*-value bounds are $P < 0.05$.

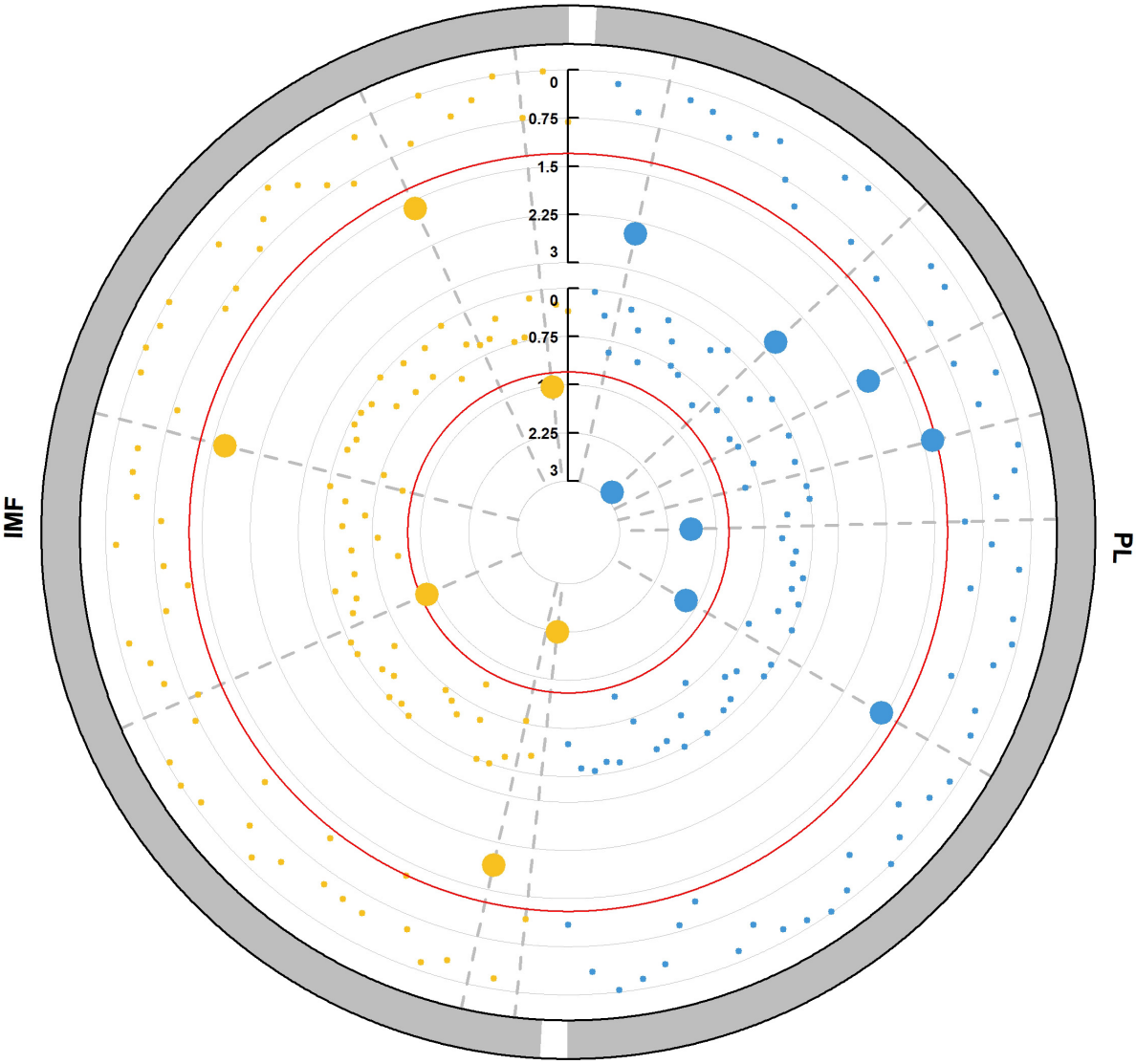

FIGURE 2
Microbial detections *via* Wilcoxon rank-sum tests between divergent groups. Microbial abundance in the highest 20% group with lowest 20% group traits. Displayed from the outer to the inner circle is the trait, the significance test in trait between the two groups with the highest and lowest microbial abundance ($P_{m-trait}$), the significance test in each microbial abundance between the highest and lowest trait ($P_{trait-m}$), where *p-values* are plotted as −log10 (*p-value*); the red line shows the significance threshold ($P < 0.05$). Each point represents a microbe, and the big point indicates the *p*-value passed the significance threshold. The dot on the same gray dashed line indicates that the $P_{m-trait}$ and $P_{trait-m}$ values for one microbe are all <0.05.

significantly associated PL and IMF was 4 and 2, respectively ($P < 0.05$, **Table 5**). Notably, some genera showed high significant associations with traits. For example, *Anaeroplasma* was significantly associated with PL ($P < 0.05$), whereas *Sharpea* with IMF. Moreover, *Paraprevotella*, *Pasteurella*, and *Streptococcus* were also significantly associated with PL ($P < 0.05$), while *Helicobacter* exhibited significant association with IMF ($P < 0.05$).

We adopted two methods (divergent Wilcoxon rank-sum test and MWAS) to screen microbes affecting PL and IMF at the genus level and found that *Paraprevotella* was significantly associated with PL in both methods ($P < 0.05$). As a significant candidate genus, *Paraprevotella* is one of the most important butyric acid-producing bacteria, and it may affect visceral fat deposition by producing butyric acid (a short-chain fatty acid).

Discussion

Fat deposition trait is closely related to carcass and meat quality traits in pigs, and it affects economic income and feed consumption. Pig fat deposition traits are influenced by host

TABLE 4 Microbiome relative abundance and trait Wilcoxon test of highest 20% and lowest 20% groups in the resource population.

Trait	Micro	The 20% pigs of highest trait		The 20% pigs of lowest trait		*P-value*	The 20% pigs of highest micro		The 20% pigs of lowest micro		*P-value*
		Micro	Micro	Micro	Micro		Trait	Trait	Trait	Trait	
		mean	SD	mean	SD		mean	SD	mean	SD	
PL	*Anaeroplasma*	0.04	0.05	0.03	0.04	0.12	7.01	1.12	6.28	1.08	<0.01
	Campylobacter	0.31	0.81	0.65	0.9	<0.01	6.18	1.2	7.08	1.29	<0.01
	Desulfovibrio	0.44	1.03	0.39	0.52	0.15	6.49	1.17	7.14	1.42	0.01
	Escherichia	0.91	2.13	1.71	4.82	0.11	6.3	1.25	6.79	1.28	0.04
	Haemophilus	0.01	0.02	0.03	0.08	0.01	6.23	1.12	6.68	1.64	0.09
	Paraprevotella	0.03	0.06	0.08	0.23	0.02	6.25	1.36	6.95	1.39	0.03
IMF	*Actinobacillus*	0.05	0.09	0.05	0.18	0.01	2.09	0.84	1.82	0.7	0.07
	Anaeroplasma	0.04	0.04	0.03	0.04	0.16	2.22	0.84	1.83	0.51	0.01
	Dialister	0.04	0.11	0.03	0.1	0.04	2.24	0.82	2	0.54	0.12
	Megasphaera	0.43	1.72	0.11	0.3	0.07	2.22	0.78	1.91	0.51	0.02
	Succinivibrio	0.01	0.02	0.04	0.09	0.27	1.78	0.66	2.07	0.65	0.02
	YRC22	1.01	1.02	0.65	0.64	0.03	2.08	0.8	1.89	0.61	0.2

PL, percentage of leaf fat; IMF, intramuscular fat content; SD, standard deviation. The significant *P*-value bounds are $P < 0.05$.

genetics and gut microbiome. Our study found that PL and IMF were influenced by the interactions between host genetics and gut microbiome. Several studies have identified that host genetics have interacted with gut microbiota and some host genetic variations affect the gut microbiota (Li et al., 2019; Bergamaschi et al., 2020; Wen et al., 2021). In our study, the IMF showed 0.29 effect of interactions between host genetics and gut microbiome, but no independent effect of gut microbiome. The reason that the IMF showed no independent effect of gut microbiome may be that gut microbiota affects IMF by interacting with host genetics, but not alone. Then, we estimated the heritability and microbiability of PL and IMF. In this study, a total of 14,139,625 SNPs were obtained from whole-genome sequencing of 239 samples from the resource population. GCTA was used to construct the GRM and estimate heritability of PL and IMF. The heritability of PL and IMF was estimated as 0.71 and 0.89, respectively. The proportion of SNP variance has been reported to be SNP heritability of traits (Yang et al., 2017). Heritability is calculated by genome sequencing data to analyze the effect of genetics on human body weight (Yang et al., 2010). The heritability is influenced by breed (Lopez et al., 2018), sample size (Tang et al., 2020), and sequencing methods (Uemoto et al., 2017). In addition, the heritability depends on the population, because both the variation in additive and non-additive genetic factors of each trait, and the environmental variance are population-specific (Visscher et al., 2008). The study results showed that when environmental factors of the resource population were consistent, most of the variation that is observed in the present population is caused by variation in genotypes. Besides, PL and IMF of this resource population were not strongly selected, and their genetic variation was large. The pedigree information (Costa et al., 2015) and chip data (Won et al., 2018; Wurtz et al., 2018) were widely applied for quantitative trait locus (QTL) mapping. So far, no report on more than 10 million SNP markers used for estimating the heritability of quantitative traits in livestock and poultry is available. This study provides a reference for heritability estimation based on genome-wide SNP data.

TABLE 5 Microbes significantly associated with PL and IMF.

Trait	Genus	Beta	*P-value*
PL	*Anaeroplasma*	3.16	0.03
	Paraprevotella	−0.83	0.03
	Pasteurella	−1.01	0.04
	Streptococcus	0.04	0.03
IMF	*Helicobacter*	0.12	0.01
	Sharpea	2.53	<0.01

PL, percentage of leaf fat; IMF, intramuscular fat content. The significant *P*-value bounds are $P < 0.05$.

In our study, heritability estimation model was consistent with microbiability estimation model. Both sex and BW were used as covariates to explore the influence of cecal microbiome on traits. To correct the effect of host genome on traits, the first five PCs generated by the GRM and the first two PCs generated at SNPs which were significantly associated with PL and IMF are considered as covariates. In the previous study, the first two PCs and the first five PCs of population structure were used as covariates to estimate microbiability (Wen et al., 2019b). In our study, the host heredity had major effect on traits.

Several studies have reported that the microbiability of traits was lower than the heritability of traits in pigs (Camarinha-Silva et al., 2017; Tang et al., 2020; Khanal et al., 2021), chicken (Wen et al., 2019b), and cattle (Difford et al., 2018). In previous studies, the microbiability of the IMF was estimated as 0.13 in Enshi pigs (Tang et al., 2020), estimated as 0.03–0.06 following different models in commercial F1 sows composed of Yorkshire × Landrace or Landrace × Yorkshire (Khanal et al., 2021). The microbiability of IMF in the resource population was estimated to be 0.26, which was higher than that in the previous study. The reason for the difference in these studies' results is that estimation of microbiability is affected by breed, environment, sample size, sequencing method, and estimation algorithm (Wen et al., 2019a). So far, few studies have described the microbiability of fat deposition traits in pigs, and estimation of microbiability of fat deposition traits in pigs needs to be further studied. Our estimated microbiability suggested that the gut microbiome had an influence on PL and IMF and provided a reference for microbiability estimation.

Pig fat deposition traits are affected by a large number of complex microbes and their metabolites which are closely related to host immune diseases, nutritional metabolism, and body behavior (Patil et al., 2020). To select microbes affecting traits, divergent Wilcoxon rank-sum test and MWAS were applied in our study. The divergent Wilcoxon rank-sum test has been used to analyze microbes in previous studies (Yang et al., 2016; Gardiner et al., 2020). MWAS has been proposed with reference to genome-wide association analysis to establish the relationship between traits and gut microbes, and it has been applied in basic research (Gilbert et al., 2016; Vollmar et al., 2020). In our study, the divergent Wilcoxon rank-sum test showed that *Campylobacter* and *Paraprevotella* were significantly associated with PL, and the MWAS results showed that *Anaeroplasma*, *Paraprevotella*, *Pasteurella*, and *Streptococcus* were significantly associated with PL. Among these genera, *Streptococcus* is reported as one of the most abundant bacteria in the gut microbes of Jinhua Pigs (Yang et al., 2018). Jinhua pig is an obese-type breed characterized by higher levels of intramuscular fat (Miao et al., 2009). MWAS results indicated that *Helicobacter* and *Sharpea* were significantly associated with IMF. *Sharpea azabuensis* has been reported to affect methane emissions in rumen, and it was viewed as one of the important driving factors of lactic acid production and utilization (Kamke et al., 2016). In previous studies, lactic acid can reduce fat synthesis and accumulation (Yonejima et al., 2013; Gan et al., 2020).

Divergent Wilcoxon rank-sum test and MWAS results indicated that *Paraprevotella* was significantly associated with PL, suggesting the influence of single genus on host phenotype. *Paraprevotella* belongs to *Bacteroidetes* phylum which could degrade cellulose and produce butyric acid (Gao et al., 2018; Hasan et al., 2018). Butyric acid is a short-chain fatty acid (SCFA), and SCFAs are closely related to glucose and lipid metabolism and energy metabolism (Dabke et al., 2019). It has been demonstrated that SCFAs enhance adipocyte differentiation in porcine adipose tissue (Li et al., 2014). The content of butyric acid has been reported to be positively correlated with the relative abundance of *Paraprevotella* in mouse feces (Fei et al., 2019). Butyric acid is a major energy source for intestinal epithelial cells and plays key functional roles in maintaining intestinal homeostasis and in overall health status. It can promote the development of the intestine and has antioxidant and anti-inflammatory effects (Fu et al., 2019). Our data revealed a significant negative correlation between the relative abundance of *Paraprevotella* and PL. *Paraprevotella* may affect the intestinal homeostasis by influencing the anabolism of butyric acid, thereby affecting the visceral fat deposition in pigs, but the mechanism of *Paraprevotella* on affecting fat deposition in pig needs to be further studied.

Conclusion

This study revealed that PL and IMF were influenced by the host genetics–gut microbiome interaction. Through divergent Wilcoxon rank-sum test and microbiome-wide association analysis, we screened out *Paraprevotella* which were significantly associated with PL. Overall, this study reveals the effect of host genetics and gut microbiome on pig fat deposition traits and provides a reference for the genetic improvement of pig fat deposition traits, which can affect pig fat deposition by altering the gut microbiome.

Data availability statement

The genotyping data in PLINK binary format is available from the Figshare database (https://figshare.com/s/c0ece21cf32f35833569). The 16S ribosomal RNA sequencing data are available in the Sequence Read Archive (SRA) repository (SRA accession number PRJNA868520). Further information on the original data can be directed to the corresponding author.

Ethics statement

This animal study was reviewed and approved by the Animal Care and Use Committee of Huazhong Agricultural University.

Author contributions

YW collected the samples, performed the data analysis and interpretation, and wrote the manuscript.

PZ performed the data analysis and wrote the manuscript. MF, ZL, and TW measured pig phenotype and collected samples. ZW and XL participated in constructing mathematical models. BL and XZ conceived and designed the study and manuscript revision. All authors contributed to manuscript revision, read, and approved the submitted version.

Funding

This study was supported by the National Natural Science Foundation of China (31930104) and the Fundamental Research Funds for the Central Universities (2662022DKPY008).

Conflict of interest

The authors declare that the research was conducted in the absence of any commercial or financial relationships that could be construed as a potential conflict of interest.

Publisher's note

Supplementary material

The Supplementary Material for this article can be found online at: https://www.frontiersin.org/articles/10.3389/fmicb.2022.925200/full#supplementary-material

SUPPLEMENTARY FIGURE 1
Distribution of fat deposition traits. **(A–H)** Distribution of backfat thickness at shoulder (SBFT), backfat thickness at loin (LBFT), backfat thickness at rump (RBFT), average backfat thickness (ABFT), percentage of leaf fat (PL), percentage of caul fat (PC), percentage of leaf fat, and caul (PLC), and intramuscular fat content (IMF).

References

Bergamaschi, M., Maltecca, C., Schillebeeckx, C., McNulty, N. P., Schwab, C., Shull, C., et al. (2020). Heritability and genome-wide association of swine gut microbiome features with growth and fatness parameters. *Sci. Rep.* 10:10134. doi: 10.1038/s41598-020-66791-3

Camarinha-Silva, A., Maushammer, M., Wellmann, R., Vital, M., Preuss, S., and Bennewitz, J. (2017). Host genome influence on gut microbial composition and microbial prediction of complex traits in pigs. *Genetics* 206, 1637–1644. doi: 10.1534/genetics.117.200782

Costa, E. V., Diniz, D. B., Veroneze, R., Resende, M. D. V., Azevedo, C. F., Guimaraes, S. E. F., et al. (2015). Estimating additive and dominance variances for complex traits in pigs combining genomic and pedigree information. *Genet. Mol. Res.* 14, 6303–6311. doi: 10.4238/2015.Jun e.11.4

Dabke, K., Hendrick, G., and Devkota, S. (2019). The gut microbiome and metabolic syndrome. *J. Clin. Invest.* 129, 4050–4057. doi: 10.1172/JCI129194

Difford, G. F., Plichta, D. R., Lovendahl, P., Lassen, J., Noel, S. J., Hojberg, O., et al. (2018). Host genetics and the rumen microbiome jointly associate with methane emissions in dairy cows. *PLoS Genet.* 14:e1007580. doi: 10.1371/journal.pgen.1007580

Fei, Y., Wang, Y., Pang, Y., Wang, W., Zhu, D., Xie, M., et al. (2019). Xylooligosaccharide modulates gut microbiota and alleviates colonic inflammation caused by high fat diet induced obesity. *Front. Physiol.* 10:1601. doi: 10.3389/fphys.2019.01601

Fortin, A., Robertson, W. M., and Tong, A. K. W. (2005). The eating quality of Canadian pork and its relationship with intramuscular fat. *Meat Sci.* 69, 297–305. doi: 10.1016/j.meatsci.2004.07.011

Fu, X., Liu, Z., Zhu, C., Mou, H., and Kong, Q. (2019). Nondigestible carbohydrates, butyrate, and butyrate-producing bacteria. *Crit. Rev. Food Sci. Nutr.* 59(sup1), S130–S152. doi: 10.1080/10408398.2018.1542587

Gan, Y., Tang, M. W., Tan, F., Zhou, X. R., Fan, L., Xie, Y. X., et al. (2020). Anti-obesity effect of *Lactobacillus plantarum* CQPC01 by modulating lipid metabolism in high-fat diet-induced C57BL/6 mice. *J. Food Biochem.* 44:e13491. doi: 10.1111/jfbc.13491

Gao, B. B., Wang, R. J., Peng, Y., and Li, X. B. (2018). Effects of a homogeneous polysaccharide from Sijunzi decoction on human intestinal microbes and short chain fatty acids in vitro. *J. Ethnopharmacol.* 224, 465–473. doi: 10.1016/j.jep.2018.06.006

Gao, S. Z., and Zhao, S. M. (2009). Physiology, affecting factors and strategies for control of pig meat intramuscular fat. *Recent Pat Food Nutr. Agric.* 1, 59–74. doi: 10.2174/2212798410901010059

Gardiner, G. E., Metzler-Zebeli, B. U., and Lawlor, P. G. (2020). Impact of intestinal microbiota on growth and feed efficiency in pigs: A review. *Microorganisms* 8:1886. doi: 10.3390/microorganisms8121886

Gilbert, J. A., Quinn, R. A., Debelius, J., Xu, Z. Z., Morton, J., Garg, N., et al. (2016). Microbiome-wide association studies link dynamic microbial consortia to disease. *Nature* 535, 94–103. doi: 10.1038/nature18850

Hasan, S., Junnikkala, S., Peltoniemi, O., Paulin, L., Lyyski, A., Vuorenmaa, J., et al. (2018). Dietary supplementation with yeast hydrolysate in pregnancy influences colostrum yield and gut microbiota of sows and piglets after birth. *PLoS One* 13:e0197586. doi: 10.1371/journal.pone.0197586

Hishikawa, D., Hong, Y. H., Roh, S., Miyahara, H., Nishimura, Y., Tomimatsu, A., et al. (2005). Identification of genes expressed differentially in subcutaneous and visceral fat of cattle, pig, and mouse. *Physiol. Genomics* 21, 343–350. doi: 10.1152/physiolgenomics.00184.2004

Kamke, J., Kittelmann, S., Soni, P., Li, Y., Tavendale, M., Ganesh, S., et al. (2016). Rumen metagenome and metatranscriptome analyses of low methane yield sheep reveals a Sharpea-enriched microbiome characterised by lactic acid formation and utilisation. *Microbiome* 4:56. doi: 10.1186/s40168-016-0201-2

Khanal, P., Maltecca, C., Schwab, C., Fix, J., and Tiezzi, F. (2021). Microbiability of meat quality and carcass composition traits in swine. *J. Anim. Breed. Genet.* 138, 223–236. doi: 10.1111/jbg.12504

Li, F., Li, C., Chen, Y., Liu, J., Zhang, C., Irving, B., et al. (2019). Host genetics influence the rumen microbiota and heritable rumen microbial features associate with feed efficiency in cattle. *Microbiome* 7:92. doi: 10.1186/s40168-019-0699-1

Li, G., Yao, W., and Jiang, H. (2014). Short-chain fatty acids enhance adipocyte differentiation in the stromal vascular fraction of porcine adipose tissue. *J. Nutr.* 144, 1887–1895. doi: 10.3945/jn.114.198531

Lopez, B. I. M., Song, C., and Seo, K. (2018). Genetic parameters and trends for production traits and their relationship with litter traits in Landrace and Yorkshire pigs. *Anim. Sci. J.* 89, 1381–1388. doi: 10.1111/asj.13090

Merlotti, C., Ceriani, V., Morabito, A., and Pontiroli, A. E. (2017). Subcutaneous fat loss is greater than visceral fat loss with diet and exercise, weight-loss promoting drugs and bariatric surgery: A critical review and meta-analysis. *Int. J. Obes.* 41, 672–682. doi: 10.1038/ijo.2017.31

Miao, Z. G., Wang, L. J., Xu, Z. R., Huang, J. F., and Wang, Y. R. (2009). Developmental changes of carcass composition, meat quality and organs in the Jinhua pig and Landrace. *Animal* 3, 468–473. doi: 10.1017/S1751731108003613

Patil, Y., Gooneratne, R., and Ju, X. H. (2020). Interactions between host and gut microbiota in domestic pigs: A review. *Gut Microbes* 11, 310–334. doi: 10.1080/19490976.2019.1690363

Quan, J., Cai, G., Ye, J., Yang, M., Ding, R., Wang, X., et al. (2018). A global comparison of the microbiome compositions of three gut locations in commercial pigs with extreme feed conversion ratios. *Sci. Rep.* 8:4536. doi: 10.1038/s41598-018-22692-0

Savage, D. C. (1977). Microbial ecology of the gastrointestinal tract. *Annu. Rev. Microbiol.* 31, 107–133. doi: 10.1146/annurev.mi.31.100177.000543

Tang, S., Xin, Y., Ma, Y., Xu, X., Zhao, S., and Cao, J. (2020). Screening of microbes associated with swine growth and fat deposition traits across the intestinal tract. *Front. Microbiol.* 11:586776. doi: 10.3389/fmicb.2020.586776

Uemoto, Y., Sato, S., Kikuchi, T., Egawa, S., Kohira, K., Sakuma, H., et al. (2017). Genomic evaluation using SNP- and haplotype-based genomic relationship matrices in a closed line of Duroc pigs. *Anim. Sci. J.* 88, 1465–1474. doi: 10.1111/asj.12805

Visscher, P. M., Hill, W. G., and Wray, N. R. (2008). Heritability in the genomics era–concepts and misconceptions. *Nat. Rev. Genet.* 9, 255–266. doi: 10.1038/nrg2322

Vollmar, S., Wellmann, R., Borda-Molina, D., Rodehutscord, M., Camarinha-Silva, A., and Bennewitz, J. (2020). The gut microbial architecture of efficiency traits in the domestic poultry model species Japanese Quail (*Coturnix japonica*) assessed by mixed linear models. *G3 Genes Genomes Genet.* 10, 2553–2562. doi: 10.1534/g3.120.401424

Wen, C. L., Yan, W., Sun, C. J., Ji, C. L., Zhou, Q. Q., Zhang, D. X., et al. (2019b). The gut microbiota is largely independent of host genetics in regulating fat deposition in chickens. *ISME J.* 13, 1422–1436. doi: 10.1038/s41396-019-0367-2

Wen, C. L., Sun, C. J., and Yang, N. (2019a). [The concepts and research progress: From heritability to microbiability]. *Yi Chuan* 41, 1023–1040. doi: 10.16288/j.yczz.19-130

Wen, C., Yan, W., Mai, C., Duan, Z., Zheng, J., Sun, C., et al. (2021). Joint contributions of the gut microbiota and host genetics to feed efficiency in chickens. *Microbiome* 9:126. doi: 10.1186/s40168-021-01040-x

Won, S., Jung, J., Park, E., and Kim, H. (2018). Identification of genes related to intramuscular fat content of pigs using genome-wide association study. *Asian Australas. J. Anim. Sci.* 31, 157–162. doi: 10.5713/ajas.17.0218

Wurtz, K. E., Siegford, J. M., Ernst, C. W., Raney, N. E., Bates, R. O., and Steibel, J. P. (2018). Genome-wide association analyses of lesion counts in group-housed pigs. *Anim. Genet.* 49, 628–631. doi: 10.1111/age.12713

Xiao, L., Estelle, J., Kiilerich, P., Ramayo-Caldas, Y., Xia, Z., Feng, Q., et al. (2016). A reference gene catalogue of the pig gut microbiome. *Nat. Microbiol* 1:16161. doi: 10.1038/nmicrobiol.2016.161

Yang, H., Huang, X., Fang, S., Xin, W., Huang, L., and Chen, C. (2016). Uncovering the composition of microbial community structure and metagenomics among three gut locations in pigs with distinct fatness. *Sci. Rep.* 6:27427. doi: 10.1038/srep27427

Yang, H., Xiao, Y. P., Wang, J. J., Xiang, Y., Gong, Y. J., Wen, X. T., et al. (2018). Core gut microbiota in Jinhua pigs and its correlation with strain, farm and weaning age. *J. Microbiol.* 56, 346–355. doi: 10.1007/s12275-018-7486-8

Yang, J. A., Benyamin, B., McEvoy, B. P., Gordon, S., Henders, A. K., Nyholt, D. R., et al. (2010). Common SNPs explain a large proportion of the heritability for human height. *Nat. Genet.* 42, 565–569. doi: 10.1038/ng.608

Yang, J. A., Lee, S. H., Goddard, M. E., and Visscher, P. M. (2011). GCTA: A tool for genome-wide complex trait analysis. *Am. J. Hum. Genet.* 88, 76–82. doi: 10.1016/j.ajhg.2010.11.011

Yang, J., Zeng, J., Goddard, M. E., Wray, N. R., and Visscher, P. M. (2017). Concepts, estimation and interpretation of SNP-based heritability. *Nat. Genet.* 49, 1304–1310. doi: 10.1038/ng.3941

Yonejima, Y., Ushida, K., and Mori, Y. (2013). Effect of lactic acid bacteria on lipid metabolism and fat synthesis in mice fed a high-fat diet. *Biosci. Microbiota Food Health* 32, 51–58. doi: 10.12938/bmfh.32.51

Zhu, B. L., Wang, X., and Li, L. J. (2010). Human gut microbiome: The second genome of human body. *Protein Cell* 1, 718–725. doi: 10.1007/s13238-010-0093-z

frontiers | Frontiers in Microbiology

TYPE Original Research
PUBLISHED 06 October 2022
DOI 10.3389/fmicb.2022.1002738

OPEN ACCESS

EDITED BY
François J. M. A. Meurens,
INRA Ecole Nationale Vétérinaire, Agroalimentaire et de l'alimentation de Nantes-Atlantique (Oniris), France

REVIEWED BY
Qiugang Ma,
China Agricultural University, China
Bert Devriendt,
Ghent University, Belgium

*CORRESPONDENCE
Jun Bao
jbao@neau.edu.cn

SPECIALTY SECTION
This article was submitted to Microorganisms in Vertebrate Digestive Systems, a section of the journal Frontiers in Microbiology

RECEIVED 26 July 2022
ACCEPTED 20 September 2022
PUBLISHED 06 October 2022

CITATION
Han Q, Zhang X, Nian H, Liu H, Li X, Zhang R and Bao J (2022) Artificial rearing alters intestinal microbiota and induces inflammatory response in piglets. *Front. Microbiol.* 13:1002738. doi: 10.3389/fmicb.2022.1002738

Artificial rearing alters intestinal microbiota and induces inflammatory response in piglets

Qi Han[1], Xiaohong Zhang[1], Haoyang Nian[1], Honggui Liu[1,2], Xiang Li[1,2], Runxiang Zhang[1] and Jun Bao[1,2]*

[1]College of Animal Science and Technology, Northeast Agricultural University, Harbin, China, [2]Key Laboratory of Swine Facilities Engineering, Ministry of Agriculture and Rural Affairs, Harbin, China

With the ongoing genetic selection for high prolificacy in sow lines and the improvements in environment and farm management, litter size has increased in recent years. Artificial rearing is becoming widely used to raise the surplus piglets in pig industry. This study aimed to investigate the changes that happened in the morphology, microbiota, mucosal barrier function, and transcriptome caused by artificial rearing in piglet colon. Two hundred and forty newborn piglets were randomly assigned into three treatments, sow rearing until weaning (CON group), artificial rearing from day 21 (AR21 group), and artificial rearing from day 7 (AR7 group). On day 35, the piglets were euthanized to collect colon samples. The results showed that the artificially reared-piglets displayed increased pre-weaning diarrhea incidence and reduced growth performance. Artificial rearing changed the diversity and structure of colonic microbiota and increased relative abundance of harmful bacteria, such as *Escherichia-Shigella*. In addition, the morphological disruption was observed in AR7 group, which was coincided with decreased tight junction proteins and goblet cell numbers. Moreover, the expression of TNFSF11, TNF-α, IL-1β, TLR2, TLR4, MyD88, NF-κB, COX-2, PTGEs, iNOS, IL-2, IL-6, IL-17A, and IFN-γ was upregulated in the colon of the artificially reared-piglets, while the expression of IL-1Ra and IκBα was downregulated, indicating that artificial rearing induced inflammatory response through the activation of NF-κB pathway. Furthermore, artificial rearing regulated SLC family members, which affected solute transport and destroyed intestinal homeostasis. In conclusion, artificial rearing caused microbiota alteration, morphology disruption, the destruction of mucosal barrier function, and inflammatory response, and thus, led to subsequent increased diarrhea incidence and reduced growth performance.

KEYWORDS

artificial rearing, piglet, diarrhea, microbiota, NF-κB pathway

Introduction

In recent years, genetic selection toward hyper-prolificacy has elevated the number of born piglets per litter, routinely exceeding the number of functional teats (Lanferdini et al., 2018). Unfortunately, larger litter size was linked to lower birth weight and growth rate, which ultimately resulted in higher pre-weaning mortality (Quesnel et al., 2008;

Peltoniemi et al., 2021). Artificial rearing is a common practice to improve piglet survival. An investigation found that 31% of pig farmers adopted this strategy to raise the surplus piglets and 85% supplemented formula milk to piglets in the Flemish region of Belgium (Vandenberghe, 2012). A recent study reported the adverse effects of artificial rearing on growth performance, behavior, and emotional state of piglets (Schmitt et al., 2019). In the artificial rearing system, milk replacer can meet the nutritional requirements of piglets to the greatest extent, but still lack multiple functional and bioactive components (Salmon et al., 2009; Levast et al., 2014). Rasmussen et al. (2016) reported that diarrhea frequently occurred in artificially reared-piglets. Vergauwen et al. (2017) found that artificial rearing altered the morphology, permeability, and redox state in the small intestine of piglets. Epidemiological studies reported that formula milk and prolonged duration of enteral feeding led to an increased risk of necrotizing enterocolitis (NEC) in infants (Lucas and Cole, 1990; Berkhout et al., 2018). NEC most commonly affects the proximal ascending colon and the terminal ileum (Di Lorenzo et al., 1995). It could be hypothesized that artificial rearing might mediate intestinal dysfunction in piglets.

Gut microbiota is implicated in a range of host physiological processes, including nutrition absorption, energy utilization, and immune modulation (Nicholson et al., 2012). A stable and diverse gut microbiota is essential for intestinal health and pig growth. The composition of gut microbiota can be affected by many factors, such as diet, age, environment, and antibiotics (Rinninella et al., 2019). The presence of sow feces can influence piglet microbiota development, growth, and survival (Nowland et al., 2021). Piccolo et al. (2017) compared the intestinal microbiota of piglets fed with the dairy or soy infant formulas and found that soy formula feeding resulted in lower community richness in jejunum. The rats fed with formula milk had a lower microbial diversity and decreased acetic acid concentration in cecum (Liu et al., 2016). Underwood et al. (2014) found that formula feeding altered microbiota composition and triggered inflammatory response and mucosal disease in rat ileum. In this study, we are particularly interested in the effects of artificial rearing on the intestinal microbiota of piglets and consequently, on the incidence of diarrhea and growth performance.

Artificial rearing has been widely adopted in the Netherlands, the United States, and increasingly in Germany (ŠPinka, 2018). So far, the scientific evidences regarding the effects of artificial rearing on intestinal health, especially colon remain scanty and require further investigation. Moreover, the pigs share many similarities with humans in anatomy, morphology, and physiology of the gastrointestinal tract (Gonzalez et al., 2015) and have been used with increasing frequency in NEC research (Mendez et al., 2020). In the present study, we established a piglet model of artificial rearing, and then measured growth performance of piglets, observed colon morphology, and analyzed the structural and functional changes of intestinal microbiota. The next-generation sequencing was performed to illustrate the molecular mechanism of colonic dysfunction. Hopefully, our study will give a comprehensive understanding of the pathogenesis of artificial rearing-induced colonic dysfunction and provide a reference for comparative medicine.

Materials and methods

Ethics statement

This study was approved by the Institutional Animal Care and Use Committee of Northeast Agricultural University. All procedures were performed in accordance with the EU Directive 2010/63/EU on the protection of animals used for scientific purposes.

Animals and experimental design

Thirty sows (Duroc × Min) were artificially inseminated with semen sourced from the same Yorkshire boar. Two hundred and forty newborn piglets (Yorkshire × Duroc × Min) were used in this animal experiment. The piglets were randomly divided into three treatments at birth (eight piglets per litter and 10 litters per group), artificial rearing from 7 days of age (AR7 group), artificial rearing from 21 days of age (AR21 group), and sow rearing until weaning (CON group). All piglets were weaned on day 35. During the period of 1–35 days of age, the CON piglets suckled the sows, whereas AR7 and AR21 piglets were fed with milk replacer (Joosten Products B.V., Netherlands) after being moved away from the sows. The milk replacer was made by mixing 150 g of milk replacer powder into 1 L of water at 45°C, which was provided using a milk cup with an inside diameter of 16 cm. The daily intake of milk replacer was 360 ml/kg body weight (BW). The nutrient composition of milk replacer was shown in Supplementary Table 1. Milk cup was cleaned and disinfected once daily. Feces and urine were cleaned twice daily. The piglets with a BW lower than 700 g were classified as runt and excluded from this study.

The individual farrowing crate consisted of a pen (2.0 m × 4.5 m) for sow to lie down, rest, and stand up and a protected area (1.0 m × 2.0 m) for piglets. Each farrowing crate was equipped with a feeder and a nipple drinker for the sows, and a 100 W infrared (IR) lamp, an electric heating plate, and a nipple drinker for the piglets. The ambient temperature was on average 25.7°C (range: min. 24.2°C to max. 27.5°C) and the temperature in protected area was maintained at approximately 30°C. Relative humidity varied from 65 to 75%. Daily photoperiod was 16 h light:8 h darkness.

Growth performance measurements

All piglets were individually weighed on day 0 and weekly during the experiment. The average daily gain (ADG) was calculated for each week and the entire experimental period.

Diarrhea incidence

From 7 days of age, the diarrhea episodes were daily recorded. The diarrhea was defined as loose and watery stool or stool attached to the skin around the anus. The diarrhea incidence of each week was calculated as follows:

$$\text{Diarrhea incidence}(\%) = \frac{A}{M} \times 100\%$$

where A = the number of piglets with diarrhea recorded for each week. M = Total number of piglets × 7 days.

Sample collection

On day 35, 10 piglets were randomly selected from each group (one piglet from each litter) and euthanized. The luminal contents of the ascending colon were collected, rapidly frozen in liquid nitrogen, and then stored at −80°C. The colon segments (approximately 1 cm) were fixed in 4% paraformaldehyde for histological examination. After washing with PBS solution twice, the mucosa samples were scraped on an ice bag using sterile glass microscope slides. Then, the samples were rapidly frozen in liquid nitrogen and stored at −80°C for further analysis.

16S rDNA sequencing

16S rDNA sequencing was conducted on 10 biological replicates in each group. Total genomic DNA was extracted from the colon content using the EZNA® Stool DNA Kit (Omega Inc., United States) according to the manufacturer's instructions. DNA was amplified by using the 341F/805R primer set for the variable region of V3 and V4 (341F: 5′-CCTACGGGNGGCWGCAG-3′, 805R: 5′-GACTACHVGGGTATCTAATCC-3′). Then, PCR products were confirmed with 2% agarose gel electrophoresis. Amplicons were purified using AMPure XT beads (Beckman Coulter Genomics, Danvers, MA, United States) and quantified by Qubit (Invitrogen, United States). Finally, the library was sequenced on a NovaSeq PE250 platform (Illumina, Inc., SanDiego, CA, United States).

The raw data were pre-processed to obtain the high-quality clean tags according to the fqtrim (v0.94). Chimeric sequences were filtered using the Vsearch (v2.3.4). After being filtered, the reads were processed by the DADA2 method using the default parameters to produce a set of denoised amplicon sequence variants (ASVs). ASVs were then annotated to the species with the SILVA 138 database. Alpha diversity was assessed using the Chao 1, Shannon, and Simpson indices. Beta diversity was measured using principal coordinate analysis (PCoA) by the distance between groups based on the unweight UniFrac distance and the hierarchical clustering algorithm. Linear discriminant analysis effect size (LEfSe) and random forest analysis were executed to determine the differences in the bacterial taxa at the genus or higher taxonomy levels between groups. The bacterial function was predicted *via* the phylogenetic analysis of community by reconstruction of unobserved states (PICRUSt2). The predicted sequences were aligned to the Kyoto Encyclopedia of Genes and Genomes (KEGG) database.

Examination of intestinal histology

The colon segments were dehydrated with a graded ethanol series, cleared in xylene, and embedded in paraffin. The paraffin sections were dewaxed routinely, rehydrated in a graded ethanol series, and stained with hematoxylin and eosin (H&E) and periodic acid-Schiff (PAS), respectively. The slides were digitized with Pannoramic MIDI scanner (3DHISTECH; Budapest, Hungary), and the micrographs were read using CaseViewer software (Version 2.4, 3D HISTECH, Budapest, Hungary). Crypt depth was measured and the expression of mucin in goblet cells was observed by PAS staining. The crypt depth and the number of PAS positive cells were evaluated for five different crypts per section.

Determination of iNOS activity and NO content

The mucosa samples (0.5 g) were homogenized in 4.5 ml cold PBS solution and then centrifuged at 1,280 × *g* for 10 min to collect supernatants. The assay kits were used to detect iNOS activity and NO content following the manufacturer's instructions (Shanghai Hengyuan Biological Technology Co., Ltd., China). Absorbance values were measured at 450 nm using a microplate reader (Molecular Devices, CA, United States).

RNA sequencing

RNA sequencing (RNA-seq) was performed on three biological replicates in each group. Total RNA was extracted using the animal tissue RNA purification kit (LC Science, Houston, TX, United States). The total RNA samples were analyzed by RNA-seq (LC-Bio, China) based on the manufacturer's protocols. Briefly, poly (A)-containing mRNA molecules were purified from total RNA using poly (T) oligo-attached magnetic beads using two rounds of purification. The purified mRNA was fragmented and reversely transcribed to create the final cDNA library using the mRNA-seq sample preparation kit (Illumina, San Diego, CA, United States). The cDNA libraries were then sequenced using the Illumina sequencing technology on an Illumina Hiseq 4000 system (Illumina, San Diego, CA, United States).

The differentially expressed genes (DEGs) were selected with |log2 fold change (FC)| ≥ 1.0 and $p < 0.05$ using Ballgown R

package (R Studio, Inc., Boston, MA, United States). All DEGs were subject to Gene Ontology (GO) enrichment analysis[1] and KEGG enrichment analysis.[2]

Real-time quantitative PCR

Real-time quantitative PCR (RT-qPCR) was conducted on eight biological replicates in each group. The mucosa samples (0.1 g) were used for total RNA isolation with TRIzol reagent (15,596,026; Invitrogen, Carlsbad, CA, United States). RNA integrity was verified with 1.1% agarose gel electrophoresis. RNA quantity and quality were determined through detecting optical density at 260 and 280 nm using a micro-spectrophotometer (Hangzhou Allsheng Instruments Co., Ltd., China). RT-PCR was performed with a RT kit (BL699A; Biosharp, China) using a thermal cycler (Bio-Rad, Hercules, CA, United States). A 20 μl reaction mixture consisted of 1 μg of total RNA, 4 μl of RT MasterMix, 1 μl of 20 × Oligo dT & Random Primer, and RNase-free water to bring the final volume to 20 μl. The RT-PCR procedure consisted of 25°C for 10 min, 55°C for 60 min, and 85°C for 5 min. Obtained cDNA was diluted into 10 ng/μl by adding RNase-free water.

The primers were synthesized by Sangon Biotech Co., Ltd. (Shanghai, China), as shown in Supplementary Table 2. RT-qPCR was performed on a LightCycler® 480 System (Roche Diagnostics, Mannheim, Germany). PCR amplification was carried out at a final volume of 20 μl containing 20 ng of cDNA template, 10 μl of FastStart Universal SYBR Green Master (ROX; Roche Applied Science, Mannheim, Germany), 0.06 μl of each primer (100 μM), and RNase-free water to bring the final volume to 20 μl. PCR amplification was performed using the following conditions: 95°C for 1 min, followed by 40 cycles of 95°C for 15 s, and 60°C for 1 min. The geNorm[3] was used to select the most optimal reference gene by calculating the ranking of three candidate housekeeping genes β-actin, GAPDH, and 18 s (Vandesompele et al., 2002). The most stable candidate housekeeping gene β-actin was selected as the reference gene. Expression levels were determined by the $2^{-\triangle\triangle Ct}$ method (Livak and Schmittgen, 2001), accounting for gene-specific efficiencies and normalized to β-actin.

Western blot

Western blot was carried out using eight biological replicates in each group. Total protein was extracted with the lysis buffer for Western and IP (Biosharp, Beijing, China) plus protease inhibitor (Beyotime, Beijing, China) and PhosSTOP (Roche, Basel, Switzerland). The protein concentration was determined with the enhanced BCA protein assay kit (Beyotime, China). 20 μg of total protein was separated on 10 and 12% SDS-PAGE gel and transferred to nitrocellulose membranes. The membranes were blocked with 5% BSA and then incubated with primary antibodies. The primary antibodies used in this experiment were listed in Supplementary Table 3. The membranes were incubated with a horse-radish peroxidase (HRP) conjugated secondary antibody against rabbit IgG at 1:8,000 dilution (Beijing Zhongshan Golden Bridge Biotechnology Co., Ltd. Beijing, China). The protein bands were visualized using an Amersham Imager 600 RGB (General Electric Company, United States) after being treated with an enhanced chemiluminescence (ECL) reagent (Beyotime, China). Obtained bands were quantified using Image J (Version 1.8.0, Rasband, MD, United States). Relative band intensities of target genes were normalized to β-actin expression.

Immunohistochemistry

Paraffin-embedded tissues were used to detect ZO-1 expression. The paraffin-embedded tissues were cut into 5-μm thick sections, deparaffinized with xylene, and rehydrated in a graded ethanol series. Antigen retrieval was performed by placing the sections in a repair box filled with citric acid, boiling them in a microwave, and then cooling to room temperature. Blocking endogenous peroxidase activity was performed by placing the sections in 3% H_2O_2 at room temperature for 25 min. The sections were incubated with mouse anti-pig ZO-1 antibody at 1:500 dilution (Servicebio, China) at 4°C overnight and followed by incubation with a HRP-labeled secondary antibody at 1:1,000 dilution at room temperature for 50 min. The sections stained were visualized with a microscope (Nikon, Tokyo, Japan).

Statistical analysis

Statistical analyses were performed using SPSS (Version 20.0, SPSS Inc., Chicago, United States). Normality was assessed using the Shapiro–Wilk test and variance homogeneity was tested using Bartlett's test. Differences between groups were analyzed using one-way ANOVA followed by Tukey's *post hoc* test. The correlation between the mean diarrhea incidences and the ADG was examined using the Pearson correlation method. Heatmap was generated with pheatmap R package (R Studio, Inc., Boston, MA, United States).

Results

Growth performance

The BW and ADG of piglets are shown in Table 1. The BW in the AR21 group was significantly lower than that in the CON group on day 28 ($p < 0.05$) and day 35 ($p < 0.01$). And the BW in

1 http://geneontology.org/
2 https://www.genome.jp/kegg/
3 http://medgen.ugent.be/~jvdesomp/genorm/

the AR7 group was significantly lower than the CON group on days 14, 21, 28, and 35 ($p < 0.01$). Besides, the ADG in the AR21 group was significantly decreased ($p < 0.01$) compared with the CON group from day 21 to day 28, day 28 to day 35, and day 0 to day 35. The ADG in the AR7 group was significantly decreased ($p < 0.01$) compared with the CON group from day 7 to day 14, day 21 to day 28, day 28 to day 35, and day 0 to day 35.

Diarrhea occurrence

During the experiment period, the diarrhea occurrence of piglets was recorded and the data are shown in Figures 1A,B. In the AR21 group, the diarrhea incidence was significantly higher ($p < 0.01$) than that in the CON group from day 21 to day 27 and from day 28 to day 34. In the AR7 group, the diarrhea incidence was significantly higher ($p < 0.05$) than that in the CON group at all four periods. The mean diarrhea incidence from day 7 to day 34 was calculated (Figure 1C). To sum up, the diarrhea incidence in the AR7 group was the highest (46.5%); followed by AR21 group (31.1%) and CON group (11.9%). In addition, Pearson correlation analysis was performed between the mean diarrhea incidence and the ADG for each week. The correlation coefficient was −0.645 ($p < 0.05$), indicating a strong negative correlation.

TABLE 1 Effect of artificial rearing on growth performance of piglets.

Items	Treatment			SEM	*p*-Value
	CON	AR21	AR7		
BW (g)[1]					
day 0	1,215	1,242	1,292	19.0	0.248
day 7	2,173	2,205	2,225	31.0	0.802
day 14	3,402	3,379	2,860**	60.1	<0.001
day 21	4,727	4,666	3,986**	89.0	<0.001
day 28	6,616	5,950*	5,385**	139.7	<0.001
day 35	9,133	7,550**	7,111**	218.2	<0.001
ADG (g/day)[2]					
day 0 to day 7	136.9	137.5	133.2	3.33	0.859
day 7 to day 14	175.6	167.8	90.8**	7.55	<0.001
day 14 to day 21	189.2	183.8	160.8	5.60	0.085
day 21 to day 28	269.9	183.5**	199.8**	10.08	<0.001
day 28 to day 35	359.7	228.6**	246.6**	13.32	<0.001
day 0 to day 35	226.2	180.2**	166.2**	6.19	<0.001

[1]$n = 10$ litters.
[2]$n = 10$ litters.
*means $p < 0.05$ compared with the CON group.
**means $p < 0.01$ compared with the CON group.

Relative abundance and diversity of colonic microbiota in piglets

As shown in Figure 2A, the alpha diversity of microbial community was evaluated using Chao 1 index, Shannon index, and Simpson index, respectively. The Chao 1, Shannon, and Simpson indices in the AR7 and AR21 groups were significantly lower ($p < 0.05$) than those in the CON group, indicating that artificial rearing reduced the microbial abundance and diversity. PCoA analysis based on the unweight UniFrac distance revealed a significant difference in beta diversity of microbial community between three groups (Figure 2B). The results of hierarchical cluster analysis by UPGMA (Figure 2C) showed that all the samples were divided into three clusters according to different treatments and the level of the AR21 group was closer to that of the AR7 group.

Figures 3A,B showed the composition of microbial community at the phylum and genus levels. *Muribaculaceae* (6.56%) was the most abundant genera in the CON group, followed by *Eubacterium coprostanoligenes group* (5.96%) and *Ruminococcaceae* UCG-005 (5.95%). In the AR21 group, the three most abundant genera were *Ruminococcaceae* UCG-005 (9.77%), *Clostridia* UCG-014 (8.28%), and *Muribaculaceae* (6.72%). In the AR7 group, *Faecalibacterium* (14.94%) was the most abundant genera, followed by *Escherichia-Shigella* (12.78%), and *Subdoligranulum* (6.82%). LEfSe analysis (Figure 3C) further indicated the relative abundance of *Catenibacterium*, *Clostridia* UCG-014, *Ruminococcaceae*, *Bacteroidetes*, and *Muribaculaceae* showed an upward trend ($p < 0.05$) in the AR21 group. There was a significant increase ($p < 0.05$) in the relative abundance of *Holdemanella*, *Megasphaera*, *Escherichia Shigella*, *Collinsella*, and *Prevotella* in the AR7 group. The potential functions of microbial community were predicted by the PICRUSt2 (Figure 3D). At KEGG level 2, carbohydrate metabolism, membrane transport, and xenobiotics biodegradation and metabolism were significantly increased ($p < 0.05$) in AR7 and AR21 groups compared to the CON group. Cell motility, environmental adaptation, immune system, metabolism of cofactors and vitamins, metabolism of terpenoids and polyketides, signaling molecules and interaction, and folding, sorting, and degradation were significantly decreased ($p < 0.05$) in AR7 and AR21 groups compared to the CON group.

Histology in piglet colon

To evaluate the effects of artificial rearing on intestinal morphology, we observed the microstructure of colon stained with H&E (Figure 4A). The colon tissue from the CON piglets displayed the absence of inflammatory cells and normal villous architecture with orderly arrangement of intestinal epithelial cells, long and slender villus, as well as smooth villus border. In the AR21 group, we observed leukocyte infiltration (green arrow) in the mucosa. In the AR7 group, the colon tissue revealed the infiltrations of red blood cells (red arrow) and leukocytes (green

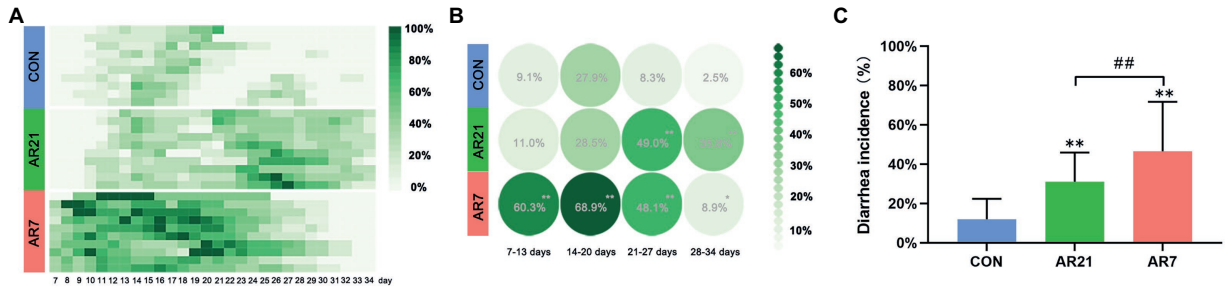

FIGURE 1
Effects of artificial rearing on the diarrhea incidence in piglets. **(A)** Recorded diarrhea occurrence of piglets from day 7 to day 34. **(B)** Mean diarrhea incidences of piglets for each week. **(C)** Mean diarrhea incidences of piglets from day 7 to day 34. Data are presented with mean±SD. $^{**}p < 0.01$ versus the CON group; $^{\#\#}p < 0.01$ versus the AR21 group. n=10 litters.

arrow) in the mucosa. Given the role of mucin in maintaining protective mucus barriers, the goblet cells were stained with PAS and then counted (Figure 4B). There was a significant reduction ($p < 0.05$) of the number of goblet cells in the AR7 group when compared with the CON group.

Mucosal barrier function in piglet colon

Then, we detected the mRNA and protein expression of tight junction proteins including ZO-1, Claudin-2, and JEAP (Figure 5). In the AR21 group, the mRNA expression of ZO-1 and Claudin-2 was lower ($p < 0.05$) than the CON group. And the protein expression of Claudin-2 in the AR21 group was lower ($p < 0.05$) than the CON group. In the AR7 group, the mRNA and protein expression of ZO-1, Claudin-2, and JEAP was significantly lower ($p < 0.01$) than that in the CON group.

DEGs, KEGG, and GO enrichment analysis

Genes conformed to false discovery rate (FDR) < 0.05 and |log2 fold change (FC)| ≥ 1.0 were considered to be DEGs between two groups. As shown in Figures 6A,B, 868 DEGs were identified between the AR21 group and the CON group, including 281 upregulated DEGs and 587 downregulated DEGs. And 833 DEGs were identified between the AR7 group and the CON group, including 231 upregulated DEGs and 602 downregulated DEGs.

As shown in Figure 6C, the DEGs were annotated with the GO enrichment analysis, with one or more GO terms, including biological process (840 subclasses), cellular component (96 subclasses), and molecular function (172 subclasses). For biological process, the major categories represented were positive regulation of transcription by RNA polymerase II (GO:0045944) and regulation of transcription, DNA-templated (GO:0006355). For the cellular components, the major categories were membrane (GO:0016020) and integral component of membrane (GO:0016021). For the molecular function, the major categories were protein binding (GO:0005515) and metal ion binding (GO:0046872). A number of interesting categories were also obtained, such as oxidation–reduction process (GO:0055114), immune response (GO:0006955), and inflammatory response (GO:0006954), which may play a role in artificial rearing-caused diarrhea and colon injury.

The DEGs were further annotated with the KEGG pathway analysis and classified into 86 subclasses. Figure 6D illustrated the scatterplot of KEGG enrichment analysis. The four most enriched pathways were Focal adhesion (ko04510), NF-κB signaling pathway (ko04064), Hematopoietic cell lineage (ko04640), and Cytokine-cytokine receptor interaction (ko04060). A number of interesting pathways were also obtained, such as bile secretion (ko04976), mineral absorption (ko04978), and carbohydrate digestion and absorption (ko04973), which is closely related to the digestion and absorption of nutrients.

NF-κB signaling pathway

NF-κB signaling pathway (ko04064) was found to be highly enriched and the DEGs were verified by RT-qPCR and western blot, including TNFSF11, TNF (TNF-α), IL-1Ra, TLR2, NFKBIA (IκBα), and PTGS2 (COX-2). As presented in Figure 7A, compared with the CON group, the mRNA expression of TNFSF11, TNF-α, IL-1β, TLR2, TLR4, MyD88, NF-κB (p65), COX-2, PTGEs, and iNOS was significantly increased ($p < 0.01$), whereas the mRNA expression of IL-1Ra and IκBα was significantly decreased ($p < 0.01$) in AR21 and AR7 groups. Besides, iNOS activity and NO content were detected using the assay kits (Figure 7B). There were significant increases in iNOS activity in AR21 and AR7 groups ($p < 0.01$) as well as NO content in the AR7 group ($p < 0.01$) when compared to the CON group. These results indicated an activation of NF-κB pathway, which could result in the production of cytokines and thereby promote inflammatory response. As expected, the protein expression was indeed consistent with their corresponding transcription status (Figures 7C,D).

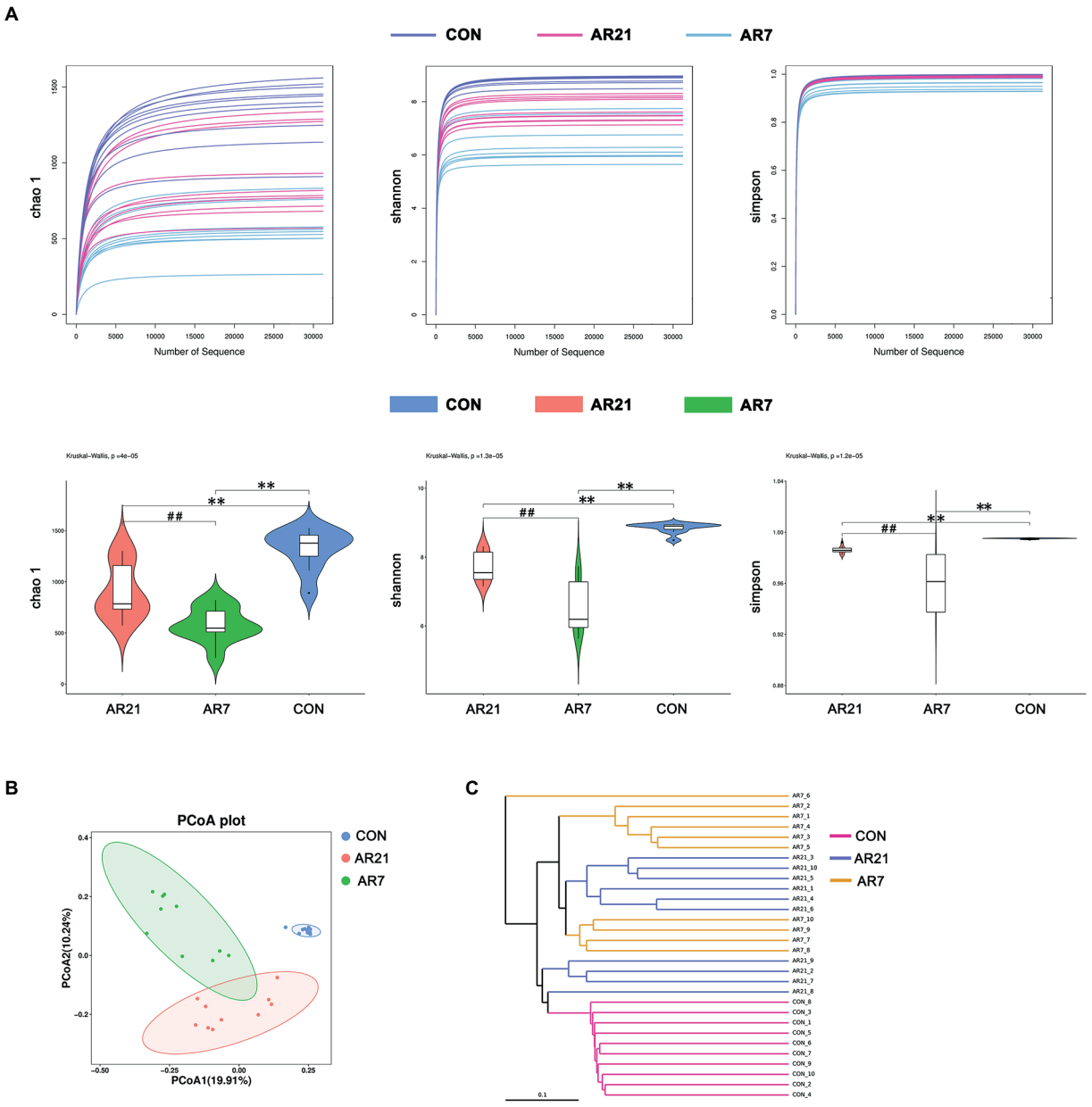

FIGURE 2
Effects of artificial rearing on the abundance and diversity of colonic microbiota in piglets. **(A)** The alpha diversity determined by Chao 1, Shannon, and Simpson. **(B)** The principal coordinate analysis (PCoA) score based on the unweight UniFrac distance. **(C)** UPGMA hierarchical clustering analysis based on the unweighted UniFrac distance. Data are presented with mean±SD. $^{**}p < 0.01$ versus the CON group; $^{\#\#}p < 0.01$ versus the AR21 group. n=10 piglets.

Cytokine secretion

Cytokine-cytokine receptor interaction (ko04060) was also found to be highly enriched and the DEGs were verified by RT-qPCR and western blot, including IL-2, IL-6, IL-17A, and IFN-γ (Figure 8). In the AR21 and AR7 groups, relative mRNA and protein expression of IL-2, IL-6, IL-17A, and IFN-γ were significantly higher ($p < 0.01$) than those in the CON group. In the AR7 group, relative mRNA and protein expression of the detected cytokines were significantly higher ($p < 0.01$) than those in the AR21 group.

SLC family

To investigate the mechanism of artificial rearing-induced diarrhea and colon injury, eight DEGs were verified by RT-qPCR, which was related to the digestion and absorption of

10.3389/fmicb.2022.1002738

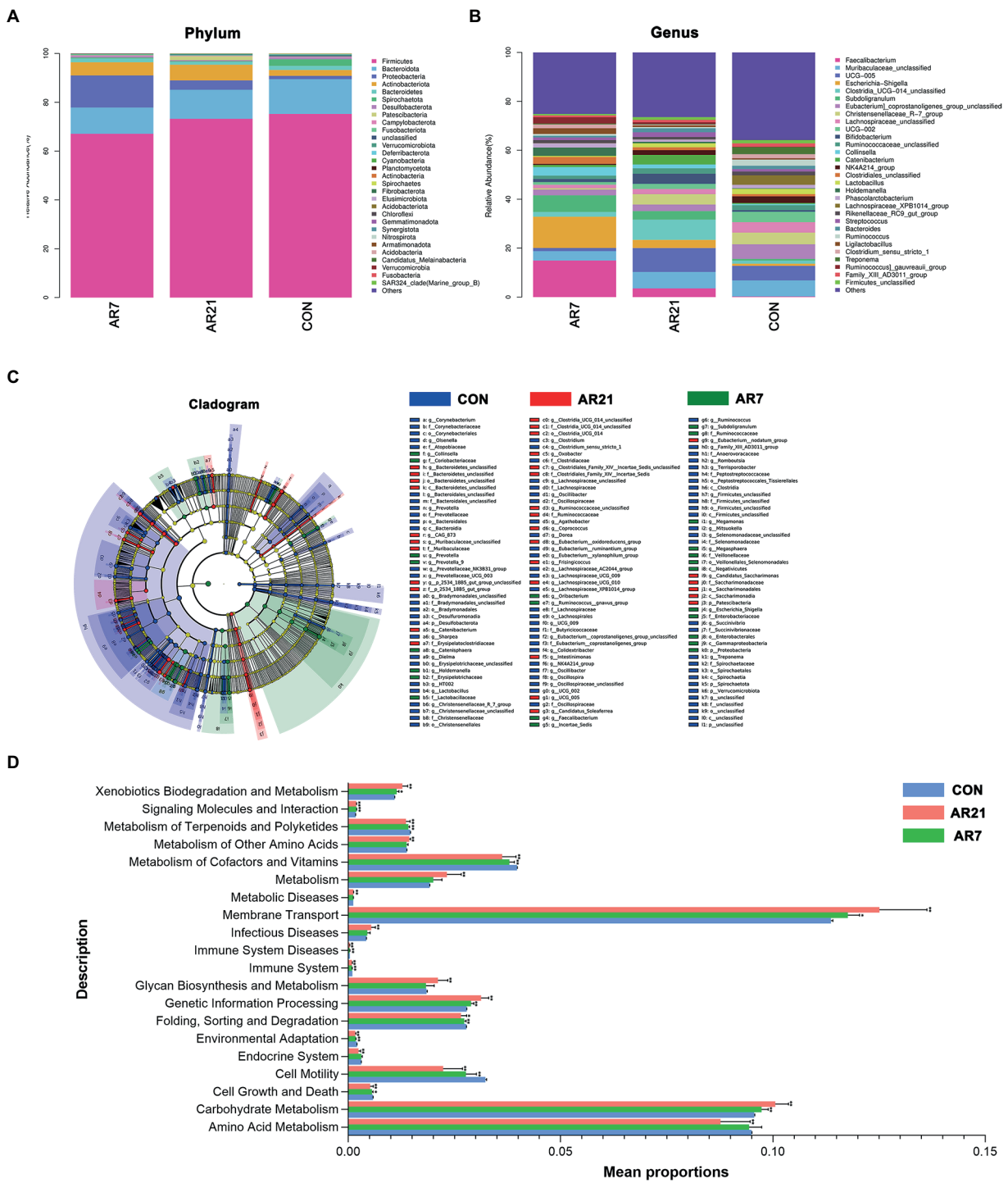

FIGURE 3
Effects of artificial rearing on the structure and function of colonic microbiota in piglets. **(A)** Relative abundance of microbiota at the phylum level. **(B)** Relative abundance of microbiota at the genus level. **(C)** Cladogram of enriched taxa based on linear discriminant analysis effect size (LEfSe) analysis. **(D)** Differences in bacterial function at Kyoto Encyclopedia of Genes and Genomes (KEGG) level 2 using PICRUSt2. Data are presented with mean±SD. *p<0.05 versus the CON group; **p < 0.01 versus the CON group. n=10 piglets.

nutrients. As presented in Figure 9, all detected SLC family members were significantly downregulated (p < 0.01) in the AR21 and AR7 groups compared with the CON group. It is noteworthy that the mRNA expression of SLC51B, SLC2A5, and SLC26A3 in the AR7 group was significantly higher (p < 0.01) than that in the AR21 group. The protein expression of SLC9A3 and SLC26A3 was indeed consistent with their corresponding transcription status.

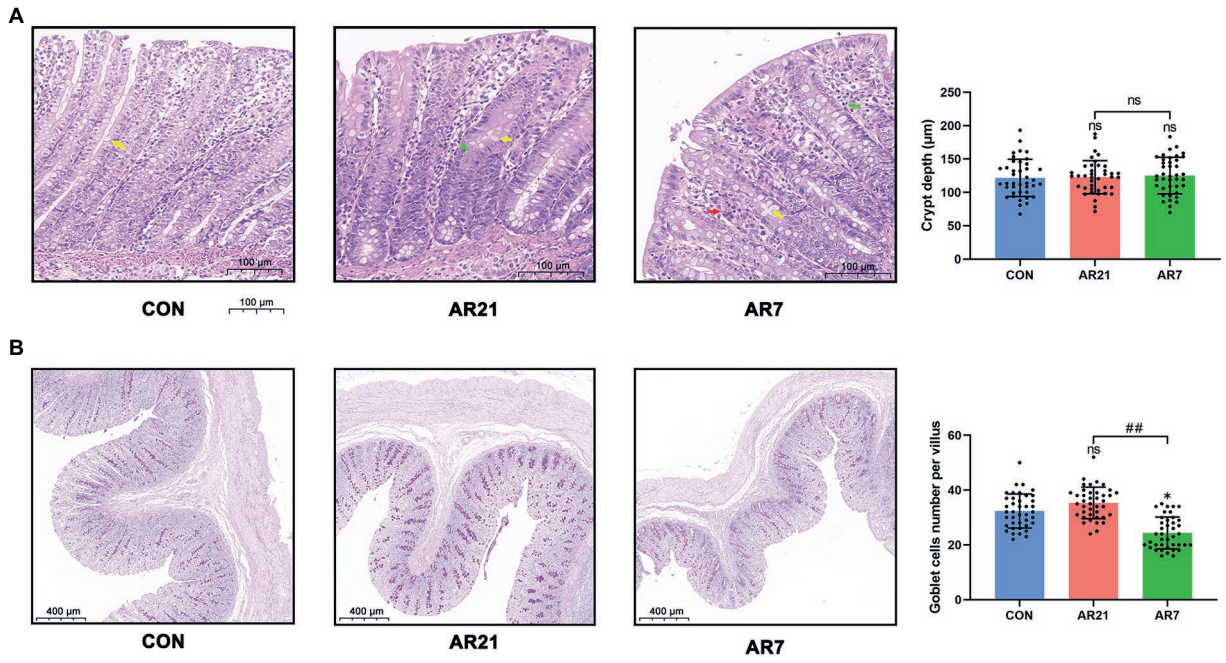

FIGURE 4
Effects of artificial rearing on the histology in piglet colon. **(A)** Microstructure of piglet colon (H&E staining). Yellow arrow indicates vacuoles. Green arrow indicates leukocyte infiltration. Red arrow indicates red blood cell infiltration. **(B)** Mean number of goblet cells (PAS staining). Data are presented with mean±SD. $^{ns}p > 0.05$; $^{*}p<0.05$ versus the CON group; $^{\#\#}p < 0.01$ versus the AR21 group. n=8 piglets.

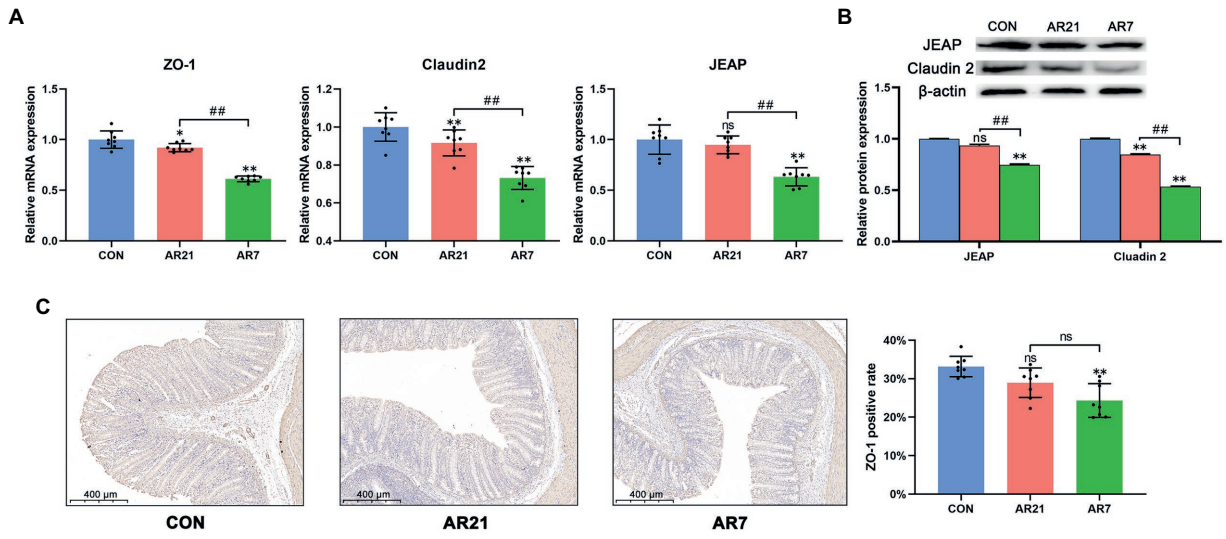

FIGURE 5
Effects of artificial rearing on the tight junction proteins in piglet colon. **(A)** Relative mRNA expression of tight junction proteins. **(B)** Relative protein expression of tight junction proteins. **(C)** ZO-1 positive cells by IHC staining. Data are presented with mean±SD. $^{ns}p > 0.05$; $^{*}p<0.05$ versus the CON group; $^{**}p < 0.01$ versus the CON group; $^{\#\#}p < 0.01$ versus the AR21 group. n=8 piglets.

In addition, the expression patterns of the 11 DEGs were generally consistent with the expression patterns identified by RNA-seq, suggesting that the RNA-seq results were accurate and reliable (Supplementary Table 4).

Discussion

Previous studies have shown the adverse effects of early weaning on the growth performance of pigs (Leliveld et al., 2013;

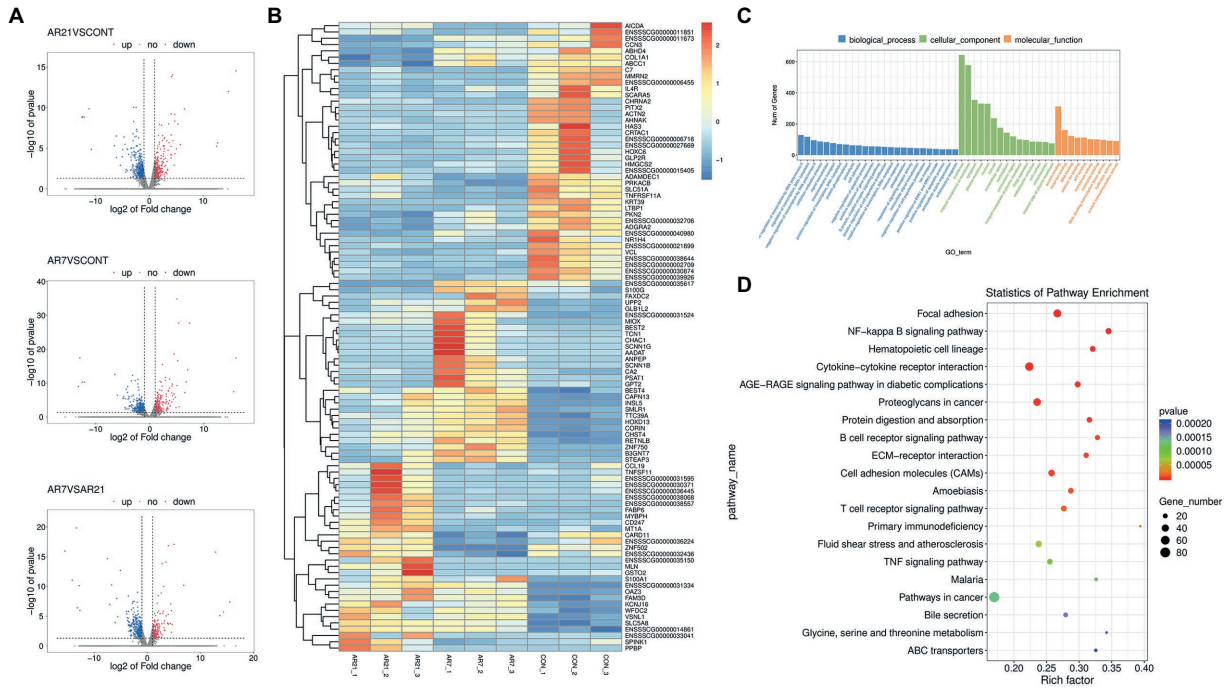

FIGURE 6
Effects of artificial rearing on the transcriptome profile in piglet colon. **(A)** The volcano plot for the DEGs. Blue dots mean the up-regulated genes. Red dots mean the down-regulated genes. Grey dots mean the genes with no significant changes. **(B)** Heatmap of DEGs in RNA-seq. Relative expression of DEGs where red hues represent comparatively upregulated genes and blue hues represent comparatively downregulated genes (scale at right). **(C)** GO enrichment analysis of DEGs. **(D)** KEGG pathway enrichment analysis of DEGs. *n*=3 piglets.

Ming et al., 2021). Similar to early weaning, artificial rearing also brought about a number of stressors, such as an abrupt separation from the sow and a different food source (Baxter et al., 2013). Schmitt et al. (2019) found that artificial rearing from 7 days of age reduced weaning BW of piglets. In this study, both AR21 and AR7 piglets had lower weaning weight and ADG during the entire experimental period compared with the CON piglets. Furthermore, the pre-weaning diarrhea incidence in AR7 group (46.5%) was higher than that in the AR21 group (31.1%) and the CON group (11.9%) during the entire experimental period, while there was a strong negative correlation between ADG and diarrhea incidence. These results indicated that artificial rearing increased the incidence of diarrhea and thus reduced growth performance in piglets.

The establishment of a healthy intestinal microbiota is required in maintaining intestinal homeostasis in the newborn, a time that is critical for immunological development (Koleva et al., 2015). The diversity of intestinal microbiota is an indicator for evaluating microbiota's health status. According to the alpha diversity analysis of 16S rDNA sequencing results, the microbial abundance and diversity were the highest in the CON group, followed by AR21 group and then AR7 group. Meanwhile, it was found by PCoA score that the difference in microbial community was obvious between three groups. This showed that artificial rearing reduced the microbial diversity and altered the structure of colonic microbiota, which is consistent with several studies reporting that artificial rearing reduced the abundance and diversity of ruminal microbiota in lambs (Belanche et al., 2019; Huang et al., 2022).

Moreover, this study also revealed the effects of artificial rearing on the composition of microbial community at the genus level. We noticed that *Ruminococcaceae* UCG-005, *Catenibacterium*, and *Muribaculaceae* increased significantly in the AR21 group. *Faecalibacterium*, *Escherichia-Shigella*, *Subdoligranulum*, and *Prevotella* increased significantly in the AR7 group. Fu et al. (2021) reported that the rise in *Ruminococcaceae* UCG-005 was correlated with intestinal inflammation and injury in piglets. *Muribaculaceae* was capable of degrading carbohydrates (Wang et al., 2020). *Catenibacterium*, *Faecalibacterium*, *Subdoligranulum*, and *Prevotella* were typical post-weaning microbial groups, which was associated with the introduction of non-breast foods and the digestion of dietary fibers (Kageyama and Benno, 2000; Luu et al., 2019; Parada Venegas et al., 2019; Van Hul et al., 2020). The genus of *Escherichia-Shigella* was a gram-negative pathogenic bacterium, which was responsible for Crohn's disease (Pascal et al., 2017). In addition, the prediction of bacterial function showed that artificial rearing changed a wide range of pathways, such as carbohydrate metabolism, xenobiotics biodegradation and metabolism, environmental adaptation, and immune system. Similar results were also reported in two other studies that formula feeding promoted carbohydrate metabolism in infant feces (Edwards et al., 1994; Bridgman et al., 2017). Based

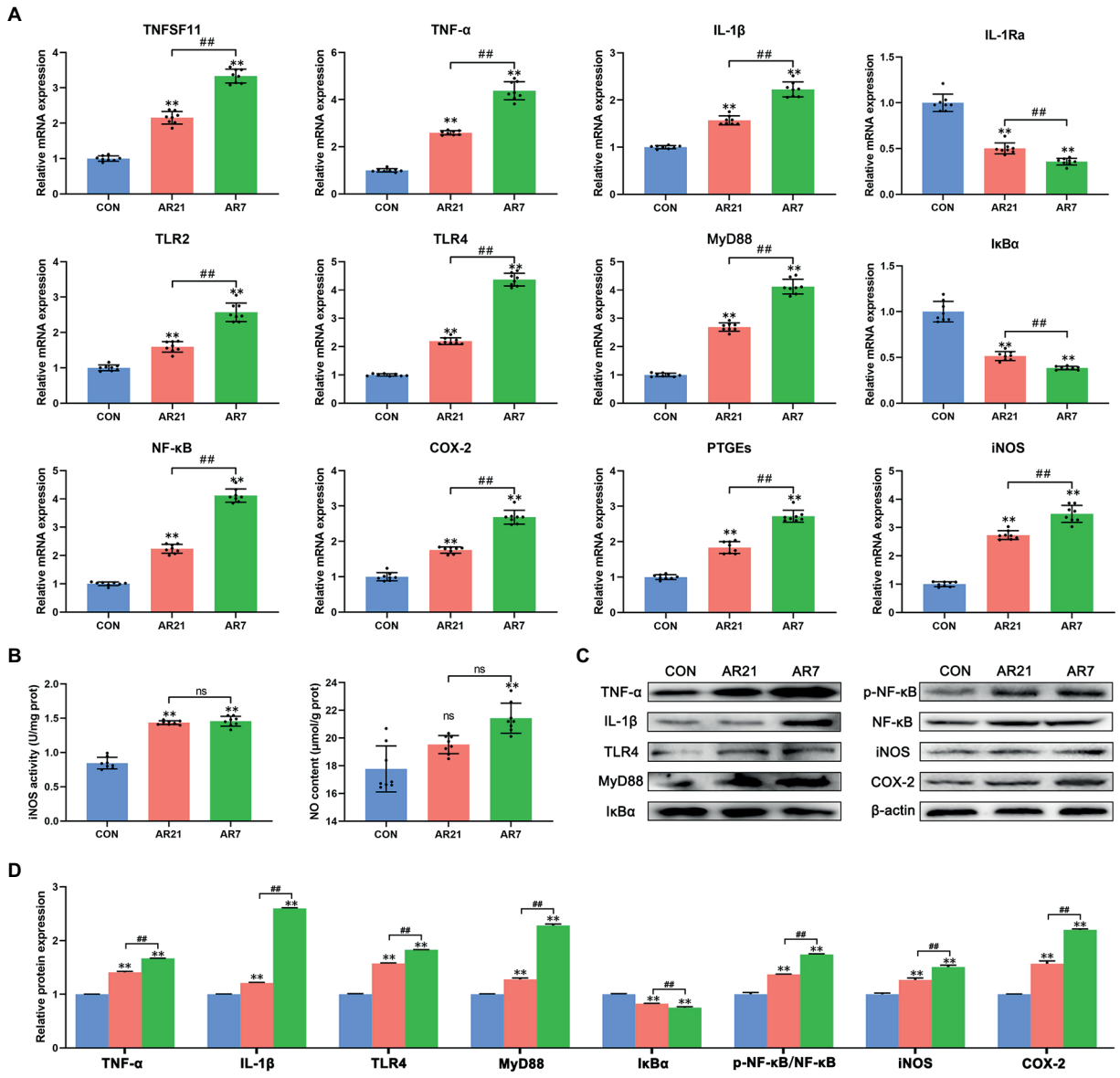

FIGURE 7
Effects of artificial rearing on NF-κB pathway and its downstream genes in piglet colon. **(A)** Relative mRNA expression of NF-κB pathway genes. **(B)** iNOS activity and NO content. **(C,D)** Relative expression of NF-κB pathway proteins and it downstream proteins. Data are presented with mean±SD. $^{ns}p > 0.05$; $^{**}p < 0.01$ versus the CON group; $^{\#\#}p < 0.01$ versus the AR21 group. n=8 piglets.

on these results, we concluded that artificial rearing could increase relative abundance of harmful bacteria and influence metabolic processes, which might led to the diarrhea of piglets.

The mucosa is the first line of defense against invading pathogens, which is composed of colonocytes and goblet cells in colon. The goblet cells are responsible for mucus secretion that form a protective mucus layer (Birchenough et al., 2015). Clinical data indicated a strong link between goblet cell loss and the development of ulcerative colitis (Gersemann et al., 2009). Besides, the spaces between colonocytes are sealed by tight junction proteins, including ZO proteins and Claudins, which provides a physical barrier to selectively allow nutrient absorption while excluding bacteria (Buckley and Turner, 2018). Prior work reported that artificial rearing from 7 days of age caused villus atrophy and deeper crypt in the small intestine of piglets (Vergauwen et al., 2017). In rats, infant formula feeding led to stunted villus and decreased the expression of ZO-1, Claudin-3, and Claudin-4 in the ileum (Gong et al., 2020). Singh et al. (2020) found that formula feeding resulted in villus loss, a decrease in ZO-1, and apoptosis of intestinal epithelial cells in rat ileum. In this study, we observed the infiltrations of red blood cells and leukocytes accompanied by a reduction of goblet cells and the decreases of ZO-1, Claudin-2 and JEAP in the AR7 group. It can thus be concluded that

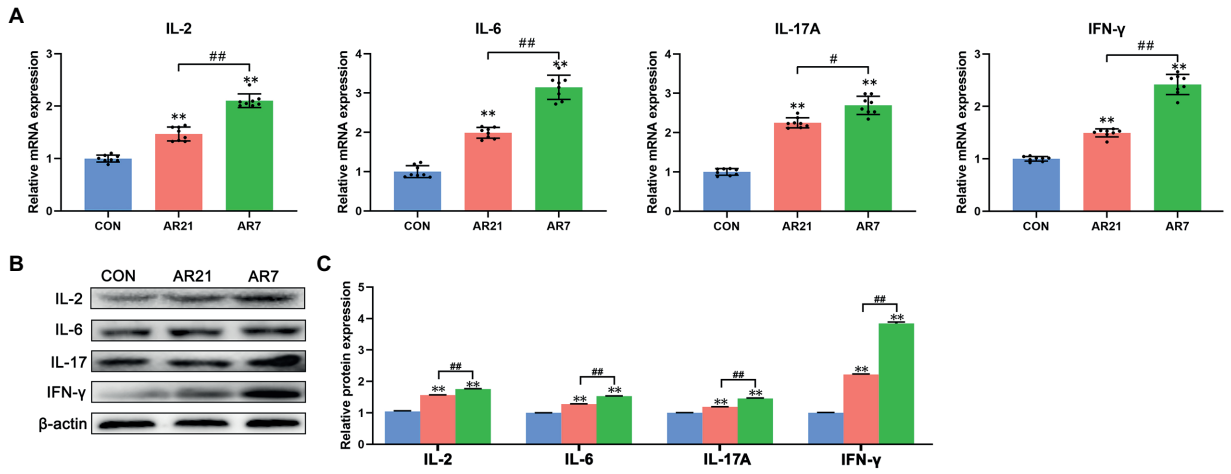

FIGURE 8
Effects of artificial rearing on cytokines in piglet colon. **(A)** Relative mRNA expression of IL-2, IL-6, IL-17A, and IFN-γ. **(B,C)** Relative protein expression of IL-2, IL-6, IL-17A, and IFN-γ. Data are presented with mean±SD. $^{**}p < 0.01$ versus the CON group; $^{\#\#}p < 0.01$ versus the AR21 group. n=8 piglets.

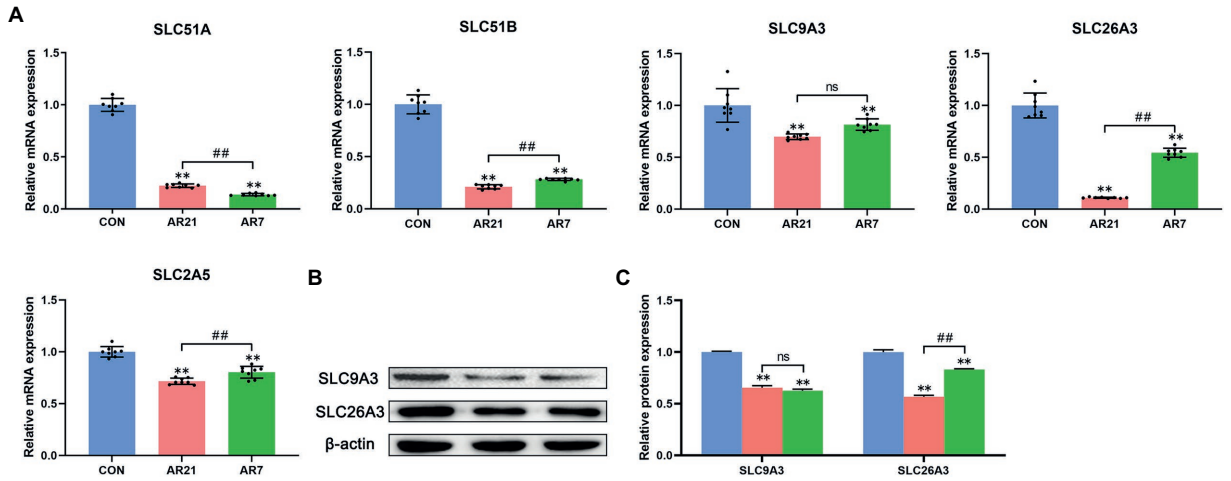

FIGURE 9
Effects of artificial rearing on SLC family members in piglet colon. **(A)** Relative mRNA expression of SLC51A, SLC51B, SLC9A3, SLC26A3, and SLC2A5. **(B,C)** Relative protein expression of SLC9A3 and SLC26A3. Data are presented with mean±SD. $^{ns}p > 0.05$; $^{**}p < 0.01$ versus the CON group; $^{\#}p < 0.05$ versus the AR21 group; $^{\#\#}p < 0.01$ versus the AR21 group. n=8 piglets.

artificial rearing from 7 days of age caused morphology disruption and disrupted barrier function in colonic mucosa. It is noteworthy that artificial rearing from 21 days of age had no significant effects on the number of goblet cells and the expression of ZO-1 and JEAP. These findings supported the notion that earlier weaning caused more serious physiological changes in structure and function of intestine (Pluske et al., 1997; Levast et al., 2010; Campbell et al., 2013).

NF-κB signaling pathway plays an essential role in immune response and inflammatory process. TLRs mediate the activation of NF-κB through the recognition of pathogen-associated molecular patterns (PAMPs) present on various microbes (Duncan et al., 2017). As the adapters for TLRs and IL-1R, MyD88 can lead to IκBα degradation and NF-κB nuclear translocation, which initiates the transcription and production of pro-inflammatory cytokines and chemokines (Kawasaki and Kawai, 2014). Previous study reported that the upregulation of TLR4, MyD88, and NF-κB was involved in lipopolysaccharide (LPS)-induced inflammatory injury through the enhanced production of pro-inflammatory cytokines including IL-1β, TNF-α, and IL-6 in the colonic mucosa of piglets (Gao et al., 2021).

Tang et al. (2021) found that early weaning induced inflammation and impaired intestinal barrier function through the upregulation of TLR4, IL-1β, IL-6, and TNF-α in piglet colon. Pie et al. (2004) also reported that weaning increased the expression of IL-1β, IL-6, and TNF-α in the mid-small intestine and up-regulated the expression of IL-1β in the proximal colon of piglets. In line with these findings, artificial rearing from 21 and 7 days of age induced colonic inflammation through the activation of NF-κB pathway and the induction of pro-inflammatory cytokines in piglets.

The SLC family constitutes a group of membrane transport proteins that transports diverse solutes across biological membranes and participates in many physiological functions, including nutrient absorption, metabolic transformation, energy homeostasis, and host defense (Lin et al., 2015). For instance, SLC51A, SLC51B, and SLC9A3 are involved in bile acid reclamation and bile secretion. Song et al. (2021) reported that the expression of SLC9A3 was decreased in the small intestine of piglets after porcine epidemic diarrhea virus infection and severe diarrhea occurred. SLC2A5 is a fructose transporter and engages in the digestion and absorption of complex carbohydrates (Iizuka, 2017). Deoxynivalenol contamination reduced SLC2A5 expression in chicken jejunum and led to growth depression (Dietrich et al., 2012). SLC26A3 is a key Cl^-/HCO_3^- exchanger protein and the patients with inflammatory bowel disease (IBD) showed a reduction in SLC26A3 in colonic epithelial cells compared with the healthy controls (Farkas et al., 2011). In the present study, the mRNA expression of SLC51A, SLC51B, SLC9A3, SLC2A5, and SLC26A3 decreased in the AR7 group. These observations indicated that the dysfunction of SLC family affected solute transport and destroyed intestinal homeostasis, contributing to diarrhea. Notably, the mRNA expression of SLC51B, SLC2A5, and SLC26A3 in the AR21 group was lower than that in the AR7 group, which might explain a higher diarrhea incidence in the AR21 group from days 28 to 34.

Concluding remarks

Collectively, our results indicated that artificial rearing both from 21 and 7 days of age reduced growth performance and increased diarrhea incidence in piglets. In addition, artificial rearing changed the diversity, structure, and function of microbial community in piglets. Meanwhile, artificial rearing mediated inflammatory response and affected solute transport through the dysfunction of SLC family.

Data availability statement

The datasets presented in this study can be found in online repositories. The names of the repository/repositories and accession number(s) can be found at: http://www.ncbi.nlm.nih.gov/bioproject/, 855325; http://www.ncbi.nlm.nih.gov/bioproject/, 855587.

Ethics statement

The animal study was reviewed and approved by Institutional Animal Care and Use Committee of Northeast Agricultural University.

Author contributions

JB, HL, XL, and RZ made substantial contributions to the conception or design of the work. QH conducted data analysis and drafted the work. JB, XZ, and HN revised the work critically for important intellectual content. All authors contributed to the article and approved the submitted version.

Funding

The study was supported by the China Agriculture Research System of MOF and MARA (No. CARS-35-05B).

Acknowledgments

The authors gratefully acknowledge the technical support of Lianchuan Biotechnology CO., Ltd. (Hangzhou, China).

Conflict of interest

The authors declare that the research was conducted in the absence of any commercial or financial relationships that could be construed as a potential conflict of interest.

Publisher's note

Supplementary material

The Supplementary material for this article can be found online at: https://www.frontiersin.org/articles/10.3389/fmicb.2022.1002738/full#supplementary-material

References

Baxter, E. M., Rutherford, K. M. D., D'eath, R. B., Arnott, G., Turner, S. P., Sandoe, P., et al. (2013). The welfare implications of large litter size in the domestic pig II: management factors. *Anim. Welf.* 22, 219–238. doi: 10.7120/09627286.22.2.219

Belanche, A., Yanez-Ruiz, D. R., Detheridge, A. P., Griffith, G. W., Kingston-Smith, A. H., and Newbold, C. J. (2019). Maternal versus artificial rearing shapes the rumen microbiome having minor long-term physiological implications. *Environ. Microbiol.* 21, 4360–4377. doi: 10.1111/1462-2920.14801

Berkhout, D. J. C., Klaassen, P., Niemarkt, H. J., De Boode, W. P., Cossey, V., Van Goudoever, J. B., et al. (2018). Risk factors for necrotizing enterocolitis: a prospective multicenter case-control study. *Neonatology* 114, 277–284. doi: 10.1159/000489677

Birchenough, G. M. H., Johansson, M. E. V., Gustafsson, J. K., Bergstrom, J. H., and Hansson, G. C. (2015). New developments in goblet cell mucus secretion and function. *Mucosal Immunol.* 8, 712–719. doi: 10.1038/mi.2015.32

Bridgman, S. L., Azad, M. B., Field, C. J., Haqq, A. M., Becker, A. B., Mandhane, P. J., et al. (2017). Fecal short-chain fatty acid variations by breastfeeding status in infants at 4 months: differences in relative versus absolute concentrations. *Front. Nutr.* 4:11. doi: 10.3389/fnut.2017.00011

Buckley, A., and Turner, J. R. (2018). Cell biology of tight junction barrier regulation and mucosal disease. *Cold Spring Harb. Perspect. Biol.* 10:a029314. doi: 10.1101/cshperspect.a029314

Campbell, J. M., Crenshaw, J. D., and Polo, J. (2013). The biological stress of early weaned piglets. *J. Anim. Sci. Biotechnol.* 4:19. doi: 10.1186/2049-1891-4-19

Di Lorenzo, M., Bass, J., and Krantis, A. (1995). An intraluminal model of necrotizing enterocolitis in the developing neonatal piglet. *J. Pediatr. Surg.* 30, 1138–1142. doi: 10.1016/0022-3468(95)90006-3

Dietrich, B., Neuenschwander, S., Bucher, B., and Wenk, C. (2012). Fusarium mycotoxin-contaminated wheat containing deoxynivalenol alters the gene expression in the liver and the jejunum of broilers. *Animal* 6, 278–291. doi: 10.1017/S1751731111001601

Duncan, S. A., Baganizi, D. R., Sahu, R., Singh, S. R., and Dennis, V. A. (2017). SOCS proteins as regulators of inflammatory responses induced by bacterial infections: a review. *Front. Microbiol.* 8:2431. doi: 10.3389/fmicb.2017.02431

Edwards, C. A., Parrett, A. M., Balmer, S. E., and Wharton, B. A. (1994). Faecal short chain fatty acids in breast-fed and formula-fed babies. *Acta Paediatr.* 83, 459–462. doi: 10.1111/j.1651-2227.1994.tb13059.x

Farkas, K., Yeruva, S., Rakonczay, Z., Ludolph, L., Molnar, T., Nagy, F., et al. (2011). New therapeutic targets in ulcerative colitis: the importance of ion transporters in the human colon. *Inflamm. Bowel Dis.* 17, 884–898. doi: 10.1002/ibd.21432

Fu, Q. Y., Tan, Z., Shi, L. G., and Xun, W. J. (2021). Resveratrol attenuates diquat-induced oxidative stress by regulating gut microbiota and metabolome characteristics in piglets. *Front. Microbiol.* 12:695155. doi: 10.3389/fmicb.2021.695155

Gao, R., Tian, S., Wang, J., and Zhu, W. (2021). Galacto-oligosaccharides improve barrier function and relieve colonic inflammation via modulating mucosa-associated microbiota composition in lipopolysaccharides-challenged piglets. *J. Anim. Sci. Biotechnol.* 12:92. doi: 10.1186/s40104-021-00612-z

Gersemann, M., Becker, S., Kubler, I., Koslowski, M., Wang, G. X., Herrlinger, K. R., et al. (2009). Differences in goblet cell differentiation between Crohn's disease and ulcerative colitis. *Differentiation* 77, 84–94. doi: 10.1016/j.diff.2008.09.008

Gong, H., Yuan, Q. C., Pang, J. Z., Li, T. G., Li, J. F., Zhan, B. Y., et al. (2020). Dietary milk fat globule membrane restores decreased intestinal mucosal barrier development and alterations of intestinal flora in infant-formula-fed rat pups. *Mol. Nutr. Food Res.* 64:e2000232. doi: 10.1002/mnfr.202000232

Gonzalez, L. M., Moeser, A. J., and Blikslager, A. T. (2015). Porcine models of digestive disease: the future of large animal translational research. *Transl. Res.* 166, 12–27. doi: 10.1016/j.trsl.2015.01.004

Huang, W., Cui, K., Han, Y., Chai, J., Wang, S., Lu, X., et al. (2022). Long term effects of artificial rearing before weaning on the growth performance, ruminal microbiota and fermentation of fattening lambs. *J. Integr. Agric.* 21, 1146–1160. doi: 10.1016/S2095-3119(21)63763-2

Iizuka, K. (2017). The role of carbohydrate response element binding protein in intestinal and hepatic fructose metabolism. *Nutrients* 9:181. doi: 10.3390/nu9020181

Kageyama, A., and Benno, Y. (2000). Catenibacterium mitsuokai gen. Nov., sp. nov., a gram-positive anaerobic bacterium isolated from human faeces. *Int. J. Syst. Evol. Microbiol.* 50, 1595–1599. doi: 10.1099/00207713-50-4-1595

Kawasaki, T., and Kawai, T. (2014). Toll-like receptor signaling pathways. *Front. Immunol.* 5:461. doi: 10.3389/fimmu.2014.00461

Koleva, P. T., Kim, J. S., Scott, J. A., and Kozyrskyj, A. L. (2015). Microbial programming of health and disease starts during fetal life. *Birth Defects Res. Part C-Embryo Today-Rev.* 105, 265–277. doi: 10.1002/bdrc.21117

Lanferdini, E., Andretta, I., Fonseca, L. S., Moreira, R. H. R., Cantarelli, V. S., Ferreira, R. A., et al. (2018). Piglet birth weight, subsequent performance, carcass traits and pork quality: a meta-analytical study. *Livest. Sci.* 214, 175–179. doi: 10.1016/j.livsci.2018.05.019

Leliveld, L. M. C., Riemensperger, A. V., Gardiner, G. E., O'doherty, J. V., Lynch, P. B., and Lawlor, P. G. (2013). Effect of weaning age and postweaning feeding programme on the growth performance of pigs to 10 weeks of age. *Livest. Sci.* 157, 225–233. doi: 10.1016/j.livsci.2013.06.030

Levast, B., Berri, M., Wilson, H. L., Meurens, F., and Salmon, H. (2014). Development of gut immunoglobulin A production in piglet in response to innate and environmental factors. *Dev. Comp. Immunol.* 44, 235–244. doi: 10.1016/j.dci.2013.12.012

Levast, B., De Monte, M., Chevaleyre, C., Melo, S., Berri, M., Mangin, F., et al. (2010). Ultra-early weaning in piglets results in low serum IgA concentration and IL17 mRNA expression. *Vet. Immunol. Immunopathol.* 137, 261–268. doi: 10.1016/j.vetimm.2010.06.004

Lin, L., Yee, S. W., Kim, R. B., and Giacomini, K. M. (2015). SLC transporters as therapeutic targets: emerging opportunities. *Nat. Rev. Drug Discov.* 14, 543–560. doi: 10.1038/nrd4626

Liu, Z., Roy, N. C., Guo, Y., Jia, H., Ryan, L., Samuelsson, L., et al. (2016). Human breast milk and infant formulas differentially modify the intestinal microbiota in human infants and host physiology in rats. *J. Nutr.* 146, 191–199. doi: 10.3945/jn.115.223552

Livak, K. J., and Schmittgen, T. D. (2001). Analysis of relative gene expression data using real-time quantitative PCR and the 2(-Delta Delta C(T)) method. *Methods* 25, 402–408. doi: 10.1006/meth.2001.1262

Lucas, A., and Cole, T. J. (1990). Breast milk and neonatal necrotising enterocolitis. *Lancet* 336, 1519–1523. doi: 10.1016/0140-6736(90)93304-8

Luu, M., Pautz, S., Kohl, V., Singh, R., Romero, R., Lucas, S., et al. (2019). The short-chain fatty acid pentanoate suppresses autoimmunity by modulating the metabolic-epigenetic crosstalk in lymphocytes. *Nat. Commun.* 10:760. doi: 10.1038/s41467-019-08711-2

Mendez, Y. S., Khan, F. A., Perrier, G. V., and Radulescu, A. (2020). Animal models of necrotizing enterocolitis. *World J. Pediatr. Surg.* 3:e000109. doi: 10.1136/wjps-2020-000109

Ming, D. X., Wang, W. H., Huang, C. Y., Wang, Z. J., Shi, C. Y., Ding, J., et al. (2021). Effects of weaning age at 21 and 28 days on growth performance, intestinal morphology and redox status in piglets. *Animals* 11:2169. doi: 10.3390/ani11082169

Nicholson, J. K., Holmes, E., Kinross, J., Burcelin, R., Gibson, G., Jia, W., et al. (2012). Host-gut microbiota metabolic interactions. *Science* 336, 1262–1267. doi: 10.1126/science.1223813

Nowland, T. L., Kirkwood, R. N., Plush, K. J., Barton, M. D., and Torok, V. A. (2021). Exposure to maternal feces in lactation influences piglet enteric microbiota, growth, and survival preweaning. *J. Anim. Sci.* 99:skab170. doi: 10.1093/jas/skab170

Parada Venegas, D., De La Fuente, M. K., Landskron, G., Gonzalez, M. J., Quera, R., Dijkstra, G., et al. (2019). Short chain fatty acids (SCFAs)-mediated gut epithelial and immune regulation and its relevance for inflammatory bowel diseases. *Front. Immunol.* 10:277. doi: 10.3389/fimmu.2019.00277

Pascal, V., Pozuelo, M., Borruel, N., Casellas, F., Campos, D., Santiago, A., et al. (2017). A microbial signature for Crohn's disease. *Gut.* 66, 813–822. doi: 10.1136/gutjnl-2016-313235

Peltoniemi, O., Yun, J., Bjorkman, S., and Han, T. (2021). Coping with large litters: the management of neonatal piglets and sow reproduction. *J. Anim. Sci. Technol.* 63, 1–15. doi: 10.5187/jast.2021.e3

Piccolo, B. D., Mercer, K. E., Bhattacharyya, S., Bowlin, A. K., Saraf, M. K., Pack, L., et al. (2017). Early postnatal diets affect the bioregional small intestine microbiome and ileal metabolome in neonatal pigs. *J. Nutr.* 147, 1499–1509. doi: 10.3945/jn.117.252767

Pie, S., Lalles, J. P., Blazy, F., Laffitte, J., Seve, B., and Oswald, I. P. (2004). Weaning is associated with an upregulation of expression of inflammatory cytokines in the intestine of piglets. *J. Nutr.* 134, 641–647. doi: 10.1093/jn/134.3.641

Pluske, J. R., Hampson, D. J., and Williams, I. H. (1997). Factors influencing the structure and function of the small intestine in the weaned pig: a review. *Livest. Prod. Sci.* 51, 215–236. doi: 10.1016/S0301-6226(97)00057-2

Quesnel, H., Brossard, L., Valancogne, A., and Quiniou, N. (2008). Influence of some sow characteristics on within-litter variation of piglet birth weight. *Animal* 2, 1842–1849. doi: 10.1017/S175173110800308X

Rasmussen, S. O., Martin, L., Ostergaard, M. V., Rudloff, S., Li, Y. Q., Roggenbuck, M., et al. (2016). Bovine colostrum improves neonatal growth, digestive function, and gut immunity relative to donor human milk and infant

formula in preterm pigs. *Am. J. Physiol. Gastrointest. Liver Physiol.* 311, G480–G491. doi: 10.1152/ajpgi.00139.2016

Rinninella, E., Raoul, P., Cintoni, M., Franceschi, F., Miggiano, G. A. D., Gasbarrini, A., et al. (2019). What is the healthy gut microbiota composition? a changing ecosystem across age, environment, diet, and diseases. *Microorganisms* 7:14. doi: 10.3390/microorganisms7010014

Salmon, H., Berri, M., Gerdts, V., and Meurens, F. (2009). Humoral and cellular factors of maternal immunity in swine. *Dev. Comp. Immunol.* 33, 384–393. doi: 10.1016/j.dci.2008.07.007

Schmitt, O., O'driscoll, K., Boyle, L. A., and Baxter, E. M. (2019). Artificial rearing affects piglets pre-weaning behaviour, welfare and growth performance. *Appl. Anim. Behav. Sci.* 210, 16–25. doi: 10.1016/j.applanim.2018.10.018

Singh, P., Sanchez-Fernandez, L. L., Ramiro-Cortijo, D., Ochoa-Allemant, P., Perides, G., Liu, Y., et al. (2020). Maltodextrin-induced intestinal injury in a neonatal mouse model. *Dis. Model. Mech.* 13:dmm044776. doi: 10.1242/dmm.044776

Song, Z. H., Yan, T., Ran, L., Niu, Z., Zhang, Y. L., Kan, Z. F., et al. (2021). Reduced activity of intestinal surface Na^+/H^+ exchanger NHE3 is a key factor for induction of diarrhea after PEDV infection in neonatal piglets. *Virology* 563, 64–73. doi: 10.1016/j.virol.2021.08.011

ŠPinka, M. (2018). *Advances in Pig Welfare*. Duxford, United Kingdom: Woodhead Publishing, an imprint of Elsevier

Tang, W., Liu, J., Ma, Y., Wei, Y., Liu, J., and Wang, H. (2021). Impairment of intestinal barrier function induced by early weaning via autophagy and apoptosis associated with gut microbiome and metabolites. *Front. Immunol.* 12:804870. doi: 10.3389/fimmu.2021.804870

Underwood, M. A., Arriola, J., Gerber, C. W., Kaveti, A., Kalanetra, K. M., Kananurak, A., et al. (2014). Bifidobacterium longum subsp. infantis in experimental necrotizing enterocolitis: alterations in inflammation, innate immune response, and the microbiota. *Pediatr. Res.* 76, 326–333. doi: 10.1038/pr.2014.102

Van Hul, M., Le Roy, T., Prifti, E., Dao, M. C., Paquot, A., Zucker, J. D., et al. (2020). From correlation to causality: the case of Subdoligranulum. *Gut Microbes* 12, 1–13. doi: 10.1080/19490976.2020.1849998

Vandenberghe, H. (2012). Opfokmanagement voor overtallige biggen bij de Vlaamse zeugenhouder. Faculty of Biosciences and Landscape Architecture, University College Ghent, Ghent.

Vandesompele, J., De Preter, K., Pattyn, F., Poppe, B., Van Roy, N., De Paepe, A., et al. (2002). Accurate normalization of real-time quantitative RT-PCR data by geometric averaging of multiple internal control genes. *Genome Biol.* 3:RESEARCH0034. doi: 10.1186/gb-2002-3-7-research0034

Vergauwen, H., Degroote, J., Prims, S., Wang, W., Fransen, E., De Smet, S., et al. (2017). Artificial rearing influences the morphology, permeability and redox state of the gastrointestinal tract of low and normal birth weight piglets. *J. Anim. Sci. Biotechnol.* 8:30. doi: 10.1186/s40104-017-0159-3

Wang, B. T., Kong, Q. M., Li, X., Zhao, J. X., Zhang, H., Chen, W., et al. (2020). A high-fat diet increases gut microbiota biodiversity and energy expenditure due to nutrient difference. *Nutrients* 12:3197. doi: 10.3390/nu12103197

frontiers | Frontiers in Microbiology

TYPE Original Research
PUBLISHED 13 October 2022
DOI 10.3389/fmicb.2022.970470

OPEN ACCESS

EDITED BY
Silvia Arboleya,
Institute of Dairy Products of Asturias (CSIC), Spain

REVIEWED BY
Judit Cabana-Domínguez,
University of Barcelona, Spain
Jingbo Liu,
Southwest University of Science and Technology, China

*CORRESPONDENCE
Renli Qi
qirenli1982@163.com
Zuohua Liu
liuzuohua66@163.com

SPECIALTY SECTION
This article was submitted to Microorganisms in Vertebrate Digestive Systems, a section of the journal Frontiers in Microbiology

RECEIVED 17 June 2022
ACCEPTED 29 September 2022
PUBLISHED 13 October 2022

CITATION
Qi R, Wang J, Sun J, Qiu X, Liu X, Wang Q, Yang F, Ge L and Liu Z (2022) The effects of gut microbiota colonizing on the porcine hypothalamus revealed by whole transcriptome analysis.
Front. Microbiol. 13:970470.
doi: 10.3389/fmicb.2022.970470

The effects of gut microbiota colonizing on the porcine hypothalamus revealed by whole transcriptome analysis

Renli Qi[1,2]*, Jing Wang[1], Jing Sun[1], Xiaoyu Qiu[1], Xin Liu[3], Qi Wang[1], Feiyun Yang[1], Liangpeng Ge[1,2] and Zuohua Liu[1,2]*

[1]Chongqing Academy of Animal Science, Chongqing, China, [2]Key Laboratory of Pig Industry Sciences, Ministry of Agriculture, Chongqing, China, [3]College of Animal Science and Technology, Southwest University, Chongqing, China

The roles of the microbe-gut-brain axis in metabolic homeostasis, development, and health are well-known. The hypothalamus integrates the higher nerve center system and functions to regulate energy balance, feeding, biological rhythms and mood. However, how the hypothalamus is affected by gut microbes in mammals is unclear. This study demonstrated differences in hypothalamic gene expression between the germ-free (GF) pigs and pigs colonized with gut microbiota (CG) by whole-transcriptome analysis. A total of 938 mRNAs, 385 lncRNAs and 42 miRNAs were identified to be differentially expressed between the two groups of pigs. An mRNA-miRNA-lncRNA competing endogenous RNA network was constructed, and miR-22-3p, miR-24-3p, miR-136-3p, miR-143-3p, and miR-545-3p located in the net hub. Gene function and pathway enrichment analysis showed the altered mRNAs were mainly related to developmental regulation, mitochondrial function, the nervous system, cell signaling and neurodegenerative diseases. Notably, the remarkable upregulation of multiple genes in oxidative phosphorylation enhanced the GF pigs' hypothalamic energy expenditure. Additionally, the reduction in ATP content and the increase in carnitine palmitoyl transterase-1 (CPT1) protein level also confirmed this fact. Furthermore, the hypothalamic cell apoptosis rate in the CG piglets was significantly higher than that in the GF piglets. This may be due to the elevated concentrations of pro-inflammatory factors produced by gut bacteria. The obtained results collectively suggest that the colonization of gut microbes has a significant impact on hypothalamic function and health.

KEYWORDS

whole transcriptome, gene expression, germ-free pig, non-coding RNA genes, hypothalamus, microbiota-gut-brain axis

Introduction

The bacterial community living in the intestine is closely related to the growth, development, metabolism, health and disease of the host (Buffie and Pamer, 2013; Bibbò et al., 2016; Zafar and Saier, 2021). The intestinal microbiota dominated by the bacteria in the *Firmicutes* and *Bacteroides* phyla not only helps their host digest nutrients that are difficult to decompose, such as dietary fiber, but can also produce various bacterial metabolites, such as short-chain fatty acids (SCFAs), biogenic amines, and amino acid derivatives (Han et al., 2021; Jia et al., 2021; Qi et al., 2021a,b). These metabolites are transported into the blood circulation or immune system and then reach the brain, liver, pancreas, muscle and other tissues to play different physiological regulatory roles. Of note, the reduction in microbiota diversity or the invasion by pathogenic bacteria not only destroys gut health directly but may also lead to immune disorders and the formation of various of metabolic diseases (Kim and Jazwinski, 2018; Wang et al., 2021).

Many studies have demonstrated complex and efficient information exchange and interaction in the microbiota-gut-brain axis (Kelly et al., 2016; Dinan and Cryan, 2017; Agirman et al., 2021; Zhao et al., 2021). Bacteria in the gut affect the brain and central nervous system (CNS), mainly by bacterial functional metabolites. In addition, the bacteria can stimulate and induce diverse peptide hormones secreted by the gastrointestinal tract, such as gastrin, ghrelin, and PYY, which participate in CNS signaling (Gribble and Reimann, 2019; Martchenko et al., 2020; Farhadipour and Depoortere, 2021). Accumulating studies have pointed out that the colonization and succession of the intestinal bacterial community affect brain development and signal delivery in the CNS in humans and animals, which affects the cognition, emotion and appetite of the host (Dinan and Cryan, 2017; Ceppa et al., 2019; Rutsch et al., 2020; Han et al., 2021). More recently, a study indicated that a bacterial structural component, muropeptides from the cell wall, can directly reach the host's brain, especially the hypothalamus, to play a regulatory role in appetite and body temperature by activating the receptor protein NOD2 (Gabanyi et al., 2022). In addition, the dysbiosis of gut microbiota caused by aging or drugs has been shown to be related to many cerebral and neurological diseases such as autism, Parkinson's disease, emotional and affective disorders, and bulimia (Quigley, 2017; Sun and Shen, 2018). Therefore, uncovering how the gut microbiota affects brain development and function has important implications for maintaining and improving our health.

Clearly, understanding how the gut microbiota affects brain gene expression is very helpful to gain insights into the interaction in the microbiota-gut-brain axis. Some previous studies based on germ-free (GF) mice have shown that the deletion and colonization of intestinal microbiota directly changed the gene expression and metabolic function of the cerebral cortex or hippocampus using transcriptome and metabolome analysis (Chen et al., 2017; Zhou et al., 2020). The hypothalamus is located in the center of the brain and is considered to be the intersection center of the endocrine system and nervous system. The hypothalamus has important functions in regulating body temperature, food intake, hormone secretion and biological rhythm. However, there is no report on the effect of intestinal microbes on the hypothalamic gene expression profile to date.

In this study, a GF pig model without any intestinal bacteria was used to study the effect of bacterial colonization on gene expression in the hypothalamus. We analyzed and compared the profiles of mRNA, lncRNA and miRNA expression in the hypothalamus of GF pigs and pigs that colonized the gut microbiota (CG pigs) by whole transcriptome analysis, which can synchronously analyze the expression of protein-coding and noncoding genes (Li et al., 2018; Gu et al., 2020; Ma et al., 2020). Our results reveal the significant effects on the porcine hypothalamic gene expression profile caused directly by the change in gut microbe introduction; thus, the findings are helpful for finding new targets for information interactions in the microbiota-gut-brain axis.

Materials and methods

Animal and sample collection

Eight newborn GF piglets were obtained *via* hysterectomy from a multiparous Chinese Bama sow (a common local Chinese small pig breed). Four of them were introduced to gut microorganisms through the fecal microbiota transplant (FMT) method for colonization (CG piglets). GF piglets and CG piglets were reared in positive-pressure sterile fiberglass isolators (Class Biologically Clean Ltd., WI, United States; three piglets per isolator) with a heated floor at 32°C–35°C before 25 days and 28°C–30°C during 26–42 days. They were fed to satiety 5–7 times a day with an autoclave-sterilized cow's milk-based formula prepared from condensed milk (Co60 γ-irradiated sterile, including 21% protein) before 25 days of age and then fed sterile compound feed until the 42nd day. All the GF and CG piglets were euthanized under isoflurane anesthesia at 42 days of age. Their hypothalamus were collected and cryopreserved for subsequent analyses. The study was approved by Ethics Committee of the Chongqing Academy of Animal Science (No. 2020012B).

FMT

FMT in piglets was performed as our described previously (Qi et al., 2021a,b). Five candidate adult donor mother pigs were used in the current study and consumed a regular diet without antibiotics and probiotics for 6 weeks prior to feces collection. Hog cholera virus, porcine parvovirus, porcine circovirus-2, porcine reproductive syndrome virus, respiratory syndrome virus, pseudorabies virus, foot and mouth disease virus, and mycoplasma hyopneumoniae were detected in the pigs. Finally, one pig without any pathogen was used as the trial donor for FMT.

FMT was performed five times on four GF infant pigs from day 3 to day 7. Briefly, 2 g of fresh stool was collected from the donor pig and placed in an anaerobic sampling tube. The stool was homogenized in 100 ml of cold saline water, filtered and then settled by gravity for 5 min. Resuspend the bacterial community using 20 ml sterile saline after centrifugation and washing 2 times. The bacteria in suspension were mean count 8×10^8 CFU/ml. All the operations were carried out in an anaerobic workstation. The bacterial suspension was administered *via* gavage to each recipient piglet for 1 ml per day.

Total RNA extraction, RNA library preparation, and sequencing

Total RNA from the hypothalamus was extracted using TRIzol (Invitrogen, United States) according to the manufacturer's instructions. Three hypothalamus tissue samples (1/4 hypothalamus) from each group were used for RNA extraction. The RNA concentration and purity were checked by OD A260/A280 (>1.8) and A260/A230 (>1.6), and the yield and quality were assessed using an Agilent 2100 Bioanalyzer (Agilent Technologies, United States) and RNA 6000 Nano LabChip Kit (Agilent Technologies, United States). The RNA integrity number (RIN) of extracted RNA was >7.0.

The preparation of whole transcriptome libraries and deep sequencing were performed by Marjorbio Technology Corp., Ltd. (Shanghai, China). Whole transcriptome libraries were constructed using the Ribo-Zero Magnetic Gold Kit (Illumina, United States) and the NEBNext® Ultra™ RNA Library Prep Kit for Illumina according to the manufacturer's instructions. The paired-end libraries were prepared by Illumina TruSeq_RNA Library Preparation Kit v2 (Illumina, USA) and were sequenced following the standard procedure on an Illumina HiSeq platform, and paired-end reads with 150 nucleotides were generated.

Raw sequencing reads were checked for potential sequencing issues and contaminants using FastQC. Adapter sequences, primers, number of fuzzy bases (Ns), and reads with quality scores below 30 were trimmed. Clean reads were aligned to the reference genome (Sus scrofa 11.1, http://asia.ensembl.org/Sus_scrofa/Info/Index) using the TopHat 2.1 program and the resulting alignment files were reconstructed with the Cufflinks 2.0 program.

Small RNA library construction and sequencing

Approximately 1 μg of total RNA was used to prepare small RNA library according to protocol of NEBNext® Small RNA Library Prep Set for Illumina. Single-end sequencing (50 bp) was performed on an Illumina Hiseq 2500 following the vendor's recommended protocol. Raw reads obtained by the sequencing were checked for potential sequencing issues and contaminants using FastQC. Reads with a length < 10 and > 34 nt were discarded. The clean reads were aligned against the miRNA precursor/mature miRNA in miRBase 20.0[1] to identify known miRNAs. The unannotated sequences were mapped to the pig genome to analyze their expression and distribution in the genome, and then used to predict potential novel miRNA candidates by Mireap.[2] The read counts of each known miRNA were then normalized to the total counts of sequence reads mapped to the miRBase version 20.0 database.

Sequencing data analyses

HTseq was used to count the genes and calculate the transcripts per kilobase million reads (TPMs) to evaluate the gene expression level. The differentially expressed mRNAs, lncRNAs, and miRNAs in GF and CG pigs were screened using the edgeR R package in the R software (version 3.5.2). Statistical significance was defined as $\log_2|$ (fold change) $| \geq 1$ and *Padjust* < 0.05. Volcano plots and heatmaps of DERNAs were plotted using the ggplots and heatmap packages.

Gene function and pathway enrichment analysis

Gene Ontology (GO) enrichment analysis, Kyoto Encyclopedia of Genes and Genomes (KEGG) pathway enrichment analysis and Reactome pathway enrichment analysis of DEGs, were performed using the OmicShare tools, a free online platform for data analysis.[3] The GO enrichment analysis was performed by the enriched GO function, in which DEGs were divided into three groups: molecular function (MF), cellular component (CC), and biology process (BP) *Padjust* < 0.05 was the threshold for significantly enriched GO terms and KEGG pathways. A *q*-value < 0.05 was the threshold for significantly enriched Reactome pathways. The potential contribution of the whole altered gene expression in the hypothalamus was also explored *via* Gene Set Enrichment Analysis (GSEA) software (version 4.1.0), especially on the KEGG analysis.

Transcription factors analysis and lncRNA target analysis

Transcription factors (TFs) can potentially affect the DEGs in the dataset, which can be identified by regulatory impact factor (RIF) metrics. To identify TFs in all DEGs, all 158 TFs in 11 families of Sus scrofa were obtained at AnimalTFDB 3.0.[4] The

1 http://www.mirbase.org/
2 http://sourceforge.net/projects/mireap/
3 https://www.omicshare.com/tools/
4 http://bioinfo.life.hust.edu.cn/AnimalTFDB/

target relationship between lncRNAs and TFs was analyzed using RNAplex software.[5] For the cis-regulation analysis, we predicted the target coding genes within 10 kb upstream and downstream of lncRNA; for the trans-regulation analysis, the target genes were predicted based on the free energy that is needed to form secondary structures between lncRNAs and mRNA sequences.

Construction of the mRNA-DE miRNA-lncRNA triple regulatory network

According to the hypothesis of the ceRNA network, all potential connections among the differentially expressed mRNAs, miRNAs, and lncRNAs were examined. Using DE miRNA as a bridge, we linked the DE mRNAs and DE lncRNAs by searching the miRNA complementary sequences, and a triple network among DE miRNAs and their targeted lncRNAs and mRNAs was constructed. The target genes of the DE miRNAs were predicted using the microT scoring method (paring score ≥ 0.8) *via* the DIANA platform, and lncRNAs regulated by the DE miRNAs were identified through alignment with lncBase Version 2.0. The Pearson correlation coefficient between lncRNAs and mRNAs was calculated and only the pairs with coefficients greater than 0.4 were involved in the triple network. Finally, a topological network of DE mRNAs-DE miRNAs-DE lncRNAs was visualized using Cytoscape Version 3.7.1.

Protein–protein interaction network construction

The Search Tool for the Retrieval of Interacting Genes (STRING)[6] is a database for searching interactions that can show the direct physical interaction and the indirect functional correlation between proteins. We used the STRING database to identify pairwise relationships among the 17 DE mRNAs related to oxidative phosphorylation, and then a protein–protein interaction (PPI) network was built.

Real-time quantitative PCR

Real time quantitative PCR (RT-qPCR) was performed to verify the expression levels of genes DE by the method of RNA-Seq. The total RNA was reverse-transcribed to cDNA using a PrimeScript™ RT reagent Kit (TaKaRa, Japan). PCR was performed using a Q6 qRT-PCR system (ABI, United States) with SYBR Premix Ex Taq. II (TaKaRa). The *β-actin* gene was used as reference gene. All of the reactions were prepared while using three replicates and the expression levels of genes were expressed as fold change using the $2^{-\triangle\triangle CT}$ method. Primer sequences are showed in Supplementary Table S1.

ATP content and ATPase activity detection

Four tissue samples from each group (1/4 hypothalamus) were used for ATP content detection and ATPase activity analysis by using an ATP Content Assay Kit (BC0305), and a Micro Na^+K^+-ATPase Assay Kit (BC0065) according to the manufacturer's protocol (Solarbio, China). The tissue samples were incubated with extraction reagent and then homogenized by ultrasonic cracking on ice. After centrifugation for 10 min, the supernatant was collected for ATP content and ATPase activity determinations, respectively.

The working principle of the ATP Content Assay Kit is briefly described as follows. The Glucose and ATP are catalyzed by hexokinase to produce glucose 6-phosphate, which is further catalytically dehydrogenated to produce NADPH. The NADPH shows a characteristic absorption peak at 340 nm. The content of ATP is proportional to that of NADPH.

The working principle of the ATPase Assay Kit is briefly described as follows. Na^+K^+-ATPase decomposes the intracellular ATP to generate ADP and inorganic phosphorus, and so the ATPase activity is determined by measuring the amount of inorganic phosphorus.

Cell apoptosis analysis

Four tissue samples each group (1/4 hypothalamus) were used for the cell apoptosis analysis. Apoptotic cells can be detected by terminal deoxynucleotidyl transferase (TdT)-mediated dUTP nick end labeling (TUNEL) assay referenced the methods of Brannelly et al. (2018). The hypothalamus tissue of pigs was assayed using a TUNEL Apoptosis Assay Kit (Solarbio) according to the manufacturer's protocol. Frozen tissue sections of 5 μm thickness were incubated with H_2O_2 (0.3% H_2O_2 in methanol) at room temperature (RT) for 30 min. After rinsing with 0.01 mol/l PBS for three times, the sections were treated with TUNEL working solution (Component A) at 37°C for 60 min, and then rinsed twice with PBS. Add 100 ul reaction buffer (Component B) to each sections for 30s and remove it. Finally, the sections were observed under fluorescence microscope (DMi8, Leica, Germany).

Western blotting assay

Three tissue samples (1/4 hypothalamus) were used for the WB detection. Total protein in the tissue was extracted by using an RIPA buffer (Beyotime, China). The standard western blotting method was used to determine the protein levels of CPT1, UCP2, total and cleaved of Caspase 3. GAPDH was used as a reference protein. Briefly, total

5 http://www.tbi.univie.ac.at/software/
6 http://string-db.org

protein extracts were separated by 12% SDS-PAGE and transferred to polyvinylidene membranes. The membranes were blocked with 5% nonfat milk in Tris-buffered saline containing 0.1% Tween 20 (TBST) at RT for 2 h, and probed overnight with primary antibodies at 4°C. After washing with TBST, the membranes were probed with the secondary antibody at RT for 2 h. The primary antibody for Caspase 3 was purchased from the Cell Signaling Technology (CST, #9664, United States). The primary antibodies for other protein were purchased from the Proteintech Group Co (UCP2, 11,081-1-AP; CPT1, 15,184-1-AP; GAPDH, 60004-1-Ig). Blots were visualized with a chemiluminescence reagent (Millipore, MA, USA) using an automatic imaging system (BioRad, CA, United States).

Blood concentrations of ILS and IL-1 detection

The venous blood of pigs was left standing for 6 h and then centrifuged to separate the serum. The concentrations of ILS and IL-1 in the serum samples were evaluated using commercial swine enzyme linked immune sorbent assay (ELISA) kits (Mlbio Co. Ltd., Shanghai, China) following the manufacturer's instructions.

Statistical analysis

Data are presented as the mean ± standard error of the mean (SEM). GraphPad Prism 8.5 software was used for statistical analysis and graph creation. The differences between groups were determined by the non-parametric Mann–Whitney test. Differences were considered statistically significant at $p < 0.05$.

Results

Results of sequencing and characteristics of transcripts

We determined tissue morphology of the hypothalamus, and all the hypothalamic histomorphology was good and with no obvious lesions. There was no clear difference between the two groups of pigs (Supplementary Figure 1).

From the whole-transcriptome sequencing, we identified a total of 50,167 transcripts for 19,256 known protein-coding genes (mRNAs), 14,393 known and 2,245 novel lncRNA transcripts, and 373 known and 539 novel miRNAs by sequencing (Figure 1).

Principal component analysis (PCA) showed that the gene expression profiles of the two groups of pigs, including long RNAs and small RNAs, were clearly distinguished (Figures 1A,B). In comparison, the two groups of pigs showed more differences in the expression profiles of long RNAs. Meanwhile, Spearman correlation analysis showed that the samples had high repeatability within the group (Figure 1C). This also reflected the good reproducibility of the sequencing results.

Expression levels of genes were indicated by the TPM values. By the comparison of the whole expression levels of mRNA, miRNA and lncRNA between groups, CG pigs had slightly higher expression levels of lncRNAs and mRNAs than GF pigs (Figure 1D). We found 25,575 (83.3%) mRNAs, 1,916 (57.9%) lncRNAs, and 387 (92.1%) miRNAs that were shared by both GF and CG pigs that showed in the Venn diagram in Figure 1E.

Differentially expressed transcripts and genes

The significant differences in transcript expression between GF and CG pigs are represented by a volcano plot (Figure 2A). There were 938 known mRNAs (including 414 upregulated and 524 downregulated protein-coding genes), 385 LncRNAs (including 75 upregulated and 315 downregulated transcripts) and 42 miRNAs (including 20 upregulated and 22 downregulated transcripts) that showed differential expression in the GF pigs relative to the CG pigs with $\log_2|$ (fold change) $|\geq 1$ and $Padjust < 0.05$. The heatmap in Figure 2B shows that the entire expression profiles of genes or transcripts in the two groups of pigs exhibited extremely significant differences. The top 10 upregulated and downregulated mRNAs, lncRNAs and miRNAs are shown in Supplementary Table S2. Obviously, the existence of a large number of differential expressed genes (DEGs) indicated the huge differences in the physiological status of the hypothalamus between the two groups of pigs.

Gene ontology and Kyoto encyclopedia of genes and genomes analysis of DGEs

To better comprehend the mechanisms involved in hypothalamic development and function, gene ontology (GO) function and Kyoto encyclopedia of genes and genomes (KEGG) pathway enrichment analyses for the altered protein-coding genes were performed. According to the results of GO analysis, the DEGs were distributed across 136 significantly enriched functional terms with $Padjust < 0.05$, including 117 BP terms, 11 CC terms, and 8 MF terms. The top 20 significantly enriched terms are shown in Figure 3A. The five most significantly enriched GO terms were membrane part (CC, GO: 0044425, $Padjust = 0.000$), developmental process (BP, GO: 0032502, $Padjust = 0.0002$), cell–cell signaling (BP, GO: 0007267, $Padjust = 0.0006$), multicellular organism development (BP, GO: 0007275, $Padjust = 0.0006$) and system development (GO: 0048731, $Padjust = 0.0006$). The three most significantly enriched MF terms were hormone activity (MF, GO: 0005179, $Padjust = 0.0080$), NADH dehydrogenase (ubiquinone) activity (MF, GO: 0008137, $Padjust = 0.0080$), and NADH dehydrogenase (quinone) activity (MF, GO: 0050136, $Padjust = 0.0006$).

According to the results of KEGG analysis, the DEGs were significantly enriched in 21 pathways with $Padjust < 0.05$, which

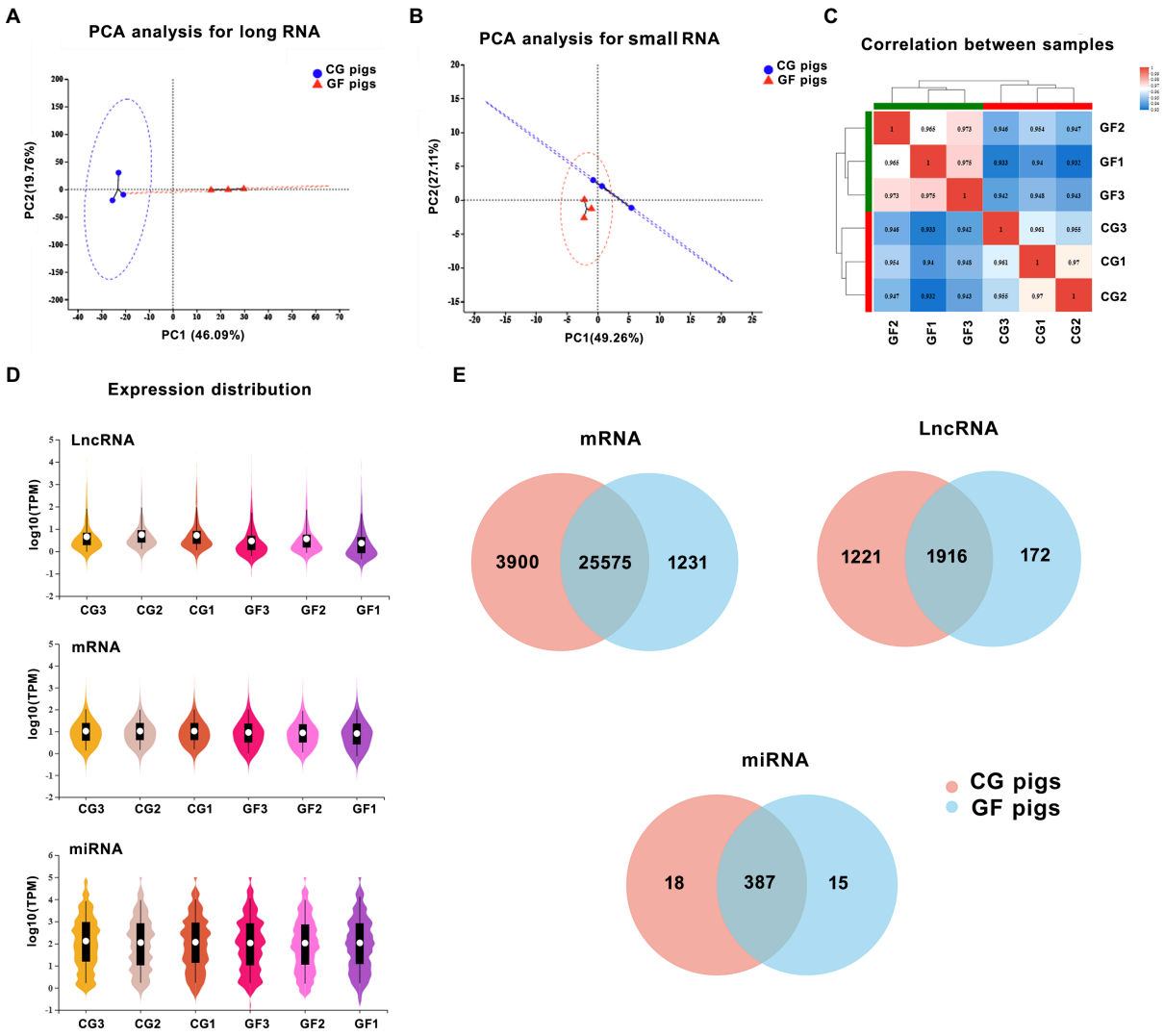

FIGURE 1
The features of the expression of long noncoding RNAs (lncRNAs), mRNAs, and microRNAs (miRNAs). **(A)** Principal component analysis (PCA) of two groups of samples based on the expression of long RNAs. **(B)** PCA of two groups of samples based on the expression of small RNAs. **(C)** The correlation analysis of samples. **(D)** The total expression levels of mRNAs, miRNAs, and lncRNAs between groups. **(E)** The number of identified lncRNAs, mRNAs, and miRNAs in the hypothalamus of the two groups of pigs.

are shown in Figure 3B. The top 10 enriched pathways included neuroactive ligand–receptor interaction, ovarian steroidogenesis, protein digestion and absorption, thyroid hormone synthesis, ECM-receptor interaction, Wnt signaling pathway, amyotrophic lateral sclerosis (ALS), melanogenesis, oxytocin signaling pathway, cholinergic synapse, vascular smooth muscle contraction, and oxidative phosphorylation. Based on the analysis, we observed that there were 33 DEGs enriched in the neuroactive ligand–receptor interaction pathway, which was the 1st most significantly enriched pathway. Figure 3C shows the core composited factors and interactions in the pathway. This result suggests that the deletion of gut bacteria has a dramatic effect on hypothalamic neural signaling activated by multiple receptor proteins such as G protein-coupled receptors (GPCRs).

In addition, similar to the enriched MF terms in GO analysis, KEGG analysis also revealed dozens of DEGs related to the change in energy turnover by enrichment of the oxidative phosphorylation pathway. Figure 3D shows the core composited factors and interactions in the pathway.

RT-qPCR confirmation of the DE genes

Next, to validate RNA-seq results, four DE genes (*NPFFR1*, *GABRA1*, *LEPR*, and *TSHR*) in the neuroactive ligand–receptor interaction and three DE genes (*COX2*, *ATP6*, and *CYTB*) in oxidative phosphorylation were selected for RT-qPCR assay. As shown in Figure 4, qPCR data for the expression of selected genes

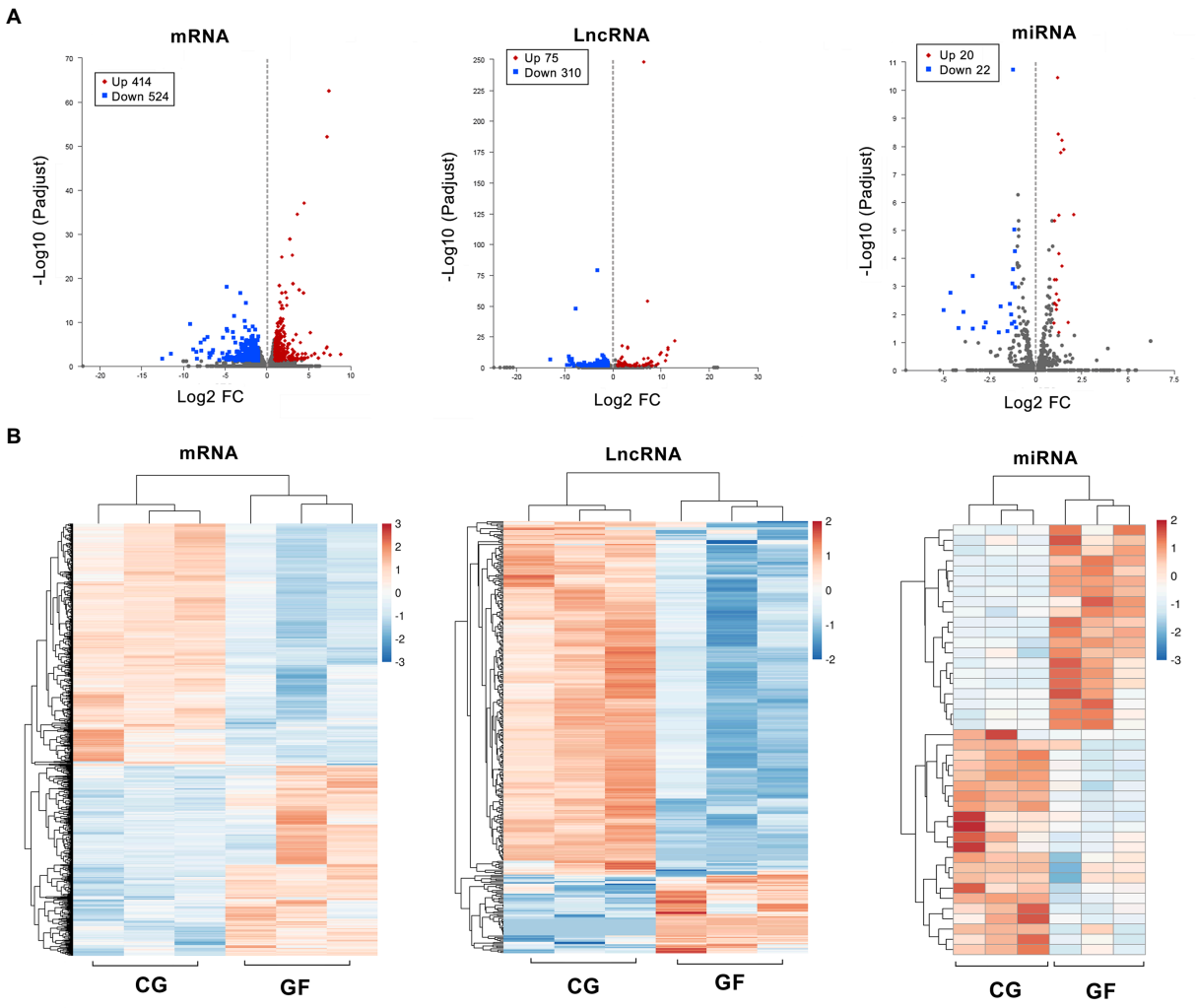

FIGURE 2
Differentially expressed transcripts and gene profiles in GF and CG pigs. **(A)** Volcano plots showing significantly different expression levels of different genes (mRNA) and transcripts (lncRNA and miRNA) between groups. **(B)** Clustering analysis of all differentially expressed genes and transcripts. The heatmap is based on expression values with $\log_2$| (fold change) |≥1 and *Padjust* <0.05.

were coincided with the RNA-seq result, thereby indicating that our transcript identification and abundance estimation are highly reliable.

Reactome pathway enrichment analysis of DEGs

Reactome is a knowledgebase of reactions and pathways for humans and dozens of other creatures, including pigs. Reactome provides an integrated view of the molecular details of biological processes ranging from metabolism to DNA replication and repair to signaling cascades (Fabregat et al., 2017; Jassal et al., 2020). Our Reactome analysis indicated that the DEGs were involved in 23 Reactome pathways with q-value < 0.05 (Figure 5). The Top 10 Reactome pathways were GPCR ligand binding (R-SSC-500792); Class A/1 (Rhodopsin-like receptors; R-SSC-373076); Respiratory electron transport, ATP synthesis by chemiosmotic coupling, and heat production by uncoupling proteins (R-SSC-163200); Hormone ligand-binding receptors (R-SSC-375281); Peptide hormone biosynthesis (R-SSC-209952); Complex I oxidizes NADH to NAD+, reduces CoQ to QH2 (R-SSC-6799197); ND4, ND5 bind the 550 kDa complex to form the 815 kDa complex (R-SSC-163217); Luteinizing hormone receptor can bind LH (R-SSC-391377); Removal of fibrillar collagen N-propeptides (R-SSC-2002428); Peripheral arm subunits bind the 815 kDa complex to form a 980 kDa complex (R-SSC-6799179). From the analysis of results, we found that GPCR protein family-mediated signaling, hormone signaling, heat production and mitochondrial oxidative metabolism showed clear differences in GF pigs compared to CG pigs.

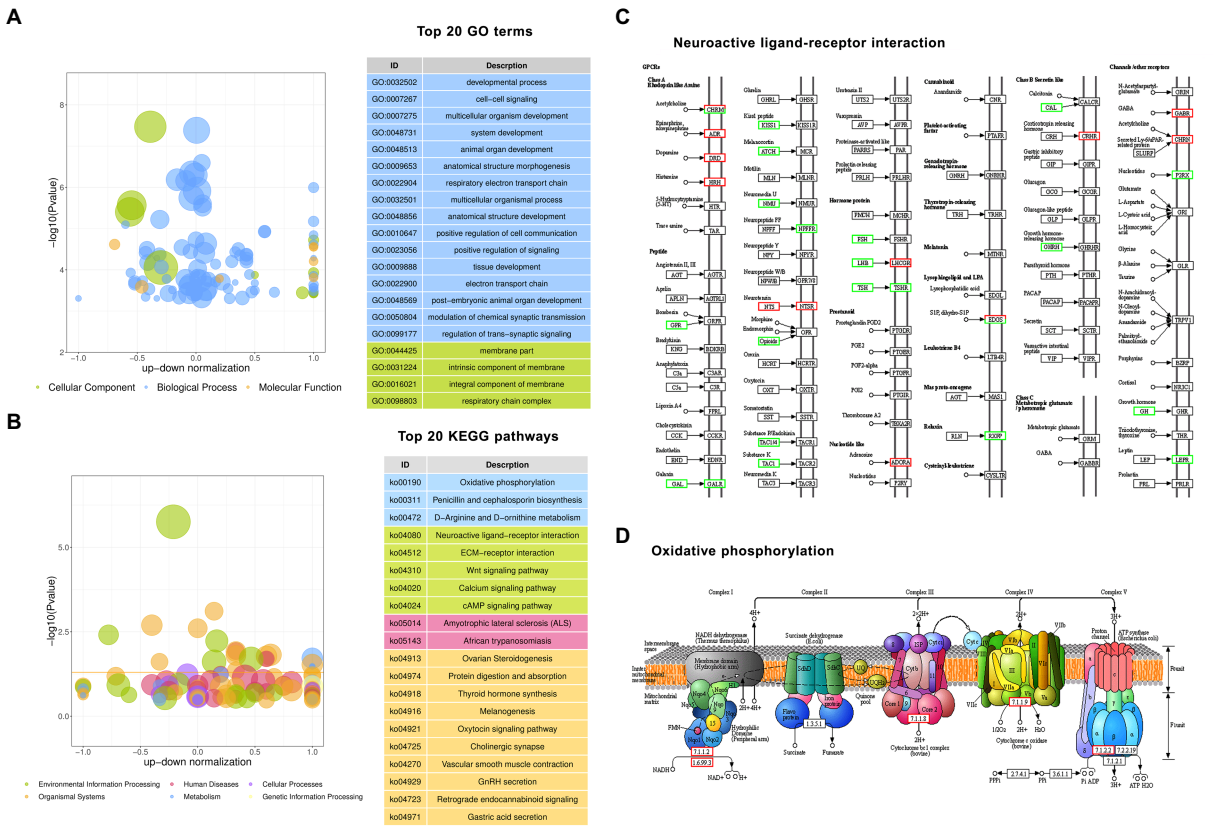

FIGURE 3
Gene Ontology (GO) and Kyoto Encyclopedia of Genes and Genomes (KEGG) enrichment analyses of differentially expressed protein-coding genes. **(A)** The top 20 enriched GO terms. **(B)** The top 20 enriched KEGG pathways. **(C)** The pathway of neuroactive ligand–receptor interaction. **(D)** The pathway of oxidative phosphorylation. Red boxes are upregulated genes, and green boxes are downregulated genes in GF pigs relative to CG pigs.

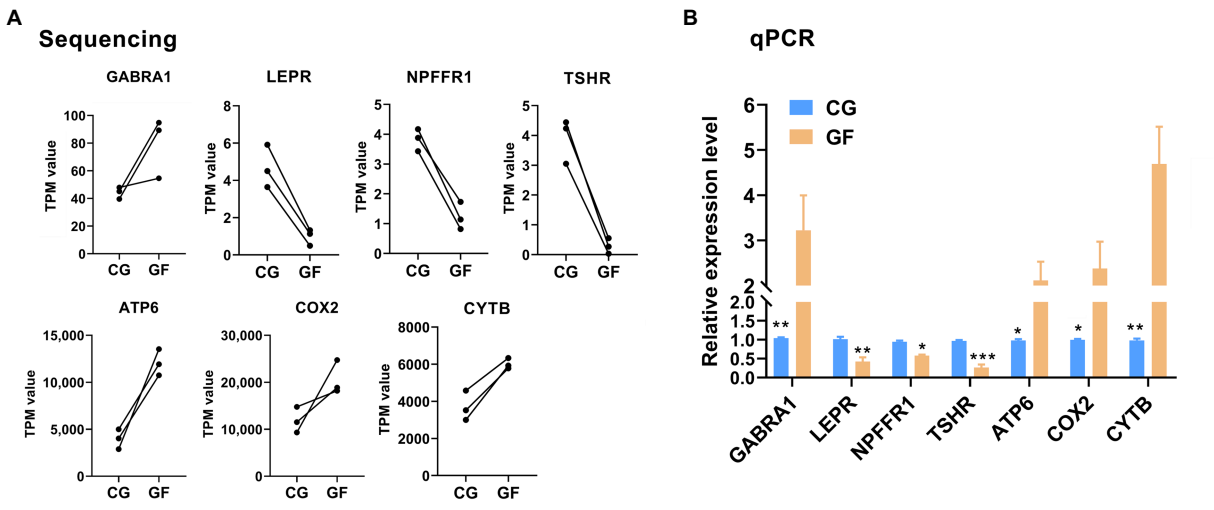

FIGURE 4
RT-qPCR validation of the RNA-Seq expression results. **(A)** The sequencing data for four DE genes (*NPFFR1*, *GABRA1*, *LEPR*, and *TSHR*) in the neuroactive ligand–receptor interaction and three DE genes (*COX2*, *ATP6*, and *CYTB*) in oxidative phosphorylation. **(B)** RT-qPCR data for the genes. The data are presented as the means ± SEM. $n = 3$. **indicates $p < 0.01$, * indicates $p < 0.05$ between CG pigs and GF pigs. *** indicates $p < 0.001$.

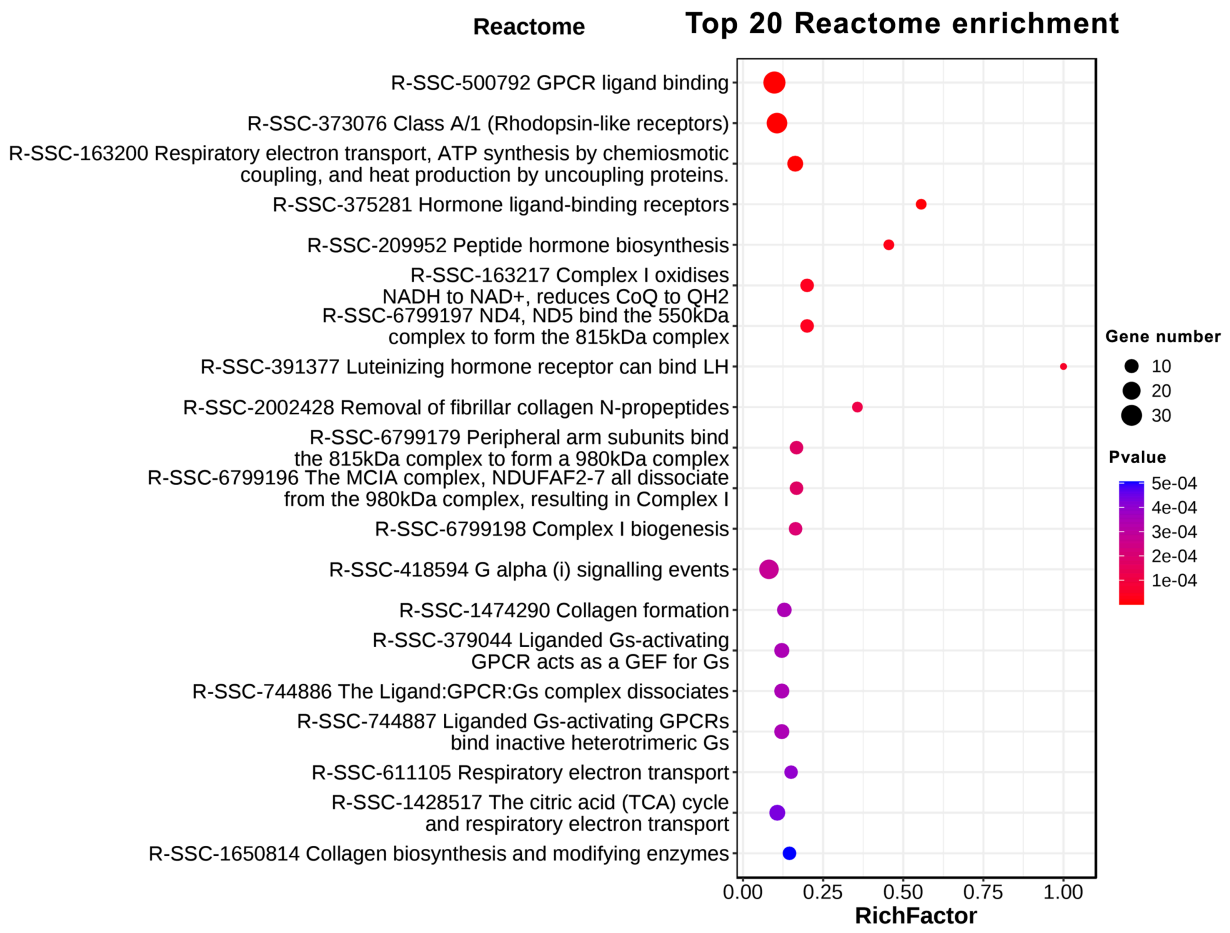

FIGURE 5
Reactome enrichment analysis of differentially expressed protein-coding genes.

Transcription factor analysis

In this study, the prediction of transcription factors (TFs) for the whole dataset of DEGs was performed, and 158 TFs were found among 938 DEGs, which showed differences in expression levels between CG and GF pigs. The differentially expressed TFs mainly included members of the *zf-C2H2* (47 TFs), *ZBTB* (15 TFs), *Homeobox* (11 TFs), *bHLH* (9 TFs), and *ARID* (5 TFs) gene families. The zf-C2H2 TF family has hundreds of members and is the largest superfamily in mammalian genomes, and these TFs are widely involved in the processes of cell proliferation, differentiation, death and intracellular signaling. The heatmap in Figure 6 shows the expression profiles of 47 TFs in the *zf-C2H2* family. More than 2/3 of the TFs in the *zf-C2H2* family showed significant reductions in expression levels in GF pigs, including multiple *ZNF* genes and *ZBTB* genes. These findings reveal the importance of gut microbiota for the normal expression and functions of *zf-C2H2* TFs. In addition, 170 lncRNAs have significant regulatory relationship with 6 of 47 *zf-C2H2* TFs according to the target prediction analysis shown in Supplementary Table S3. It has been observed that *INSM2* endured the most lncRNA regulation in the *zf-C2H2* family.

Construction of a competing endogenous RNA regulatory network

To investigate the interaction between different subtypes of DE RNAs, we constructed a competing endogenous RNA (ceRNA) network using DE miRNAs as a bridge for DE mRNAs and DE lncRNAs and identified the putative interactive pairs of DE miRNA – DE mRNA – DE lncRNA. 56 DE lncRNAs and 81 DE mRNAs were targeted by 5 DE miRNAs that were filtered according to *Padjust* < 0.05 and correlation > 0.90, and then these DE RNAs were used to construct an lncRNA-miRNA-mRNA triple network (Figure 7). In the regulatory ceRNA network, miR-22-3p, miR-24-3p, miR-136-3p, miR-143-3p, and miR-545-3p were located in the center and may play pivotal regulatory roles in the triple network. It is worth noting that all the five miRNAs were significantly downregulated in the

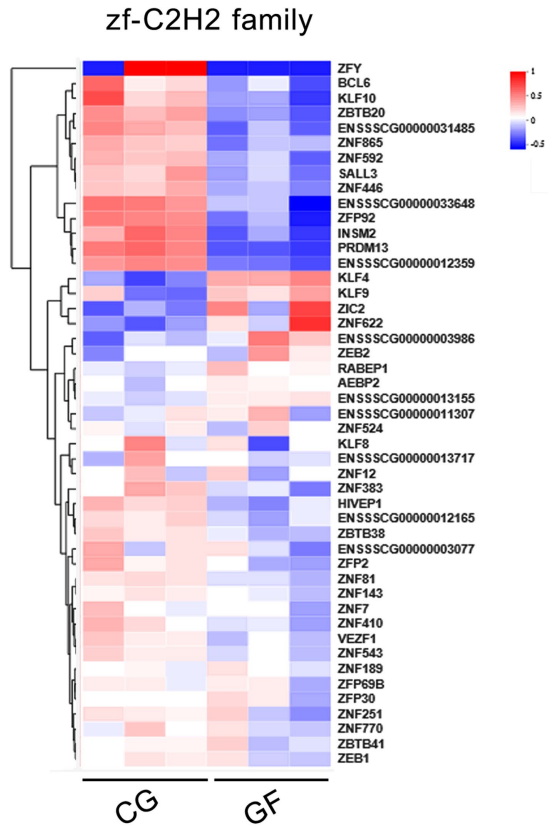

FIGURE 6
Clustering heatmap showing 47 altered *zf-C2H2* TFs.

hypothalamus of CG pigs. Target relationship between the five miRNAs and miRNAs or lncRNAs was showed in the Supplementary Table S4.

Energic consumption was increased in GF pigs' hypothalamus

Gene set enrichment analysis (GSEA) was also performed to identify the genes and cognitive pathways in the hypothalamus most affected by gut microbe colonization. Our GSEA results indicated that oxidative phosphorylation and thermogenesis were the most significantly enriched pathways (Figures 8A,B). This result was highly consistent with the KEGG and Reactome analyses. The two pathways share 17 altered genes. A protein–protein interaction (PPI) network was generated with the 17 genes and several mitochondrial DNA ND family genes located in the center of the network with the most neighbors and expanded nodes (Figure 8C). All of the genes were highly expressed in the GF pigs (Figure 8D), revealing that the requirement of energy expenditure was exorbitant.

To verify this result, we further evaluated the content of adenosine 5′-triphosphate (ATP), the principal energy currency of the cell, and the activity of ATPase in the hypothalamus. The obtained data showed that the ATP content in the GF pigs was significantly less than that in the CG pigs, with $p < 0.05$ (Figure 8E). However, the catalytic activity of Na^+/K^+ ATPase was almost 1.7-fold higher in the GF pigs than in the CG pigs (Figure 8F). Furthermore, protein level of carnitine palmitoyl transterase-1 (CPT-1) was clearly increased while protein level of uncoupling protein 2 (UCP2) was reduced in the GF pigs' hypothalamus that was showed by the western blotting assay (Figures 8G–I). Previous studies indicated that CPT1 is a key rate-limiting enzyme in the process of mitochondrial fatty acid oxidation, while UCP2 has a role in the ATP production (Qu et al., 2016; Kim et al., 2019). Therefore, these findings indicating that ATP production was decreased, however, ATP consumption was enhanced in the pigs without gut microbes.

Hypothalamic cell apoptosis was increased in the pigs with gut microbes

We noticed that the GSEA analysis also showed that dozens of DEGs were significantly enriched in apoptosis (Figure 9A). Therefore, we examined the hypothalamic cell apoptosis level in the two groups of pigs. The TdT-mediated dUTP nick end labeling (TUNEL) analysis showed that the number of apoptosis-positive cells in the hypothalamus of CG pigs was significantly greater than that of GF pigs (approximately 5–7-fold for GF pigs, Figure 9B). Furthermore, we analyzed the hypothalamic expression level of Caspase3, a key regulator and executor of programmed cell death (Jiang et al., 2020). The results of western blotting analysis showed that the protein levels of total caspase3 protein and cleaved Caspase3 (activated) were significantly increased in CG piglets with $p < 0.05$ (Figures 9C,D). It was speculated that the colonization of intestinal microbe increased the cell apoptosis rate in the hypothalamus in CG pigs may cause by the raise of circulating pro-inflammatory molecules. To confirm the speculation, blood concentrations of bacterial lipopolysaccharide (LPS) and interleukin-1 (IL-1) were detected by the ELISA method. The results showed that the blood concentration of LPS and IL-1 in CG pigs were about 5- and 2.3-fold of that of GF pigs, respectively (Figures 9E,F). Undoubtedly, these findings suggest that the colonization of gut microbes increases cell apoptosis in the hypothalamus, which may have a certain impact on brain health.

Discussion

Accumulating evidence suggests that the colonization and proliferation of gut microbes closely affect and alter the brain and CNS in humans and animals (Kelly et al., 2016; Rutsch et al., 2020; Zafar and Saier, 2021). A healthy gut with diverse microbes is vital for normal brain functions and emotional behavior (Suganya and Koo, 2020). The brain is the most complex organ in our body, and it is indisputably difficult to clearly distinguish the subtle structural

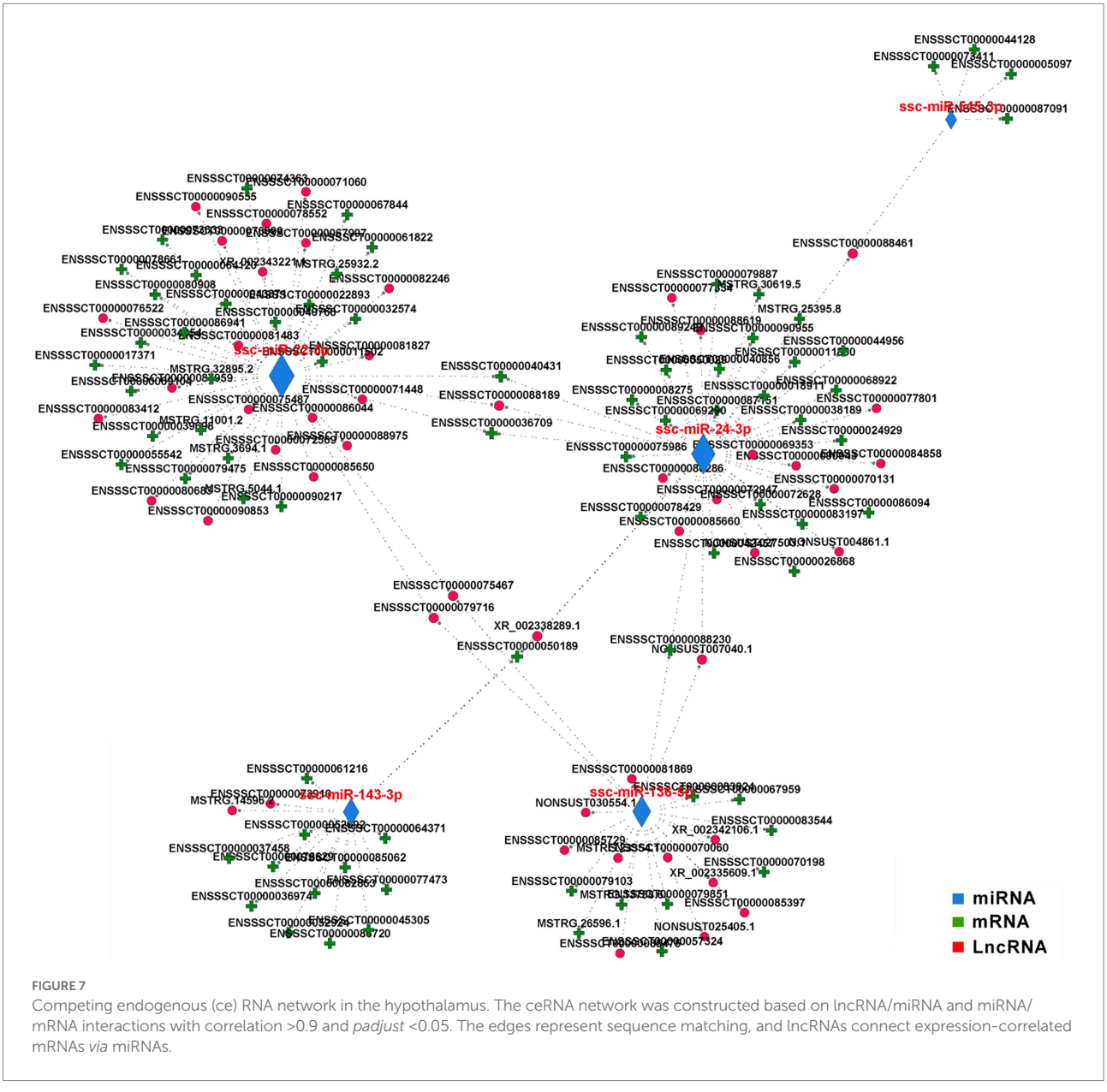

FIGURE 7
Competing endogenous (ce) RNA network in the hypothalamus. The ceRNA network was constructed based on lncRNA/miRNA and miRNA/mRNA interactions with correlation >0.9 and *padjust* <0.05. The edges represent sequence matching, and lncRNAs connect expression-correlated mRNAs *via* miRNAs.

and physiological changes in the brain caused by gut microbiota. GF animals without gut microbes are ideal models for studying the microbe-gut-brain axis. Lu et al. (2018) investigated the differences in brain development and behaviors between GF mice and mice with a gut microbiota (Lu et al., 2018). They found that the mice with gut microbiota showed better brain structural maturation, better contextual memory, and better spatial and learning memory than GF mice. This suggests that commensal bacteria are necessary for normal morphological development and maturation of the brain.

To explore the molecules related to brain development and function, high-throughput omics analysis has been widely used, especially transcriptome analysis. Recently, several studies based on rodents have given explanatory notes about the effects of gut microbial deletion on the morphology, function, and gene expression profiles of the brain using transcriptome analysis. A previous study has showed that 50 miRNAs and 4,623 mRNAs were differentially expressed in the hippocampi of GF mice compared with those of specific pathogen-free (SPF) mice (Chen et al., 2017). Colonization with the gut bacterial community of SPF mice could partially correct the variation in mRNA and miRNA expression profiles in the hippocampus of GF mice, but that was not sufficient to reverse the behavioral alterations of GF mice. Similarly, Zhou investigated 2,230 differentially expressed lncRNAs in the hippocampus of GF mice relative to SPF mice. Most of these lncRNAs and their target mRNAs were highly associated with cardiac hypertrophy, nuclear factors of activated T cells (NFAT), gonadotropin-releasing hormone (GnRH), calcium, and cAMP-response element binding protein (CREB) signaling pathways (Zhou et al., 2020). These gene expression

10.3389/fmicb.2022.970470

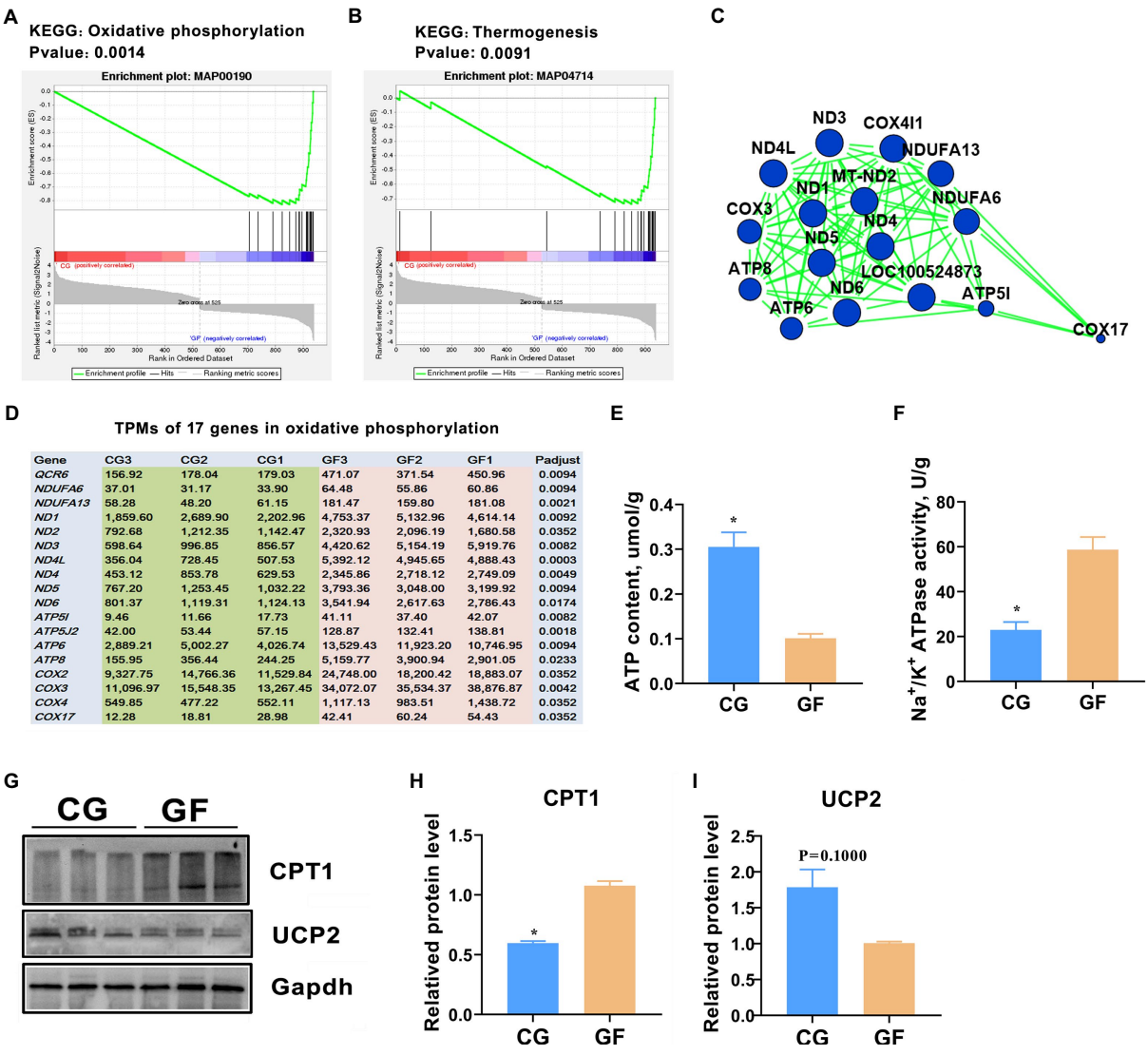

Gene	CG3	CG2	CG1	GF3	GF2	GF1	Padjust
QCR6	156.92	178.04	179.03	471.07	371.54	450.96	0.0094
NDUFA6	37.01	31.17	33.90	64.48	55.86	60.86	0.0094
NDUFA13	58.28	48.20	61.15	181.47	159.80	181.08	0.0021
ND1	1,859.60	2,689.90	2,202.96	4,753.37	5,132.96	4,614.14	0.0092
ND2	792.68	1,212.35	1,142.47	2,320.93	2,096.19	1,680.58	0.0352
ND3	598.64	996.85	856.57	4,420.62	5,154.19	5,919.76	0.0082
ND4L	356.04	728.45	507.53	5,392.12	4,945.65	4,888.43	0.0003
ND4	453.12	853.78	629.53	2,345.86	2,718.12	2,749.09	0.0049
ND5	767.20	1,253.45	1,032.22	3,793.36	3,048.00	3,199.92	0.0094
ND6	801.37	1,119.31	1,124.13	3,541.94	2,617.63	2,786.43	0.0174
ATP5I	9.46	11.66	17.73	41.11	37.40	42.07	0.0082
ATP5J2	42.00	53.44	57.15	128.87	132.41	138.81	0.0018
ATP6	2,889.21	5,002.27	4,026.74	13,529.43	11,923.20	10,746.95	0.0094
ATP8	155.95	356.44	244.25	5,159.77	3,900.94	2,901.05	0.0233
COX2	9,327.75	14,766.36	11,529.84	24,748.00	18,200.42	18,883.07	0.0352
COX3	11,096.97	15,548.35	13,267.45	34,072.07	35,534.37	38,876.87	0.0042
COX4	549.85	477.22	552.11	1,117.13	983.51	1,438.72	0.0352
COX17	12.28	18.81	28.98	42.41	60.24	54.43	0.0352

FIGURE 8
Hypothalamic energy consumption in pigs. GSEA analysis showed that oxidative phosphorylation **(A)** and thermogenesis **(B)** were significantly changed in GF pigs. **(C)** Protein–protein interaction (PPI) network of the 17 changed genes involved in oxidative phosphorylation and thermogenesis. **(D)** Expression levels (TPMs) of the 17 genes related to oxidative phosphorylation and thermogenesis. **(E)** ATP contents in the hypothalamus; **(F)** ATPase activity in the hypothalamus. **(G)** Western blotting (WB) analysis the protein levels of carnitine palmitoyl transterase-1 (CPT1) and uncoupling protein 2 (UCP2) in hypothalamus. **(H,I)** Quantitative analysis of the protein levels of CPT 1 and UCP2. The data are presented as the means ± SEM. *indicates $p < 0.05$ between CG pigs and GF pigs, $n = 4$ for the ATP content and ATPase activity assay and $n = 3$ for WB analysis.

studies provide references for subsequent functional research on the microbiota-gut-brain axis.

Due to the similar organ size and similar metabolic characteristics of pigs and humans, pigs are considered to be a more suitable model for studying human-related metabolic diseases than mice and rats (Koopmans and Schuurman, 2015). In this study, the effects and details of the deletion and colonization of gut microbes on the pig hypothalamus, the core of the intersection of the nervous system and endocrine system, were demonstrated by whole transcriptome analysis; thus, this study provides a lot of valid information for future studies on brain development and metabolism. Our results showed that thousands of protein-coding RNAs and noncoding RNAs were clearly differentially expressed in GF pigs compared to pigs with gut microbes. These altered genes were involved in the regulation of the nervous system, signal transduction, developmental regulation, and neurological diseases, reflecting how gut microbes affect the health and function of the hypothalamus. Notably, the transcriptome analysis highlighted that ligand–receptor-mediated neural signaling systems, such as GPCR-mediated signaling

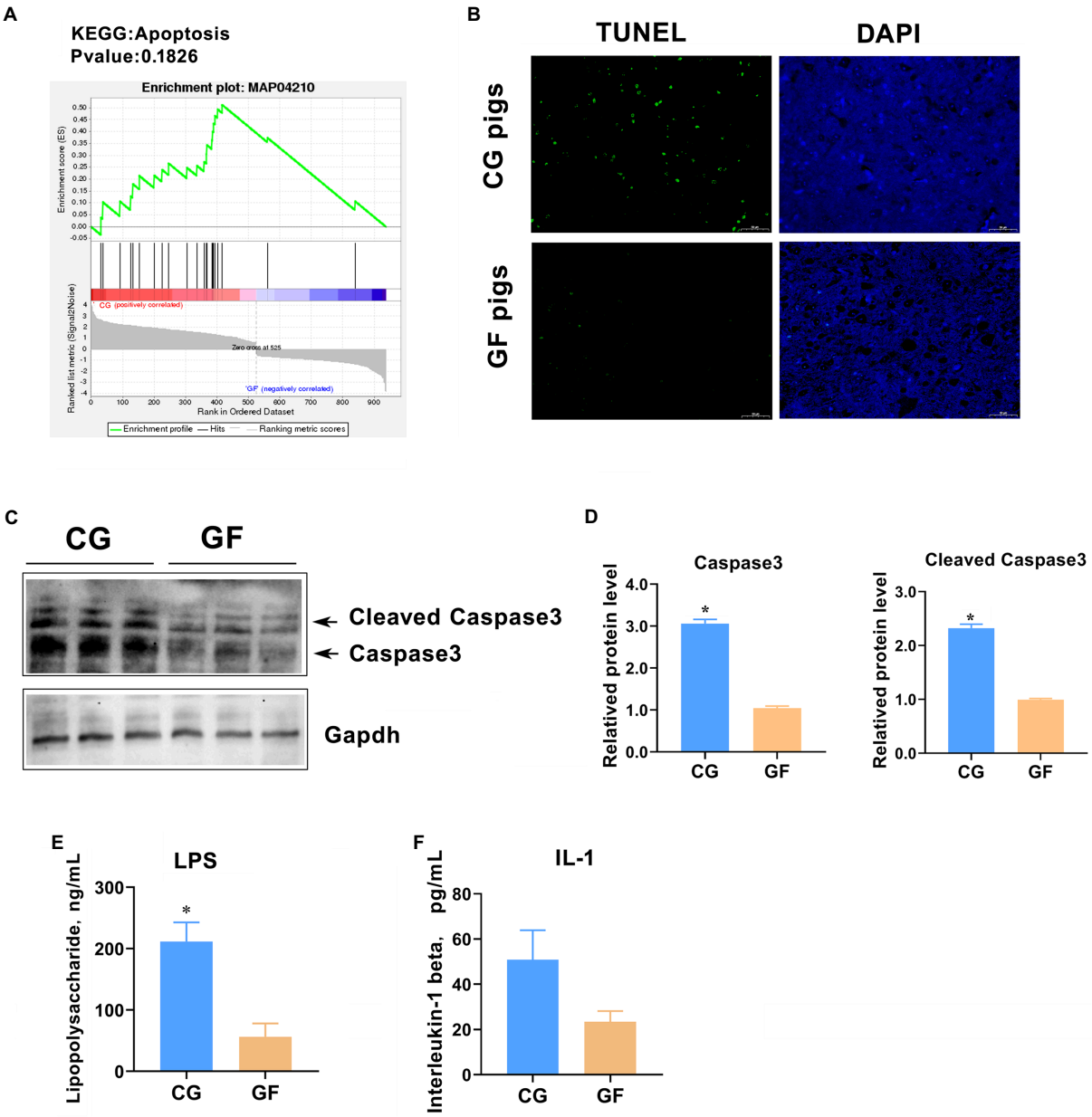

FIGURE 9
Hypothalamic cell apoptotic level between groups. **(A)** Apoptosis enrichment indicated by GSEA. **(B)** TUNEL analysis of cell apoptosis in the hypothalamus. Green color indicates TUNEL-positive cells. **(C)** Western blotting analysis of total and cleaved Caspase3. **(D)** Quantitative analysis of the protein levels of total and cleaved Caspase3. **(E)** Blood concentration of bacterial lipopolysaccharide (LPS). **(F)** Blood concentration of interleukin-1 (IL-1). The data are presented as the means ± SEM. *indicates p <0.05 between CG pigs and GF pigs. n =4 for the detection of LPS and IL-1 concentrations and n =3 for WB analysis.

networks, were significantly changed by gut microbe deletion. Undoubtedly, this leads to corresponding changes in CNS signaling and will affect the animal's behavior and mood. In addition, we speculate that the changes in the ligand–receptor-activated neural signaling system in GF pigs were mainly due to the lack of bacterial metabolites such as short-chain fatty acids (SCFAs). As we all known that SCFAs could activate many members of GPCR protein family by receptor-ligand binding and then make an impact on activation of brain neural signals and keep of blood brain barrier (BBB; Silva et al., 2020). Moreover, some other types of compounds produced by gut bacteria, such as amino acid derivatives (i.e., melatonin and GABA) and secondary bile acids have similar effects on the switching in neural signaling.

Previous GF animal-based studies have indicated those energy homeostasis and glycolipid metabolisms are significantly altered in animals without any gut microbes

(Krisko et al., 2020). A study showed that GF mice have a lower body fat weight and lower metabolic rate than mice with gut microbiota (Bäckhed et al., 2004). Nevertheless, Bäckhed found that compared to mice with a gut microbiota, GF mice are protected against the obesity that develops after consuming a high-fat, sugar-rich diet (Bäckhed et al., 2007). Mechanistically, GF mice have significantly increased levels of phosphorylated AMP-activated protein kinase (AMPK) and its downstream targets involved in fatty acid oxidation (acetyl-CoA carboxylase, ACC; carnitine palmitoyl transferase, CPT) in muscle and liver. A similar study reported that diet-induced obesity resistance in GF mice was conveyed by increased energy expenditure, preferential carbohydrate oxidation, and increased fecal fat and energy excretion (Kübeck et al., 2016). Our previous study also showed that GF piglets have smaller muscle and fat sizes than pigs with gut microbiota of the same age. Muscle cell mitochondria have dysregulated expression of multiple genes involved in oxidative metabolism (Qi et al., 2021a,b). The brain is the main organ for energy consumption in mammals, accounting for approximately 20% of the body's energy expenditure (Bélanger et al., 2011; Engl and Attwell, 2015). This study found that the hypothalamus of GF and CG pigs showed large differences in oxidative phosphorylation and energy utilization. Gene expression analysis indicated that hypothalamic oxidative phosphorylation and mitochondrial function were significantly enhanced in GF pigs. Similarly, 31 genes related to oxidative phosphorylation and mitochondrial function was upregulated in the ilea of GF mice, as revealed by transcriptome analysis (Manes et al., 2017). These findings suggested that the gut microbiota could control bioenergetics for the host within the metabolic network by regulating various factors in energy turnover.

It is known that gut-residing microbes in the disease or disruption state may be involved in the progression of neurological disorders (Quigley, 2017; Sun and Shen, 2018). McVey-Neufeld et al. reported that colonization of gut microbiota restores normal intrinsic and extrinsic nerve function and gut–brain signaling in GF mice (McVey-Neufeld et al., 2015). Here, we unexpectedly found that colonization of the gut microbiota resulted in a significant increase in the number of apoptotic cells in the hypothalamus of piglets. This may be due to the increase in pro-inflammatory factors such as lipopolysaccharide (LPS) produced by gut microbes or by the imbalance of the cell repair process mediated by the immune system that was also affected by gut microorganisms. The significant elevation of blood concentrations of LPS and IL-1 in the CG pigs confirmed this speculation to a large extent. This study has not accurately explored and reflected the underlying molecular mechanism of cell apoptosis in the hypothalamus caused by gut microbiota, which is an important topic for our future research. This finding provides new evidence that the gut microbiota is inextricably linked to the health of the brain through crosstalk in the microbe-gut-brain axis.

We must state the limitations for this study. Limited by the experimental conditions, the sample size in this study is small, which may have a certain impact on the accuracy of results. In addition, the authenticity of the numerous changed genes and signaling targets obtained by the sequencing should to be verified through in-depth functional assays. We will continue to investigate the effects of gut microbes on hypothalamic function and health based on the GF pig model.

Conclusion

To summarize, this study demonstrates the significant effects of gut microbe colonization on the porcine hypothalamus. The whole-transcriptome analysis showed thousands of protein coding and noncoding genes differentially expressed in GF pigs related to the pigs having a gut microbiota and therefore comprehensively affecting the development, function and health of the hypothalamus. Importantly, this study also provides new candidate target molecules for subsequent functional research.

Data availability statement

The datasets presented in this study can be found in online repositories. The names of the repository/repositories and accession number(s) can be found at: NCBI GEO - GSE207675.

Ethics statement

The study was approved by Ethics Committee of the Chongqing Academy of Animal Science (No. 2020012B).

Author contributions

ZL and RQ: conceptualization. RQ, JW, XQ, XL, and JS: data curation. JS and XL: formal analysis. ZL, XQ, and RQ: funding acquisition. JW, QW, and XQ: investigation. JS, FY, and RQ: methodology. RQ and ZL: project administration. LG and RQ: resources. RQ: supervision and writing—original draft. XL and JW: visualization. LG and ZL: writing—review and editing. All authors contributed to the article and approved the submitted version.

Funding

This research was supported by the National Natural Science Foundation of China (U21A20245) and the Financial Resourced Program of Chongqing (nos. 20238 and 21515).

Conflict of interest

The authors declare that the research was conducted in the absence of any commercial or financial relationships that could be construed as a potential conflict of interest.

Publisher's note

All claims expressed in this article are solely those of the authors and do not necessarily represent those of their affiliated organizations, or those of the publisher, the editors and the reviewers. Any product that may be evaluated in this article, or claim that may be made by its manufacturer, is not guaranteed or endorsed by the publisher.

Supplementary material

The Supplementary material for this article can be found online at: https://www.frontiersin.org/articles/10.3389/fmicb.2022.970470/full#supplementary-material

References

Agirman, G., Yu, K. B., and Hsiao, E. Y. (2021). Signaling inflammation across the gut-brain axis. *Science* 374, 1087–1092. doi: 10.1126/science.abi6087

Bäckhed, F., Ding, H., Wang, T., Hooper, L. V., Koh, G. Y., Nagy, A., et al. (2004). The gut microbiota as an environmental factor that regulates fat storage. *Proc. Natl. Acad. Sci. U. S. A.* 101, 15718–15723. doi: 10.1073/pnas.0407076101

Bäckhed, F., Mancheste, J. K., Semenkovich, C. F., and Gordon, J. I. (2007). Mechanisms underlying the resistance to diet-induced obesity in germ-free mice. *Proc. Natl. Acad. Sci. U. S. A.* 104, 979–984. doi: 10.1073/pnas.0605374104

Bélanger, M., Allaman, I., and Magistretti, P. J. (2011). Brain energy metabolism: focus on astrocyte-neuron metabolic cooperation. *Cell Metab.* 14, 724–738. doi: 10.1016/j.cmet.2011.08.016

Bibbò, S., Ianiro, G., Giorgio, V., Scaldaferri, F., Masucci, L., Gasbarrini, A., et al. (2016). The role of diet on gut microbiota composition. *Eur. Rev. Med. Pharmacol. Sci.* 20, 4742–4749.

Brannelly, L. A., Roberts, A. A., Skerratt, L. F., and Berger, L. (2018). Using terminal transferase-mediated dutp nick end-labelling (TUNEL) and caspase 3/7 assays to measure epidermal cell death in frogs with chytridiomycosis. *J. Vis. Exp.* 135:57345. doi: 10.3791/57345

Buffie, C. G., and Pamer, E. G. (2013). Microbiota-mediated colonization resistance against intestinal pathogens. *Nat. Rev. Immunol.* 13, 790–801. doi: 10.1038/nri3535

Ceppa, F., Mancini, A., and Tuohy, K. (2019). Current evidence linking diet to gut microbiota and brain development and function. *Int. J. Food Sci. Nutr.* 70, 1–19. doi: 10.1080/09637486.2018.1462309

Chen, J. J., Zeng, B. H., Li, W. W., Zhou, C. J., Fan, S. H., Cheng, K., et al. (2017). Effects of gut microbiota on the microRNA and mRNA expression in the hippocampus of mice. *Behav. Brain Res.* 322, 34–41. doi: 10.1016/j.bbr.2017.01.021

Dinan, T. G., and Cryan, J. F. (2017). The microbiome-gut-brain axis in health and disease. *Gastroenterol. Clin. North Am.* 46, 77–89. doi: 10.1016/j.gtc.2016.09.007

Engl, E., and Attwell, D. (2015). Non-signaling energy use in the brain. *J. Physiol.* 593, 3417–3429. doi: 10.1113/jphysiol.2014.282517

Fabregat, A., Sidiropoulos, K., Viteri, G., Forner, O., Marin-Garcia, P., Arnau, V., et al. (2017). Reactome pathway analysis: a high performance in-memory approach. *BMC Bioinformatics* 18:142. doi: 10.1186/s12859-017-1559-2

Farhadipour, M., and Depoortere, I. (2021). The function of gastrointestinal hormones in obesity-implications for the regulation of energy intake. *Nutrients* 13:1839. doi: 10.3390/nu13061839

Gabanyi, I., Lepousez, G., Wheeler, R., Vieites-Prado, A., Nissant, A., Wagner, S., et al. (2022). Bacterial sensing via neuronal Nod2 regulates appetite and body temperature. *Science* 376:eabj3986. doi: 10.1126/science.abj3986

Gribble, F. M., and Reimann, F. (2019). Function and mechanisms of enteroendocrine cells and gut hormones in metabolism. *Nat. Rev. Endocrinol.* 15, 226–237. doi: 10.1038/s41574-019-0168-8

Gu, X. F., Li, H. B., Sha, L., and Zhao, W. (2020). Construction and comprehensive analyses of a competing endogenous rna network in tumor-node-metastasis stage I hepatocellular carcinoma. *Biomed. Res. Int.* 2020:5831064. doi: 10.1155/2020/5831064

Han, H., Yi, B., Zhong, R., Wang, M., Zhang, S., Ma, J., et al. (2021). From gut microbiota to host appetite: gut microbiota-derived metabolites as key regulators. *Microbiome* 9:162. doi: 10.1186/s40168-021-01093-y

Jassal, B., Matthews, L., Viteri, G., Gong, C., Lorente, P., Fabregat, A., et al. (2020). The reactome pathway knowledgebase. *Nucleic Acids Res.* 48, D498–D503. doi: 10.1093/nar/gkz1031

Jia, X., Xu, W., Zhang, L., Li, X., Wang, R., and Wu, S. (2021). Impact of gut microbiota and microbiota-related metabolites on hyperlipidemia. *Front. Cell. Infect. Microbiol.* 11:634780. doi: 10.3389/fcimb.2021.634780

Jiang, M., Qi, L., Li, L., and Li, Y. (2020). The caspase-3/GSDME signal pathway as a switch between apoptosis and pyroptosis in cancer. *Cell Death Discov.* 6:112. doi: 10.1038/s41420-020-00349-0

Kelly, J. R., Clarke, G., Cryan, J. F., and Dinan, T. G. (2016). Brain-gut-microbiota axis: challenges for translation in psychiatry. *Ann. Epidemiol.* 26, 366–372. doi: 10.1016/j.annepidem.2016.02.008

Kim, S., and Jazwinski, S. M. (2018). The gut microbiota and healthy aging: a mini-review. *Gerontology* 64, 513–520. doi: 10.1159/000490615

Kim, J. D., Yoon, N. A., Jin, S., and Diano, S. (2019). Microglial UCP2 mediates inflammation and obesity induced by high-fat feeding. *Cell Metab.* 30, 952–962.e5. doi: 10.1016/j.cmet.2019.08.010

Koopmans, S. J., and Schuurman, T. (2015). Considerations on pig models for appetite, metabolic syndrome and obesetype 2 diabetes: from food intake to metabolic disease. *Eur. J. Pharmacol.* 759, 231–239. doi: 10.1016/j.ejphar.2015.03.044

Krisko, T. I., Nicholls, H. T., Bare, C. J., Holman, C. D., Putzel, G. G., Jansen, R. S., et al. (2020). Dissociation of adaptive thermogenesis from glucose homeostasis in microbiome-deficient mice. *Cell Metab.* 31, 592–604.e9. doi: 10.1016/j.cmet.2020.01.012

Kübeck, R., Bonet-Ripoll, C., Hoffmann, C., Walker, A., Müller, V. M., Schüppel, V. L., et al. (2016). Dietary fat and gut microbiota interactions determine diet-induced obesity in mice. *Mol. Metab.* 5, 1162–1174. doi: 10.1016/j.molmet.2016.10.001

Li, M. S., Liu, Y. L., Zhang, X. L., Liu, J., and Wang, P. (2018). Transcriptomic analysis of high-throughput sequencing about circRNA, lncRNA and mRNA in bladder cancer. *Gene* 677, 189–197. doi: 10.1016/j.gene.2018.07.041

Lu, J., Synowiec, S., Lu, L., Yu, Y., Bretherick, T., Takada, S., et al. (2018). Microbiota influence the development of the brain and behaviors in C57BL/6J mice. *PLoS One* 13:e0201829. doi: 10.1371/journal.pone.0201829

Ma, N., Tie, C. R., Yu, B., Zhang, W., and Wan, J. (2020). Identifying lncRNA–miRNA–mRNA networks to investigate Alzheimer's disease pathogenesis and therapy strategy. *Aging* 12, 2897–2920. doi: 10.18632/aging.102785

Manes, N. P., Shulzhenko, N., Nuccio, A. G., Azeem, S., Morgun, A., and Nita-Lazar, A. (2017). Multiomics comparative analysis reveals multiple layers of host signaling pathway regulation by the gut microbiota. *mSystems* 2, e00107–e00117. doi: 10.1128/mSystems.00107-17

Martchenko, A., Martchenko, S. E., Biancolin, A. D., and Brubaker, P. L. (2020). Circadian rhythms and the gastrointestinal tract: relationship to metabolism and gut hormones. *Endocrinology* 161:bqaa167. doi: 10.1210/endocr/bqaa167

McVey-Neufeld, K. A., Perez-Burgos, A., Mao, Y. K., Bienenstock, J., and Kunze, W. A. (2015). The gut microbiome restores intrinsic and extrinsic nerve function in germ-free mice accompanied by changes in calbindin. *Neurogastroenterol. Motil.* 27, 627–636. doi: 10.1111/nmo.12534

Qi, R. L., Qiu, X., Du, L., Wang, J., Wang, Q., Huang, J., et al. (2021a). Changes of gut microbiota and its correlation with short chain fatty acids and bioamine in piglets at the early growth stage. *Front. Vet. Sci.* 7:617259. doi: 10.3389/fvets.2020.617259

Qi, R. L., Sun, J., Qiu, X. Y., Zhang, Y., Wang, J., Wang, Q., et al. (2021b). The intestinal microbiota contributes to the growth and physiological state of muscle tissue in piglets. *Sci. Rep.* 11:11237. doi: 10.1038/s41598-021-90881-5

Qu, Q., Zeng, F., Liu, X., Wang, Q. J., and Deng, F. (2016). Fatty acid oxidation and carnitine palmitoyltransferase I: emerging therapeutic targets in cancer. *Cell Death Dis.* 7:e2226. doi: 10.1038/cddis.2016.132

Quigley, E. M. M. (2017). Microbiota-brain-gut axis and neurodegenerative diseases. *Curr. Neurol. Neurosci. Rep.* 17:94. doi: 10.1007/s11910-017-0802-6

Rutsch, A., Kantsjö, J. B., and Ronchi, F. (2020). The gut-brain axis: how microbiota and host inflammasome influence brain physiology and pathology. *Front. Immunol.* 11:604179. doi: 10.3389/fimmu.2020.604179

Silva, Y. P., Bernardi, A., and Frozza, R. L. (2020). The role of short-chain fatty acids from gut microbiota in gut-brain communication. *Front. Endocrinol.* 11:25. doi: 10.3389/fendo.2020.00025

Suganya, K., and Koo, B. S. (2020). Gut–brain Axis: role of gut microbiota on neurological disorders and how probiotics/prebiotics beneficially modulate microbial and immune pathways to improve brain functions. *Int. J. Mol. Sci.* 21:7551. doi: 10.3390/ijms21207551

Sun, M. F., and Shen, Y. Q. (2018). Dysbiosis of gut microbiota and microbial metabolites in Parkinson's disease. *Ageing Res. Rev.* 45, 53–61. doi: 10.1016/j.arr.2018.04.004

Wang, B., Wan, L., Wang, H., Dai, H., Lu, X., Lee, Y. K., et al. (2021). Targeting the gut microbiota for remediating obesity and related metabolic disorders. *J. Nutr.* 151, 1703–1716. doi: 10.1093/jn/nxab103

Zafar, H., and Saier, M. H. (2021). Gut bacteroides species in health and disease. *Gut Microbes* 13, 1–20. doi: 10.1080/19490976.2020.1848158

Zhao, Z., Ning, J., Bao, X. Q., Shang, M., Ma, J., Li, G., et al. (2021). Fecal microbiota transplantation protects rotenone-induced Parkinson's disease mice via suppressing inflammation mediated by the lipopolysaccharide-TLR4 signaling pathway through the microbiota-gut-brain axis. *Microbiome* 9:226. doi: 10.1186/s40168-021-01107-9

Zhou, C. J., Rao, X. C., Wang, H. Y., Zeng, B. H., Yu, Y., Chen, J. J., et al. (2020). Hippocampus-specific regulation of long non-coding RNA and mRNA expression in germ-free mice. *Funct. Integr. Genomics* 20, 355–365. doi: 10.1007/s10142-019-00716-w

frontiers | Frontiers in Microbiology

TYPE Original Research
PUBLISHED 15 September 2023
DOI 10.3389/fmicb.2023.1250891

OPEN ACCESS

EDITED BY
Lifeng Zhu,
Nanjing University of Chinese Medicine, China

REVIEWED BY
Zunji Shi,
Lanzhou University, China
Lenan Zhuang,
Zhejiang University, China
Xuguang Du,
China Agricultural University, China

*CORRESPONDENCE
Jianguo Zhao
✉ zhaojg@ioz.ac.cn
Guangliang Liu
✉ LiuGuangLiang01@caas.cn

†These authors have contributed equally to this work

RECEIVED 30 June 2023
ACCEPTED 17 August 2023
PUBLISHED 15 September 2023

CITATION
Qiao C, He M, Wang S, Jiang X, Wang F, Li X, Tan S, Chao Z, Xin W, Gao S, Yuan J, Li Q, Xu Z, Zheng X, Zhao J and Liu G (2023) Multi-omics analysis reveals substantial linkages between the oral-gut microbiomes and inflamm-aging molecules in elderly pigs.
Front. Microbiol. 14:1250891.
doi: 10.3389/fmicb.2023.1250891

Multi-omics analysis reveals substantial linkages between the oral-gut microbiomes and inflamm-aging molecules in elderly pigs

Chuanmin Qiao[1,2,3†], Maozhang He[4†], Shumei Wang[4†], Xinjie Jiang[2], Feng Wang[2], Xinjian Li[2], Shuyi Tan[2], Zhe Chao[2], Wenshui Xin[2], Shuai Gao[2], Jingli Yuan[2], Qiang Li[2], Zichun Xu[2], Xinli Zheng[2], Jianguo Zhao[1*] and Guangliang Liu[2*]

[1]Institute of Zoology, Chinese Academy of Sciences, Beijing, China, [2]Institute of Animal Science and Veterinary Medicine, Academy of Agricultural Sciences, Haikou, China, [3]Hainan Yazhou Bay Seed Laboratory, Sanya, China, [4]Department of Microbiology, School of Basic Medical Sciences, Anhui Medical University, Hefei, China

Introduction: The accelerated aging of the global population has emerged as a critical public health concern, with increasing recognition of the influential role played by the microbiome in shaping host well-being. Nonetheless, there remains a dearth of understanding regarding the functional alterations occurring within the microbiota and their intricate interactions with metabolic pathways across various stages of aging.

Methods: This study employed a comprehensive metagenomic analysis encompassing saliva and stool samples obtained from 45 pigs representing three distinct age groups, alongside serum metabolomics and lipidomics profiling.

Results: Our findings unveiled discernible modifications in the gut and oral microbiomes, serum metabolome, and lipidome at each age stage. Specifically, we identified 87 microbial species in stool samples and 68 in saliva samples that demonstrated significant age-related changes. Notably, 13 species in stool, including *Clostridiales bacterium*, *Lactobacillus johnsonii*, and *Oscillibacter* spp., exhibited age-dependent alterations, while 15 salivary species, such as *Corynebacterium xerosis*, *Staphylococcus sciuri*, and *Prevotella intermedia*, displayed an increase with senescence, accompanied by a notable enrichment of pathogenic organisms. Concomitant with these gut-oral microbiota changes were functional modifications observed in pathways such as cell growth and death (necroptosis), bacterial infection disease, and aging (longevity regulating pathway) throughout the aging process. Moreover, our metabolomics and lipidomics analyses unveiled the accumulation of inflammatory metabolites or the depletion of beneficial metabolites and lipids as aging progressed. Furthermore, we unraveled a complex interplay linking the oral-gut microbiota with serum metabolites and lipids.

Discussion: Collectively, our findings illuminate novel insights into the potential contributions of the oral-gut microbiome and systemic circulating metabolites and lipids to host lifespan and healthy aging.

KEYWORDS

swine, aging, oral-gut axis, multi-omics, inflammation

1. Introduction

The escalating number of elderly individuals is an escalating public health concern globally, with a particular emphasis on China, where it is estimated that there will be around 402 million older adults by 2040 (Wang and Chen, 2022). The swift aging of the population, stimulated by recent declines in fertility and mortality rates, spark concerns regarding the health and quality of life of elderly individuals, and will pose significant challenges for the healthcare system. The process of aging is intricate and dynamic, involving the restructuring of various physiological systems that are intricately associated with systemic inflammation, metabolism, and immunity across diverse cells and tissues (Fulop et al., 2017; Finger et al., 2022). However, the process of aging and lifespan is tremendously influenced by host genetics and environmental factors. The symbiotic commensal microbiota has been recognized as an influential environmental factor in the development of aging-related metabolic and immune diseases. Accumulating evidence supports the role of microbiota in the development of these diseases (Belkaid and Hand, 2014; Thaiss et al., 2016; Zheng et al., 2020; Ansaldo et al., 2021), and further research is needed to better understand the relationship between the microbiome and aging.

Altered gut microbiome and host metabolism have been implicated in the process of aging (Cruz-Pereira et al., 2022; Ghosh et al., 2022). Aging is associated with changes in the gut microbiota, which in turn can affect host metabolism (Gao et al., 2018). The gut microbiota is a complex community of microorganisms that live in the gastrointestinal tract and play an important role in maintaining human health (Thursby and Juge, 2017; Gomaa, 2020). As we age, the diversity and composition of the gut microbiota can change, with a decrease in beneficial bacteria and an increase in harmful bacteria. These changes in the gut microbiota can contribute to a number of age-related health problems, such as impaired immune function, inflammation, and metabolic dysfunction (Kong et al., 2019; Badal et al., 2020; Ghosh et al., 2022; Yin et al., 2023). For example, alterations in the gut microbiota have been linked to age-related diseases such as type 2 diabetes, cardiovascular disease, and cognitive decline (Pascale et al., 2019; Ghosh et al., 2020; Pellanda et al., 2021). The gut microbiome plays a critical role in host metabolism through a variety of mechanisms, including fermentation of dietary fibers, regulation of intestinal barrier function, regulation of immune function and bile acid metabolism, for instance, microbial derived SCFAs can modulate various metabolic pathways in the host, including glucose and lipid metabolism, and can also affect immune function and inflammation (Gasaly et al., 2021; Ohtani and Hara, 2021; Zhang, 2022). Overall, the relationship between the gut microbiota and host metabolism is complex and their joint action on aging still not fully understood. However, there is growing evidence to suggest that interventions aimed at modulating the gut microbiota, such as dietary changes or probiotics, may have potential therapeutic benefits for age-related metabolic disorders.

The study of aging and the host microbiome is a relatively new field of research. Though there have been many studies of the human microbiome and aging, there are still several deficiencies that need to be addressed since human gut microbiota extremely dynamic and influenced by a number of confounding factors, such as diet, medications, lifestyle factors, which can make it difficult to isolate the effects of aging on the gut microbiota (Bana and Cabreiro, 2019; Manor et al., 2020; Molinero et al., 2023). Further, many studies of the human, and others animal microbiome and aging focus on taxonomic changes, but do not investigate functional changes in the microbiome. Functional studies are needed to better understand the mechanisms by which the human microbiome influences aging-related processes. Besides, scarce researches investigate the process of aging using multi-omics, which involved metagenomics, metabolomics, lipidomics, and transcriptomics to provide a more comprehensive understanding of biological systems that are involved in the aging process. By integrating these different types of data, researchers can identify key molecular and cellular changes that occur during aging, and can use this information to develop new approaches for preventing or treating age-related diseases. In addition, previous researches mainly focus on the role of gut microbiota in the host aging. However, the importance of the oral microbiome in the aging process is increasingly recognized, as the oral microbiome plays a key role in maintaining oral health and is also implicated in various systemic diseases (Sedghi et al., 2021; Peng et al., 2022).

Hence, a well-controlled model system that reproduces faithfully the trajectories in the oral and gut microbiota with age is warranted and will provide a better understanding of the role played by them in the healthy development and aging of the host. Pigs are used as an excellent model to study the interaction between host microbiome and aging by combining multi-omics, because pigs share many similarities with humans in terms of their anatomy, physiology, and nutritional requirements. For example, the structure and function of the pig gut is similar to that of humans, as well as in organ development and disease progression (Lunney et al., 2021; Rose et al., 2022). In addition, swine can be raised in a controlled environment and are readily available and relatively inexpensive compared to other animal models, which allows researchers to manipulate their diet and other environmental factors that may influence the host microbiome and aging process. Previous research has also been identified that pigs have a gut microbiome that is similar in composition to that of humans, with a high degree of microbial diversity and similar microbial taxa (Lim et al., 2019; Yang et al., 2022). Overall, the use of pigs as a model for studying the interaction between host microbiome and aging provides a valuable tool for understanding the complex interplay between these factors, and for developing interventions and therapies that can improve healthspan and reduce the burden of age-related diseases in humans.

To date, there is a paucity of data investigating the progression of aging through the integration of metagenomics analyses of oral and gut microbial species, with metabolomics and lipidomics profiling of blood molecules. In this study, we recruited a cohort of 45 pigs and collected 45 fecal and 45 salivary samples, as well as 30 blood samples at three different age points: (1) 1 year old, (2) 4 years old, and (3) 8 years old (Tohyama and Kobayashi, 2019). The use of this animal model allowed us to explore the potential correlations among these factors and their possible roles in the observed changes associated with aging (Figure 1A). Our primary objective was to determine the complex molecular changes that occur at different stages of age in pigs, and how they contribute to age-related alteration in host metabolism and decline in physiological functions. Multi-omics approaches can provide a more comprehensive understanding of the aging process, as different types of molecules are interconnected and influence each other in complex ways. By analyzing multiple omics data sets, we can identify molecular signatures and pathways that are associated with aging and age-related diseases. This can lead to the development of new biomarkers and therapeutic targets for age-related conditions, as well as strategies for promoting healthy

10.3389/fmicb.2023.1250891

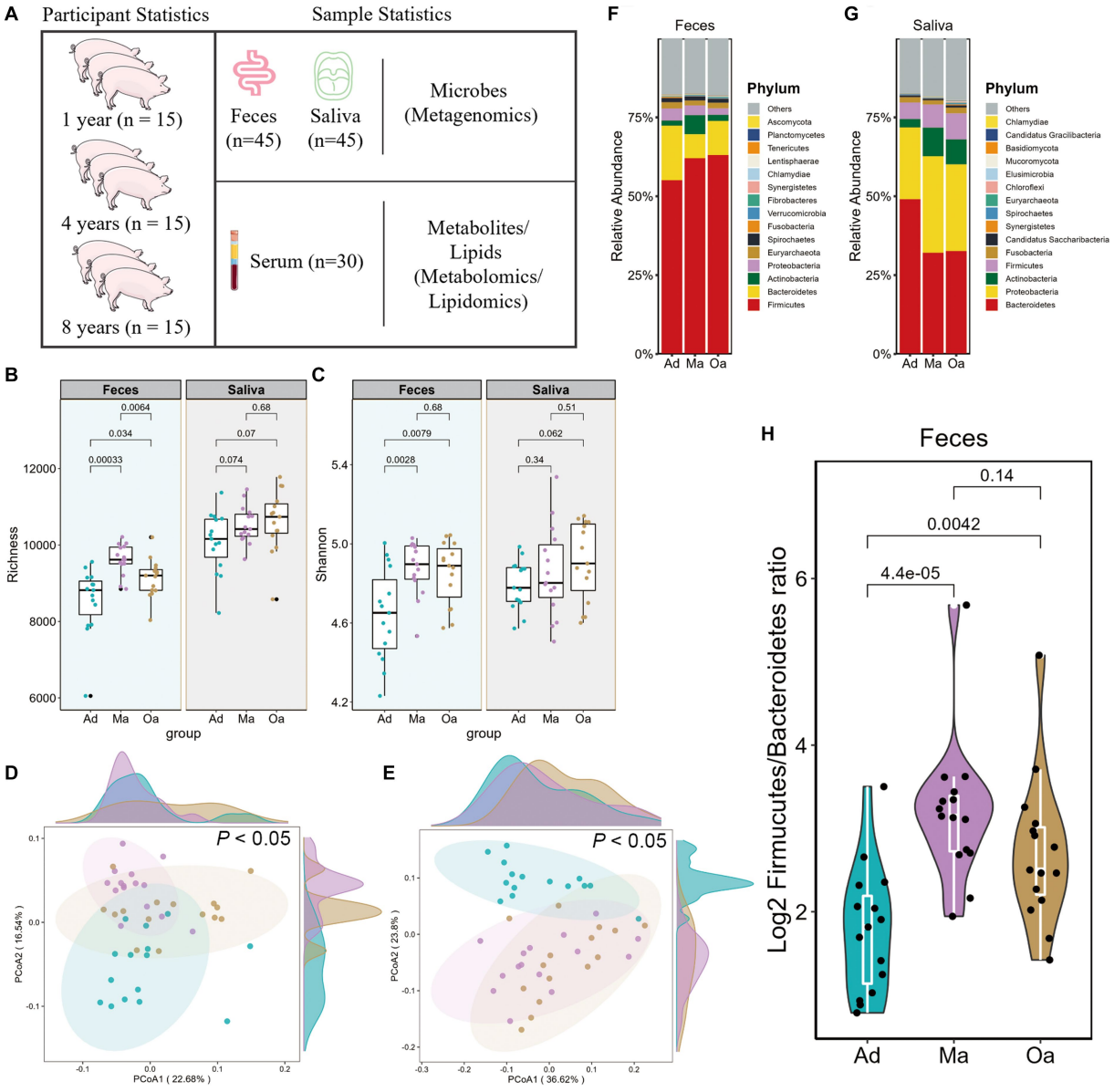

FIGURE 1
Alterations of gut microbial composition in relation to aging in pigs. **(A)** Workflow overview of the metagenomic, metabolomic, and lipidomics strategies used in this study. Comparison of α-diversity by **(B)** richness and **(C)** Shannon indices using Wilcoxon rank sum test in pigs at adult (Ad), middle age (Ma), and old age (Oa). **(D,E)** Principal coordinate analysis (PCoA) based on the Bray–Curtis dissimilarity metric derived from feces and saliva showed a significant difference in gut and salivary microbial composition among Ad, Ma, and Oa groups. Statistical significance and variance of Bray–Curtis dissimilarity data were assessed using PERMANOVA. **(F,G)** Relative abundance of bacterial phyla in gut and oral microbiotas of individuals with Ad, Ma, and Oa. **(H)** Log_2 Firmicutes/Bacteroidota ratios in gut samples from individuals in Ad, Ma, and Oa groups (Wilcoxon rank-sum test).

aging and extending lifespan. In general, the study of aging by multi-omics is an important and rapidly growing field that has the potential to revolutionize our understanding of aging and age-related diseases, and ultimately improve human health and well-being.

2. Materials and methods

2.1. Study design and sample collection

A cohort of 45 pigs was enrolled in this study, and fecal and salivary samples were collected from each pig. The pigs were categorized into three age groups, with 15 pigs in each group: one-year-old pigs, those approximately 4 years old, and those approximately 8 years old. Additionally, serum samples were randomly collected from 10 pigs in each age group. This study design allowed for the collection of comprehensive and representative biological samples across different age points, which is essential for investigating the complexities of the aging process.

2.2. Shotgun metagenomic sequencing and analysis

In this study, the microbial alterations induced by age were determined by extracting DNA from saliva and fecal samples using

QIAamp DNA mini kit (QIAGEN, Germany). Shotgun metagenomic sequencing of porcine saliva and fecal DNA was performed on an Illumina HiSeq 2000 platform (Illumina, United States). To process the raw sequence reads, Trimmomatic (version 0.39) (Bolger et al., 2014) was used to remove low-quality reads and adaptors. The resulting trimmed reads were aligned to the porcine genome (*sus scrofa*, Sscrofa11.1) using Bowtie 2 (version 2.4.4) (Langmead and Salzberg, 2012) to remove host reads. The non-swine reads were assembled using MEGAHIT (v.1.1.3) with default parameters (Li et al., 2015), and taxonomy classification was performed using Kraken2 (version 2.0.8). Bracken was utilized to improve species-level abundance estimation based on Kraken2 results (Wood et al., 2019). Functional annotation of genes was performed by aligning to KEGG database using DIAMOND (v.0.9.32.133) (Buchfink et al., 2015), and the best-hit with identity ≥30% and coverage ≥70% was selected. The Chao1 and Shannon indices were calculated using the R packages picante and vegan based on the microbial abundance matrix at the species level. The dissimilarity matrix constructed using the Bray–Curtis method was employed to visualize the differences in microbiota composition between different groups.

2.3. Chemicals and regents

Sigma Aldrich provided Ammonium acetate (NH_4AC), Merck provided Acetonitrile, and Fisher provided ammonium hydroxide (NH_4OH) and methanol. Thermo Fisher provided MS-grade methanol, MS-grade acetonitrile, and HPLC-grade 2-propanol. Sigma provided HPLC-grade formic acid and HPLC-grade ammonium formate. All chemicals used in this study were of high purity and quality, ensuring the reliability and reproducibility of the results.

2.4. Analysis of plasma metabolomics

Untargeted metabolomic and lipidomic profiles of fasting serum and stool samples were measured by combining two UHPLC-MS/MS methods, including metabolites in both positive and negative ionization modes. The raw data files were processed using Compound Discoverer 3.1 (CD3.1, Thermo Fisher) to perform peak alignment, peak picking, and metabolite quantitation. The main parameters included: a retention time tolerance of 0.2 min; actual mass tolerance, 5 ppm; signal intensity tolerance of 30%; signal/noise ratio of 3; and minimum intensity of 100,000. Peak intensities were normalized to the total spectral intensity and used to predict the molecular formula based on additive ions, molecular ion peaks and fragment ions. Peaks were then matched with the mzCloud,[1] HMDB, mzVault and MassList databases for untargeted metabolomic analysis, and with the Lipidmaps and Lipidblast databases for lipidomic analysis. Accurate qualitative and relative quantitative results were thus obtained. Partial least squares discriminant analysis (PLS-DA) was used to reveal the metabolites changes in groups by R package *ropls* (Thevenot et al., 2015) and the abundance of significant metabolites with variable important in projection (VIP) >1 and with corrected *p*-value (Wilcoxon test) <0.05 were selected for enrichment analysis. The enrichment pathway of differential plasma metabolite profile between any two groups in pigs was analyzed by MetaboAnalyst 5.0[2] (Pang et al., 2022), respectively.

2.5. Sample preparation for lipidomics analyses

For the purpose of non-targeted lipid profiling, lipids were isolated from plasma samples using established techniques, as described previously (Zhou et al., 2017). Briefly, a 200 μL volume of water was added to sample and vortexed for 5 s. Subsequently, 240 μL of precooling methanol was added and the mixture vortexed for 30 s. After that, 800 μL of MTBE was added and the mixture was ultrasound 20 min at 4°C followed by sitting still for 30 min at room temperature. The solution was centrifuged at 14,000 g for 15 min at 10°C and the upper organic solvent layer was obtained and dried under nitrogen. Reverse phase chromatography was selected for LC separation using CSH C18 column (1.7 μm, 2.1 mm × 100 mm, Waters). The lipid extracts were re-dissolved in 200 μL 90% isopropanol/acetonitrile, centrifuged at 14,000 g for 15 min, finally 3 μL of sample was injected. Solvent A was acetonitrile–water (6:4, v/v) with 0.1% formic acid and 0.1 mM ammonium formate and solvent B was acetonitrile–isopropanol (1,9, v/v) with 0.1% formic acid and 0.1 mM ammonium formate. The initial mobile phase was 30% solvent B at a flow rate of 300 μL/min. It was held for 2 min, and then linearly increased to 100% solvent B in 23 min, followed by equilibrating at 5% solvent B for 10 min. Mass spectra was acquired by Q-Exactive Plus in positive and negative mode, respectively. ESI parameters were optimized and preset for all measurements as follows: source temperature, 300°C; capillary temperature, 350°C, the ion spray voltage was set at 3000 V, S-Lens RF Level was set at 50% and the scan range of the instruments was set at m/z 200–1800. "Lipid Search" is a search engine for the identification of lipid species based on MS/MS math. Lipid Search contains more than 30 lipid classes and more than 1,500,000 fragment ions in the database. Both mass tolerance for precursor and fragment were set to 5 ppm.

2.6. Statistical analysis

All statistical analyses were conducted in R platform (version 4.0). For statistic in multiple groups, we utilized Kruskal–Wallis one-way ANOVA to evaluate the difference among three groups. Only the remarkably different indices in three groups were evaluated by further Mann–Whitney *U* test with Bonferroni correction as post-hoc test between each of two groups. Values of adjusted *p*-value less than 0.05 were considered statistically significant. Error bars indicate mean ± standard error (se). The Mfuzz package in R to conduct the cluster analysis. Spearman's rank correlation coefficients were calculated and corrected for multiple testing using the Benjamini–Hochberg method. For the correlations between differentially microbial species, KO genes, metabolites, and lipidomics, a significance threshold of 0.05 and an absolute correlation threshold of 0.6 were applied.

1 https://www.mzcloud.org/

2 http://www.metaboanalyst.ca

3. Results

3.1. Description of the study

In the present research, we performed a multi-omic oral and gut microbiome study of pigs at 1 year old, 4 years old, and 8 years old. This extended previous studies that based on 16S rRNA gene sequencing and limited in gut region. This study additionally includes metagenomics analyses of the oral cavity, metabolomics, and lipidomics of serum in tested subjects (Figure 1A). We generated metagenomic data for 45 faeces and 45 saliva, while metabolomics, and lipidomics data for 30 serum samples, respectively. In sum, a total of 575.6 Gbp of DNA sequencing data was acquired.

Across all samples with available metagenomic data, the total clean DNA sequencing data amounted to 292.0096 Gbp for fecal specimens and 282.64 Gbp for sputum samples. Each sample yielded an average of 6.49 Gbp for feces and 6.28 Gbp for saliva. For serum samples, we identified 1,150 metabolites in positive ion mode and 496 in negative ion mode, and 2,402 lipids through lipidomics. By integrating these multi-omics datasets, we provide a comprehensive analysis of the changing trajectory of aging-related gut-oral microbial species, functional genes, and pathways, along with their intimate correlations with serum metabolites and lipids.

3.2. Increased alpha-diversity and altered overall saliva-faeces microbial composition in swine across different stages of age

We performed metagenomic analyses in pigs with nearly 1 year old (adult, Ad group), 4 years old (middle age, Ma) and 8 years old (old age, Oa) to explore the link between the oral-gut microbiome and different stage of ages. In faeces, Chao1 index showed significant difference among the porcine age groups, while there was no significant alteration in Shannon's diversity index between Ma and Oa groups except between Ad and Ma groups. However, in saliva samples, both alpha diversity indexes showed no statistical difference among these three groups, though consistently exhibited higher alpha diversity from Ad to Oa stage (Figures 1B,C). Furthermore, principal coordinate analysis (PCoA) based on Bray–Curtis distances from gut and oral microbiota at species showed significant separation among the three groups ($p < 0.05$; Figures 1D,E). These results all suggested that age played a great role in the composition of oral and gut microbiota of swine.

At the phylum level, we observed considerable differences in the oral and gut microbial profiles among the Ad, Ma and Oa groups. In the stool sample, the relative abundance of Firmicutes was increased in parallel with age, whereas Bacteroidetes was more abundant in the Ad group and Actinobacteria was more abundant in the Ma group (Figure 1F). In the saliva sample, we observed the relative abundance of Bacteroidetes decreased with aging. Inversely, Proteobacteria and Actinobacteria increased in the Ma and Oa groups as compared with Ad group (Figure 1G). In addition, the Firmicutes/Bacteroidetes (F/B) ratio was a measure of the relative abundance of Firmicutes and Bacteroidetes bacteria in the gut microbiome. It has been suggested that this ratio may be a useful indicator of overall gut health and may also be associated with various health conditions, we compared the ratio in the three groups. The relative abundance of Firmicute was higher in subjects of Ma and Oa groups than in the Ad group, whereas the proportion of Bacteroidetes was lower in Ma group, accordingly, we found a higher Firmicutes/Bacteroidetes ratio in the pigs of Ma group than in the Oa and Ad groups (Figure 1H).

3.3. Age-dependent taxonomic signatures of oral and gut microbial species

Previous investigations have primarily relied on 16S rDNA microbiome profiling, which has imposed limitations on the comprehensive assessment of age-related variations in the abundance of microbial species and their functional capacities within the microbial community. In the present study, our objective was to investigate the alterations in compositions and functions of the oral-gut axis microbiota associated with age. To achieve this, we employed shotgun metagenomics to analyze sputum and fecal specimens obtained from swine, enabling a more in-depth exploration of the microbial community. Furthermore, we conducted a comparative analysis of microbial abundance across different age groups to elucidate the potential impact of age on the oral-gut axis microbiota. Among the top 10 species in the Ad, Ma, and Oa groups, the most abundant in the gut were *Lactobacillus reuteri*, *Lactobacillus johnsonii*, *Lactobacillus amylovorus* (each belonging to the genus *Lactobacillus*), *Ruminococcus flavefaciens*, *Bacteroides fragilis*, and *Corynebacterium xerosis* (Figure 2A). Next, we determined differentially abundant species among the three groups and between any two groups by using Kruskal–Wallis and Wilcoxon rank-sum test analyses, respectively. Furthermore, we only considered those species that make up at least 0.05% of the relative abundance of the entire community and have adjusted *p*-values <0.05. Examination of the microbiota at the species level identified a consortium of bacteria that were significantly altered by the effect of age. When comparing the top 30 different species in each group, the majority of only Ad-enriched bacteria were from genus Bacteroides, including *Bacteroides fragilis, Bacteroides plebeius CAG:211*, and *Bacteroides plebeius*. On the other hand, the abundances of several species from genus Clostridium, comprising *Clostridium perfringens, Clostridium celatum, Clostridium disporicum*, as well as *Bifidobacterium pseudolongum* were notably enhanced in Ma group. What's more, the abundances of *Oscillibacter* sp. *57_20 s*, *Oscillibacter* sp. *CAG:155*, and *Oscillibacter* sp. *1–3* were also found increased with age (Figure 2B and Supplementary Table S1). Further, pairwise comparisons identified 62 microbial species that showed differential expression between Ma and Ad groups, 36 species between Oa and Ad groups, and 43 species between Oa and Ma groups (Supplementary Figures S1A–C and Supplementary Table S2).

We next investigated which salivary microbes show significant differences across age. We observed *Chryseobacterium taklimakanense*, *Moraxella pluranimalium, Flavobacterium ummariense,* and *Moraxella porci* were the top abundant species in the saliva samples of pigs in Ad, Ma, and Oa groups (Figures 2C). In particular, our results show a number of taxa that increase with age, including the species *Corynebacterium xerosis, Staphylococcus sciuri, Actinobacillus seminis, Escherichia coli*, and *Corynebacterium pollutisoli*, or decrease with age, including the species *Flavobacterium marinum, Flavobacterium ummariense*, *Chryseobacterium bovis*, and *Chryseobacterium hominis*

10.3389/fmicb.2023.1250891

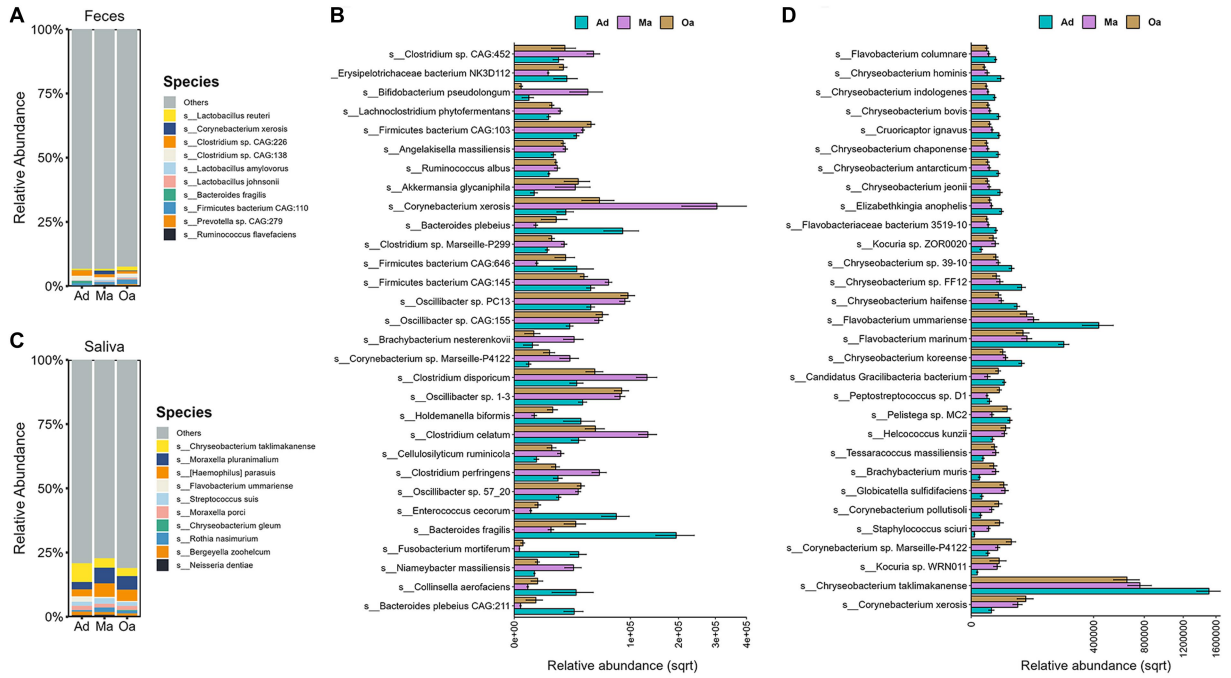

FIGURE 2
Taxonomic signatures of oral and gut microbial species showed age-dependent. **(A)** Stacked bar chart displays the top 10 most abundant microbes at species level in stool sample among the three groups. **(B)** The Kruskal–Wallis test was employed to identify microbes that differed significantly among three groups (with corrected *p*-value <0.05). The grouping error bar plot displays the top 30 microbes with the largest differences in stool samples. **(C)** The stacked bar chart displays the top 10 most abundant microbes in different groups of saliva samples, ranked by their relative abundances. **(D)** The Kruskal–Wallis test was employed to identify microbes that differed significantly among three groups (with corrected *p*-value <0.05). The grouping error bar plot displays the top 30 microbes with the largest differences in salivary samples.

(Figure 2D; Supplementary Figures S1D–F and Supplementary Table S3). In addition, a total of 66 salivary microbes were found as significantly different between Ma and Ad groups, 66 species between Oa and Ad groups, and 8 microbes between Oa and Ma groups (Supplementary Figures S1D–F and Supplementary Table S4).

3.4. Age-specific serum metabolomic and lipidomic features in domestic pigs

Serum metabolites and lipids are known to play a key role in mediating the metabolic and immune interactions between the microbiome and its host, thus providing a fundamental view into the complex dynamics of host age and physiology. To refine the metabolomic and lipidomic features across age, we performed untargeted metabolomic and lipidomic profiling by UHPLC-MS/MS analysis. A subset of 30 participants (each 10 pigs from Ad, Ma, and Oa groups) from this study was included in the serum metabonomic and lipidomic study. In serum samples, 1,646 known metabolites and 2,402 lipids were yielded. Both qualitative PCA and PLS-DA analyses were performed to evaluate metabolomic and lipidomic composition. From the prospective of serum metabolites, overall metabolic abundance of swine at different stages of age was different from that of each other as indicated by PCA analysis (Figures 3A $p < 0.05$, PERMANOVA test) and PLS-DA analysis (Supplementary Figure S2A). To identify significantly altered metabolites that may be important across the stages of age, we performed pairwise comparisons between groups. When Ma was compared with Ad, a sum of 121 metabolites were significantly altered (Figure 3B). These include the enrichment of deoxycholic acid, 1-palmitoylphosphatidylcholine, 1-methylhistidine, lipoxin a4, phenaceturic acid, and 1h-indole-3-propanoic acid. In contrast, succinate, taurine, leucine, L-isoleucine, and glutamic acid was depleted in Ma pigs compared with Ad (Supplementary Figure S2B and Supplementary Table S5). With the comparison of Oa with Ad, 113 metabolites were detected differentially abundant (Figure 3C), including the depletion of taurine, succinate, phenylalanine, glutamic acid and folinic acid in Oa. Particularly, deoxycholic acid, salicylic acid, phenaceturic acid, chenodeoxycholate, 1-palmitoyllysophosphatidylcholine, hippuric acid, and valine betaine were enriched in Oa and Ma when both compared to Ad subjects (Supplementary Figure S2C and Supplementary Table S6). Moreover, 40 metabolites were identified with differential expression in Oa and Ma groups. Notably, sarcosine, 1-palmitoyl-lysophosphatidylcholine and histamine were found to show increasing trends from Ad, through Ma, to Oa (Figure 3D; Supplementary Figure S2D and Supplementary Table S7). Among them, four metabolites (5-methoxymethylone, pro-hyp, 1-palmitoyl-lysophosphatidylcholine, and 17,20-dimethyl prostaglandin F1alpha) overlapped with those of aging correlations (Figures 3E,F), suggesting their potential contribution to the progression of different stages of age. Furthermore, MetaboAnalyst was used for searching KEGG database to explore the most relevant metabolic pathways based on differential metabolites from each pair of inter-group differential analyses. Valine, leucine and isoleucine biosynthesis, and Histidine metabolism were significantly influenced by age (Figure 3G).

10.3389/fmicb.2023.1250891

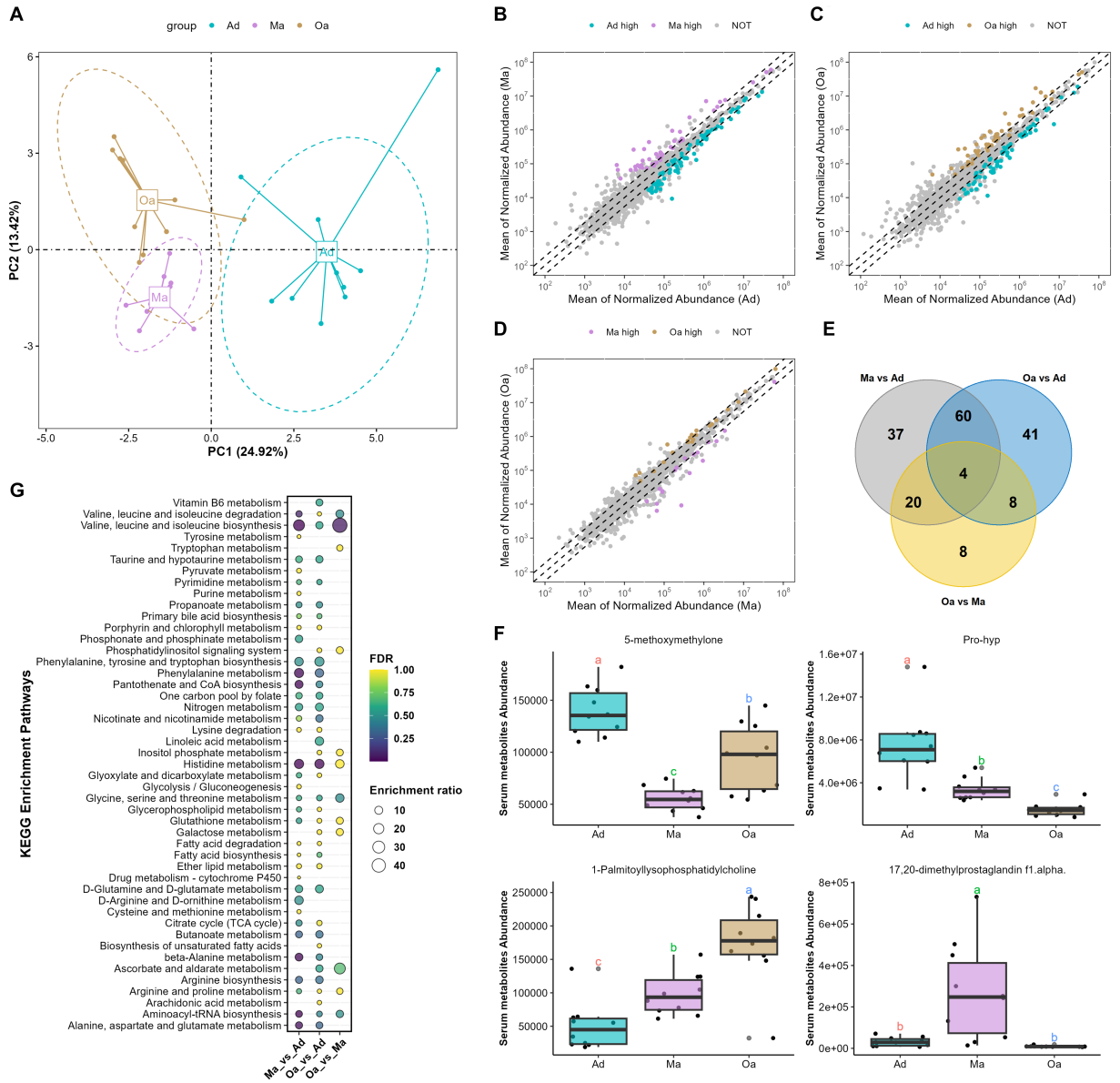

FIGURE 3
Aging altered the overall serum metabolites composition. **(A)** Principal component analysis (PCA) of serum metabolomics data revealed a significant deviation in metabolite composition among different age groups. **(B)** Compared Ma with Ad group, scatter plot showed that 44 metabolites with significantly higher abundance in Ma group are indicated with purple, while the 77 metabolites with significantly higher abundance in Ad group are in cyan. **(C)** Scatter plot showed that 48 metabolites with significantly higher abundance in Oa group are indicated with brown, while the 65 metabolites with significantly higher abundance in Ad group are in cyan. **(D)** Scatter plot showed that 22 metabolites with significantly higher abundance in Oa group are indicated with brown, while the 18 metabolites with significantly higher abundance in Ma group are in purple. **(E)** The Venn diagram illustrated the intersection based on significant differential metabolites derived from any two groups, and revealing that 4 metabolites were present in the differential results of all 3 pairwise comparisons. **(F)** The box plot displays the relative abundances of intersecting 4 metabolites across different age groups, with letters above the plot indicating significant differences between groups. Different letters between two groups indicate significant differences. **(G)** A metabolic pathway analysis was performed based on metabolites showing differences between pairwise groups. The size of the circles represents the degree of pathway enrichment, while the color of the circles indicates the significance of the pathway.

Next, among these lipids detected in different stages of pigs, the top 5 classes were represented as following: triacylglycerols (TGs), phosphatidylcholines (PCs), sphingomyelins (SMs), (DG), and (ChE) (Supplementary Figures S2A–C). PLS-DA analysis of differentially altered lipids (DALs) indicated that serum lipid profiles were dramatically shifted from Ad, through Ma to Oa pigs (Supplementary Figure S2D). To determine the temporal characteristics of the complete lipidomic dataset, Mfuzz was used for clustering analysis of 1,087 DALs across different stages of age, which divided all the DALs into 4 clusters (Figure 4A and Supplementary Table S8). As shown in Figure 4B, Cluster 1 and Cluster 4 were presented with an increasing trend in Ma and Oa groups when compared to the Ad group. We next found the DALs in Cluster 2 were exhibited a progressively declined in over the course of aging. However, it is also noteworthy that the levels of DALs in Cluster 3 were all dramatically decreased in Ma group.

10.3389/fmicb.2023.1250891

We then found that 35.98, 14.29, and 12.17% of DALs in Cluster 1 belongs to the lipid classes of triglyceride (TG), phosphatidylcholine (PC), and diradylglycerols (DG), respectively (Figure 4C). Within Cluster 2, 9.13% of DALs are TG, 19.8% are sphingomyelins (SM), 16.89% are ceramide (Cer), and 6.59% are PC (Figure 4D). These DALs were gradually decreased over age, suggesting that these DALs were specific diminished in response to the physiological alteration in relating to aging. The lipidomic analysis also showed that 20.82% of DALs in Cluster 3 were TG, and 17.14% were SM (Figure 4E). Additionally, when compared to pigs in Ad and Ma groups, swine in Oa was more profoundly in increasing the abundances of DALs in Cluster 4, in which 18.89% were TG, 27.42% were PC, and 13.13% were DG (Figure 4F). Furthermore, paired comparisons revealed 32 lipids exhibited significant differences between the Oa and Ma group, whereas 82 and 67 features showed obvious differences between the Ad versus the Ma and the Oa group, respectively (FDR <0.05, Supplementary Table S9). Of these significantly changed lipids, we screened out three lipids with significant differences in expression among the three groups (Figure 4G). The abundance of these three lipids were displayed in Figures 4H–J.

3.5. Summary of age-associated changes in microbial genes through KO genes and KEGG pathway modules

Considering the multi-omics shift of the gut microbiome and metabolome with age, we hypothesized that metabolite and lipid differences might reflect differences in microbial enzyme gene expression. To further determine the microbial metabolic processes occurring in swine at different stages of age, we annotated metagenome-analysed microbial genes in the KEGG orthology (KO) database. Firstly, PCA analyses based on KO genes and functional ko pathways in faeces and saliva samples displayed a significantly different distribution of KO genes among three groups (Figures 5A,B; Supplementary Figures S3A,B). To examine the effect of age on influencing the prevalence of microbial enzymatic genes, we compared the relative abundance of KO genes among the three groups and between each of two groups. Notably, we observed a sum of 99 KO genes within the intestinal microbiota were showed significantly different in abundance in swine among three groups (Figure 5C and Supplementary Table S10). Among the differentially abundant genes, *gluA* and *pgm* gene abundance showed a tendency to rise gradually with increasing age. In the saliva samples of swine, 35 differentially

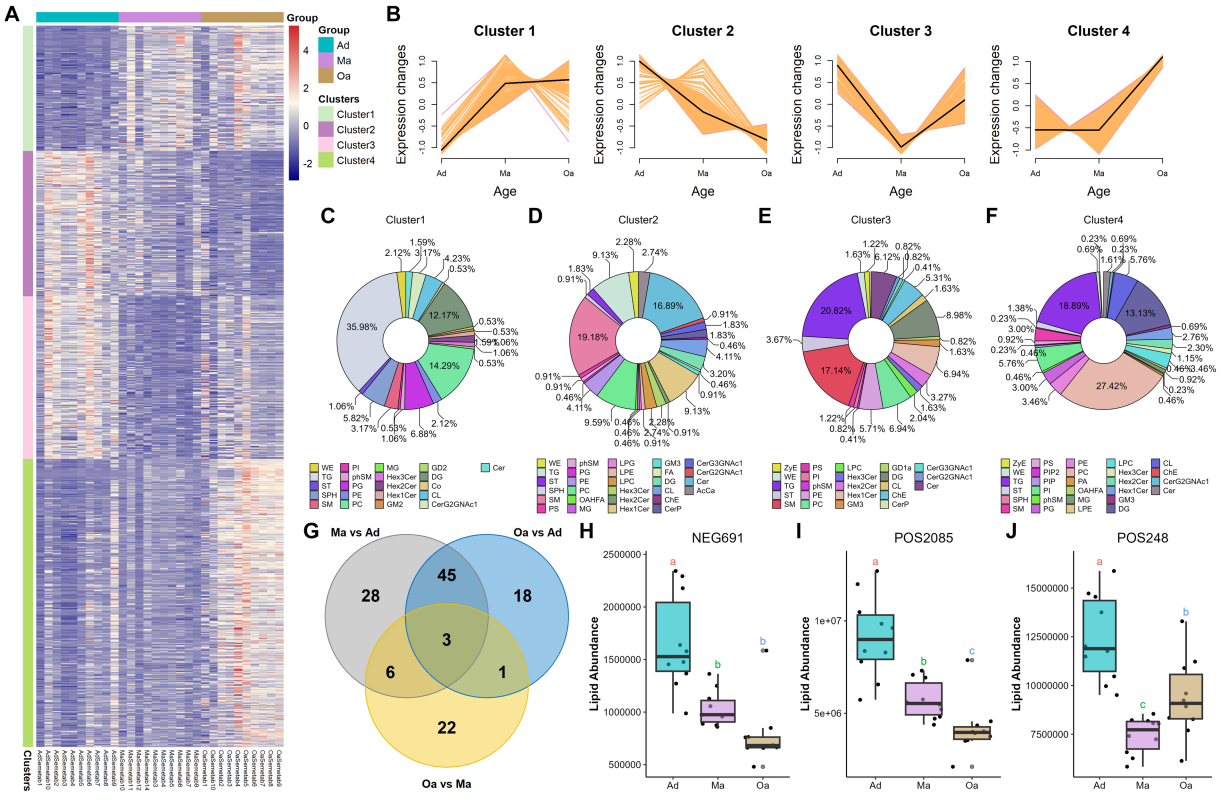

FIGURE 4
Significant differences in lipid profiles among different age groups. **(A)** The differentially altered lipids (DALs) that showed significant changes were clustered and represented in a heatmap. **(B)** Four clusters (Clusters 1–4) were highlighted, and the trend lines indicating the change in serum levels of these differentially altered lipids (DALs) were displayed. **(C–F)** The differentially altered lipids (DALs) in each cluster were further subcategorized based on their lipid classes. **(G)** The Venn diagram illustrated the intersection based on significant differential lipids derived from any two groups, and revealing that 3 lipids were present in the differential results of all 3 pairwise comparisons. **(H–J)** The box plot displays the relative abundances of intersecting 3 lipids across different age groups, with letters above the plot indicating significant differences between groups. Different letters between two groups indicate significant differences.

expressed KO genes encoded by oral microbiota were detected (Supplementary Figure S3C and Supplementary Table S11), such as *glnA*, which dominant in Oa group, but had the lowest abundance in Ma group. Intriguingly, we found 13 discrepant KO genes that were intersected in the intestinal and salivary microbiota (Figure 5D). For instance, K03496 and K06180 were simultaneously enriched in the gut and salivary microbiome of Ad group. Overall, these intersecting differential genes are not similarly enriched across groups (Figures 5E,F). In the KO map analyses of gut microbial metabolism in the three stages of age, which revealed that the abundance of ko04217 (cell growth and death; necroptosis), ko05152 (infection disease; bacterial; tuberculosis) and ko04727 (nervous system; GABAergic synapse) were progressively increased from Ad group, through Ma group, to Oa group (Figure 5G and Supplementary Table S12). Among the differentially abundant pathways in salivary microbiota, we identified the dominant KEGG pathways that were enriched in the Oa group as the following, including ko01523 (drug resistance: antineoplastic; antifolate resistance), ko04211 and ko04213 (aging: longevity regulating pathway), and ko05134 (infectious diseases: bacterial; legionellosis), while amino acid metabolism (ko00200, ko00430, ko00471), cofactors and vitamins (ko00670), as well as Carbohydrate metabolism (ko00053, ko00520, ko00052) were mainly increased in Ma group (Supplementary Figure S3D and Supplementary Table S13). Furthermore, Venn diagram analysis revealed that 26 discriminatorily abundant ko maps that were present in both the oral and gut microbiota (Supplementary Figure S3E), of which the Pyruvate metabolism (ko00620) was increased progressively, and Peroxisome (ko04146) was declined gradually from Ad to Ma and then to Oa group (Supplementary Figures S3F,G).

3.6. The association between metabolites, lipids, and oral-gut microbiome in swine at different stages of age

The present investigation employed an intrinsic multi-omics analysis to elucidate the microbial features present in saliva, stool, serum metabolites, and lipids, demonstrating varied expression patterns among pigs at different age stages. Moreover, an association analysis was performed to comprehend the interplay between the altered oral-gut microbiota and the differentially abundant serum metabolites and lipids, utilizing Spearman rank correlation analysis. This analytical strategy facilitated the identification of co-varying features that relied on their mutual covariation with the ageing process. These findings provide valuable insights into the intricate interactions among diverse biological systems while highlighting potential avenues for further research in this domain. Notably, we observed significant disparities in the distribution of associations between paired microbial species and serum metabolites and lipids across various age stages. Specifically, when initially correlating these paired features to distinguish between pigs in the Ad group and Ma group, a multitude of positively and negatively associated features were detected (absolute coefficients >0.7 and FDR <0.05) (Figure 6A

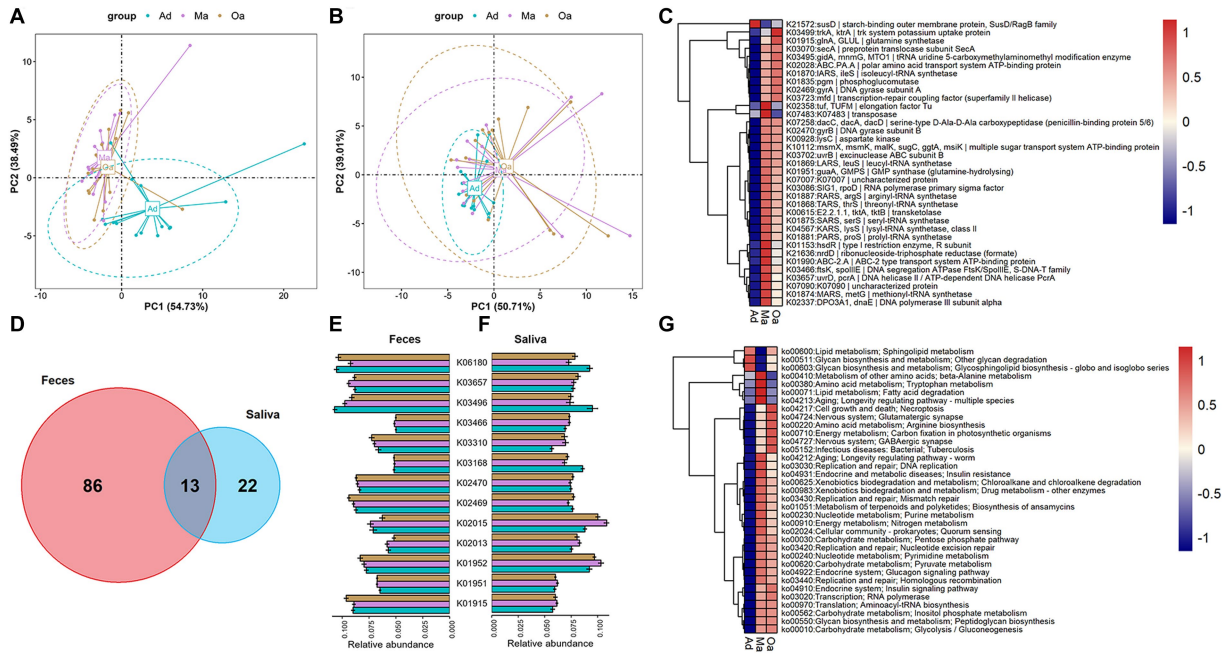

FIGURE 5
The alterations in the KO functional genes and pathways of the oral-gut microbiome that occur with aging. **(A,B)** Principal component analysis (PCA) based on KO genes and pathways of the microbiome in stool revealed a distinct separation trend between different groups. **(C)** The heatmap displays the abundance of differentially expressed KO genes in the microbiome of fecal samples across three groups. The abundance of each KO gene is represented by the mean value of the samples in each group. **(D)** A Venn diagram illustrates the intersection of differentially expressed KO genes in fecal samples across three groups and differentially expressed KO genes in saliva samples across three groups. **(E,F)** The bar chart (with error bars) displays the abundance of 13 differentially expressed KO genes that are present in both fecal **(E)** and saliva samples **(F)**. **(G)** The heatmap displays the abundance of differentially expressed KO pathways in the microbiome of fecal samples across three groups. The abundance of each KO pathways is represented by the mean value of the samples in each group.

10.3389/fmicb.2023.1250891

and Supplementary Table S14). Among the four metabolites that significantly discriminate between any two comparisons, it was observed that the abundance of several microbial species, such as *Bacteroides fragilis*, *Bacteroides plebeius* CAG:211, *Enterococcus cecorum*, *Oscillibacter* sp. CAG:241, *Oscillibacter* sp. CAG:241_62_21, *Firmicutes bacterium* CAG:83, *Fusobacterium mortiferum*, and *Fusobacterium necrophorum*, exhibited a negative correlation with 1-palmitoyl-lysophosphatidylcholine (Figures 6B–I). Similarly, species of *Clostridium botulinum*, *Clostridium celatum*, and *Clostridium disporicum* also exhibited an anticorrelation with the serum level of pro-hyp (Figures 6K,L). Additionally, a total of 161 associations between stool microbial species and serum lipids were identified (Supplementary Figure S4A and Supplementary Table S15). We further examined the association patterns between two lipids that significantly decreased from Ad, through Ma, to Oa, and stool microbes. It was observed that *Bacteroides fragilis*, *Bacteroides plebeius* CAG:211, and *Fusobacterium mortiferum* were positively associated with SM(d36:1) + HCOO (Supplementary Figures S4B,D). Interestingly, we also observed that the relative abundance of *Bacteroides fragilis*, *Bacteroides plebeius* CAG:211, and *Fusobacterium mortiferum* were positively correlated with SM(d38:4) + H (Supplementary Figures S4E–G). We also evaluated the associations between salivary microbes and serum metabolites and lipids, as described above. The number of correlations reached 301 and 476, respectively, by the time the association analysis was conducted between salivary microbes and serum metabolites and lipids (Supplementary Figures S5A, S6A and Supplementary Tables S16, S17). As shown in Supplementary Figures S5B–D, 1-palmitoyl-lysophosphatidylcholine was positively correlated with salivary *Kocuria* sp. ZOR0020, *Nigerium massiliense*, and *Staphylococcus sciuri*. Additionally, pro-hyp exhibited a positive association with *Flavobacterium columnare* and *Flavobacterium marinum* (Supplementary Figures S5E,F). Additionally, our investigation revealed that SM(d36:1) + HCOO declined with age and exhibited a negative correlation with eight salivary microbes. Notably, we observed a positive association between SM(d36:1) + HCOO and *Pelistega* sp. MC2 (Supplementary Figures S6B–J). Besides, we observed that SM(d38:4) + H exhibited an inverse correlation with

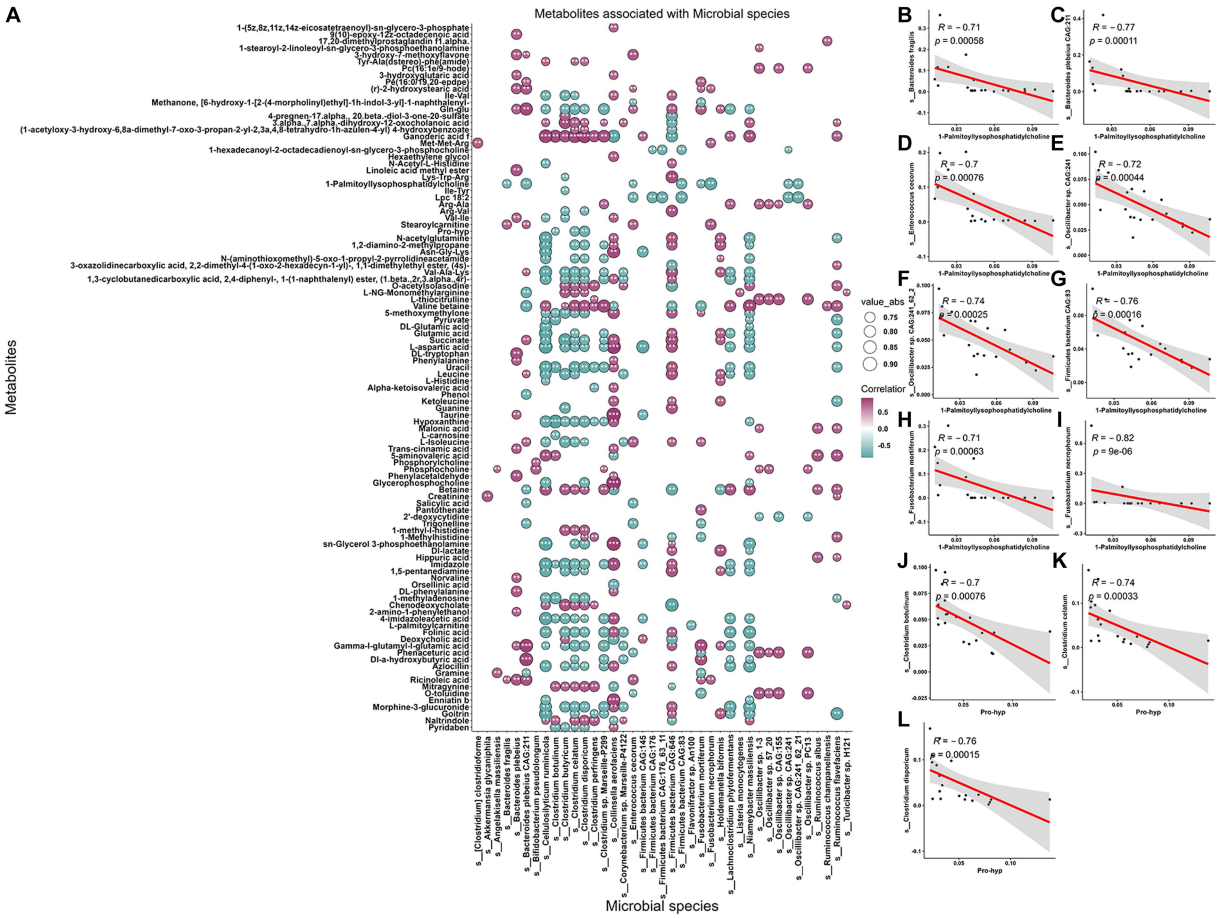

FIGURE 6
Association between metabolites, and gut microbiome of the swine in Ad and Ma groups. **(A)** The correlations between fecal microbes and serum metabolites were calculated. The absolute correlation coefficient (|*r*|) is represented by the size of the circle, and the adjusted *p*-value is indicated by an asterisk ("*", $p < 0.05$, "**", $p < 0.01$, "***", $p < 0.001$). **(B–I)** Scatter plot representing the relationship between 1-palmitoyl-lysophosphatidylcholine and *Bacteroides fragilis*, *Bacteroides plebeius* CAG:211, *Enterococcus cecorum*, *Oscillibacter* sp. CAG:241, *Oscillibacter* sp. CAG:241_62_21, *Firmicutes bacterium* CAG:83, *Fusobacterium mortiferum*, and *Fusobacterium necrophorum*, respectively, by using Spearman rank sum test. **(J–L)** The relationship between pro-hyp and *Clostridium botulinum, Clostridium celatum, and Clostridium disporicum* was analyzed using a scatter plot and Spearman rank sum test.

four salivary microbes and a positive association with one salivary microbe (Supplementary Figures S6K–O). Furthermore, the results of the association analysis for paired microbiome, metabolites, and lipids in others any two groups are presented in Supplementary Tables S18–S25.

4. Discussion

Ageing is a significant risk factor for several age-related diseases, such as non-alcoholic fatty liver disease (NAFLD), type 2 diabetes mellitus, cardiovascular disease, neurodegenerative diseases, and cancer (Guo et al., 2022). To gain a better understanding of the ageing process, researchers have identified twelve hallmarks that contribute to this process. These hallmarks encompass genomic instability, telomere attrition, epigenetic alterations, loss of proteostasis, disabled macroautophagy, deregulated nutrient sensing, mitochondrial dysfunction, cellular senescence, stem cell exhaustion, altered intercellular communication, chronic inflammation, and dysbiosis. By comprehending these hallmarks and their underlying mechanisms, strategies can be developed to promote healthy ageing and, potentially, prevent or treat age-related diseases (Lopez-Otin et al., 2023). While the significant role of gut microbiota in influencing host health and disease has been well-established (Lynch and Pedersen, 2016), a comprehensive understanding of the intricate structure of the gut microbiome and the underlying mechanisms that interact with host aging in domestic pigs is still lacking. Therefore, the primary aim of this investigation is to discern the age-related alterations in both the oral and gut microbiome, as well as blood metabolites and lipids. By conducting this study under relatively uniform conditions, we seek to unravel the inter-relationships among these factors and shed light on the complex dynamics of host-microbiota interactions during the aging process.

In the current study, we investigated the effects of aging on oral-gut microbiome by utilizing multi-omics approaches, including shotgun metagenomics, LC-MS untargeted metabolomics and lipidomics analysis, and proteomics. In summary, our findings demonstrate that the elderly swine, particularly the Oa group, exhibited higher gut microbial diversity in both saliva and stool samples compared to the younger group living in the same farm, which in accordance with previous studies. Nevertheless, recent studies have revealed that centenarians are commonly associated with lower alpha diversity in their gut microbiome, as well as a decrease in butyrate-producing bacteria such as *Faecalibacterium*, *Roseburia*, and *Eubacterium*, instead with increased opportunistic pathogens (Biagi et al., 2017). Additionally, it is common for individuals to experience an upsurge in opportunistic pathogens within their gut microbiome, potentially due to a reduction in immune system function that results in a decrease in the population of beneficial gut bacteria. This decline in beneficial bacteria can lead to an amplification of opportunistic bacteria that may exert detrimental effects on health (Bosco and Noti, 2021). The observed increase in microbial diversity may signify a compensatory mechanism in response to the decline in beneficial gut bacteria, as the body endeavors to maintain a microbial equilibrium within the gut. Moreover, the greater alpha diversity observed in elderly individuals may be linked to longer colonic transit times and heightened exposure to environmental influences relative to younger individuals (Graff et al., 2001; Roager et al., 2016). Our research has revealed distinctive structural and functional traits of the gut microbiome in Oa pigs, highlighting an elevated abundance of specific beneficial bacterial species, including *Akkermansia*, in elderly swine. On the other hand, our study has demonstrated that aging is correlated with an increasing prevalence of pathogenic bacteria in the salivary microbiome, suggesting that alterations in the salivary microbiome may serve as a more precise indicator of the aging process within the body. Despite the clinical significance of gut microbiota composition, there is a paucity of research investigating the age-related dynamics of the microbiota, including changes in the F/B ratio. Only a limited number of researches have focused on examining the age-related changes in the F/B ratio in swine. This highlights the need for further research to better understand the dynamics of the gut microbiota throughout the aging process and its impact on host health and diseases. In this research, the F/B ratio was found to sharply increase from Ad to Ma, and then just as slightly decreased from Ma to Oa group, which exhibited controversy against previous reports (Makivuokko et al., 2010; Claesson et al., 2011; Kim et al., 2019). Research has shown that individuals with obesity and metabolic diseases typically have a higher F/B ratio, whereas those who are healthy have a lower ratio (Crovesy et al., 2020; Magne et al., 2020). Pigs belonging to the Oa group exhibited a higher F/B ratio compared to adult pigs, indicating dysbiosis in the gut microbiota of elderly swine, which may be linked to age-related diseases in pigs. Moreover, some studies have suggested that a higher F/B ratio could lead to increased energy harvest from the diet, subsequently resulting in weight gain, which may explain why pigs in the Ma group in the production phase require more energy to support their reproductive performance. During this period, sows generally gain weight and participate in reproductive and lactation activities, which necessitate greater nutrient intake, particularly energy. Therefore, further research is required to fully comprehend the intricate relationship between the F/B ratio and host aging.

Notably, it has been documented that aging is accompanied with chronic inflammation and inflamm-aging provided the possibility of studying aging-related diseases from a promising viewpoint (Kovtonyuk et al., 2016). 1-palmitoyl-lysophosphatidylcholine (1-PC) is reported as a bioactive lipid molecule that has been shown to play a role in inflammation (Hung et al., 2012; Liu et al., 2020). It is a type of lysophosphatidylcholine (LPC), which is a class of phospholipids that are involved in various physiological processes (Schmitz and Ruebsaamen, 2010; Law et al., 2019; Liu et al., 2020). Studies have found that 1-PC can activate immune cells such as macrophages and neutrophils, leading to the production of pro-inflammatory cytokines and chemokines (Liu et al., 2020). In addition, 1-PC has been shown to stimulate the production of reactive oxygen species (ROS), which can contribute to inflammation and tissue damage (Yoder et al., 2014). Furthermore, elevated levels of 1-PC have been observed in various inflammatory conditions such as atherosclerosis, and joint pain (Liu et al., 2020; Jacquot et al., 2022). In these conditions, 1-PC is thought to contribute to the pathogenesis of the disease by promoting inflammation and tissue damage. Overall, the available evidence suggests that 1-PC is involved in the regulation of inflammation and may contribute to the development and progression of various inflammatory conditions. The present study identified that the abundance of 1-PC was increased progressively with porcine age and negatively associated with gut *Bacteroides*

fragilis, Bacteroides plebeius CAG:211, Enterococcus cecorum, but positively correlated with oral pathogenic *Staphylococcus sciuri*, and *Nigerium massiliense*. The observed increase in 1-PC levels in the bloodstream of elderly pigs may signify the manifestation of inflammaging, a chronic low-grade inflammatory state that is linked to aging. The upsurge in 1-PC may trigger the recruitment of lymphocytes and macrophages, resulting in the production of multiple inflammatory factors that can induce oxidative stress, amplify the level of inflammation in the body, and potentially fuel the onset of various age-related ailments. The correlation analyses revealed that there may be a complex interplay between these microbial species and this particular serum metabolite, which could potentially have implications for pig health and well-being. However, further research is needed to fully understand the mechanisms underlying these associations and their potential impact on pig health.

Pro-hyp is a dipeptide composed of proline and hydroxyproline that is found in collagen, a major component of connective tissues such as skin, tendons, and cartilage (Ohara et al., 2010; Ide et al., 2021). Collagen is produced by fibroblasts in various tissues throughout the body and is subsequently broken down into smaller peptides, predominantly pro-hyp, through various enzymatic processes (Ohara et al., 2007). Pro-hyp could be absorbed into circulation and transported to other tissues, where it exerts various beneficial effects, including anti-inflammatory, improve skin anti-decrepitude function and ameliorated joint condition (Zhang et al., 2010; Sontakke et al., 2016; Lee et al., 2019; Aguirre-Cruz et al., 2020). Osteoporosis is a disease characterized by low bone mass and structural deterioration of bone tissue, leading to increased bone fragility and a higher risk of fractures. Aging is a major risk factor for osteoporosis, as bone mass tends to decline with age. This is due to a combination of factors, including hormonal changes, decreased physical activity, and altered microbial composition. Studies have found that changes in the gut microbiota composition are associated with changes in bone density and structure. For example, some studies have found that the presence of certain bacterial species, such as *Lactobacillus*, is associated with increased bone density, while other species, such as *Prevotella*, are associated with decreased bone density. In our study, we discovered the declined level of pro-hyp in pigs progressively with age. In addition, we also found a significant negative correlation between decreased levels of pro-hyp and the abundance of gut *Clostridium botulinum*, *Clostridium disporicum* and *Clostridium celatum*, while showed a significant positive association with salivary *Flavobacterium columnare*, and *Flavobacterium marinum*. This could be due to the fact that gut bacteria, which are significantly negatively correlated with pro-hyp levels, increase in abundance with age, while oral microbiota, which are positively correlated with pro-hyp levels, decrease with age. In summary, the findings of this study suggest that supplementation with pro-hyp and probiotics that have the capacity to produce or process pro-hyp may represent a potential strategy for ameliorating age-related skeletal and skin aging. Notably, the interaction between pro-hyp and host microbiota shows promise as a novel avenue for the development of therapeutic interventions for aging-related disorders, including improved joint health and skin elasticity. These results have implications for the development of targeted therapies aimed at mitigating the negative effects of aging on the musculoskeletal and integumentary systems.

In summary, this investigation employed a unique approach by utilizing pigs residing in a controlled farm environment to mitigate confounding variables. The study revealed notable age-dependent modifications in both the structure and function of the oral and gut microbiota, as well as alterations in circulating levels of metabolites and lipids. Furthermore, we identified numerous interrelationships between perturbed microbial species and serum molecules, potentially influencing the maintenance of health and the development of diseases throughout different stages of host development and aging. However, the challenge of mitigating harmful inflamm-aging factors to promote healthy aging remains a significant obstacle. These findings hold significant implications for the advancement of therapeutic interventions and the progress of clinical applications targeting age-related diseases, utilizing pigs as a naturally aging animal model.

Data availability statement

The original contributions presented in the study are publicly available. This data can be found here: NCBI SRA, PRJNA1015378.

Ethics statement

The animal study was approved by All procedures were conducted according to the Regulations for the Administration of Affairs Concerning Experimental Animals (Ministry of Science and Technology, China, revised in March 2017), and approved by the Institutional Animal Care and Use Committee at the Experimental Animal Center of Hainan Academy of Agricultural Science (HNXMSY-20210503). The study was conducted in accordance with the local legislation and institutional requirements.

Author contributions

GL and JZ conceived and designed the experiments and revised the manuscript. CQ, MH, and SW performed the experiments, analyzed the data, and wrote the manuscript. XJ, FW, XL, ST, ZC, WX, SG, JY, QL, XZ, and ZX collected the samples and performed the experiments. All authors contributed to the article and approved the submitted version.

Funding

This work was supported by the grant from the Science and Technology Planning Project of Hainan Province (SQKY2022-0015), National Natural Science Foundation of China (Grant number 32260138), Project of Sanya Yazhou Bay Science and Technology City (Grant number SCKJ-JYRC-2022-97), Seed Laboratory of Yazhou Bay, Hainan Province (Grant number B22C11209), and UNDP-GEF Participatory *in-situ* conservation and sustainable use of agrobiodiversity in Hainan and Scientific Research of BSKY (XJ201922) from Anhui Medical University.

Conflict of interest

The authors declare that the research was conducted in the absence of any commercial or financial relationships that could be construed as a potential conflict of interest.

Publisher's note

All claims expressed in this article are solely those of the authors and do not necessarily represent those of their affiliated organizations, or those of the publisher, the editors and the reviewers. Any product that may be evaluated in this article, or claim that may be made by its manufacturer, is not guaranteed or endorsed by the publisher.

Supplementary material

The Supplementary material for this article can be found online at: https://www.frontiersin.org/articles/10.3389/fmicb.2023.1250891/full#supplementary-material

References

Aguirre-Cruz, G., Leon-Lopez, A., Cruz-Gomez, V., Jimenez-Alvarado, R., and Aguirre-Alvarez, G. (2020). Collagen hydrolysates for skin protection: oral administration and topical formulation. *Antioxidants* 9:181. doi: 10.3390/antiox9020181

Ansaldo, E., Farley, T. K., and Belkaid, Y. (2021). Control of immunity by the microbiota. *Annu. Rev. Immunol.* 39, 449–479. doi: 10.1146/annurev-immunol-093019-112348

Badal, V. D., Vaccariello, E. D., Murray, E. R., Yu, K. E., Knight, R., Jeste, D. V., et al. (2020). The gut microbiome, aging, and longevity: a systematic review. *Nutrients* 12:3759. doi: 10.3390/nu12123759

Bana, B., and Cabreiro, F. (2019). The microbiome and aging. *Annu. Rev. Genet.* 53, 239–261. doi: 10.1146/annurev-genet-112618-043650

Belkaid, Y., and Hand, T. W. (2014). Role of the microbiota in immunity and inflammation. *Cells* 157, 121–141. doi: 10.1016/j.cell.2014.03.011

Biagi, E., Rampelli, S., Turroni, S., Quercia, S., Candela, M., and Brigidi, P. (2017). The gut microbiota of centenarians: signatures of longevity in the gut microbiota profile. *Mech. Ageing Dev.* 165, 180–184. doi: 10.1016/j.mad.2016.12.013

Bolger, A. M., Lohse, M., and Usadel, B. (2014). Trimmomatic: a flexible trimmer for illumina sequence data. *Bioinformatics* 30, 2114–2120. doi: 10.1093/bioinformatics/btu170

Bosco, N., and Noti, M. (2021). The aging gut microbiome and its impact on host immunity. *Genes Immun.* 22, 289–303. doi: 10.1038/s41435-021-00126-8

Buchfink, B., Xie, C., and Huson, D. H. (2015). Fast and sensitive protein alignment using DIAMOND. *Nat. Methods* 12, 59–60. doi: 10.1038/nmeth.3176

Claesson, M. J., Cusack, S., O'Sullivan, O., Greene-Diniz, R., de Weerd, H., Flannery, E., et al. (2011). Composition, variability, and temporal stability of the intestinal microbiota of the elderly. *Proc. Natl. Acad. Sci. U. S. A.* 108, 4586–4591. doi: 10.1073/pnas.1000097107

Crovesy, L., Masterson, D., and Rosado, E. L. (2020). Profile of the gut microbiota of adults with obesity: a systematic review. *Eur. J. Clin. Nutr.* 74, 1251–1262. doi: 10.1038/s41430-020-0607-6

Cruz-Pereira, J. S., Moloney, G. M., Bastiaanssen, T. F. S., Boscaini, S., Tofani, G., Borras-Bisa, J., et al. (2022). Prebiotic supplementation modulates selective effects of stress on behavior and brain metabolome in aged mice. *Neurobiol. Stress* 21:100501. doi: 10.1016/j.ynstr.2022.100501

Finger, C. E., Moreno-Gonzalez, I., Gutierrez, A., Moruno-Manchon, J. F., and McCullough, L. D. (2022). Age-related immune alterations and cerebrovascular inflammation. *Mol. Psychiatry* 27, 803–818. doi: 10.1038/s41380-021-01361-1

Fulop, T., Larbi, A., Dupuis, G., le Page, A., Frost, E. H., Cohen, A. A., et al. (2017). Immunosenescence and inflamm-aging as two sides of the same coin: friends or foes? *Front. Immunol.* 8:1960. doi: 10.3389/fimmu.2017.01960

Gao, J., Xu, K., Liu, H., Liu, G., Bai, M., Peng, C., et al. (2018). Impact of the gut microbiota on intestinal immunity mediated by tryptophan metabolism. *Front. Cell. Infect. Microbiol.* 8:13. doi: 10.3389/fcimb.2018.00013

Gasaly, N., de Vos, P., and Hermoso, M. A. (2021). Impact of bacterial metabolites on gut barrier function and host immunity: a focus on bacterial metabolism and its relevance for intestinal inflammation. *Front. Immunol.* 12:658354. doi: 10.3389/fimmu.2021.658354

Ghosh, T. S., Das, M., Jeffery, I. B., and O'Toole, P. W. (2020). Adjusting for age improves identification of gut microbiome alterations in multiple diseases. *eLife* 9:e50240. doi: 10.7554/eLife.50240

Ghosh, T. S., Shanahan, F., and O'Toole, P. W. (2022). The gut microbiome as a modulator of healthy ageing. *Nat. Rev. Gastroenterol. Hepatol.* 19, 565–584. doi: 10.1038/s41575-022-00605-x

Gomaa, E. Z. (2020). Human gut microbiota/microbiome in health and diseases: a review. *Antonie Van Leeuwenhoek* 113, 2019–2040. doi: 10.1007/s10482-020-01474-7

Graff, J., Brinch, K., and Madsen, J. L. (2001). Gastrointestinal mean transit times in young and middle-aged healthy subjects. *Clin. Physiol.* 21, 253–259. doi: 10.1046/j.1365-2281.2001.00308.x

Guo, J., Huang, X., Dou, L., Yan, M., Shen, T., Tang, W., et al. (2022). Aging and aging-related diseases: from molecular mechanisms to interventions and treatments. *Signal Transduct. Target. Ther.* 7:391. doi: 10.1038/s41392-022-01251-0

Hung, N. D., Sok, D. E., and Kim, M. R. (2012). Prevention of 1-palmitoyl lysophosphatidylcholine-induced inflammation by polyunsaturated acyl lysophosphatidylcholine. *Inflamm. Res.* 61, 473–483. doi: 10.1007/s00011-012-0434-x

Ide, K., Takahashi, S., Sakai, K., Taga, Y., Ueno, T., Dickens, D., et al. (2021). The dipeptide prolyl-hydroxyproline promotes cellular homeostasis and lamellipodia-driven motility via active beta1-integrin in adult tendon cells. *J. Biol. Chem.* 297:100819. doi: 10.1016/j.jbc.2021.100819

Jacquot, F., Khoury, S., Labrum, B., Delanoe, K., Pidoux, L., Barbier, J., et al. (2022). Lysophosphatidylcholine 16:0 mediates chronic joint pain associated to rheumatic diseases through acid-sensing ion channel 3. *Pain* 163, 1999–2013. doi: 10.1097/j.pain.0000000000002596

Kim, B. S., Choi, C. W., Shin, H., Jin, S. P., Bae, J. S., Han, M., et al. (2019). Comparison of the gut microbiota of centenarians in longevity villages of South Korea with those of other age groups. *J. Microbiol. Biotechnol.* 29, 429–440. doi: 10.4014/jmb.1811.11023

Kong, F., Deng, F., Li, Y., and Zhao, J. (2019). Identification of gut microbiome signatures associated with longevity provides a promising modulation target for healthy aging. *Gut Microbes* 10, 210–215. doi: 10.1080/19490976.2018.1494102

Kovtonyuk, L. V., Fritsch, K., Feng, X., Manz, M. G., and Takizawa, H. (2016). Inflamm-aging of hematopoiesis, hematopoietic stem cells, and the bone marrow microenvironment. *Front. Immunol.* 7:502. doi: 10.3389/fimmu.2016.00502

Langmead, B., and Salzberg, S. L. (2012). Fast gapped-read alignment with Bowtie 2. *Nat. Methods* 9, 357–359. doi: 10.1038/nmeth.1923

Law, S. H., Chan, M. L., Marathe, G. K., Parveen, F., Chen, C. H., and Ke, L. Y. (2019). An updated review of lysophosphatidylcholine metabolism in human diseases. *Int. J. Mol. Sci.* 20:1149. doi: 10.3390/ijms20051149

Lee, H. J., Jang, H. L., Ahn, D. K., Kim, H. J., Jeon, H. Y., Seo, D. B., et al. (2019). Orally administered collagen peptide protects against UVB-induced skin aging through the absorption of dipeptide forms, gly-pro and pro-hyp. *Biosci. Biotechnol. Biochem.* 83, 1146–1156. doi: 10.1080/09168451.2019.1580559

Li, D., Liu, C. M., Luo, R., Sadakane, K., and Lam, T. W. (2015). MEGAHIT: an ultra-fast single-node solution for large and complex metagenomics assembly via succinct de Bruijn graph. *Bioinformatics* 31, 1674–1676. doi: 10.1093/bioinformatics/btv033

Lim, M. Y., Song, E. J., Kang, K. S., and Nam, Y. D. (2019). Age-related compositional and functional changes in micro-pig gut microbiome. *Geroscience* 41, 935–944. doi: 10.1007/s11357-019-00121-y

Liu, P., Zhu, W., Chen, C., Yan, B., Zhu, L., Chen, X., et al. (2020). The mechanisms of lysophosphatidylcholine in the development of diseases. *Life Sci.* 247:117443. doi: 10.1016/j.lfs.2020.117443

Lopez-Otin, C., Blasco, M. A., Partridge, L., Serrano, M., and Kroemer, G. (2023). Hallmarks of aging: an expanding universe. *Cells* 186, 243–278. doi: 10.1016/j.cell.2022.11.001

Lunney, J. K., Van Goor, A., Walker, K. E., Hailstock, T., Franklin, J., and Dai, C. (2021). Importance of the pig as a human biomedical model. *Sci. Transl. Med.* 13:eabd5758. doi: 10.1126/scitranslmed.abd5758

Lynch, S. V., and Pedersen, O. (2016). The human intestinal microbiome in health and disease. *N. Engl. J. Med.* 375, 2369–2379. doi: 10.1056/NEJMra1600266

Magne, F., Gotteland, M., Gauthier, L., Zazueta, A., Pesoa, S., Navarrete, P., et al. (2020). The Firmicutes/Bacteroidetes ratio: a relevant marker of gut dysbiosis in obese patients? *Nutrients* 12:1474. doi: 10.3390/nu12051474

Makivuokko, H., Tiihonen, K., Tynkkynen, S., Paulin, L., and Rautonen, N. (2010). The effect of age and non-steroidal anti-inflammatory drugs on human intestinal microbiota composition. *Br. J. Nutr.* 103, 227–234. doi: 10.1017/S0007114509991553

Manor, O., Dai, C. L., Kornilov, S. A., Smith, B., Price, N. D., Lovejoy, J. C., et al. (2020). Health and disease markers correlate with gut microbiome composition across thousands of people. *Nat. Commun.* 11:5206. doi: 10.1038/s41467-020-18871-1

Molinero, N., Antón-Fernández, A., Hernández, F., Ávila, J., Bartolomé, B., and Moreno-Arribas, M. V. (2023). Gut microbiota, an additional hallmark of human aging and neurodegeneration. *Neuroscience* 518, 141–161. doi: 10.1016/j.neuroscience.2023.02.014

Ohara, H., Ichikawa, S., Matsumoto, H., Akiyama, M., Fujimoto, N., Kobayashi, T., et al. (2010). Collagen-derived dipeptide, proline-hydroxyproline, stimulates cell proliferation and hyaluronic acid synthesis in cultured human dermal fibroblasts. *J. Dermatol.* 37, 330–338. doi: 10.1111/j.1346-8138.2010.00827.x

Ohara, H., Matsumoto, H., Ito, K., Iwai, K., and Sato, K. (2007). Comparison of quantity and structures of hydroxyproline-containing peptides in human blood after oral ingestion of gelatin hydrolysates from different sources. *J. Agric. Food Chem.* 55, 1532–1535. doi: 10.1021/jf062834s

Ohtani, N., and Hara, E. (2021). Gut-liver axis-mediated mechanism of liver cancer: a special focus on the role of gut microbiota. *Cancer Sci.* 112, 4433–4443. doi: 10.1111/cas.15142

Pang, Z., Zhou, G., Ewald, J., Chang, L., Hacariz, O., Basu, N., et al. (2022). Using MetaboAnalyst 5.0 for LC-HRMS spectra processing, multi-omics integration and covariate adjustment of global metabolomics data. *Nat. Protoc.* 17, 1735–1761. doi: 10.1038/s41596-022-00710-w

Pascale, A., Marchesi, N., Govoni, S., Coppola, A., and Gazzaruso, C. (2019). The role of gut microbiota in obesity, diabetes mellitus, and effect of metformin: new insights into old diseases. *Curr. Opin. Pharmacol.* 49, 1–5. doi: 10.1016/j.coph.2019.03.011

Pellanda, P., Ghosh, T. S., and O'Toole, P. W. (2021). Understanding the impact of age-related changes in the gut microbiome on chronic diseases and the prospect of elderly-specific dietary interventions. *Curr. Opin. Biotechnol.* 70, 48–55. doi: 10.1016/j.copbio.2020.11.001

Peng, X., Cheng, L., You, Y., Tang, C., Ren, B., Li, Y., et al. (2022). Oral microbiota in human systematic diseases. *Int. J. Oral Sci.* 14:14. doi: 10.1038/s41368-022-00163-7

Roager, H. M., Hansen, L. B., Bahl, M. I., Frandsen, H. L., Carvalho, V., Gøbel, R. J., et al. (2016). Colonic transit time is related to bacterial metabolism and mucosal turnover in the gut. *Nat. Microbiol.* 1:16093. doi: 10.1038/nmicrobiol.2016.93

Rose, E. C., Blikslager, A. T., and Ziegler, A. L. (2022). Porcine models of the intestinal microbiota: the translational key to understanding how gut commensals contribute to gastrointestinal disease. *Front. Vet. Sci.* 9:834598. doi: 10.3389/fvets.2022.834598

Schmitz, G., and Ruebsaamen, K. (2010). Metabolism and atherogenic disease association of lysophosphatidylcholine. *Atherosclerosis* 208, 10–18. doi: 10.1016/j.atherosclerosis.2009.05.029

Sedghi, L., DiMassa, V., Harrington, A., Lynch, S. V., and Kapila, Y. L. (2021). The oral microbiome: role of key organisms and complex networks in oral health and disease. *Periodontol.* 87, 107–131. doi: 10.1111/prd.12393

Sontakke, S. B., Jung, J. H., Piao, Z., and Chung, H. J. (2016). Orally available collagen tripeptide: enzymatic stability, intestinal permeability, and absorption of gly-pro-hyp and pro-hyp. *J. Agric. Food Chem.* 64, 7127–7133. doi: 10.1021/acs.jafc.6b02955

Thaiss, C. A., Zmora, N., Levy, M., and Elinav, E. (2016). The microbiome and innate immunity. *Nature* 535, 65–74. doi: 10.1038/nature18847

Thevenot, E. A., Roux, A., Xu, Y., Ezan, E., and Junot, C. (2015). Analysis of the human adult urinary metabolome variations with age, body mass index, and gender by implementing a comprehensive workflow for univariate and OPLS statistical analyses. *J. Proteome Res.* 14, 3322–3335. doi: 10.1021/acs.jproteome.5b00354

Thursby, E., and Juge, N. (2017). Introduction to the human gut microbiota. *Biochem. J.* 474, 1823–1836. doi: 10.1042/BCJ20160510

Tohyama, S., and Kobayashi, E. (2019). Age-appropriateness of porcine models used for cell transplantation. *Cell Transplant.* 28, 224–228. doi: 10.1177/0963689718817477

Wang, H., and Chen, H. (2022). Aging in China: challenges and opportunities. *China CDC Wkly.* 4, 601–602. doi: 10.46234/ccdcw2022.130

Wood, D. E., Lu, J., and Langmead, B. (2019). Improved metagenomic analysis with Kraken 2. *Genome Biol.* 20:257. doi: 10.1186/s13059-019-1891-0

Yang, H., Wu, J., Huang, X., Zhou, Y., Zhang, Y., Liu, M., et al. (2022). ABO genotype alters the gut microbiota by regulating GalNAc levels in pigs. *Nature* 606, 358–367. doi: 10.1038/s41586-022-04769-z

Yin, X.-J., Ji, S.-K., Duan, C.-H., Tian, P.-Z., Ju, S.-S., Yan, H., et al. (2023). The succession of fecal bacterial community and its correlation with the changes of serum immune indicators in lambs from birth to 4 months. *J. Integr. Agric.* 22, 537–550. doi: 10.1016/j.jia.2022.08.055

Yoder, M., Zhuge, Y., Yuan, Y., Holian, O., Kuo, S., van Breemen, R., et al. (2014). Bioactive lysophosphatidylcholine 16:0 and 18:0 are elevated in lungs of asthmatic subjects. *Allergy Asthma Immunol. Res.* 6, 61–65. doi: 10.4168/aair.2014.6.1.61

Zhang, P. (2022). Influence of foods and nutrition on the gut microbiome and implications for intestinal health. *Int. J. Mol. Sci.* 23:9588. doi: 10.3390/ijms23179588

Zhang, Y., Kouguchi, T., Shimizu, K., Sato, M., Takahata, Y., and Morimatsu, F. (2010). Chicken collagen hydrolysate reduces proinflammatory cytokine production in C57BL/6.KOR-ApoEshl mice. *J. Nutr. Sci. Vitaminol.* 56, 208–210. doi: 10.3177/jnsv.56.208

Zheng, D., Liwinski, T., and Elinav, E. (2020). Interaction between microbiota and immunity in health and disease. *Cell Res.* 30, 492–506. doi: 10.1038/s41422-020-0332-7

Zhou, J., Li, Y., Chen, X., Zhong, L., and Yin, Y. (2017). Development of data-independent acquisition workflows for metabolomic analysis on a quadrupole-orbitrap platform. *Talanta* 164, 128–136. doi: 10.1016/j.talanta.2016.11.048

frontiers | Frontiers in Microbiology

TYPE Mini Review
PUBLISHED 09 October 2023
DOI 10.3389/fmicb.2023.1284603

OPEN ACCESS

EDITED BY
Wen-Chao Liu,
Guangdong Ocean University, China

REVIEWED BY
Yongjie Wang,
North Carolina Agricultural and Technical State University, United States
Xiao-Xuan Zhang,
Qingdao Agricultural University, China

*CORRESPONDENCE
Feilong Deng
✉ fdeng@fosu.edu.cn
Ying Li
✉ yingli@fosu.edu.cn

†These authors share first authorship

RECEIVED 28 August 2023
ACCEPTED 22 September 2023
PUBLISHED 09 October 2023

CITATION
Yang J, Chen R, Peng Y, Chai J, Li Y and Deng F (2023) The role of gut archaea in the pig gut microbiome: a mini-review. *Front. Microbiol.* 14:1284603. doi: 10.3389/fmicb.2023.1284603

The role of gut archaea in the pig gut microbiome: a mini-review

Jianbo Yang[1,2†], Routing Chen[1,2†], Yunjuan Peng[1,2], Jianmin Chai[1,2,3], Ying Li[1,2*] and Feilong Deng[1,2*]

[1]Guangdong Provincial Key Laboratory of Animal Molecular Design and Precise Breeding, College of Life Science and Engineering, Foshan University, Foshan, China, [2]School of Life Science and Engineering, Foshan University, Foshan, Guangdong, China, [3]State Key Laboratory of Swine and Poultry Breeding Industry, Guangzhou, China

The gastrointestinal microbiota of swine harbors an essential but often overlooked component: the gut archaea. These enigmatic microorganisms play pivotal roles in swine growth, health, and yield quality. Recent insights indicate that the diversity of gut archaea is influenced by various factors including breed, age, and diet. Such factors orchestrate the metabolic interactions within the porcine gastrointestinal environment. Through symbiotic relationships with bacteria, these archaea modulate the host's energy metabolism and digestive processes. Contemporary research elucidates a strong association between the abundance of these archaea and economically significant traits in swine. This review elucidates the multifaceted roles of gut archaea in swine and underscores the imperative for strategic interventions to modulate their population and functionality. By exploring the probiotic potential of gut archaea, we envisage novel avenues to enhance swine growth, health, and product excellence. By spotlighting this crucial, yet under-investigated, facet of the swine gut microbiome, we aim to galvanize further scientific exploration into harnessing their myriad benefits.

KEYWORDS

pig gut microbiota, gut archaea, probiotics, pig, feed efficiency

1. Introduction

The gastrointestinal tract (GIT) of pigs, similar to other livestock, hosts a complex and dynamic microbial community consisting of bacteria, fungi, viruses, and archaea, which plays a crucial role in enhancing host health and performance (Upadhaya and Kim, 2022; Vasquez et al., 2022; Zhao et al., 2023; Zhuang et al., 2023). The gut microbiota in pigs mediates nutrient metabolism, modulates the immune system, and provides colonization resistance against pathogens, functioning as a key determinant in the symbiotic relationship between the pig host and its microbial inhabitants. In recent years, numerous studies have examined the influence of the gut microbiome on the health (De Vries and Smidt, 2020; Duarte and Kim, 2022; Deng et al., 2023) and economically significant traits of pigs, identifying several key bacteria and potential probiotics that affect pig growth performance (Giang et al., 2011; Wang et al., 2019; Lee et al., 2022). In summary, research on the interactions among the complex microbiota residing in the pig gastrointestinal tract, as well as the interplay between bacteria and host, is proving valuable for improving pig farming efficiency.

Archaea are prokaryotic microorganisms that are distinct from eukaryotes and bacteria, and are commonly found in the bodies of human and animals (Matarazzo et al., 2012; Bang and Schmitz, 2015). While archaea share morphological features with bacteria, they have developed unique biochemical and metabolic characteristics (Pace, 1997; Schleifer, 2009), such as thermophily and heat resistance, during their long evolutionary history (Macario et al., 1999;

Baker et al., 2020). In humans, archaea colonize the infant gut at birth and interact with bacteria, viruses, and the human body, thereby exerting an influence on health (Wampach et al., 2017; Korpela and de Vos, 2018). Trimethylamine N-oxide (TMAO) is a molecule produced from choline, betaine, and carnitine through gut microbial metabolism. Elevated levels of TMAO have been associated with cardiovascular risks (Janeiro et al., 2018). Studies suggest that intestinal archaea may contribute to obesity and reduce TMAO-related diseases like heart failure (Zhang et al., 2009; Wang and Zhao, 2018). Therefore, researchers have proposed "archaeabiotics" as the next generation of probiotics (Hania et al., 2017) to contribute to human health. Rumen archaea may have positive effects on livestock, with certain groups being significantly enriched in high-feed-utilization beef cattle, sheep rumen, and high-producing dairy cows. Li and colleagues found that archaea such as *M. smithii* are significantly enriched in the rumen of beef cattle with high feed efficiency (Li and Guan, 2017). Another study by Li et al. (2019) based on meta-transcriptomics, revealed that archaeal groups such as Methanomassiliicoccales exhibit heightened expression in the rumen of beef cattle with high feed efficiency. McLoughlin et al. (2020) identified three archaea associated with *Methanobrevibacter* spp. in the sheep rumen, and these archaea showed a significant positive correlation with feed efficiency. Xue et al.'s (2020) study identified the significant enrichment of 12 archaeal species in the rumen of high milk-yielding and high-milk-protein dairy cows. Feedback inhibition in fermentation by hydrogen gas arises from the accumulation of hydrogen, which in turn hinders the microbial activities generating it. These archaea help overcome the challenge of feedback inhibition of fermentation by hydrogen gas, maintaining a low hydrogen environment for efficient fermentation.

In pigs, archaea constitute a common component of the resident microbiota and actively participate in digestive and metabolic processes within the intestinal tract (Borrel et al., 2020). However, in comparison to ruminants, our understanding of the diversity of archaea in the pig gut, their potential functions, and their associations with economically significant traits remains limited. In this review, we summarize the current knowledge on pig gut archaea and their potential applications in the pig industry.

2. Diversity of gut archaea in pigs

Within the labyrinthine microbiome environment of the porcine digestive system, the Archaea—an extraordinary domain of life, distinct in phylogenetic, morphological, and physiological attributes—comprise a smaller fragment yet contribute significantly to microbial diversity. The genus *Methanocorpusculum* is particularly notable, and its relative abundance fluctuation is influenced by investigative parameters and sample diversity.

The 16S rRNA, found in bacterial and archaeal cells, possesses conserved sequences and is commonly employed as a marker gene (Liu et al., 2008). Trailblazing studies like those conducted by Mao et al. (2011) utilized 16S rRNA gene clone libraries to probe into the archaeal diversity present in pig fecal matter, revealing a dominance of *Methanobrevibacter* and *Methanosphaera stadtmanae* (Table 1). Concurrently, Luo and associates (Luo et al., 2012) emphasized the significant sequence homology between most archaeal sequences in Erhualian and Landrace pigs and *Methanobrevibacter*. Advancing beyond clone-based methodologies, Yong et al. (2014) employed DGGE (denaturing gradient gel electrophoresis) and RT-PCR (Reverse Transcription Polymerase Chain Reaction), illuminating *Methanosarcina* and *Methanobrevibacter* as the chief methane-producing archaea in fecal specimens. Their study also uncovered how porcine growth stages affect these archaea presences, along with *Methanosmithii* species. Yet, clone-based strategies might underrepresent archaeal diversity. Utilizing high-throughput sequencing technologies, Lamendella et al. (2011) and Su et al. (2014) revealed a diverse spectrum of methanogen-related operational taxonomic units (OTUs), with a significant majority aligning with the *Methanobacteria* class.

2.1. Exploring archaea through metagenomics

Recently, shotgun metagenomic sequencing has gained traction due to its comprehensive and insightful data (Sharpton, 2014; Quince et al., 2017). Xiong et al. (2022) wielded this method to scrutinize gut archaea's influence on bacterial colonization and succession in piglets, identifying Euryarchaeota as the predominant phylum and *Methanobrevibacter smithii* as the leading species. Deng et al.'s (2021) metagenomic examination of 276 samples corroborated these findings, naming *Methanobrevibacter* and *Methanobrevibacter A smithii* as the most copious archaeal genus and species, respectively. Deng et al.'s (2022) longitudinal analysis uncovered the temporal evolution of archaeal diversity in the swine gut, with weaning signifying a marked shift in community dynamics. The analysis revealed a significant positive correlation between the relative abundance of *Methanobrevibacter A sp900319535* and weight gain observed between days 70 and 140 ($p = 0.005$). Similarly, a potential positive correlation was noted between the relative abundance of *Methanobrevibacter A smithii* and weight gain ($p = 0.005$). These pivotal findings have implications for augmenting the economic efficacy of the livestock sector. Concurrently, Wei et al. (2022) elucidated the impact of domestication on archaeal abundance in the porcine gut, denoting a notable reduction in specific archaeal taxa.

2.2. Dynamic and differential characteristics of gut archaea

Research implies that archaea could significantly influence pig nutrition, metabolism, and growth performance, especially during weaning (Deng et al., 2022). The symbiotic relationship between methanogens and the host during the intestinal colonization of newborn piglets appears mutually selective (Su et al., 2014). Studies further note that gut fungal and archaeal communities exhibit high dynamism during lactation and weaning, with methanogens and parasites impeding piglets' adaptation during the weaning transition (Xiong et al., 2022). Additionally, archeological traces have been found in various segments of the pig digestive tract, including the cecum, colon, rectum, and feces (Gresse et al., 2019). The dominance of the genus *Methanobrevibacter* was consistently observed, with the early colonization of methane-producing archaea in the intestines of piglets showing breed-specific variations and dramatic changes with age [18; 29]. Feehan et al. (2023) collected fecal samples from seven pigs at 22

TABLE 1 Primary archaeal taxa in the pig gut.

Study number	Archaea taxa	Breeds	Age (day)	Technology	Citation
1	Methanobrevibacter (46%)	Duroc × Landrace × Yorkshire	Not given	16S rRNA sequencing	Borrel et al. (2020)
2	141 sequences (37%) related to *Methanobrevibacter gottschalkii* and *Methanobrevibacter millerae* 111 sequences (29%) related to *Methanobrevibacter smithii*	Erhualian × Landrace	40,50,70,330 ~ 360	16S rRNA sequencing	Liu et al. (2008)
4	*Methanomicrobia* and *Thermococci* account for 1% of the total rRNA sequences	Yorkshire	180	Metagenomic sequencing	Luo et al. (2012)
5	Across all reads, 99.91% were identified as class *Methanobacteria*	Meishan × Yorkshire	1,3,7,14	16S rRNA sequencing	Yong et al. (2014)
6	Euryarchaeota was the most abundance phylum Methanobacteriaceae, Methanosarcinaceae, and Candidatus Methanomethylophilaceae were the most abundant families *Methanobrevibacter smithii* was the most abundance species	Large White	14,21,28	Shotgun metagenomic sequencing	Quince et al. (2017)
7	*Methanobrevibacter* (23.02%) *Candidatus methanomethylophilus* (10.52%)	17 breeds from 11farms	Not given	Shotgun metagenomic sequencing	Sharpton (2014)
8	*Methanobrevibacter* A (0.23% of the total rRNA sequences) *Methanobrevibacter* (0.067% of the total rRNA sequences) *Methanomethylophilus* (0.062% of the total rRNA sequences) and *Methanosphaera* (0.023% of the total rRNA sequences)	Not given	7, 14, 21, 28, 35, 70, and 140	Shotgun metagenomic sequencing	Xiong et al. (2022)
10	Methanobacteriaceae family reaching 98.1% Methanomassiliicoccales reaching 1.8%	Landrace × Large White	28	16S rRNA sequencing	Deng et al. (2022)

time points for metagenomic sequencing. They found differences in the MAGs (Metagenome-Assembled Genomes) of the *Methanobacteriales* and *Methanomassiliicoccales* bacteria. The former predominantly existed in the gut of pre-weaning hosts, while the latter was mainly present in adult hosts, suggesting a potential relationship between specific groups of methanogenic archaea (Methanobacteriales and Methanomassiliicoccales) and the diet of the host at different life stages. Interestingly, the structure of archaeal communities in pig intestines seems heavily influenced by dietary patterns. Cao et al. (2016) provided Lantang pigs with varying fiber levels and documented significant alterations in the intestinal tract's archaeal structure, notably *Methanobrevibacter*. Luo et al. (2012) also unveiled a higher diversity and density of archaea in fecal samples from lean-type pigs as compared to obese-type pigs, suggesting a possible role of intestinal archaea in pig fat deposition. These discoveries highlight the intricate, dynamic nature and potential roles of archaeal communities within the porcine gut, potentially influencing host health and productivity. Given the complexities presented, it is paramount to pursue further research endeavors that seek to delineate the intricate interplay between intestinal archaea, bacteria, and their respective hosts. Such investigations could potentially pave the way for innovative microbiota-centric interventions, thereby enhancing swine health and productivity.

3. Potential function of gut archaea in pigs

Archaea are crucial bacteria for ruminants. Numerous studies have focused on the function of archaea in the rumen. While certain archaeal taxonomies are beneficial for ruminants, most research suggests that rumen archaea, especially methanogenic archaea, reduce production efficiency (Huang et al., 2016; Kim et al., 2017; Huws et al., 2018; Xie et al., 2021). Even though the archaeal constituents within the pig gut microbiome may seem less significant in comparison to ruminants, it's becoming increasingly clear that these microorganisms exhibit a unique dynamism and functionality. Peng et al. (2022) re-analyzed several datasets involved in metagenomic and meta-transcriptomic sequencing data of livestock, revealed a greater prevalence of 'active archaeal species' with a statistically significant p-adjust value of ≤ 0.05 and a fold change of ≥ 2, in pigs compared to sheep, cattle, and chicken. This finding suggests that archaea play crucial and active roles within the porcine gut, even when present in lower relative abundance compared with bacteria or fungi.

3.1. Potential role of gut archaea in fat metabolism

The heightened presence of specific *Methanobrevibacter* species in the colonic environment of pigs, particularly when subjected to high-fat dietary conditions, has been noted. Zhao and colleagues collected samples of colonic contents from five high-fat pigs and low-fat pigs to explore the potential of link between gut microbiome and fat deposit (Zhao et al., 2022). Future studies with larger sample sizes are recommended to further elucidate the relationship between archaea and SCFA concentration, ensuring the results are more statistically significant and generalizable (Figure 1).

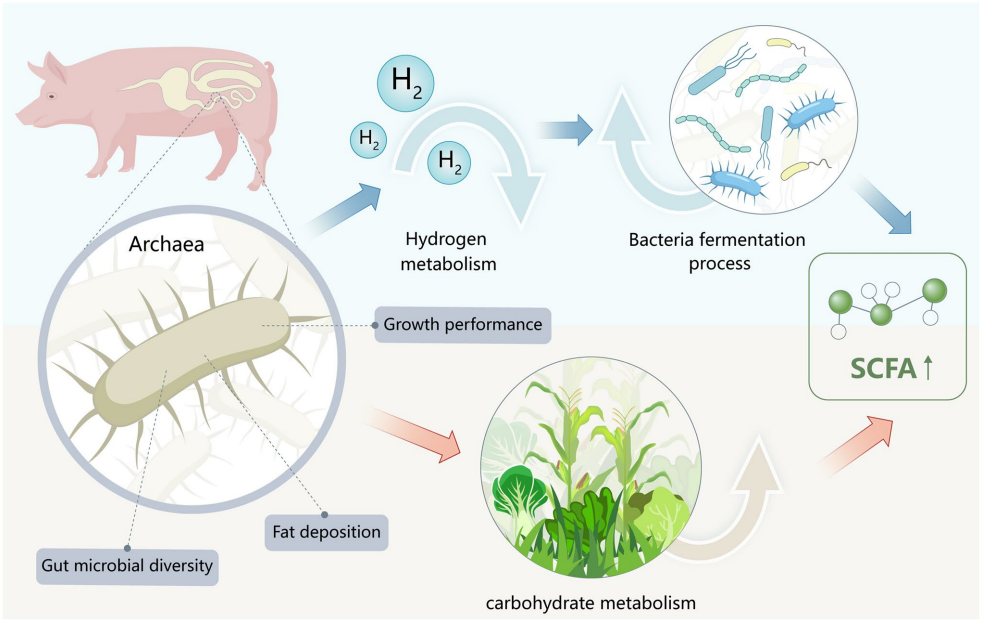

FIGURE 1
Potential functions and mechanisms of gut archaea in swine digestive systems.

3.2. Impact of dietary composition on gut archaea in pigs

Dietary makeup significantly shapes the archaeal profile in pigs. For instance, levels of dietary fiber have been shown to adjust the abundance of *Methanobrevibacter* (Cao et al., 2016). Furthermore, researched by Luo et al. (2017) shows that the addition of dietary pea fiber boosts the diversity of methanogenic archaea and transforms the archaeal community structure. Lean and obese pigs display notable differences in the density and variety of fecal methanogens, implying a potential impact of archaea on fat deposition (Luo et al., 2012). In a study conducted by Xu et al. (2023), the increase of methane-inhibiting archaeal genera in experimental pig cohorts demonstrates the direct effect of dietary manipulation on gut archaeal diversity. However, the consequences of such shifts in the archaeal community on pig growth, development, and health call for further investigation.

3.3. Enhancing fermentation efficiency and growth performance

Our team's scrutiny of the potential of pig gut archaea reveals their essential role in amplifying fermentation efficiency via hydrogen metabolism. A comprehensive examination of 276 pig fecal metagenomes discloses an exclusive hydrogen-consuming metabolic route in archaea, accompanied by a matching hydrogen-producing pathway in gut bacteria. This suggests a symbiotic interaction between archaea and bacteria, where archaea promote efficient gut fermentation by maintaining a low hydrogen environment (Deng et al., 2021). Additionally, the effects of weaning on the gut archaea of pigs demonstrate a positive correlation between archaeal species richness and pig body weight. The rise in functional potential, indicated by the increase in KEGG KOs over time, and the significant association of *Methanobrevibacter A smithii* and *Methanobrevibacter A sp900769095* with body weight, point toward archaea's potential in enhancing pig performance (Deng et al., 2022). It is noteworthy to mention that the regression analysis utilized for these findings was based on a limited dataset of fewer than 25 samples, which may necessitate further studies for more comprehensive insights.

4. Potential application in the pig industry

Archaea, key components of the pig gut microbiome and primarily inhabitants of anaerobic environments, are central to host health and digestion. Despite receiving less attention than gut bacteria in research, current literature, inclusive of our findings, underscores their role in breaking down complex carbohydrates and producing vital short-chain fatty acids (SCFAs) (Samuel and Gordon, 2006). Our investigations suggest that enhancing *Methanosphaera* in pig diets can bolster feed efficiency (Deng et al., 2021). This endorses the manipulation of gut archaea as a promising approach toward sustainable pig farming. Moreover, archaea could serve as representatives of these traits. Associations have been noted between the abundance of certain archaea, specifically *Methanobrevibacter A smithii* and *Methanobrevibacter A sp900769095*, and traits like feed efficiency, growth rate, and meat quality (Lin and Miller, 1998; Deng et al., 2022; Zhao et al., 2022). Therefore, we propose that in the future, certain beneficial archaea could serve as "Archaebiotics" and play a crucial role in the swine industry. However, it's important to recognize that this perspective is based on a few association studies. Further direct evidence is needed to firmly establish the influence of archaea on economically significant traits.

5. Outlook

Indeed, Archaea, often viewed as the linchpin species of the gut microbiome, orchestrate the functional establishment of bacterial communities within the host intestines. Their distinct metabolic capabilities and intimate interactions with bacteria regulate myriad vital processes connected to host health and growth. A more profound exploration of these intricate relationships could bring about transformational insights, shedding light on innovative strategies for bolstering animal health and productivity. However, unlike their extensively studied ruminant counterparts, pig gut archaea have been largely sidelined, obscuring their likely pivotal role in swine health and productivity.

Probiotic microorganisms, as living microbes, hold the capacity to regulate the equilibrium and dynamics of the gastrointestinal microbiota. Their constructive impacts on host health and productivity have led them to become one of the most favored additions to animal feed formulations (Retta et al., 2016; Markowiak and Śliżewska, 2018). The investigations by Peng et al. (2023) identified four strains of probiotics that exhibit potential inhibitory effects against pathogenic microorganisms. These inquiries highlight the pivotal role of probiotics in preserving the stability of the microbial community. Yet, of greater intrigue is the advent of 'archaeal probiotics,' which signals a pioneering phase in microbiome research. Initial indications hint at the potential of specific archaeal species to enhance host energy metabolism without inducing adverse effects (Luo et al., 2012), thus paving the way for their application as probiotics. Leveraging the strides in metagenomics and metabolomics could further illuminate the complex symbiotic relationships between archaea and their hosts. However, a significant challenge remains in the realm of archaeal research: the difficulty in culturing and isolating new archaeal species. This limitation not only hampers the comprehensive study of these microorganisms but also restricts their potential applications in various domains.

To summarize, our understanding of pig gut archaea is in its nascent stages, but existing evidence compellingly suggests the substantial roles these prokaryotes could play in swine health and productivity. As we progress, focused efforts should be aimed at better comprehending the ecological role of archaea, their interplay with other gut microbes, and their prospective benefits as probiotics. The untapped potential of gut archaea in pigs awaits our exploration.

6. Conclusion

This review has underscored the substantial yet understudied potential of pig gut archaea in the swine industry. The nascent understanding of the influence of archaea on pig nutrition, metabolism, and growth underscores their potential utility in augmenting swine health and productivity. The advent of sophisticated metagenomic studies, along with the isolation and functional verification of specific archaeal species, holds significant promise. This strategy may unearth the intricate roles these archaea play within pig gut ecosystems, leading to the development of innovative feed additives or probiotics. By encouraging further research into this area, we hope to fully exploit the beneficial aspects of these gut archaea and open up new avenues for sustainable and efficient pig farming.

Author contributions

JY: Writing – original draft. RC: Writing – original draft. YP: Writing – review & editing. JC: Writing – review & editing. YL: Conceptualization, Writing – review & editing. FD: Conceptualization, Writing – original draft.

Funding

The author(s) declare financial support was received for the research, authorship, and/or publication of this article. This work was supported by the Youth Project of Guangdong Foshan joint fund of the Guangdong Natural Science Foundation (2022A1515110819), National Natural Science Foundation of China (no. 32170430), and State Key Laboratory of Swine and Poultry Breeding Industry (2023GZ25).

Conflict of interest

The authors declare that the research was conducted in the absence of any commercial or financial relationships that could be construed as a potential conflict of interest.

Publisher's note

References

Baker, B. J., De Anda, V., Seitz, K. W., Dombrowski, N., Santoro, A. E., and Lloyd, K. G. (2020). Diversity, ecology and evolution of Archaea. *Nat. Microbiol.* 5, 887–900. doi: 10.1038/s41564-020-0715-z

Bang, C., and Schmitz, R. A. (2015). Archaea associated with human surfaces: not to be underestimated. *FEMS Microbiol. Rev.* 39, 631–648. doi: 10.1093/femsre/fuv010

Borrel, G., Brugère, J.-F., Gribaldo, S., Schmitz, R. A., and Moissl-Eichinger, C. (2020). The host-associated archaeome. *Nat. Rev. Microbiol.* 18, 622–636. doi: 10.1038/s41579-020-0407-y

Cao, Z., Liang, J., Liao, X., Wright, A., Wu, Y., and Yu, B. (2016). Effect of dietary fiber on the methanogen community in the hindgut of Lantang gilts. *Animal* 10, 1666–1676. doi: 10.1017/S1751731116000525

De Vries, H., and Smidt, H. (2020). Microbiota development in piglets. *The suckling and weaned piglet* 179–205. doi: 10.3920/978-90-8686-894-0_7

Deng, F., Li, Y., Peng, Y., Wei, X., Wang, X., Howe, S., et al. (2021). The diversity, composition, and metabolic pathways of archaea in pigs. *Animals* 11:2139. doi: 10.3390/ani11072139

Deng, F., Peng, Y., Zhang, Z., Howe, S., Wu, Z., Dou, J., et al. (2022). Weaning time affects the archaeal community structure and functional potential in pigs. *Front. Microbiol.* 13:845621. doi: 10.3389/fmicb.2022.845621

Deng, F., Wang, C., Li, D., Peng, Y., Deng, L., Zhao, Y., et al. (2023). The unique gut microbiome of giant pandas involved in protein metabolism contributes to the host's dietary adaption to bamboo. *Microbiome* 11:180. doi: 10.1186/s40168-023-01603-0

Duarte, M. E., and Kim, S. W. (2022). Intestinal microbiota and its interaction to intestinal health in nursery pigs. *Anim. Nutr.* 8, 169–184. doi: 10.1016/j.aninu.2021.05.001

Feehan, B., Ran, Q., Dorman, V., Rumback, K., Pogranichniy, S., Ward, K., et al. (2023). Novel complete methanogenic pathways in longitudinal genomic study of monogastric age-associated archaea. *Animal Microbiome* 5:35. doi: 10.1186/s42523-023-00256-6

Giang, H. H., Viet, T. Q., Ogle, B., and Lindberg, J. E. (2011). Effects of supplementation of probiotics on the performance, nutrient digestibility and faecal microflora in growing-finishing pigs. *Asian Australas. J. Anim. Sci.* 24, 655–661. doi: 10.5713/ajas.2011.10238

Gresse, R., Chaucheyras Durand, F., Dunière, L., Blanquet-Diot, S., and Forano, E. (2019). Microbiota composition and functional profiling throughout the gastrointestinal tract of commercial weaning piglets. *Microorganisms* 7:343. doi: 10.3390/microorganisms7090343

Hania, W. B., Ballet, N., Vandeckerkove, P., Ollivier, B., O'Toole, P. W., and Brugère, J.-F., *Archaebiotics: archaea as pharmabiotics for treating chronic disease in humans. Archaea—new biocatalysts, novel pharmaceuticals and various biotechnological applications*. IntechOpen: Rijeka, Croatia (2017) 41–62.

Huang, X. D., Martinez-Fernandez, G., Padmanabha, J., Long, R., Denman, S. E., and McSweeney, C. S. (2016). Methanogen diversity in indigenous and introduced ruminant species on the Tibetan plateau. *Archaea* 2016:5916067. doi: 10.1155/2016/5916067

Huws, S. A., Creevey, C. J., Oyama, L. B., Mizrahi, I., Denman, S. E., Popova, M., et al. (2018). Addressing global ruminant agricultural challenges through understanding the rumen microbiome: past, present, and future. *Front. Microbiol.* 9:2161. doi: 10.3389/fmicb.2018.02161

Janeiro, M. H., Ramírez, M. J., Milagro, F. I., Martínez, J. A., and Solas, M. (2018). Implication of trimethylamine N-oxide (TMAO) in disease: potential biomarker or new therapeutic target. *Nutrients* 10:1398. doi: 10.3390/nu10101398

Kim, M., Park, T., and Yu, Z. (2017). Metagenomic investigation of gastrointestinal microbiome in cattle. *Asian Australas. J. Anim. Sci.* 30, 1515–1528. doi: 10.5713/ajas.17.0544

Korpela, K., and de Vos, W. M. (2018). Early life colonization of the human gut: microbes matter everywhere. *Curr. Opin. Microbiol.* 44, 70–78. doi: 10.1016/j.mib.2018.06.003

Lamendella, R., Santo Domingo, J. W., Ghosh, S., Martinson, J., and Oerther, D. B. (2011). Comparative fecal metagenomics unveils unique functional capacity of the swine gut. *BMC Microbiol.* 11:103. doi: 10.1186/1471-2180-11-103

Lee, J. H., Kim, S., Kim, E. S., Keum, G. B., Doo, H., Kwak, J., et al. (2022). Comparative analysis of the pig gut microbiome associated with the pig growth performance. *J. Anim. Sci. Technol.*, 65, 856–864. doi: 10.5187/jast.2022.e122

Li, F., and Guan, L. L. (2017). Metatranscriptomic profiling reveals linkages between the active rumen microbiome and feed efficiency in beef cattle. *Appl. Environ. Microbiol.* 83:e00061-17. doi: 10.1128/AEM.00061-17

Li, F., Hitch, T. C., Chen, Y., Creevey, C. J., and Guan, L. L. (2019). Comparative metagenomic and metatranscriptomic analyses reveal the breed effect on the rumen microbiome and its associations with feed efficiency in beef cattle. *Microbiome* 7, 1–21. doi: 10.1186/s40168-019-0618-5

Lin, C., and Miller, T. L. (1998). Phylogenetic analysis of methanobrevibacter isolated from feces of humans and other animals. *Arch. Microbiol.* 169, 397–403. doi: 10.1007/s002030050589

Liu, Z., DeSantis, T. Z., Andersen, G. L., and Knight, R. (2008). Accurate taxonomy assignments from 16S rRNA sequences produced by highly parallel pyrosequencers. *Nucleic Acids Res.* 36:e120. doi: 10.1093/nar/gkn491

Luo, Y., Chen, H., Yu, B., He, J., Zheng, P., Mao, X., et al. (2017). Dietary pea fiber increases diversity of colonic methanogens of pigs with a shift from Methanobrevibacter to Methanomassiliicoccus-like genus and change in numbers of three hydrogenotrophs. *BMC Microbiol.* 17:17. doi: 10.1186/s12866-016-0919-9

Luo, Y.-H., Su, Y., Wright, A.-D. G., Zhang, L.-l., Smidt, H., and Zhu, W.-Y. (2012). Lean breed landrace pigs harbor fecal methanogens at higher diversity and density than obese breed Erhualian pigs. *Archaea* 2012:605289. doi: 10.1155/2012/605289

Macario, A. J., Lange, M., Ahring, B. K., and De Macario, E. C. (1999). Stress genes and proteins in the archaea. *Microbiol. Mol. Biol. Rev.* 63, 923–967. doi: 10.1128/MMBR.63.4.923-967.1999

Mao, S.-Y., Yang, C.-F., and Zhu, W.-Y. (2011). Phylogenetic analysis of methanogens in the pig feces. *Curr. Microbiol.* 62, 1386–1389. doi: 10.1007/s00284-011-9873-9

Markowiak, P., and Śliżewska, K. (2018). The role of probiotics, prebiotics and synbiotics in animal nutrition. *Gut Pathog.* 10:21. doi: 10.1186/s13099-018-0250-0

Matarazzo, F., Ribeiro, A., Faveri, M. D., Taddei, C., Martinez, M. B., and Mayer, M. P. A. (2012). The domain Archaea in human mucosal surfaces. *Clin. Microbiol. Infect.* 18, 834–840. doi: 10.1111/j.1469-0691.2012.03958.x

McLoughlin, S., Spillane, C., Claffey, N., Smith, P. E., O'Rourke, T., Diskin, M. G., et al. (2020). Rumen microbiome composition is altered in sheep divergent in feed efficiency. *Front. Microbiol.* 11:1981. doi: 10.3389/fmicb.2020.01981

Pace, N. R. (1997). A molecular view of microbial diversity and the biosphere. *Science* 276, 734–740. doi: 10.1126/science.276.5313.734

Peng, Y., Chen, R., Zhang, Z., Jin, R., Xie, T., Liu, X., et al. (2023). Metagenomic and meta-transcriptomic analysis reveal the colonization and expression profile of probiotic strains in humans and animals. *Fermentation* 9:417. doi: 10.3390/fermentation9050417

Peng, Y., Xie, T., Wu, Z., Zheng, W., Zhang, T., Howe, S., et al. (2022). Archaea: an under-estimated kingdom in livestock animals. *Front. Vet. Sci.* 9:973508. doi: 10.3389/fvets.2022.973508

Quince, C., Walker, A. W., Simpson, J. T., Loman, N. J., and Segata, N. (2017). Shotgun metagenomics, from sampling to analysis. *Nat. Biotechnol.* 35, 833–844. doi: 10.1038/nbt.3935

Retta, K. S. (2016). Role of probiotics in rumen fermentation and animal performance: a review. *Int. J. Livestock Prod.* 7, 24–32. doi: 10.5897/IJLP2016.0285

Samuel, B. S., and Gordon, J. I. (2006). A humanized gnotobiotic mouse model of host–archaeal–bacterial mutualism. *Proc. Natl. Acad. Sci.* 103, 10011–10016. doi: 10.1073/pnas.0602187103

Schleifer, K. H. (2009). Classification of Bacteria and Archaea: past, present and future. *Syst. Appl. Microbiol.* 32, 533–542. doi: 10.1016/j.syapm.2009.09.002

Sharpton, T. J. (2014). An introduction to the analysis of shotgun metagenomic data. *Front. Plant Sci.* 5:209. doi: 10.3389/fpls.2014.00209

Su, Y., Bian, G., Zhu, Z., Smidt, H., and Zhu, W. (2014). Early methanogenic colonisation in the faeces of Meishan and Yorkshire piglets as determined by pyrosequencing analysis. *Archaea* 2014:547908. doi: 10.1155/2014/547908

Upadhaya, S. D., and Kim, I. H. (2022). Maintenance of gut microbiome stability for optimum intestinal health in pigs–a review. *J. Anim. Sci. Biotechnol.* 13, 1–11. doi: 10.1186/s40104-022-00790-4

Vasquez, R., Oh, J. K., Song, J. H., and Kang, D.-K. (2022). Gut microbiome-produced metabolites in pigs: a review on their biological functions and the influence of probiotics. *J. Anim. Sci. Technol.* 64, 671–695. doi: 10.5187/jast.2022.e58

Wampach, L., Heintz-Buschart, A., Hogan, A., Muller, E. E., Narayanasamy, S., Laczny, C. C., et al. (2017). Colonization and succession within the human gut microbiome by archaea, bacteria, and microeukaryotes during the first year of life. *Front. Microbiol.* 8:738. doi: 10.3389/fmicb.2017.00738

Wang, X., Tsai, T., Deng, F., Wei, X., Chai, J., Knapp, J., et al. (2019). Longitudinal investigation of the swine gut microbiome from birth to market reveals stage and growth performance associated bacteria. *Microbiome* 7, 1–18. doi: 10.1186/s40168-019-0721-7

Wang, Z., and Zhao, Y. (2018). Gut microbiota derived metabolites in cardiovascular health and disease. *Protein Cell* 9, 416–431. doi: 10.1007/s13238-018-0549-0

Wei, L., Zhou, W., and Zhu, Z. (2022). Comparison of changes in gut microbiota in wild boars and domestic pigs using 16S rRNA gene and metagenomics sequencing technologies. *Animals* 12:2270. doi: 10.3390/ani12172270

Xie, F., Jin, W., Si, H., Yuan, Y., Tao, Y., Liu, J., et al. (2021). An integrated gene catalog and over 10,000 metagenome-assembled genomes from the gastrointestinal microbiome of ruminants. *Microbiome* 9:137. doi: 10.1186/s40168-021-01078-x

Xiong, X., Rao, Y., Tu, X., Wang, Z., Gong, J., Yang, Y., et al. (2022). Gut archaea associated with bacteria colonization and succession during piglet weaning transitions. *BMC Vet. Res.* 18:243. doi: 10.1186/s12917-022-03330-4

Xu, R., Li, Q., Wang, H., Su, Y., and Zhu, W. (2023). Reduction of redox potential exerts a key role in modulating gut microbial taxa and function by dietary supplementation of pectin in a pig model. *Microbiol. Spectr.* 11:e0328322. doi: 10.1128/spectrum.03283-22

Xue, M.-Y., Sun, H.-Z., Wu, X.-H., Liu, J.-X., and Guan, L. L. (2020). Multi-omics reveals that the rumen microbiome and its metabolome together with the host metabolome contribute to individualized dairy cow performance. *Microbiome* 8:64. doi: 10.1186/s40168-020-00819-8

Yong, S., Smidt, H., and Wei-Yun, Z. (2014). Comparison of fecal methanogenic archaeal community between Erhualian and landrace pigs using denaturing gradient gel electrophoresis and real-time PCR analysis. *J. Integr. Agric.* 13, 1340–1348. doi: 10.1016/S2095-3119(13)60529-8

Zhang, H., DiBaise, J. K., Zuccolo, A., Kudrna, D., Braidotti, M., Yu, Y., et al. (2009). Human gut microbiota in obesity and after gastric bypass. *Proc. Natl. Acad. Sci.* 106, 2365–2370. doi: 10.1073/pnas.0812600106

Zhao, W., Abdelsattar, M. M., Wang, X., Zhang, N., and Chai, J. (2023). In vitro modulation of rumen fermentation by microbiota from the recombination of rumen fluid and solid phases. *Microbiol. Spectr.* 11:e0338722. doi: 10.1128/spectrum.03387-22

Zhao, G., Xiang, Y., Wang, X., Dai, B., Zhang, X., Ma, L., et al. (2022). Exploring the possible link between the gut microbiome and fat deposition in pigs. *Oxidative Med. Cell. Longev.* 2022:1098892. doi: 10.1155/2022/1098892

Zhuang, Y., Lv, X., Cui, K., Chai, J., and Zhang, N. (2023). Early solid diet supplementation influences the proteomics of rumen epithelium in goat kids. *Biology* 12:684. doi: 10.3390/biology12050684

frontiers | Frontiers in Microbiology

TYPE Original Research
PUBLISHED 20 October 2023
DOI 10.3389/fmicb.2023.1239847

OPEN ACCESS

EDITED BY
Lifeng Zhu,
Nanjing University of Chinese Medicine, China

REVIEWED BY
David C. B. Taras,
Boehringer Ingelheim, Germany
Limei Lin,
Nanjing Agricultural University, China

*CORRESPONDENCE
Long Jin
✉ longjin@sicau.edu.cn
Mingzhou Li
✉ mingzhou.li@sicau.edu.cn

†These authors have contributed equally to this work

RECEIVED 14 June 2023
ACCEPTED 28 September 2023
PUBLISHED 20 October 2023

CITATION
Zeng B, Chen L, Kong F, Zhang C, Chen L, Qi X, Chai J, Jin L and Li M (2023) Dynamic changes of fecal microbiota in a weight-change model of Bama minipigs.
Front. Microbiol. 14:1239847.
doi: 10.3389/fmicb.2023.1239847

Dynamic changes of fecal microbiota in a weight-change model of Bama minipigs

Bo Zeng[1†], Li Chen[2†], Fanli Kong[3], Chengcheng Zhang[1], Long Chen[1], Xu Qi[1], Jin Chai[1], Long Jin[1*] and Mingzhou Li[1*]

[1]Key Laboratory of Livestock and Poultry Multi-omics, Ministry of Agriculture and Rural Affairs, and Farm Animal Genetic Resources Exploration and Innovation Key Laboratory of Sichuan Province, College of Animal Science and Technology, Sichuan Agricultural University, Chengdu, China, [2]Chongqing Academy of Animal Science, Chongqing, China, [3]College of Life Science, Sichuan Agricultural University, Ya'an, China

Introduction: Obesity is closely related to gut microbiota, however, the dynamic change of microbial diversity and composition during the occurrence and development process of obesity is not clear.

Methods: A weight-change model of adult Bama pig (2 years, 58 individuals) was established, and weight gain (27 weeks) and weight loss (9 weeks) treatments were implemented. The diversity and community structures of fecal microbiota (418 samples) was investigated by using 16S rRNA (V3-V4) high-throughput sequencing.

Results: During the weight gain period (1~27 week), the alpha diversity of fecal microbiota exhibited a "down-up-down" fluctuations, initially decreasing, recovering in the mid-term, and decreasing again in the later stage. Beta diversity also significantly changed over time, indicating a gradual deviation of the microbiota composition from the initial time point. *Bacteroides*, *Clostridium sensu stricto* 1, and *Escherichia-Shigella* showed positive correlations with weight gain, while *Streptococcus*, *Oscillospira*, and Prevotellaceae UCG-001 exhibited negative correlations. In the weight loss period (30~38 week), the alpha diversity further decreased, and the composition structure underwent significant changes compared to the weight gain period. Christensenellaceae R-7 group demonstrated a significant increase during weight loss and showed a negative correlation with body weight. *Porphyromonas* and *Campylobacter* were positively correlated with weight loss.

Discussion: Both long-term fattening and weight loss induced by starvation led to substantial alterations in porcine gut microbiota, and the microbiota changes observed during weight gain could not be recovered during weight loss. This work provides valuable resources for both obesity-related research of human and microbiota of pigs.

KEYWORDS

Bama pig, obesity, dietary restriction, gut microbiota, 16S rRNA

1. Introduction

Obesity is a major public health problem worldwide with related epidemics poses a threat to human health and quality of life (WHO, 2021). Gut microbiota is closely related to host obesity. Differences in fecal microbiota were found between obese and lean/normal humans in both European (Turnbaugh et al., 2009; Goodrich et al., 2014) and Asian (Liu et al., 2017; Yun

et al., 2017). For mechanism and therapeutic purpose, diverse animal models have been used to investigate obesity and associated microbiota, typically including mouse, rat, and pigs (Lecomte et al., 2015; Chang et al., 2018; Kleinert et al., 2018). Pigs are recognized as important animal models in gastrointestinal tract studies due to having a similar anatomy and immune system to humans (Hvistendahl, 2012).

Studies on porcine gut microbiome indicated that gut microbiota (e.g., *Prevotella*) has an effect on the feed efficiency (Yang H. et al., 2017; Jiang et al., 2023). Few studies have directly compared the fecal microbiota of pigs with high and low body weights (Han et al., 2017; Oh et al., 2020). In fact, these studies are more inclined to productivity and not applicable to obesity issue. Typically, high-fat diet (HFD) or high-energy diet (HED) treatments are used to construct obesity models in animals. Pedersen et al. constructed HFD-induced obesity models on two kinds of minipigs (Ossabaw and Göttingen) and many obesity-related bacteria were identified (including *Bacteroides*, *Clostridium*) (Pedersen et al., 2013). Panasevich et al. also used Ossabaw pigs and treated with HDF for 36 weeks. They found that although obesity significantly lowered alpha-diversity of both cecal and fecal microbiota, there are difference in obesity associated bacteria with distinct predicted function between cecal contents and feces (Panasevich et al., 2018). However, shortcomings remain in these studies, i.e., relatively low number of individuals and samples, single time point (only at termination point), and no dynamic monitoring of microbiota changes during obesity process. In addition, although some studies have elaborately investigated the dynamic changes of swine gut microbiota at different ages (Ban-Tokuda et al., 2017; Wang et al., 2019; Luo et al., 2022), the time-period were from lactation to finishing (< 7 month), which is also not suitable for reference as obesity model (especially to simulate obesity of adult human).

Bama minipigs, an indigenous Chinese miniature pig breed, are widely used in biomedical research (Yang et al., 2015; Ruan et al., 2016). Studies on gut microbiota of Bama pigs are mainly focused on growth promoters and probiotics (Liu et al., 2017; Wang et al., 2021; Azad et al., 2022), and microbial research based on obesity model of Bama pig has not been reported. Here, we constructed an obesity model with relatively large number of adult Bama pigs (2 years age), and fecal microbial ecosystem was analyzed using 16S rRNA gene sequencing. We aimed to address the following objectives: (1) to dynamically delineate changes in diversity and composition structure of pig gut microbiota during weight gain and weight loss, (2) to identify gut bacteria highly correlated with pig body weight. This study has great significance not only as reference for accurately understanding the relationship between human obesity process and gut microbiota, but also to provide bioinformatical resource for future comparative research in pigs.

2. Materials and methods

2.1. Animal group design and sampling

The animal experiments were conducted with design and methods similar to those used in our previous multi-omics research project (Jin et al., 2023). A total of 60 2-year-old female adult individuals were selected from a large population of purebred Bama minipigs (a closed breeding herd which originally introduced from the national conservation farm located at Bama Yao autonomous county of Guangxi Zhuang autonomous region, China) and used in this study. All pigs were raised in the same experimental field under the same environmental conditions (Hengshu Bio-Techonlogy, Yibin, Sichuan, China). The animals were not treated with any vaccines, antimicrobials or other drugs from 1 month before and throughout the experiment period. The environment was controlled throughout the experimental period at a room temperature of 18 ~ 22°C and humidity of 30 ~ 70%. Pigs were raised in separate cages and allowed *ad libitum* to water. All pigs were fed twice daily (7:00 am, 6:00 pm) with restricted feed intake. The feed formulation and daily dosage was determined according to the nutritional requirements outlined by the Feeding Standard of Swine (NY/T 65–2004) and published by the Ministry of Agriculture and Rural Affairs of the People's Republic of China.

All pigs were acclimated to a basic diet (BD, 12.9 MJ/kg) for 1 week before treatment with daily dose at 3% of their initial average body weight. Then, the animal experiment was divided into a weight gain stage (Gain) and a weight loss stage (Lose) (Figure 1). During the Gain stage, pigs were fed a high-fat diet (HFD, 15.1 MJ/kg) for 27 weeks (1 ~ 27 week), and the daily dose was monthly adjusted to 3% of their current average body weight by weighing for the next month. After that, 10 pigs were randomly selected (by drawing lots) for the weight loss experiments. Pigs in the Lose stage were transferred to a separate room (still caged individually) and stabilized by feeding basic diet for 2 weeks. In order to achieve weight loss, pigs were then subjected to starvation treatment for 9 weeks (30 ~ 38 week). They continued to be fed with basic diet, but daily dose was reduced to 10% of before (0.3% of their average body weight at week 27, not changed thereafter). The above feed macronutrient content is shown in Supplementary Table S1. The pigs were observed daily to determine their health conditions, and two individuals with abnormal physical conditions were directly eliminated.

Body weight was measured regularly by moving pigs to an electronic cage scale. In order to ensure the consistency of sampling process at different time points, both the sampling time (to avoid circadian effect) and fecal sample quality were strictly controlled. Fecal samples were collected on the next day after weighing during 9:00 ~ 10:00 am with fecal container pre-cleaned the night before sampling. Feces with abnormal shape, color or volume was not included. All pigs ($n = 58$) were participated in the sampling, but only a part of individuals obtained the samples under the above conditions. Fresh feces were directly loaded into 50 mL screw-cap centrifuge tubes and immediately snap-frozen in a dry ice box, then transported to a laboratory and stored at −76°C until further analysis.

2.2. Sequencing and bioinformatics

Total bacterial DNA was extracted directly from each 200 mg thawed sample (scooped from the center part of feces) using TIANamp Bacteria DNA Kit (TIANGEN Biotech, Beijing, China) according to the manufacturer's instructions. DNA concentration was measured using a NanoDrop spectrophotometer (Thermo Scientific), as well as quantified through agarose gel electrophoresis. We only selected samples from part of individuals for subsequent library construction and sequencing. Among them, all samples from 10 pigs that used for weight loss study were included, and out of the remaining

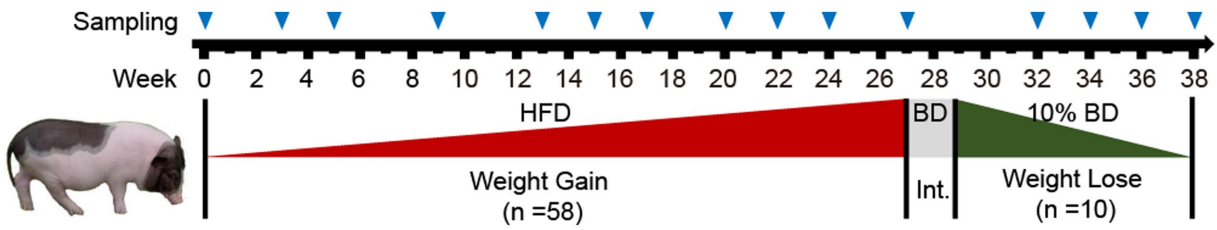

FIGURE 1
Experimental design and sampling. Animal experiments are divided into weight gain and weight loss periods, with a 2-week intermittent period (Int.) in between. Apart from the initial time point (week 0), the time point at the end of each week was used as name for labeling and describing the processing week. Bama pigs in the weight gain period (1 ~ 27) received a high-fat diet (HFD) for 27 weeks, while those in the weight loss period (30 ~ 38) were fed only 10% of a basic diet (BD) for 9 weeks. Fecal samples were collected at the time points marked by blue triangles, and body weight was recorded.

48 pigs, 30 pigs were randomly selected and their samples were sequenced (Supplementary Table S2). 16S rRNA gene amplicons were produced and sequenced at the Beijing Genomics Institute (BGI: Shenzhen, China) using the Illumina HiSeq 2 × 250 protocol. The V3-V4 region of the 16S rRNA gene was amplified using the 341f/806r barcoded primer pair (341f: 5′-XXXXXX CCT AYG GGR BGC ASC AG-3′, 806r: 5′-XXXXXX GGA CTA CHV GGG TWT CTA AT-3′).

The sequencing data analysis was performed using the QIIME2[1] (Bolyen et al., 2019). The DADA2 method was used for sequence quality control (Callahan et al., 2016). Barcode and primer sequences were removed from the 5′ ends and low-quality bases were truncated from the 3′ ends according to the Q20 standard. The clean fasta sequences were overlapped and the feature table was constructed after de-redundancy. Features with very low sequence reads were filtered out ($n > 30$). The final high-quality representative feature sequences were used for taxonomic annotation with the SILVA rRNA database (132_99 release) used as reference[2].

Before the diversity analysis, the feature table was collapsed to the genus level (silva taxonomy level '5_') to improve biological reliability (the 16S V3-V4 region study may be not accurate at the species level). The Shannon's diversity index and the 'Number of Genus' were computed for alpha-diversity, and differences between time points were tested using the Kruskal-Wallis H test with FDR based multiple comparisons adjustment (Kruskal and Wallis, 1952; Benjamini and Hochberg, 1995). Binary Jaccard and Bray-Curtis distances for each pair of samples were calculated to represent similarity relationships of the gut microbiota, and visualized using principal coordinates analysis (PCoA). PERMANOVA was used for group significance tests of beta-diversity.

Microbial composition was studied at three levels: phylum, family and genus. The relative abundances of dominant bacteria are displayed in stacked bar charts. The relative abundances data matrix at phylum and genus level were used for subsequent analysis, and low-abundance taxa (total average relative abundance <0.1%) were filtered out. The LEfSe (Linear discriminant analysis Effect Size) software was used with default parameters (factorial Kruskal-Wallis test α <0.05, logarithmic LDA score > 2.0) to identify differentially abundant taxa between the Gain and Loss periods (https://huttenhower.sph.harvard.edu/lefse) (Segata et al., 2011). SparCC software (Friedman and Alm, 2012) was used to calculate the Pearson and Spearman correlations between bacterial taxa (genus level) and pig body weight (bootstraps, $n = 100$). The dynamic change in relative abundance of these weight-related taxa was analyzed.

PICRUSt2 (Phylogenetic Investigation of Communities by Reconstruction of Unobserved States) was used to analyze the function of the fecal microbiota (Douglas et al., 2020). The predicted metagenomes were subjected to KEGG and MetaCyc pathway analysis. Similar to microbiota analysis, the alpha and beta diversity of KEGG Orthology (KO) terms was studied and the significance of differences between groups were tested using the Kruskal-Wallis H test and PERMANOVA test, respectively.

3. Results

The body weight of the Bama pigs changed significantly during the experiments (Figure 2A). The average weight rose from 74.2 kg at week 0 to 142.0 kg at week 27 during the Gain period. In the Lose period, it dropped from 122.2 kg at week 27 to 94.1 kg at week 38. Due to quality control of sampling and subsequent experiments (DNA extraction, library construction, etc.), a part of samples was excluded, resulting in an irregular number of samples at each time point (Supplementary Table S2). A total of 418 fecal samples were enrolled in a microbial diversity study through the 16S rRNA gene high-throughput sequencing approach, with 378 samples (13 ~ 40 per time point) in the weight gain period and 40 samples (10 per time point) in the weight loss period. After quality control of the sequence data, a total of 23,229,042 high-quality sequences were obtained with an average of 55,571 reads per sample, and the sample with the lowest sequence number has 20,636 reads. After sequence de-redundancy, we constructed the feature metadata table of all samples, which contains 7,104 high-quality features (feature min counts >30). These features were annotated and clustered into 587 taxa at the genus level, with an average of 161 genera per sample (Supplementary Table S2).

3.1. Dynamic changes in fecal microbial diversity

Two statistical measure, the Shannon index and the Number of Genus were calculated to study changes in the alpha diversity of pig

1 https://qiime2.org/
2 https://www.arb-silva.de/

10.3389/fmicb.2023.1239847

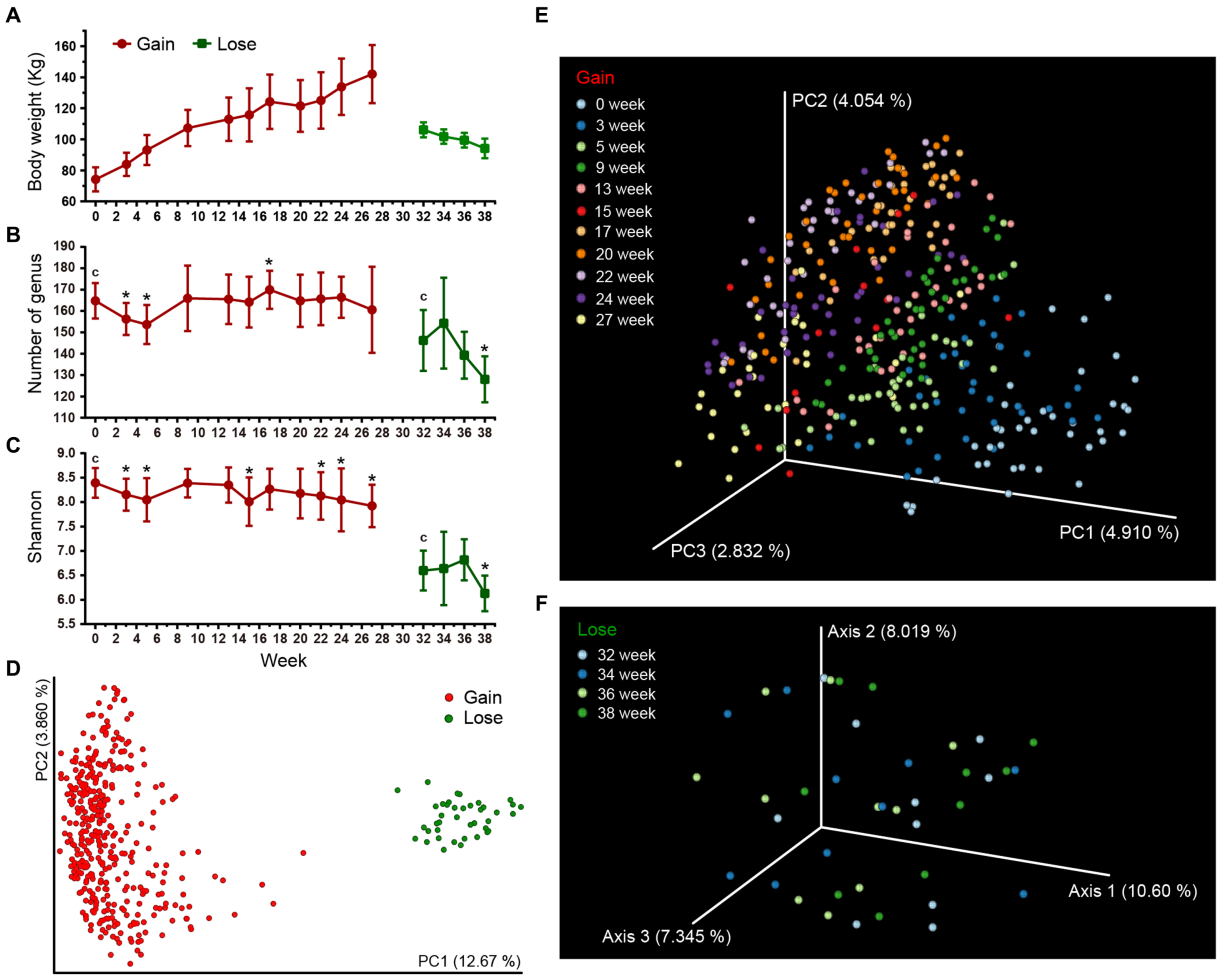

FIGURE 2
Gut microbial diversities of Bama pigs. Two different stage groups (weight gain and weight loss period) are marked with red and green colors, respectively. **(A)** Changes in the average body weight over time (only include pigs for which sequence data is available, Supplementary Table S2). **(B,C)** Alpha diversity measures of fecal microbiota using Number of Genus **(B)** and the Shannon index **(C)**. Error bars represent standard deviation (SD). Kruskal-Wallis H test was used to compare the intra-group differences between the initial time point (c) and other time points (*$q < 0.05$). **(D–F)** PCoA plots of beta-diversity analysis using binary Jaccard distance metrics. Each node represents the fecal microbiota of one single sample. Microbiota differences between weight gain and weight loss periods were calculated **(D)**, and the changes across time within each period are separately illustrated **(E,F)**.

microbiota over time. The diversity difference between initial and other time points in respective stages were compared. The high-fat diet (HFD) of the Gain period caused a "down-up-down' fluctuation in diversity indices (Figures 2B,C). Both the Shannon index and the Number of Genus were significantly lower after 3 ~ 5 weeks of HFD treatment. By the week 9, they rose and returned to their original levels. For remaining 13–27 week, the Number of genus remained stable (one exception that increased at week 17), but the Shannon index decreased significantly by week 22 ~ 27 (Supplementary Table S3A, $q < 0.05$). After 3 weeks of starvation in the Lose period (30 ~ 32 week), the fecal microbial diversity was further sharply reduced compared to the Gain period (Supplementary Table S3A). No significant differences were found during the 32 ~ 36 week period, but by the end of the experiment at week 38, the diversity index dropped to its lowest point. In addition, we separately tracked the changes of microbial diversity of 10 individuals selected for lose period, and found that there was no significant difference from other individuals (Supplementary Figure S1), indicating that random selection had minimal impact on the diversity results.

We next assessed beta diversity with PCoA analysis and microbial composition differences of all samples were measured based on the binary Jaccard and Bray-Curtis distances of all taxa metadata. Overall, there was a significant difference between the Gain and Lose periods (Figure 2D; Supplementary Figure S2A; Supplementary Table S3B). During the Gain period, differences in microbiota between each pair of time points were all significant (Supplementary Table S3B), and the degree of distance gradually increased (compared to week 0, Supplementary Figure S3) as the Gain period continued, revealing the change of microbiota underwent a dynamic alienation process over time (Figure 2E; Supplementary Figure S2B). In the Lose period, although the overall difference among all time groups was significant (Figure 2F; Supplementary Table S3B, All between vs. All within, $p < 0.01$), there was no significant difference for pairwise comparisons between individual time groups (One exception in the Bray-Curtis

10.3389/fmicb.2023.1239847

results of week 34, Supplementary Figure S2C; Supplementary Table S3B). Moreover, we suspect that the microbiota changes early on during the initial 2-week period (week 30, 31) of food restriction and then stabilizes by week 32, so no gradient change similar to the Gain period occurs in the later time period.

3.2. Changes of the dominant gut bacteria

We analyzed changes in the relative abundance of dominant bacteria at three taxonomic levels (Phylum, Family and Genus). Overall, Firmicutes (64.3%), Bacteroidetes (27.9%), Proteobacteria (2.5%) and Spirochaetes (2.3%) were the most dominant phyla. At the family and genus level, the dominant bacteria were mainly Ruminococcaceae (29.5%, 43 taxa), Lachnospiraceae (14.6%, 64 taxa), Christensenellaceae (9.1%, 3 taxa), *Bacteroides* (3.7%), *Treponema* (2.0%), and *Lactobacillus* (1.7%).

The LEfSe analysis results revealed that the gut microbiota composition underwent extensive changes between the Gain and Lose periods (Figure 3; Supplementary Table S7). Each taxon was analyzed one at a time and presented in taxonomic order at the phylum level. Firmicutes decreased in the weight loss period, mainly due to the significant decrease of taxa in Ruminococcaceae (including *Ruminococcus*, *Oscillibacter*), Lachnospiraceae, *Lactobacillus* and *Streptococcus*. Although the total relative abundance of Bacteroidetes did not change significantly, it was actually neutralized by up and down changes of taxa in genus/family level. For example, *Bacteroides* and *Porphyromonas* increased significantly in the Lose period, while the p-251-o5 family, Prevotellaceae (including *Prevotella*), Rikenellaceae, and Muribaculaceae, were all significantly reduced. Proteobacteria increased in the Lose period due to an increase in *Escherichia-Shigella* and *Desulfovibrio*. Furthermore, the decrease of Spirochaetes was mainly due to the decrease in *Treponema*, and increase of Verrucomicrobia in the Loss period was mostly due to *Akkermansia*.

3.3. Gut bacteria related to pig body weight

We looked for gut bacteria that were correlated with body weight during the Gain and the Lose periods. Only the 85 most dominant taxa at the genus or family levels (relative abundance >0.001) were enrolled in both the Pearson and Spearman correlation tests (Supplementary Table S4). After filtering ($|R| > 0.2$, $p < 0.05$, taxa relative abundance >0.005), 9 prominent taxa were identified, and the results were completely different between the Gain and Lose periods (Figure 4). In the Gain period, *Bacteroides*, *Clostridium sensu stricto* 1, and *Escherichia-Shigella* were positively correlated with body weight and their abundances increased over time; while *Streptococcus*, *Oscillospira* and *Prevotellaceae* UCG-001 were negatively correlated (decreased during the Gain period).

In the Lose period, *Porpyromonas* and *Campylobacter* were positively correlated and decreased in relative abundance over time (Supplementary Table S4). Only one taxon, '*Christensenellaceae* R-7 group', was negatively correlated with body weight, and its average relative abundance was very high (reaching 26.3% at week 38). In

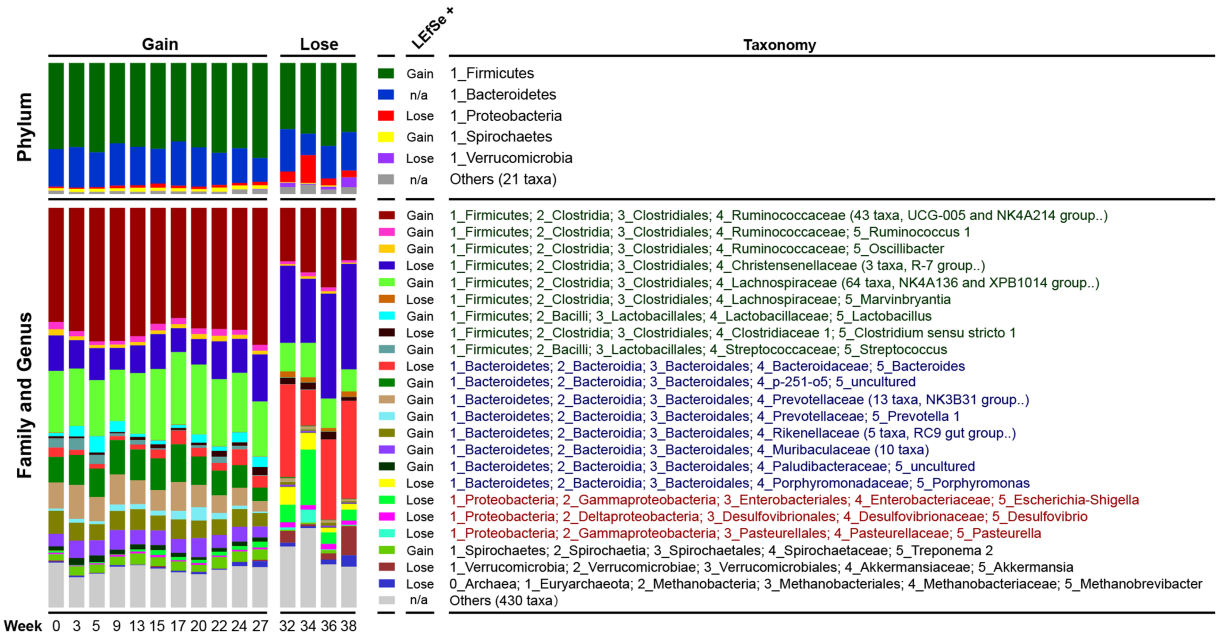

FIGURE 3
Dynamic changes in the composition of the pig microbiota. Each bar represents the average relative abundance of each taxon at a particular time point. In the 'Family and Genus' part, the genera with very low relative abundances (< 0.01) were summarized at the family level, and taxa that cannot be identified to the family level were merged into 'Others'. Abundance differences of each taxon between the Gain and Lose periods were tested by LEfSe and 'LEfSe+' indicates the group with higher abundance. n/a, not applicable. Taxa names belonging to the same phylum were marked with the same color.

10.3389/fmicb.2023.1239847

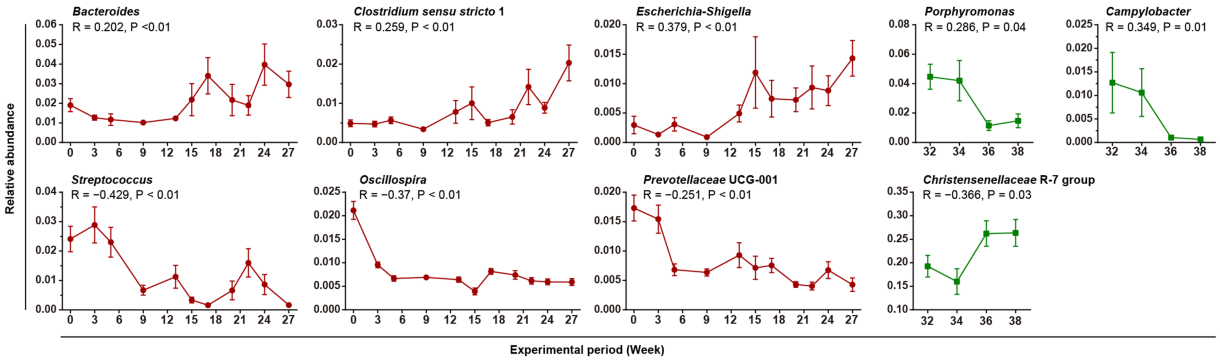

FIGURE 4
Gut bacteria correlated with body weight. Linear graphs show the average relative abundances of weight-related bacteria over time (Mean + SEM). The red and green lines indicate the Gain and Lose periods, respectively. The results of the Spearman correlation test are marked in the figure.

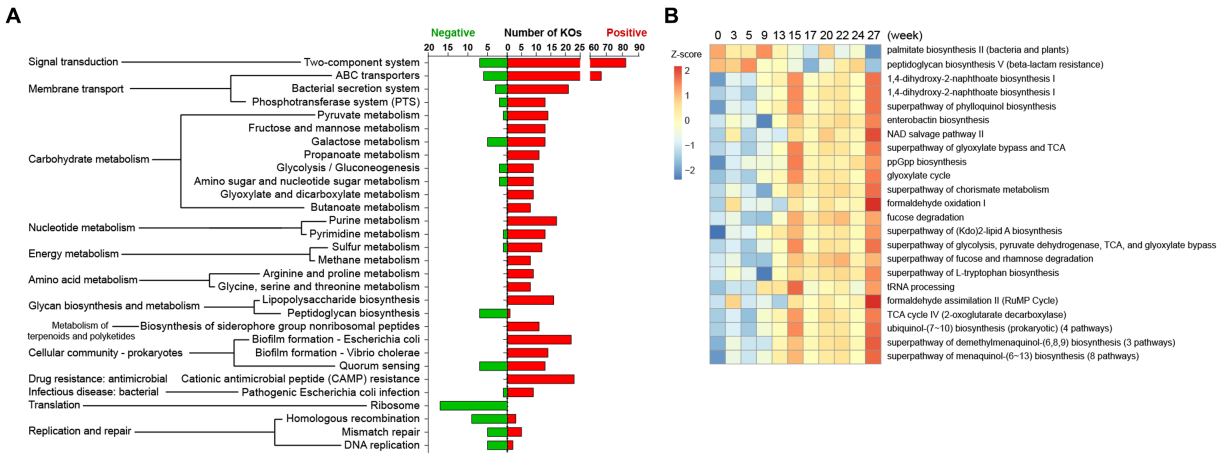

FIGURE 5
Predicted KEGG and MetaCyc pathways correlated to pig body weight in the Gain stage. Microbial metagenomic information was predicted using the PICRUSt2 package based on the 16S metadata of all samples. **(A)** KOs were tested for Spearman correlation with body weight data, and only KOs with relatively strong correlation ($|R| > 0.3$, $p < 0.01$, Average counts >100) were mapped to KEGG pathways. **(B)** Predicted metagenome was annotated as Enzyme Classification (EC) and mapped to the MetaCyc pathway. The aggregated enzyme gene counts data (Average counts >1,000) was used for Spearman correlation test ($|R| > 0.2$, $p < 0.01$), and relative abundance of these pathways were shown as a heatmap.

addition, bacteria taxa with its abundance significant changed during weight gain period were not recovered in weight loss period.

3.4. Predicted function of pig gut microbiota

We next used PICRUSt2 to explore the functional profiles of pig gut microbiota. The 16S feature metadata of all samples were loaded for metagenome prediction, and predicted genes were studied for functional annotation and pathway attribution analysis based on the KEGG and MetaCyc databases. A total of 7,088 KEGG Orthology (KO) genes were acquired. The gene alpha diversity index (both Shannon and Observer KO number) was higher in the Lose group than the Gain group (Supplementary Table S5A-1, Shannon index: 10.9 vs. 10.5, KOs: ~5,384 vs. ~5,126), indicating that although starvation-related weight loss led to a significant decrease of gut microbial species, the remaining bacteria carry more types of genes and may have relatively more complex functions. Meanwhile, comparisons across time points (week groups) revealed that both alpha and beta diversity of KOs varied significantly over time (Supplementary Table S5A-2, 3, test on "week" factor).

A correlation analysis was conducted on 4,556 abundant KOs (counts >100). In the weight gain period, 1,081 KOs were positively correlated with body weight, and 149 KOs were negatively correlated (Supplementary Table S5B). KEGG pathway affiliations of these weight-related KOs are shown in Figure 5A. However, only 6 KOs were significantly (all positive) related to body weight in the Lose period (Supplementary Table S5B), and it was not possible to find any weighted-related KOs that changed in the Gain period and recovered during the Lose period.

For the MetaCyc analysis, 2,138 predicted Enzyme genes were attributed to 415 MetaCyc pathways. Likewise, 35 pathways were corelated with body weight in the Gain period (Figure 5B, 33 positive and 2 negative) and 72 pathways were weight-related in the Lose period (Supplementary Table S5C).

4. Discussion

4.1. The influence of weight gain and weight loss on microbial diversity

The high-fat diet (HFD) treatment is commonly used to construct obesity models of experimental animals (de La Serre et al., 2010; Fei et al., 2020). Here, we do not intend to distinguish the HFD and HED (high-energy diet) in discussion, as different studies have used inconsistent ingredient and fat ratios or indeterminate energy criteria (Matteo et al., 2012; Lecomte et al., 2015; Wan et al., 2019) sIn previous studies on mice and pigs, HFD significantly reduced the alpha diversity of animal intestinal microbiota (Chang et al., 2018; Panasevich et al., 2018; Yin et al., 2018), but not significantly so in human cases, e.g., Shannon diversity was not significantly changed in young Chinese adults after a long-term HFD lasting for 6 months (Wan et al., 2019). In addition, a short-term animal-based diet (4 days, high fat and protein) also did not significantly change the alpha-diversity index (David et al., 2014). In light of these results, the influence of HFD on gut microbial diversity remains unclear. Differences in species, HFD formulations, and duration may all have impact on microbial diversity and lead to inconsistent results. In addition to HFD, the obesity traits of host may also affect gut microbiota. Several studies have shown that obese individuals are associated with higher (Kasai et al., 2015; Chávez-Carbajal et al., 2019) or lower (Turnbaugh et al., 2009; Liu et al., 2017; Yun et al., 2017) microbial diversity. HFD and the obesity phenotype are in fact two different influencing factors for gut microbiota.

In our study, the changes of fecal microbiota in pigs during long-time HFD fattening were dynamically monitored. The "down-up-down" variation of alpha diversity has never been observed before (Figure 2C) and its explanation can only be speculative. The early reduction in alpha-diversity (after 3 weeks) was mainly due to HFD treatment (consistent finding in mice, after 2 weeks) (Yin et al., 2018). The rebound of diversity at the middle time points is hard to explain, but it's not a simple recovery, because the microbial composition has changed significantly from our beta diversity results. After a long-term HFD, excessive obesity of pigs may again lead to decrease in gut microbial diversity (consistent finding in Ossabaw pig, after 36 weeks) (Panasevich et al., 2018).

The effect of weight loss on gut microbial diversity remains controversial. In human studies, calorie-restricted diets can increase (Frost et al., 2019) or has insignificant effect (Sowah et al., 2022) on fecal bacteria diversity. Studies employing lower-fat diet (LFD) (Wan et al., 2019) and a fruit and vegetable diet (Kopf et al., 2018) were associated with increased Shannon diversity. Inconsistent reports also appeared in mouse model studies, e.g., increased (Cignarella et al., 2018) or not changed (Beli et al., 2018) in alpha diversity. Moreover, a study on obese women with very-low-calorie diets showed that although the diversity (observed ASVs) increased after diet restriction, the total bacteria copies decreased (von Schwartzenberg et al., 2021). In our weight loss experiments, we applied extreme dietary restriction (reduce 90%), a treatment that approximates the starvation model and led to a dramatic decline of alpha diversity. One study found that starvation of hybrid grouper led to significantly decreased abundance and diversity of intestinal microbiota (Liu et al., 2020). The gut bacteria diversity of brown bears was lower after hibernation, a process that may constitute a model similar to starvation (Sommer et al., 2016). Overall, we speculate that distinct weight loss strategies may results in diverse changes in microbial diversity.

4.2. Gut bacteria related to body weight

In the current study, *Bacteroides* was positively correlated with pig body weight in the Gain period (Figure 4, increase with weight gain) while its relative abundance still extremely increased in Lose period (Figure 3), an apparently contradictory result. HFD can cause a significant increase in *Bacteroides* in adult human (Wan et al., 2019), and research has shown that multiple species of *Bacteroides* (*B. fragilis*, *B. ovatus*, *B. vulgatus*, etc.) are positively correlated with children's BMI (Korpela et al., 2017; Indiani et al., 2018). Interestingly, some *Bacteroides* species are negatively related to obesity and in fact are used to reverse obesity. For example, *B. acidifaciens* can prevent obesity and improve insulin sensitivity in mice (Yang J. Y. et al., 2017), and *B. thetaiotaomicron* can reduce plasma glutamate concentration and alleviate diet-induced body-weight gain and adiposity in mice (Liu et al., 2017). Therefore, we speculate that the changes in *Bacteroides* in the Gain and Lose periods in our study resulted from contributions from different *Bacteroides* species.

Multiple weight gain related bacterial taxa have also been reported in previous related studies. *Escherichia coli* was found to be higher in obese people (Gao et al., 2015; Pinart et al., 2022). A monocolonization study in mice found that *E. coli* colonization led to increased inflammation of host tissue, and aggravates HFD induced obesity and insulin resistance (Ju et al., 2023). *Oscillospira* is positively associated with leanness and health, and both HFD and inflammatory diseases can lead to a significant decrease of *Oscillospira* (Tims et al., 2013; Konikoff and Gophna, 2016; Khan et al., 2018). Similarly, the abundance of Prevotellaceae was reduced in children consuming a western-style diet (high-fat and low fiber) (Davis et al., 2020), and also in patients with urinary and nervous system diseases (Gerhardt and Mohajeri, 2018; Sanada et al., 2020; Stanford et al., 2020).

Regarding the issue of weight loss, there are variations in the changes observed in Firmicutes across different reports. In a mouse model, a significant decrease in Firmicutes was discovered when obesity was reversed through Resveratrol supplementation (Sung et al., 2017). Similar patterns have been observed in studies on hibernating animals, including grizzly bears, squirrels, and frogs, where a reduction in Firmicutes and an increase in Bacteroidetes and Verrucomicrobia were consistently observed (Dill-McFarland et al., 2014; Sommer et al., 2016; Weng et al., 2016), aligning closely with our findings in pigs (Figure 3). However, contradictory outcomes have been reported in mice subjected to intermittent fasting (Beli et al., 2018; Cignarella et al., 2018).

Christensenellaceae, as evident from our pig model study (Figures 3, 4), emerges as the most crucial bacterium associated with weight loss. It has also been found to be enriched in human individuals with a low BMI. Studies involving whole fecal bacteria transplantation (Zhou et al., 2017) and the transplantation of a single bacterium (*C. minuta*) (Goodrich et al., 2014) have demonstrated that Christensenellaceae possesses the ability to modify the composition of the microbiome associated with obesity and reduce body weight. Additionally, *Akkermansia* has garnered considerable attention (Figure 3). Consistently, fasting in mice has been shown to significantly increase the abundance of *Akkermansia* (Beli et al., 2018). Furthermore, it has been observed that both *Akkermansia* and

Christensenellaceae were significantly up-regulated in a study involving the use of weight-loss drugs (quercetin and resveratrol) to alleviate obesity in mice fed a high-fat diet (Zhao et al., 2017).

4.3. Function of weight-related gut microbiota

In a study involving intestinal metagenomics conducted on Chinese individuals (23), it was observed that obese individuals have a lower gene count of gut bacteria compared to lean individuals. Interestingly, several obesity-upregulated KEGG pathways aligned with our findings in pigs, including 'ABC transporters', 'Phosphotransferase system (PTS)', 'Galactose metabolism', 'Lipopolysaccharide biosynthesis', and 'Fructose and mannose metabolism'. Furthermore, two pathways, namely 'Sulfur metabolism' and 'Methane metabolism', were found to be upregulated following a high-fat diet in mice (Hong et al., 2020). Notably, the 'Ribosome' pathway exhibited downregulation in studies involving diabetic mice fed a high-fat diet (Liu et al., 2019) and in obese women with liver steatosis (Hoyles et al., 2018), highlighting its consistent downregulation across various obesity-related conditions. These repeatedly validated pathways warrant attention, while further investigation is needed to explore other pathways in detail.

5. Conclusion

The long-term HFD-fattening of Bama pigs can induce significant dynamic changes in their gut microbiota and eventually lead to a decrease in microbial diversity. The weight gain process was accompanied by an increased abundance of *Bacteroides* and *Clostridium sensu stricto* 1, and a decrease of *Streptococcus*, *Oscillospira*, and Prevotellaceae UCG-001. Weight loss through starvation did not restore the gut microbiota to its previous structure, but further reduced microbial diversity and the abundance of *Porphyromonas* and *Campylobacter*. Notably, Christensenellaceae R-7 group exhibits a significant association with weight loss. These weight-related gut bacteria in pigs could still be investigated as potential and functionally relevant microbial resources for pigs. This obesity model study based on Bama pigs revalidate many existing findings, and the original results again demonstrate the complexity of the relationship between gut microbiota and body weight.

Data availability statement

All sequencing data are available in the NCBI Sequence Read Archive (SRA) under the bioproject number PRJNA889082, submission: SUB12136091.

Ethics statement

All experimental procedures involving animals were performed according to Regulations for the Administration of Affairs Concerning Experimental Animals (Ministry of Science and Technology, China, revised in March 2017), and approved by the animal ethical and welfare committee (AEWC) of Sichuan Agricultural University under permit No. DKY-B20161707.

Author contributions

LJ and ML designed the study and provided the funding support. LiC, CZ, LoC, XQ, and JC contributed to the animal experiments and sample collection. BZ performed the data analysis and wrote the manuscript. FK provided the reference analysis and constructive discussions. All authors contributed to the article and approved the submitted version.

Funding

This work was supported by the National Key R&D Program of China (2021YFA0805903 to LJ and 2020YFA0509500 to ML), the Tackling Project for Agricultural Key Core Technologies of China (NK2022110602), the Sichuan Science and Technology Program (2021ZDZX0008 to LJ and 2021YFYZ0009 to ML), the National Natural Science Foundation of China (32225046 to ML and 32202630 to FK).

Acknowledgments

We would like to thank Diyan Li from the School of Pharmacy at Chengdu University for help in data analysis. We also thank Jideng Ma and Kereng Long from Sichuan Agricultural University for animal management and sample collection.

Conflict of interest

The authors declare that the research was conducted in the absence of any commercial or financial relationships that could be construed as a potential conflict of interest.

Publisher's note

Supplementary material

The Supplementary material for this article can be found online at: https://www.frontiersin.org/articles/10.3389/fmicb.2023.1239847/full#supplementary-material

References

Azad, M. A. K., Gao, Q., Ma, C., Wang, K., and Kong, X. (2022). Betaine hydrochloride addition in Bama mini-pig's diets during gestation and lactation enhances immunity and alters intestine microbiota of suckling piglets. *J. Sci. Food Agric.* 102, 607–616. doi: 10.1002/jsfa.11389

Ban-Tokuda, T., Maekawa, S., Miwa, T., Ohkawara, S., and Matsui, H. (2017). Changes in faecal bacteria during fattening in finishing swine. *Anaerobe* 47, 188–193. doi: 10.1016/j.anaerobe.2017.06.006

Beli, E., Yan, Y., Moldovan, L., Vieira, C. P., Gao, R., Duan, Y., et al. (2018). Restructuring of the gut microbiome by intermittent fasting prevents retinopathy and prolongs survival in mice. *Diabetes* 67, 1867–1879. doi: 10.2337/db18-0158

Benjamini, Y., and Hochberg, Y. (1995). Controlling the false discovery rate: a practical and powerful approach to multiple testing. *J. Royal Stat. Soc.: Ser. B* 57, 289–300. doi: 10.1111/j.2517-6161.1995.tb02031.x

Bolyen, E., Rideout, J. R., Dillon, M. R., Bokulich, N. A., Abnet, C. C., Al-Ghalith, G. A., et al. (2019). Reproducible, interactive, scalable and extensible microbiome data science using QIIME 2. *Nat. Biotechnol.* 37, 852–857. doi: 10.1038/s41587-019-0209-9

Callahan, B. J., McMurdie, P. J., Rosen, M. J., Han, A. W., Johnson, A. J. A., and Holmes, S. P. (2016). DADA2: high-resolution sample inference from Illumina amplicon data. *Nat. Methods* 13, 581–583. doi: 10.1038/nmeth.3869

Chang, C. J., Lu, C. C., Lin, C. S., Martel, J., Ko, Y. F., Ojcius, D. M., et al. (2018). Antrodia cinnamomea reduces obesity and modulates the gut microbiota in high-fat diet-fed mice. *Int. J. Obes.* 42, 231–243. doi: 10.1038/ijo.2017.149

Chávez-Carbajal, A., Nirmalkar, K., Pérez-Lizaur, A., Hernández-Quiroz, F., Ramírez-del-Alto, S., García-Mena, J., et al. (2019). Gut microbiota and predicted metabolic pathways in a sample of Mexican women affected by obesity and obesity plus metabolic syndrome. *Int. J. Mol. Sci.* 20:438. doi: 10.3390/ijms20020438

Cignarella, F., Cantoni, C., Ghezzi, L., Salter, A., Dorsett, Y., Chen, L., et al. (2018). Intermittent fasting confers protection in CNS autoimmunity by altering the gut microbiota. *Cell Metab.* 27, 1222–1235.e6. doi: 10.1016/j.cmet.2018.05.006

David, L. A., Maurice, C. F., Carmody, R. N., Gootenberg, D. B., Button, J. E., Wolfe, B. E., et al. (2014). Diet rapidly and reproducibly alters the human gut microbiome. *Nature* 505, 559–563. doi: 10.1038/nature12820

Davis, E. C., Dinsmoor, A. M., Wang, M., and Donovan, S. M. (2020). Microbiome composition in pediatric populations from birth to adolescence: impact of diet and prebiotic and probiotic interventions. *Dig. Dis. Sci.* 65, 706–722. doi: 10.1007/s10620-020-06092-x

de La Serre, C. B., Ellis, C. L., Lee, J., Hartman, A. L., Rutledge, J. C., and Raybould, H. E. (2010). Propensity to high-fat diet-induced obesity in rats is associated with changes in the gut microbiota and gut inflammation. *American journal of physiology-gastrointestinal and liver. Physiology* 299, G440–G448. doi: 10.1152/ajpgi.00098.2010

Dill-McFarland, K. A., Neil, K. L., Zeng, A., Sprenger, R. J., Kurtz, C. C., Suen, G., et al. (2014). Hibernation alters the diversity and composition of mucosa-associated bacteria while enhancing antimicrobial defence in the gut of 13-lined ground squirrels. *Mol. Ecol.* 23, 4658–4669. doi: 10.1111/mec.12884

Douglas, G. M., Maffei, V. J., Zaneveld, J. R., Yurgel, S. N., Brown, J. R., Taylor, C. M., et al. (2020). PICRUSt2 for prediction of metagenome functions. *Nat. Biotechnol.* 38, 685–688. doi: 10.1038/s41587-020-0548-6

Fei, Y., Wang, Y., Pang, Y., Wang, W., Zhu, D., Xie, M., et al. (2020). Xylooligosaccharide modulates gut microbiota and alleviates colonic inflammation caused by high fat diet induced obesity. *Front. Physiol.* 10:1601. doi: 10.3389/fphys.2019.01601

Friedman, J., and Alm, E. J. (2012). Inferring correlation networks from genomic survey data. *PLoS Comput. Biol.* 8:e1002687. doi: 10.1371/journal.pcbi.1002687

Frost, F., Storck, L. J., Kacprowski, T., Gärtner, S., Rühlemann, M., Bang, C., et al. (2019). A structured weight loss program increases gut microbiota phylogenetic diversity and reduces levels of Collinsella in obese type 2 diabetics: a pilot study. *PLoS One* 14:e0219489. doi: 10.1371/journal.pone.0219489

Gao, X., Jia, R., Xie, L., Kuang, L., Feng, L., and Wan, C. (2015). Obesity in school-aged children and its correlation with gut E.Coli and Bifidobacteria: a case–control study. *BMC Pediatr.* 15:64. doi: 10.1186/s12887-015-0384-x

Gerhardt, S., and Mohajeri, M. H. (2018). Changes of colonic bacterial composition in Parkinson's disease and other neurodegenerative diseases. *Nutrients* 10:708. doi: 10.3390/nu10060708

Goodrich, J. K., Waters, J. L., Poole, A. C., Sutter, J. L., Koren, O., Blekhman, R., et al. (2014). Human genetics shape the gut microbiome. *Cells* 159, 789–799. doi: 10.1016/j.cell.2014.09.053

Han, G. G., Lee, J.-Y., Jin, G.-D., Park, J., Choi, Y. H., Chae, B. J., et al. (2017). Evaluating the association between body weight and the intestinal microbiota of weaned piglets via 16S rRNA sequencing. *Appl. Microbiol. Biotechnol.* 101, 5903–5911. doi: 10.1007/s00253-017-8304-7

Hong, Y., Li, B., Zheng, N., Wu, G., Ma, J., Tao, X., et al. (2020). Integrated metagenomic and Metabolomic analyses of the effect of Astragalus polysaccharides on alleviating high-fat diet-induced metabolic disorders. *Front. Pharmacol.* 11:833. doi: 10.3389/fphar.2020.00833

Hoyles, L., Fernández-Real, J.-M., Federici, M., Serino, M., Abbott, J., Charpentier, J., et al. (2018). Molecular phenomics and metagenomics of hepatic steatosis in non-diabetic obese women. *Nat. Med.* 24, 1070–1080. doi: 10.1038/s41591-018-0061-3

Hvistendahl, M. (2012). Pigs as stand-ins for microbiome studies. *Science* 336:1250. doi: 10.1126/science.336.6086.1250

Indiani, C. M. D. S. P., Rizzardi, K. F., Castelo, P. M., Ferraz, L. F. C., Darrieux, M., and Parisotto, T. M. (2018). Childhood obesity and Firmicutes/Bacteroidetes ratio in the gut microbiota: a systematic review. *Child. Obes.* 14, 501–509. doi: 10.1089/chi.2018.0040

Jiang, Q., Xie, C., Chen, L., Xiao, H., Xie, Z., Zhu, X., et al. (2023). Identification of gut microbes associated with feed efficiency by daily-phase feeding strategy in growing-finishing pigs. *Animal Nutrition* 12, 42–53. doi: 10.1016/j.aninu.2022.09.005

Jin, L., Wang, D., Zhang, J., Liu, P., Wang, Y., Lin, Y., et al. (2023). Dynamic chromatin architecture of the porcine adipose tissues with weight gain and loss. *Nat. Commun.* 14:3457. doi: 10.1038/s41467-023-39191-0

Ju, T., Bourrie Benjamin, C. T., Forgie Andrew, J., Pepin Deanna, M., Tollenaar, S., Sergi Consolato, M., et al. (2023). The gut commensal *Escherichia coli* aggravates high-fat-diet-induced obesity and insulin resistance in mice. *Appl. Environ. Microbiol.* 89, e0162822–e0101622. doi: 10.1128/aem.01628-22

Kasai, C., Sugimoto, K., Moritani, I., Tanaka, J., Oya, Y., Inoue, H., et al. (2015). Comparison of the gut microbiota composition between obese and non-obese individuals in a Japanese population, as analyzed by terminal restriction fragment length polymorphism and next-generation sequencing. *BMC Gastroenterol.* 15:100. doi: 10.1186/s12876-015-0330-2

Khan, T. J., Ahmed, Y. M., Zamzami, M. A., Mohamed, S. A., Khan, I., Baothman, O. A. S., et al. (2018). Effect of atorvastatin on the gut microbiota of high fat diet-induced hypercholesterolemic rats. *Sci. Rep.* 8:662. doi: 10.1038/s41598-017-19013-2

Kleinert, M., Clemmensen, C., Hofmann, S. M., Moore, M. C., Renner, S., Woods, S. C., et al. (2018). Animal models of obesity and diabetes mellitus. *Nat. Rev. Endocrinol.* 14, 140–162. doi: 10.1038/nrendo.2017.161

Konikoff, T., and Gophna, U. (2016). Oscillospira: a central, enigmatic component of the human gut microbiota. *Trends Microbiol.* 24, 523–524. doi: 10.1016/j.tim.2016.02.015

Kopf, J. C., Suhr, M. J., Clarke, J., Eyun, S. I., Riethoven, J. M., Ramer-Tait, A. E., et al. (2018). Role of whole grains versus fruits and vegetables in reducing subclinical inflammation and promoting gastrointestinal health in individuals affected by overweight and obesity: a randomized controlled trial. *Nutr. J.* 17:72. doi: 10.1186/s12937-018-0381-7

Korpela, K., Zijlmans, M. A. C., Kuitunen, M., Kukkonen, K., Savilahti, E., Salonen, A., et al. (2017). Childhood BMI in relation to microbiota in infancy and lifetime antibiotic use. *Microbiome* 5:26. doi: 10.1186/s40168-017-0245-y

Kruskal, W. H., and Wallis, W. A. (1952). Use of ranks in one-criterion variance analysis. *J. Am. Stat. Assoc.* 47, 583–621. doi: 10.1080/01621459.1952.10483441

Lecomte, V., Kaakoush, N. O., Maloney, C. A., Raipuria, M., Huinao, K. D., Mitchell, H. M., et al. (2015). Changes in gut microbiota in rats fed a high fat diet correlate with obesity-associated metabolic parameters. *PLoS One* 10:e0126931. doi: 10.1371/journal.pone.0126931

Liu, R., Hong, J., Xu, X., Feng, Q., Zhang, D., Gu, Y., et al. (2017). Gut microbiome and serum metabolome alterations in obesity and after weight-loss intervention. *Nat. Med.* 23, 859–868. doi: 10.1038/nm.4358

Liu, S., Qin, P., and Wang, J. (2019). High-fat diet alters the intestinal microbiota in Streptozotocin-induced type 2 diabetic mice. *Microorganisms* 7:176. doi: 10.3390/microorganisms7060176

Liu, X., Shi, H., He, Q., Lin, F., Wang, Q., Xiao, S., et al. (2020). Effect of starvation and refeeding on growth, gut microbiota and non-specific immunity in hybrid grouper (*Epinephelus fuscoguttatus*♀×*E. lanceolatus*♂). *Fish Shellfish Immunol.* 97, 182–193. doi: 10.1016/j.fsi.2019.11.055

Luo, Y., Ren, W., Smidt, H., Wright André-Denis, G., Yu, B., Schyns, G., et al. (2022). Dynamic distribution of gut microbiota in pigs at different growth stages: composition and contribution. *Microbiol. Spectrum* 10, e0068821–e0000621. doi: 10.1128/spectrum.00688-21

Matteo, S., Elodie, L., Sandra, G., Audrey, B., Mathieu, B., Claire, C., et al. (2012). Metabolic adaptation to a high-fat diet is associated with a change in the gut microbiota. *Gut* 61, 543–553. doi: 10.1136/gutjnl-2011-301012

Oh, J. K., Chae, J. P., Pajarillo, E. A. B., Kim, S. H., Kwak, M.-J., Eun, J.-S., et al. (2020). Association between the body weight of growing pigs and the functional capacity of their gut microbiota. *Anim. Sci. J.* 91:e13418. doi: 10.1111/asj.13418

Panasevich, M. R., Wankhade, U. D., Chintapalli, S. V., Shankar, K., and Rector, R. S. (2018). Cecal versus fecal microbiota in Ossabaw swine and implications for obesity. *Physiol. Genomics* 50, 355–368. doi: 10.1152/physiolgenomics.00110.2017

Pedersen, R., Ingerslev, H.-C., Sturek, M., Alloosh, M., Cirera, S., Christoffersen, B. Ø., et al. (2013). Characterisation of gut microbiota in Ossabaw and Göttingen Minipigs as

models of obesity and metabolic syndrome. *PLoS One* 8:e56612. doi: 10.1371/journal.pone.0056612

Pinart, M., Dötsch, A., Schlicht, K., Laudes, M., Bouwman, J., Forslund, S. K., et al. (2022). Gut microbiome composition in obese and non-obese persons: a systematic review and Meta-analysis. *Nutrients* 14:12. doi: 10.3390/nu14010012

Ruan, J., Zhang, Y., Yuan, J., Xin, L., Xia, J., Liu, N., et al. (2016). A long-term high-fat, high-sucrose diet in Bama minipigs promotes lipid deposition and amyotrophy by up-regulating the myostatin pathway. *Mol. Cell. Endocrinol.* 425, 123–132. doi: 10.1016/j.mce.2016.02.001

Sanada, K., Nakajima, S., Kurokawa, S., Barceló-Soler, A., Ikuse, D., Hirata, A., et al. (2020). Gut microbiota and major depressive disorder: a systematic review and meta-analysis. *J. Affect. Disord.* 266, 1–13. doi: 10.1016/j.jad.2020.01.102

Segata, N., Izard, J., Waldron, L., Gevers, D., Miropolsky, L., Garrett, W. S., et al. (2011). Metagenomic biomarker discovery and explanation. *Genome Biol.* 12:R60. doi: 10.1186/gb-2011-12-6-r60

Sommer, F., Ståhlman, M., Ilkayeva, O., Arnemo, J. M., Kindberg, J., Josefsson, J., et al. (2016). The gut microbiota modulates energy metabolism in the hibernating Brown bear *Ursus arctos*. *Cell Rep.* 14, 1655–1661. doi: 10.1016/j.celrep.2016.01.026

Sowah, S. A., Milanese, A., Schübel, R., Wirbel, J., Kartal, E., Johnson, T. S., et al. (2022). Calorie restriction improves metabolic state independently of gut microbiome composition: a randomized dietary intervention trial. *Genome Med.* 14:30. doi: 10.1186/s13073-022-01030-0

Stanford, J., Charlton, K., Stefoska-Needham, A., Ibrahim, R., and Lambert, K. (2020). The gut microbiota profile of adults with kidney disease and kidney stones: a systematic review of the literature. *BMC Nephrol.* 21:215. doi: 10.1186/s12882-020-01805-w

Sung, M. M., Kim, T. T., Denou, E., Soltys, C.-L. M., Hamza, S. M., Byrne, N. J., et al. (2017). Improved glucose homeostasis in obese mice treated with resveratrol is associated with alterations in the gut microbiome. *Diabetes* 66, 418–425. doi: 10.2337/db16-0680

Tims, S., Derom, C., Jonkers, D. M., Vlietinck, R., Saris, W. H., Kleerebezem, M., et al. (2013). Microbiota conservation and BMI signatures in adult monozygotic twins. *ISME J.* 7, 707–717. doi: 10.1038/ismej.2012.146

Turnbaugh, P. J., Hamady, M., Yatsunenko, T., Cantarel, B. L., Duncan, A., Ley, R. E., et al. (2009). A core gut microbiome in obese and lean twins. *Nature* 457, 480–484. doi: 10.1038/nature07540

von Schwartzenberg, R. J., Bisanz, J. E., Lyalina, S., Spanogiannopoulos, P., Ang, Q. Y., Cai, J., et al. (2021). Caloric restriction disrupts the microbiota and colonization resistance. *Nature* 595, 272–277. doi: 10.1038/s41586-021-03663-4

Wan, Y., Wang, F., Yuan, J., Li, J., Jiang, D., Zhang, J., et al. (2019). Effects of dietary fat on gut microbiota and faecal metabolites, and their relationship with cardiometabolic risk factors: a 6-month randomised controlled-feeding trial. *Gut* 68, 1417–1429. doi: 10.1136/gutjnl-2018-317609

Wang, K., Hu, C., Tang, W., Azad, M. A. K., Zhu, Q., He, Q., et al. (2021). The enhancement of intestinal immunity in offspring piglets by maternal probiotic or Synbiotic supplementation is associated with the alteration of gut microbiota. *Front. Nutr.* 8:6053. doi: 10.3389/fnut.2021.686053

Wang, X., Tsai, T., Deng, F., Wei, X., Chai, J., Knapp, J., et al. (2019). Longitudinal investigation of the swine gut microbiome from birth to market reveals stage and growth performance associated bacteria. *Microbiome* 7:109. doi: 10.1186/s40168-019-0721-7

Weng, F. C.-H., Yang, Y.-J., and Wang, D. (2016). Functional analysis for gut microbes of the brown tree frog (*Polypedates megacephalus*) in artificial hibernation. *BMC Genomics* 17:1024. doi: 10.1186/s12864-016-3318-6

WHO (2021). *Obesity and overweight*. Available online: www.who.int/news-room/fact-sheets/detail/obesity-and-overweight.

Yang, H., Huang, X., Fang, S., He, M., Zhao, Y., Wu, Z., et al. (2017). Unraveling the fecal microbiota and metagenomic functional capacity associated with feed efficiency in pigs. *Front. Microbiol.* 8:1555. doi: 10.3389/fmicb.2017.01555

Yang, J. Y., Lee, Y. S., Kim, Y., Lee, S. H., Ryu, S., Fukuda, S., et al. (2017). Gut commensal *Bacteroides acidifaciens* prevents obesity and improves insulin sensitivity in mice. *Mucosal Immunol.* 10, 104–116. doi: 10.1038/mi.2016.42

Yang, S.-L., Xia, J.-H., Zhang, Y.-Y., Fan, J.-G., Wang, H., Yuan, J., et al. (2015). Hyperinsulinemia shifted energy supply from glucose to ketone bodies in early nonalcoholic steatohepatitis from high-fat high-sucrose diet induced Bama minipigs. *Sci. Rep.* 5:13980. doi: 10.1038/srep13980

Yin, J., Li, Y., Han, H., Chen, S., Gao, J., Liu, G., et al. (2018). Melatonin reprogramming of gut microbiota improves lipid dysmetabolism in high-fat diet-fed mice. *J. Pineal Res.* 65:e12524. doi: 10.1111/jpi.12524

Yun, Y., Kim, H.-N., Kim, S. E., Heo, S. G., Chang, Y., Ryu, S., et al. (2017). Comparative analysis of gut microbiota associated with body mass index in a large Korean cohort. *BMC Microbiol.* 17:151. doi: 10.1186/s12866-017-1052-0

Zhao, L., Zhang, Q., Ma, W., Tian, F., Shen, H., and Zhou, M. (2017). A combination of quercetin and resveratrol reduces obesity in high-fat diet-fed rats by modulation of gut microbiota. *Food Funct.* 8, 4644–4656. doi: 10.1039/C7FO01383C

Zhou, D., Pan, Q., Shen, F., Cao, H.-X., Ding, W.-J., Chen, Y.-W., et al. (2017). Total fecal microbiota transplantation alleviates high-fat diet-induced steatohepatitis in mice via beneficial regulation of gut microbiota. *Sci. Rep.* 7:1529. doi: 10.1038/s41598-017-01751-y

frontiers | Frontiers in Microbiology

TYPE Original Research
PUBLISHED 20 November 2023
DOI 10.3389/fmicb.2023.1257295

OPEN ACCESS

EDITED BY
Congying Chen,
Jiangxi Agricultural University, China

REVIEWED BY
Yu Pi,
Chinese Academy of Agricultural Sciences, China
Zhigang Song,
Shandong Agricultural University, China

*CORRESPONDENCE
Dong Xia
✉ xiadong@saas.sh.cn

RECEIVED 18 July 2023
ACCEPTED 07 November 2023
PUBLISHED 20 November 2023

CITATION
Jiang X, Deng S, Lu N, Yao W, Xia D, Tu W, Lei H, Jia P and Gan Y (2023) Fecal microbial composition associated with testosterone in the development of Meishan male pigs. *Front. Microbiol.* 14:1257295. doi: 10.3389/fmicb.2023.1257295

Fecal microbial composition associated with testosterone in the development of Meishan male pigs

Xueyuan Jiang[1], Shaoshan Deng[1,2], Naisheng Lu[1], Wen Yao[2], Dong Xia[1]*, Weilong Tu[1], Hulong Lei[1], Peng Jia[1] and Yeqing Gan[3]

[1]Shanghai Engineering Research Center of Breeding Pig, Livestock and Poultry Resources (Pig) Evaluation and Utilization Key Laboratory of Ministry of Agriculture and Rural Affairs, Institute of Animal Husbandry and Veterinary Science, Shanghai Academy of Agricultural Sciences, Shanghai, China, [2]College of Animal Science and Technology, Nanjing Agricultural University, Nanjing, China, [3]Meishan Pig Breeding Center of Jiading, Shanghai, China

Introduction: The gut microbiota closely relates to host health, whereas the relationship between gut microbiota and testosterone during the development of Meishan male pigs remains unclear. This study investigated the fecal microbiota composition and testosterone level during development in Meishan male pigs.

Methods: Fresh fecal samples of 20 healthy Meishan male pigs were individually collected at 10 and 22 weeks (wk) of age for testosterone content detection and bacteria pyrosequencing analysis. Anaerobic culture experiment of fecal bacteria in vitro was performed for bacteria pyrosequencing analysis.

Results: The fecal testosterone content increased significantly from 10 weeks (wk) to 22 wk of age ($P < 0.05$). Meanwhile, the boars at 22 wk had a lower abundance of phylum *Bacteroidetes* and *Proteobacteria*, and genus *Alloprevotella*, *Prevotella_1*, *Prevotellaceae_NK3B31_group*, and *Streptococcus* in the fecal microbiota composition ($P < 0.05$). but higher proportions of the phylum *Actinobacteria*, *Firmicutes*, *Kiritimatiellaeota*, and *Tenericutes*, and genus *Clostridium_sensu_stricto_1*, *Muribaculaceae* and *Terrisporobacter* than that at 10 wk ($P < 0.05$), and the Firmicutes to Bacteroidetes ratio was higher at 22 wk than 10 wk ($P < 0.05$). Moreover, the fecal testosterone level significantly correlated with the relative abundance of the phylum *Actinobacteria*, *Firmicutes*, and *Tencuteseri*, and genus *Alloprevotella*, *Clostridium_sensu_stricto_1*, *Muribaculaceae*, *Prevotella_1* and *Streptococcus*. Furthermore, the *in vitro* experiments indicated that the abundance of the phylum *Proteobacteria* and genus *Escherichia-Shigella* reduced with the increase of supplemental testosterone level. In contrast, the proportion of *Firmicutes* phylum increased with additional testosterone levels.

Discussion: Testosterone could modulate the microflora structure. Meanwhile, the bacteria could degrade the testosterone in a dose testosterone-dependent manner. These results provide us with new insights into the relationship between the gut microbiome and testosterone and the contributions of the gut microbiome in physiological regulation in response to gonad development.

KEYWORDS

Meishan male pigs, testosterone, microbiome, development, interaction

1 Introduction

It is well known that the gut microbiome plays a vital role in the health status of the host. Describing the complexity and changes of the intestinal microbiota may help understand its effects on overall animal health. Moreover, the gut microbiome is regulated by many factors, including environmental variables, host genetics, and even steroid hormones. For instance, cortisol increases the proliferation of *Salmonella* in primary porcine alveolar macrophages (Verbrugghe et al., 2011). Mudd et al. (2017) observed that the fecal *Ruminococcus* population negatively correlated to the serum cortisol level in piglets. Experiments on weaning piglets showed a significant correlation between elevated cortisol levels and pathogenic bacteria at weaning (Moeser et al., 2007; Tuchscherer et al., 2018). Estradiol and progesterone inhibited the growth of *Helicobacter pylori in vitro* culture (Hosoda et al., 2011). Progesterone could increase the relative abundance of the *Bifidobacterium* genus in the gut microbial composition (Nuriel-Ohayon et al., 2019). All these studies suggest that steroid hormones may influence the proliferation and metabolism of bacteria.

Testosterone is a steroid hormone secreted from the Leydig cells of the testes in males or the ovaries of females, and in small amounts by the adrenal glands. Testosterone plays an essential role in male sex maturation and spermatogenesis. Interestingly, sex differences in gut microbiota were reduced between emasculated male and female mice (Qin et al., 2010; Yurkovetskiy et al., 2013). Germ-free and SPF mice had differences in serum testosterone levels (Markle et al., 2013). Gonadectomy and hormone replacement significantly affected rodent intestinal microbiota composition (Org et al., 2016). These suggest that testosterone may interact with the gut microbiome.

The synthesis and secretion of testosterone in males vary with gonadal development. It has been reported that the plasma concentration of testosterone gradually increases during pubertal development and reaches peak level at sexual maturation in pigs (Allrich et al., 1983; Schwarzenberger et al., 1993). However, whether such developmental changes of testosterone affect intestinal microbial structure and function is yet to be being determined. Meishan pig is known as an early maturation breed, and the plasma testosterone level positively increases with age, even after sexual maturation (Kanematsu et al., 2006). Therefore, this study investigated the changes in the gut microbiome composition from 10 wk. to 22 wk. in Meishan male pigs, when the plasma testosterone concentration nearly increased twice (Kanematsu et al., 2006). Further, vitro experiments were conducted to verify the effect of testosterone on the gut microbiome. The discoveries will establish a foundation for understanding the interaction of testosterone and the gut microbiota in males.

2 Materials and methods

2.1 Animals and sampling

This experiment was approved by the Institutional Animal Care and Use Committee (IACUC) of the Shanghai Academy of Agricultural Sciences (Grant number: SAASPZ0520013). All animal care and experimental protocols followed the guidelines of the Laboratory Animal Guideline for Ethical Review of Animal Welfare (GB/T 35892-2018) set by the Standardization Administration of China.

A total of 20 healthy Meishan male pigs were investigated in this study, and all animals were given the same basal diet throughout the whole experiment. Fresh fecal samples were individually collected via rectal massage without contamination with the barn floor at 10 and 22 weeks (wk) of age, respectively. Each fecal sample was mixed homogeneously individually over ice and distributed for different analyses. The fecal sample for microbiome pyrosequencing analysis was filled in a tube with ethanol (1:3, v/v) and stored at −20°C until DNA extraction. The fecal sample for hormone analysis was stored at −20°C.

2.2 Determination of fecal testosterone concentration

Compared with blood sampling, fecal sample collection is non-invasive with less interference from acute stress (Sheriff et al., 2010). Fecal steroid hormones concentration can represent the systemic steroid hormones synthesis and secretion, especially for periodic investigation, and now it is commonly used and accepted as a means to study the changes of hormones in domestic and wild animals (Fujita et al., 2001; Sheriff et al., 2010; SankarGanesh et al., 2014). The fecal sample extraction and testosterone measurement followed the protocol described previously (Fujita et al., 2001). In brief, fecal samples were frozen-dried for 72 h, the sample weight before and after frozen-dried was recorded for the calculation of stool water content, and then 100 mg dried fecal powder was extracted in 3 mL of 80% aqueous methanol by vortex for 15 min. Following extraction, we centrifuged the suspension and recovered the supernatant liquid for testosterone measurement. The fecal testosterone was measured by using commercial enzyme-linked immunoassay (EIA) kits of testosterone (Cayman, Item No. 582701, inter-assay CV < 10.7%, intra-assay CV < 14.0%).

2.3 Anaerobic culture experiment of fecal bacteria *in vitro*

Fresh feces from 5 experimental castration boars were collected via rectal massage without contamination with the barn floor. In the laboratory, the feces were mixed evenly and sterilized with physiological saline at 1:9 (mass: volume). The diluted material was then homogenized and strained through a four-layer of cheesecloth. After centrifuging at 1,500 rpm for 15 min, the supernatant was taken for inoculation.

The medium for *in vitro* anaerobic culture was modified from that of Williams et al. (2005). The medium contained 4.0 g glucose, 1.0 g trypticase, 1.5 g Pipes, 0.6 g KCl, 0.6 g NaCl, 0.2 g $CaCl_2{\cdot}2H_2O$, 0.5 g $MgSO_4{\cdot}7H_2O$, 0.54 g NH_4Cl, 1.0 mg resazurin solution, 4.1 g Na_2CO_3, 1.0 mg Haemin, 2.5 mg $NiCl_2{\cdot}6H_2O$, 2.5 mg H_3BO_3, 2.5 mg $Na_2MoO_4{\cdot}2H_2O$, 0.5 mg SeO_2, 0.5 mg $CoCl_2{\cdot}6H_2O$, 0.314 mg $NaVO_3$, 0.25 mg $MnCl_2{\cdot}4H_2O$, 0.25 mg $ZnCl_2$, 0.25 mg $CuCl{\cdot}2H_2O$, 0.2 mg $FeSO_4{\cdot}7H_2O$, 68.5 µL acetic acid, 30 µL propionic, 18.4 µL butyric, 5.5 µL valeric, 5.5 µL 2-methyl-butyric, 4.7 µL iso-butyric, and 5.5 µL iso-valeric acids. The solution was filtered and sterilized by 0.22 µm.

The reducing agent contained 20.5 g $Na_2S{\cdot}9H_2O$ and 20.5 cysteines HCl dissolved in 1 L of boiled distilled water with nitrogen gas bubbling through it. This procedure was completed in a fume

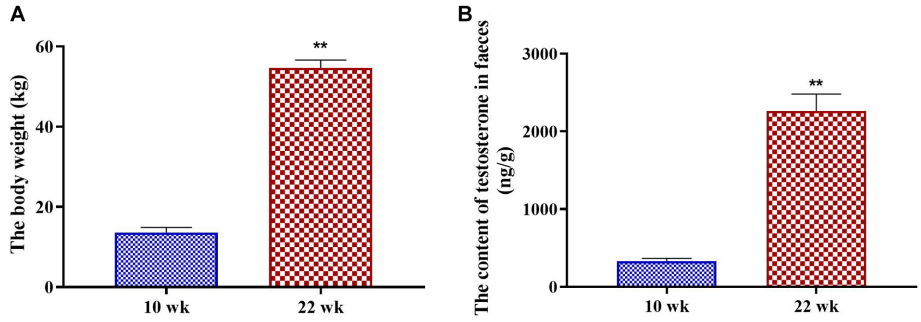

FIGURE 1
The developmental changes in male pigs. **(A)** The body weight; **(B)** the fecal testosterone content. Graph shows mean value ± SEM ($N = 20$). ** ($p < 0.01$) means significant difference between the males at the age of 10 weeks (10 wk) and 22 weeks (22 wk).

cupboard due to the danger of inhalation of toxic fumes. The vitamin/phosphate solution contained 0.0204 g biotin, 0.0205 g folic acid, 0.1640 g calcium D-pantothenate, 0.1640 g nicotinamide, 0.1640 g riboflavin, 0.1640 g thiamin HCl, 0.1640 g pyridoxine HCl, 0.0204 g para-aminobenzoic acid, 0.0205 g cyanocobalamin, dissolved in a 1 L of solution containing 54.7 g KH_2PO_4. This solution was then filter-sterilized into sterile bottles.

The anaerobic culture trial of fecal bacteria *in vitro* was designed with single factor variance, and the final concentrations of testosterone in the treatments were 200 μg/mL, 400 μg/mL, 800 μg/mL, and 1,200 μg/mL (The solvent for testosterone is DMSO). At the same time, the control group contained the same amount of DMSO as the treatments. Each treatment had six replicates, and each replicate had an 80 mL medium. After 10 min of carbon dioxide flushing, 1 mL reducing agent, 1 mL vitamin-phosphate solution, and 5 mL inoculant were added. After that, the culture was incubated in a shaker at 37°C and 180 rpm for 8 h.

2.4 Bacteria pyrosequencing analysis

The total DNA of the fecal microbial community was extracted from individual fecal samples and *in vitro* culture samples, as described previously (Jiang et al., 2020). Illumina Miseq PE250 sequencing was performed based on the bacterial 16S rRNA sequence V3-V4. The data were analyzed on the online platform of Majorbio Cloud Platform.[1] The operational taxonomic units (OTU) picking with a 97% similarity cut-off was compiled with Qiime using default parameters. Taxonomic classification was performed based on the OTU database. The alpha-diversity indices, including Chao, Ace, Shannon, and Simpson, were calculated with the Mothur program[2] and Rarefaction software. The community difference at 10 wk. and 22 wk. was evaluated using Principal Co-ordinates Analysis (PCoA) and Adonis test, and a significant difference was assigned at $p < 0.05$.

1 http://www.majorbio.com
2 http://www.mothur.org

2.5 Statistical analysis

The statistical analyses were performed using SPSS 17.0 for Windows. Independent-Samples *T*-test was used to analyze the significant differences in different treatments. The results were presented as the mean ± standard error of the mean (SEM). Statistical significance was considered at $p \leq 0.05$ for all analyses. Graph Pad Prism Version 5.01 software (Graph Pad Software, Inc., La Jolla, CA, United States) was used for mapping.

3 Results

3.1 Experiment *in vivo*

3.1.1 Testosterone concentration

As the male pigs grew from 10 wk. to 22 wk., the body weight increased significantly ($p = 0.00$, Figure 1A). Meanwhile, the fecal testosterone concentration of the male pigs increased significantly from 10 wk. to 22 wk. ($p = 0.00$, Figure 1B).

3.1.2 Fecal microbiota analysis

The 16S ribosomal RNA gene sequencing obtained 2,251,025 high-quality sequencing reads from 40 samples. Based on 97% species similarity, 1815 OTUs were obtained, which involved 476 different OTU classifications. The bacterial DNA pyrosequencing profile (Figure 2) observed that the Ace, Chao, and Simpson were higher at 22 wk. than at 10 wk. ($p < 0.05$). Principal Component Analysis (PCA)(a) and Principal Co-ordinates Analysis (PCoA) visually confirmed that the fecal microbial communities at 22 wk. distinctly separated from those at 10 wk. (Figure 3).

At the phylum level (Figure 4A), the majority proportions of sequences attributed to *Bacteroidetes* (>41.94%) and *Firmicutes* (>40.12%). Following the growth of the pigs from 10 wk. to 22 wk. (Figure 4B), there was a significant reduction of *Bacteroidetes* ($p = 0.02$) and *Proteobacteria* ($p = 0.01$) but a pronounced increase of *Firmicutes* ($p = 0.02$), *Tenericutes* ($p = 0.01$), *Kiritimatiellaeota* ($p = 0.01$) and *Actinobacteria* ($p = 0.02$). Moreover, the *Firmicutes* / *Bacteroidetes* ratio at 10 wk. was significantly lower than at 22 wk. ($p = 0.02$, Figure 4C).

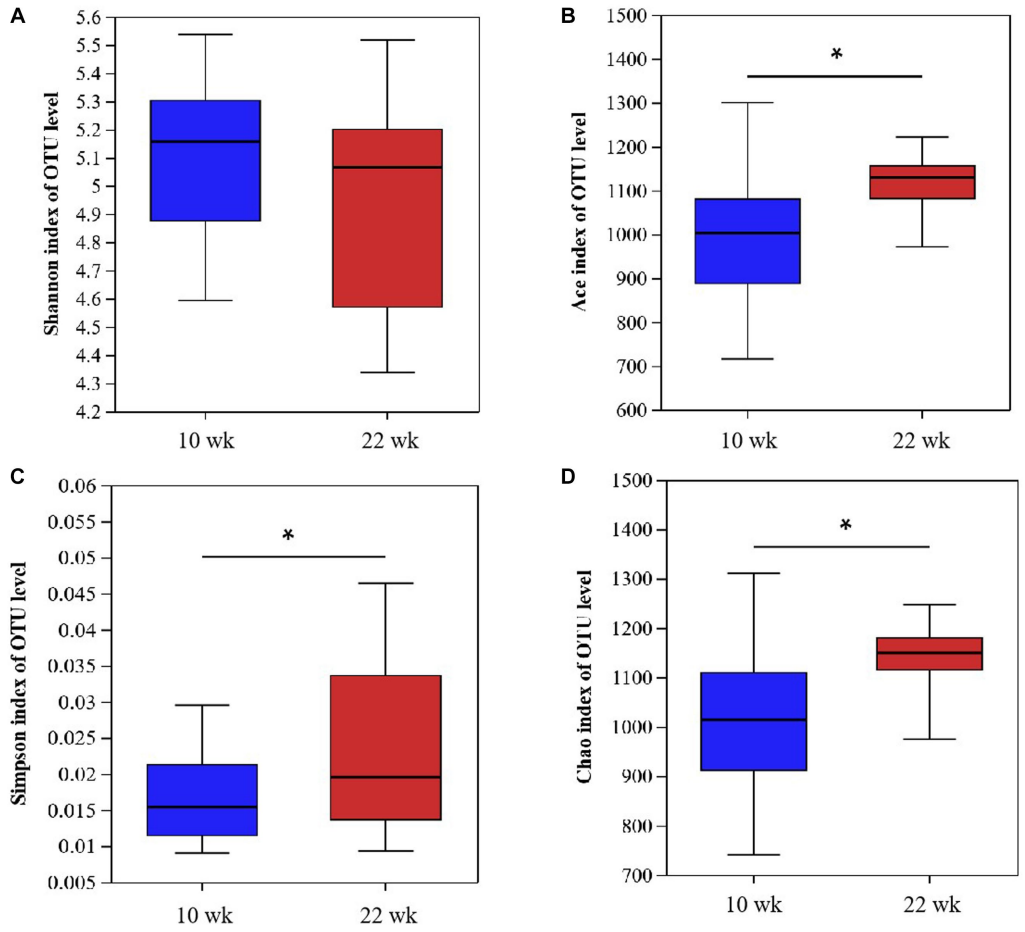

FIGURE 2
Fecal bacterial richness and alpha diversity index. **(A)** Shannon; **(B)** Ace; **(C)** Simpson; **(D)** Chao. *($p < 0.05$) means significant difference between the males at the age of 10 weeks (10 wk) and 22 weeks (22 wk). $N = 20$.

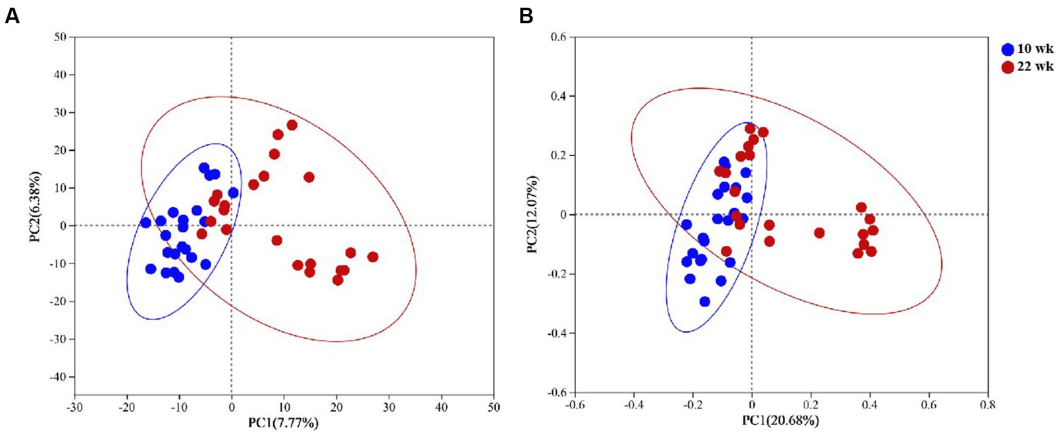

FIGURE 3
Principal Component Analysis (PCA, **A**) and Principal Co-ordinates Analysis (PCoA, **B**) plots on OTU level. Adonis test showed sexual development time has a significant impact on the fecal microbial community. **(A)** Based on Bray-Curtis distance and $R^2 = 0.09$, $p = 0.00$; **(B)** Based on weighted unifrac distance and $R^2 = 0.12$, $p = 0.00$ at the OTU level. Red dots represent the male pigs at 10 weeks (10 wk), blue triangles represent the male pigs at 22 weeks (22). $N = 20$.

At the genus level (Figure 5), the proportions of *Prevotellaceae_NK3B31_group* ($p = 0.00$), *Streptococcus* ($p = 0.00$), *Alloprevotella* ($p = 0.01$), and *Prevotella_1* ($p = 0.00$) of the fecal microbial composition were significantly lower at 22 wk. than that at 10 wk., while *Clostridium_sensu_stricto_1* ($p = 0.00$), *Muribaculaceae* ($p = 0.02$) and *Terrisporobacter* ($p = 0.03$) were higher at 22 wk. than that at 10 wk.

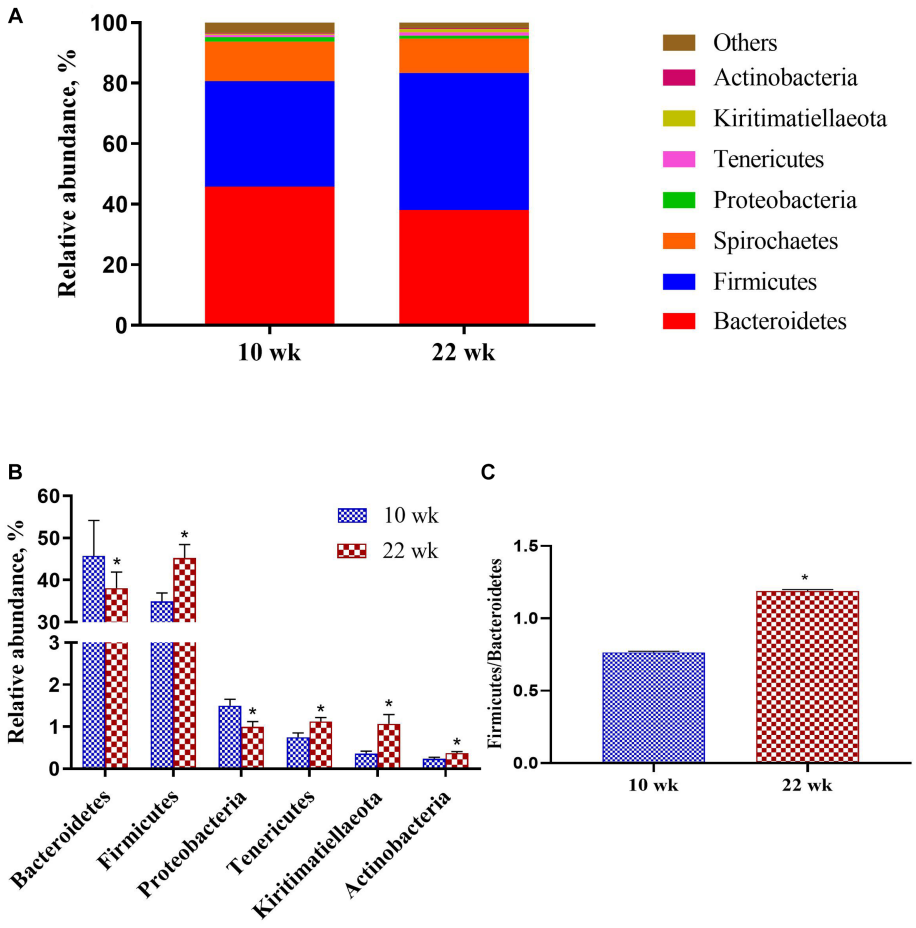

FIGURE 4
Taxonomic classification of the 16S rRNA gene sequences at the phylum level. **(A)** Fecal microbiota composition; **(B)** Composition difference; **(C)** the *Firmicutes/Bacteroidetes* ratio. Graph shows means value ± SEM ($N = 20$). * ($p < 0.05$) means significant difference between the males at the age of 10 weeks (10 wk) and 22 weeks (22 wk).

Additionally, LEfSe analysis was performed to determine the abundance of specific microbial taxa between the male pigs at 10 wk. and 22 wk. (Figure 6). An LDA score (log10) greater than 3.5 was considered the threshold. The genera *Prevotellaceae_NK3B31_group*, *Prevotella_1*, *Prevotellaceae*, *Streptococcus*, *Lachnospiraceae*, *Alloprevotella*, *Agathobacter*, *Sphaerochaeta*, and *Succinivibrio* enriched at 10 wk., and the genera *Ruminococcaceae_UCG-002*, *Turicibacter*, *Romboutsia*, *Muribaculaceae*, *Ruminococcaceae_NK4A214_group*, *Christensenellaceae_R-7_group* and *Lachnospiraceae_XPB1014_group* improved at 22 wk.

3.1.3 Correlation analysis between testosterone level and fecal differential microbe

Pearson's correlation coefficient analysis (Figure 7) observed that the fecal testosterone level was significantly positively associated with the relative abundance of phylum *Firmicutes* ($r = 0.56$, $p = 0.00$), *Tenericutes* ($r = 0.44$, $p = 0.00$), and *Actinobacteria* ($r = 0.72$, $p = 0.00$), and genus *Muribaculaceae* ($r = 0.52$, $p = 0.00$), *Clostridium_sensu_stricto_1* ($r = 0.48$, $p = 0.00$). However, the fecal testosterone level was significantly negatively associated with the relative abundance of genus *Alloprevotella* ($r = -0.36$, $p = 0.02$), *Prevotella_1* ($r = -0.43$, $p = 0.00$), and *Streptococcus* ($r = -0.47$, $p = 0.00$).

3.2 Experiment *in vitro*

3.2.1 Depletion rate of testosterone in the microbial communities culture medium

The EIA assay determined the testosterone concentration in the culture solution and did not observe testosterone in the control group. However, the testosterone levels in the culture medium of the testosterone treatments (200 μg/mL, 400 μg/mL, 800 μg/mL, and 1,200 μg/mL) decreased significantly ($p < 0.05$) after 8 h culture, the depletion rate inclined with the increase of supplemental testosterone level (50.76 ± 2.61%, 66.20 ± 2.63%, 79.24 ± 1.14%, and 80.68 ± 1.01%, respectively, Figure 8).

3.2.2 Changes in bacterial diversity

The bacterial DNA pyrosequencing profile (Figure 9) observed that testosterone had no significant effect on richness estimators (Ace and Chao) of microbial communities of the *in vitro* culture. Nevertheless, the 400 μg/mL testosterone treatment achieved the most extensive Shannon index, higher than the 200 μg/mL testosterone and 1,200 μg/mL testosterone treatment ($p < 0.05$). Moreover, the Simpson of the 200 μg/mL testosterone treatment was significantly higher than other treatments ($p < 0.05$).

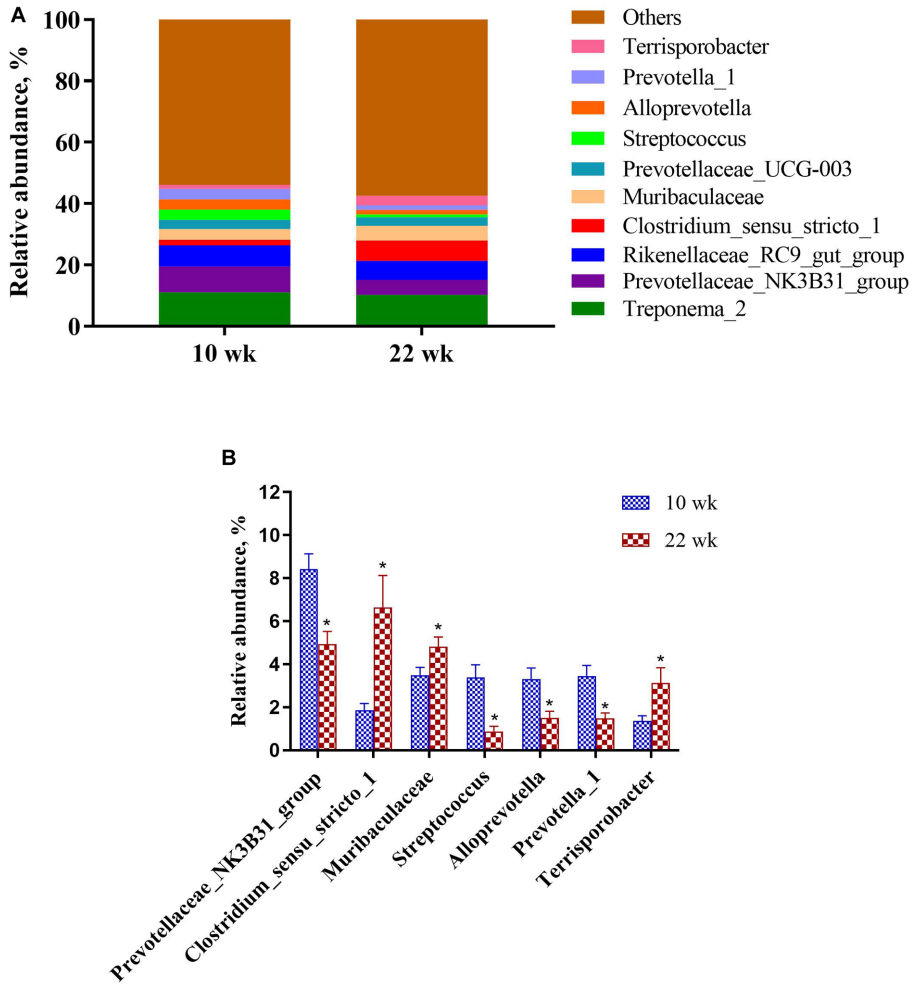

FIGURE 5
The column chart identifying the significantly different taxa between the different age at the genus level. **(A)** Gut microbiota composition; **(B)** Composition difference. Graph shows means value ± SEM ($N = 20$). * ($p < 0.05$) means significant difference between the males at the age of 10 weeks (10 wk) and 22 weeks (22 wk).

Although there was no clear visual separation of groups within the testosterone treatments in Figure 10, the inter-group variation was higher than the inter-individual variation of the treatment. The PCA (Figure 10A) and PCoA (Figure 10B) visually confirmed the distinct separation of microbial communities at the OTU level ($p = 0.00$ and $p = 0.03$) among the five groups.

3.2.3 Microbiota analysis

The *in vitro* culture trial observed that *Proteobacteria* and *Firmicutes* were the dominant phylum (Figure 11A). The abundance of *Proteobacteria* in the 800 and 1,200 μg/mL testosterone treatments was significantly lower than in the 200 and 400 μg/mL testosterone treatments ($p < 0.05$, Figure 11B). The abundance of *Firmicutes* in the 800 and 1,200 μg/mL testosterone treatments was significantly higher than the 200 and 400 μg/mL testosterone ($p < 0.05$, Figure 11B).

At the genus level (Figure 12), with the increase in supplemental testosterone level, the proportion of *Escherichia-Shigella* decreased. In contrast, the abundance of *Erysipelatoclostridium* in the 800 μg/mL testosterone treatment was higher than the 200 and 400 μg/mL testosterone ($p = 0.04$ and $p = 0.03$).

4 Discussion

The present study revealed the relationship between testosterone and the composition of intestinal microorganisms during the gonad development of Meishan male pigs. It is well known that testosterone has a significant effect on the physiology and behavior of animals. Still, it has been more challenging to show that testosterone differences lead to differences in the gut microbiome of animals. In the present study, male Meishan pigs had higher fecal testosterone at 22 wk. of age than 10 wk. of age, which is consistent with previous studies that the plasma testosterone level in male Meishan pigs increased gradually from birth to 30 wk. of age and positively correlated with the bodyweight development (Kanematsu et al., 2006). Meanwhile, the fecal microbiome had higher Ace, Chao, and Simpson at 22 wk. of age than that at 10 wk., and the microbial communities at 22 wk. of age grouped differently from 10 wk. in the PCA and PCoA. Furthermore, *in vitro* trials confirmed that the different testosterone treatments (0, 200, 400, 800, 1,200 μg/mL) had distinct separation of microbial communities at the OTU level of PCoA. The present study via *in vivo* and *in vitro* trials showed that the intestinal microbial composition changed with testosterone levels.

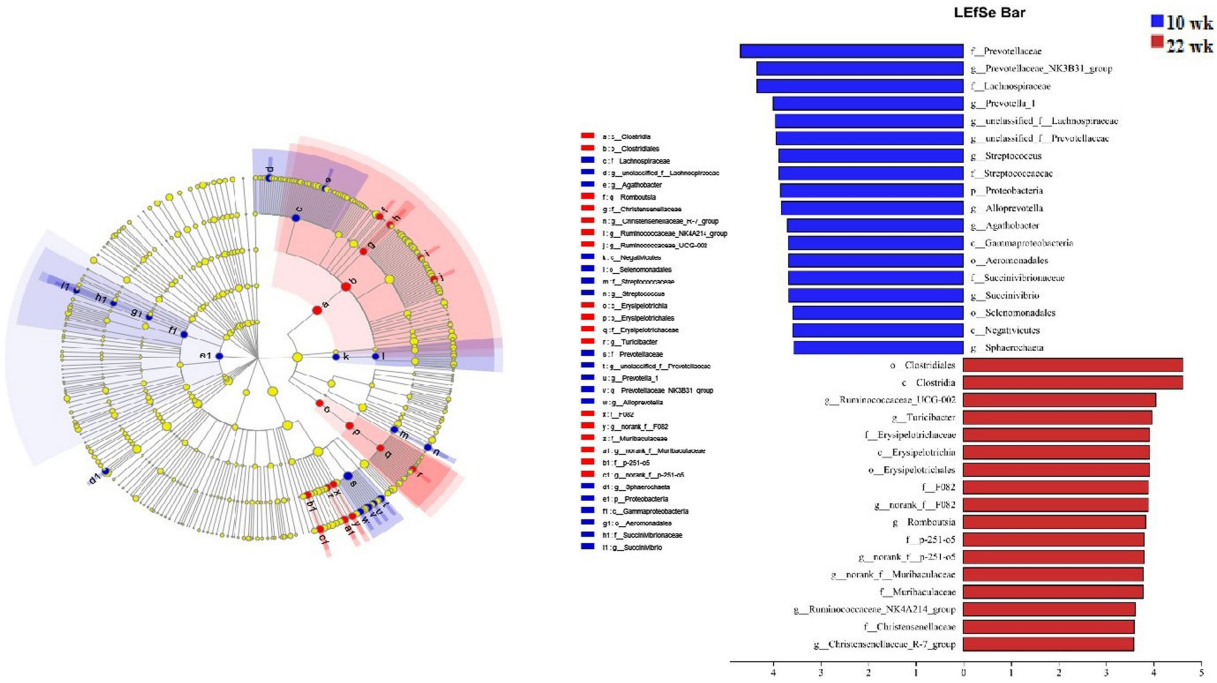

FIGURE 6
Linear Discriminant Analysis Effect Size (LEfSe) of the most dominant bacteria in the fecal microbiota of the males at the age of 10 weeks (10 wk) (red) and 22 weeks (22 wk) (blue) at genus level ($N = 20$; all linear discriminant analysis [LDA] scores (log10) >3.5).

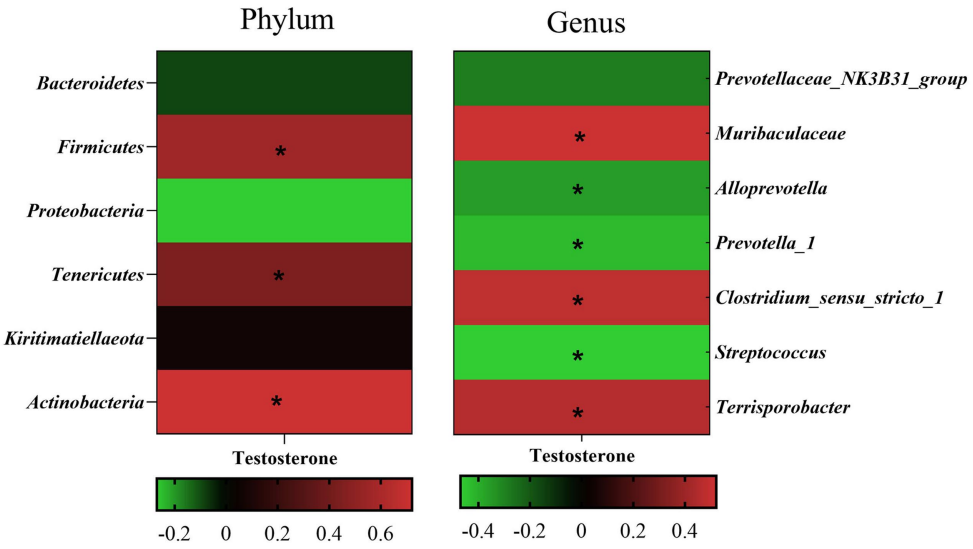

FIGURE 7
Pearson correlation analysis between fecal testosterone level and differential microbe at phylum level and genus level. The cells are colored based on the Pearson correlation coefficient between the testosterone level and differential microbe between different age, red represents positive correlation, green represents negative correlation, and * represents that the correlation was significant ($p < 0.05$).

As previously reported, *Firmicutes* and *Bacteroidetes* dominated the fecal microbiota at the phylum level (Xiao et al., 2017; Wang H. et al., 2019; Guo et al., 2020). The *Firmicutes* to *Bacteroidetes* ratio was relevant in signaling human gut microbiota status (Ley et al., 2006). It can be linked to overall changes in bacterial profiles at different stages of life (Mariat et al., 2009). The study of Mariat et al. (2009) also showed that the *Firmicutes* to *Bacteroidetes* ratio undergoes an increase from birth to adulthood. Consistently, the *Firmicutes* to *Bacteroidetes* ratio was higher at 22 wk. of male pigs, and the abundance of phylum *Firmicutes* positively correlated with testosterone content. Furthermore, the *in vitro* trial indicated that the mass of *Firmicutes* increased parallel to the increase in testosterone dosage. These suggest that the development of

testosterone secretion may be attributed to changes in the fecal microbiota associated with advancing age.

The phylum *Proteobacteria* includes several gastrointestinal pathogens, such as diarrheagenic *Escherichia coli* (Cordonnier et al., 2016; Wang X. et al., 2019). Morgan et al. (2012) observed expansive *Proteobacteria* in intestinal inflammation, including irritable bowel syndrome and metabolic syndrome. Moreover, high abundances, or 'blooms' of *Proteobacteria* in the gastrointestinal tract, have been suggested as a microbial signature of dysbiosis in mammals (Shin et al., 2015). Numerous studies indicated that the abnormal expansion of *Proteobacteria* is a potential diagnostic microbial characteristic of gut microbiota imbalance and epithelial dysfunction (Litvak et al., 2017). *Streptococcus* is an early colonizer in the gut of pigs, and an increase in the abundance of *Streptococcus* may also initiate infection. Here, as male pigs developed from 10 wk. to 22 wk., the fecal testosterone level increased, while the proportion of *Proteobacteria* phylum and *Streptococcus* genera decreased. Moreover, the *in vitro* trial indicated that testosterone treatments inhibited *Escherichia-Shigella* growth. These suggest that testosterone may be advantageous for formatting a healthy gut microbial community in male pigs, combined with the developmental changes in the *Firmicutes* to *Bacteroidetes* ratio and fecal testosterone.

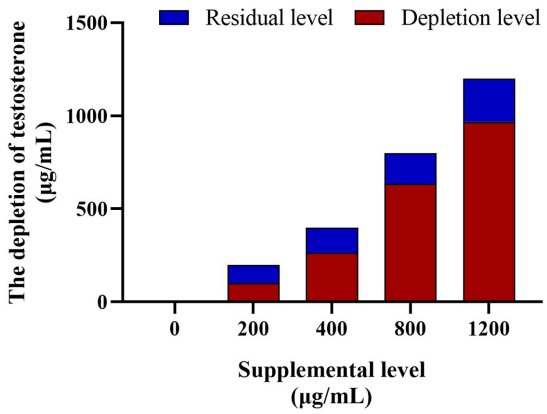

FIGURE 8
The testosterone depletion in culture medium among the different testosterone treatment group. The depletion rates of testosterone are 60.27, 66.20, 71.37%, and 78.23 in turn. $N = 6$.

In addition, the present study observed that the abundance of the phylum *Actinobacteria*, *Kiritimatiellaeota*, and *Tenericutes*, and genera *Alloprevotella*, *Clostridium_sensu_stricto_1*, *Muribaculaceae*, *Prevotellaceae_NK3B31_group*, *Prevotella_1*, and *Terrisporobacter* differed from 10 wk. to 22 wk. The abundance of phylum *Actinobacteria* and *Tenericutes*, and genera *Clostridium_sensu_stricto_1* and *Muribaculaceae* positively correlated with the fecal testosterone content, whereas genera *Alloprevotella*, *Prevotella_1* negatively correlated with the fecal testosterone level. However, data about the changes in bacteria and testosterone were inconsistent. The phylum *Actinobacteria* is associated with synthesizing antibiotics, immunomodulatory compounds, and metabolites, which are essential for animal health. Niu et al. (2015) observed that the abundance of *Clostridium* and *Tenericutes* in the gut positively correlated with the apparent crude fiber digestibility in pigs. *Muribaculaceae* may be associated with carbohydrate degradation (Lagkouvardos et al., 2019). Zhang et al. (2022) observed that the proportion of *Alloprevotella* and *Muribaculaceae* increased in the gut of

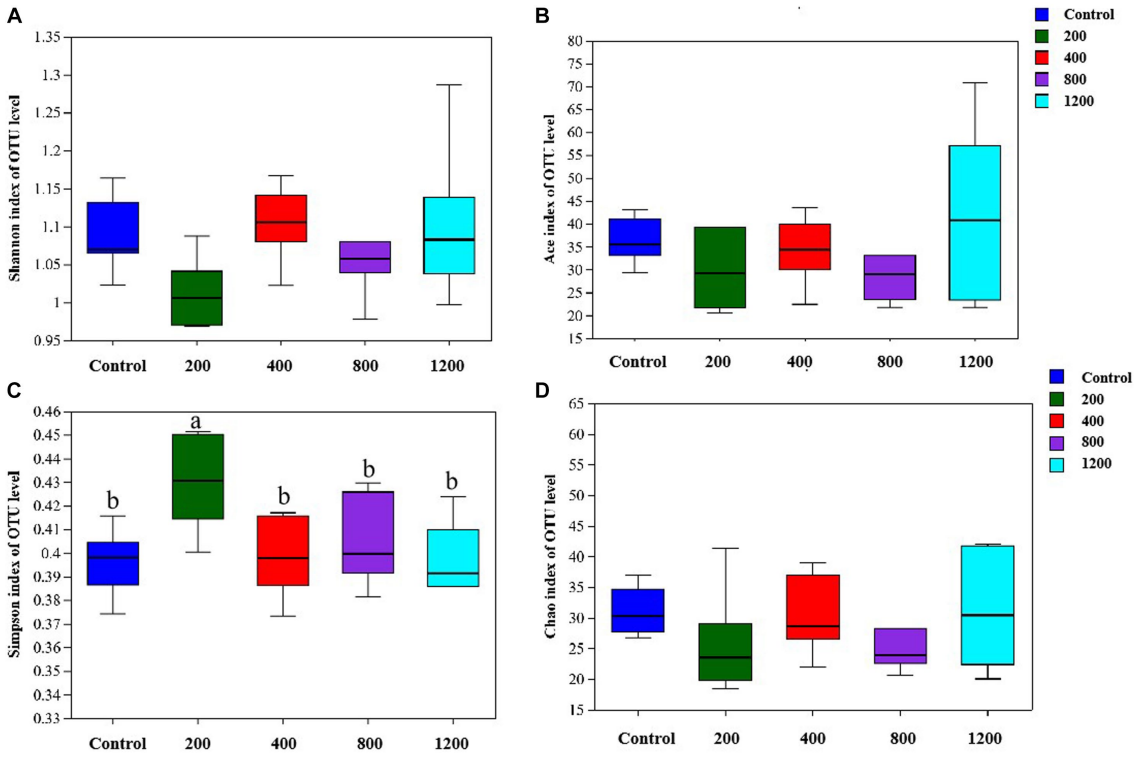

FIGURE 9
The richness and alpha diversity index of the culture microbial communities. **(A)** Shannon; **(B)** Ace; **(C)** Simpson; **(D)** Chao. Graph shows means value ± SEM ($N = 6$), and the bars with different letters indicate significant difference ($p < 0.05$).

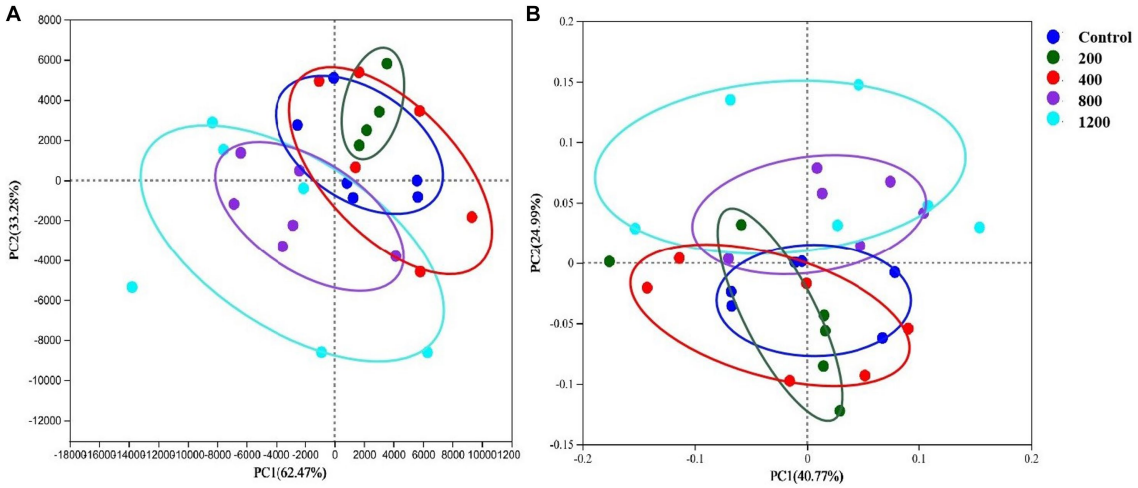

FIGURE 10
Principal Component Analysis (PCA, **A**) and Principal Co-ordinates Analysis (PCoA, **B**) plots on OTU level. Adonis test showed testosterone has a significant impact on the microbial community. **(A)** $R^2 = 0.37$, $p = 0.00$; **(B)** $R^2 = 0.27$, $p = 0.03$ at the OTU level. $N = 6$.

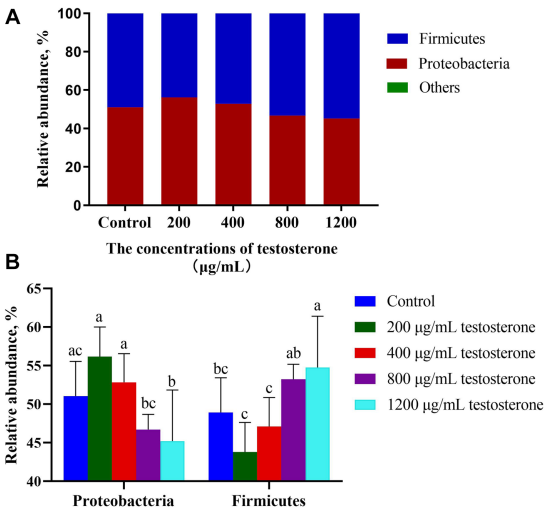

FIGURE 11
Taxonomic classification of the 16S rRNA gene sequences at the phylum level for the testosterone treatment. **(A)** Gut microbiota composition; **(B)** Composition difference. Graph shows means value ± SEM ($N = 6$), and the bars with different letters indicate significant difference ($p < 0.05$).

piglets under cold stress. Women with Polycystic Ovary Syndrome had a reduced relative abundance of the phylum *Tenericutes* in the fecal microbiome (Lindheim et al., 2017). A clinical study showed that *Alloprevotella* was enriched in obese participants (Insenser et al., 2018). Diethylhexylphthalate-exposed mice had a decrease in blood testosterone levels and a reduction of *Firmicutes* and *Paraprevotella* in the fecal microbiota, while an increase in *Bacteroidetes* and *Prevotella* (Tian et al., 2019). A previous study showed that *Prevotella* could produce succinate and acetate, which could improve the gut barrier and exhibit anti-inflammatory function, the abundance of *Prevotella* decreased from 30% of all bacteria to 4.0% as pigs aged (Xiao et al., 2017). These discrepant data suggest that the relationship between testosterone and gut microbiota may differ in the developmental stage and health status.

While steroid hormones model the gut microbiome composition and diversity, the bacteria may influence testosterone secretion and metabolism. Neuman et al. (2015) reported that transplantation of male microbiome to females caused an increase in the testosterone and enrichment of *E. coli* and *Shigella-like* bacteria in females. *Clostridium* can convert glucocorticoids to androgens, a group of male steroid hormones. Genera *Prevotella* can use estradiol and progesterone as alternative sources for growth (Kornman and Loesche, 1982). The *Firmicutes*, *Proteobacteria*, and *Actinobacteria* can metabolize and degrade steroid hormones (García-Gómez et al., 2013). Fecal bacteria, such as *Bacillus*, *Brevibacterium*, *Streptomyces*, and *Pseudomonas*, could degrade testosterone (Yang et al., 2010; Shih et al., 2017). Present data agreed with the above that the consumption rate of testosterone increased gradually with the treated testosterone dosage in the culture medium, further illustrating that the bacteria could degrade testosterone.

To conclude, the present study found a significant correlation between the change in testosterone content and microflora. The vitro

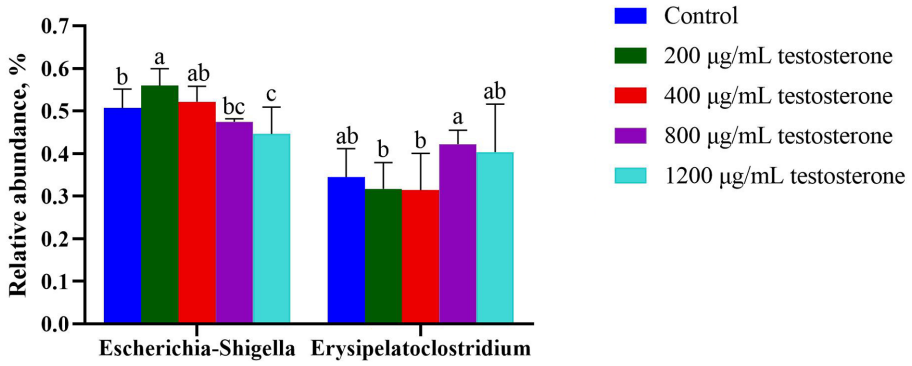

FIGURE 12
The column chart identifying the significantly different taxa among the testosterone treatment group at the genus level. Graph shows means value ± SEM ($N = 6$), and the bars with different letters indicate significant difference ($p < 0.05$).

trials showed that testosterone could modulate the microflora structure. Meanwhile, the bacteria could degrade the testosterone in a dose testosterone-dependent manner. Whether such interaction contributes to testosterone and gut microbiome development changes remains unclear and further studies are needed.

Data availability statement

The datasets presented in this study can be found in online repositories. The names of the repository/repositories and accession number(s) can be found below: Raw read sequences of the 16S rRNA gene from Meishan pig feces-associated microbiota in this study are publicly available in the NCBI SRA depository within BioProject PRJNA998586, with BioSample accession numbers SAMN36707203-SAMN36707246.

Ethics statement

The animal study was approved by Institutional Animal Care and Use Committee (IACUC) of Shanghai Academy of Agricultural Sciences Shanghai Academy of Agricultural Sciences. The study was conducted in accordance with the local legislation and institutional requirements.

Author contributions

XJ: Conceptualization, Data curation, Formal Analysis, Project administration, Writing – original draft, Writing – review & editing. SD: Investigation, Methodology, Writing – review & editing. NL: Investigation, Validation, Writing – review & editing. WY: Formal Analysis, Writing – review & editing. DX: Supervision, Writing – review & editing. WT: Formal Analysis, Writing – review & editing. HL: Formal Analysis, Writing – review & editing. PJ: Investigation, Writing – review & editing. YG: Resources, Writing – review & editing.

Funding

The author(s) declare financial support was received for the research, authorship, and/or publication of this article. The work was supported by Youth Program of National Natural Science Foundation of China (Grant No. 32100033 and Grant No. 32002177).

Conflict of interest

The authors declare that the research was conducted in the absence of any commercial or financial relationships that could be construed as a potential conflict of interest.

Publisher's note

All claims expressed in this article are solely those of the authors and do not necessarily represent those of their affiliated organizations, or those of the publisher, the editors and the reviewers. Any product that may be evaluated in this article, or claim that may be made by its manufacturer, is not guaranteed or endorsed by the publisher.

References

Allrich, R. D., Christenson, R. K., Ford, J. J., and Zimmerman, D. R. (1983). Pubertal development of the boar: age-related changes in testicular morphology and *in vitro* production of testosterone and estradiol-17β. *Biol. Reprod.* 28, 902–909. doi: 10.1095/biolreprod28.4.902

Cordonnier, C., Le Bihan, G., Emond-Rheault, J. G., Garrivier, A., Harel, J., and Jubelin, G. (2016). Vitamin B12 uptake by the gut commensal bacteria *Bacteroides thetaiotaomicron* limits the production of Shiga toxin by enterohemorrhagic *Escherichia coli*. *Toxins* 8, 11–19. doi: 10.3390/toxins8010014

Fujita, S., Mitsunaga, F., Sugiura, H., and Shimizu, K. (2001). Measurement of urinary and fecal steroid metabolites during the ovarian cycle in captive and wild Japanese macaques, *Macaca fuscata*. *Am. J. Primatol.* 53, 167–176. doi: 10.1002/ajp.3

García-Gómez, E., González-Pedrajo, B., and CamachoArroyo, I. (2013). Role of sex steroid hormones in bacterial-host interactions. *Biomed. Res. Int.* 2013:928290. doi: 10.1155/2013/928290

Guo, L., Wu, Y., and Wang, C. (2020). Gut microbiological disorders reduce semen utilization rate in Duroc boars. *Front. Microbiol.* 11:581926. doi: 10.3389/fmicb.2020.581926

Hosoda, K., Shimomura, H., Hayashi, S., Yokota, K., and Hirai, Y. (2011). Steroid hormones as bactericidal agents to *Helicobacter pylori*. *FEMS Microbiol. Lett.* 318, 68–75. doi: 10.1111/j.1574-6968.2011.02239.x

Insenser, M., Murri, M., Del Campo, R., Martínez-García, M. Á., Fernández-Durán, E., and Escobar-Morreale, H. F. (2018). Gut microbiota and the polycystic ovary syndrome: influence of sex, sex hormones, and obesity. *J. Clin. Endocrinol. Metab.* 103, 2552–2562. doi: 10.1210/jc.2017-02799

Jiang, X., Lu, N., Zhao, H., Yuan, H., Xia, D., and Lei, H. (2020). The microbiome-metabolome response in the colon of piglets under the status of weaning stress. *Front. Microbiol.* 11:2055. doi: 10.3389/fmicb.2020.02055

Kanematsu, N., Jin, W. Z., Watanabe, G., and Taya, K. (2006). Age-related changes of reproductive hormones in young Meishan boars. *J. Reprod. Dev.* 52, 651–656. doi: 10.1262/jrd.18013

Kornman, K. S., and Loesche, W. J. (1982). Effects of estradiol and progesterone on *Bacteroides* melaninogenicus and *Bacteroides gingivalis*. *Infect. Immun.* 35, 256–263. doi: 10.1128/iai.35.1.256-263.1982

Lagkouvardos, I., Lesker, T. R., Hitch, T. C. A., Gálvez, E. J. C., Smit, N., Neuhaus, K., et al. (2019). Sequence and cultivation study of Muribaculaceae reveals novel species, host preference, and functional potential of this yet undescribed family. *Microbiome* 7:28. doi: 10.1186/s40168-019-0637-2

Ley, R. E., Turnbaugh, P., Klein, S., and Gordon, J. I. (2006). Microbial ecology: human gut microbes associated with obesity. *Nature* 444, 1022–1023. doi: 10.1038/4441022a

Lindheim, L., Bashir, M., Münzker, J., Trummer, C., Zachhuber, V., Leber, B., et al. (2017). Alterations in gut microbiome composition and barrier function are associated with reproductive and metabolic defects in women with polycystic ovary syndrome (PCOS): a pilot study. *PLoS One* 12:e0168390. doi: 10.1371/journal.pone.0168390

Litvak, Y., Byndloss, M. X., Tsolis, R. M., and Baumler, A. J. (2017). Dysbiotic *proteobacteria* expansion: a microbial signature of epithelial dysfunction. *Curr. Opin. Microbiol.* 39, 1–6. doi: 10.1016/j.mib.2017.07.003

Mariat, D., Firmesse, O., Levenez, F., and Guimarăes, V. (2009). The *Firmicutes* / *Bacteroidetes* ratio of the human microbiota changes with age. *BMC Microbiol.* 9:123. doi: 10.1186/1471-2180-9-123

Markle, J. G., Frank, D. N., Mortin-Toth, S., Robertson, C. E., Feazel, L. M., Rolle-Kampczyk, U., et al. (2013). Sex differences in the gut microbiome drive hormone-dependent regulation of autoimmunity. *Science* 339, 1084–1088. doi: 10.1126/science.1233521

Moeser, A. J., Ryan, K. A., Nighot, P. K., and Blikslager, A. T. (2007). Gastrointestinal dysfunction induced by early weaning is attenuated by delayed weaning and mast cell blockade in pigs. *Am. J. Physiol Gastr. L.* 293, G413–G421. doi: 10.1152/ajpgi.00304.2006

Morgan, X. C., Tickle, T. L., Sokol, H., Gevers, D., Devaney, K. L., Ward, D. V., et al. (2012). Dysfunction of the intestinal microbiome in inflammatory bowel disease and treatment. *Genome Biol.* 13:R79. doi: 10.1186/gb-2012-13-9-r79

Mudd, A. T., Berding, K., Wang, M., Donovan, S. M., and Dilger, R. N. (2017). Serum cortisol mediates the relationship between fecal *Ruminococcus* and brain N-acetylaspartate in the young pig. *Gut Microbes* 8, 589–600. doi: 10.1080/19490976.2017.1353849

Neuman, H., Debelius, J. W., Knight, R., and Koren, O. (2015). Microbial endocrinology: the interplay between the microbiota and the endocrine system. *FEMS Microbiol. Rev.* 39, 509–521. doi: 10.1093/femsre/fuu010

Niu, Q., Li, P., Hao, S., Zhang, Y., and Huang, R. (2015). Dynamic distribution of the gut microbiota and the relationship with apparent crude fiber digestibility and growth stages in pigs. *Sci. Rep.* 5:9938. doi: 10.1038/srep09938

Nuriel-Ohayon, M., Neuman, H., Ziv, O., Belogolovski, A., Barsheshet, Y., Bloch, N., et al. (2019). Progesterone increases bifidobacterium relative abundance during late pregnancy. *Cell Rep.* 27, 730–736.e3. doi: 10.1016/j.celrep.2019.03.075

Org, E., Mehrabian, M., Parks, B. W., Shipkova, P., Liu, X., Drake, T., et al. (2016). Sex differences and hormonal effects on gut microbiota composition in mice. *Gut Microbes* 7, 313–322. doi: 10.1080/19490976.2016.1203502

Qin, J., Li, R., Raes, J., Arumugam, M., Burgdorf, K., Manichanh, C., et al. (2010). A human gut microbial gene catalogue established by metagenomic sequencing. *Nature* 464, 59–65. doi: 10.1038/nature08821

SankarGanesh, D., Ramachandran, R., Muniasamy, S., Saravanakumar, V. R., Suriyakalaa, U., Kannan, S., et al. (2014). A correlation of fecal volatiles and steroid hormone profiles with behavioral expression during estrous cycle of goat, *Capra hircus*. *Gen. Comp. Endocrinol.* 206, 178–183. doi: 10.1016/j.ygcen.2014.07.028

Schwarzenberger, F., Toole, G. S., Christie, H. L., and Raes, J. I. (1993). Plasma levels of several androgens and estrogens from birth to puberty in male domestic pigs. *Acta Endocrinol.* 128, 173–177. doi: 10.1530/acta.0.1280173

Sheriff, M. J., Krebs, C. J., and Boonstra, R. (2010). Assessing stress in animal populations: do fecal and plasma glucocorticoids tell the same story? *Gen. Comp. Endocrinol.* 166, 614–619. doi: 10.1016/j.ygcen.2009.12.017

Shih, C. J., Chen, Y. L., Wang, C. H., Wei, T. S., Lin, I. T., Ismail, W. A., et al. (2017). Biochemical mechanisms and microorganisms involved in anaerobic testosterone metabolism in estuarine sediments. *Front. Microbiol.* 8:15. doi: 10.3389/fmicb.2017.01520

Shin, N.-R., Whon, T. W., and Bae, J.-W. (2015). *Proteobacteria*: microbial signature of dysbiosis in gut microbiota. *Trends Biotechnol.* 33, 496–503. doi: 10.1016/j.tibtech.2015.06.011

Tian, X., Yu, Z., Feng, P., Ye, Z., Li, R., Liu, J., et al. (2019). *Lactobacillus plantarum TW1-1* alleviates diethylhexylphthalate-induced testicular damage in mice by modulating gut microbiota and decreasing inflammation. *Front. Cell. Infect. Microbiol.* 9:221. doi: 10.3389/fcimb.2019.00221

Tuchscherer, M., Puppe, B., Tuchscherer, A., and Kanitz, E. (2018). Psychosocial stress sensitizes neuroendocrine and inflammatory responses to *Escherichia coli* challenge in domestic piglets. *Brain Behav. Immun.* 68, 274–287. doi: 10.1016/j.bbi.2017.10.026

Verbrugghe, E., Boyen, F., Van Parys, A., Van Deun, K., Croubels, S., Thompson, A., et al. (2011). Stress induced *Salmonella Typhimurium* recrudescence in pigs coincides with cortisol induced increased intracellular proliferation in macrophages. *Vet. Res.* 42:118. doi: 10.1186/1297-9716-42-118

Wang, H., Shou, Y., Zhu, X., Xu, Y., Shi, L., Xiang, S., et al. (2019). Stability of vitamin B12 with the protection of whey proteins and their effects on the gut microbiome. *Food Chem.* 276, 298–306. doi: 10.1016/j.foodchem.2018.10.033

Wang, X., Tsai, T., Deng, F., Wei, X., Chai, J., Knapp, J., et al. (2019). Longitudinal investigation of the swine gut microbiome from birth to market reveals stage and growth performance associated bacteria. *Microbiome* 7:109. doi: 10.1186/s40168-019-0721-7

Williams, B. A., Bosch, M. W., Verstegen, M. H. B., and Tamminga, S. (2005). An *in vitro* batch culture method to assess potential fermentability of feed ingredients for monogastric diets. *Anim. Feed. Sci. Tech.* 123-124, 445–462. doi: 10.1016/j.anifeedsci.2005.04.031

Xiao, Y., Li, K., Xiang, Y., and Zhou, W. (2017). The fecal microbiota composition of boar Duroc, Yorkshire, landrace and Hampshire pigs. *Asian Australas. J. Anim. Sci.* 30, 1456–1463. doi: 10.5713/ajas.16.0746

Yang, Y. Y., Borch, T., Young, R. B., Goodridge, L. D., and Davis, J. G. (2010). Degradation kinetics of testosterone by manure-borne bacteria: influence of temperature, pH, glucose amendments, and dissolved oxygen. *J. Environ. Qual.* 39, 1153–1160. doi: 10.2134/jeq2009.0112

Yurkovetskiy, L., Burrows, M., Khan, A. A., and Graham, L., Volchkov, P., Becker, L., Antonopoulos, D., Umesaki, Y., and Chervonsky, A. V. (2013). Gender bias in autoimmunity is influenced by microbiota. *Immunity* 39: 400–412. doi: 10.1016/j.immuni.2013.08.013

Zhang, Y., Sun, L., Zhu, R., Zhang, S., Liu, S., Wang, Y., et al. (2022). Porcine gut microbiota in mediating host metabolic adaptation to cold stress. *NPJ Biofilms. Microbiol.* 8:18. doi: 10.1038/s41522-022-00283-2

frontiers | Frontiers in Microbiology

TYPE Original Research
PUBLISHED 22 November 2023
DOI 10.3389/fmicb.2023.1293333

OPEN ACCESS

EDITED BY
Lifeng Zhu,
Nanjing University of Chinese Medicine, China

REVIEWED BY
María Linares,
Universidad Complutense de Madrid, Spain
Jing Chen,
Shanghai University of Traditional Chinese Medicine, China

*CORRESPONDENCE
Jianchang Li
✉ lijianchang111@163.com

RECEIVED 13 September 2023
ACCEPTED 08 November 2023
PUBLISHED 22 November 2023

CITATION
Chen G, Kuang Z, Li F and Li J (2023) The causal relationship between gut microbiota and leukemia: a two-sample Mendelian randomization study.
Front. Microbiol. 14:1293333.
doi: 10.3389/fmicb.2023.1293333

The causal relationship between gut microbiota and leukemia: a two-sample Mendelian randomization study

Guanjun Chen[1], Zheshu Kuang[1], Fan Li[2] and Jianchang Li[1]*

[1]Affiliated Hospital of Binzhou Medical University, Binzhou, China, [2]Department of Gastroenterology, The First Hospital of Jilin University, Changchun, China

Background: The association between gut microbiota and leukemia has been established, but the causal relationship between the two remains unclear.

Methods: A bidirectional two-sample Mendelian randomization (MR) was used to analyze the causal relationship between gut microbiota and leukemia. Microbiome data ($n = 14,306$) and leukemia ($n = 1,145$) data were both sourced from European populations. Single nucleotide polymorphisms (SNPs) were selected as instrumental variables based on several criteria. We employed various MR methods, such as the inverse variance weighted (IVW) method, to evaluate the causal effect between exposure and outcomes and conducted sensitivity analyses to validate the heterogeneity and pleiotropy of the instrumental variables.

Results: 5,742 qualified instrumental variables were included. In the primary MR results, a total of 10 gut microbial taxa were associated with leukemia risk. Genus Blautia and genus Lactococcus are risk factors for acute lymphoblastic leukemia [genus Blautia odds ratio (OR): 1.643, 95% confidence interval (CI): 1.592 ~ 1.695, Adjusted $p < 0.001$; genus Lactococcus OR: 2.152, 95% CI: 1.447 ~ 3.199, Adjusted $p = 0.011$]. Genus Rikenellaceae RC9 gut group, genus Anaerostipes, genus Slackia, and genus Lachnospiraceae ND3007 group are risk factors for acute myeloid leukemia [genus Rikenellaceae RC9 gut group OR: 1.964, 95% CI: 1.573 ~ 2.453, Adjusted $p < 0.001$; genus Anaerostipes OR: 2.515, 95% CI: 1.503 ~ 4.209, Adjusted $p = 0.017$; genus Slackia OR: 2.553, 95% CI: 1.481 ~ 4.401, Adjusted $p = 0.022$; genus Lachnospiraceae ND3007 group OR: 3.417, 95% CI: 1.960 ~ 5.959, Adjusted $p = 0.001$]. Genus Ruminococcaceae UCG011 and genus Ruminococcaceae UCG014 were risk factors for chronic myeloid leukemia (genus Ruminococcaceae UCG011 OR: 2.010, 95% CI: 1.363 ~ 2.963, Adjusted $p = 0.044$; genus Ruminococcaceae UCG014 OR: 3.101, 95% CI: 1.626 ~ 5.915, Adjusted $p = 0.044$). Genus Slackia was a protective factor for acute lymphoblastic leukemia (genus Slackia OR: 0.166, 95% CI: 0.062 ~ 0.443, Adjusted $p = 0.017$). Family Acidaminococcaceae was a protective factor for acute myeloid leukemia (family Acidaminococcaceae OR: 0.208, 95% CI: 0.120 ~ 0.361, Adjusted $p < 0.001$). Genus Desulfovibrio was a protective factor for chronic lymphoblastic leukemia (genus Desulfovibrio OR: 0.581, 95% CI: 0.440 ~ 0.768, Adjusted $p = 0.020$). Sensitivity analysis revealed no heterogeneity or pleiotropy between SNPs.

Conclusion: This study revealed the causal relationship between the gut microbiota and leukemia, and identified potential pathogenic bacteria and probiotic taxa associated with the onset of leukemia. This research may aid in the early detection of various types of leukemia and offer a new direction for the prevention and treatment of leukemia.

KEYWORDS

gut microbiota, leukemia, mendelian randomization, acute lymphoblastic leukemia, acute myeloid leukemia, chronic lymphoblastic leukemia, chronic myeloid leukemia

1 Introduction

Leukemia is a malignant hematologic tumor, characterized by the metabolic dysregulation of leukemia cells and leukemia stem cells relative to non-cancerous stem cells (Nemkov et al., 2019). According to global cancer statistics, the incidence of Acute Lymphoblastic Leukemia (ALL) is approximately 1.7–4.6 individuals per 100,000 population, Acute Myeloid Leukemia (AML) is approximately 1.2–4.2 individuals per 100,000 population, Chronic Lymphocytic Leukemia (CLL) is approximately 2.0–5.0 individuals per 100,000 population, and Chronic Myeloid Leukemia (CML) is approximately 0.8–2.1 individuals per 100,000 population, with a continuing upward trend in recent years (Bray et al., 2018; Sung et al., 2021).

Currently, leukemia treatments primarily involve chemotherapy, radiation therapy, and hematopoietic stem cell transplantation. However, due to the complexity and heterogeneity of leukemia, therapeutic outcomes still have limitations. Hence, further research and exploration into the pathogenesis of leukemia and new therapeutic strategies are essential.

While the etiology and pathogenesis of leukemia are not fully understood, factors like immune dysfunction, genetic predispositions, and environmental elements play significant roles in its onset and progression. Moreover, increasing evidence suggests that alterations in the composition and function of gut microbiota are closely related to the onset, treatment, and prognosis of leukemia (Ma et al., 2021; Wang et al., 2022; Zhou et al., 2022). The gut microbiota refers to the microbial community living within the human gastrointestinal tract. Its symbiotic relationship with the host is intricate and is closely related to human health (Valdes et al., 2018).

In many leukemia studies, gut microbial dysbiosis has been observed. For instance, Bai L and colleagues found that ALL induces structural changes in the gut microbial community. Antibiotics significantly reduced α-diversity, but β-diversity remained unchanged. Bacteroidales and Enterococcaceae can be considered as biological markers for ALL (Bai et al., 2017). A case–control study reported that the diversity of the gut microbiota (Anaerostipes, Coprococcus, Roseburia, and Ruminococcus2) in children and adolescents with ALL is significantly lower than that in the control group (Rajagopala et al., 2016). Rashidi A and colleagues discovered that in AML patients, gut microbiota like acteroides, Alistipes, and Faecalibacterium are disrupted during induction chemotherapy. This disruption is persistent, and normal levels cannot be restored after chemotherapy completion (Rashidi et al., 2022). However, most studies are designed as case–control studies, making it challenging to determine exposure time and outcomes. Furthermore, in observational studies, the association between gut microbiota and leukemia can be easily confounded by factors such as age, environment, dietary patterns, and lifestyle (Rinninella et al., 2019). Thus, whether there is a causal relationship between gut microbiota and leukemia remains uncertain.

Mendelian randomization (MR) as a natural randomization approach is increasingly utilized to integrate summary data from genome-wide association studies (GWAS) (Greenland, 2018). It employs genetic variations associated with the exposure as proxies for the exposure to assess the association between exposure and outcome, and is widely adopted in researching the causal relationships of disease etiology. Additionally, MR can effectively eliminate potential biases and confounders (such as immune dysfunction, genetic factors, environmental factors, etc.), ensuring the reliability and validity of the experimental results (Davey Smith and Hemani, 2014). In this study, we employed a two-sample MR to analyze whether there's a causal relationship between the composition of gut microbiota and the risk of leukemia.

2 Materials and methods

2.1 Data sources

This study utilizes a two-sample MR to explore the causal relationship between different types of gut microbiota and the onset of leukemia, with data sourced from publicly available GWAS summary statistics.

We obtained the GWAS summary data related to individual gut microbiota from the MiBioGen global consortium database. To ensure minimal heterogeneity, we selected only 150 datasets of genus and species, with an average of 5,376,402 available SNPs. Participants were from 24 countries, including the United States, Canada, and Germany, with a total sample size of 18,340 (Kurilshikov et al., 2021).[1]

The study acquired the 16S rRNA gene sequencing profiles and genotyping data of these participants. We incorporated the data from European ancestry participants of this study as exposure in the MR analysis.

The FinnGen project in the Finnish biobank aims to collect and analyze genomic and health data of 500,000 participants (Kurki et al., 2023).[2] From FINNGEN, we obtained GWAS datasets of various leukemias, with each dataset containing nearly 287,136 individuals, among which 1,145 were leukemia patients. The dataset information used for the MR analysis is shown in Table 1, Supplementary Tables S1, S8 (Kurilshikov et al., 2021). No additional ethical approval or consent to participate was required because we used published studies and public summary statistics.

The study flowchart is illustrated in Figure 1. In essence, the gut microbiota is the exposure, and leukemia is the outcome. The leukemia diagnoses conform to the International Disease Classifications for ALL, AML, CLL, and CML, with their respective ICD10 codes being C910, C920, C911, and C921. Population stratification is a common source of bias in MR studies. To minimize

1 https://mibiogen.gcc.rug.nl/

2 https://r9.finngen.fi/

TABLE 1 Dataset information.

Datasets	Authors	Year	Population	Gender	ICD-10 coding	sample size	NSNP	Number of individuals			Median age at first event		
								All	Female	Male	All	Female	Male
Acute lymphocytic leukaemia	FinnGen	2023	European	Males and females	C910	287,320	20,167,370	184	102	82	19.82	16.49	23.97
Acute myeloid leukaemia	FinnGen	2023	European	Males and females	C920	287,367	20,167,370	231	88	143	61.52	55.02	65.53
Chronic lymphocytic leukaemia	FinnGen	2023	European	Males and females	C911	287,757	20,167,370	624	193	431	67.41	66.63	67.75
Chronic myeloid leukaemia	FinnGen	2023	European	Males and females	C921	287,242	20,167,370	106	51	55	55.51	54.58	56.37
Abundance of 150 Gut microbiota	Kurilshikov A	2021	European	Males and females	-	14,306	5,331,372(Ave.)	-	-	-	-	-	-

this stratification, samples included in this MR study are exclusively from European populations, thereby reducing bias arising from population stratification (Larsson et al., 2019).

2.2 Basic assumptions of MR and instrumental variable (IV) selection

MR analysis employs Instrumental Variables (IVs) to estimate the relationship between exposure (gut microbiota) and outcomes (ALL, AML, CLL, CML), examining whether gut microbiota promotes or inhibits the onset of leukemia.

This study utilizes Single Nucleotide Polymorphisms (SNPs) as IVs. The instrumental variables used in MR analysis must meet the following basic assumptions: Assumption 1 (Relevance): The instrumental variable is significantly associated with the risk factor; Assumption 2 (Independence): The instrumental variable is not associated with any confounders; Assumption 3 (Exclusivity): The instrumental variable influences the outcome only indirectly through the risk factor. Using instrumental variables (SNPs), risk factors (gut microbiota), and outcomes (ALL, AML, CLL, CML), we constructed a Directed Acyclic Graph (DAG, Figure 2) to elucidate the aforementioned assumptions.

We applied a series of SNP selection criteria to the acquired GWAS summary data to ensure they met the three aforementioned assumptions:

Assumption 1: We selected SNPs associated with risk factors at p-value $<1\times10^{-5}$. Considering the limited number of SNPs, we slightly adjusted the threshold based on the genome-wide significance level (5×10^{-8}) to meet the requirements for further analysis (Gou et al., 2023; Yue et al., 2023). We calculated the proportion of variance in exposure explained by SNP using the formula r2 = 2 * eaf * (1 − eaf) * beta^2 (Codd et al., 2013). To ensure the instrumental variables are independent genetic SNPs, we applied parameters r2 = 0.001 and physical distance = 10,000 base pairs to eliminate SNPs with linkage disequilibrium (LD). Using SNPs associated with risk factors, we extracted associated data from the outcome summary data and performed data matching. In this study, we removed ambiguous SNPs and palindromic SNPs during the matching process. Given the inevitable missing data in the outcome database and the spatiotemporal consistency among high-LD SNPs, we substituted missing SNPs in the outcome data with high-LD proxy SNPs, enhancing the model's ability to interpret the true causal relationship. The criteria for selecting high linkage disequilibrium SNPs were r2 > 0.8 and window<10,000 kb. We calculated the F-statistic between SNP and exposure using the formula F = beta^2/se^2 to measure its strength as IVs (Burgess and Thompson, 2011). The F-statistic, used to gauge the strength of the instrumental variable in explaining the risk factor, considers SNPs with an F-statistic < 10 as weak instruments (Burgess et al., 2017), and these are excluded. The aforementioned filtering ensures a strong correlation between the SNP and the risk factors.

Assumption 2: We utilized phenoscanner to test potential associations of each SNP with confounders (Staley et al., 2016). SNPs that may violate the independence assumption need to be removed, ensuring the selected SNPs are not associated with any potential confounders. Mendelian Randomization Pleiotropy Residual Sum and

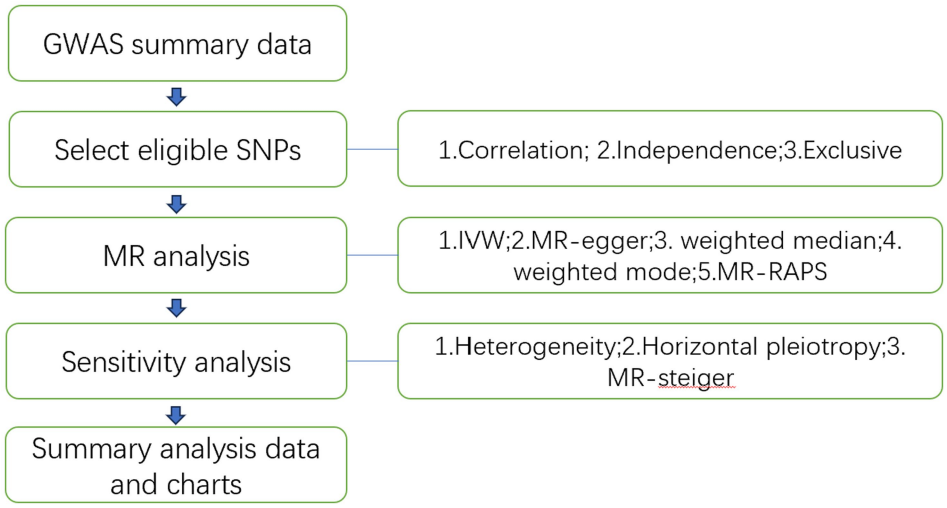

FIGURE 1
Study flowchart.

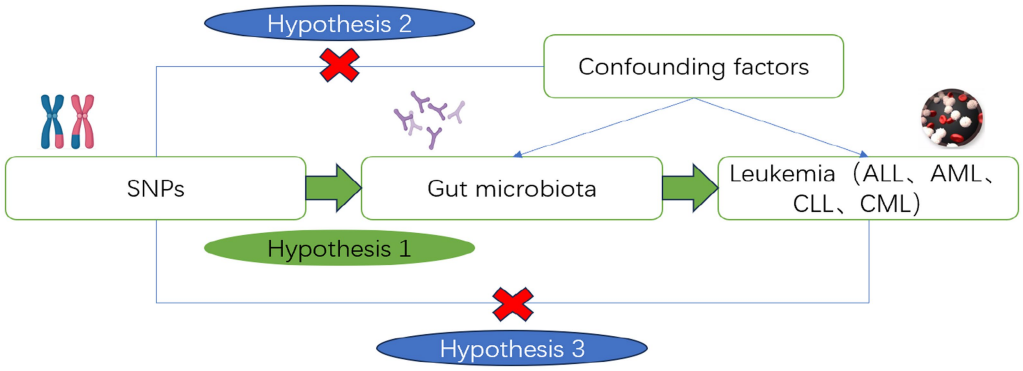

FIGURE 2
Directed acyclic diagram of the MR analysis principle. Created with MedPeer (www.medpeer.cn).

Outlier (MR-PRESSO) analysis can detect and identify outliers and SNPs with pleiotropy (Verbanck et al., 2018), which are then excluded.

Assumption 3: Incorrect SNP selection might lead to outcomes directly associated with SNPs, eventually resulting in erroneous conclusions about reverse causal relationships. Therefore, we employed MR-steiger to test the causal estimation direction of SNPs (Hemani et al., 2017). SNPs with incorrect directions are excluded. Finally, based on the Bonferroni correction ($p < 0.05/n$, n: the number of remaining SNPs), we removed SNPs directly associated with the outcome. By following the above methods, we ensured that SNPs indirectly influence the outcome only through risk factors.

In summary, after the stringent filtering described above, the remaining SNPs were considered valid instrumental variables.

2.3 MR analysis study design

In this study, we employed the Inverse Variance Weighted (IVW) method, MR-Egger, Weighted Median, Weighted Mode and MR-RAPS to infer whether there's a causal relationship between human gut microbiome composition and leukemia risk.

Essentially, IVW is a meta-analysis method, combining wald ratio estimates obtained from each SNP calculation using inverse variance weighting. This provides an overall estimate of the impact of the gut microbiota on leukemia risk, which is determined by dividing the effect estimate of the SNP result by the exposure effect estimate of the SNP (Burgess et al., 2013; Lee et al., 2016; Choi et al., 2019). When horizontal pleiotropy is absent, IVW can avoid the influence of confounders.

MR-Egger is similar to the IVW method, but the intercept term in the former can evaluate horizontal pleiotropy. Hence, MR-Egger regression was employed to assess whether the included SNPs have potential horizontal pleiotropy. The MR-Egger method is based on the NOME (No Measurement Error) assumption. Therefore, we calculated its I^2 value to quantify the extent to which MR-Egger violates the NOME assumption. When I^2 is less than 90%, the results require correction (Bowden et al., 2016). Moreover, given the lower accuracy and statistical power of the MR-Egger regression, we employed the MR-PRESSO method to detect outliers with pleiotropic bias and to correct for horizontal pleiotropy.

The weighted median and weighted mode methods can provide consistent causal effect estimates. Even if the majority of similar individual instrumental causal effect estimates come from valid instruments, the weighted median and weighted mode methods remain effective, even when other instruments do not meet the causal inference requirements of the MR method (Bowden et al., 2016; Hartwig et al., 2017). Compared to the MR-Egger method, the weighted median and weighted mode methods improve the accuracy of the results (Ooi et al., 2019).

Additionally, we also employed the MR-RAPS method, which directly uses a random-effects distribution to simulate the pleiotropy of genetic variants, making it more robust than traditional MR methods (Wu et al., 2020).

In the absence of heterogeneity and horizontal pleiotropy, the IVW MRE model serves as the primary analytical method. If heterogeneity is present, results from the IVW random-effects model and the weighted median method are discussed collectively. If horizontal pleiotropy exists among SNPs, the MR-Egger method is used as the primary analytical approach. Non-primary MR analytical methods serve as sensitivity analyses to assess the reliability of the aforementioned models. The final results of this study are considered statistically significant at a significance level of $p < 0.05$.

2.4 Sensitivity analysis

Sensitivity analysis serves as the assessment of uncertain factors in a model to reduce their impact on the results in subsequent operations. Therefore, in addition to using comprehensive MR-steiger analysis to ensure the overall direction of causal effects and various MR analyses to explore the causal relationship between human gut microbiota composition and leukemia risk, we also conducted heterogeneity tests, pleiotropy analyses, and other sensitivity analyses.

We employed Cochran's Q test to quantify the heterogeneity among the selected SNPs. A p-value <0.05 for the Q statistic indicates the presence of heterogeneity. The intercept term of MR-Egger can assess horizontal pleiotropy. When the analysis results show significant horizontal pleiotropy, the causal estimation results of MR-Egger are preferred.

2.5 Statistical software and data visualization

All statistical analyses in this study were performed using R software (version 4.1.2) and employed the R package "TwoSampleMR" along with some basic R packages.

The study produced scatter plots for each SNP's impact on risk factors and outcomes, as well as regression curves for causal estimates. Forest plots, scatter plots of MR analysis, and fitted curve diagrams were drawn based on the final causal estimation results. Additionally, we produced plots using the leave-one-out method to assess whether the MR conclusion is dependent on a particular SNP. If such an SNP exists in a significant MR conclusion, consideration should be given to removing that instrumental variable.

3 Results

3.1 Filtering qualified SNPs

To investigate the causal influence of gut microbiota on leukemia, we selected 7,291 significantly associated SNPs. Due to missing data for some SNPs in the result dataset, we removed 368 associated SNPs. The F-statistics for each SNP was >10, indicating that there were no weak instrumental variables. Subsequently, we eliminated 1,120 palindromic and ambiguous SNPs. Using Phenoscanner, we manually removed 20 SNPs related to confounding factors, such as viral infections (Bartenhagen et al., 2017), immune abnormalities (Rutella et al., 2022), chemical exposure (Beane Freeman et al., 2009), ionizing radiation exposure (Metz-Flamant et al., 2012), and alcohol consumption (Engen et al., 2015). The MR-PRESSO analysis identified and removed 19 SNPs with horizontal pleiotropy and outliers. The MR-steiger analysis did not identify SNPs with incorrect causal directions. 22 SNPs directly associated with the outcome were removed after Bonferroni correction.

After rigorous selection, a total of 5,742 SNPs were included as qualified IVs for subsequent MR analysis. Detailed information about the selected instrumental variables is presented in Supplementary Tables S3–S5.

3.2 MR analysis results

As shown in Figures 3, 4, the MR analysis results using the IVW method revealed 10 gut microbiota genera associated with the risk of leukemia.

Genus Blautia and genus Lactococcus were risk factors for ALL (genus Blautia OR: 1.643, 95% CI: 1.592 ~ 1.695, Adjusted $p < 0.001$; genus Lactococcus OR: 2.152, 95% CI: 1.447 ~ 3.199, Adjusted $p = 0.011$). Genus Rikenellaceae RC9 gut group, genus Anaerostipes, genus Slackia, and genus Lachnospiraceae ND3007 group were risk factors for AML (genus Rikenellaceae RC9 gut group OR: 1.964, 95% CI: 1.573 ~ 2.453, Adjusted $p < 0.001$; genus Anaerostipes OR: 2.515, 95% CI: 1.503 ~ 4.209, Adjusted $p = 0.017$; genus Slackia OR: 2.553, 95% CI: 1.481 ~ 4.401, Adjusted $p = 0.022$; genus Lachnospiraceae ND3007 group OR: 3.417, 95% CI: 1.960 ~ 5.959, Adjusted $p = 0.001$). Genus Ruminococcaceae UCG011 and genus Ruminococcaceae UCG014 were risk factors for CML (genus Ruminococcaceae UCG011 OR: 2.010, 95% CI: 1.363 ~ 2.963, Adjusted $p = 0.044$; genus Ruminococcaceae UCG014 OR: 3.101, 95% CI: 1.626 ~ 5.915, Adjusted $p = 0.044$). Genus Slackia was a protective factor for ALL (genus Slackia OR: 0.166, 95% CI: 0.062 ~ 0.443, Adjusted $p = 0.017$). Family Acidaminococcaceae was a protective factor for AML (family Acidaminococcaceae OR: 0.208, 95% CI: 0.120 ~ 0.361, Adjusted $p < 0.001$). Genus Desulfovibrio was a protective factor for CLL (genus Desulfovibrio OR: 0.581, 95% CI: 0.440 ~ 0.768, Adjusted $p = 0.020$).

Additionally, as indicated in Supplementary Figure S4, preliminary MR results suggest an association between leukemia occurrence and the gut microbiota such as genus Christensenellaceae R 7 group, family Family XIII, and family Family XI. However, these associations were no longer significant after FDR correction (Adjusted $p > 0.05$).

10.3389/fmicb.2023.1293333

Exposures	NExp	Outcomes	NOut	NSNP	Method	OR (95% CI)	P value	Adjusted P value
genus Slackia	14306	Acute lymphocytic leukaemia (controls excluding all cancers)	287320	6	IVW(MRE)	0.166 (0.062 ~ 0.443)	<0.001	0.017
genus Blautia	14306	Acute lymphocytic leukaemia (controls excluding all cancers)	287320	2	IVW(MRE)	1.643 (1.592 ~ 1.695)	<0.001	<0.001
genus Lactococcus	14306	Acute lymphocytic leukaemia (controls excluding all cancers)	287320	7	IVW(MRE)	2.152 (1.447 ~ 3.199)	<0.001	0.011
family Acidaminococcaceae	14306	Acute myeloid leukaemia (controls excluding all cancers)	287367	6	IVW(MRE)	0.208 (0.120 ~ 0.361)	<0.001	<0.001
genus Rikenellaceae RC9 gut group	14306	Acute myeloid leukaemia (controls excluding all cancers)	287367	9	IVW(MRE)	1.964 (1.573 ~ 2.453)	<0.001	<0.001
genus Anaerostipes	14306	Acute myeloid leukaemia (controls excluding all cancers)	287367	10	IVW(MRE)	2.515 (1.503 ~ 4.209)	<0.001	0.017
genus Slackia	14306	Acute myeloid leukaemia (controls excluding all cancers)	287367	7	IVW(MRE)	2.553 (1.481 ~ 4.401)	0.001	0.022
genus Lachnospiraceae ND3007 group	14306	Acute myeloid leukaemia (controls excluding all cancers)	287367	2	IVW(MRE)	3.417 (1.960 ~ 5.959)	<0.001	0.001
genus Desulfovibrio	14306	Chronic lymphocytic leukaemia (controls excluding all cancers)	287757	8	IVW(MRE)	0.581 (0.440 ~ 0.768)	<0.001	0.020
genus Ruminococcaceae UCG011	14306	Chronic myeloid leukaemia (controls excluding all cancers)	287242	8	IVW(MRE)	2.010 (1.363 ~ 2.963)	<0.001	0.044
genus Ruminococcaceae UCG014	14306	Chronic myeloid leukaemia (controls excluding all cancers)	287242	10	IVW(MRE)	3.101 (1.626 ~ 5.915)	0.001	0.044

* refer to existence of heterogeneity between SNPs, # refer to existence of pleiotropy of SNPs

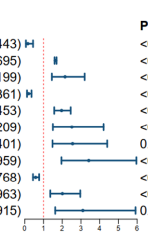

FIGURE 3
MR results and its forest plot.

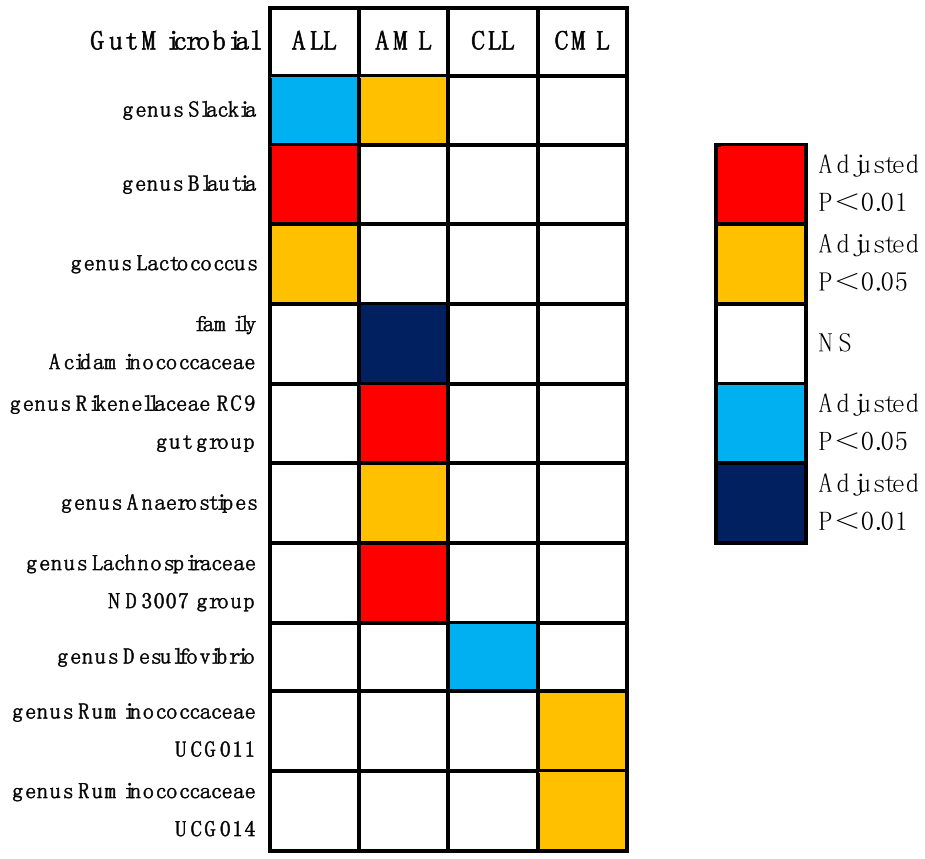

FIGURE 4
Causal effects of gut microbiota on leukemia ($p < 0.05/0.01$). Red indicates risk factors for leukemia, blue represents protective factors for leukemia, and white signifies non-causal factors for leukemia. NS, not significantly associated.

Supplementary Figure S1 presents the forest plot of the final causal estimation results. The scatter plot in Supplementary Figure S2 illustrates the causal effects of SNPs on the gut microbiota and leukemia. The leave-one-out analysis in Supplementary Figure S3 did not identify any SNPs that significantly influenced the outcome.

3.3 Sensitivity analysis results

In the sensitivity analysis, we conducted heterogeneity tests, horizontal pleiotropy analysis, and a comprehensive MR-steiger analysis, with the results presented in Table 2.

The heterogeneity test revealed no apparent heterogeneity among the SNP groups within the investigated gut microbiota variables. We calculated the intercept term of the MR-Egger regression and found no evidence of horizontal pleiotropy. Lastly, to ensure the overall causal effect direction of the MR analysis, we applied the MR-steiger model to validate the direction of the causal estimation. The results confirmed that the direction of causality in every MR analysis was correct.

The estimations of the association between the gut microbiota and leukemia using various MR methods are presented in Supplementary Table S2. Results for heterogeneity tests and horizontal pleiotropy analysis are shown in Supplementary Tables S6, S7, respectively. The power of each MR study can be found in Supplementary Table S2.

10.3389/fmicb.2023.1293333

TABLE 2 Tests of MR-Steiger casual direction, MR-Egger I2, heterogeneity and pleiotropy.

Exposures	Outcomes	Q from IVW	Q from MR-Egger	Pval_Q from IVW	Pval_Q from MR-Egger	MR-Steiger	Pval of MR-Egger interception	I2 of MR-Egger
Genus Blautia	Acute lymphocytic leukaemia (controls excluding all cancers)	–	–	–	–	True	–	0.55
Genus Rikenellaceae RC9 gut group	Acute myeloid leukaemia (controls excluding all cancers)	1.36	0.97	0.99	1.00	True	0.55	0.95
Family Acidaminococcaceae	Acute myeloid leukaemia (controls excluding all cancers)	1.16	0.94	0.95	0.92	True	0.67	0.96
Genus Lachnospiraceae ND3007 group	Acute myeloid leukaemia (controls excluding all cancers)	–	–	–	–	True	–	0.00
Genus Lactococcus	Acute lymphocytic leukaemia (controls excluding all cancers)	1.50	1.50	0.96	0.91	True	0.95	0.89
Genus Slackia	Acute lymphocytic leukaemia (controls excluding all cancers)	4.46	4.24	0.49	0.37	True	0.67	0.98
Genus Anaerostipes	Acute myeloid leukaemia (controls excluding all cancers)	1.72	1.70	1.00	0.99	True	0.89	0.83
Genus Desulfovibrio	Chronic lymphocytic leukaemia (controls excluding all cancers)	1.66	1.66	0.98	0.95	True	0.99	0.93
Genus Slackia	Acute myeloid leukaemia (controls excluding all cancers)	2.43	2.41	0.88	0.79	True	0.89	0.92
Genus Ruminococcaceae UCG011	Chronic myeloid leukaemia (controls excluding all cancers)	1.51	1.51	0.98	0.96	True	0.98	0.92
Genus Ruminococcaceae UCG014	Chronic myeloid leukaemia (controls excluding all cancers)	2.07	1.99	0.99	0.98	True	0.78	0.90

MR studies with fewer than 3 SNPs cannot undergo Q-test and MR-Egger intercept analysis.

4 Discussion

The relationship between the gut microbiota and leukemia is a research area that has garnered significant attention. As mentioned in the background, several studies have indicated that the gut microbiota may play a role in the onset and progression of leukemia.

To the best of our knowledge, this study is among the first to systematically assess the causal relationship between the gut

microbiota and various types of leukemia. Our MR research, utilizing a large-scale GWAS database, fills a gap in this research domain from a novel perspective.

Two-sample MR studies provide compelling evidence suggesting that specific gut microbes play a substantial role in the onset and progression of various leukemias, with metabolites from these microbiota playing a crucial role. Traditional observational studies, influenced by confounders like dietary habits and age, as well as reverse causality (Davies et al., 2018), may present biased findings. Therefore, utilizing SNPs as IVs in MR analysis to explore the causal relationship between gut microbiota and leukemia substantially mitigates these interferences, rendering the conclusions more convincing.

Traditional observational studies have reported associations between variations in gut microbiota and leukemia. A prospective clinical study involving 29 AML patients, 17 CML patients, and 33 healthy participants found an increased relative abundance of Actinobacteria, Acidobacteria, and Chloroflexi at the phylum level, while a decrease in Tenericutes. At the genus level, especially in AML patients, there was an increase in Streptococcus and a decrease in Megamonas, Lachnospiraceae NC2004 group, and Prevotella 9 (Yu et al., 2021). Another study, using a 16S rRNA quantitative array and bioinformatic analysis to examine fecal samples from participants, found significant bacterial variations in the fecal specimens of ALL patients compared to healthy controls. For instance, there was a notable enrichment of *Bacteroides clarus* in ALL patients (Song and Gyarmati, 2020). Moreover, leukemia treatments can alter the gut microbiota. For instance, antibiotic treatment that down-regulates the gut microbiota can restore the anti-leukemia efficacy of APO866 (ElMokh et al., 2022). Using B-cell receptor inhibitors (BCRi) as targeted therapy can up-regulate the Bacteroidia levels in CLL patients (Zuccaro et al., 2023). This also seems to underscore the association between the gut microbiota and leukemia.

The molecular mechanisms through which gut microbiota induce leukemia onset and progression have attracted significant research attention. Studies have shown that dysbiosis of the gut microbiota may lead to immune system abnormalities, thereby increasing the risk of leukemia onset (Rooks and Garrett, 2016). A case–control study found that gastrointestinal infections increase the risk of AML, potentially due to immune dysregulation caused by the imbalance in the gut microbiota brought about by the infections (Østgård et al., 2018).

Secondly, metabolites derived from the gut microbiota play a pivotal role in the occurrence and progression of leukemia in relation to the gut microbiota. The gut microbiota can break down dietary fiber, producing short-chain fatty acids (SCFAs) like acetate, propionate, and butyrate. These SCFAs play a crucial role in the health of intestinal cells and the regulation of the immune system (Ganapathy et al., 2013; Swanson et al., 2020). Gut microbes such as genus Slackia, genus Blautia, genus Anaerostipes, genus Rikenellaceae RC9 gut group, genus Lachnospiraceae ND3007 group, and genus Ruminococcaceae UCG014 can produce substantial amounts of butyrate through various metabolic pathways. Research has shown that SCFAs are particularly crucial in inducing T lymphocyte differentiation and development, thereby driving anti-pathogen immunity or immune tolerance based on the immune environment, indirectly promoting the onset of leukemia (Zhang et al., 2019). For instance, SCFAs can promote microbial antigen-specific Th1 cells to produce IL-10 via the GPR43 signaling pathway. Furthermore, SCFAs can accelerate the expression of B-lymphocyte-induced maturation protein 1 (Blimp-1) in Th1 cells by activating the STAT3 and mTOR pathways, thereby enhancing Th1 cell production of IL-10, resulting in immune suppression (Sun et al., 2018). Butyrate, via the GPR41 and GPR43 signaling pathways, accelerates the metabolism of antigen-activated CD8+ T cells, thereby enhancing their memory potential (Bachem et al., 2019).

Tet2 gene is a tumor-suppressor gene, and Tet2 gene mutation is one of the factors that can trigger AML and CML (Chiba, 2016). Meisel et al. (2018) found that mutations in the Tet2 gene disrupt the integrity of the intestinal barrier, leading to the entry of gut microbiota into the bloodstream or local lymph nodes. The body's immune system produces the corresponding inflammatory cytokine IL-6, which subsequently stimulates the proliferation of leukemia cells. Additionally, studies have indicated that inflammatory stimuli weaken the integrity of the intestinal barrier. The direct contact of gut microbiota and their metabolites (e.g., SCFAs) with the intestinal epithelium leads to the overactivation of NF-KB in intestinal epithelial cells. This promotes the production of cytokines such as TNF, IL-1, and IL-6, thereby inducing and exacerbating leukemia (Gerloff et al., 2015; Tsilimigras et al., 2017; Zhang et al., 2017).

A study found that in an ALL mouse model, the proportion of bacteria with dietary flavonoid conversion functions, such as the genus Lactococcus, increased (Song and Gyarmati, 2020). Dietary bioflavonoids have been shown to induce mixed-lineage leukemia (MLL) gene cleavage by targeting topoisomerase II, and they might lead to pediatric leukemia (Strick et al., 2000).

The aforementioned findings are consistent with our experimental results, strongly confirming that the abnormal composition of the gut microbiota is related to the pathogenesis of leukemia.

Probiotics are a class of active microorganisms that, by reducing gut dysbiosis, promoting nutrient absorption, protecting the intestinal mucosal barrier, modulating immunity, or inhibiting intestinal inflammation, have a positive impact on gut health (Fredricks, 2019).

The genus Desulfovibrio is a sulfate-reducing bacterium (SRB), and its metabolic pathways help maintain the sulfur cycle in the gut environment. In previous studies, the genus Desulfovibrio has been regarded as a "double-edged sword," being both beneficial (Chen et al., 2015; Zhao et al., 2016) and harmful (Singh et al., 2023). The family Acidaminococcaceae consists of bacteria that play a crucial role in amino acid metabolism in the gut. Its imbalance is associated with the onset and progression of various diseases, including oral infections (Luo et al., 2020) and inflammatory bowel diseases (Gevers et al., 2014). However, no current research explicitly indicates a direct relationship between the two and leukemia.

Our study revealed that genus Desulfovibrio and family Acidaminococcaceae serve as protective factors for CLL and AML, potentially acting as probiotics to reduce the risk of CLL and AML. However, previous studies have demonstrated differential effects of both on human health, necessitating further randomized controlled trials to validate these findings. Additionally, the potential mechanisms through which genus Desulfovibrio and family Acidaminococcaceae inhibit leukemia development require further investigation.

Interestingly, the genus Slackia acts as a risk factor for ALL while serving as a protective factor for AML in the development and progression of leukemia. One possible reason is that ALL is more prevalent in children and adolescents, while AML mainly occurs in adults; thus, there are variations in gut microbiota across different age groups. Furthermore, the etiology, pathogenesis, and immune phenotypes of the two diseases differ. As a result, the relationship between different diseases and the same gut microbiota can vary, sometimes even being completely opposite.

Implementing the MR method can elucidate causal relationships from exposure to outcome, unaffected by confounding factors and reverse causation, potentially providing more convincing evidence than observational studies.

The MR conducted in our study has several advantages: Firstly, this research represents the first attempt to infer the causal relationship between the gut microbiota and leukemia using comprehensive GWAS data, offering a novel approach to select candidate gut microbiota for subsequent functional studies. Secondly, it is based on publicly available large-scale GWAS summary statistics, thus offering an efficient option without additional experimental costs to extract reliable genetic information. Thirdly, our research is comprehensive in its investigation of leukemia, having conducted a holistic analysis of the four primary types of leukemia. This affords us the opportunity to evaluate common gut microbiota that have causal relationships with various leukemias.

However, certain limitations should be mentioned: Firstly, the gut microbiota GWAS is still in its nascent phase in terms of sample size, which offers insufficient information at the species or strain level. Secondly, further subgroup analyses are not feasible due to the absence of stratified summary data (e.g., gender and ethnicity) in the initial studies. Thirdly, our study lacks *in vivo* or *in vitro* models. Future research directions can build upon this to establish a direct link between gut microbiota and the origins of leukemia. Fourthly, the power of some aspects of this study is relatively low, which may increase the probability of Type II errors. Lastly, given that the majority of GWAS participants are of European ancestry, extrapolating the study results to other ethnic groups may be limited.

5 Conclusion

In summary, through two-sample MR analyses using publicly available GWAS summary data, we evaluated the causal relationship between the gut microbiota and leukemia, and identified potential pathogenic bacteria and probiotic taxa that influence the onset of leukemia. This research may aid in the early detection of various types of leukemia and offer a new direction for the prevention and treatment of leukemia.

Data availability statement

The datasets presented in this study can be found in online repositories. The names of the repository/repositories and accession number(s) can be found in the article/Supplementary material.

Author contributions

GC: Conceptualization, Investigation, Writing – original draft, Writing – review & editing. ZK: Formal analysis, Supervision, Writing – review & editing. FL: Data curation, Software, Writing – review & editing. JL: Supervision, Validation, Writing – review & editing.

Funding

The author(s) declare that no financial support was received for the research, authorship, and/or publication of this article.

Acknowledgments

We express our gratitude to the participants and researchers of the FinnGen study and thank the MiBioGen consortium for releasing the gut microbiota GWAS summary statistics.

Conflict of interest

The authors declare that the research was conducted in the absence of any commercial or financial relationships that could be construed as a potential conflict of interest.

Publisher's note

Supplementary material

The Supplementary material for this article can be found online at: https://www.frontiersin.org/articles/10.3389/fmicb.2023.1293333/full#supplementary-material

References

Bachem, A., Makhlouf, C., Binger, K. J., de Souza, D. P., Tull, D., Hochheiser, K., et al. (2019). Microbiota-derived short-chain fatty acids promote the memory potential of antigen-activated CD8(+) T cells. *Immunity* 51, 285–297.e285. doi: 10.1016/j.immuni.2019.06.002

Bai, L., Zhou, P., Li, D., and Ju, X. (2017). Changes in the gastrointestinal microbiota of children with acute lymphoblastic leukaemia and its association with antibiotics in the short term. *J. Med. Microbiol.* 66, 1297–1307. doi: 10.1099/jmm.0.000568

Bartenhagen, C., Fischer, U., Korn, K., Pfister, S. M., Gombert, M., Chen, C., et al. (2017). Infection as a cause of childhood leukemia: virus detection employing whole genome sequencing. *Haematologica* 102, e179–e183. doi: 10.3324/haematol.2016.155382

Beane Freeman, L. E., Blair, A., Lubin, J. H., Stewart, P. A., Hayes, R. B., Hoover, R. N., et al. (2009). Mortality from lymphohematopoietic malignancies among workers in formaldehyde industries: the National Cancer Institute cohort. *J. Natl. Cancer Inst.* 101, 751–761. doi: 10.1093/jnci/djp096

Bowden, J., Davey Smith, G., Haycock, P. C., and Burgess, S. (2016). Consistent estimation in Mendelian randomization with some invalid instruments using a weighted median estimator. *Genet. Epidemiol.* 40, 304–314. doi: 10.1002/gepi.21965

Bowden, J., Del Greco, M. F., Minelli, C., Davey Smith, G., Sheehan, N. A., and Thompson, J. R. (2016). Assessing the suitability of summary data for two-sample Mendelian randomization analyses using MR-egger regression: the role of the I2 statistic. *Int. J. Epidemiol.* 45, 1961–1974. doi: 10.1093/ije/dyw220

Bray, F., Ferlay, J., Soerjomataram, I., Siegel, R. L., Torre, L. A., and Jemal, A. (2018). Global cancer statistics 2018: GLOBOCAN estimates of incidence and mortality worldwide for 36 cancers in 185 countries. *CA Cancer J. Clin.* 68, 394–424. doi: 10.3322/caac.21492

Burgess, S., Butterworth, A., and Thompson, S. G. (2013). Mendelian randomization analysis with multiple genetic variants using summarized data. *Genet. Epidemiol.* 37, 658–665. doi: 10.1002/gepi.21758

Burgess, S., Small, D. S., and Thompson, S. G. (2017). A review of instrumental variable estimators for Mendelian randomization. *Stat. Methods Med. Res.* 26, 2333–2355. doi: 10.1177/0962280215597579

Burgess, S., and Thompson, S. G. (2011). Avoiding bias from weak instruments in Mendelian randomization studies. *Int. J. Epidemiol.* 40, 755–764. doi: 10.1093/ije/dyr036

Chen, S. W., Zhu, J., Zuo, S., Zhang, J. L., Chen, Z. Y., Chen, G. W., et al. (2015). Protective effect of hydrogen sulfide on TNF-α and IFN-γ-induced injury of intestinal epithelial barrier function in Caco-2 monolayers. *Inflamm. Res.* 64, 789–797. doi: 10.1007/s00011-015-0862-5

Chiba, S. (2016). Significance of TET2 mutations in myeloid and lymphoid neoplasms. *Rinsho Ketsueki* 57, 715–722. doi: 10.11406/rinketsu.57.715

Choi, K. W., Chen, C. Y., Stein, M. B., Klimentidis, Y. C., Wang, M. J., Koenen, K. C., et al. (2019). Assessment of bidirectional relationships between physical activity and depression among adults: a 2-sample Mendelian randomization study. *JAMA Psychiatry* 76, 399–408. doi: 10.1001/jamapsychiatry.2018.4175

Codd, V., Nelson, C. P., Albrecht, E., Mangino, M., Deelen, J., Buxton, J. L., et al. (2013). Identification of seven loci affecting mean telomere length and their association with disease. *Nat. Genet.* 45, 422–427. doi: 10.1038/ng.2528

Davey Smith, G., and Hemani, G. (2014). Mendelian randomization: genetic anchors for causal inference in epidemiological studies. *Hum. Mol. Genet.* 23, R89–R98. doi: 10.1093/hmg/ddu328

Davies, N. M., Holmes, M. V., and Davey Smith, G. (2018). Reading Mendelian randomisation studies: a guide, glossary, and checklist for clinicians. *BMJ* 362:k601. doi: 10.1136/bmj.k601

ElMokh, O., Matsumoto, S., Biniecka, P., Bellotti, A., Schaeuble, K., Piacente, F., et al. (2022). Gut microbiota severely hampers the efficacy of NAD-lowering therapy in leukemia. *Cell Death Dis.* 13:320. doi: 10.1038/s41419-022-04763-3

Engen, P. A., Green, S. J., Voigt, R. M., Forsyth, C. B., and Keshavarzian, A. (2015). The gastrointestinal microbiome: alcohol effects on the composition of intestinal microbiota. *Alcohol Res.* 37, 223–236.

Fredricks, D. N. (2019). The gut microbiota and graft-versus-host disease. *J. Clin. Invest.* 129, 1808–1817. doi: 10.1172/jci125797

Ganapathy, V., Thangaraju, M., Prasad, P. D., Martin, P. M., and Singh, N. (2013). Transporters and receptors for short-chain fatty acids as the molecular link between colonic bacteria and the host. *Curr. Opin. Pharmacol.* 13, 869–874. doi: 10.1016/j.coph.2013.08.006

Gerloff, D., Grundler, R., Wurm, A. A., Bräuer-Hartmann, D., Katzerke, C., Hartmann, J. U., et al. (2015). NF-κB/STAT5/miR-155 network targets PU.1 in FLT3-ITD-driven acute myeloid leukemia. *Leukemia* 29, 535–547. doi: 10.1038/leu.2014.231

Gevers, D., Kugathasan, S., Denson, L. A., Vázquez-Baeza, Y., Van Treuren, W., Ren, B., et al. (2014). The treatment-naive microbiome in new-onset Crohn's disease. *Cell Host Microbe* 15, 382–392. doi: 10.1016/j.chom.2014.02.005

Gou, Y., Zhang, J., Li, C., Liu, Y., Hui, J., Zhou, R., et al. (2023). Causal relationship between gut microbiota and rheumatoid arthritis: a two-sample Mendelian randomisation study. *Clin. Exp. Rheumatol.* doi: 10.55563/clinexprheumatol/p9ig7c

Greenland, S. (2018). An introduction to instrumental variables for epidemiologists. *Int. J. Epidemiol.* 47:358. doi: 10.1093/ije/dyx275

Hartwig, F. P., Davey Smith, G., and Bowden, J. (2017). Robust inference in summary data Mendelian randomization via the zero modal pleiotropy assumption. *Int. J. Epidemiol.* 46, 1985–1998. doi: 10.1093/ije/dyx102

Hemani, G., Tilling, K., and Davey Smith, G. (2017). Orienting the causal relationship between imprecisely measured traits using GWAS summary data. *PLoS Genet.* 13:e1007081. doi: 10.1371/journal.pgen.1007081

Kurilshikov, A., Medina-Gomez, C., Bacigalupe, R., Radjabzadeh, D., Wang, J., Demirkan, A., et al. (2021). Large-scale association analyses identify host factors influencing human gut microbiome composition. *Nat. Genet.* 53, 156–165. doi: 10.1038/s41588-020-00763-1

Kurki, M. I., Karjalainen, J., Palta, P., Sipilä, T. P., Kristiansson, K., Donner, K. M., et al. (2023). FinnGen provides genetic insights from a well-phenotyped isolated population. *Nature* 613, 508–518. doi: 10.1038/s41586-022-05473-8

Larsson, S. C., Michaëlsson, K., and Burgess, S. (2019). Mendelian randomization in the bone field. *Bone* 126, 51–58. doi: 10.1016/j.bone.2018.10.011

Lee, C. H., Cook, S., Lee, J. S., and Han, B. (2016). Comparison of two meta-analysis methods: inverse-variance-weighted average and weighted sum of Z-scores. *Genomics Inform.* 14, 173–180. doi: 10.5808/gi.2016.14.4.173

Luo, Y. X., Sun, M. L., Shi, P. L., Liu, P., Chen, Y. Y., and Peng, X. (2020). Research progress in the relationship between Veillonella and oral diseases. *Hua Xi Kou Qiang Yi Xue Za Zhi* 38, 576–582. doi: 10.7518/hxkq.2020.05.018

Ma, T., Chen, Y., Li, L. J., and Zhang, L. S. (2021). Opportunities and challenges for gut microbiota in acute leukemia. *Front. Oncol.* 11:692951. doi: 10.3389/fonc.2021.692951

Meisel, M., Hinterleitner, R., Pacis, A., Chen, L., Earley, Z. M., Mayassi, T., et al. (2018). Microbial signals drive pre-leukaemic myeloproliferation in a Tet2-deficient host. *Nature* 557, 580–584. doi: 10.1038/s41586-018-0125-z

Metz-Flamant, C., Samson, E., Caër-Lorho, S., Acker, A., and Laurier, D. (2012). Leukemia risk associated with chronic external exposure to ionizing radiation in a French cohort of nuclear workers. *Radiat. Res.* 178, 489–498. doi: 10.1667/rr2822.1

Nemkov, T., D'Alessandro, A., and Reisz, J. A. (2019). Metabolic underpinnings of leukemia pathology and treatment. *Cancer Rep. (Hoboken)* 2:e1139. doi: 10.1002/cnr2.1139

Ooi, B. N. S., Loh, H., Ho, P. J., Milne, R. L., Giles, G., Gao, C., et al. (2019). The genetic interplay between body mass index, breast size and breast cancer risk: a Mendelian randomization analysis. *Int. J. Epidemiol.* 48, 781–794. doi: 10.1093/ije/dyz124

Østgård, L. S. G., Nørgaard, M., Pedersen, L., Østgård, R. D., Medeiros, B. C., Overgaard, U. M., et al. (2018). Autoimmune diseases, infections, use of antibiotics and the risk of acute myeloid leukaemia: a national population-based case-control study. *Br. J. Haematol.* 181, 205–214. doi: 10.1111/bjh.15163

Rajagopala, S. V., Yooseph, S., Harkins, D. M., Moncera, K. J., Zabokrtsky, K. B., Torralba, M. G., et al. (2016). Gastrointestinal microbial populations can distinguish pediatric and adolescent acute lymphoblastic leukemia (ALL) at the time of disease diagnosis. *BMC Genomics* 17:635. doi: 10.1186/s12864-016-2965-y

Rashidi, A., Ebadi, M., Rehman, T. U., Elhusseini, H., Halaweish, H. F., Kaiser, T., et al. (2022). Lasting shift in the gut microbiota in patients with acute myeloid leukemia. *Blood Adv.* 6, 3451–3457. doi: 10.1182/bloodadvances.2021006783

Rinninella, E., Raoul, P., Cintoni, M., Franceschi, F., Miggiano, G. A. D., Gasbarrini, A., et al. (2019). What is the healthy gut microbiota composition? A changing ecosystem across age, environment, diet, and diseases. *Microorganisms* 7:14. doi: 10.3390/microorganisms7010014

Rooks, M. G., and Garrett, W. S. (2016). Gut microbiota, metabolites and host immunity. *Nat. Rev. Immunol.* 16, 341–352. doi: 10.1038/nri.2016.42

Rutella, S., Vadakekolathu, J., Mazziotta, F., Reeder, S., Yau, T. O., Mukhopadhyay, R., et al. (2022). Immune dysfunction signatures predict outcomes and define checkpoint blockade-unresponsive microenvironments in acute myeloid leukemia. *J. Clin. Invest.* 132:e159579. doi: 10.1172/jci159579

Singh, S. B., Carroll-Portillo, A., and Lin, H. C. (2023). Desulfovibrio in the gut: the enemy within? *Microorganisms* 11:1772. doi: 10.3390/microorganisms11071772

Song, Y., and Gyarmati, P. (2020). Microbiota changes in a pediatric acute lymphocytic leukemia mouse model. *Microbiology* 9:e982. doi: 10.1002/mbo3.982

Staley, J. R., Blackshaw, J., Kamat, M. A., Ellis, S., Surendran, P., Sun, B. B., et al. (2016). PhenoScanner: a database of human genotype-phenotype associations. *Bioinformatics* 32, 3207–3209. doi: 10.1093/bioinformatics/btw373

Strick, R., Strissel, P. L., Borgers, S., Smith, S. L., and Rowley, J. D. (2000). Dietary bioflavonoids induce cleavage in the MLL gene and may contribute to infant leukemia. *Proc. Natl. Acad. Sci. U. S. A.* 97, 4790–4795. doi: 10.1073/pnas.070061297

Sun, M., Wu, W., Chen, L., Yang, W., Huang, X., Ma, C., et al. (2018). Microbiota-derived short-chain fatty acids promote Th1 cell IL-10 production to maintain intestinal homeostasis. *Nat. Commun.* 9:3555. doi: 10.1038/s41467-018-05901-2

Sung, H., Ferlay, J., Siegel, R. L., Laversanne, M., Soerjomataram, I., Jemal, A., et al. (2021). Global Cancer statistics 2020: GLOBOCAN estimates of incidence and mortality worldwide for 36 cancers in 185 countries. *CA Cancer J. Clin.* 71, 209–249. doi: 10.3322/caac.21660

Swanson, G. R., Siskin, J., Gorenz, A., Shaikh, M., Raeisi, S., Fogg, L., et al. (2020). Disrupted diurnal oscillation of gut-derived short chain fatty acids in shift workers drinking alcohol: possible mechanism for loss of resiliency of intestinal barrier in disrupted circadian host. *Transl. Res.* 221, 97–109. doi: 10.1016/j.trsl.2020.04.004

Tsilimigras, M. C., Fodor, A., and Jobin, C. (2017). Carcinogenesis and therapeutics: the microbiota perspective. *Nat. Microbiol.* 2:17008. doi: 10.1038/nmicrobiol.2017.8

Valdes, A. M., Walter, J., Segal, E., and Spector, T. D. (2018). Role of the gut microbiota in nutrition and health. *BMJ* 361:k2179. doi: 10.1136/bmj.k2179

Verbanck, M., Chen, C. Y., Neale, B., and Do, R. (2018). Detection of widespread horizontal pleiotropy in causal relationships inferred from Mendelian randomization between complex traits and diseases. *Nat. Genet.* 50, 693–698. doi: 10.1038/s41588-018-0099-7

Wang, R., Yang, X., Liu, J., Zhong, F., Zhang, C., Chen, Y., et al. (2022). Gut microbiota regulates acute myeloid leukaemia via alteration of intestinal barrier function mediated by butyrate. *Nat. Commun.* 13:2522. doi: 10.1038/s41467-022-30240-8

Wu, F., Huang, Y., Hu, J., and Shao, Z. (2020). Mendelian randomization study of inflammatory bowel disease and bone mineral density. *BMC Med.* 18:312. doi: 10.1186/s12916-020-01778-5

Yu, D., Yu, X., Ye, A., Xu, C., Li, X., Geng, W., et al. (2021). Profiling of gut microbial dysbiosis in adults with myeloid leukemia. *FEBS Open Bio* 11, 2050–2059. doi: 10.1002/2211-5463.13193

Yue, M., Jin, C., Jiang, X., Xue, X., Wu, N., Li, Z., et al. (2023). Causal effects of gut microbiota on sleep-related phenotypes: a two-sample Mendelian randomization study. *Clocks Sleep* 5, 566–580. doi: 10.3390/clockssleep5030037

Zhang, Z., Tang, H., Chen, P., Xie, H., and Tao, Y. (2019). Demystifying the manipulation of host immunity, metabolism, and extraintestinal tumors by the gut microbiome. *Signal Transduct. Target. Ther.* 4:41. doi: 10.1038/s41392-019-0074-5

Zhang, Y., Yu, X., Lin, D., Lei, L., Hu, B., Cao, F., et al. (2017). Propiece IL-1α facilitates the growth of acute T-lymphocytic leukemia cells through the activation of NF-κB and SP1. *Oncotarget* 8, 15677–15688. doi: 10.18632/oncotarget.14934

Zhao, H., Yan, R., Zhou, X., Ji, F., and Zhang, B. (2016). Hydrogen sulfide improves colonic barrier integrity in DSS-induced inflammation in Caco-2 cells and mice. *Int. Immunopharmacol.* 39, 121–127. doi: 10.1016/j.intimp.2016.07.020

Zhou, Y., Zhou, C., and Zhang, A. (2022). Gut microbiota in acute leukemia: current evidence and future directions. *Front. Microbiol.* 13:1045497. doi: 10.3389/fmicb.2022.1045497

Zuccaro, V., Petazzoni, G., Mileto, I., Corbella, M., Asperges, E., Sacchi, P., et al. (2023). Gut microbiota and B cell receptor (BCR) inhibitors for the treatment of chronic lymphocytic leukemia: is biodiversity correlated with clinical response or immune-related adverse event occurrence? A cross-sectional study. *Microorganisms* 11:1305. doi: 10.3390/microorganisms11051305

frontiers | Frontiers in Microbiology

TYPE Original Research
PUBLISHED 20 February 2024
DOI 10.3389/fmicb.2024.1314528

OPEN ACCESS

EDITED BY
Edoardo Pasolli,
University of Naples Federico II, Italy

REVIEWED BY
Samara Paula Mattiello,
University of Tennessee Southern,
United States
Chuanfa Liu,
The Chinese University of Hong Kong, China

*CORRESPONDENCE
Wei Liu
✉ liuw@zaas.ac.cn
Feng Ye
✉ fengye@njmu.edu.cn

†These authors have contributed equally to this work

RECEIVED 10 October 2023
ACCEPTED 31 January 2024
PUBLISHED 20 February 2024

CITATION
Liu W, Li Z, Ze X, Deng C, Xu S and Ye F (2024) Multispecies probiotics complex improves bile acids and gut microbiota metabolism status in an *in vitro* fermentation model. *Front. Microbiol.* 15:1314528. doi: 10.3389/fmicb.2024.1314528

Multispecies probiotics complex improves bile acids and gut microbiota metabolism status in an *in vitro* fermentation model

Wei Liu[1*†], Zhongxia Li[2†], Xiaolei Ze[2], Chaoming Deng[2], Shunfu Xu[3] and Feng Ye[3*]

[1]Institute of Plant Protection and Microbiology, Zhejiang Academy of Agricultural Sciences, Hangzhou, China, [2]BYHEALTH Institute of Nutrition and Health, Guangzhou, China, [3]Department of Gastroenterology, The First Affiliated Hospital of Nanjing Medical University, Nanjing, China

The consumption of probiotics has been extensively employed for the management or prevention of gastrointestinal disorders by modifying the gut microbiota and changing metabolites. Nevertheless, the probiotic-mediated regulation of host metabolism through the metabolism of bile acids (BAs) remains inadequately comprehended. The gut-liver axis has received more attention in recent years due to its association with BA metabolism. The objective of this research was to examine the changes in BAs and gut microbiota using an *in vitro* fermentation model. The metabolism and regulation of gut microbiota by commercial probiotics complex containing various species such as *Lactobacillus*, *Bifidobacterium*, and *Streptococcus* were investigated. The findings indicated that the probiotic strains had produced diverse metabolic profiles of BAs. The probiotics mixture demonstrated the greatest capacity for Bile salt hydrolase (BSH) deconjugation and 7α-dehydroxylation, leading to a significant elevation in the concentrations of Chenodeoxycholic acid, Deoxycholic acidcholic acid, and hyocholic acid in humans. In addition, the probiotic mixtures have the potential to regulate the microbiome of the human intestines, resulting in a reduction of isobutyric acid, isovaleric acid, hydrogen sulfide, and ammonia. The probiotics complex intervention group showed a significant increase in the quantities of *Lactobacillus* and *Bifidobacterium* strains, in comparison to the control group. Hence, the use of probiotics complex to alter gut bacteria and enhance the conversion of BAs could be a promising approach to mitigate metabolic disorders in individuals.

KEYWORDS

Bile acids, gut microbiota, metabolism, probiotics, *in vitro* fermentation model

Introduction

The human gut provides a dynamic habitat for microbial communities. In normal bodily conditions, external nourishment and internal substances enter the digestive system to supply sufficient materials for the host and its microbiota. Bile acids (BAs) are many endogenous amphiphilic molecules combined with taurine or glycine. Bile acids are synthesized in the liver through a complex enzymatic reaction, which is catalyzed by cholesterol (Singh et al., 2019).

While eating, the gallbladder releases bile salt into the intestine to aid in the digestion of nutrients from food, which is constantly present in the intestine along with chyme.

Eventually, it is absorbed again at the ileum's conclusion and sent back to the pool of bile salts via circulation. Around 95% of bile salts are efficiently absorbed again during the process of intestinal liver circulation. During the process, only a limited quantity of bile salts is permitted to be released into the large intestine, where they engage in the metabolic transformation process of gut microbiota (Trauner and Boyer, 2003).

Maintaining an optimal composition within the bile acid pool and metabolic homeostasis is heavily influenced by the interaction between the gut and liver. These mechanisms may contribute to the hindrance of high blood sugar, abnormal blood lipid levels, excessive body weight, and the development of diabetes. BAs, which are generated by the host and altered by gut microbiota, serve as a crucial factor in the absorption of nutrients, transmission of hormonal signals, control of lipids and cholesterol, inflammation, and maintenance of energy balance (Tian et al., 2020).

The liver initiates the production of BA through the synthesis of cholesterol. The majority of BAs are taken in by the intestine through the hepatic portal vein and subsequently return to the liver to initiate the cycle once more. Rodents have primary bile acids including cholic acid (CA), chenodeoxycholic acid (CDCA), and α- and β-muricholic acids, as well as secondary BAs such as murideoxycholic acid (MDCA), hyodeoxycholic acid (HDCA), and ω-Muricholic acid (ω-MCA) (De Aguiar et al., 2013). In comparison to other mammals, the liver of humans generates two main bile acids, namely CA and CDCA, while the bile acid pool contains secondary BAs including deoxycholic acid (DCA) and lithocholic acid (LCA). CA and CDCA are significant biological agents in the human body (Li et al., 2020). In the gut, the primary bile acids undergo a conversion process to become secondary bile acids during digestion. Apart from being characterized as primary or secondary BAs, each BA can be conjugated or unconjugated (Puri et al., 2018). Furthermore, the gut microbiome plays a crucial role in the breakdown of BAs. Bacteria that metabolize BAs, especially gut commensals that catalyze the dehydroxylation of primary BAs into7-dehydroxylation BA, offer a hopeful opportunity to regulate the BAs reservoir and thereby influence the physiology of the host (Marion et al., 2019).

Nevertheless, in the case of humans, the buildup of BAs has been linked to harm to the liver, long-term liver illness, inflammation, and the development of tumors (Zhou and Hylemon, 2014). Elevated concentrations of secondary BAs in both feces and blood have been linked to the development of cholesterol gallstones and colon cancer (Li et al., 2019). In addition to cancer, the disruption of the intestinal microecological balance is connected to the majority of chronic illnesses in humans, encompassing conditions linked to inflammation, metabolism, heart health, immune system, nervous system, and mental health. The majority of symbiotic microorganisms inhabit the human intestine directly, and alterations in the equilibrium of the population are the main cause of intestinal diseases. As a result, there is a growing emphasis on the management of gut bacteria to prevent and treat specific illnesses (Baker et al., 2011).

Intestinal health is significantly influenced by the interaction of probiotics and BAs, as indicated by recent research. The intestinal microbiota transforms conjugated bile acids into unconjugated bile acids through the action of bacterial bile salt hydrolase (BSH). These unconjugated bile acids are then subjected to various modifications such as 7-dehydroxylation or 12-dehydroxylation, amidation, oxidation-reduction, esterification, and desulfation, resulting in the formation of secondary bile acids. For example, *Bacteroides intestinalis* has been recognized for transforming primary BAs into secondary BAs, which could potentially cause cancerous effects, through the process of deconjugation and dehydration (Fukiya et al., 2009). *Lactobacillus delbrueckii* subsp. *bulgaricus* (LDB) has been shown its ability to actively acquire BAs through various mechanisms, such as transportation driven by the bacterial transmembrane proton gradient and binding facilitated by bacterial S-layer proteins (Hou et al., 2020). Furthermore, the study revealed that *Lactobacillus rhamnosus* GG (LGG) not only suppressed the synthesis of hepatic BAs but also increased their secretion by activating the FXR/FGF15 signaling pathway and controlling the deconjugation of primary BAs mediated by gut microbiota. In mice, these impacts hinder the occurrence of excessive liver damage and fibrosis caused by BAs (Liu et al., 2020b). It was noted that the administration of VSL#3, a blend of probiotics, resulted in elevated excretion and detachment levels of fecal BAs in mice. Additionally, there was an increase in the production of liver BAs and alterations in the gut microbiota of the mice (Degirolamo et al., 2014).

Currently, there is a wealth of data on the tolerance of probiotics to BAs, but little information exists regarding the impact of probiotic metabolism on BAs. The present study aimed to examine the alterations in structure and levels of

Abbreviations: 12-KLCA, 12-ketolithocholic acid; 12-oxo-CDCA, 12-Oxochenodeoxycholic acid; 23-DCA, Nor-Deoxycholic Acid; 3-oxo-CA, 3-Oxocholic acid; 3-oxo-DCA, 3-oxodeoxycholic acid; 3β-CA, 3β-Cholic Acid;3β-DCA, 3β-deoxycholic acid; 3β-HDCA, β-Hyodeoxycholic Acid; 3β-UDCA, 3β-Ursodeoxycholic Acid; 6,7-DKLCA, 6,7-diketolithocholic acid; 6-ketoLCA, 5-β-Cholanic Acid-3α-ol-6-one; 7,12-DKLCA, 7,12-diketolithocholic acid; 7-KDCA, 7-Ketodeoxycholic acid; 7-KLCA, 7-ketolithocholic acid; CA, cholic acid; CA-3S, Cholic Acid 3 Sulfate Sodium Salt; CDCA, Chenodeoxycholic acid; CDCA-3S, Chenodeoxycholic acid3-sulfate disodium salt; DCA, Deoxycholic acid; DCA-3-O-S, Deoxycholic Acid 3-O-Sulfate Disodium Salt; DHCA, Dehydrocholic acid; DLCA, Dehydrolithocholic acid; GCDCA-3S, Glycochenodeoxycholic Acid 3 Sulfate Disodium Salt; GHDCA, Glycohyodeoxycholic Acid; GUDCA-3S, Glycoursodeoxycholic Acid 3 Sulfate Sodium; HCA, hyocholic acid; HDCA, Hyodeoxycholic acid; isoCDCA, Isochenodeoxycholic Acid; LCA, Lithocholic acid; LCA-3S, lithocholic acid-3-sulfate; MDCA, murideoxycholic acid; NCA, norcholic acid; UCA, Ursocholic acid; UDCA, Ursodeoxycholic acid;α-MCA, α-muricholic acid; βGCA, 3β-Glycocholic Acid, β-MCA, β-muricholic acid; ω-MCA, ω-muricholic acid; TCA, Taurocholic acid; TCA-3S, Taurocholic Acid 3 sulfate sodium salt; TCDCA, aurochenodeoxycholic acid; TDCA, Taurodeoxycholic acid; TDHCA, Taurodehydrocholic acid; THCA, Taurohyocholic acid; THDCA, Taurohyodeoxycholic Acid (sodium salt); TLCA, taurolithocholic acid; TLCA-3S, taurolithocholic acid-3-sulfate; TUDCA, Tauroursodeoxycholic acid; Tβ-MCA, Tauro-β-muricholic acid; Tω-MCA, Tauro-ω-muricholic Acid sodium salt; GCA, Glycocholic acid; GCDCA, Glycochenodeoxycholic acid; GDHCA, Glycodehydrocholic acid; GHCA, Glycohyocholic acid; GLCA, Glycolithocholic acid; GLCA-3S, Glycolithocholic acid-3-sulfate; GUDCA, Glycoursodeoxycholic acid; CDCA-3Gln, Chenodeoxycholic acid-3-β-D-glucuronide.

short-chain fatty acids (SCFAs) in a probiotic complex following a 24-hour fermentation period. In an *in vitro* fermentation model, the metabolism of individual probiotics and a mixture of probiotics were investigated both before and after fermentation. This research aims to clarify the connection between probiotics and BAs metabolism, indicating that probiotics with the ability to regulate BAs could be used as an alternative approach to enhance liver metabolism.

Materials and methods

Probiotic complex and reagents

Mixed probiotic products tested in this study were provided by BYHEALTH Co., LTD, namely Yep. There are four strains in the probiotics complex: *L. acidophilus* DDS-1 (9×10^9 CFU/g), *L. rhamnosus* UALR-06 (4×10^9 CFU/g), *B. lactis* UABIA-12 (3.5×10^9 CFU/g), *B. longum* UABI-14 (5×10^8 CFU/g). The complex probiotics were used to evaluate the effect on gut microbiota and the ability to metabolize BAs. All of the standard bile acids were purchased from CNW (Shanghai, China) and IsoReag (Shanghai, China). Before analysis, the stock solutions were diluted using methanol (MeOH) to create working solutions.

Stool sample collection

Samples of fresh feces from 20 individuals in good health, consisting of 10 males and 10 females, were collected. Every volunteer had to adhere to their regular diet and had no previous or current use of antibiotics, probiotics, or any other supplementary medications in the past 3 months. Prior to sample collection for this study, these volunteers, who are free from any intestinal diseases, provided their informed consent. The specimens were kept at a temperature of 4°C and were handled within a time frame of 4 h after being gathered.

Anaerobic fermentation broth preparation

The necessary culture medium was formulated based on previously published literature (Liu et al., 2020a). In brief, Yeast extract-Casein hydrolysate-Fatty Acids (YCFA) and MRS-L (Man-Rogosa-Sharpe with 1.5% L-cysteine) media as the fermentation medium was aliquoted into 5 mL bottles using a peristaltic pump under anaerobic conditions through nitrogen filling and then sealed with a rubber plug. The culture media were autoclaved before use. Individual probiotics were grown in MRS-L medium.

Batch *in vitro* fermentation

One gram of fecal samples was weighed into centrifuge tubes and diluted in 10 ml of phosphate buffer solution (PBS). To achieve thorough blending, the samples underwent oscillation on a vortex shaker and were subsequently filtered twice using a double-layer sterile filter screen to eliminate any insoluble large particles. Afterward, a fecal suspension with a concentration of 10% was prepared using PBS to serve as the initial stock solution for the gut microbiota.

A YCFA medium was prepared according to a method reported in the literature (Tidjani Alou et al., 2020), and the final pH of the medium was adjusted to 6.8 ± 0.1. On an ultra-clean workbench, a sterile syringe was used to inoculate YCFA basic medium with 500 μL of fecal suspension in PBS. Next, the probiotics complex was inoculated with 1% (w/w) solution and injected into the anaerobic fermentation vial. Samples not inoculated with probiotics served as the blank control (CK). All anaerobic fermentation vials were placed inside the anaerobic workstation under an 85% N_2/10% H_2/ 5% CO_2 Atmosphere to undergo fermentation at 37°C for 24 h. The experimental scheme of fermentation *in vitro* is shown in Supplementary Figure 1.

BAs sample preparation and detection

Fresh BAs from cattle and pig were purchased from farmhouse local specialty store in Changsha. Human bile samples were obtained from patients who had undergone endoscopic retrograde cholangiopancreatography (ERCP) procedures within the Department of Gastroenterology at the First Affiliated Hospital of Nanjing Medical University. Bile aspirations were acquired subsequent to the cannulation of the papilla, facilitated by the insertion of a sterile 7 French standard endoscopic retrograde cholangiography catheter into the common bile duct (Cook, Ireland), followed by the extraction of bile into a sterile 20 mL syringe. The study protocol and informed consent form were approved by the ethics committee of the First Affiliated Hospital of Nanjing Medical University (2024-SR-037). A total of three types of BAs derived from cattle, pigs, and humans were collected. The pig group contained five samples each, while the human group provided six samples. The control and treatment groups were subjected to the BAs assay in the *in vitro* fermentation model. In the control group, there was 50 μL of human bile mixed with 5 mL of MRS-L medium, whereas in the treatment group, there was a mixture of 50 μL of overnight bacterial suspension, 50 μL of human bile, and 5 mL of MRS-L medium. BA experiment was done in triplicate for each sample. Furthermore, a volume of 1 mL from suspensions co-cultured for 24 h was obtained and then centrifuged at 10,000×g for 3 min. Subsequently, 500 μL of the resultant supernatant was utilized for BA detection.

The quantification of the BAs was performed using the ACQUITY UPLC-Xevo TQ-S system (Waters Corp., USA), which combines ultra-performance liquid chromatography with tandem mass spectrometry (UPLC-MS/MS). The cryopreserved BAs were first removed and dissolved on ice before being pipetted into 5 μL samples of BAs with 15 μL pure water.

The suspensions were combined in a tube for centrifugation, followed by the addition of 180 μL of the solvent containing the internal standard acetonitrile (ACN)/MeOH = 80/20 (v/v). To ensure sufficient protein precipitation, the samples were homogenized at a speed of 1,450 × g at 10°C, followed by freezing storage at −20°C. Afterward, the specimens were spun at 13,500 × g at a temperature of 4°C for 20 min.

Determination of SCFA and gases of fermentation products

The analysis of SCFAs was conducted utilizing a Shimadzu GC2010 gas chromatograph (GC) manufactured by Shimadzu Corporation in Kyoto, Japan. For the analysis of SCFAs, the supernatant was removed. Initially, 500 μL supernatant was combined with 100 μL crotonic acid / metaphosphoric acid, thoroughly mixed, and then placed in a freezer at −30°C for 24 h to complete the acidification of the samples. Samples treated with acid were subjected to centrifugation at 4°C using a speed of 10,000×g for 3 min. at 4°C. Following passage through a 0.22 μm millipore filter, an injection of 10 μL of the supernatant was made using an Agilent DB-FFAP column (0.32 mm×30 m×0.5 μm; Agilent, USA). The nitrogen flow rate as the carrier gas remained constant at 12 mL/min while the split ratio was adjusted to 8.0. The detector was supplied with hydrogen, air, and tail at flow rates of 40 mL/min, 400 mL/min, and 30 mL/min, respectively. GC was conducted using a temperature gradient that started at 80°C and increased to 190°C at a rate of 10°C per minute. After reaching 240°C at a speed of 40°C/min for 5 min, it was then kept constant for an extra 0.5 min. The FID and gasification chamber were both set to 240°C. Following a 24-h period, the fermentation vials were assessed for gas production (CO_2, CH_4, H_2, H_2S, and NH_3) using an APES-BC5-B fermentation gas analyzer manufactured by Empaer Technology Co., Ltd. (located in Shenzhen, China) and equipped with five highly responsive gas transducers.

Sequencing the gut microbiota using 16s rRNA

To remove the liquid above, the 24-h fermentation mixture was spun at a speed of 9000×g for 3 min. DNA extraction and analysis of 16S rRNA sequencing were performed on the pellet. After the completion of the experiment, the DNA samples obtained were measured using agarose gel electrophoresis and a microplate reader called Nanodrop 2000. The DNA amplification technique was used to obtain the v3-v4 region of the 16sRNA. Subsequently, PCR primers were designed to flank the v3-v4 region of the bacterial 16S rDNA, with primer 343F (5'-tacggraggcagcag-3') and primer 798R (5'-agggtatctaatcct-3') bands being utilized.

The PCR amplification conditions were as follows: initial denaturation at 94°C for 5 min, followed by seven cycles of denaturation at 94°C for 30 s, annealing at 56°C for 30 s, extension at 72°C for 20 s, another extension at 72°C for 5 min, and a final hold at 4°C. Agarose gel electrophoresis was employed to analyze the PCR products, followed by purification of the amplification products using magnetic bead purification and quantification using Qubit. Libraries were constructed using a Bioanalyzer (Aglient 2100).

The original double-ended sequence was generated by sequencing Illumina MiSeq and then de-hybridized using Trimmomatic software. The full sequence was obtained by splicing the double-ended sequence using Flash software (version 1.2.11) after complete generation. To eliminate sequences with N bases, single base repetition times >8, and insufficient length, the split_libraries (version 1.8.0) software in QIIME was employed for spliced sequences. Afterward, the UCHIME program (2.4.2 version) was employed to eliminate chimeras from the sequences, acquiring top-notch sequences for the division of Operational Taxonomic Units (OTU) in the following steps. The National Center for Biotechnology Information Short Read Archive received all human consensus sequencing data with accession no. PRJNA1003221.

Statistical analysis

Graph Pad Prism8 and IBM SPSS Statistics 25 were used to statistically analyze the experimental data, which were then presented as the mean ± SD. The data with normal distribution underwent a comparative analysis among multiple groups using the Friedman M non-parametric test, considering the Bonferroni corrected significance value for multiple tests. The results of the test for homogeneity of variance and their statistical significance were indicated by the p-value ($^{*}p < 0.05$, $^{**}p < 0.01$, $^{***}p < 0.001$). Significantly regulated metabolites of BAs between groups were determined by VIP and absolute Log_2FC (fold change). VIP values were extracted from OPLS-DA result, which also contains score plots and permutation plots, and were generated using R package MetaboAnalystR.

Using the Vsearch software (version 2.4.2), the high-quality sequences obtained were categorized into OTUs with a similarity of at least 97%. The representative sequence of each OTU was determined by selecting the most abundant sequence through the QIIME software. The OTU annotation information was obtained by comparing the representative sequences with the database using the Naive Bayesian classification algorithm of the RDP classifier. To build the phylogenetic tree, we utilized the Pynast (v0.1) program for constructing the phylogenetic relationship of representative sequences of OTUs and obtaining the resulting tree.

Results

Characteristics of BAs

Utra-performance liquid chromatography coupled with triple quadrupole mass spectrometry (UPLC–TQMS) was used to collect and analyze five fecal samples obtained from pig, cattle, and human sources. Figure 1 illustrates that the three distinct host samples exhibited variations in both the content and types of total bile acids (TBAs). Specifically, when comparing the BAs of pigs and cows, the levels of TBAs in humans, pigs, and cattle were in a ratio of 1:11:10. Previous studies have demonstrated that the TBAs of pigs and cattle are roughly 11 and 10 times greater than those of humans, respectively. The TBAs of pigs were most abundant, followed by cattle and humans. In pigs, TωMCA, TβMCA, βUDCA, βDCA, ωMCA, HCA, αMCA, βMCA, and CDCA-24Gln stood out as distinct from the BAs species found in cattle.

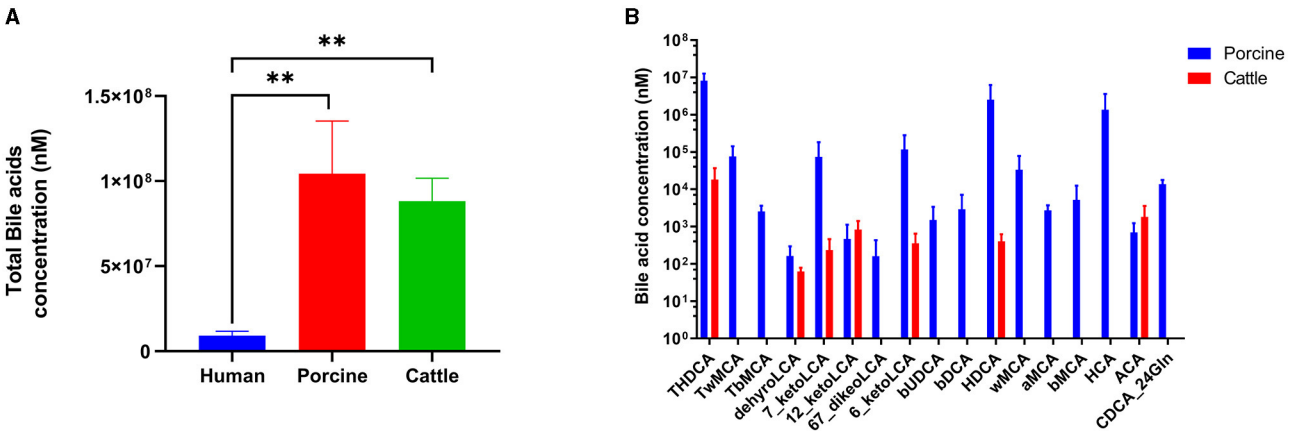

FIGURE 1
Bile acid profiles in humans, pigs, and cattle. **(A)** Content of total bile acid. **(B)** Unique bile acids in pigs and cattle. Significance was determined as $*p < 0.05$ (significant), $**p < 0.01$ (very significant) using one-way ANOVA (*Post-hoc* Dunnett's test).

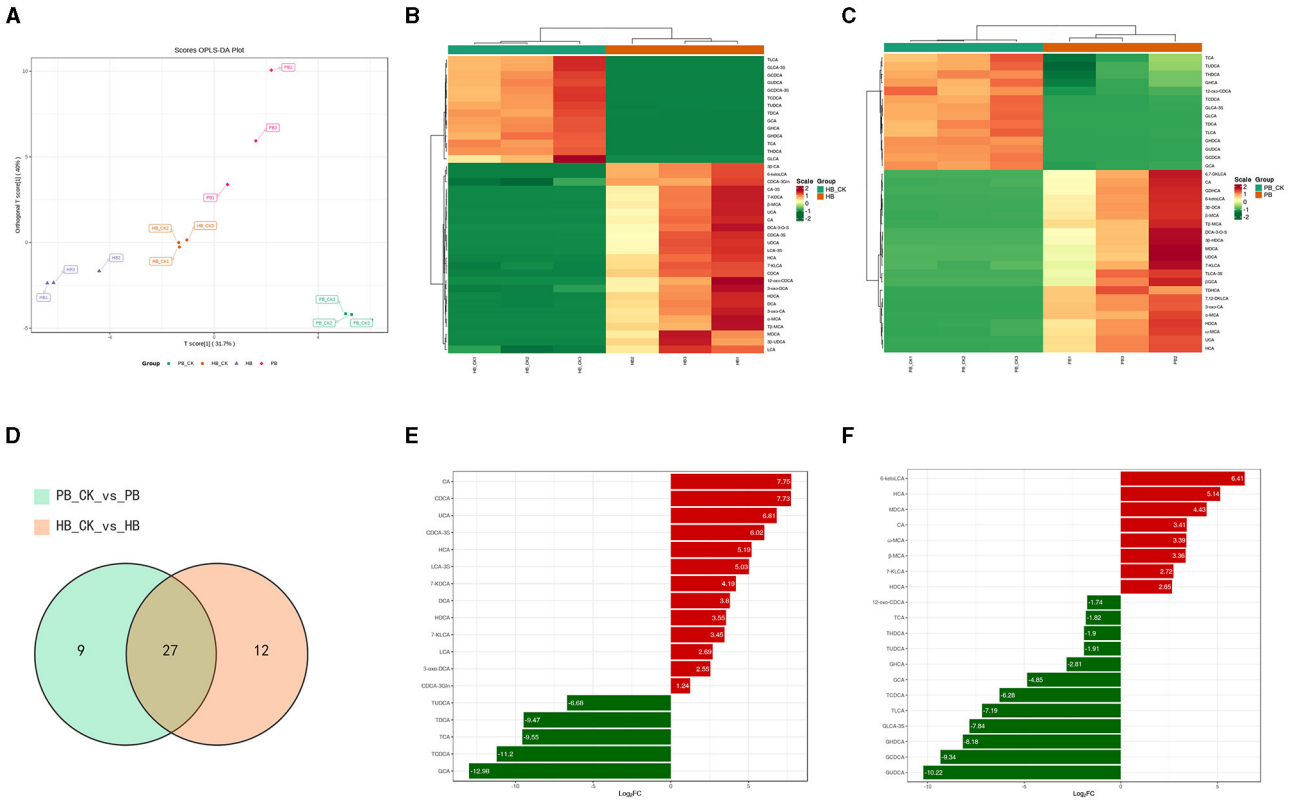

FIGURE 2
Metabolism characterization of bile acids against complex probiotics in pigs and humans. **(A)** Orthogonal partial least squares discriminant analysis (OPLS-DA) of BA in the human (HB) and pig groups (PB). **(B)** Heatmap of BAs metabolism in humans. **(C)** Heatmap of BAs metabolism in pig. The red color shows an increased expression level while the blue color displays decreased expression level. Hierarchical classification was performed to group metabolites from each group. Dendrograms show clustering between metabolites which were closely related based on their estimated Euclidean distance. **(D)** Venn diagram comparison analysis of BA metabolism in the presence of probiotics. **(E)** up-regulated BA levels in humans compared with the control group. **(F)** down-regulated BA levels in pigs compared with the control group.

Bacterial alteration of BA profiles

To explore the disparity in BA metabolism between pigs and humans, we analyzed the range of BAs in a laboratory-based fermentation model. To evaluate the level of expression, a system of color coding was used, which involved the utilization of red and blue. Red was used to indicate a higher level of expression, while blue was used to represent a lower level of expression. White

was used to signify no change. After 24 h of fermentation with probiotics, Figure 2A clearly distinguishes the metabolic variety of human BAs from that of porcine BAs. The OPLSDA model was used to assess the diversity in the metabolite composition of BA varieties. The evaluation parameters of the model, $R^2 = 0.97$ and $Q^2 = 0.939$, demonstrated the reliability and validity of the OPLSDA model. Within the porcine category, there was a notable decrease in 14 BA species and a significant increase in 22 BA species. Similarly, the human BA group experienced a significant decrease in 14 BA species and a noteworthy increase in 25 BA species. Regarding the metabolism of BAs, both of them exhibit a comparable pattern of change, where secondary BAs undergo modification through conjugation with either glycine (forming glyco-conjugated bile acids) or taurine (forming tauro-conjugated bile acids) during probiotic fermentation (as shown in Figures 2B, 2C). In Figure 2D, a total of 27 BA species were found to be present in both the metabolism of human BA and porcine BA. Among these metabolites, the concentrations of CA, HCA, and HDCA exhibited a significant increase, while the levels of GCA, TCDCA, and TUDCA showed a substantial decrease in the top 20 metabolites with the highest fold change when probiotics were present (as shown in Figures 2E, F, Supplementary Tables 1, 2). Complex probiotics Yep had varied outcomes for different derived BAs. The findings may suggest that these characteristics of probiotics possess a strong capacity to alter the metabolism of BAs, rendering them promising candidates for interventions aimed at enhancing wellbeing.

Effects of probiotics complex on SCFAs and intestinal gases

The determination involved SCFAs such as acetic acid, propionic acid, isobutyric acid, butyric acid, isovaleric acid, and valeric acid, as depicted in Figure 3. The levels of isobutyric acid ($p = 0.009$) and isovaleric acid ($p = 0.002$) in the complex probiotics Yep were notably reduced when compared to the CK group. In comparison to the CK group, the complex probiotics Yep exhibited a notable reduction in the concentration of NH_3.

Effects of probiotics complex on gut microbiota

The PCoA analysis based on the plot of the weighted unifrac distance matrix showed no apparent cluster differentiation between the CK group and the probiotics complex. On the other hand, the probiotics mixture was far apart from the rest of the groups and exhibited a greater level of variation. The data indicate that the probiotics complex caused noticeable alterations in the gut microbiota (Figure 4). After 24 h of fermentation, *Firmicutes*, *Bacteroidetes, Actinobacteria*, and *Proteobacteria* were the predominant gut microbiota in each group at the phylum level. Furthermore, there were slight alterations noticed in the proportion of *Firmicutes* and *Bacteroidetes*. Specifically, when compared to the other groups, complex probiotics Yep notably enhanced both this ratio and the ratio of *Actinobacteria* simultaneously.

At the level of genus, the probiotic mixture changed the gut microbiota and notably boosted the presence of *Bacteroides*, *Lactobacillus*, and *Bifidobacterium* genera in comparison to the control group (Figure 4). Furthermore, the complex group exhibited significantly lower levels of various opportunistic pathogens, such as *Escherichia-Shigella* and *Sutterella* genera, in comparison to the CK group.

Correlation between SCFAs and gas production

To explore the correlation between the microbiota involved in fermentation and the resulting SCFAs and gases, this study conducted a correlation analysis between the top 20 various bacterial genera with the greatest abundance and fermentation metabolites. Figure 5 displayed that various bacteria exhibited distinct associations with the production of gases and SCFAs. The amounts of isobutyric acid and isovaleric acid exhibited an inverse relationship with the genera *Lactobacillus*, *Lachnoclostridium*, and *Roseburia*, while displaying a positive correlation with the genera *Dialister*, *Megasphaera*, and *Collinsella*. Similarly, the levels of NH_3 and H_2S synthesis exhibited an inverse relationship with the *Bifidobacterium* and *Lactobacillus* species, and they displayed a positive correlation with the *Blautia* species. Conversely, *Escherichia-Shigella* showed a negative correlation with NH_3.

Discussion

Bile consists of compounds that are produced by the liver, gallbladder, and bile duct cells. These compounds can be either endogenous or exogenous, reflecting both typical and atypical metabolic processes of these organs. Studying the composition of bile can offer valuable insights into biomarkers of hepatobiliary diseases, aiding in their diagnosis and therapeutic utilization.

Research has shown that BAs have a vital function in maintaining balance in the liver, gallbladder, intestines, and aiding in the process of digestion. Moreover, the intestinal flora greatly affects the variety of bile acid collections by breaking down conjugates and removing hydroxyl groups or changing their configuration, which has important consequences for the host. As a major contributor to BAs metabolism, BSH produces secondary BAs. Of the many gut microbiota, *Lactobacilli* and *Bifidobacteria* have been most frequently studied for BSH activity.

Nevertheless, research is scarce on the correlation between BAs derived from humans and certain probiotics. The metabolism of BAs and the changes in gut microbiota were investigated in this study using an *in vitro* fermentation model and by introducing external probiotics for intervention. Typically, the *in vitro* BAs assay models solely consist of pigs, cattle, or mice, and BAs were employed to assess the resistance and tolerance of probiotic strains, disregarding the definitive host. In contrast to BAs found in pigs and cows, the composition of BAs in humans is completely different (Begley et al., 2005), whereby the concentration of total BAs in pig and cow bile is ~10 times greater than that in human bile. Moreover, selected BAs are unique in pigs compared with cattle bile, such as TβMCA, TωMCA, etc. This suggests that pig BA

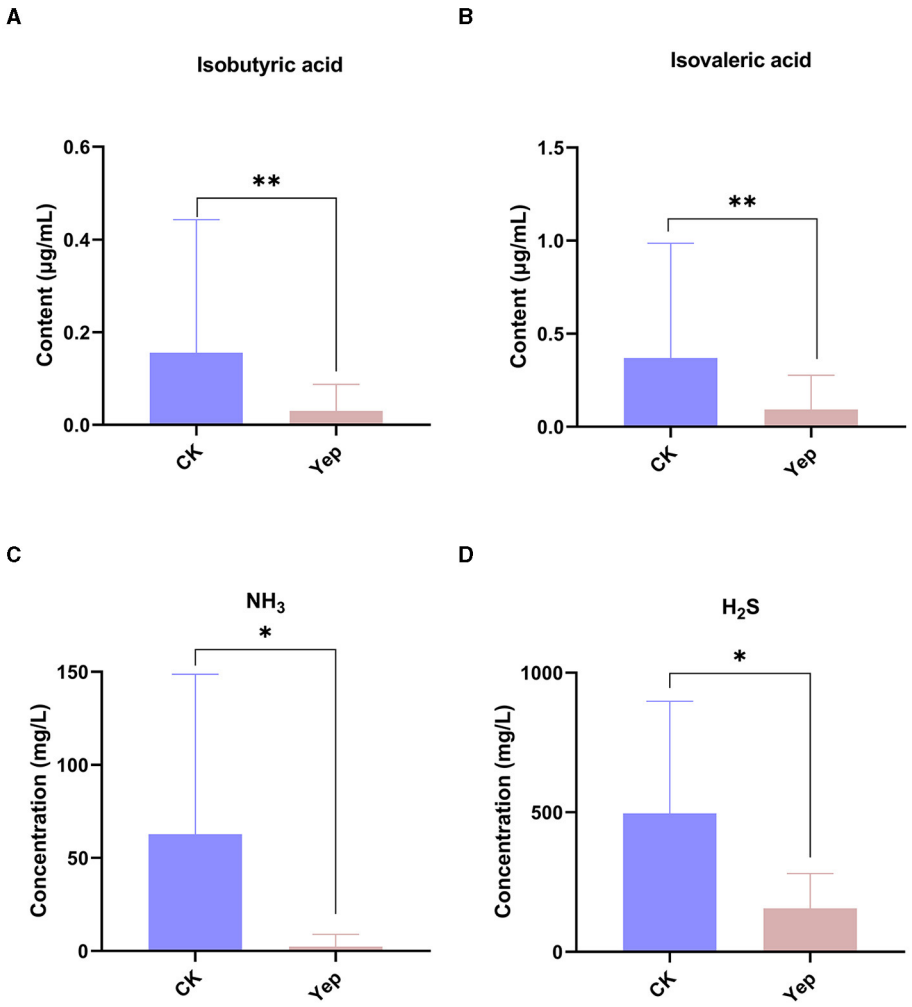

FIGURE 3
The levels of short-chain fatty acid and gases produced by gut microbiota after 24-h fermentation processes under the probiotics complexes intervention. CK represents the control group, Yep represents the probiotics complex, *$p < 0.05$, significant. **$p < 0.01$, very significant. ***$p < 0.001$, extremely significant.

models can be utilized to evaluate and forecast the efficacy of various interventions on BA metabolism, particularly in the bile of humans.

Intestinal BAs have the potential to impact the composition of the gut microbiota, subsequently exerting an influence on it. Deconjugation is the process by which the conjugated BAs, like CA and CDCA, are metabolized and ultimately converted into secondary BAs, including DCA, HDCA, HCA, or THDCA. The BA profiles underwent significant changes over time following the introduction of probiotics complex Yep. In a previous study by Bansal et al. (2020) it was found that DCA, which is a microbial metabolic byproduct obtained from secondary bile acids, effectively decreased the colonization and inflammation induced by *C. perfringens* in necrotic enteritis among chickens. Several BAs, such as chenodeoxycholic, lithocholic, and ursodeoxycholic acids, were discovered to hinder spore germination in a separate investigation (Davis et al., 2016). Furthermore, bacteria possessing BSH activity are responsible for the deconjugation of BAs. In previous studies, *Lactobacilli*, *Clostridium*, *Bacteroides*, and *Bifidobacteria* were found to possess functional BSH (Jones et al., 2008).

The regulation of BAs is governed by a wide range of nuclear and membrane receptors. Wan and Sheng (2018) identified FXR and TGR5 as the main representatives of nuclear and membrane receptors, respectively. Activation of the FXR and TGR5 receptors by CDCA, DCA, CA, and LCA regulates various host processes, such as energy metabolism, reduction of hepatic BAs burden, and alleviation of toxic cellular damage induced by BAs in cholestasis. Additionally, these receptors also influence glucose, lipids, and anti-inflammatory reactions (Gonzalez et al., 2015). Moreover, the TGR5 receptor gets activated by the LCA, DCA, TLCA, and TCDCA bile acids. According to recent research, it has been found that the TGR5 ligand reduces the production of inflammatory cytokines when exposed to lipopolysaccharides (LPS) (Hogenauer et al., 2014). The HCA types serve as new indicators for metabolic disorders and enhance the regulation of glucose balance by means of a unique TGR5 and FXR communication pathway, resulting in potential benefits for diabetes prevention (Zheng et al., 2021). It was reported that the control of THDCA levels has been found to regulate rheumatoid arthritis in a persistent cold climate (Liu et al., 2023). Inhibiting the PPARα nucleus cytoplasm pathway, the

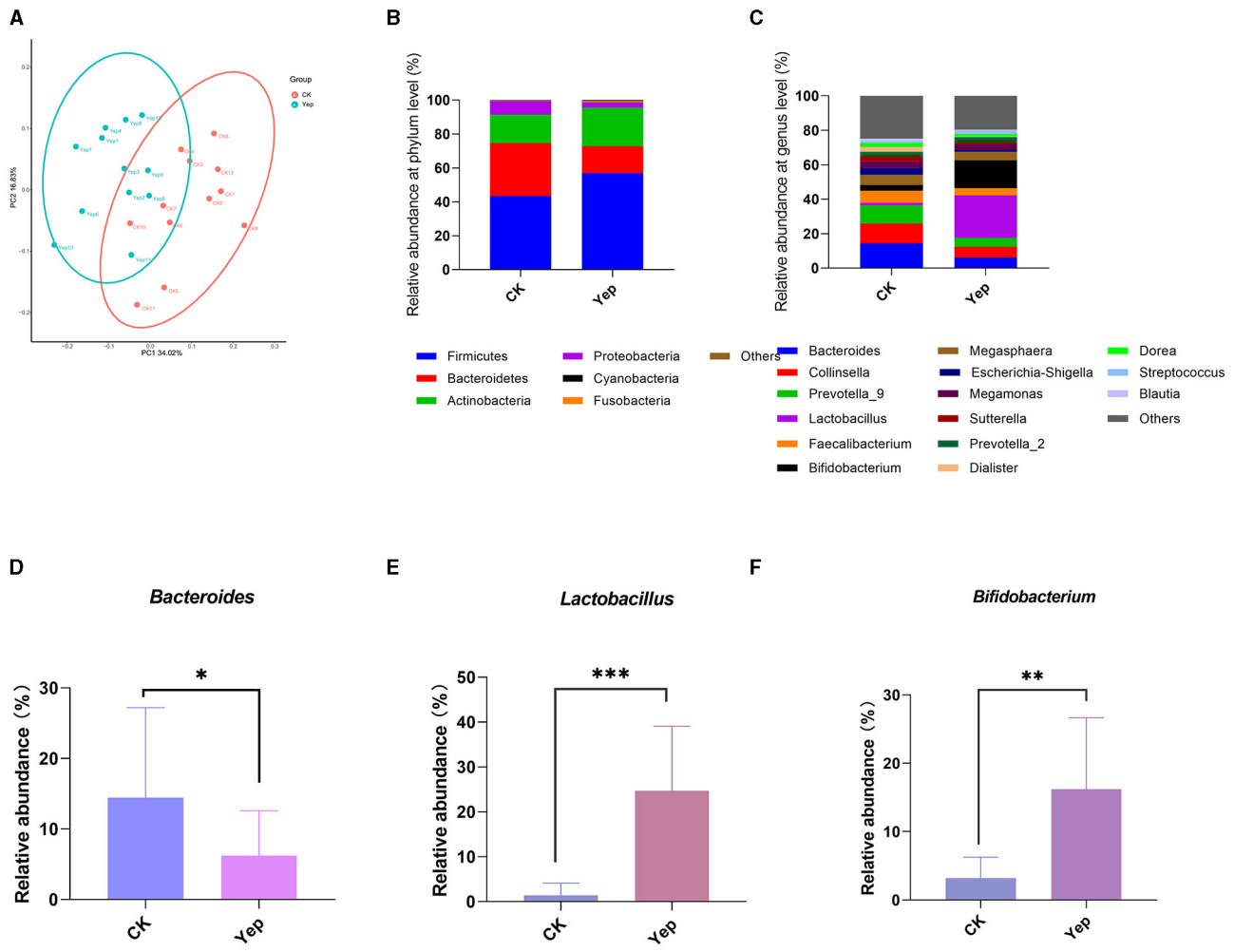

FIGURE 4
Effect of complex probiotics on gut microbiota in humans. **(A)** PCoA analysis based on weighted unifrac distances. **(B)** The profiles of human gut microbiota on phylum level after the probiotics complex intervention. **(C)** The profiles of human gut microbiota on genus level after the probiotics complex intervention. **(D–F)** Relative abundance of *Bacteroides*, *Lactobacillus*, and *Bifidobacterium* in different groups. Compared between the CK and Yep group; significance was determined as $*p < 0.05$ (significant), $**p < 0.01$ (very significant) using Student's t-test.

diet supplemented with HDCA was separately analyzed and found to improve non-alcoholic fatty liver disease (Kuang et al., 2023). Consistent with this observation, we noticed a significant increase in the levels of CDCA, DCA, CA, and HCA in this study when the probiotics complex Yep was administered.

Bile acids (BAs), suggested as a possible indicator of liver damage, have been under consideration for many years. Elevated concentrations of linked BAs in cirrhosis or chronic hepatitis may serve as useful markers of liver impairment for hepatocellular carcinoma in individuals with liver cirrhosis. Elevated serum levels of TCDCA, TUDCA, GCA, TCA, and GCDCA were found in women suffering from severe intrahepatic cholestasis of pregnancy, as indicated by a study (Ovadia et al., 2019). The presence of alterations in BAs is closely connected to the pathological changes that occur during the advancement of cirrhosis. The findings of this research were indistinguishable from those of another study (Liu et al., 2019a). Individuals diagnosed with early cirrhosis showed a significant rise in the levels of overall BAs, such as GCA, GCDCA, TCA, TCDCA, and TUDCA, compared to those diagnosed with chronic hepatitis. Furthermore, these increased levels were discovered to have a strong correlation with the identification of cirrhosis. Moreover, these elevated concentrations were found to be closely linked to the diagnosis of cirrhosis. There were notable associations between the fibrosis stages and TCDCA, GCDCA, GCA, and TCA, indicating positive correlations. Higher concentrations of GCDCA, TCDCA, GCA, and TCA exhibited a positive correlation with the advancement of alcoholic liver disease in individuals (Sugita et al., 2015). Additionally, it was hypothesized that GCDCA, GCA, and GUDCA could serve as more reliable indicators of abstaining from alcohol (Wang et al., 2020). The patients with alcoholic cirrhosis showed a significant rise in the levels of conjugated primary bile acid metabolites (GCDCA, TCDCA, GCA, TCA) compared to secondary bile acid metabolites (except for glycohyocholate), indicating a correlation between disease severity and the progressive increase of these subsets. Furthermore, mice that were consistently fed a high-fat diet

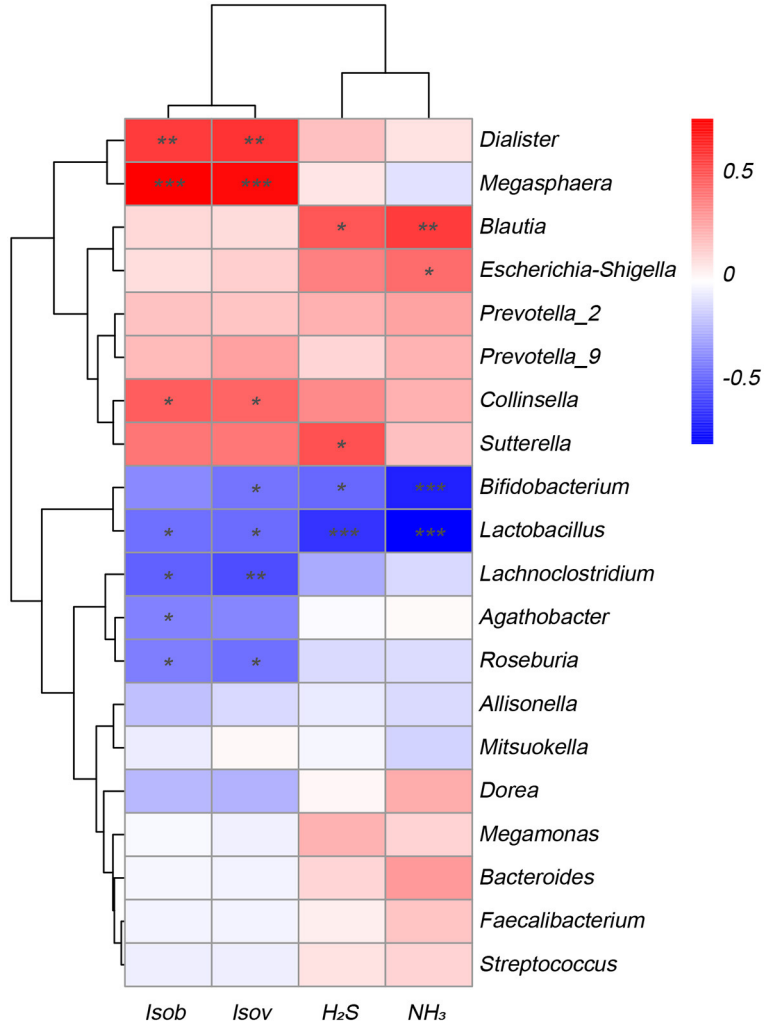

FIGURE 5
Correlation analysis of fecal microbiota at the genus level with metabolites SCFAs and gases in the Yep-treated samples. Isob, isobutyric acid; Isov, isovaleric acid; The correlation heatmap was measured using the Spearman correlation coefficient. *$0.01 < p \leq 0.05$; **$0.001 < p \leq 0.01$; ***$p \leq 0.001$.

(HFD) also exhibited the spontaneous formation of liver tumors, accompanied by a notable rise in levels of bile acids within the liver. The probiotics complex intervention in humans resulted in a significant decrease in the levels of TUDCA, TDCA, TCA, TCDCA, and GCA, which was quite fascinating. The BAs metabolism is believed to be improved by the physiological activities of the probiotics complex Yep, which are considered beneficial for human health in this study.

In the present study, the administration of the probiotics complex decreased isobutyric acid and isovaleric acid levels. These branched short-chain fatty acids are derived from the degradation of amino acids valine, leucine, or isoleucine and have been shown to enhance insulin-stimulated glucose uptake and improve insulin sensitivity (Qu et al., 2017). Consequently, the findings potentially imply a transition from a carbohydrate-based to a protein-based fermentation milieu, thereby indicating alterations in the microbial composition (Liu et al., 2019b). In addition, the isobutyric acid and isovaleric acid levels were correlated negatively with *Lactobacillus*, *Lachnoclostridium*, and *Roseburia*, while correlated positively with *Dialister, Megasphaera,* and *Collinsella*. Similarly, the concentrations of H_2S and NH_3 exhibited a reduction after fermentation, indicating that the probiotics complex exerts a modulatory influence on gut microbiota, resulting in a decrease in the abundance of detrimental bacteria associated with gas production. Importantly, a negative association was found between H_2S and NH_3 and the genera *Bifidobacterium* and *Lactobacillus*, while a positive association was observed with the genus *Blautia*, which has been linked to inflammation (Maeda and Takeda, 2017).

A symbiotic gut microbiota consists of numerous bacteria and metabolites expressed by bacteria and the host, and they can regulate the microecological balance of the intestinal tract, protect intestinal mucosa, and decrease inflammation while enhancing the metabolism of lipids. Compared with the discoveries in existing literature, there are some novelties in our study. This study represents the first attempt to compare the variations in BAs between human, pig, and cattle species. Additionally, comparison

studies *in vitro* on BAs and multi-species probiotics in humans and pigs have never been investigated. However, it is imperative to recognize that the existing research is still in its nascent phases and poses numerous unresolved enigmas and obstacles. In our study, only two independent assessments to determine the effects of the probiotics complex on BAs and gut microbiota were conducted, we didn't account for the potential impact of the simultaneous presence of both factors on microbial metabolism, which serves as a limitation of our study. To enhance comprehension of the probiotics' mechanism of action, further inquiries are imperative, encompassing supplementary clinical trials, identification of bioactive constituents, and optimization studies to treatment dosages and durations. Moreover, comprehensive evaluations of the interactions and safety of BAs and probiotics are also indispensable to provide additional avenues and alternatives for the treatment of liver ailments.

Conclusion

The current research found that the complex probiotics Yep had an impact on the microbiota in the human gut. It led to an increase in the prevalence of *Bacteroides*, *Lactobacillus*, and *Bifidobacterium*, while reducing the prevalence of the opportunistic pathogens *Escherichia-Shigella* and *Sutterella*. At the same time, the intricate probiotics regulated the metabolism of BAs and intestinal gases. The present findings indicate the possibility of using probiotic intervention to enhance gut microbiota and support gastrointestinal wellbeing.

Data availability statement

The datasets presented in this study can be found in online repositories. The names of the repository/repositories and accession number(s) can be found at: https://www.ncbi.nlm.nih.gov/, PRJNA1003221.

Ethics statement

Ethical approval was attained by the ethics committee of the First Affiliated Hospital of Nanjing Medical University (2024-SR-037). Ethical approval was not required for the studies involving animals in accordance with the local legislation and institutional requirements because The bile acids from porcine and cattle were commercially available and used as purchased. Written informed consent was obtained from the owners for the participation of their animals in this study.

Author contributions

WL: Writing—original draft, Writing—review & editing, Conceptualization, Funding acquisition. ZL: Writing—original draft, Writing— review & editing, Conceptualization. XZ: Writing—review & editing, Formal analysis. CD: Writing—review & editing, Formal analysis. SX: Writing—review & editing, Formal analysis. FY: Writing—review & editing, Supervision, Conceptualization, Formal analysis, Resources.

Funding

The author(s) declare financial support was received for the research, authorship, and/or publication of this article. The study received funding from the BYHEALTH Nutrition and Health Research Foundation (no. TY0191106).

Conflict of interest

The authors declare that the research was conducted in the absence of any commercial or financial relationships that could be construed as a potential conflict of interest.

Publisher's note

Supplementary material

The Supplementary Material for this article can be found online at: https://www.frontiersin.org/articles/10.3389/fmicb.2024.1314528/full#supplementary-material

References

Baker, R. G., Hayden, M. S., and Ghosh, S. (2011). NF-kappaB, inflammation, and metabolic disease. *Cell Metab.* 13, 11–22. doi: 10.1016/j.cmet.2010.12.008

Bansal, M., Fu, Y., Alrubaye, B., Abraha, M., Almansour, A., Gupta, A., et al. (2020). A secondary bile acid from microbiota metabolism attenuates ileitis and bile acid reduction in subclinical necrotic enteritis in chickens. *J. Anim. Sci. Biotechnol.* 11, 37. doi: 10.1186/s40104-020-00441-6

Begley, M., Gahan, C. G., and Hill, C. (2005). The interaction between bacteria and bile. *FEMS Microbiol. Rev.* 29, 625–651. doi: 10.1016/j.femsre.2004.09.003

Davis, M. Y., Zhang, H., Brannan, L. E., Carman, R. J., and Boone, J. H. (2016). Rapid change of fecal microbiome and disappearance of Clostridium difficile in a colonized infant after transition from breast milk to cow milk. *Microbiome* 4, 53. doi: 10.1186/s40168-016-0198-6

De Aguiar, V., Tarling, T. Q. E. J., and Edwards, P. A. (2013). Pleiotropic roles of bile acids in metabolism. *Cell Metab.* 17, 657–669. doi: 10.1016/j.cmet.2013.03.013

Degirolamo, C., Rainaldi, S., Bovenga, F., Murzilli, S., and Moschetta, A. (2014). Microbiota modification with probiotics induces hepatic bile acid synthesis via downregulation of the Fxr-Fgf15 axis in mice. *Cell Rep.* 7, 12–18. doi: 10.1016/j.celrep.2014.02.032

Fukiya, S., Arata, M., Kawashima, H., Yoshida, D., Kaneko, M., Minamida, K., et al. (2009). Conversion of cholic acid and chenodeoxycholic acid into their 7-oxo derivatives by Bacteroides intestinalis AM-1 isolated from human feces. *FEMS Microbiol. Lett.* 293, 263–270. doi: 10.1111/j.1574-6968.2009.01531.x

Gonzalez, F. J., Jiang, C., Bisson, W. H., and Patterson, A. D. (2015). Inhibition of farnesoid X receptor signaling shows beneficial effects in human obesity. *J. Hepatol.* 62, 1234–1236. doi: 10.1016/j.jhep.2015.02.043

Hogenauer, K., Arista, L., Schmiedeberg, N., Werner, G., Jaksche, H., Bouhelal, R., et al. (2014). G-protein-coupled bile acid receptor 1 (GPBAR1, TGR5) agonists reduce the production of proinflammatory cytokines and stabilize the alternative macrophage phenotype. *J. Med. Chem.* 57, 10343–10354. doi: 10.1021/jm501052c

Hou, G., Peng, W., Wei, L., Li, R., Yuan, Y., Huang, X., et al. (2020). *Lactobacillus delbrueckii* interfere with bile acid enterohepatic circulation to regulate cholesterol metabolism of growing-finishing pigs via its bile salt hydrolase activity. *Front. Nutr.* 7, 617676. doi: 10.3389/fnut.2020.617676

Jones, B. V., Begley, M., Hill, C., Gahan, C. G., and Marchesi, J. R. (2008). Functional and comparative metagenomic analysis of bile salt hydrolase activity in the human gut microbiome. *Proc. Natl. Acad. Sci. U. S. A.* 105, 13580–13585. doi: 10.1073/pnas.0804437105

Kuang, J., Wang, J., Li, Y., Li, M., Zhao, M., Ge, K., et al. (2023). Hyodeoxycholic acid alleviates non-alcoholic fatty liver disease through modulating the gut-liver axis. *Cell Metab.* 18, 11. doi: 10.1016/j.cmet.2023.07.011

Li, D., Wang, P., Wang, P., Hu, X., and Chen, F. (2019). Targeting the gut microbiota by dietary nutrients: a new avenue for human health. *Crit. Rev. Food Sci. Nutr.* 59, 181–195. doi: 10.1080/10408398.2017.1363708

Li, S., Ung, T. T., Nguyen, T. T., Sah, D. K., Park, S. Y., Jung, Y. D., et al. (2020). Cholic acid stimulates MMP-9 in human colon cancer cells via activation of MAPK, AP-1, and NF-kappaB activity. *Int. J. Mol. Sci.* 21, 420. doi: 10.3390/ijms21103420

Liu, J., Peng, F., Cheng, H., Zhang, D., Zhang, Y., Wang, L., et al. (2023). Chronic cold environment regulates rheumatoid arthritis through modulation of gut microbiota-derived bile acids. *Sci. Total Environ.* 903, 166837. doi: 10.1016/j.scitotenv.2023.166837

Liu, N., Feng, J., Lv, Y., Liu, Q., Deng, J., Xia, Y., et al. (2019a). Role of bile acids in the diagnosis and progression of liver cirrhosis: a prospective observational study. *Exp. Ther. Med.* 18, 4058–4066. doi: 10.3892/etm.2019.8011

Liu, W., Li, X., Zhao, Z., Pi, X., Meng, Y., Fei, D., et al. (2020a). Effect of chitooligosaccharides on human gut microbiota and antiglycation. *Carbohydr. Polym.* 242, 116413. doi: 10.1016/j.carbpol.2020.116413

Liu, W., Zhou, Y., Qin, Y., Li, Y., Yu, L., Li, R., et al. (2019b). Sex-dependent effects of PM(2.5.) maternal exposure and quercetin intervention on offspring's short chain fatty acids. *Int J. Environ. Res. Pub. Health* 16, 371. doi: 10.3390/ijerph16224371

Liu, Y., Chen, K., Li, F., Gu, Z., Liu, Q., He, L., et al. (2020b). Probiotic *Lactobacillus rhamnosus* GG prevents liver fibrosis through inhibiting hepatic bile acid synthesis and enhancing bile acid excretion in mice. *Hepatology* 71, 2050–2066. doi: 10.1002/hep.30975

Maeda, Y., and Takeda, K. (2017). Role of gut microbiota in rheumatoid arthritis. *J. Clin. Med.* 6, 60. doi: 10.3390/jcm6060060

Marion, S., Studer, N., Desharnais, L., Menin, L., Escrig, S., Meibom, A., et al. (2019). *In vitro* and *in vivo* characterization of *Clostridium scindens* bile acid transformations. *Gut Microbes* 10, 481–503. doi: 10.1080/19490976.2018.1549420

Ovadia, C., Seed, P. T., Sklavounos, A., Geenes, V., Ilio, D. i., Chambers, C., et al. (2019). Association of adverse perinatal outcomes of intrahepatic cholestasis of pregnancy with biochemical markers: results of aggregate and individual patient data meta-analyses. *Lancet* 393, 899–909. doi: 10.1016/S0140-6736(18)31877-4

Puri, P., Daita, K., Joyce, A., Mirshahi, F., Santhekadur, P. K., Cazanave, S., et al. (2018). The presence and severity of nonalcoholic steatohepatitis is associated with specific changes in circulating bile acids. *Hepatology* 67, 534–548. doi: 10.1002/hep.29359

Qu, W., Yuan, X., Zhao, J., Zhang, Y., Hu, J., Wang, J., et al. (2017). Dietary advanced glycation end products modify gut microbial composition and partially increase colon permeability in rats. *Mol. Nutr. Food Res.* 61, 118. doi: 10.1002/mnfr.201700118

Singh, J., Metrani, R., Shivanagoudra, S. R., Jayaprakasha, G. K., and Patil, B. S. (2019). Review on bile acids: effects of the gut microbiome, interactions with dietary fiber, and alterations in the bioaccessibility of bioactive compounds. *J. Agric. Food Chem.* 67, 9124–9138. doi: 10.1021/acs.jafc.8b07306

Sugita, T., Amano, K., Nakano, M., Masubuchi, N., Sugihara, M., Matsuura, T., et al. (2015). Analysis of the serum bile acid composition for differential diagnosis in patients with liver disease. *Gastroenterol. Res. Pract.* 2015, 717431. doi: 10.1155/2015/717431

Tian, Y., Gui, W., Koo, I., Smith, P. B., Allman, E. L., Nichols, R. G., et al. (2020). The microbiome modulating activity of bile acids. *Gut Microbes* 11, 979–996. doi: 10.1080/19490976.2020.1732268

Tidjani Alou, M., Naud, S., Khelaifia, S., Bonnet, M., Lagier, J. C., Raoult, D., et al. (2020). State of the art in the culture of the human microbiota: new interests and strategies. *Clin. Microbiol. Rev.* 34, 1–19. doi: 10.1128/CMR.00129-19

Trauner, M., and Boyer, J. L. (2003). Bile salt transporters: molecular characterization, function, and regulation. *Physiol Rev* 83, 633–671. doi: 10.1152/physrev.00027.2002

Wan, Y. Y., and Sheng, L. (2018). Regulation of bile acid receptor activity(?). *Liver Res.* 2, 180–185. doi: 10.1016/j.livres.2018.09.008

Wang, X., Chen, L., Wang, H., Cai, W., and Xie, Q. (2020). Modulation of bile acid profile by gut microbiota in chronic hepatitis B. *J. Cell Mol. Med.* 24, 2573–2581. doi: 10.1111/jcmm.14951

Zheng, X., Chen, T., Zhao, A., Ning, Z., Kuang, J., Wang, S., et al. (2021). Hyocholic acid species as novel biomarkers for metabolic disorders. *Nat. Commun.* 12, 1487. doi: 10.1038/s41467-021-21744-w

Zhou, H., and Hylemon, P. B. (2014). Bile acids are nutrient signaling hormones. *Steroids* 86, 62–68. doi: 10.1016/j.steroids.2014.04.016

frontiers | Frontiers in Microbiology

TYPE Original Research
PUBLISHED 26 March 2024
DOI 10.3389/fmicb.2024.1352586

OPEN ACCESS

EDITED BY
Ganji Purnachandra Nagaraju,
University of Alabama at Birmingham,
United States

REVIEWED BY
Seema Kumari,
Gandhi Institute of Technology and Management (GITAM), India
Suresh Chava,
University of Alabama at Birmingham,
United States

*CORRESPONDENCE
Jiali Liu
✉ liujiali006@163.com
Sheng Cui
✉ cuisheng@yzu.edu.cn

RECEIVED 08 December 2023
ACCEPTED 28 February 2024
PUBLISHED 26 March 2024

CITATION
Zheng J, Zhou Y, Zhang D, Ma K, Gong Y, Luo X, Liu J and Cui S (2024) Intestinal melatonin levels and gut microbiota homeostasis are independent of the pineal gland in pigs. *Front. Microbiol.* 15:1352586. doi: 10.3389/fmicb.2024.1352586

Intestinal melatonin levels and gut microbiota homeostasis are independent of the pineal gland in pigs

Jiaming Zheng[1,2], Yewen Zhou[1,2], Di Zhang[1,2], Kezhe Ma[1,2], Yuneng Gong[1,2], Xuan Luo[3], Jiali Liu[3]* and Sheng Cui[1,2,4]*

[1]College of Veterinary Medicine, Yangzhou University, Yangzhou, China, [2]Jiangsu Co-Innovation Center for Prevention and Control of Important Animal Infectious Diseases and Zoonoses, Yangzhou University, Yangzhou, China, [3]State Key Laboratory of Animal Biotech Breeding, College of Biological Sciences, China Agricultural University, Beijing, China, [4]Institute of Reproduction and Metabolism, Yangzhou University, Yangzhou, China

Introduction: Melatonin (MEL) is a crucial neuroendocrine hormone primarily produced by the pineal gland. Pinealectomy (PINX) has been performed on an endogenous MEL deficiency model to investigate the functions of pineal MEL and its relationship with various diseases. However, the effect of PINX on the gastrointestinal tract (GIT) MEL levels and gut microbiome in pigs has not been previously reported.

Methods: By using a newly established pig PINX model, we detected the levels of MEL in the GIT by liquid chromatography–tandem mass spectrometry. In addition, we examined the effects of PINX on the expression of MEL synthesis enzymes, intestinal histomorphology, and the intestinal barrier. Furthermore, 16S rRNA sequencing was performed to analyze the colonic microbiome.

Results: PINX reduced serum MEL levels but did not affect GIT MEL levels. Conversely, MEL supplementation increased MEL levels in the GIT and intestinal contents. Neither PINX nor MEL supplementation had any effect on weight gain, organ coefficient, serum biochemical indexes, or MEL synthetase arylalkylamine N-acetyltransferase (AANAT) expression in the duodenum, ileum, and colon. Furthermore, no significant differences were observed in the intestinal morphology or intestinal mucosal barrier function due to the treatments. Additionally, 16S rRNA sequencing revealed that PINX had no significant impact on the composition of the intestinal microbiota. Nevertheless, MEL supplementation decreased the abundance of Fibrobacterota and increased the abundance of Actinobacteriota, Desulfobacterota, and Chloroflexi.

Conclusion: We demonstrated that synthesis of MEL in the GIT is independent of the pineal gland. PINX had no influence on intestinal MEL level and microbiota composition in pigs, while exogenous MEL alters the structure of the gut microbiota.

KEYWORDS

pig, pinealectomy, melatonin, intestine, gut microbiota

1 Introduction

Melatonin (MEL), a crucial neurohormone derived from tryptophan, is mainly synthesized by the pineal gland during the dark phase of the light/dark cycles (Claustrat and Leston, 2015; Yin et al., 2020). Synthesis of extra-pineal MEL was reported in the retina (Wiechmann and Sherry, 2013), skin (Rusanova et al., 2019), Harderian gland (Santillo et al., 2020), and, importantly, the gastrointestinal tract (GIT) (Bubenik, 2002; Pan et al., 2021). MEL is synthesized in the enterochromaffin cells of the GIT (Huether, 1993; Kvetnoy et al., 2002), and it is known that the GIT contains approximately 400 times more MEL than the pineal gland (Bubenik, 2002; Chen et al., 2011). Therefore, MEL is not only important in regulating the circadian rhythm but is also involved in regulating multiple gastrointestinal functions, such as intestinal motility (De Filippis et al., 2008), barrier permeability (Sommansson et al., 2013; Swanson et al., 2015), energy expenditure (Prezotto et al., 2014; Xu et al., 2022), and bicarbonate secretion (Sommansson et al., 2013, 2014). In addition, it was reported that MEL deficiency is closely associated with the development of intestinal diseases (Gong et al., 2022; Xia et al., 2022). Furthermore, MEL improved sleep deprivation-induced intestinal mucosal injury by altering the composition of the gut microbiota (Gao et al., 2019, 2021). More importantly, clinical studies show that sleep disturbances increase disease activity in patients with gastrointestinal disorders (Sochal et al., 2020), indicating an association between MEL deficiency and gastrointestinal diseases.

Gut microbiota is crucial for the homeostatic maintenance of gastrointestinal function. Studies have demonstrated that MEL could influence the swarming and motility of *Enterobacter aerogenes* (Paulose et al., 2016). Moreover, in high-fat diet-fed mice, MEL has been proven to prevent obesity and obesity-related disorders by modulating the diversity and composition of gut microbiota, including *Firmicutes*, *Bacteroides*, and *Akkermansia* (Xu P. et al., 2017). Although it is clear from these studies that administration of exogenous MEL affects the gut microbiota, it is unclear whether deficiency of endogenous MEL affects intestinal barrier integrity and gut microbiota dysbiosis. Previous research has reported that some MEL in the intestine may originate from the pineal gland through circulation, especially at nighttime (Huether et al., 1998). On the contrary, other research studies have shown that MEL is locally synthesized in the intestine and is independent of the pineal gland since PINX has no influence on its concentration (Huether, 1993; Bubenik and Brown, 1997; Kvetnoy et al., 2002). Thus, it is necessary and meaningful to understand the effect of PINX and MEL supplementation on intestinal MEL levels and gut microbiota.

PINX was performed on an endogenous MEL deficiency model to evaluate the regulation of circadian rhythms in the pineal gland (de Farias et al., 2015; Tchekalarova et al., 2020), immunity (Sahin et al., 2018; Luo et al., 2020), Alzheimer's disease (Tzoneva et al., 2021), and inflammation and oxidative stress (Ballur et al., 2022). However, most of these studies were performed on rodents (Al Gburi et al., 2022; Demir et al., 2022), so it is difficult to use the findings of these studies to explain various MEL deficiency disorders in humans because nocturnal rodents and diurnal humans have different circadian rhythms in terms of behavior and physiology (Cheung et al., 2005; Slawik et al., 2016). Pigs are highly similar to humans in terms of physiological anatomy, nutritional metabolism, cardiovascular system structure, and immune response, making them one of the ideal experimental animal models for the study of human diseases (Walters et al., 2017; Pabst, 2020). Previously, PINX was found to promote small intestine crypt cell proliferation in rats (Callaghan, 1991). However, to date, no experimental studies have been conducted on pigs to assess the impact of PINX on intestinal function and gut microbiota.

In this study, we used a newly established pig PINX model to evaluate the effects of pineal and exogenous MEL on growth performance, biochemical parameters, GIT MEL levels, intestinal mucosal barrier function, and subsequent gut microbiome composition. These findings demonstrate that MEL synthesis in the GIT is independent of the pineal gland in pigs. Exogenous MEL, not pineal MEL, affects the gut microbiota.

2 Materials and methods

2.1 Reagents and antibodies

Antibodies against arylalkylamine N-acetyltransferase (AANAT) (ab108508) and GAPDH (ab15580) were purchased from Abcam (Cambridge, UK). ZO-1 (TA5145) and claudin-1 (T56872) were purchased from Abmart (Shanghai, China). MEL and formic acid were purchased from Macklin Biochemical Co., Ltd. (Shanghai, China). Methanol was purchased from Sigma (St. Louis, MO, USA).

2.2 Animals

A total of 18 male Bama pigs (5–6 months old), with an initial body weight of approximately 18–20 kg, were obtained from Beijing Farm Animal Research Center, Beijing, China. They were housed in the SPF lab of Yangzhou University, with a temperature of 24 ± 2°C and humidity of 60 ± 5%, under a 12-h light–dark cycle. The animals were fed with standard diet at 8:00 a.m., 12:00 p.m., and 18:00 p.m. based on their weight, with *ad libitum* access to drinking water. Experiments were approved by the Animal Ethics Association of Yangzhou University (approval ID: SYXK (Su) 2022-0044).

2.3 Experimental design and treatment with MEL

Eighteen pigs were divided on average into three groups: sham–pinealectomy group (Control), pinealectomy group (PINX), and pinealectomy + melatonin supplementation group (PINX+MEL). A total of 12 pigs underwent stereotaxic surgery with the removal of the pineal gland, and other six pigs received the same procedure without the removal of the pineal gland. Two weeks after the PINX operation, PINX pigs were randomly divided into two groups: the PINX group receiving equal amounts of ethanol and the PINX+MEL group receiving 10 mg/kg of body weight MEL daily at 18:00 pm in drinking water for 4 months, according to the earlier

literature (Agil et al., 2011). The MEL was dissolved in ethanol and further diluted in 2,000 mL water. The body weights were monitored every 2 weeks.

2.4 Surgery procedure

The surgical procedure of PINX on pigs has recently been established in our laboratory by applying a parieto-occipital approach (unpublished data) (Dempsey et al., 1982; Egermann et al., 2011). First, a near circular-shaped incision was made above the parietal bone by using a circular drill and an angled rongeur. The bone flap was delicately removed to expose the dura mater, which was then opened to expose the bilateral parietal lobes. The parieto-occipital lobes were retracted bilaterally by using a brain retractor. Dissection was performed down to the pineal recess, and the pineal gland was then observed medial to the internal cerebral veins. The pineal gland was grasped with delicate forceps and removed in one motion. Successful removal of the pineal gland was confirmed by autopsy and a decrease in serum MEL levels.

2.5 Collection of samples

Four months after surgery, the animals were euthanized by the carotid artery bleeding under anesthesia with 2% pentobarbital sodium (0.5 mL/kg) at 20:00 p.m. After laparotomy, the brain, heart, liver, spleen, lung, kidney, and testis were excised and weighted. The middle part of the GIT from the stomach to the rectum and samples of the digesta from six intestinal segments were collected as previously described (Zhang et al., 2022). After washing with phosphate-buffered saline, one part of the GIT was fixed with 4% paraformaldehyde and the other was frozen in liquid nitrogen. The relative organ weight was calculated according to the formula (Xia et al., 2022): relative organ weight: organ weight/body weight × 100.

2.6 Serum lipid indexes

Blood samples were collected from the anterior vena cava after 12 h of fasting, and serum was separated by centrifuging at 3,500 rpm according to previous literature (Xia et al., 2022). An automatic biochemistry analyzer (C16000; Abbott Architect, IL, USA) was used to test alanine aminotransferase (ALT), aspartate aminotransferase (AST), total cholesterol (TC), triglyceride (TG), high-density lipoprotein (HDL-C), and low-density lipoprotein (LDL-C) levels.

2.7 Hematoxylin and eosin (H&E) staining

The duodenum and ileum were dehydrated in gradient alcohol series, cleared in xylene, and then processed into paraffin sections. Paraffin blocks of 7 mm were cut and stained with H&E. The sections were analyzed by using a light microscope (IX71; Olympus, Tokyo, Japan). Villus length and crypt depth were measured according to previous literature (Ren et al., 2018).

TABLE 1 Elution programs of MEL analysis.

Time (min)	Flow rate (mL/min)	%A	%B
Initial	0.6	60	40
0.8	0.6	60	40
2.0	0.6	20	80
4.0	0.6	20	80
4.5	0.6	60	40
5.5	0.6	60	40

2.8 MEL analysis

A volume of 300 μL of serum was suspended in 1 mL ethyl acetate, vortexed fully for 3 min, and ultrasonicated for 1 min to extract the MEL. For intestine and intestinal contents, 0.1 g of samples was ground to a fine powder with liquid nitrogen and suspended in ethyl acetate. After centrifuging at 12,000 g for 15 min under 4°C, the supernatants were collected and dried using nitrogen gas. Furthermore, the samples were redissolved in 150 μL mobile phase (0.1% formic acid–methanol = 65: 35, v/v), vortexed, and centrifuged. After filtration with a 0.22-um filter, the supernatants were transferred to an autosampler vial. LC-MS/MS was performed according to the method described by Magliocco et al. (2021). Briefly, samples were analyzed by an ExionLC high-performance liquid chromatography (HPLC) system coupled to a 6500 QTRAP mass spectrometer (ABI Sciex, Foster City, CA, USA). An Agilent ZORBAX Eclipse Plus C18 column (4.6 mm x 100 mm, 3.5 um particle size) (Agilent Technologies, Santa Clara, CA, USA) was used with a temperature of 40°C. The mobile phase was water with 0.1% formic acid (A) and methanol with 0.1% formic acid (B). The elution programs are detailed in Table 1. The ion spray voltage was 5.5 kV in the ESI mode. Quantitation was performed in the positive ionization mode by multiple reaction monitoring at *m/z* 233.1/174.0.

2.9 Western blotting

Western blotting was performed as described in previous literature (Zhang et al., 2018). First, the sample was electrophoresed using 12% SDS-PAGE gel and transferred to the PVDF membrane. After blocking with 5% skim milk, the membrane was incubated with AANAT, ZO-1, claudin-1, and GAPDH at 4°C overnight. After washing with TBST, they were incubated with the secondary antibody for 2 h at room temperature. The protein bands were detected with electrochemiluminescence (Vazyme Biotech, Nanjing, China). Band intensities were quantified by using ImageJ software.

2.10 Gut microbiota analysis

Fresh colonic contents (~200 mg of each sample) were collected from each animal at the same time. Bacterial genomic DNA was extracted from samples using the Power Fecal® DNA Isolation Kit (MoBio Carlsbad, CA USA). The V3–V4 regions of the 16S rRNA gene were amplified using primers 341F and 806R (5′-CCTAYGGGRBGCASCAG-3′ and 5′-GGACTACNNGGGTATCTAAT-3′), respectively. The Illumina NovaSeq platform was used to generate 250-bp paired-end reads. The sequencing was performed on the QIIME2 platform of Beijing Novogene Biotech Co., Ltd. (Beijing, China) and analyzed based on amplicon sequence variants (ASVs) (Li et al., 2020). QIIME2 was used for the analysis of alpha diversity (including Chao1, Observed_otus, Shannon, and Simpson) and principal component analysis (PCA). The dominant microbiota of all groups was detected using LEfSe analysis.

2.11 Statistical analysis

The data were analyzed using GraphPad Prism 8 (GraphPad Inc., La Jolla, CA) and presented as mean ± SEM. A one-way ANOVA was used to evaluate statistical differences among experimental groups. Experiments were performed with at least three independent biological replicates, and a p-value of < 0.05 was considered statistically significant.

3 Results

3.1 PINX has no effect on pig weight gain, organ coefficient, and serum biochemical indexes

To confirm the successful establishment of the pig PINX model, the MEL concentration in serum was first assayed. The results showed that PINX dramatically decreased the global MEL level and omitted the diurnal pattern compared with the control (unpublished data) but did not affect the body weight gain (Figure 1A). In addition, PINX and MEL supplementation had no significant effects on the indexes of brain, heart, liver, spleen, lung, kidney, and testis (Figure 1B) and the serum levels of ALT, AST, TC, TG, HDL-C, and LDL-C (Figures 1C–H). These findings suggest that PINX and MEL supplementation do not affect the growth performance in pigs.

3.2 PINX does not affect MEL levels in GIT and intestinal contents

To explore the effect of PINX on the MEL levels in the GIT, the concentration of MEL in different segments of the GIT and intestinal contents was detected. The results showed that the MEL levels in the stomach and duodenum were higher than those in other segments in the control group, but no significant differences were found among the segments of the PINX pigs compared to the control group. In addition, PINX did not affect the MEL levels in the intestinal contents (Figure 2). Furthermore, the AANAT protein expressions in the duodenum, ileum, and colon had no significant differences among the three groups (Figure 3), indicating that MEL synthesis in the GIT is independent of the pineal gland in pigs.

3.3 PINX had little effect on the intestinal morphology and intestinal mucosal barrier

The histological examination showed that PINX and MEL supplementation did not affect the villus height and villus/crypt ratio in the duodenum and ileum, although PINX increased the duodenal crypt depth (Figure 4). Therefore, we explored the cellular mucosal barrier of the duodenum in different groups of pigs. The Western blotting assay revealed that no difference was observed in the protein expression of ZO-1 and claudin-1 among the three groups (Figure 5), suggesting that PINX and MEL supplementation had little effect on duodenal and ileal mucosal morphology and on the mucosal barrier.

3.4 Effects of PINX on intestinal microbiota

The Venn diagram showed common and unique ASVs among the treatment groups. A total of 4,196 ASVs were determined, and there were 916 common ASVs among the three groups. In addition, 752, 712, and 955 unique ASVs were specifically identified in the control, PINX, and PINX+MEL groups, respectively (Figure 6A). We further determined four indexes (Chao1, Observed_otus, Shannon, and Simpson) to evaluate the alpha diversity of the microbiome in each group, but no significant differences were observed in the intestinal microbiota α diversity index among the three groups, indicating that PINX and MEL supplementation did not have a significant effect on the richness and diversity of the colonic microbiota (Figures 6B–E). The PCA results showed that the distance between the control and the PINX sample was close, indicating their similarities in the microorganisms. However, the PINX+MEL group showed a distinctive separation from control and PINX treatments (Figure 6F), suggesting that the MEL supplementation changed the microbiota composition of pigs.

The relative abundance of microbiota is given in Figure 7. The phylum level analysis showed that Firmicutes, Bacteroidota, Spirochaetota, Euryarchaeota, Proteobacteria, and Actinobacteriota were the top six phyla. Compared with the control, although PINX decreased the abundance of Actinobacteriota, Desulfobacterota, Fibrobacterota, and Chloroflexi at the phylum level, it was not significant. However, compared to the PINX group, MEL treatment decreased Fibrobacterota abundance and increased Actinobacteriota, Desulfobacterota, and Chloroflexi abundance. At the genus level, PINX and MEL supplementation had no effect on the relative abundances of microbiota. To identify the distinct gut microbiota of the three groups, we conducted the linear discriminant analysis (LDA) effect size (LEfSe). The results showed that Negativicutes, Clostridia_vadinBB60, Prevotellaceae_bacterium,

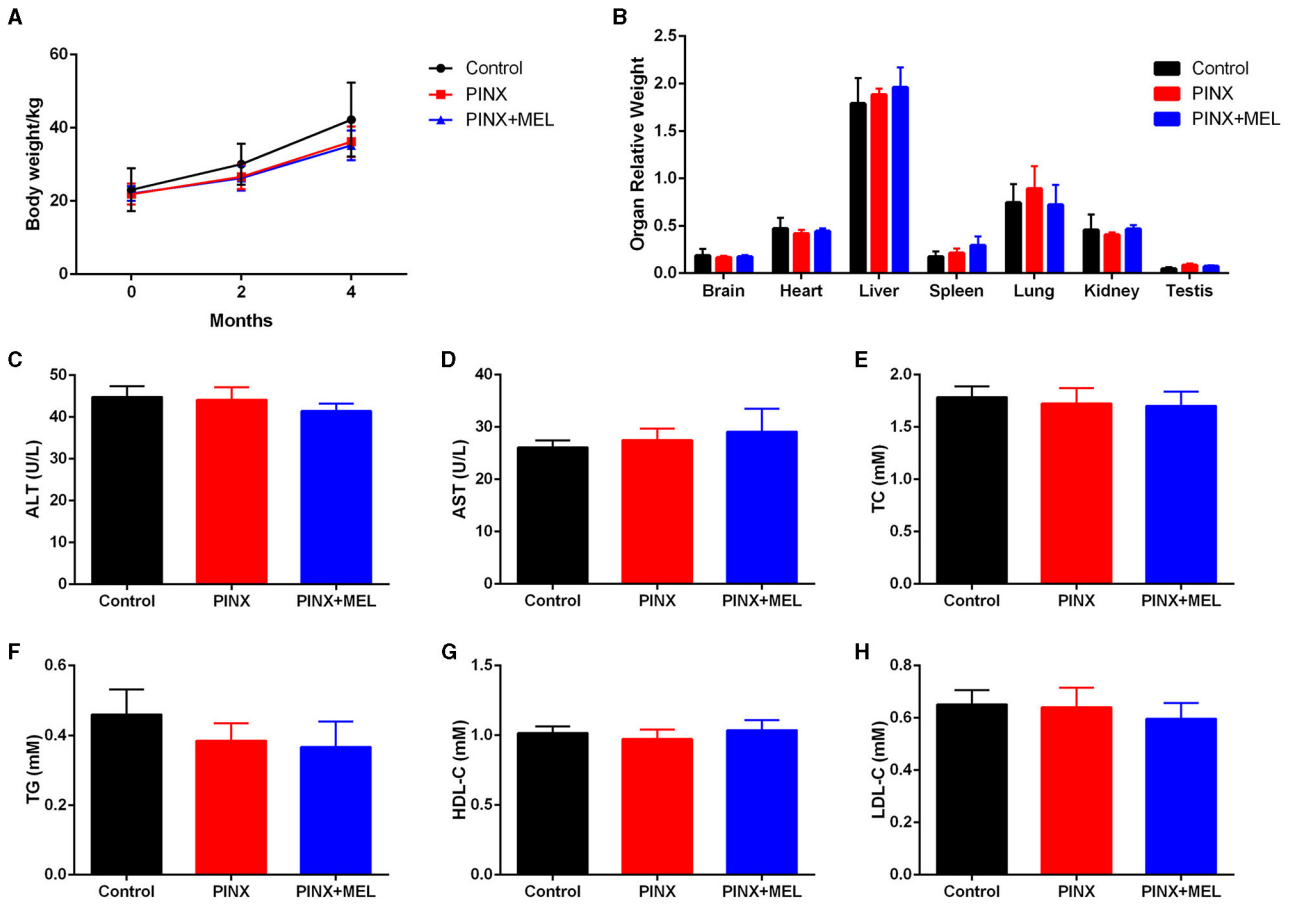

FIGURE 1
Effects of PINX on body weight, organ coefficients, and serum biochemical indexes in pigs. **(A)** The body weights of three groups of pigs were recorded. **(B)** Effect of PINX on the relative organ weights of the brain, heart, liver, spleen, lungs, kidneys, and testes after 4 months. The effect of PINX on serum levels of ALT **(C)**, AST **(D)**, total cholesterol (TC) **(E)**, triglycerides (TG) **(F)**, high-density lipoprotein cholesterol (HDL-C) **(G)**, and low-density lipoprotein cholesterol (LDL-C) **(H)**. Control, sham–pinealectomy group; PINX, pinealectomy group; PINX+MEL, pinealectomy + melatonin supplementation group.

Acidaminococcaceae, and *Phascolarctobacterium* were significantly more abundant in the control group. In addition, Faecalibacterium and Peptostreptococcales_Tissierellales are domainant in PINX pigs. MEL supplementation significantly elevated the relative abundance of bacterium_MD2012, *Monoglobus* (Monoglobaceae, Monoglobales), Ruminococcus_champanellensis, Actinobacteriota, Chloroflexi, Anaerolineae, Desulfobacterota, and *Methanobacterium* (Figure 8). Collectively, these results demonstrated that PINX does not affect the gut microbiota in pigs, but MEL supplementation changed the composition of the gut microbiota.

4 Discussion

It has been documented that MEL supplementation affects the gut microbiota composition in mice (Xu P. et al., 2017), rat (Lv et al., 2020), and suckling piglets (Xia et al., 2022). In this study, the effect of endogenous MEL deficiency on gut microbiota has been studied using a new established pig PINX model. The results demonstrate that PINX has no significant effect on MEL concentration in the intestine and intestinal contents, as well as on the intestinal microbiota, suggesting that MEL synthesis in the GIT is independent of the pineal gland, supported by the findings of Bubenik and Brown (1997) that PINX has no influence on MEL levels in the intestine. Meanwhile, MEL supplementation has considerable effect on shaping the composition of the intestinal microbiota.

In the current study, we observed that PINX significantly reduced nighttime serum MEL levels, confirming the successful removal of the pineal gland. However, GIT enterochromaffin cells were reported to synthesize MEL and contribute to plasmatic MEL concentration (Huether et al., 1992; Bubenik and Brown, 1997), so the serum MEL is detectable even after PINX. Studies have shown that MEL has anti-obesity effects, reducing TG and TC concentrations and liver steatosis in mice fed with a high-fat diet (Xu P. et al., 2017). However, the current study found that PINX and MEL supplementation had no effect on body weight gain and serum biochemical indexes of pigs fed with basic diets, which was similar to the results observed in PINX rats (Buonfiglio et al., 2018) and MEL-supplemented mice (Haridas et al., 2013) and piglets (Xia et al., 2022). Possible explanations for this difference may include

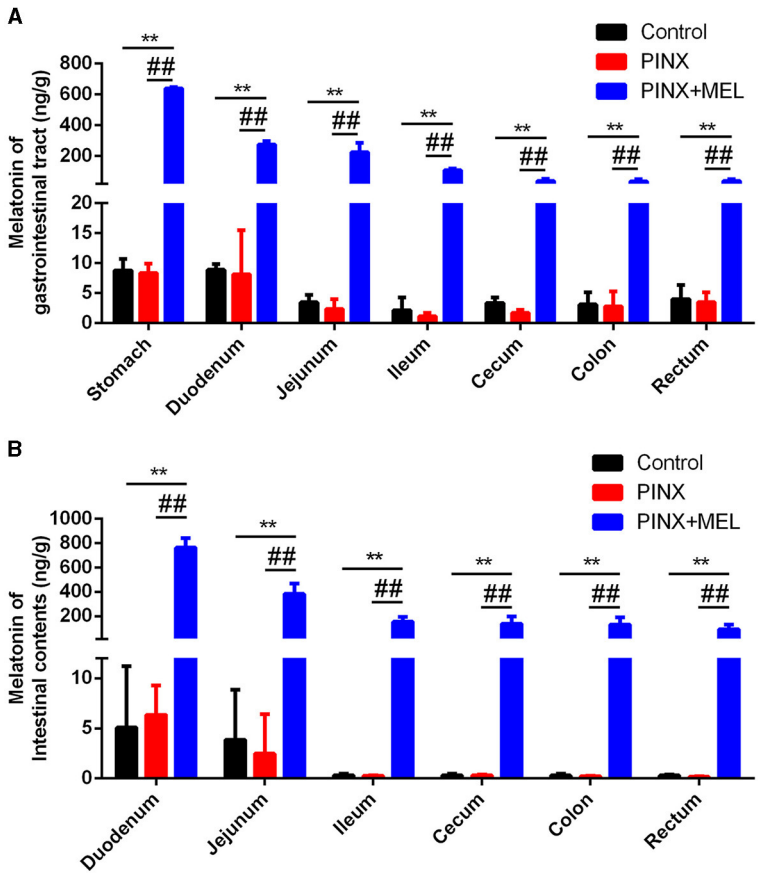

FIGURE 2
Effect of PINX on MEL concentration in the gastrointestinal tract and intestinal contents. **(A)** MEL levels in different segments of gastrointestinal tract tissues of three groups of pigs. **(B)** MEL levels in different segments of intestinal contents of three groups of pigs. Data are represented as mean ± SEM. $^{**}p < 0.01$ compared with the control group, $^{\#\#}p < 0.01$ compared with the PINX group.

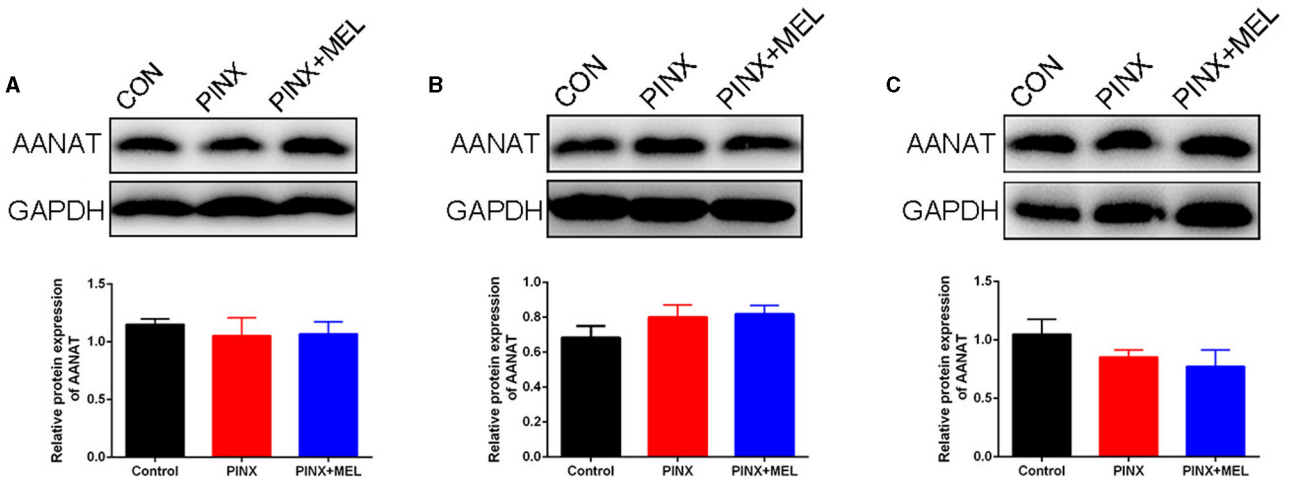

FIGURE 3
Effect of PINX on AANAT expression in the gastrointestinal tract. Immunoblots (up) and quantification (down) of AANAT in the duodenum **(A)**, ileum **(B)**, and colon **(C)**.

the animal species, experimental duration, and feeding regimes. In our study, it should be noted that the pigs were fed with a basic diet according to their weight, while the mice or rats had *ad libitum* access to food in other studies. These results indicate that PINX and MEL supplementation has no effect on growth performance in pigs.

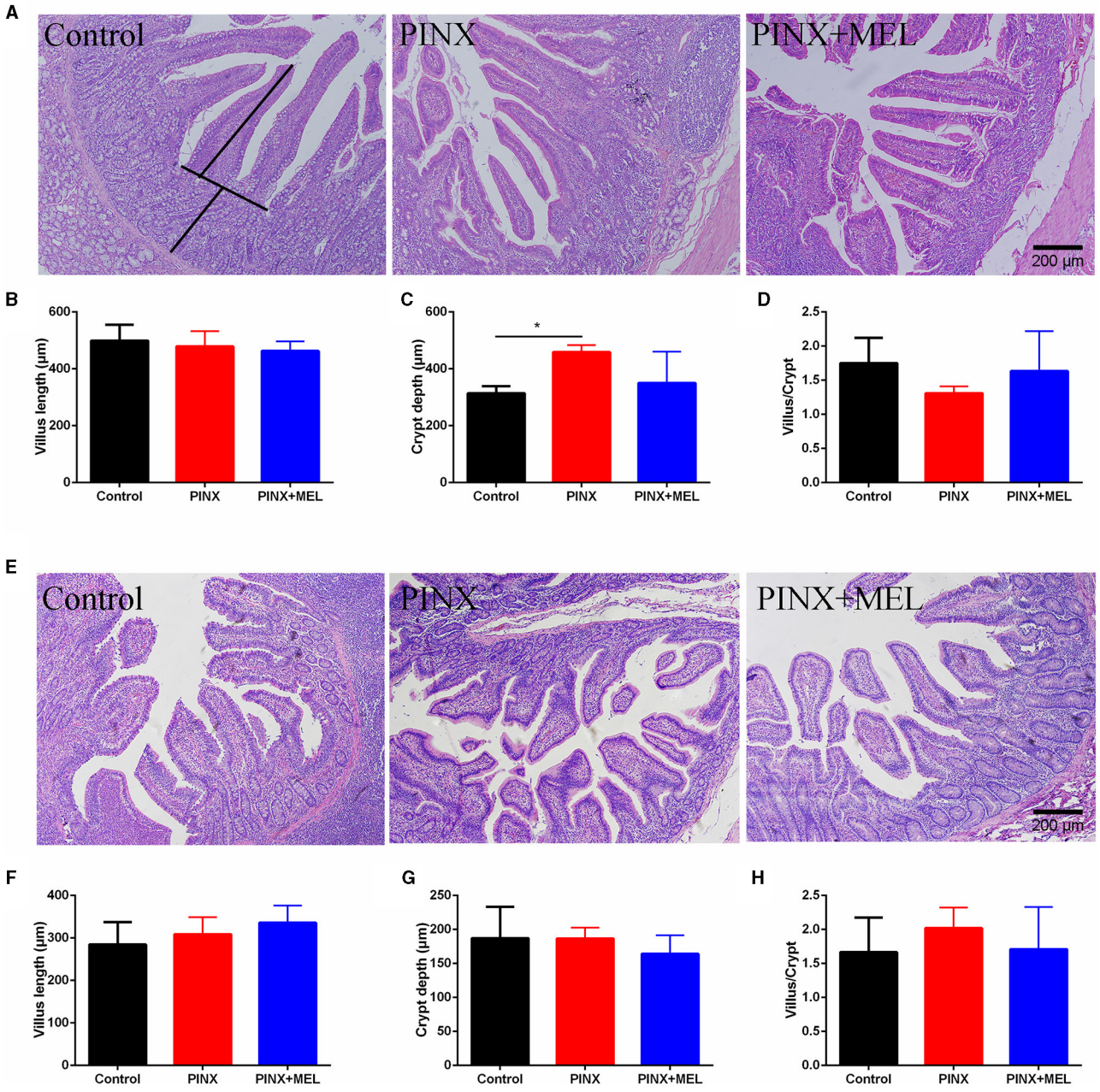

FIGURE 4
Effect of PINX on duodenal and ileum morphology. **(A)** Representative images of H&E staining in the duodenum. The villus length and crypt depth were measured as indicated in the image. **(B–D)** Statistical analysis of villus length, crypt depth, and the ratio of the villus to crypt of the duodenum. **(E)** Representative images of H&E staining in the ileum. **(F–H)** The statistical analysis of villus length, crypt depth, and the ratio of the villus to crypt of the ileum. Scale bar: 200 μm. Data are represented as mean ± SEM. *$p < 0.05$ compared with the control group.

The mucosal morphology parameters, such as villus height, crypt depth, and tight junction protein, are often used to evaluate intestinal barrier function (Ding and Li, 2003). Ren et al. (2018) found that MEL increased the ratio of the villus to crypt in the ileum, promoted nutrient absorption, and consequently improved body weight gain in mice with weanling stress. Gao et al. (2019) found that sleep deprivation damaged the tight junction proteins, resulting in a loss of intestinal mucosal integrity. In this study, although PINX decreased the MEL levels in serum and sleep time in pigs during the dark phases (data not shown), PINX did not influence the intestinal integrity, as reflected by the levels of proteins ZO-1 and claudin-1. These inconsistent results may be due to the differences in the duration of the experiment. Gao et al. conducted an acute sleep deprivation experiment with a duration of 3 days, while in our study, the pineal gland was removed for 4 months.

Recently, an interesting study showed a new role of the pineal gland in regulating seasonal alterations of gut microbiota in Siberian hamsters (Shor et al., 2020). In this study, we demonstrated that PINX had no significant effects on the alpha diversity and beta

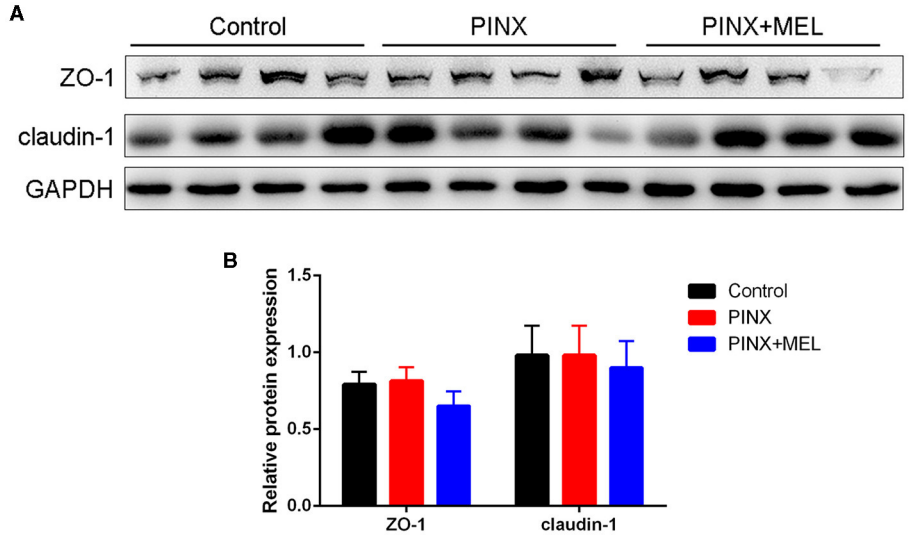

FIGURE 5
Effect of PINX on the duodenal mucosal barrier. Immunoblots **(A)** and quantification **(B)** of ZO-1 and claudin-1 in the duodenum.

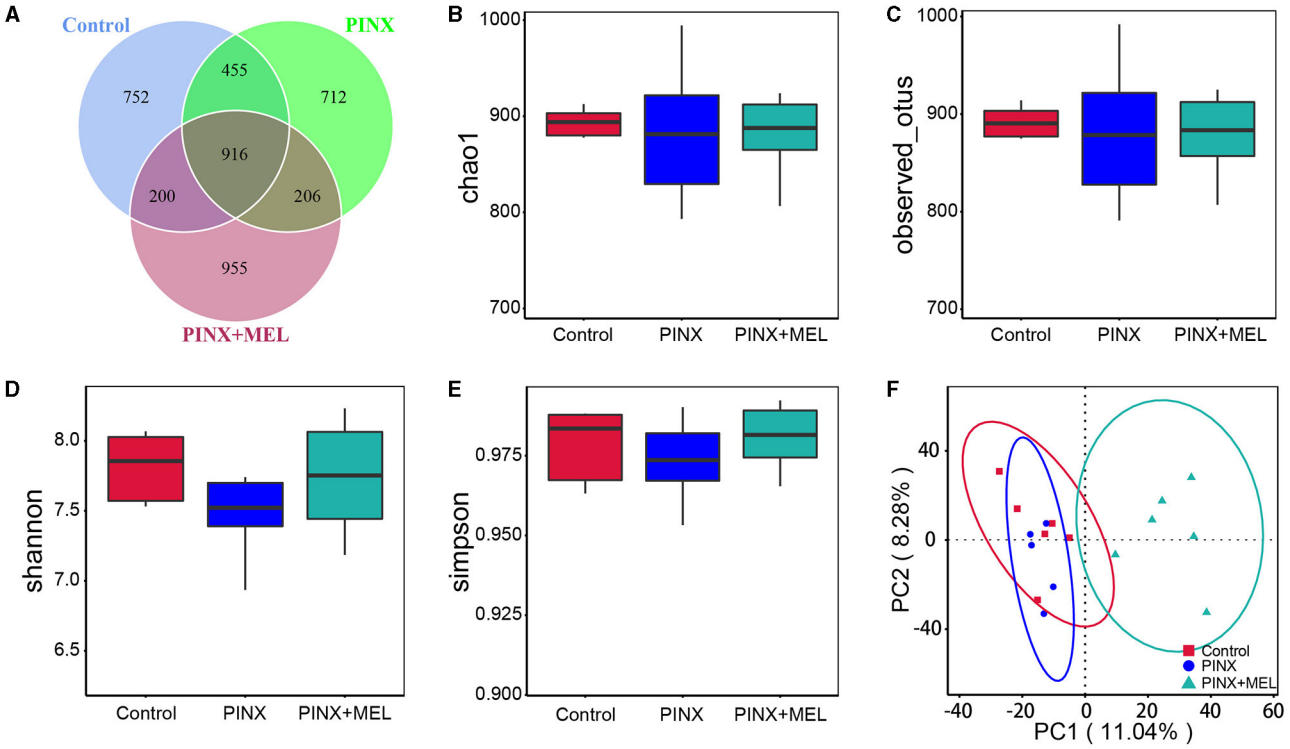

FIGURE 6
Effect of PINX on colonic microbiota alpha diversity and beta diversity. **(A)** Venn diagram showing overlapping ASVs identified in pig's microbiota of each group. Alpha diversity analysis of Chao1 **(B)**, Observed_otus **(C)**, Shannon **(D)**, and Simpson **(E)**. **(F)** Principal component analysis (PCA) of colonic microbiota.

diversity of the intestinal microbiota, whereas the beta diversity analysis showed that MEL supplementation altered the microbial community structure. It is acknowledged that the Firmicutes-to-Bacteroidetes ratio is considered to be an important indicator for the state of the intestinal microbiota, and previous studies have reported that MEL affects the Firmicutes-to-Bacteroidetes ratio (Xu P. et al., 2017; Yin et al., 2018, 2020). In this study, the abundance of Firmicutes and Bacteroidetes was not significantly different after MEL supplementation; this finding is consistent with previous results in suckling piglets (Xia et al., 2022). This discrepancy may

10.3389/fmicb.2024.1352586

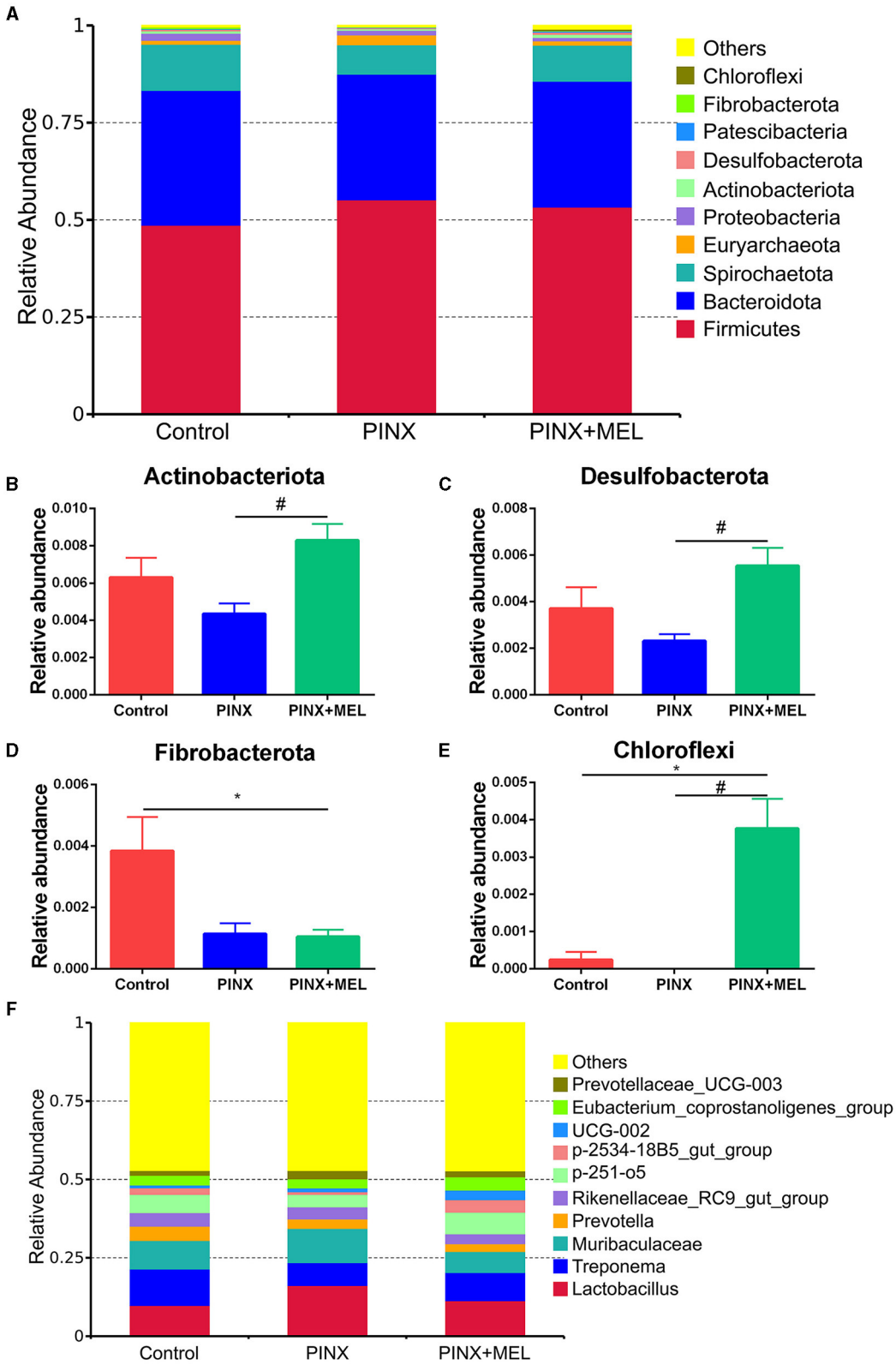

FIGURE 7
Effects of PINX on gut microbiome composition. **(A)** Relative contribution of the top 10 phyla in each group. **(B–E)** Comparison of the relative abundance at the phylum levels among each group. **(F)** Relative contribution of the top 10 genera in each group. Data are represented as mean ± SEM. *$p < 0.05$ compared with the control group, $^{\#}p < 0.05$ compared with the PINX group.

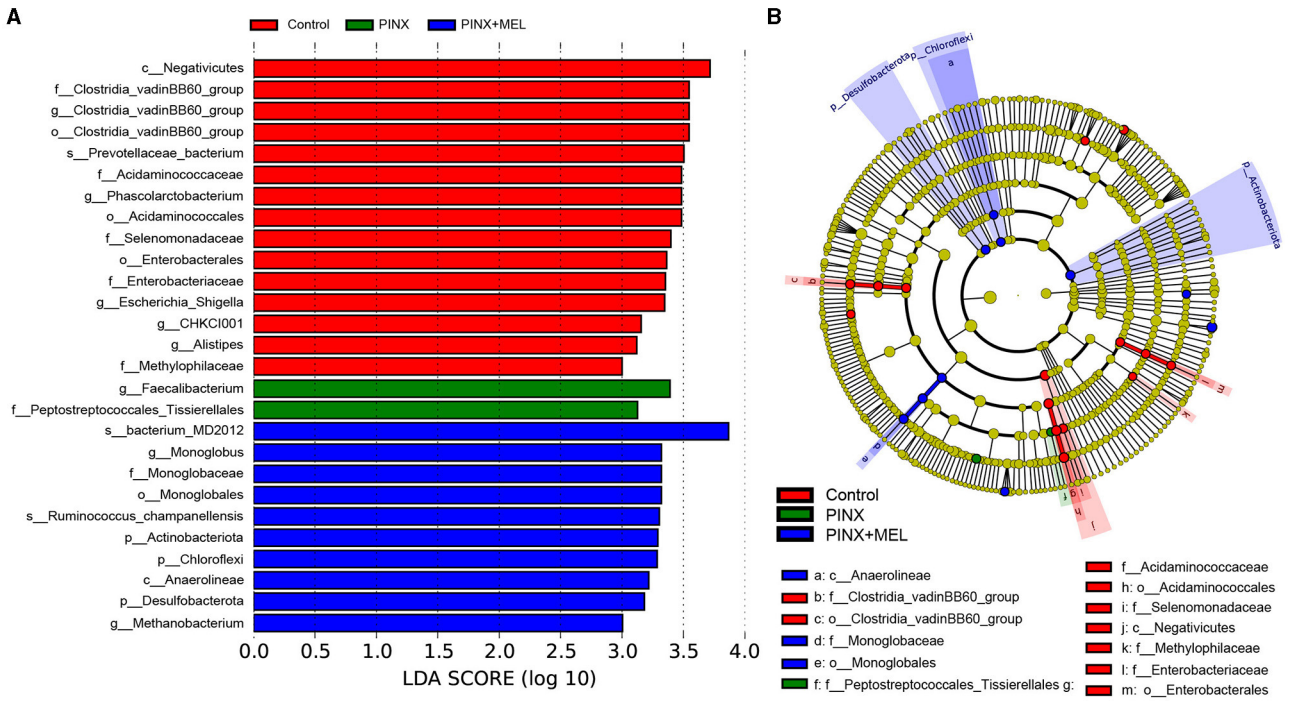

FIGURE 8
Different taxa microbe analysis based on the LEfSe method. **(A)** Linear discriminant analysis (LDA) score in each group (LDA ≥ 3.0). **(B)** Cladogram of gut microbiota in each group. Each circle's diameter reflects the abundance of that taxa in the community.

be caused by differences in model organisms (mice versus pigs). However, Ruminococcaceae, a beneficial bacterium belonging to the phylum Firmicutes, may ameliorate intestinal inflammation (Wang L. et al., 2021; Wang Y. et al., 2021). Butyrate, a primary product of intestinal microbial fermentation of dietary fiber, serves as an essential energy source for intestinal epithelial cells and protects colonic epithelial cells from tumorigenesis (Hamer et al., 2008; Xu S. et al., 2017; Yang and Yu, 2018). Ruminococcaceae is a major producer of butyrate, which is dramatically reduced in individuals suffering from inflammatory bowel disease (Darnaud et al., 2018; Ma et al., 2023). A previous study revealed that MEL effectively ameliorated sleep deprivation-induced colitis by restoring intestinal microbiota homeostasis and improving the production of butyrate (Gao et al., 2021). In this study, LEfSe analysis showed that *Ruminococcus* was much more abundant in the MEL supplementation group. The increase in the abundance of *Ruminococcus* may increase the production of butyrate, which contributes to a healthier intestinal environment. In addition, MEL supplementation decreased Fibrobacterota abundance and increased the relative abundance of Actinobacteriota, Desulfobacterota, and Chloroflexi. Fibrobacterota is important for the degradation of cellulose in the gastrointestinal tracts, best known for its role in rumen function, and is a potential source of novel enzymes for bioenergy applications (Jewell et al., 2013). It is believed that cellulose hydrolysis, anerobic metabolism, and the absence of motility are the unified characteristics of Fibrobacterota (Abdul Rahman et al., 2015). A recent study suggests that indole-3-carboxaldehyde, a tryptophan metabolite produced by bacteria, decreased the abundance of phylum Fibrobacterota, which had a beneficial role in intestinal health in weaned piglets (Zhang et al., 2022). Thus, we speculated that MEL, which is also a tryptophan derivative and an indole-like neuroendocrine hormone, may have the same inhibitory mechanism on Fibrobacterota and improve intestinal health. Another bacteria phylum, Actinobacteria, is known to generate various antimicrobial compounds and maintain mucosal immunity (Arango et al., 2016), which have a variety of anti-tumor and anti-biofilm properties (Azman et al., 2019). It is estimated that over 80% of medicinal antibiotics are derived from Actinobacteria, especially the *Streptomyces* genus (Procópio et al., 2012). Importantly, butyrate can ameliorate the progression of colorectal cancer induced by AOM/DSS in mice, partially by promoting the colonization of Actinobacteriota (Kang et al., 2023). Our findings are supported by those of a recent study on piglets, which revealed that MEL treatment enhanced the proportion of Actinobacteria, potentially augmenting aspects such as barrier integrity, nutrient absorption, and microbial balance (Xia et al., 2022). Members of the Desulfobacterota phylum exhibit a predilection for anoxic environments, with many using sulfur compounds or iron as the terminal electron acceptors during respiration and/or disproportionation reactions (Simon and Kroneck, 2013; Murphy et al., 2021). This process is essential for the host's energy metabolism, as sulfate is a key source of sulfur for protein synthesis and other cellular processes. It is worth noting that rice bran diet improved intestinal digestive enzyme activities, increased Desulfobacterota abundance, and promoted growth in pigs (Li et al., 2023). In addition, polysaccharides can increase the relative abundance of Verrucomicrobiota, Desulfobacterota, and Actinobacteriota; generate short-chain fatty acids; and benefit

intestinal health (Hu et al., 2021). While the role of Chloroflexi in the mammalian gut is less understood, the increased abundance of Chloroflexi following MEL supplementation may suggest its potential role in shaping the gut environment or metabolite profile. Collectively, our study sheds light on the multifaceted impact of MEL supplementation on the gut microbiome. These shifts in microbial communities likely contribute to an overall enhancement of gut health and function.

In summary, to the best of our knowledge, this is the first study to investigate the effects of PINX on GIT MEL levels and the composition of intestinal microbiota in pigs. The results support that MEL synthesis and gut microbiota homeostasis in the GIT are independent of the pineal gland in pigs. MEL supplementation modulates the composition of intestinal flora. However, future research studies are needed to elucidate the molecular mechanism by which MEL participates in host–bacteria interactions.

Data availability statement

The datasets presented in this study can be found in the NCBI SRA Repository (https://www.ncbi.nlm.nih.gov/sra), accession number PRJNA1086051.

Ethics statement

The animal study was approved by Animal Ethics Association of Yangzhou University [approval ID: SYXK (Su) 2022-0044]. The study was conducted in accordance with the local legislation and institutional requirements.

Author contributions

JZ: Writing – original draft, Project administration, Methodology, Data curation. YZ: Writing – original draft, Project administration, Methodology. DZ: Writing – review & editing, Project administration, Methodology. KM: Writing – review & editing, Project administration, Methodology. YG: Writing – review & editing, Project administration, Methodology. XL: Writing – review & editing, Project administration, Methodology. JL: Methodology, Writing – review & editing, Supervision, Funding acquisition. SC: Methodology, Writing – review & editing, Supervision, Funding acquisition.

Funding

The author(s) declare financial support was received for the research, authorship, and/or publication of this article. This work was supported by National Key Research and Development Program of China (2021YFF1000603), National Natural Science Foundation of China (32130098), and the Postgraduate Research and Practice Innovation Program of Jiangsu Province (Yangzhou University, KYCX21_3271, SJCX21_1638).

Conflict of interest

The authors declare that the research was conducted in the absence of any commercial or financial relationships that could be construed as a potential conflict of interest.

Publisher's note

References

Abdul Rahman, N., Parks, D., Vanwonterghem, I., Morrison, M., Tyson, G., and Hugenholtz, P. (2015). A phylogenomic analysis of the bacterial phylum fibrobacteres. *Front. Microbiol.* 6, 1469. doi: 10.3389/fmicb.2015.01469

Agil, A., Navarro-Alarcón, M., Ruiz, R., Abuhamadah, S., El-Mir, M., and Vázquez, G. (2011). Beneficial effects of melatonin on obesity and lipid profile in young Zucker diabetic fatty rats. *J. Pineal Res.* 50, 207–212. doi: 10.1111/j.1600-079X.2010.00830.x

Al Gburi, M. R. A., Altinoz, E., Elbe, H., Onal, M., Yilmaz, U., Yilmaz, N., et al. (2022). Pinealectomy and melatonin administration in rats: their effects on pulmonary edema induced by α-naphthylthiourea. *Drug Chemi. Toxicol.* 46, 1024–1034. doi: 10.1080/01480545.2022.2119994

Arango, R., Carlson, C., Currie, C., McDonald, B., Book, A., Green, F., et al. (2016). Antimicrobial activity of actinobacteria isolated from the guts of subterranean termites. *Environ. Entomol.* 45, 1415–1423. doi: 10.1093/ee/nvw126

Azman, A., Mawang, C., Khairat, J., and AbuBakar, S. (2019). Actinobacteria-a promising natural source of anti-biofilm agents. *Int. Microbiol.* 22, 403–409. doi: 10.1007/s10123-019-00066-4

Ballur, A., Altinoz, E., Yigitturk, G., Onal, M., Elbe, H., Bicer, Y., et al. (2022). Influence of pinealectomy and long-term melatonin administration on inflammation and oxidative stress in experimental gouty arthritis. *Inflammation* 45, 1332–1347. doi: 10.1007/s10753-022-01623-2

Bubenik, G. A. (2002). Gastrointestinal melatonin: localization, function, and clinical relevance. *Dig. Dis. Sci.* 47, 2336–2348. doi: 10.1023/A:1020107915919

Bubenik, G. A., and Brown, G. M. (1997). Pinealectomy reduces melatonin levels in the serum but not in the gastrointestinal tract of rats. *Biol. Signals* 6, 40–44. doi: 10.1159/000109107

Buonfiglio, D., Parthimos, R., Dantas, R., Cerqueira Silva, R., Gomes, G., Andrade-Silva, J., et al. (2018). Melatonin absence leads to long-term leptin resistance and overweight in rats. *Front. Endocrinol.* 9, 122. doi: 10.3389/fendo.2018.00122

Callaghan, B. D. (1991). The effect of pinealectomy and autonomic denervation on crypt cell proliferation in the rat small intestine. *J. Pineal Res.* 10, 180–185. doi: 10.1111/j.1600-079X.1991.tb00813.x

Chen, C., Fichna, J., Bashashati, M., Li, Y., and Storr, M. (2011). Distribution, function and physiological role of melatonin in the lower gut. *World J. Gastroenterol.*17, 3888–3898. doi: 10.3748/wjg.v17.i34.3888

Cheung, K., Wang, T., Poon, A., Carl, A., Tranmer, B., Hu, Y., et al. (2005). The effect of pinealectomy on scoliosis development in young nonhuman primates. *Spine* 30, 2009–2013. doi: 10.1097/01.brs.0000179087.38730.5d

Claustrat, B., and Leston, J. (2015). Melatonin: physiological effects in humans. *Neurochirurgie*. 61, 77–84. doi: 10.1016/j.neuchi.2015.03.002

Darnaud, M., Dos Santos, A., Gonzalez, P., Augui, S., Lacoste, C., Desterke, C., et al. (2018). Enteric delivery of regenerating family member 3 alpha alters the intestinal microbiota and controls inflammation in mice with colitis. *Gastroenterology* 154, 1009–1023. doi: 10.1053/j.gastro.2017.11.003

de Farias, T. S., de Oliveira, A., Andreotti, S., do Amaral, F., Chimin, P., de Proença, A., et al. (2015). Pinealectomy interferes with the circadian clock genes expression in white adipose tissue. *J. Pineal Res.* 58, 251–261. doi: 10.1111/jpi.12211

De Filippis, D., Iuvone, T., Esposito, G., Steardo, L., Arnold, G., Paul, A., et al. (2008). Melatonin reverses lipopolysaccharide-induced gastro-intestinal motility disturbances through the inhibition of oxidative stress. *J. Pineal Res.* 44, 45–51. doi: 10.1111/j.1600-079X.2007.00526.x

Demir, M., Altinoz, E., Elbe, H., Bicer, Y., Yigitturk, G., Karayakali, M., et al. (2022). Effects of pinealectomy and crocin treatment on rats with isoproterenol-induced myocardial infarction. *Drug Chem. Toxicol.* 45, 2576–2585. doi: 10.1080/01480545.2021.1977025

Dempsey, R., Hopkins, J., Bittman, E., and Kindt, G. (1982). Total pinealectomy by an occipital parasagittal approach in sheep. *Surg. Neurol.* 18, 377–380. doi: 10.1016/0090-3019(82)90157-4

Ding, L. A., and Li, J. S. (2003). Gut in diseases: physiological elements and their clinical significance. *World J. Gastroenterol.* 9, 2385–2389. doi: 10.3748/wjg.v9.i11.2385

Egermann, M., Gerhardt, C., Barth, A., Maestroni, G., Schneider, E., and Alini, M. (2011). Pinealectomy affects bone mineral density and structure–an experimental study in sheep. *BMC Musculoskelet. Disord.* 12, 271. doi: 10.1186/1471-2474-12-271

Gao, T., Wang, Z., Dong, Y., Cao, J., and Chen, Y. (2021). Melatonin-mediated colonic microbiota metabolite butyrate prevents acute sleep deprivation-induced colitis in mice. *Int. J. Mol. Sci.* 22, 21. doi: 10.3390/ijms222111894

Gao, T., Wang, Z., Dong, Y., Cao, J., Lin, R., Wang, X., et al. (2019). Role of melatonin in sleep deprivation-induced intestinal barrier dysfunction in mice. *J. Pineal Res.* 67, e12574. doi: 10.1111/jpi.12574

Gong, Y., Hou, F., Xiang, C., Li, C., Hu, G., and Chen, C. (2022). The mechanisms and roles of melatonin in gastrointestinal cancer. *Front. Oncol.* 12, 1066698. doi: 10.3389/fonc.2022.1066698

Hamer, H., Jonkers, D., Venema, K., Vanhoutvin, S., Troost, F., and Brummer, R. (2008). Review article: the role of butyrate on colonic function. *Aliment. Pharmacol. Ther.* 27, 104–119. doi: 10.1111/j.1365-2036.2007.03562.x

Haridas, S., Kumar, M., and Manda, K. (2013). Melatonin ameliorates chronic mild stress induced behavioral dysfunctions in mice. *Physiol. Behav.* 119, 201–207. doi: 10.1016/j.physbeh.2013.06.015

Hu, B., Liu, C., Jiang, W., Zhu, H., Zhang, H., Qian, H., et al. (2021). Chronic in vitro fermentation and in vivo metabolism: extracellular polysaccharides from Sporidiobolus pararoseus regulate the intestinal microbiome of humans and mice. *Int. J. Biol. Macromol.* 192, 398–406. doi: 10.1016/j.ijbiomac.2021.09.127

Huether, G. (1993). The contribution of extrapineal sites of melatonin synthesis to circulating melatonin levels in higher vertebrates. *Experientia* 49, 665–670. doi: 10.1007/BF01923948

Huether, G., Messner, M., Rodenbeck, A., and Hardeland, R. (1998). Effect of continuous melatonin infusions on steady-state plasma melatonin levels in rats under near physiological conditions. *J. Pineal Res.* 24, 146–151. doi: 10.1111/j.1600-079X.1998.tb00527.x

Huether, G., Poeggeler, B., Reimer, A., and George, A. (1992). Effect of tryptophan administration on circulating melatonin levels in chicks and rats: evidence for stimulation of melatonin synthesis and release in the gastrointestinal tract. *Life Sci.* 51, 945–953. doi: 10.1016/0024-3205(92)90402-B

Jewell, K., Scott, J., Adams, S., and Suen, G. (2013). A phylogenetic analysis of the phylum Fibrobacteres. *Syst. Appl. Microbiol.* 36, 376–382. doi: 10.1016/j.syapm.2013.04.002

Kang, J., Sun, M., Chang, Y., Chen, H., Zhang, J., Liang, X., et al. (2023). Butyrate ameliorates colorectal cancer through regulating intestinal microecological disorders. *Anticancer. Drugs* 34, 227–237. doi: 10.1097/CAD.0000000000001413

Kvetnoy, I., Ingel, I., Kvetnaia, T., Malinovskaya, N., Rapoport, S., Raikhlin, N., et al. (2002). Gastrointestinal melatonin: cellular identification and biological role. *Neuro Endocrinol. Lett.* 23, 121–132.

Li, M., Shao, D., Zhou, J., Gu, J., Qin, J., Chen, W., et al. (2020). Signatures within esophageal microbiota with progression of esophageal squamous cell carcinoma. *Chin. J. Cancer Res.* 32, 755–767. doi: 10.21147/j.issn.1000-9604.2020.06.09

Li, Z., Zhang, F., Zhao, Y., Liu, X., Xie, J., and Ma, X. (2023). Effects of different starch diets on growth performance, intestinal health and faecal microbiota of growing pigs. *J. Anim. Physiol. Anim. Nutr.* doi: 10.1111/jpn.13810

Luo, J., Zhang, Z., Sun, H., Song, J., Chen, X., Huang, J., et al. (2020). Effect of melatonin on T/B cell activation and immune regulation in pinealectomy mice. *Life Sci.* 242, 117191. doi: 10.1016/j.lfs.2019.117191

Lv, W., Liu, C., Yu, L., Zhou, J., Li, Y., Xiong, Y., et al. (2020). Melatonin alleviates neuroinflammation and metabolic disorder in DSS-induced depression rats. *Oxid. Med. Cell. Longev.* 2020, 1241894. doi: 10.1155/2020/1241894

Ma, L., Yang, Y., Liu, W., and Bu, D. (2023). Sodium butyrate supplementation impacts the gastrointestinal bacteria of dairy calves before weaning. *Appl. Microbiol. Biotechnol.* 107, 3291–3304. doi: 10.1007/s00253-023-12485-5

Magliocco, G., Le Bloc'h, F., Thomas, A., Desmeules, J., and Daali, Y. (2021). Simultaneous determination of melatonin and 6-hydroxymelatonin in human overnight urine by LC-MS/MS. *J. Chromatogr. B Analyt. Technol. Biomed. Life Sci.* 1181, 122938. doi: 10.1016/j.jchromb.2021.122938

Murphy, C., Biggerstaff, J., Eichhorn, A., Ewing, E., Shahan, R., Soriano, D., et al. (2021). Genomic characterization of three novel Desulfobacterota classes expand the metabolic and phylogenetic diversity of the phylum. *Environ. Microbiol.* 23, 4326–4343. doi: 10.1111/1462-2920.15614

Pabst, R. (2020). The pig as a model for immunology research. *Cell Tissue Res.* 380, 287–304. doi: 10.1007/s00441-020-03206-9

Pan, J., Li, F., Wang, C., Li, X., Zhang, S., Zhang, W., et al. (2021). Effects of duodenal 5-hydroxytryptophan perfusion on melatonin synthesis in GI tract of sheep. *Molecules* 26, 17. doi: 10.3390/molecules26175275

Paulose, J. K., Wright, J. M., Patel, A., and Cassone, V. (2016). Human gut bacteria are sensitive to melatonin and express endogenous circadian rhythmicity. *PLoS ONE* 11, e0146643. doi: 10.1371/journal.pone.0146643

Prezotto, L. D., Lemley, C., Camacho, L., Doscher, F., Meyer, A., Caton, J., et al. (2014). Effects of nutrient restriction and melatonin supplementation on maternal and foetal hepatic and small intestinal energy utilization. *J. Anim. Physiol. Anim. Nutr.* 98, 797–807. doi: 10.1111/jpn.12142

Procópio, R., Silva, I., Martins, M., Azevedo, J., and Araújo, J. (2012). Antibiotics produced by Streptomyces. *Brazil. J. Infect. Dis.* 16, 466–471. doi: 10.1016/j.bjid.2012.08.014

Ren, W., Wang, P., Yan, J., Liu, G., Zeng, B., Hussain, T., et al. (2018). Melatonin alleviates weanling stress in mice: Involvement of intestinal microbiota. *J. Pineal Res.* 64, 2. doi: 10.1111/jpi.12448

Rusanova, I., Martínez-Ruiz, L., Florido, J., Rodríguez-Santana, C., Guerra-Librero, A., Acuña-Castroviejo, D., et al. (2019). Protective effects of melatonin on the skin: future perspectives. *Int. J. Mol. Sci.* 20(19). doi: 10.3390/ijms20194948

Sahin, Z., Sandal, S., Yilmaz, B., Bulmus, O., Ozdemir, G., Kutlu, S., et al. (2018). Pinealectomy alters IFN-γ and IL-10 levels in primary thymocyte culture of rats. *Cellul. Mol. Biol.* 64, 25–30. doi: 10.14715/cmb/2018.64.14.5

Santillo, A., Chieffi Baccari, G., Minucci, S., Falvo, S., Venditti, M., and Di Matteo, L. (2020). The Harderian gland: Endocrine function and hormonal control. *Gen. Comp. Endocrinol.* 297, 113548. doi: 10.1016/j.ygcen.2020.113548

Shor, E. K., Brown, S. P., and Freeman, D. A. (2020). A novel role for the pineal gland: Regulating seasonal shifts in the gut microbiota of Siberian hamsters. *J. Pineal Res.* 69, e12696. doi: 10.1111/jpi.12696

Simon, J., and Kroneck, P. (2013). Microbial sulfite respiration. *Adv. Microb. Physiol.* 62, 45–117. doi: 10.1016/B978-0-12-410515-7.00002-0

Slawik, H., Stoffel, M., Riedl, L., Vesel,ý, Z., Behr, M., Lehmberg, J., et al. (2016). Prospective study on salivary evening melatonin and sleep before and after pinealectomy in humans. *J. Biol. Rhythms* 31, 82–93. doi: 10.1177/0748730415616678

Sochal, M., Małecka-Panas, E., Gabryelska, A., Talar-Wojnarowska, R., Szmyd, B., Krzywdzińska, M., et al. (2020). Determinants of sleep quality in inflammatory bowel diseases. *J. Clin. Med.* 9(9). doi: 10.3390/jcm9092921

Sommansson, A., Nylander, O., and Sjöblom, M. (2013). Melatonin decreases duodenal epithelial paracellular permeability via a nicotinic receptor-dependent pathway in rats in vivo. *J. Pineal Res.* 54, 282–291. doi: 10.1111/jpi.12013

Sommansson, A., Yamskova, O., Schiöth, H. B., Nylander, O., and Sjöblom, M. (2014). Long-term oral melatonin administration reduces ethanol-induced increases in duodenal mucosal permeability and motility in rats. *Acta Physiologica (Oxford, England)* 212, 152–165. doi: 10.1111/apha.12339

Swanson, G. R., Gorenz, A., Shaikh, M., Desai, V., Forsyth, C., Fogg, L., et al. (2015). Decreased melatonin secretion is associated with increased intestinal permeability and marker of endotoxemia in alcoholics. *Am. J. Physiol. Gastrointest. Liver Physiol.* 308, G1004–1011. doi: 10.1152/ajpgi.00002.2015

Tchekalarova, J., Atanasova, M., Ivanova, N., Boyadjiev, N., Mitreva, R., and Georgieva, K. (2020). Endurance training exerts time-dependent modulation on depressive responses and circadian rhythms of corticosterone and BDNF in the rats with pinealectomy. *Brain Res. Bull.* 162, 40–48. doi: 10.1016/j.brainresbull.2020.05.012

Tzoneva, R., Georgieva, I., Ivanova, N., Uzunova, V., Nenchovska, Z., Apostolova, S., et al. (2021). The role of melatonin on behavioral changes and concomitant oxidative stress in icvAβ rat model with pinealectomy. *Int. J. Mol. Sci.* 22(23). doi: 10.3390/ijms222312763

Walters, E., Wells, K., Bryda, E., Schommer, S., and Prather, R. (2017). Swine models, genomic tools and services to enhance our understanding of human health and diseases. *Lab Anim.* 46, 167–172. doi: 10.1038/laban.1215

Wang, L., Liao, Y., Yang, R., Zhu, Z., Zhang, L., Wu, Z., et al. (2021). An engineered probiotic secreting Sj16 ameliorates colitis via Ruminococcaceae/butyrate/retinoic acid axis. *Bioeng. transl. Med.* 6, e10219. doi: 10.1002/btm2.10219

Wang, Y., Nan, X., Zhao, Y., Jiang, L., Wang, H., Zhang, F., et al. (2021). Dietary supplementation of inulin ameliorates subclinical mastitis via regulation of rumen microbial community and metabolites in dairy cows. *Microbiol. Spect.* 9, e0010521. doi: 10.1128/Spectrum.00105-21

Wiechmann, A. F., and Sherry, D. M. (2013). Role of melatonin and its receptors in the vertebrate retina. *Int. Rev. Cell Mol. Biol.* 300, 211–242. doi: 10.1016/B978-0-12-405210-9.00006-0

Xia, S., Gao, W., Li, Y., Ma, J., Gong, S., Gao, Z., et al. (2022). Effects of melatonin on intestinal function and bacterial compositions in sucking piglets. *J. Anim. Physiol. Anim. Nutr.* 106, 1139–1148. doi: 10.1111/jpn.13675

Xu, L., Li, D., Li, H., Zhang, O., Huang, Y., Shao, H., et al. (2022). Suppression of obesity by melatonin through increasing energy expenditure and accelerating lipolysis in mice fed a high-fat diet. *Nutr. Diabetes* 12, 42. doi: 10.1038/s41387-022-00222-2

Xu, P., Wang, J., Hong, F., Wang, S., Jin, X., Xue, T., et al. (2017). Melatonin prevents obesity through modulation of gut microbiota in mice. *J. Pineal Res.* 62, 4. doi: 10.1111/jpi.12399

Xu, S., Liu, C., Xu, W., Huang, L., Zhao, J., and Zhao, S. (2017). Butyrate induces apoptosis by activating PDC and inhibiting complex I through SIRT3 inactivation. *Signal Transd. Target. Thera.* 2, 16035. doi: 10.1038/sigtrans.2016.35

Yang, J., and Yu, J. (2018). The association of diet, gut microbiota and colorectal cancer: what we eat may imply what we get. *Protein Cell* 9, 474–487. doi: 10.1007/s13238-018-0543-6

Yin, J., Li, Y., Han, H., Chen, S., Gao, J., Liu, G., et al. (2018). Melatonin reprogramming of gut microbiota improves lipid dysmetabolism in high-fat diet-fed mice. *J. Pineal Res.* 65, e12524. doi: 10.1111/jpi.12524

Yin, J., Li, Y., Han, H., Ma, J., Liu, G., Wu, X., et al. (2020). Administration of exogenous melatonin improves the diurnal rhythms of the gut microbiota in mice fed a high-fat diet. *mSystems* 5, 3. doi: 10.1128/mSystems.00002-20

Zhang, J., Qiu, J., Zhou, Y., Wang, Y., Li, H., Zhang, T., et al. (2018). LIM homeobox transcription factor Isl1 is required for melatonin synthesis in the pig pineal gland. *J. Pineal Res.* 65, e12481. doi: 10.1111/jpi.12481

Zhang, R., Huang, G., Ren, Y., Wang, H., Ye, Y., Guo, J., et al. (2022). Effects of dietary indole-3-carboxaldehyde supplementation on growth performance, intestinal epithelial function, and intestinal microbial composition in weaned piglets. *Front. Nutrit.* 9, 896815. doi: 10.3389/fnut.2022.896815

frontiers | Frontiers in Microbiology

TYPE Original Research
PUBLISHED 13 May 2024
DOI 10.3389/fmicb.2024.1362487

OPEN ACCESS

EDITED BY
Wen-Chao Liu,
Guangdong Ocean University, China

REVIEWED BY
Yuying Li,
Chinese Academy of Agricultural Sciences, China
Yuncai Xiao,
Huazhong Agricultural University, China
Nikhilesh Joardar,
Washington University in St. Louis, United States

*CORRESPONDENCE
Weifen Li
✉ weifenli@zju.edu.cn
Yang Wang
✉ yangwang@qau.edu.cn

RECEIVED 28 December 2023
ACCEPTED 22 April 2024
PUBLISHED 13 May 2024

CITATION
Yuan J, Meng H, Liu Y, Wang L, Zhu Q, Wang Z, Liu H, Zhang K, Zhao J, Li W and Wang Y (2024) *Bacillus amyloliquefaciens* attenuates the intestinal permeability, oxidative stress and endoplasmic reticulum stress: transcriptome and microbiome analyses in weaned piglets. *Front. Microbiol.* 15:1362487. doi: 10.3389/fmicb.2024.1362487

Bacillus amyloliquefaciens attenuates the intestinal permeability, oxidative stress and endoplasmic reticulum stress: transcriptome and microbiome analyses in weaned piglets

Junmeng Yuan[1], Hongling Meng[1], Yu Liu[1], Li Wang[1], Qizhen Zhu[1], Zhengyu Wang[1], Huawei Liu[1], Kai Zhang[1], Jinshan Zhao[1], Weifen Li[2]* and Yang Wang[1]*

[1]College of Animal Science and Technology, Qingdao Agricultural University, Qingdao, China, [2]College of Animal Sciences, Zhejiang University, Hangzhou, China

Endoplasmic reticulum (ER) stress is related to oxidative stress (OS) and leads to intestinal injury. *Bacillus amyloliquefaciens* SC06 (SC06) can regulate OS, but its roles in intestinal ER stress remains unclear. Using a 2 × 2 factorial design, 32 weaned piglets were treated by two SC06 levels (0 or 1×10^8 CFU/g), either with or without diquat (DQ) injection. We found that SC06 increased growth performance, decreased ileal permeability, OS and ER stress in DQ-treated piglets. Transcriptome showed that differentially expressed genes (DEGs) induced by DQ were enriched in NF-κB signaling pathway. DEGs between DQ- and SC06 + DQ-treated piglets were enriched in glutathione metabolism pathway. Ileal microbiome revealed that the SC06 + DQ treatment decreased *Clostridium* and increased *Actinobacillus*. Correlations were found between microbiota and ER stress genes. In conclusion, dietary SC06 supplementation increased the performance, decreased the permeability, OS and ER stress in weaned piglets by regulating ileal genes and microbiota.

KEYWORDS

***Bacillus amyloliquefaciens*, intestinal health, endoplasmic reticulum stress, oxidative stress, transcriptome, microbiome**

1 Introduction

During weaning, piglets encounter various stressors, such as the sudden separation from their mothers, mixing with other litters, and eating the less digestible feed (Lallès et al., 2007). These stressors can generate excessive amounts levels of reactive oxygen species (ROS) and have the potential to cause oxidative stress (OS) (Zheng et al., 2017). The small intestine performs many physiological functions, including digestion, absorption and immunoregulation (Pluske et al., 1997). In the ileal lumen, alkaline intestinal fluid that containing a variety of enzymes can break down digesta into glucose, amino acids, and fatty acids (Malik et al., 2023). Nutrients, such as bile salts and vitamin B_{12} can be absorbed by ileum (Hyder et al., 2023). In addition, immune cells in ileum can also participate in the immune response (Chen et al., 2021). It is reported that OS leads to histological and biochemical damages of small intestine, leading to post-weaning diarrhea and growth retardation in weaned piglets (Su et al., 2023).

OS and ROS production are thought to be components of endoplasmic reticulum (ER) stress. The ER is the largest organelle in the cell and is a major site for protein metabolism, lipid synthesis, carbohydrate metabolism and calcium storage (Reid and Nicchitta, 2015; Westrate et al., 2015). Report also indicated that mitigation of ER stress may be an effective strategy to alleviate OS and growth retardation (Jing et al., 2023). The ER unfolded protein response (ER-UPR) appears to be the representative biomarker of ER stress. Accumulation and aggregation of unfolded proteins can impair normal cellular function and result in cell death (Wang et al., 2019). Studies showed that various stimuli, such as porcine epidemic diarrhea virus, *Escherichia coli* and LPS, could aggravate the ER stress in weaned piglets (Jiang et al., 2017; Chen et al., 2022; Liu et al., 2022).

Strain-specific probiotics have been reported to elevate the growth performance (Wang et al., 2017a), antioxidant capacity (Wang et al., 2012) and intestinal health (Hu et al., 2018) of weaned piglets. Moreover, recent study has also demonstrated that probiotics could ameliorate the ER stress. Yang et al. (2020) reported that ER stress in the ileum of *Salmonella*-infected piglets was significantly alleviated after intragastric injection of *Lactobacillus johnsonii* L531. Zhang et al. (2021) suggested that *Lactobacillus johnsonii* attenuated *Citrobacter rodentium*-induced colitis by regulating ER stress in mice. Chen et al. (2024) showed that dietary supplementation with *Bacillus subtilis* HW2 significantly alleviated ER stress in the ileum of broilers with necrotizing enteritis. Our previous studies have proved that *Bacillus amyloliquefaciens* SC06 (SC06) improved the antioxidant capacity and intestinal barrier function of piglets and IPEC-1 cells (Wang et al., 2017b; Du et al., 2018). However, whether SC06 can attenuate the intestinal ER stress level in weaned piglets remains unclear.

Gut microbiota can affect the intestinal redox state by producing metabolites such as SCFAs and polyphenolic metabolites (Zhao et al., 2023). Lee et al. (2016) showed that the changes in gut microbiota are closely related to OS in weaned piglets. Fu et al. (2021) suggested that the relative abundance of Firmicutes and Actinobacteria, the genus *Ruminococcaceae UCG-005*, and members of *Eubacterium coprostanoligenes* was increased in the intestinal tract of oxidatively-stressed piglets.

Hence, the present study aimed to reveal the effects of dietary SC06 supplementation on the growth performance, ileal barrier function, OS and ER stress in diquat (DQ)-treated weaned piglets by using ileal mucosal transcriptome and microbiome analyses.

2 Materials and methods

2.1 Experimental design

A total of 32 weaned male piglets (Duroc × Landrace × Yorkshire, 29-day-old) with similar initial body weights (7.51 ± 0.39 kg) were assigned to a 2 × 2 factorial design with two SC06 levels (0 or 1×10^8 CFU/g) and two DQ levels (0 or 10 mg/kg body weight). Therefore, the 4 treatments were: control group (Con), basal diet; DQ group, basal diet and intraperitoneal injection of 10 mg/kg DQ; SC06 group, basal diet containing 1×10^8 CFU/g SC06; SC06 + DQ group, basal diet containing 1×10^8 CFU/g SC06 and intraperitoneal injection of DQ (10 mg/kg body weight), with 8 piglets per pen. The dosage of DQ was based on Zheng et al. (2017). At day 22 of experiment, DQ (diquat dibromide monohydrate, PS365; Sigma, United States) was intraperitoneally injected. The SC06 powder was pre-mixed with 1 kg of the basal diet and successively mixed into the remaining diet. The animal study was reviewed and approved by the Animal Care and Use Committee of Qingdao Agricultural University (protocol number 20221125374). We have followed the ARRIVE guidelines for reporting animal research. The basal diet of piglets was prepared according to NRC 2012 and the composition and nutrient levels were listed in Table 1.

2.2 Sample collection

At the 29th day of the trial, blood samples were collected from the vena cava anterior and were centrifuged for 10 min at 4°C (3,000 × g,

TABLE 1 Composition and nutrient levels of basal diets (air-dry basis) %.

Item	Content
Ingredients	
Corn	60.00
Soybean meal	12.30
Extruded soybean	3.70
Fish meal	3.46
Whey powder	5.00
Soybean protein concentrate	6.60
Soybean oil	2.60
Sucrose	3.00
Limestone	0.60
$CaHPO_4$	0.90
NaCl	0.10
L-Lys·HCl	0.50
DL-Met	0.10
L-Thr	0.10
L-Trp	0.04
Chloride choline	0.10
Premix[a]	0.50
Acidifier	0.40
Total	100.00
Nutrient levels[b]	
DE/(MJ/kg)	14.73
CP (%)	19.03
Ca (%)	0.79
AP (%)	0.37
D-Lys (%)	1.33
D-Met (%)	0.38
Thr (%)	0.74
Trp (%)	0.23

[a]The premix provided the following per kg of diets: VA 2000 IU, VD_3 300 IU, VE 20 IU, VB_1 2.0 mg, VB_2 4.0 mg, VB_6 5.0 mg, VB_{12} 0.02 mg, VK_3 3.0 mg, biotin 0.1 mg, folic acid 0.5 mg, pantothenic acid 15.0 mg, nicotinic acid 0.75 mg, Cu (as copper sulfate) 25 mg, Fe (as ferrous sulfate) 100 mg, Mn (as manganese sulfate) 10 mg, Zn (as zinc sulfate) 100 mg, I (as potassium iodide) 0.30 mg, Se (Na_2SeO_3) (as sodium selenite) 100 mg, phytase, 100 IU.
[b]The nutrient levels were calculated values.

Centrifuge 5804R, Eppendorf, Germany) to obtain the serum. Serum samples were stored at −20°C. Mid-ileal segments were carefully dissected and rinsed with sterilized saline. Part of the ileal segment was cut and fixed in 4% paraformaldehyde solution. Then, cotton swabs were used to wipe the ileal mucosa in order to obtain the mucosal bacteria. The swab tips were collected in 1.5 mL centrifuge tubes. Moreover, ileal mucosa samples were also gently scraped off. The swab tips and ileal mucosa samples were placed in liquid nitrogen immediately and then stored at −80°C for further analysis.

2.3 Biochemical analyses

Ileal mucosa samples were homogenized with ice-cold physiologic saline (1:10, w/v) and centrifuged at 2,000 × g for 10 min (4°C), and the protein concentration in the supernatant was determined using a BCA Protein Concentration Determination Kit (Beyotime Biotechnology Co., Ltd., Shanghai, China). The concentrations of malondialdehyde (MDA, Cat. YJ54526), D-Lactate (Cat. YJ75986) and the diamine oxidase (DAO, Cat. YJ98519) and the activities of catalase (CAT, Cat. YJ22695), superoxide dismutase (SOD, Cat. YJ45986) and glutathione peroxidase (GSH-Px, Cat. YJ36985) were determined using by Enzyme-linked immunosorbent assay (ELISA) kits (Enzyme-Linked Biotechnology Co., Ltd., Shanghai, China). The level of ROS was determined by ELISA kit (ROS, Cat. MM-121201) from Meimian Industrial Co., Ltd. (Jiangsu, China). The experimental procedures were performed in strict accordance with the manufacturer's instructions. The absorbance was read by a microplate reader (SpectraMax iD3, Molecular Devices, Shanghai, China).

2.4 Hematoxylin–eosin staining

The ileal segments were embedded in paraffin, and the section of each sample was mounted on glass slides for hematoxylin–eosin (HE) staining. The villus was observed under an OLYMPUS microscope (OLYMPUS, Japan) using the HMIAS-2000 (HMIAS, China) image analysis system. Villus height and crypt depth were measured according to the method of Shan et al. (2019).

2.5 Transmission electron microscope

The ileal tissue was cut (1 mm^3) and fixed with electron microscope fixative (Xavier Biotechnology Co., Ltd., Wuhan, China). The ultrathin sections were cut using a ultramicrotome (Leica EM UC7, Wetzlar, Germany) and stained with uranyl acetate. Electron micrographs of the samples were then captured by the transmission electron microscope (TEM) (HITACHI HT7700 120 kV, Tokyo, Japan).

2.6 Real-time quantitative PCR

RNA extraction and real-time quantitative PCR (RT-qPCR) were performed according to our previous study (Yuan et al., 2023a). In brief, total RNA was extracted from ileal mucosa using Trizol reagent (Tiangen Biochemical Technology Co., Ltd., Beijing, China). RT-qPCR was then performed by using the TB Green® Premix Ex Taq™ kit (TaKaRa) and BioRad CFX96™ Real-Time PCR system (Bio-Rad Laboratories, Hercules, CA). The thermal cycling protocol and primer design methods were referred to our previous report (Yuan et al., 2023b). The forward and reverse primers of the genes are presented in Supplementary Table S1. Glyceraldehyde-3-phosphate dehydrogenase (*GAPDH*) and *β-actin* as housekeeping genes were used to normalize target genes transcript levels.

2.7 Western blotting

The protocol was based on previous study (Liu et al., 2019). In brief, total protein was extracted from ileal mucosa and the protein concentration was measured by BCA kit (Beyotime Biotechnology Co., Ltd., Shanghai, China). Protein samples were separated by electrophoresis on SDS-PAGE and transferred electrophoretically to a nitrocellulose membranes membrane. The membrane was blocked and then incubated with primary antibodies overnight (4°C). The membrane was rinsed and then incubated with the secondary antibodies for 60 min at room temperature. The antibodies, including *β*-actin (1:1000, Cat. GB11001), GRP78 (1:500, Cat. GB11098), PERK (1:500, Cat. GB11510), ATF4 (1:500, Cat. GB11157), Claudin-1 (1:500, Cat. GB112543), Occludin (1:1000, Cat. GB11149) and ZO-1 (1:500, Cat. GB111402) were purchased from Servicebio Technology Co., Ltd. (Wuhan, China) and photoshop-PERK (p-PERK) was obtained from Affinity Biosciences Co., Ltd. (OH, United States). The blots were then developed with an ECL detection system (Invitrogen iBright FL1000, Thermo Fisher Scientific, New York) as per the manufacturer's instructions. Image J software (National Institutes of Health, Bethesda, United States) was used to quantitate relative protein expression.

2.8 Total RNA extraction, mRNA library construction and sequencing

Total RNA from ileal mucosa was purified by ethanol precipitation and CTAB-PBIOZOL reagent according to the manufacturer's instructions. Mucosal samples were ground with liquid nitrogen. The ground powder sample was transferred to 1.5 mL of preheated 65°C CTAB-pBIOZOL reagent, and then the sample was incubated in a Thermo mixer for 15 min at 65 ° C to allow complete dissociation of the nucleoprotein complex. After centrifuge at 12,000 × g for 5 min at 4°C, 400 μL of chloroform was added in the supernatant and centrifuged at 12,000 × g for 10 min at 4°C. The supernatant was transferred to a new 2 mL tube. Then, 700 μL acidic phenol and 200 μL chloroform were added followed by centrifuging 12,000 × g for 10 min at 4°C. Equal volume of aqueous phase of chloroform was added in aqueous phase and centrifuged at 12,000 × g for 10 min at 4°C. The supernatant was collected and equal volume of supernatant of isopropyl alcohol was added and placed at −20°C for 2 h for precipitation. After that, the mix was centrifuged at 12,000 × g for 20 min at 4°C and then supernatant was removed. After washing with 1 mL of 75% ethanol, the RNA pellet was air-dried in the biosafety cabinet and was dissolved by adding 50 μL of DEPC-treated water. Subsequently, total RNA was identified and quantified using the Nano Drop and Agilent 2100 bioanalyzer (Thermo Fisher Scientific, MA, United States).

mRNA was purified using oligo(dT) magnetic beads. Purified mRNA was cleaved into small fragments with fragmentation buffer at the appropriate temperature. Then first-strand cDNA was generated using random hexamer-primed reverse transcription, followed by a second-strand cDNA synthesis. Afterwards, A-Tailing Mix and RNA Index Adapters were added by incubating to end repair. The cDNA fragments obtained from previous step were amplified by PCR, and products were purified by Ampure XP Beads, then dissolved in EB solution. The product was validated for quality control on an Agilent 2100 bioanalyzer. The double-stranded PCR products from the previous step were denatured by heat with the splinted oligonucleotide sequence and cycled to obtain the final library. Single strand circle DNA (ssCir DNA) was formatted into the final library.

Qualified libraries were denatured to single-stranded PCR products. The reaction system and cycle program were subsequently configured and set up. Single-stranded cyclized products were produced, whereas non-cyclized linear DNA molecules were digested. Single-stranded circular DNA molecules were replicated by rolling cycle amplification technology to generate DNA nanospheres (DNBS) containing multiple copies of DNA. Then, DNB of sufficient quality was loaded into patterned nanoarrays using high-intensity DNA nanochip technology and sequenced by combinatorial probe anchored synthesis (cPAS).

2.9 Sequencing data analysis

Fastp was used to filter raw data, mainly to remove reads with adapters. When the N content of any sequencing reads exceeded 10% of the base number of the reads, the paired reads were removed. Paired bases were removed when the number of low-quality bases ($Q \leq 20$) exceeded 50% of the total number of bases. All subsequent analyses were based on clean reads.

The reference genome and its annotation files were downloaded from the website.[1] Feature Counts was used to calculate the gene alignments and then calculated the fragments per kilobase of exon model per million mapped fragments of each gene based on the gene length. DESeq2 was used to analyze the differential expression between the two groups, and the *p*-value was corrected using the Hochberg method. The corrected *p*-value <0.05 and $|\log_2 \text{foldchange}| \geq 1$ were used as a threshold expressed significant difference. Enrichment analysis was performed based on hypergeometric test. KEGG was tested for hypergeometric distribution by pathway. All genes raw data has been deposited in the NCBI with the Bioproject ID PRJNA1021385.

2.10 DNA extraction and microbiological analysis

The fecal genomic DNA extraction kit of TIANamp stool DNA kit (Tiangen Biotech Co., Ltd., Beijing, China) was used to extract the DNA of mucosa bacteria, and the experiment was carried out according to the instructions. DNA was checked for integrity and quantified. The V3–V4 region was amplified by PCR using 338F (5′-ACTCCTACGGGAGGCAGCA-3′) and 806R (5′-GGACTACHVGGGTWTCTAAT-3′) primers and finally sent to Illumina MiSeq platform for sequencing. The original tags were quality filtered using QIIME2 2019.4 software and integrated through FLASH software. After removing the chimeric sequences, the ASVs (amplicon sequence variants) were clustered by 97% similarity using uCLUST 1.2.22, and the representative sequences of each cluster were annotated according to the SILVA database. Indices of alpha diversity (Chao1, Simpson, Shannon, Pieiou_e, Observed_species, Faith_pd, Goods_coverage) of the samples were evaluated. Principal coordinate analysis (PCoA) was undertaken for all samples following analysis through application of Bray–Curtis dissimilarity and unweighted UniFrac using R packages (3.2.0).

Microbial functions were predicted by PICRUSt2 (Phylogenetic investigation of communities by reconstruction of unobserved states) KEGG[2] databases. All DNA raw data was submitted to the NCBI database under BioProject ID PRJNA1012569.

2.11 Statistical analysis

The effects of SC06, DQ and their interactions on biochemical parameters were assessed using analysis of variance (ANOVA) and the general linear model procedure using IBM SPSS Statistics 18.0 (IBM Corp., Armonk, NY, United States). Multiple mean comparisons were performed using univariate ANOVA and Duncan's multiple range test. All data was graphed by GraphPad Prism 8 (GraphPad Software, La Jolla, CA) and was expressed as the mean and standard error of the mean (SEM). The online analysis platform Biodeep[3] was used to conduct Pearson's correlation analysis between ER stress-related genes and bacterial genus abundance. All means and comparisons were considered statistically significant at $p < 0.05$.

3 Results

3.1 SC06 supplementation improved the growth performance of weaned piglets

The DQ injection significantly decreased the ADG ($p < 0.01$). The SC06 supplementation increased the ADG ($p = 0.03$). Moreover, the interaction between DQ and SC06 (SC06 × DQ) reversed DQ-induced changes in ADG ($p = 0.04$) (Table 2).

3.2 SC06 supplementation improved the ileal morphology and decreased the ileal permeability of weaned piglets

The ileal morphology was explored by HE staining and TEM. HE staining results showed that DQ injection significantly

1 https://ftp.ncbi.nlm.nih.gov/genomes/refseq/vertebrate_mammalian/Sus_scrofa/latest_assembly_versions/GCF_000003025.6_Sscrofa11.1/

2 https://www.kegg.jp/

3 https://www.biodeep.cn/home

TABLE 2 Effect of SC06 on growth performance in weaned piglets.

Item	Initial weight (kg)	Final weight (kg)	ADG (g)
Con	7.49	21.53	547.03[a]
DQ	7.49	19.16	405.36[b]
SC06	7.52	22.21	551.79[a]
SC06 + DQ	7.52	21.81	508.93[a]
SEM	0.39	1.22	39.65
Main effect			
SC06			
–			476.19
+			530.36
DQ			
–			549.41
+			457.14
p-value			
SC06			0.03
DQ			<0.01
Interaction			0.04

Mean values within a row with unlike letters are significantly different ($p < 0.05$). ADG, average daily gain; Con, control diet; DQ, control diet plus diquat injection; SC06, control diet containing 1×10^8 CFU/g *Bacillus amyloliquefaciens* SC06; SC06 + DQ, control diet containing 1×10^8 CFU/g *Bacillus amyloliquefaciens* SC06 plus diquat injection, $n = 6$.

decreased the villus height and V/C value ($p < 0.01$) and increased the crypt depth ($p = 0.03$). The SC06 supplementation increased villus height and V/C value ($p < 0.01$). Moreover, SC06 × DQ increased the villus height and V/C value ($p < 0.01$) in DQ-injected piglets (Figure 1A). According to the TEM analysis, we found that the tight junctions were clear and complete in the Con, SC06 and SC06 + DQ groups, but the tight junctions were not clear and the paracellular spaces were expanded in the DQ group (Figure 1B). Furthermore, the serum DAO and D-lactate levels were elevated by the DQ injection ($p < 0.01$). The SC06 supplementation decreased the levels of DAO and D-lactate ($p < 0.01$). SC06 × DQ also lowered the levels of DAO and D-lactate in DQ-treated piglets (Figure 1C). Protein expressions of tight junctions showed that the DQ treatment significantly down-regulated the expressions of claudin-1, occludin and ZO-1 ($p < 0.01$). The SC06 supplementation up-regulated the expressions of claudin-1, occludin and ZO-1 ($p < 0.01$). Moreover, SC06 × DQ increased these protein expressions in DQ-treated piglets (Figure 1D).

3.3 SC06 supplementation attenuated the ileal OS of weaned piglets

The DQ injection elevated the levels of MDA and ROS ($p < 0.01$), and decreased activities of CAT, SOD and GSH-Px ($p < 0.01$). The SC06 supplementation decreased the levels of MDA and ROS ($p < 0.01$), and increased activities of CAT, SOD and GSH-Px ($p < 0.01$). Moreover, SC06 × DQ reversed the changes in MDA, ROS, CAT, SOD and GSH-Px in DQ-treated piglets (Figure 2).

3.4 SC06 supplementation attenuated the ileal ER stress of weaned piglets

Figure 3A showed that the DQ treatment significantly increased the gene expressions of *GRP78* ($p < 0.01$), *PERK* ($p < 0.01$), *eIF2α* ($p < 0.01$), *IRE1-α* ($p = 0.03$), *CHOP* ($p < 0.01$), *ERO1α* ($p = 0.01$) and *ATF4* ($p < 0.01$). The SC06 supplementation significantly decreased the gene expressions of *GRP78* ($p < 0.01$), *PERK* ($p < 0.01$), *eIF2α* ($p = 0.01$), *ATF6* ($p = 0.03$), *IRE1-α* ($p < 0.01$), *CHOP* ($p < 0.01$), *ERO1α* ($p < 0.01$) and *ATF4* ($p < 0.01$). Moreover, SC06 × DQ increased the gene expressions of *GRP78* ($p < 0.01$), *PERK* ($p < 0.01$), *eIF2α* ($p < 0.01$), *ATF6* ($p = 0.03$), *IRE1-α* ($p = 0.01$), *CHOP* ($p < 0.01$), *ERO1α* ($p < 0.01$) and *ATF4* ($p < 0.01$) in DQ-treated piglets. Western blotting results further indicated that the expressions of GRP78 ($p < 0.01$), ATF4 ($p = 0.03$) and p-PERK/PERK ($p < 0.01$) were significantly up-regulated. The supplementation of SC06 down-regulated the expressions of GRP78, ATF4, PERK and p-PERK/PERK ($p < 0.01$). Besides, SC06 × DQ also decreased the expressions of GRP78 and p-PERK/PERK ($p < 0.01$) in DQ-injected piglets (Figure 3B).

3.5 Transcription changes of weaned piglets with SC06 supplementation

A total of 105 common genes were found between the Con vs. DQ and Con vs. SC06 groups, 589 common genes were found between the Con vs. DQ and DQ vs. SC06 + DQ groups, 90 common genes were found between the Con vs. SC06 and DQ vs. SC06 + DQ groups (Figure 4A). Moreover, compared with the Con group, 702 genes were upregulated (such as *ZNF473*, *GGT5*, *FBXO39*, etc.) and 191 genes were downregulated (such as *GPT2*, *NR1D1*, *SOD3*, etc.) in the DQ group ($p < 0.05$); 104 genes were upregulated (such as *SLC25A37*, *CLCN1*, *TRUB1*, etc.) and 154 genes were downregulated (such as *DPYS*, *APOA4*, *SLC25A20*, etc.) in the SC06 group ($p < 0.05$). Compared with the DQ group, 225 genes were upregulated (such as *ZNF473*, *PRDX6*, *GPT2*, etc.) and 971 genes were downregulated (such as *GGT5*, *OGT*, *CTSK*, *SLC25A37*, etc.) in the SC06 + DQ group ($p < 0.05$) (Figure 4B and Supplementary Tables S2–S4).

3.6 Functional analysis of the DEGs

KEGG analysis showed that the enriched pathways of DEGs between the DQ group and the Con group included NF-κB signaling pathway, Intestinal immune network for IgA production, Phagosome, etc. The enriched pathways of DEGs between the SC06 group and the Con group included PI3K-Akt signaling pathway, NF-κB signaling pathway, Phagosome, etc. The enriched pathways of DEGs between the SC06 + DQ group and the DQ group included Arginine biosynthesis, Protein digestion and absorption, Glutathione metabolism, etc. (Figure 5).

3.7 Validation of the expressions of DEGs by RT-qPCR

The DEGs that related to OS and ER stress were selected for validation by RT-qPCR. Results showed that the DQ treatment

10.3389/fmicb.2024.1362487

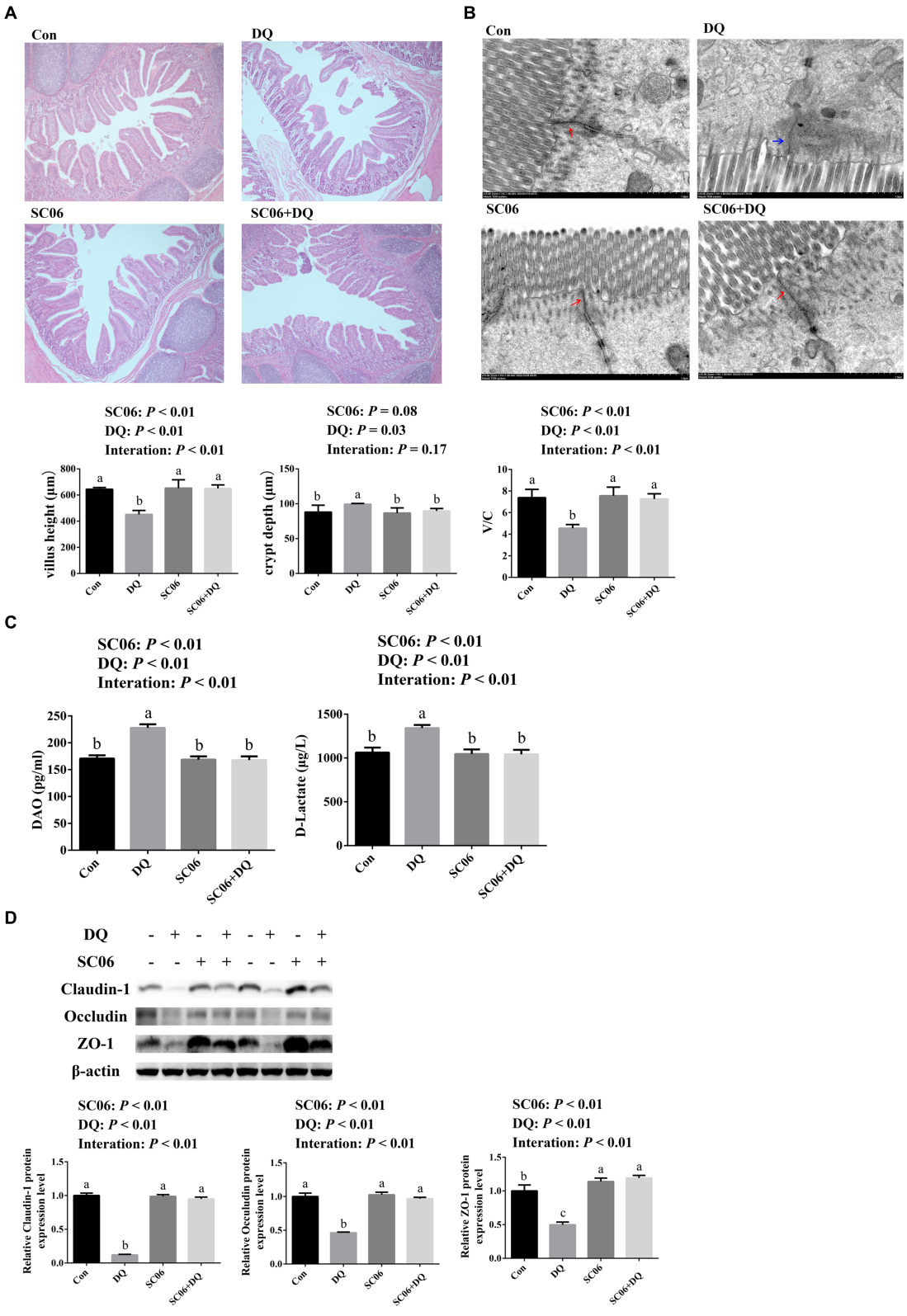

FIGURE 1
Effects of SC06 on the ileal morphology and permeability of piglets. **(A)** HE staining sections, images were photographed under 50× magnification, $n = 6$. **(B)** TEM section, images were photographed under 15 kx magnification, $n = 3$. **(C)** Serum DAO and D-lactate levels, $n = 6$. **(D)** Expressions of tight junction proteins, $n = 3$. ^{a,b,c}Mean value within a row with no common superscript differ significantly ($p < 0.05$). Red arrows indicate normal tight junctions and blue arrows indicate abnormal tight junctions, V/C, villus height/crypt depth; DAO, diamine oxidase; ZO-1, zona occludens 1; Con, control diet; DQ, control diet plus diquat injection; SC06, control diet containing 1×10^8 CFU/g *Bacillus amyloliquefaciens* SC06; SC06 + DQ, control diet containing 1×10^8 CFU/g *Bacillus amyloliquefaciens* SC06 plus diquat injection.

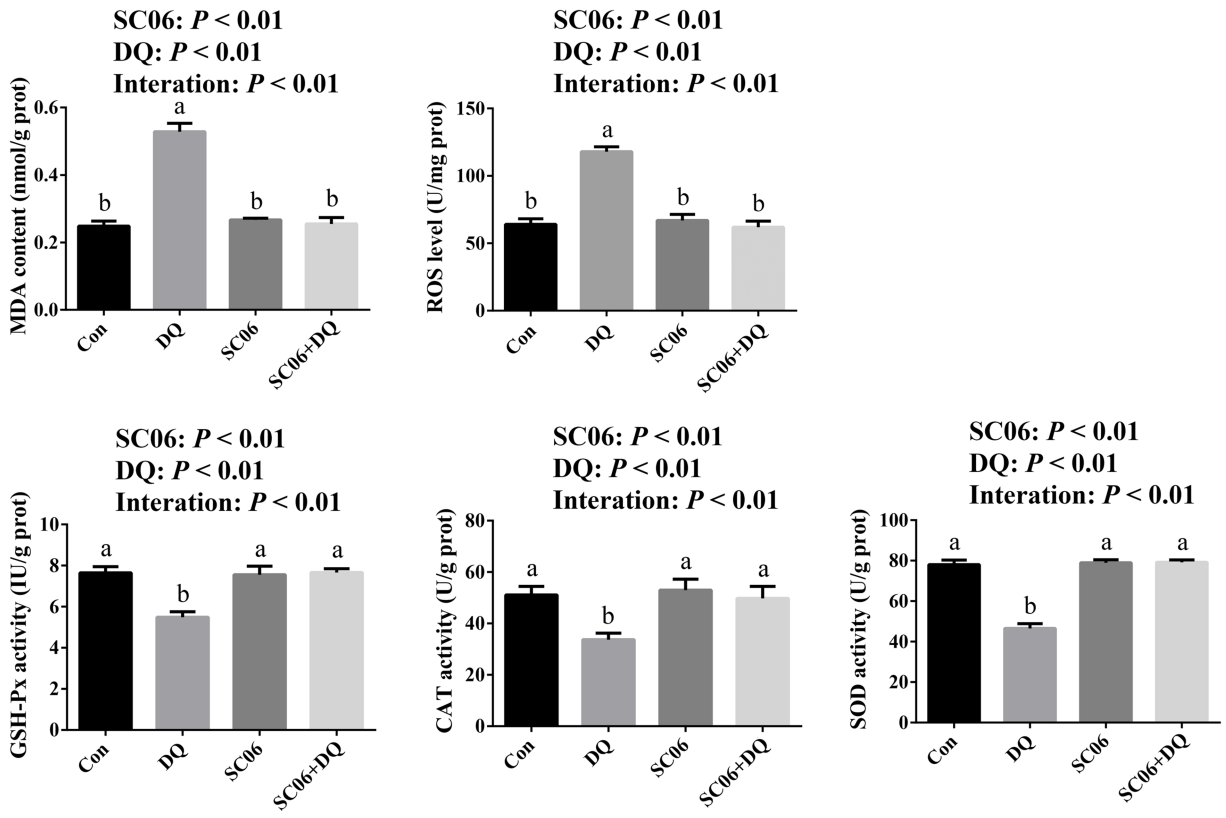

FIGURE 2
Effects of SC06 on the ileal oxidative stress of piglets. [a,b]Mean value within a row with no common superscript differ significantly ($p < 0.05$), $n = 6$. ROS, reactive oxygen species; MDA, malondialdehyde; GSH-Px, glutathione peroxidase; CAT, catalase; SOD, superoxide dismutase; Con, control diet; DQ, control diet plus diquat injection; SC06, control diet containing 1×10^8 CFU/g *Bacillus amyloliquefaciens* SC06; SC06 + DQ, control diet containing 1×10^8 CFU/g *Bacillus amyloliquefaciens* SC06 plus diquat injection.

increased the expressions of *GGT5, SLC25A37, OGT, CTSK* ($p < 0.01$) and *ZC3H7A* ($p = 0.04$), and decreased the expressions of *GPT2, SOD3, PRDX6* and *PDZK1* ($p < 0.01$). The SC06 supplementation decreased the expressions of *GGT5, SLC25A37, OGT, CTSK* ($p < 0.01$), *ZC3H7A* ($p = 0.05$), and increased the expressions of *SOD3*, *PRDX6* ($p < 0.01$) and *PDZK1* ($p = 0.02$). Moreover, SC06 × DQ reversed the changes in *GGT5, SLC25A37, OGT*, *CTSK*, *PRDX6* ($p < 0.01$) and *SOD3* ($p = 0.04$) in DQ-treated piglets (Figure 6).

3.8 Ileal mucosal microbiota changes of weaned piglets with SC06 supplementation

The α-diversity indices, including Chao1, Simpson, Shannon, Pielou_e, Observed_species, Faith_pd and Goods_coverage were not significantly different between the Con and DQ groups, Con and SC06 groups, as well as DQ and SC06 + DQ groups (Figure 7A). Moreover, there was no difference in the β-diversity among groups (Figure 7B). However, the ileal mucosal microbiota composition was significantly influenced by different treatments. At the phylum level, the DQ treatment decreased the abundance of Acidobacteria compared with the Con group ($p < 0.05$). As for the top 20 family, we found that in comparison with the Con group, the DQ treatment increased the abundance of Turicibacteraceae ($p < 0.05$); the SC06 treatment decreased the abundance of Ruminococcaceae ($p < 0.05$). Compared with the DQ group, the SC06 + DQ treatment increased the abundance of Pasteurellaceae ($p < 0.05$). As for the top 20 genus, compared with the Con group, the DQ treatment increased the abundances of *Clostridium* and *Turicibacter* ($p < 0.05$); the SC06 treatment increased the abundance of *Lactobacillus* ($p < 0.05$). Compared with the DQ group, the SC06 + DQ treatment decreased the abundance of *Clostridium* ($p < 0.01$) and increased the abundance of *Actinobacillus* ($p < 0.05$) (Figure 8 and Supplementary Table S5).

3.9 Functional analysis of the ileal mucosal microbiota

Compared with the Con group, piglets in the DQ group had lower levels of microbial genes associated with Arachidonic acid metabolism ($p < 0.05$) and Glycosphingolipid biosynthesis-lacto and neolacto series ($p < 0.05$), and higher levels of microbial genes related to Betalain biosynthesis ($p < 0.01$), Pathways in cancer ($p < 0.05$) and Hypertrophic cardiomyopathy ($p < 0.05$); piglets in the SC06 group had lower levels of microbial genes associated with Spliceosome ($p < 0.01$) and Basal transcription factors ($p < 0.05$), and higher levels of microbial genes related to Beta-alanine metabolism ($p < 0.05$), Salivary secretion ($p < 0.01$), Nitrotoluene degradation ($p < 0.05$), Flagellar assembly ($p < 0.05$) and Parkinsons disease ($p < 0.01$). Moreover, compared with the DQ group, piglets in the SC06 + DQ group had higher levels of microbial genes related to ECM-receptor interaction ($p < 0.05$) and Ethylbenzene degradation ($p < 0.01$) (Figure 9).

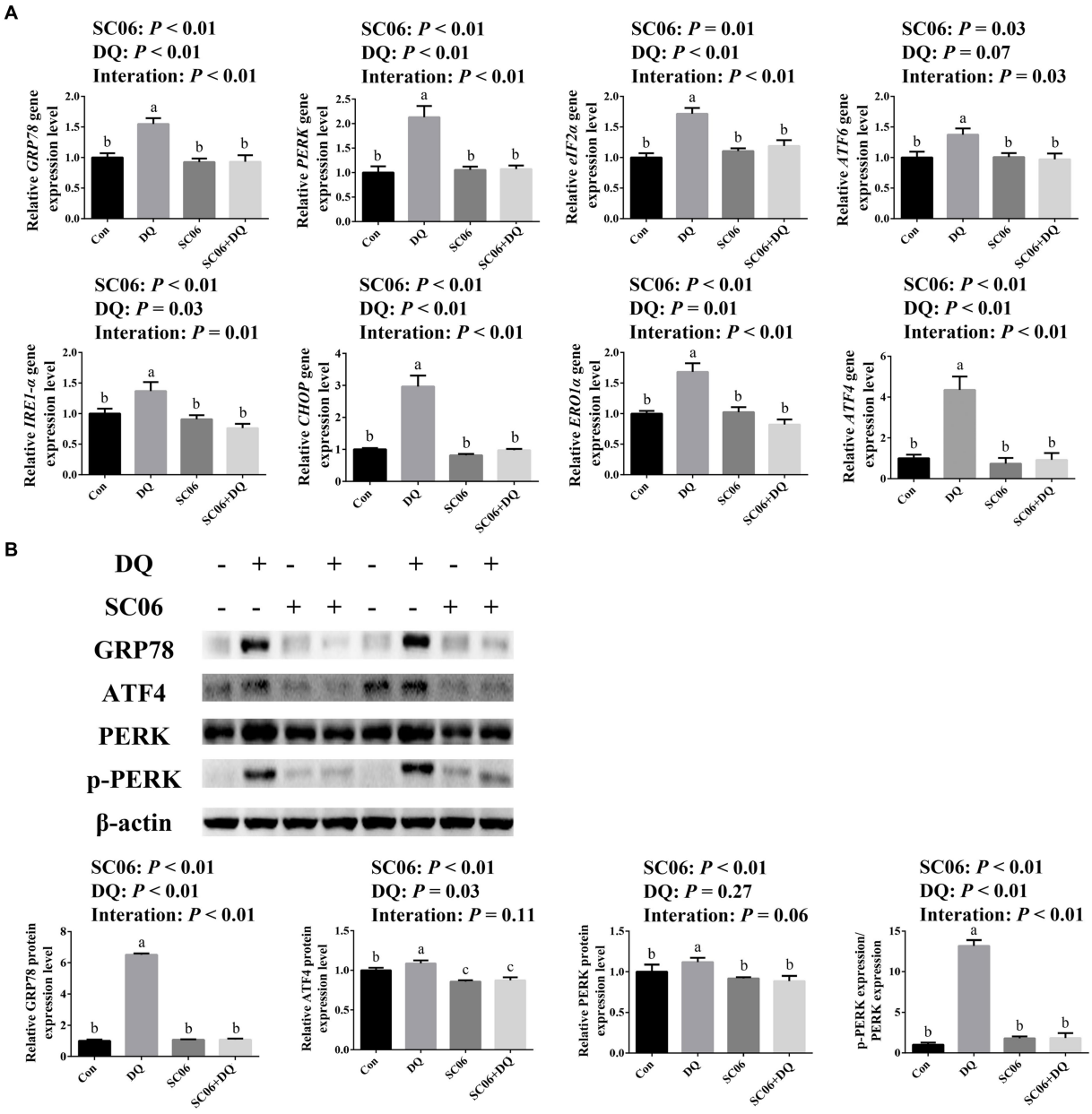

FIGURE 3
Effects of SC06 on the ileal ER stress of piglets. **(A)** Expressions of ER stress-related genes, $n = 6$. **(B)** Expressions of ER stress-related proteins, $n = 3$. [a,b,c]Mean value within a row with no common superscript differ significantly ($p < 0.05$). *GRP78*, glucose-regulated protein 78; *PERK*, protein kinase RNA-like endoplasmic reticulum kinase; *eIF2α*, phosphorylation of eukaryotic initiation factor-2α; *ATF6*, activating transcription factor 6; *IRE1-α*, inositol-requiring enzyme 1α; *CHOP*, C/EBP homologous protein; *ERO1α*, endoplasmic reticulum oxidoreductin 1α; *ATF4*, activating transcription factor 4; Con, control diet; DQ, control diet plus diquat injection; SC06, control diet containing 1×10^8 CFU/g *Bacillus amyloliquefaciens* SC06; SC06 + DQ, control diet containing 1×10^8 CFU/g *Bacillus amyloliquefaciens* SC06 plus diquat injection.

3.10 Correlation analysis between ER stress-related genes and bacterial genus abundance

The correlation between the ER stress-related genes and the significantly altered top 20 genera was shown in Figure 10. We found that *SLC25A37* ($r = 0.62$, $p < 0.01$), *ERO1α* ($r = 0.58$, $p < 0.01$), *CHOP* ($r = 0.48$, $p < 0.05$), *ATF4* ($r = 0.47$, $p < 0.05$) and *GGT5* ($r = 0.47$, $p < 0.05$) were positively correlated with the abundance of *Clostridium*. *SOD3* ($r = -0.52$, $p < 0.01$) and *PRDX6* ($r = -0.48$, $p < 0.05$) were significantly negatively correlated with *Clostridium*. Moreover, *eIF2α* was positively correlated with the abundance of *Turicibacter* ($r = 0.48$, $p < 0.05$) (Figure 10 and Supplementary Table S6).

4 Discussion

In the production of pig farming, various factors can induce intestinal OS and impair intestinal barrier function, leading to economic losses. Probiotics are well-known in regulating growth

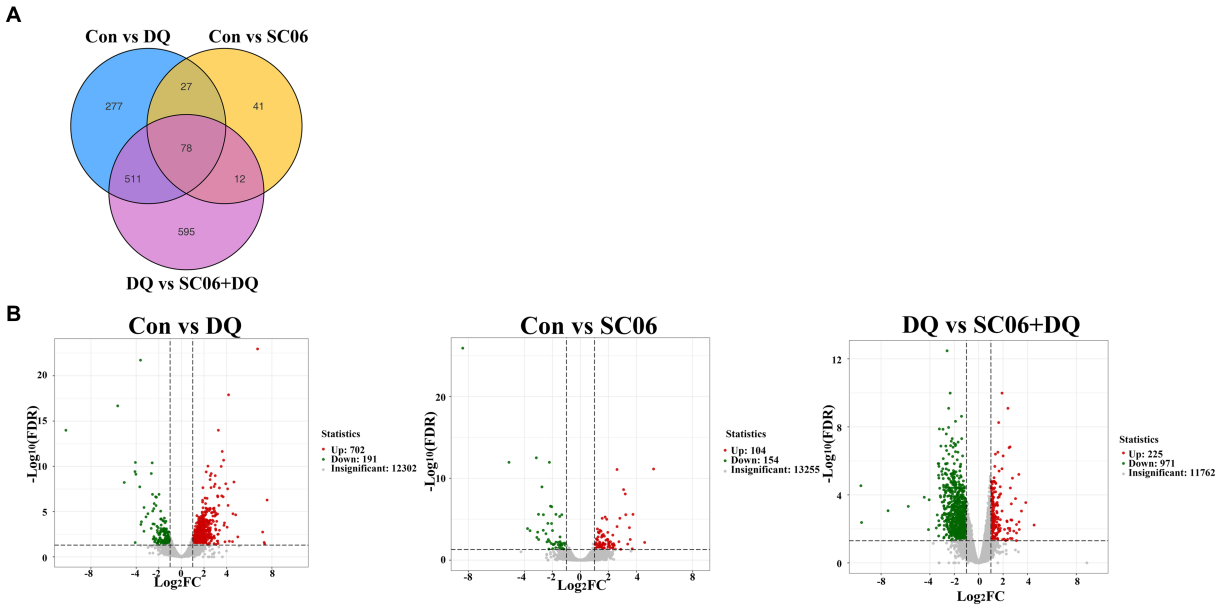

FIGURE 4
Differentially expressed genes in the ileal mucosal of weaned piglets. **(A)** Venn diagrams between different comparation groups. **(B)** Volcano plot between groups. *n* = 3. Con, control diet; DQ, control diet plus diquat injection; SC06, control diet containing 1×10^8 CFU/g *Bacillus amyloliquefaciens* SC06; SC06 + DQ, control diet containing 1×10^8 CFU/g *Bacillus amyloliquefaciens* SC06 plus diquat injection.

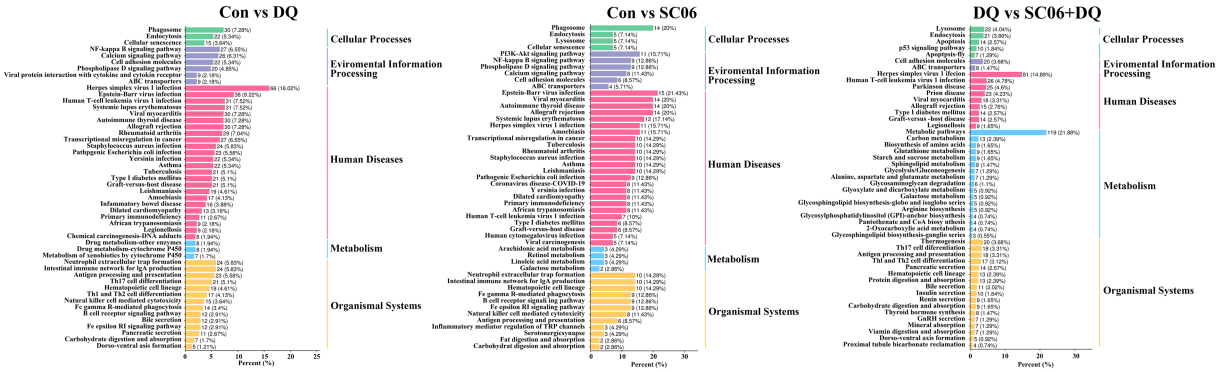

FIGURE 5
KEGG pathway analysis of genes in the ileal mucosal of weaned piglets. *n* = 3. Con, control diet; DQ, control diet plus diquat injection; SC06, control diet containing 1×10^8 CFU/g *Bacillus amyloliquefaciens* SC06; SC06 + DQ, control diet containing 1×10^8 CFU/g *Bacillus amyloliquefaciens* SC06 plus diquat injection.

performance and gut health. In the present study, the DQ injection impaired the growth performance, ileal morphology and barrier function. Supplementation of SC06 improved the morphology, increased ADG and the expressions of tight junctions and decreased the permeability of ileum. Moreover, SC06 × DQ improved ADG, ileal morphology and barrier functions in DQ-treated piglets, which were similar to the findings of previous studies on the beneficial effects of probiotics in pig growth and intestinal health (Wang et al., 2018; Sun et al., 2023).

Excessive amounts of ROS can induce OS, causing lipid peroxidation and augmenting MDA levels. Here the elevated ileal ROS and MDA levels in DQ-treated piglets indicated the increased OS. On the contrary, the SC06 supplementation and SC06 × DQ decreased the ROS and MDA levels. The major antioxidant defense machineries for most living organisms are composed of biological antioxidants and antioxidant enzymes, such as GSH-Px, CAT and SOD. Here we found that the SC06 supplementation reversed the decreased activities of GSH-Px, CAT and SOD in DQ-treated piglets. These results were consistent with the findings showing that dietary supplementation of probiotics enhanced the antioxidant capacity of piglets (Wang et al., 2017a; Yu et al., 2022).

OS is associated with ER stress (Doyle et al., 2011). Recent studies have also shown that ER stress plays important roles in intestinal barrier function and homeostasis (Wan et al., 2022; Tan et al., 2023). Therefore, the ER stress-related parameters were further detected. We found that the ER stress-related genes, including *GRP78*, *PERK*, *eIF2α*, *ATF4*, *ATF6*, *IRE1-α*, *CHOP* and *ERO1α* were increased in the DQ-treated piglets, implying the elevation of ER stress. However, the

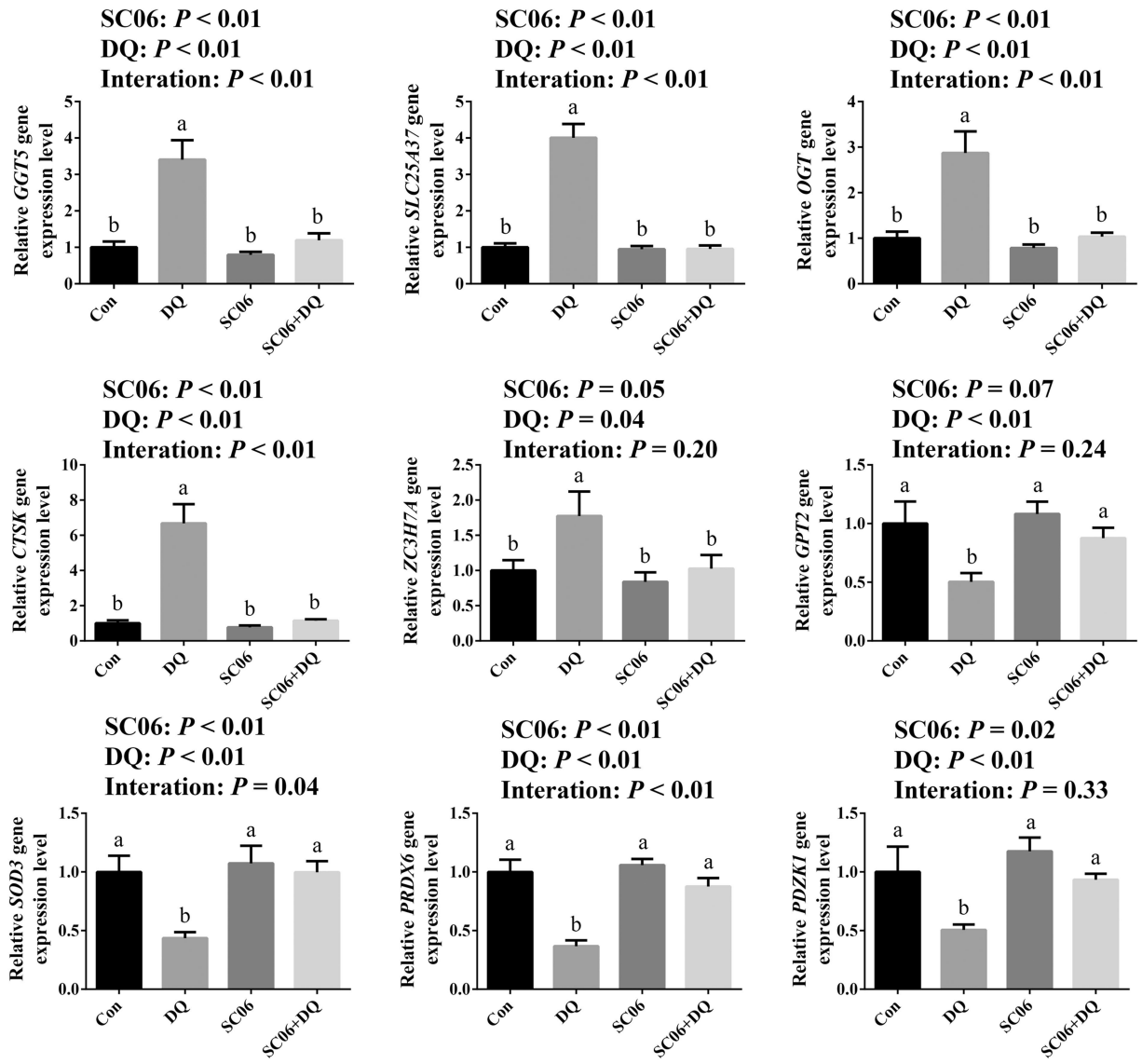

FIGURE 6
Validation of DEGs by real-time quantitative PCR. [a,b,c]Mean value within a row with no common superscript differ significantly ($p < 0.05$), $n = 6$. *GGT5*, gamma-glutamyltransferase 5; *SLC25A37*, solute carrier family 25 member 37; *OGT*, EGF domain specific O-linked N-acetylglucosamine transferase; *CTSK*, cathepsin K; *ZC3H7A*, zinc finger CCCH-type containing 7A; *GPT2*, glutamic pyruvic transaminase 2; *SOD3*, superoxide dismutase 3; *PRDX6*, peroxiredoxin 6; *PDZK1*, PDZ domain containing 1; Con, control diet; DQ, control diet plus diquat injection; SC06, control diet containing 1×10^8 CFU/g *Bacillus amyloliquefaciens* SC06; SC06 + DQ, control diet containing 1×10^8 CFU/g *Bacillus amyloliquefaciens* SC06 plus diquat injection.

SC06 supplementation or the SC06 × DQ decreased the expressions of the above genes. Western blotting further confirmed the decreased ER stress in oxidatively-stressed piglets receiving SC06.

In recent years, with the rapid development of next-generation sequencing, RNA-sequencing (RNA-seq) has become one of the important means to study genes function and screen new genes and has been widely used in animal husbandry. By using ileal transcriptome, Tang et al. (2022) identified the key differentially expressed genes (DEG) involved in the chronic heat stress-induced ER stress in growing piglets. In the study by Cui et al. (2021), transcriptome sequencing analysis revealed that OS activated the ER stress response/UPR but inhibited glutathione metabolism based on the screened DEGs. Here, ileal transcriptome demonstrated that the DEGs between the DQ and Con groups mainly included *GPT2*, *GGT5*, *SOD3*, etc. The DEGs between the SC06 and Con groups mainly included *SLC25A37*, *TRUB1*, *APOA4*, *SLC25A20*, etc. The DEGs between the SC06 + DQ and DQ groups mainly included *PRDX6*, *GGT5*, *OGT*, *CTSK*, etc. These DEGs are reported to be associated with OS or ER stress. *GGT5* is confirmed to regulate immunity and OS (Li et al., 2016). The change in *GPT2* in murine mammary cancer cells expression was accompanied by the increase of the ATF4 (Kiesel et al., 2022). SOD3 is also related to OS (Wert et al., 2018). Reduction of SOD3 was found in ursodeoxycholic acid (an ER stress inhibitor)-treated diabetic mice (Cao et al., 2016). Moreover, in the study by Bie et al. (2023), serum RNA sequencing identified *SLC25A37* is the key gene that associated with ER stress. OGT is a unique glycosyltransferase involved in metabolic reprogramming. Xu et al. (2017) indicated that OGT promotes fatty liver-associated liver

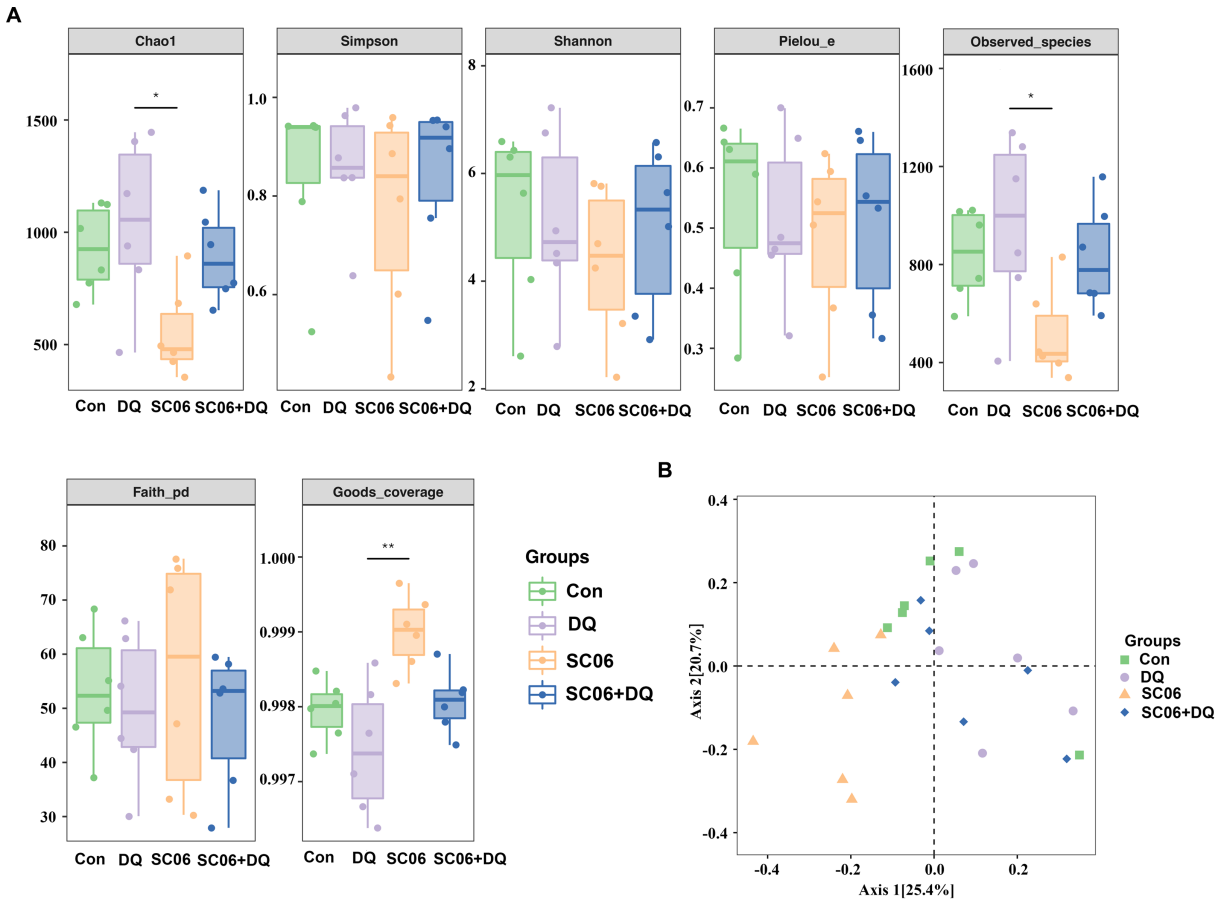

FIGURE 7
Effects of SC06 on the α- and β-diversity of ileal mucosal microbiota. **(A)** α-diversity. **(B)** β-diversity. $n = 6$. Con, control diet; DQ, control diet plus diquat injection; SC06, control diet containing 1×10^8 CFU/g *Bacillus amyloliquefaciens* SC06; SC06 + DQ, control diet containing 1×10^8 CFU/g *Bacillus amyloliquefaciens* SC06 plus diquat injection.

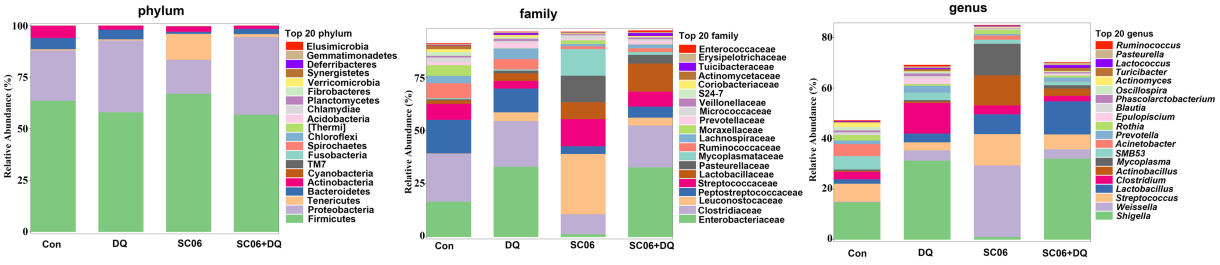

FIGURE 8
The top 20 phylum, family and genus of ileal mucosal microbiota. $n = 6$. Con, control diet; DQ, control diet plus diquat injection; SC06, control diet containing 1×10^8 CFU/g *Bacillus amyloliquefaciens* SC06; SC06 + DQ, control diet containing 1×10^8 CFU/g *Bacillus amyloliquefaciens* SC06 plus diquat injection.

cancer through inducing palmitic acid and activating ER stress. Besides, two ER stress inducers, tunicamycin and thapsigargin, induced expressions of GRP78, IRE-1, TRAP, and CTSK at both protein and mRNA levels, indicating the CTSK is also related to ER stress (Wang et al., 2011). MacLeod et al. (2019) suggested that proximal interactors of ZC3H7A were enriched in biological processes related to translation regulation, mRNA processing, cytoplasmic stress granule, and p53-mediated DNA damage signaling. PRDX6 is a cytoprotective protein by regulating intracellular ROS. Fatma et al. (2011) demonstrated that *PRDX6* deficiency in cells evoked ER stress, evidenced by increased expression or activation of proapoptotic factors, CHOP, ATF4, PERK, IRE-α and eIF2-α and by increased caspases 3 and 12 processing. PDZK1 was reported to regulate cellular apoptosis (Yu et al., 2018a), but their study also showed that leukocyte PDZK1 deficiency had no significant effect on macrophage ER stress in atherosclerotic plaques of low density lipoprotein receptor deficient

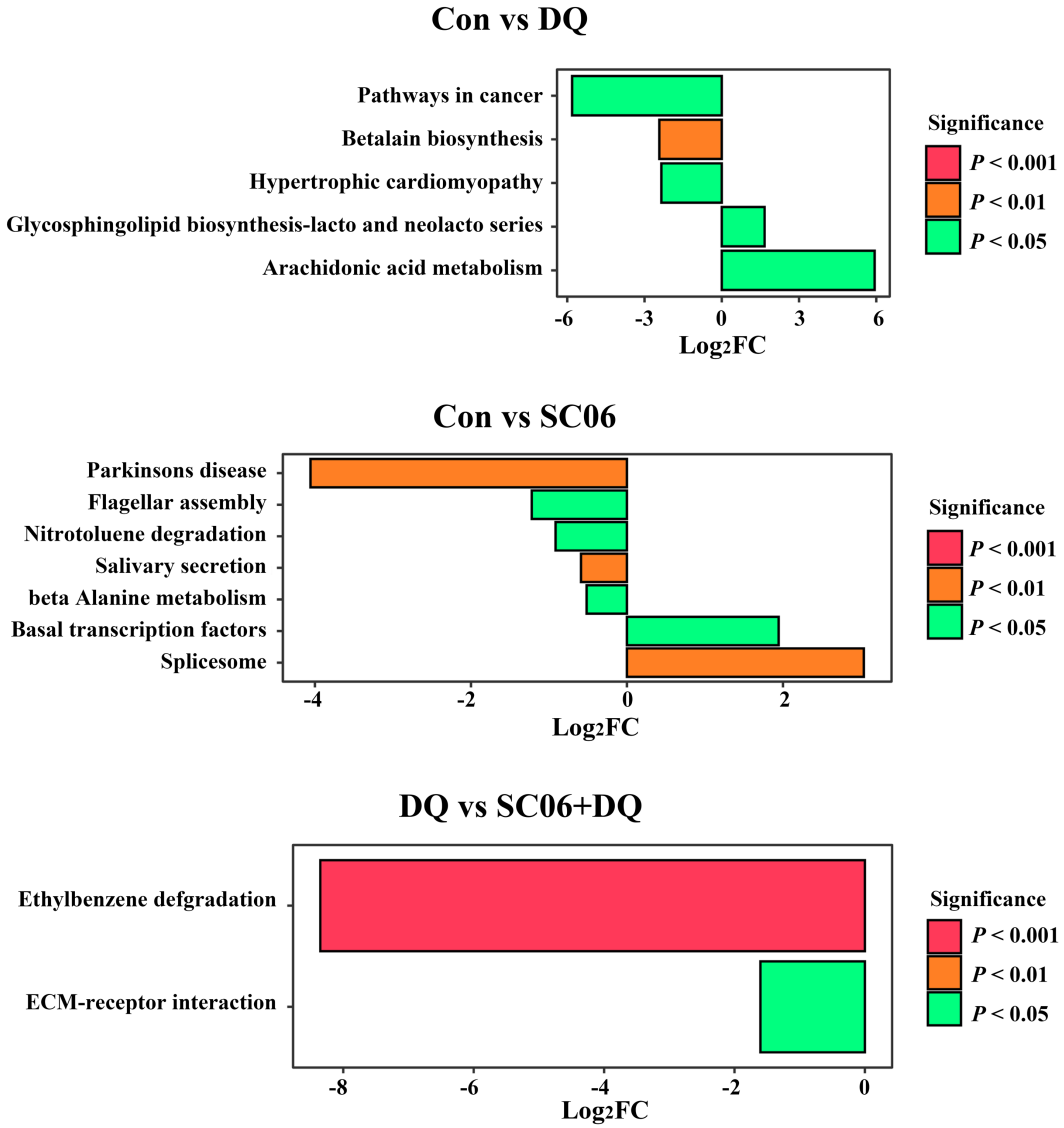

FIGURE 9
Functional prediction of ileal mucosal microbiota. *n* = 6. Con, control diet; DQ, control diet plus diquat injection; SC06, control diet containing 1×10^8 CFU/g *Bacillus amyloliquefaciens* SC06; SC06 + DQ, control diet containing 1×10^8 CFU/g *Bacillus amyloliquefaciens* SC06 plus diquat injection.

mice (Yu et al., 2018b). Taken together, the alterations of the above DEGs may be associated with the changes of OS and ER stress in different groups.

Further, KEGG analysis showed that the DEGs between the DQ and Con groups were mostly enriched in the NF-κB signaling pathway, Intestinal immune network for IgA production, Phagosome, etc. The first eukaryotic transcription factor shown to respond directly to OS was NF-κB (Schreck et al., 1991). During inflammation, ROS can mediate the activation of NF-κB, and the subsequent expression of inflammatory cytokines (Srivastava et al., 2011). In recent decades, a crosstalk between NF-κB and ER stress has been found (Li et al., 2022). ER stress can activate NF-κB by integrating functions of basal IKK activity, IRE1 and PERK (Tam et al., 2012). Therefore, the enriched NF-κB signaling pathway was in accordance with the increased OS and ER stress in the DQ group. Moreover, the DEGs between the SC06 and Con groups were mostly enriched in PI3K-Akt signaling pathway, NF-κB signaling pathway, Phagosome, etc. PI3K-Akt signaling pathway can activate Nrf2 to ameliorate OS (Wen et al., 2018). Research showed that PI3K-Akt inactivation could induce CHOP expression in ER stressed cells (Hyoda et al., 2006). Thus, the enriched PI3K-Akt signaling pathway may imply the attenuated OS and ER stress by the SC06 treatment. Additionally, the DEGs between the SC06 + DQ and DQ groups were mostly enriched in Arginine biosynthesis, Protein digestion and absorption, Glutathione metabolism, etc. Glutathione metabolism is well-known in redox regulation (Yuan et al., 2023a). Arginine, a basic amino acid, serves as an essential precursor for the synthesis of biologically important molecules such as protein, ornithine, proline, polyamines, creatine, NO and agmatine (Wu and Morris, 1998). The beneficial effects of arginine, including antioxidation were reported (Saleh and El-Demerdash, 2005). Furthermore, García-Navas et al. (2012) suggested that depletion of L-arginine induces autophagy as a cytoprotective response to endoplasmic reticulum stress in human T lymphocytes. Hence, the enriched Arginine biosynthesis and

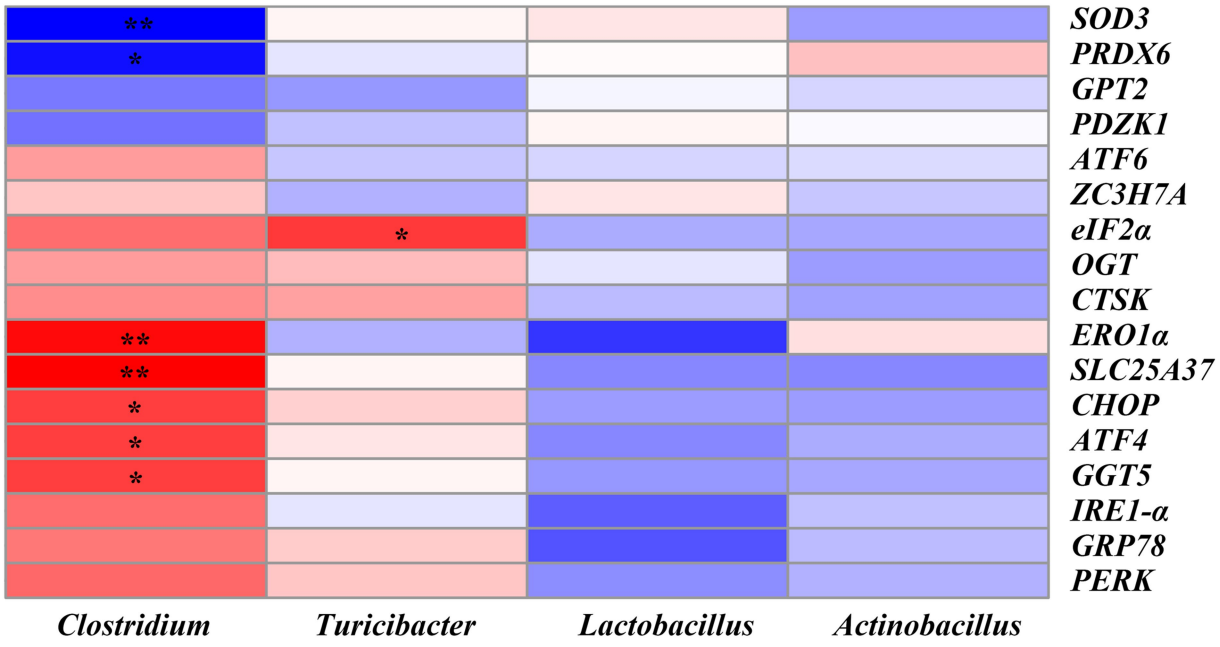

FIGURE 10
Heatmap of Pearson's correlation analysis between ER stress-related genes and the top 20 microbiota genera. * = $p < 0.05$, ** = $p < 0.01$, $n = 6$. *SOD3*, superoxide dismutase 3; *PRDX6*, peroxiredoxin 6; *GPT2*, glutamic pyruvic transaminase 2; *PDZK1*, PDZ domain containing 1; *ATF6*, activating transcription factor 6; *ZC3H7A*, zinc finger CCCH-type containing 7A; *eIF2α*, phosphorylation of eukaryotic initiation factor-2α; *OGT*, EGF domain specific O-linked N-acetylglucosamine transferase; *CTSK*, cathepsin K; *ERO1α*, endoplasmic reticulum oxidoreductin 1α; *SLC25A37*, solute carrier family 25 member 37; *CHOP*, C/EBP homologous protein; *ATF4*, activating transcription factor 4; *GGT5*, gamma-glutamyltransferase 5; *IRE1-α*, inositol-requiring enzyme 1α; *GRP78*, glucose-regulated protein 78; *PERK*, protein kinase RNA-like endoplasmic reticulum kinase.

Glutathione metabolism suggested the decrease of OS and ER stress in SC06 + DQ group compared with the DQ group.

In addition, gut microbiota protects their hosts from pathogens through competitive exclusion. When the gut microbiota is abnormal, harmful bacteria will overproliferate and induce the endotoxin in blood, causing significant OS (Wang et al., 2017a). Although numerous studies explored the cecal microbiota or fecal microbiota, the studies on intestinal mucosal microbiota are relatively little. Several research have proved that there are different in composition and diversity of microbiota in the lumen and mucosa (Wu et al., 2020). Moreover, together with intestinal mucosa, mucin, secretory immunoglobulin A and intestinal mucosal microbiota are vital in blocking and delaying the translocation and infection of various pathogens (Yap and Mariño, 2018). In the present study, altered ileal mucosal microbiota composition was observed among groups. As for the phylum, and top 20 family and genus, compared with the Con group, DQ decreased the Acidobacteria abundance and increased the abundances of Turicibacteraceae, *Clostridium* and *Turicibacter*; SC06 decreased Ruminococcaceae abundance and increased *Lactobacillus* abundance. Compared with the DQ group, SC06 + DQ decreased the *Clostridium* abundance and increased the abundances of *Pasteurellaceae* and *Actinobacillus*. *Turicibacter* belongs to the Firmicutes phylum. *Turicibacter* was associated with rat models of trinitrobenzene sulfonic acid-induced colitis and diabetes, might also affect intestinal health and cause various diseases, including diabetes, inflammation (Jones-Hall et al., 2015). *Clostridium* genera are mostly known as pathogenic microorganisms (Samul et al., 2013). Most of the studies conducted during the weaning transition have reported an increase of *Clostridium* (Gresse et al., 2017). *Acinetobacter* are dominant genera in the small intestine and considered to take part in digestion process (Zhao et al., 2015). Some species of *Acinetobacter* have been applied in the degradation of lignin and amino acids (Adegoke et al., 2012). *Lactobacillus* spp. are well-known probiotics and have beneficial role in growth promotion, antioxidation and anti-inflammation (Valeriano et al., 2017). Taken together, the increased abundances of *Clostridium* and *Turicibacter* indicated the increased ileal inflammation by the DQ treatment. The increased *Lactobacillus* abundance in the SC06 group, decreased *Clostridium* abundance and increased *Actinobacillus* abundance in the SC06 + DQ group, were related to the improved ileal health and digestive capacity of piglets.

Moreover, our KEGG results of ileal mucosal microbiota indicate that some diseases-related pathways, including the Hypertrophic cardiomyopathy and Pathways in cancer were upregulated in the DQ group compared with the Con group. Moreover, ECM-receptor interaction and Ethylbenzene degradation pathways were upregulated in the SC06 + DQ group compared with the DQ group. ECM-receptor interactions are pathways that maintain cell and tissue structure and function. ECM-receptors mediate ECM protein interactions and promote the macromolecules formation (Mo et al., 2023). Ethylbenzene is a toxic aromatic organic compound. The treatment of SC06 + DQ significantly enriched microbial functional genes related to the degradation of the ethylbenzene, suggesting that the microbes may have a better ability to degrade toxic organic compounds and maintain homeostasis of the gut environment. Similar result was found by Liu et al. (2021), in which the gut microbial genes of chickens treated with multi-enzyme were also enriched in the Ethylbenzene degradation pathway.

In addition, correlation analysis further showed that there were significant correlations between the ER stress-related genes and the abundance of microbial genus. For example, *SLC25A37* and *ERO1α* were positively correlated with, while *SOD3* was negatively correlated with the abundance of *Clostridium*. *eIF2α* was positively correlated with the abundance of *Turicibacter*. Since *Clostridium* was significantly reduced in the SC06 + DQ group, it may be the key bacterium responsible for the alleviation of OS by SC06 in weaned piglets.

5 Conclusion

In summary, our data show a significant improvement in growth performance, ileal morphology, barrier function, antioxidant and anti-ER stress capacity of dietary SC06 supplementation in DQ-treated weaned piglets. By taking advantages of microbiome and transcriptome analyses, we found significant reshaping of ileal mucosal bacteria (including *Clostridium* and *Turicibacter*) with SC06 supplementation, along with the changes in ileal genes (including *SLC25A37*, *ERO1α, SOD3* and *eIF2α*).

Data availability statement

The datasets presented in this study can be found in online repositories. The names of the repository/repositories and accession number(s) can be found at: NCBI - PRJNA1021385 and PRJNA1012569.

Ethics statement

The animal study was reviewed and approved by the Animal Care and Use Committee of Qingdao Agricultural University (protocol number 20221125374). The study was conducted in accordance with the local legislation and institutional requirements.

Author contributions

JY: Writing – original draft, Writing – review & editing. HM: Formal analysis, Writing – original draft. YL: Formal analysis, Writing – original draft. LW: Data curation, Writing – original draft. QZ: Data curation, Writing – original draft. ZW: Data curation, Writing – original draft. HL: Funding acquisition, Writing – original draft. KZ: Funding acquisition, Writing – original draft. JZ: Funding acquisition, Writing – original draft. WL: Conceptualization, Writing – original draft, Writing – review & editing. YW: Conceptualization, Writing – original draft, Writing – review & editing.

Funding

The author(s) declare financial support was received for the research, authorship, and/or publication of this article. This work was financially supported by Shandong Provincial Natural Science Foundation (Grant No. ZR2020QC183), National Natural Science Foundation of China (Grant No. 32102586), Natural Science Foundation of Zhejiang Province (Grant No. LZ20C170002).

Acknowledgments

The authors thank Yingchun Liu at Qingdao Institute of Animal Science and Veterinary Medicine for her support in animal experiment.

Conflict of interest

The authors declare that the research was conducted in the absence of any commercial or financial relationships that could be construed as a potential conflict of interest.

Publisher's note

Supplementary material

The Supplementary material for this article can be found online at: https://www.frontiersin.org/articles/10.3389/fmicb.2024.1362487/full#supplementary-material

References

Adegoke, A. A., Mvuyo, T., and Okoh, A. I. (2012). Ubiquitous *Acinetobacter* species as beneficial commensals but gradually being emboldened with antibiotic resistance genes. *J. Basic Microbiol.* 52, 620–627. doi: 10.1002/jobm.201100323

Bie, Y., Zheng, X., Chen, X., Liu, X., Wang, L., Sun, Y., et al. (2023). RNA sequencing and bioinformatics analysis of differentially expressed genes in the peripheral serum of ankylosing spondylitis patients. *J. Orthop. Surg. Res.* 18:394. doi: 10.1186/s13018-023-03871-w

Cao, A., Wang, L., Chen, X., Guo, H., Chu, S., Zhang, X., et al. (2016). Ursodeoxycholic acid ameliorated diabetic nephropathy by attenuating hyperglycemia-mediated oxidative stress. *Biol. Pharm. Bull.* 39, 1300–1308. doi: 10.1248/bpb.b16-00094

Chen, Y., Cui, W., Li, X., and Yang, H. (2021). Interaction between commensal bacteria, immune response and the intestinal barrier in inflammatory bowel disease. *Front. Immunol.* 12:761981. doi: 10.3389/fimmu.2021.761981

Chen, Y. M., Gabler, N. K., and Burrough, E. R. (2022). Porcine epidemic diarrhea virus infection induces endoplasmic reticulum stress and unfolded protein response in jejunal epithelial cells of weaned pigs. *Vet. Pathol.* 59, 82–90. doi: 10.1177/03009858211048622

Chen, P., Lv, H., Du, M., Liu, W., Che, C., Zhao, J., et al. (2024). *Bacillus subtilis* HW2 enhances growth performance and alleviates gut injury via attenuation of endoplasmic reticulum stress and regulation of gut microbiota in broilers under necrotic enteritis challenge. *Poult. Sci.* 103:103661. doi: 10.1016/j.psj.2024.103661

Cui, Y., Zhou, X., Chen, L., Tang, Z., Mo, F., Li, X., et al. (2021). Crosstalk between endoplasmic reticulum stress and oxidative stress in heat exposure-induced apoptosis is dependent on the ATF4–CHOP–CHAC1 signal pathway in IPEC-J2 cells. *J. Agri. Food Chem.* 69, 15495–15511. doi: 10.1021/acs.jafc.1c03361

Doyle, K. M., Kennedy, D., Gorman, A. M., Gupta, S., Healy, S. J., and Samali, A. (2011). Unfolded proteins and endoplasmic reticulum stress in neurodegenerative disorders. *J. Cell. Mol. Med.* 15, 2025–2039. doi: 10.1111/j.1582-4934.2011.01374.x

Du, W., Xu, H., Mei, X., Cao, X., Gong, L., Wu, Y., et al. (2018). Probiotic *Bacillus* enhance the intestinal epithelial cell barrier and immune function of piglets. *Benef. Microbes* 9, 743–754. doi: 10.3920/BM2017.0142

Fatma, N., Singh, P., Chhunchha, B., Kubo, E., Shinohara, T., Bhargavan, B., et al. (2011). Deficiency of PRDX6 in lens epithelial cells induces ER stress response-mediated impaired homeostasis and apoptosis. *Am. J. Physiol. Cell Physiol.* 301, C954–C967. doi: 10.1152/ajpcell.00061.2011

Fu, Q., Tan, Z., Shi, L., and Xun, W. (2021). Resveratrol attenuates diquat-induced oxidative stress by regulating gut microbiota and metabolome characteristics in piglets. *Front. Microbiol.* 12:695155. doi: 10.3389/fmicb.2021.695155

García-Navas, R., Munder, M., and Mollinedo, F. (2012). Depletion of L-arginine induces autophagy as a cytoprotective response to endoplasmic reticulum stress in human T lymphocytes. *Autophagy* 8, 1557–1576. doi: 10.4161/auto.21315

Gresse, R., Chaucheyras-Durand, F., Fleury, M. A., Van de Wiele, T., Forano, E., and Blanquet-Diot, S. (2017). Gut microbiota dysbiosis in postweaning piglets: understanding the keys to health. *Trends Microbiol.* 25, 851–873. doi: 10.1016/j.tim.2017.05.004

Hu, S., Cao, X., Wu, Y., Mei, X., Xu, H., Wang, Y., et al. (2018). Effects of probiotic *Bacillus* as an alternative of antibiotics on digestive enzymes activity and intestinal integrity of piglets. *Front. Microbiol.* 9:2427. doi: 10.3389/fmicb.2018.02427

Hyder, I., Reddy, P. R. K., and Mukherjee, J. (2023). "Physiology of digestion" in *Textbook of veterinary physiology* (Springer Nature: Singapore), 315–351.

Hyoda, K., Hosoi, T., Horie, N., Okuma, Y., Ozawa, K., and Nomura, Y. (2006). PI3K-Akt inactivation induced CHOP expression in endoplasmic reticulum-stressed cells. *Biochem. Biophys. Res. Commun.* 340, 286–290. doi: 10.1016/j.bbrc.2005.12.007

Jiang, Q., Chen, S., Ren, W., Liu, G., Yao, K., Wu, G., et al. (2017). *Escherichia coli* aggravates endoplasmic reticulum stress and triggers CHOP-dependent apoptosis in weaned pigs. *Amino Acids* 49, 2073–2082. doi: 10.1007/s00726-017-2492-4

Jing, J., He, Y., Liu, Y., Tang, J., Wang, L., Jia, G., et al. (2023). Selenoproteins synergistically protect porcine skeletal muscle from oxidative damage via relieving mitochondrial dysfunction and endoplasmic reticulum stress. *J. Anim. Sci. Biotechnol.* 14, 79–17. doi: 10.1186/s40104-023-00877-6

Jones-Hall, Y. L., Kozik, A., and Nakatsu, C. (2015). Ablation of tumor necrosis factor is associated with decreased inflammation and alterations of the microbiota in a mouse model of inflammatory bowel disease. *PLoS One* 10:e0119441. doi: 10.1371/journal.pone.0119441

Kiesel, V. A., Sheeley, M. P., Hicks, E. M., Andolino, C., Donkin, S. S., Wendt, M. K., et al. (2022). Hypoxia-mediated ATF4 induction promotes survival in detached conditions in metastatic murine mammary cancer cells. *Front. Oncol.* 12:767479. doi: 10.3389/fonc.2022.767479

Lallès, J. P., Bosi, P., Smidt, H., and Stokes, C. R. (2007). Nutritional management of gut health in pigs around weaning. *Proc. Nutr. Soc.* 66, 260–268. doi: 10.1017/S0029665107005484

Lee, I. K., Kye, Y. C., Kim, G., Kim, H. W., Gu, M. J., Umboh, J., et al. (2016). Stress, nutrition, and intestinal immune responses in pigs—a review. *Asian Australas. J. Anim. Sci.* 29, 1075–1082. doi: 10.5713/ajas.16.0118

Li, W., Jin, K., Luo, J., Xu, W., Wu, Y., Zhou, J., et al. (2022). NF-κB and its crosstalk with endoplasmic reticulum stress in atherosclerosis. *Front. Cardiovasc. Med.* 9:988266. doi: 10.3389/fcvm.2022.988266

Li, W., Wu, Z. Q., Zhang, S., Cao, R., Zhao, J., Sun, Z. J., et al. (2016). Augmented expression of gamma-glutamyl transferase 5 (GGT5) impairs testicular steroidogenesis by deregulating local oxidative stress. *Cell Tissue Res.* 366, 467–481. doi: 10.1007/s00441-016-2458-y

Liu, R., Liu, J., Zhao, G., Li, W., Zheng, M., Wang, J., et al. (2019). Relevance of the intestinal health-related pathways to broiler residual feed intake revealed by duodenal transcriptome profiling. *Poult. Sci.* 98, 1102–1110. doi: 10.3382/ps/pey506

Liu, G., Tao, J., Lu, J., Jia, G., Zhao, H., Chen, X., et al. (2022). Dietary tryptophan supplementation improves antioxidant status and alleviates inflammation, endoplasmic reticulum stress, apoptosis, and pyroptosis in the intestine of piglets after lipopolysaccharide challenge. *Antioxidants* 11:872. doi: 10.3390/antiox11050872

Liu, Y., Zeng, D., Qu, L., Wang, Z., and Ning, Z. (2021). Multi-enzyme supplementation modifies the gut microbiome and metabolome in breeding hens. *Front. Microbiol.* 12:711905. doi: 10.3389/fmicb.2021.711905

MacLeod, G., Bozek, D. A., Rajakulendran, N., Monteiro, V., Ahmadi, M., Steinhart, Z., et al. (2019). Genome-wide CRISPR-Cas9 screens expose genetic vulnerabilities and mechanisms of temozolomide sensitivity in glioblastoma stem cells. *Cell Rep.* 27, 971–986.e9. doi: 10.1016/j.celrep.2019.03.047

Malik, D., Narayanasamy, N., Pratyusha, V. A., Thakur, J., and Sinha, N. (2023). "Digestion and assimilation of nutrients" in *Textbook of nutritional biochemistry* (Springer Nature: Singapore), 79–111.

Mo, Q., Kulyar, M. F., Quan, C., Ding, Y., Zhang, Y., Zhang, L., et al. (2023). Thiram-induced hyperglycemia causes tibial dyschondroplasia by triggering aberrant ECM remodeling via the gut-pancreas axis in broiler chickens. *J. Hazard. Mater.* 444:130368. doi: 10.1016/j.jhazmat.2022.130368

Pluske, J. R., Hampson, D. J., and Williams, I. H. (1997). Factors influencing the structure and function of the small intestine in the weaned pig: a review. *Livest. Prod. Sci.* 51, 215–236. doi: 10.1016/s0301-6226(97)00057-2

Reid, D. W., and Nicchitta, C. V. (2015). Diversity and selectivity in mRNA translation on the endoplasmic reticulum. *Nat. Rev. Mol. Cell Biol.* 16, 221–231. doi: 10.1038/nrm3958

Saleh, S., and El-Demerdash, E. (2005). Protective effects of L-arginine against cisplatin-induced renal oxidative stress and toxicity: role of nitric oxide. *Basic Clin. Pharmacol. Toxicol.* 97, 91–97. doi: 10.1111/j.1742-7843.2005.pto_114.x

Samul, D., Worsztynowicz, P., Leja, K., and Grajek, W. (2013). Beneficial and harmful roles of bacteria from the *Clostridium* genus. *Acta Biochim. Pol.* 60, 515–521. doi: 10.18388/abp.2013_2015

Schreck, R., Rieber, P., and Baeuerle, P. A. (1991). Reactive oxygen intermediates as apparently widely used messengers in the activation of the NF-kappa B transcription factor and HIV-1. *EMBO J.* 10, 2247–2258. doi: 10.1002/j.1460-2075.1991.tb07761.x

Shan, C., Sun, B., Dalloul, R. A., Zhai, Z., Sun, P., Li, M., et al. (2019). Effect of the oral administration of astragalus polysaccharides on jejunum mucosal immunity in chickens vaccinated against Newcastle disease. *Microb. Pathog.* 135:103621. doi: 10.1016/j.micpath.2019.103621

Srivastava, S. K., Yadav, U. C., Reddy, A. B., Saxena, A., Tammali, R., Shoeb, M., et al. (2011). Aldose reductase inhibition suppresses oxidative stress-induced inflammatory disorders. *Chem. Biol. Interact.* 191, 330–338. doi: 10.1016/j.cbi.2011.02.023

Su, W., Li, Z., Gong, T., Wang, F., Jin, M., Wang, Y., et al. (2023). An alternative ZnO with large specific surface area: preparation, physicochemical characterization and effects on growth performance, diarrhea, zinc metabolism and gut barrier function of weaning piglets. *Sci. Total Environ.* 882:163558. doi: 10.1016/j.scitotenv.2023.163558

Sun, W., Chen, W., Meng, K., Cai, L., Li, G., Li, X., et al. (2023). Dietary supplementation with probiotic *Bacillus licheniformis* S6 improves intestinal integrity via modulating intestinal barrier function and microbial diversity in weaned piglets. *Biology* 12:238. doi: 10.3390/biology12020238

Tam, A. B., Mercado, E. L., Hoffmann, A., and Niwa, M. (2012). ER stress activates NF-κB by integrating functions of basal IKK activity, IRE1 and PERK. *PLoS One* 7:e45078. doi: 10.1371/journal.pone.0045078

Tan, Y. R., Shen, S. Y., Shen, H. Q., Yi, P. F., Fu, B. D., and Peng, L. Y. (2023). The role of endoplasmic reticulum stress in regulation of intestinal barrier and inflammatory bowel disease. *Exp. Cell Res.* 424:113472. doi: 10.1016/j.yexcr.2023.113472

Tang, S., Xie, J., Fang, W., Wen, X., Yin, C., Meng, Q., et al. (2022). Chronic heat stress induces the disorder of gut transport and immune function associated with endoplasmic reticulum stress in growing pigs. *Anim. Nutr.* 11, 228–241. doi: 10.1016/j.aninu.2022.08.008

Valeriano, V. D., Balolong, M. P., and Kang, D. K. (2017). Probiotic roles of *Lactobacillus* sp. in swine: insights from gut microbiota. *J. Appl. Microbiol.* 122, 554–567. doi: 10.1111/jam.13364

Wan, Y., Yang, L., Jiang, S., Qian, D., and Duan, J. (2022). Excessive apoptosis in ulcerative colitis: crosstalk between apoptosis, ROS, ER stress, and intestinal homeostasis. *Inflamm. Bowel Dis.* 28, 639–648. doi: 10.1093/ibd/izab277

Wang, M. G., Fan, R. F., Li, W. H., Zhang, D., Yang, D. B., Wang, Z. Y., et al. (2019). Activation of PERK-eIF2α-ATF4-CHOP axis triggered by excessive ER stress contributes to lead-induced nephrotoxicity. *Biochim. Biophys Acta Mol. Cell Res.* 1866, 713–726. doi: 10.1016/j.bbamcr.2018.12.002

Wang, J., Ji, H., Wang, S., Liu, H., Zhang, W., Zhang, D., et al. (2018). Probiotic *Lactobacillus plantarum* promotes intestinal barrier function by strengthening the epithelium and modulating gut microbiota. *Front. Microbiol.* 9:1953. doi: 10.3389/fmicb.2018.01953

Wang, Y., Liu, Y., Sidhu, A., Ma, Z., McClain, C., and Feng, W. (2012). *Lactobacillus rhamnosus* GG culture supernatant ameliorates acute alcohol-induced intestinal permeability and liver injury. *Am. J. Physiol. Gastrointest. Liver Physiol.* 303, G32–G41. doi: 10.1152/ajpgi.00024.2012

Wang, K., Niu, J., Kim, H., and Kolattukudy, P. E. (2011). Osteoclast precursor differentiation by MCPIP via oxidative stress, endoplasmic reticulum stress, and autophagy. *J. Mol. Cell Biol.* 3, 360–368. doi: 10.1093/jmcb/mjr021

Wang, Y., Wu, Y., Wang, B., Cao, X., Fu, A., Li, Y., et al. (2017a). Effects of probiotic *Bacillus* as a substitute for antibiotics on antioxidant capacity and intestinal autophagy of piglets. *AMB Express* 7:52. doi: 10.1186/s13568-017-0353-x

Wang, Y., Wu, Y., Wang, Y., Fu, A., Gong, L., Li, W., et al. (2017b). *Bacillus amyloliquefaciens* SC06 alleviates the oxidative stress of IPEC-1 via modulating Nrf2/Keap1 signaling pathway and decreasing ROS production. *Appl. Microbiol. Biotechnol.* 101, 3015–3026. doi: 10.1007/s00253-016-8032-4

Wen, Z., Hou, W., Wu, W., Zhao, Y., Dong, X., Bai, X., et al. (2018). 6′-O-Galloylpaeoniflorin attenuates cerebral ischemia reperfusion-induced neuroinflammation and oxidative stress via PI3K/Akt/Nrf2 activation. *Oxid. Med. Cell. Longev.* 2018:8678267. doi: 10.1155/2018/8678267

Wert, K. J., Velez, G., Cross, M. R., Wagner, B. A., Teoh-Fitzgerald, M. L., Buettner, G. R., et al. (2018). Extracellular superoxide dismutase (SOD3) regulates oxidative stress at the vitreoretinal interface. *Free Radic. Biol. Med.* 124, 408–419. doi: 10.1016/j.freeradbiomed.2018.06.024

Westrate, L. M., Lee, J. E., Prinz, W. A., and Voeltz, G. K. (2015). Form follows function: the importance of endoplasmic reticulum shape. *Annu. Rev. Biochem.* 84, 791–811. doi: 10.1146/annurev-biochem-072711-163501

Wu, M., Li, P., Li, J., An, Y., Wang, M., and Zhong, G. (2020). The differences between luminal microbiota and mucosal microbiota in mice. *J. Microbiol. Biotechnol.* 30, 287–295. doi: 10.4014/jmb.1908.08037

Wu, G., and Morris, S. M. Jr. (1998). Arginine metabolism: nitric oxide and beyond. *Biochem. J.* 336, 1–17. doi: 10.1042/bj3360001

Xu, W., Zhang, X., Wu, J. L., Fu, L., Liu, K., Liu, D., et al. (2017). O-GlcNAc transferase promotes fatty liver-associated liver cancer through inducing palmitic acid and activating endoplasmic reticulum stress. *J. Hepatol.* 67, 310–320. doi: 10.1016/j.jhep.2017.03.017

Yang, G. Y., Xia, B., Su, J. H., He, T., Liu, X., Guo, L., et al. (2020). Anti-inflammatory effects of *Lactobacillus johnsonii* L531 in a pig model of *Salmonella* infantis infection involves modulation of $CCR6^{+}$ T cell responses and ER stress. *Vet. Res.* 51, 26–13. doi: 10.1186/s13567-020-00754-4

Yap, Y. A., and Mariño, E. (2018). An insight into the intestinal web of mucosal immunity, microbiota, and diet in inflammation. *Front. Immunol.* 9:2617. doi: 10.3389/fimmu.2018.02617

Yu, X., Cui, Z., Qin, S., Zhang, R., Wu, Y., Liu, J., et al. (2022). Effects of *Bacillus licheniformis* on growth performance, diarrhea incidence, antioxidant capacity, immune function, and fecal microflora in weaned piglets. *Animals* 12:1609. doi: 10.3390/ani12131609

Yu, P., Qian, A. S., Chathely, K. M., and Trigatti, B. L. (2018a). PDZK1 in leukocytes protects against cellular apoptosis and necrotic core development in atherosclerotic plaques in high fat diet fed ldl receptor deficient mice. *Atherosclerosis* 276, 171–181. doi: 10.1016/j.atherosclerosis.2018.05.009

Yu, P., Qian, A. S., Chathely, K. M., and Trigatti, B. L. (2018b). Data on leukocyte PDZK1 deficiency affecting macrophage apoptosis but not monocyte recruitment, cell proliferation, macrophage abundance or ER stress in atherosclerotic plaques of LDLR deficient mice. *Data Brief* 19, 1148–1161. doi: 10.1016/j.dib.2018.05.128

Yuan, J., Liu, Y., Zhao, F., Mu, Y., Tian, X., Liu, H., et al. (2023a). Hepatic proteomics analysis reveals attenuated endoplasmic reticulum stress in *Lactiplantibacillus plantarum*-treated oxidatively stressed broilers. *J. Agric. Food Chem.* 71, 11726–11739. doi: 10.1021/acs.jafc.3c01534

Yuan, J., Zhao, F., Liu, Y., Liu, H., Zhang, K., Tian, X., et al. (2023b). Effects of *Lactiplantibacillus plantarum* on oxidative stress, mitophagy, and NLRP3 inflammasome activation in broiler breast meat. *Poult. Sci.* 102:103128. doi: 10.1016/j.psj.2023.103128

Zhang, Y., Mu, T., Yang, Y., Zhang, J., Ren, F., and Wu, Z. (2021). *Lactobacillus johnsonii* attenuates *Citrobacter rodentium*-induced colitis by regulating inflammatory responses and endoplasmic reticulum stress in mice. *J. Nutr.* 151, 3391–3399. doi: 10.1093/jn/nxab250

Zhao, W., Wang, Y., Liu, S., Huang, J., Zhai, Z., He, C., et al. (2015). The dynamic distribution of porcine microbiota across different ages and gastrointestinal tract segments. *PLoS One* 10:e0117441. doi: 10.1371/journal.pone.0117441

Zhao, J., Zhao, F., Yuan, J., Liu, H., and Wang, Y. (2023). Gut microbiota metabolites, redox status, and the related regulatory effects of probiotics. *Heliyon* 9:e21431. doi: 10.1016/j.heliyon.2023.e21431

Zheng, P., Yu, B., He, J., Yu, J., Mao, X., Luo, Y., et al. (2017). Arginine metabolism and its protective effects on intestinal health and functions in weaned piglets under oxidative stress induced by diquat. *Br. J. Nutr.* 117, 1495–1502. doi: 10.1017/S0007114517001519

frontiers | Frontiers in Microbiology

TYPE Original Research
PUBLISHED 27 May 2024
DOI 10.3389/fmicb.2024.1403825

OPEN ACCESS

EDITED BY
Lifeng Zhu,
Nanjing University of Chinese Medicine, China

REVIEWED BY
Zhengrui Li,
Shanghai Jiao Tong University, China
Hong Liu,
Shandong University of Technology, China

*CORRESPONDENCE
Zheng Hao
1060256010@qq.com

RECEIVED 20 March 2024
ACCEPTED 10 May 2024
PUBLISHED 27 May 2024

CITATION
Fu J and Hao Z (2024) The causality between gut microbiota and non-Hodgkin lymphoma: a two-sample bidirectional Mendelian randomization study.
Front. Microbiol. 15:1403825.
doi: 10.3389/fmicb.2024.1403825

The causality between gut microbiota and non-Hodgkin lymphoma: a two-sample bidirectional Mendelian randomization study

Jinjie Fu[1,2] and Zheng Hao[2,3,4]*

[1]Graduate School, Tianjin University of Traditional Chinese Medicine, Tianjin, China, [2]College of Traditional Chinese Medicine, Tianjin University of Traditional Chinese Medicine, Tianjin, China, [3]Tianjin Key Laboratory of Modern Chinese Medicine Theory of Innovation and Application, Tianjin, China, [4]Guo Aichun Institute of Medical History and Literature, Tianjin University of Traditional Chinese Medicine, Tianjin, China

Background: Studies have indicated an association between gut microbiota (GM) and non-Hodgkin lymphoma (NHL). However, the causality between GM and NHL remains unclear. This study aims to investigate the causality between GM and NHL using Mendelian randomization (MR).

Methods: Data on GM is sourced from the MiBioGen consortium, while data on NHL and its subtypes is sourced from the FinnGen consortium R10 version. Inverse variance weighted (IVW) was employed for the primary MR analysis method, with methods such as Bayesian weighted Mendelian randomisation (BWMR) as an adjunct. Sensitivity analyses were conducted using Cochran's Q test, MR-Egger regression, MR-PRESSO, and the "Leave-one-out" method.

Results: The MR results showed that there is a causality between 27 GMs and NHL. Among them, 20 were negatively associated (OR < 1), and 7 were positively associated (OR > 1) with the corresponding diseases. All 27 MR results passed sensitivity tests, and there was no reverse causal association.

Conclusion: By demonstrating a causal link between GM and NHL, this research offers novel ideas to prevent, monitor, and cure NHL later.

KEYWORDS

gut microbiota, non-Hodgkin lymphoma, diffuse large B-cell lymphoma, haematology system, Mendelian randomization

1 Introduction

NHL is a prevalent malignancy tumor in the haematology system, accounting for about 90% of lymphomas overall. It can be classified into three basic types: B-cell type, T-cell type, and NK-cell type (Shankland et al., 2012). The prevalence of NHL is progressively rising on an annual basis. Based on statistical data, the number of new NHL cases in 2020 was 544,000, with approximately 260,000 deaths (Mafra et al., 2022). The number of new cases is projected to reach 778,000 by 2040, an increase of about 43% compared to 2020 (Chu et al., 2023). While the etiology of NHL is not fully understood, infection, immunosuppression, immunodeficiency syndromes, and autoimmune diseases are commonly recognized as significant risk factors for the onset of

NHL (Ansell, 2015; Armitage et al., 2017). In terms of treatment, from the anti-CD20 monoclonal antibody (rituximab) in 1982 (Miller et al., 1982), to the current immune checkpoint inhibitors (ICI) and bispecific antibodies (Bock et al., 2022; Abou Dalle et al., 2024), immunotherapy combined with chemotherapy has always been a focus in the treatment of NHL. Despite some progress made in these treatment methods, the therapy of relapsed/refractory NHL is still a major dilemma in the field, with many unmet needs in NHL therapy (Chaudhari et al., 2019).

The gastrointestinal tract, as the most common extranodal site involved in NHL (Hanafy et al., 2020), harbors a large number of microbes, such as bacteria and fungi. This subset of microorganisms is collectively referred to as GM (Costea et al., 2017). Recently, the close connection between GM and NHL has been increasingly confirmed. Research has shown that the abundance of GM in diffuse large B-cell lymphoma (DLBCL) patients is markedly greater than that in healthy individuals, as revealed by 16S rRNA gene sequencing (Yuan et al., 2021). In terms of NHL occurrence, studies have found an association between mucosa-associated lymphoid tissue (MALT) lymphoma and the invasion of GM such as Burkholderia. GM like Burkholderia may influence the mechanism of MALT lymphoma occurrence through the synthesis of Mvin protein (Kuo et al., 2019; Tanaka et al., 2021). Regarding the diagnosis of NHL, some scholars have suggested that GM can serve as a diagnostic marker for NK/T cell lymphoma (Shi et al., 2023). In addition, GM can also modulate the efficacy of immunotherapy. Studies have shown that the treatment response of cancer patients receiving immune checkpoint inhibitors (ICIs) is associated with the composition of GM. For example, GM such as Bacteroides may enhance patients' anti-tumor capacity by improving the function of effector T cells in the tumor microenvironment (Gopalakrishnan et al., 2018). Furthermore, studies have shown that oral administration of *Akkermansia muciniphila* and fecal microbiota transplantation can restore the efficacy of immune checkpoint inhibitors (ICI) in drug-resistant tumor mice through an interleukin-12-dependent mechanism (Routy et al., 2018). Therefore, by modulating GM, it is possible to improve the therapeutic effect of immunotherapies such as ICB, lower associated side effects (Park E. M. et al., 2022), and mitigate the development of resistance to ICIs in cancer patients (Routy et al., 2018). Myeloablative conditioning and the use of broad-spectrum antibiotics before hematopoietic stem cell transplantation (HSCT) can damage the intestinal epithelium and mucosal barrier, leading to gastrointestinal mucositis, and consequently increasing the risk of infections in patients (Keefe et al., 2007). Meanwhile, GM can influence the immune system and maintain intestinal homeostasis by regulating cells such as Treg and TH17 (Arpaia et al., 2013; Smith et al., 2013). Based on differences in GM, it is possible to predict and assess pre-transplant risks in NHL patients undergoing HSCT, aiding in the identification and prevention of high-risk individuals (Montassier et al., 2016). For instance, assessing the diversity of gut microbiota (GM) in patients on the day of transplant surgery can predict those at high risk of mortality during HSCT (Taur et al., 2014). In the future, GM may be a novel diagnostic biomarker and therapeutic target for NHL. Therefore, research on the causal relationship between the two is necessary.

MR explores the causality between exposure and outcome by utilizing instrumental variables (IVs) (Davies et al., 2018). Under the principle of random assignment, MR studies could avoid confounding factors or reverse causation interference (Davey Smith and Hemani, 2014), resulting in more stable and reliable research outcomes. For the research, we employ a two-sample MR methodology to investigate the causality between GM and NHL.

2 Methods

2.1 Data sources

MiBioGen consortium provided genetic variation data on GM (Kurilshikov et al., 2021). This research involved 18, 340 persons and generated corresponding genetic sequencing and genotyping data. It included 211 GMs, classified into five categories: phylum, class, order, family, and genus. Three unknown families and twelve unknown genera were excluded. Eventually, the study included nine phyla, sixteen classes, twenty orders, thirty-two families, and one hundred nineteen genera, totaling 196 GMs. The genetic variation data for NHL originates from the FinnGen consortium R10 version GWAS summary data (Kurki et al., 2023). It includes NHL and its five subtypes: follicular lymphoma (FL), DLBCL, marginal zone B-cell lymphoma (MZBL), T/NK cell lymphoma, and mantle cell lymphoma (MCL) (Table 1). The diagnostic criteria for NHL refer to ICD-10 codes C82, C83, C84, C85; The diagnostic criteria for FL refer to ICD-10 code C82; The diagnostic criteria for DLBCL refer to ICD-10 code C83.3; The diagnostic criteria for MZBL refer to ICD-10 codes C83.80, C83.89; The diagnostic criteria for T/NK cell lymphoma refer to ICD-10 code C84; The diagnostic criteria for MCL refer to ICD-10 code C83.1.

2.2 Selection of IVs

IVs were screened based on the following criteria (Figure 1): (1) In order to obtain IVs that are strongly correlated with GM and have robust relationships, we set the significance threshold at $p < 1.0 \times 10^{-8}$. However, the number of obtained IVs was small and difficult to meet the requirements of this study. Therefore, we referred to previous research (Sanna et al., 2019) and set the significance threshold at $p < 1.0 \times 10^{-5}$. At the same time, to ensure the mutual independence of the selected IVs, we removed linkage disequilibrium in the IVs ($r^2 < 0.001$, kb = 10,000); (2) To ensure the independence of the IVs, the IVs are unrelated to any confounding factors; (3) IVs can only influence the occurrence of NHL through GM and cannot affect NHL through other pathways. Additionally, to avoid bias from weak IVs, we excluded weak IVs using the F-statistic ($F > 10$). We also removed palindromic sequences from the IVs.

2.3 Positive MR analysis and sensitivity analysis

We utilized six methods, including IVW, MR Egger, weighted median, simple mode, weighted mode, and BWMR, to investigate the causality between GM and NHL. However, IVW was the primary evaluation method (Hemani et al., 2018). Given the uniqueness of GWAS data, the IVW method is widely recognized as the primary method for exploring causal relationships in MR analysis. By conducting a meta-analysis of each Wald ratio of the included valid IVs, it can provide the most accurate estimate of the effect. This approach is also commonly seen in other literature (Legason et al., 2017; Lu et al., 2023; Martín-Masot et al., 2023; Ruan et al., 2023; Li et al., 2024; Zheng et al., 2024). The IVW method is divided into random-effects IVW and fixed-effects IVW, with the selection based on heterogeneity in MR results (Greco et al., 2015). Since no single

TABLE 1 Detailed information on GMs and NHLs with their subtypes.

	Trait	Year	Population	Case	Control	PMID/URL (Datadownload)
Exposure	Gut microbiota	2023	European	–	–	33462485
Outcome	Non-Hodgkin lymphoma	2023	European	1,072	314193	https://storage.googleapis.com/finngen-public-data-r10/summary_stats/finngen_R10_C3_NONHODGKIN_EXALLC.gz
	Follicular lymphoma	2023	European	1,181	324650	https://storage.googleapis.com/finngen-public-data-r10/summary_stats/finngen_R10_CD2_FOLLICULAR_LYMPHOMA_EXALLC.gz
	Diffuse large B-cell lymphoma	2023	European	1,050	314193	https://storage.googleapis.com/finngen-public-data-r10/summary_stats/finngen_R10_C3_DLBCL_EXALLC.gz
	Marginal zone B-cell lymphoma	2023	European	202	314193	https://storage.googleapis.com/finngen-public-data-r10/summary_stats/finngen_R10_C3_MARGINAL_ZONE_LYMPHOMA_EXALLC.gz
	Mantle cell lymphoma	2023	European	210	314193	https://storage.googleapis.com/finngen-public-data-r10/summary_stats/finngen_R10_C3_MANTLE_CELL_LYMPHOMA_EXALLC.gz
	T/NK-cell lymphomas	2023	European	363	324650	https://storage.googleapis.com/finngen-public-data-r10/summary_stats/finngen_R10_CD2_TNK_LYMPHOMA_EXALLC.gz

method can perfectly suit all situations, additional methods such as MR Egger and weighted median are used as supplements (Bowden et al., 2015, 2016). For instance, when there is pleiotropy present, the MR Egger method is more suitable for inferring causal relationships. Finally, to mitigate the effects of multi-genic structure and pleiotropy, we utilized the BWMR method to further validate the obtained causal relationships (Zhao et al., 2020).

Sensitivity analysis includes heterogeneity testing, leave-one-out testing, and multivariate testing (Hemani et al., 2018). We evaluated the potential bias in the results by examining the pleiotropy of genes and the heterogeneity of the data. Cochran's Q test assesses heterogeneity, based on whether the *p*-value in Cochran's IVW is less than 0.05. MR-Egger regression detects horizontal pleiotropy, determined by the difference between its intercept and 0. MR-PRESSO can detect and lower horizontal pleiotropy (Burgess et al., 2020). Additionally, "leave-one-out" analysis can identify outlier SNPs within the SNPs, thus avoiding bias introduced by individual outlier SNPs on the overall MR results and enhancing the stability of the results.

2.4 Reverse MR analysis

In order to avoid interference from reverse causal relationships on the positive MR results, we conducted a reverse MR analysis with NHL and its five subtypes as exposure and GM as the outcome.

2.5 Statistical analysis

The statistical analyses in R 4.3.0 used the "TwoSampleMR" package.

3 Results

3.1 Obtained IVs

412 IVs related to non-Hodgkin lymphoma and its subtypes were obtained through screening (Supplementary Table S1). Among them, there were no palindromic sequences, and the $F > 10$ (range 17.421–88.429). The included GMs were divided into five categories, so there may be overlaps among SNPs under each GM.

3.2 Results of positive MR analysis

The IVW results showed that there were 34 GMs associated with NHL and its subtypes. Among them, 8 were associated with NHL, 6 with FL, 4 with DLBCL, 5 with MZBL, 6 with MCL, and 5 with T/NK cell lymphoma (Figure 2).

According to the IVW analysis results, phylum Cyanobacteria (OR: 0.622, CI: 0.426–0.908, $p = 0.014$), order Bifidobacteriales (OR: 0.715, CI: 0.512–0.998, $p = 0.049$), genus *Ruminococcus gnavus* group

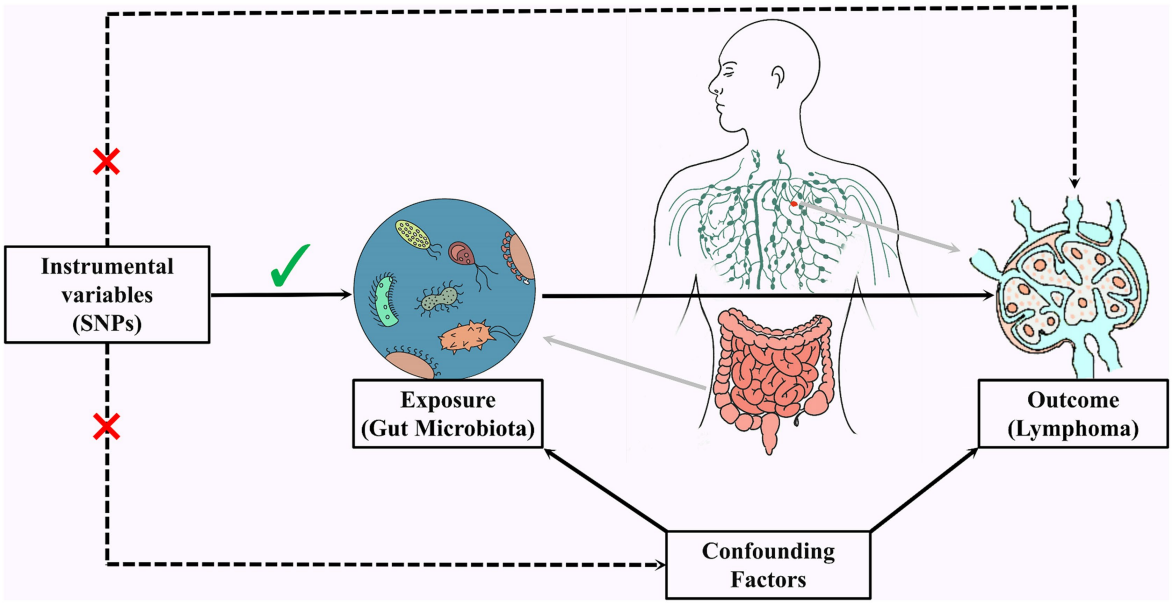

FIGURE 1
Three conditions met by filtering IVs.

(OR: 0.679, CI: 0.499–0.924, $p = 0.014$), genus *Bifidobacterium* (OR: 0.660, CI: 0.475–0.916, $p = 0.013$), and genus Lachnospiraceae UCG010 (OR: 0.570, CI: 0.352–0.923, $p = 0.022$) were negatively associated with an increased risk of NHL. Class Gammaproteobacteria (OR: 1.876, CI: 1.002–3.513, $p = 0.049$), genus *Faecalibacterium* (OR: 1.571, CI: 1.037–2.381, $p = 0.033$), and genus *Sellimonas* (OR: 1.542, CI: 1.220–1.948, $p = 0.0002$) were positively associated with an increased risk of NHL.

According to the IVW analysis results, order Pasteurellales (OR: 0.747, CI: 0.565–0.988, $p = 0.041$), genus *Alistipes* (OR: 0.554, CI: 0.327–0.939, $p = 0.028$), genus *Coprobacter* (OR: 0.728, CI: 0.537–0.987, $p = 0.041$), genus *Haemophilus* (OR: 0.702, CI: 0.502–0.983, $p = 0.040$), and genus Ruminococcaceae NK4A214 group (OR: 0.598, CI: 0.389–0.920, $p = 0.019$) were negatively associated with an increased risk of FL. Genus *Catenibacterium* (OR: 1.448, CI: 1.011–2.076, $p = 0.044$) was positively associated with an increased risk of FL.

According to the IVW analysis results, genus *Alistipes* (OR: 0.521, CI: 0.311–0.873, $p = 0.013$), genus Ruminococcaceae UCG011 (OR: 0.749, CI: 0.574–0.978, $p = 0.034$) were negatively associated with an increased risk of DLBCL. Family Desulfovibrionaceae (OR: 1.579, CI: 1.033–2.487, $p = 0.049$), genus *Bilophila* (OR: 1.777, CI: 1.053–3.000, $p = 0.031$) were positively associated with an increased risk of DLBCL.

According to the IVW analysis results, family Streptococcaceae (OR: 0.290, CI: 0.113–0.746, $p = 0.010$), genus *Eubacterium ruminantium* group (OR: 0.505, CI: 0.283–0.900, $p = 0.021$) were negatively associated with an increased risk of MZBL. Order Gastranaerophilales (OR: 2.445, CI: 1.064–5.616, $p = 0.035$), family Veillonellaceae (OR: 2.344, CI: 1.055–5.207, $p = 0.036$), genus Ruminococcaceae NK4A214 group (OR: 2.789, CI: 1.104–7.044, $p = 0.030$) were positively associated with an increased risk of MZBL.

According to the IVW analysis results, class Clostridia (OR: 0.317, CI: 0.107–0.935, $p = 0.037$), genus *Bifidobacterium* (OR: 0.441, CI: 0.211–0.920, $p = 0.029$), genus *Marvinbryantia* (OR: 0.328, CI: 0.115–0.938, $p = 0.038$), genus *Parasutterella* (OR: 0.441, CI: 0.207–0.939, $p = 0.034$), genus *Ruminiclostridium* 6 (OR: 0.397, CI: 0.70–0.926, $p = 0.032$) were negatively associated with an increased risk of MCL. Genus *Faecalibacterium* (OR: 2.755, CI: 1.084–7.005, $p = 0.033$) was positively associated with an increased risk of MCL.

According to the IVW analysis results, class Methanobacteria (OR: 0.574, CI: 0.371–0.887, $p = 0.012$), family Lactobacillaceae (OR: 0.538, CI: 0.308–0.941, $p = 0.030$), genus Christensenellaceae R 7group (OR: 0.359, CI: 0.134–0.960, $p = 0.041$), genus Lachnospiraceae UCG001 (OR: 0.350, CI: 0.196–0.627, $p = 0.0004$), genus Ruminococcaceae UCG014 (OR: 0.412, CI: 0.205–0.829, $p = 0.013$) were negatively associated with an increased risk of T/NK cell lymphoma.

Using BWMR to validate the 34 pairs of causalities between the obtained GMs and NHL (Figure 3), the results showed that class Gammaproteobacteria ($p = 0.340$) and order Bifidobacteriales ($p = 0.051$) were not causally related to NHL; genus *Catenibacterium* ($p = 0.050$) and genus *Coprobacter* ($p = 0.052$) were not causally related to FL; family Desulfovibrionaceae was not causally related to DLBCL. Comparing these 5 pairs of relationships between the results of BWMR and IVW (Table 2), it was found that although causal relationships existed in the IVW results, their *p*-values were close to 0.05. Therefore, these 5 pairs of relationships were excluded from our study.

Finally, sensitivity analysis of the MR results was conducted (Supplementary Table S1). The *p*-values of Cochran's Q test were all >0.05, indicating no heterogeneity. The *p*-values of the MR-Egger intercept (Supplementary Figures S1, S2) and MR-PRESSO results were all >0.05, indicating no horizontal pleiotropy. Results from the "leave-one-out" method (Supplementary Figures S3, S4) showed that

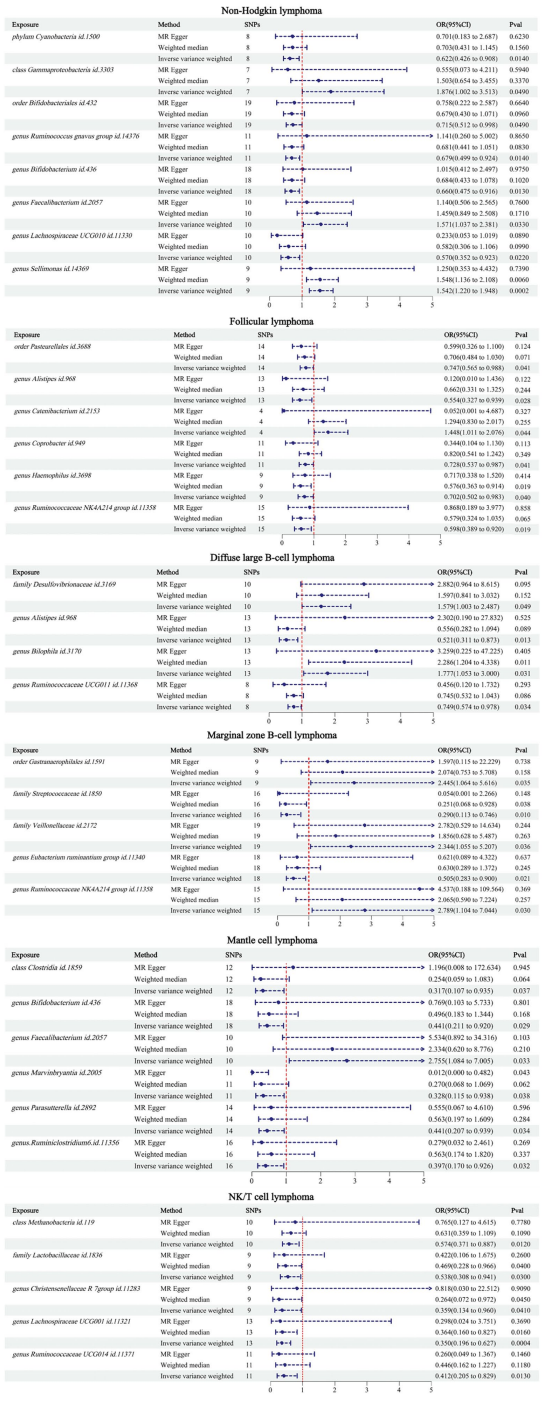

FIGURE 2
MR results between 34 GMs and NHL.

removing any single SNP would not significantly affect the MR results.

3.3 Results of reverse MR analysis

The reverse MR results showed that NHL and its subtypes were associated with 37 GMs (Supplementary Table S3). Among them, there were 7 associated with NHL, 10 with FL, 5 with DLBCL, 4 with MZBL, 9 with MCL, and 2 with T/NK cell lymphoma. Mapping the forest, see Figure 4. After comparing with the results of the forward MR, among the 34 forward MR results, FL was inversely associated with order Pasteurellales and genus *Haemophilus*, DLBCL was inversely associated with family Desulfovibrionaceae, and no other reverse causal associations were found in the remaining forward MR results. Sensitivity analysis was conducted for the three reverse causal associations mentioned above (Table 3). Except for the presence of heterogeneity in the MR results between FL and order Pasteurellales (without horizontal pleiotropy), the remaining two MR results showed no heterogeneity or horizontal pleiotropy.

Therefore, we finally identified 27 GMs with clear causal relationships with NHL and its subtypes, and presented them in the form of a heatmap (Figures 5, 6).

4 Discussion

In the 2020 cancer diagnosis statistics, NHL ranked 11th, and its incidence has been increasing year by year (Sung et al., 2021). Although GMs play important roles in the occurrence, development, diagnosis, and treatment of NHL (Upadhyay Banskota et al., 2023), the specific causality between the two is unknown. Previous studies have investigated the causal relationship between lipids (Kleinstern et al., 2020) and diet (Zhou et al., 2024), among other factors (Shi et al., 2024), and NHL through MR. Our research identified 27 GMs with causal relationships with NHL and its subtypes through forward and reverse MR analyses, as well as sensitivity analysis. Among them, phylum Cyanobacteria, genus *Ruminococcus gnavus* group, genus *Bifidobacterium*, genus Lachnospiraceae UCG010, genus *Alistipes*, genus Ruminococcaceae NK4A214 group, genus Ruminococcaceae UCG011, family Streptococcaceae, genus *Eubacterium ruminantium* group, class Clostridia, genus *Marvinbryantia*, genus *Parasutterella*, genus *Ruminiclostridium* 6, class Methanobacteria, family Lactobacillaceae, genus Christensenellaceae R 7group, genus Lachnospiraceae UCG001, and genus Ruminococcaceae UCG014 were negatively associated with the disease (OR < 1), indicating a protective effect against the corresponding types of NHL. Genus *Faecalibacterium*, genus *Sellimonas*, genus *Bilophila*, order Gastranaerophilales, family Veillonellaceae, genus Ruminococcaceae NK4A214 group, and genus *Faecalibacterium* were positively associated with the disease (OR > 1), serving as risk factors for the corresponding types of NHL. It is worth mentioning that in our positive MR analysis between GM and NHL, we observed that the absence of order Pasteurellales and genus *Haemophilus* might play a promoting role in FL occurrence. However, in the reverse MR analysis, we found that the occurrence of FL could inhibit the production of order Pasteurellales and genus *Haemophilus*. Therefore, we cannot ascertain whether the lack of order Pasteurellales and genus *Haemophilus* is the cause or the consequence of FL occurrence. To avoid interference from reverse causal relationships, we excluded the portion of results that exhibited reverse causal associations from the positive MR results.

The relationship between GM and NHL is complex. With the development of technologies in fields like 16S rRNA sequencing or shotgun metagenomics sequencing, researchers have gained a clearer understanding of the specific taxonomic groups in the GM and their relationship with diseases. Due to the involvement of numerous GM

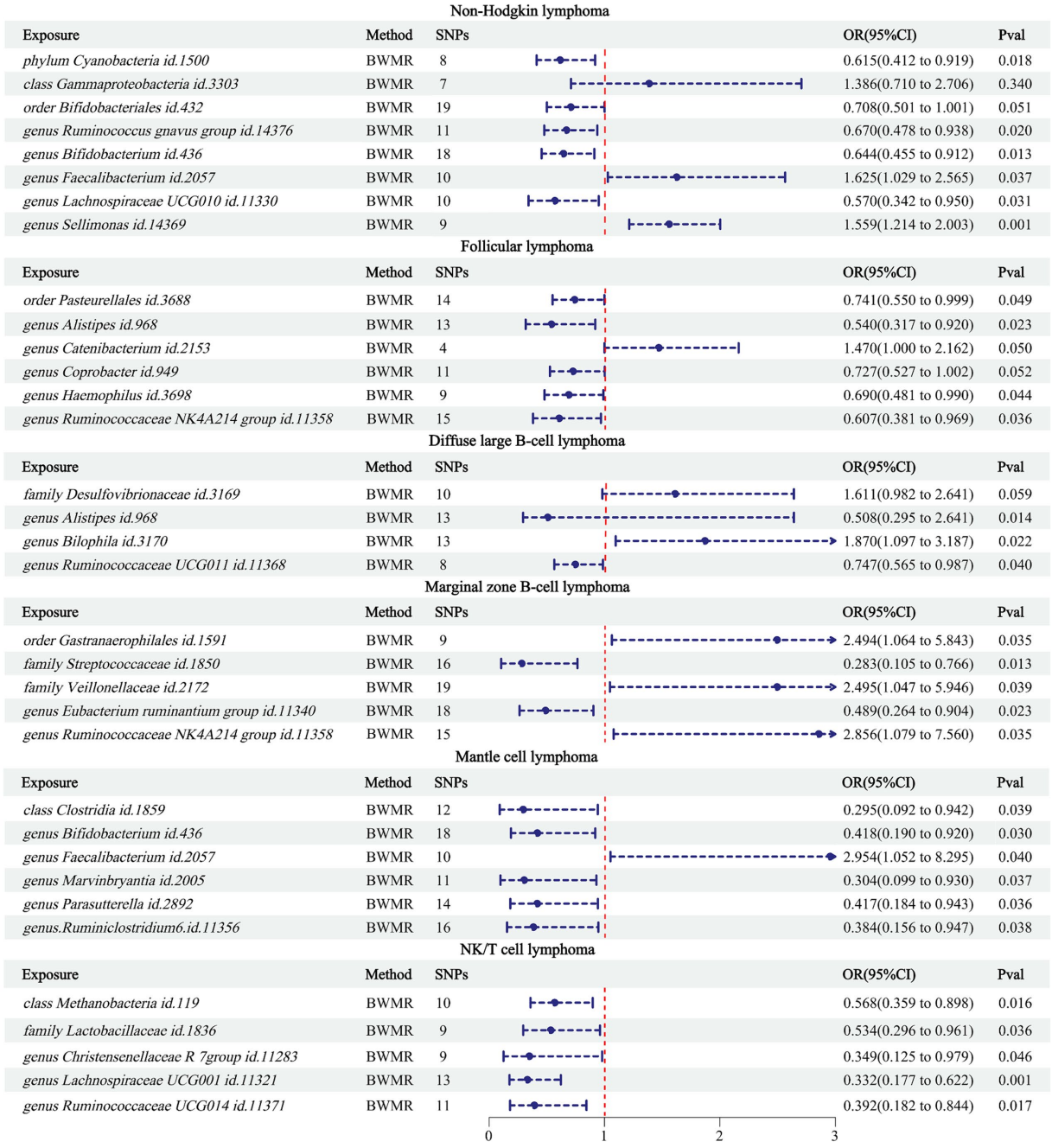

FIGURE 3
BWMR results between 34 GMs and NHL.

species in NHL and its subtypes in this study, we focused our discussion on the MR results related to NHL.

The phylum Cyanobacteria is a group of ancient and diverse prokaryotes (Schirrmeister et al., 2011) that can be divided into different genera such as Aphanothece, Leptolyngbya, and Spirulina (Walter et al., 2017). Research has found that Cyanobacteria can synthesize 1,600 types of compounds (Bohlin et al., 2010; Nagarajan et al., 2012), which play positive roles in antiviral, antibacterial, and immunomodulatory aspects (Sieber and Marahiel, 2005; De Morais et al., 2015; Sathasivam et al., 2019), thus they are widely applied in various fields. In addition, Cyanobacteria have significant anti-cancer effects, for example, Somocystinamide A (ScA), a lipopeptide compound isolated from Cyanobacteria, can inhibit tumor cell proliferation by inducing programmed cell death (Wrasidlo et al., 2008, p. 8). Curacin A, produced by Cyanobacteria, is a hybrid polyketide-peptide compound and an effective anticancer agent (Catassi et al., 2006). It can induce cancer cell death by inhibiting the activity of microtubule protein polymerization (Blokhin et al., 1995). In the results of this study, the phylum Cyanobacteria was found to decrease the risk of NHL, which is similar to the aforementioned

TABLE 2 Comparison of IVW and BWMR results for 5 pairs of GMs and NHL.

Exposure	Outcome	IVW		BWMR	
		Pval	OR(95%CI)	Pval	OR(95%CI)
class Gammaproteobacteria id.3303	Non-Hodgkin lymphoma	0.049	1.876 (1.002–3.513)	0.340	1.386 (0.710–2.706)
order Bifidobacteriales id.432		0.049	0.715 (0.512–0.998)	0.051	0.708 (0.501–1.001)
genus Catenibacterium id.2153	Follicular lymphoma	0.044	1.448 (1.011–2.076)	0.050	1.470 (1.000–2.162)
genus Coprobacter id.949		0.041	0.728 (0.537–0.987)	0.052	0.727 (0.527–1.002)
family Desulfovibrionaceae id.3169	Diffuse large B-cell lymphoma	0.049	1.579 (1.003–2.487)	0.059	1.611 (0.982–2.641)

previous research findings. Based on previous studies, we speculate that Cyanobacteria may also exhibit similar anticancer effects in NHL. Furthermore, most cancer-related chemotherapy drugs are derived from natural products in nature (Sithranga Boopathy and Kathiresan, 2010), and Cyanobacteria not only exist in the human gut but can also be obtained from marine (Mondal et al., 2020), soil, and agricultural runoff (Senousy et al., 2020). Hence, future research could delve into the anticancer mechanisms of Cyanobacteria in NHL, thereby laying the groundwork for the extraction and development of novel drugs related to NHL from natural products.

Ruminococcus gnavus is a Gram-positive anaerobic bacterium found primarily within the gastrointestinal tract of humans and animals (Qin et al., 2010). In terms of human health, *Ruminococcus gnavus* constitutes a significant proportion of the infant GM (Sagheddu et al., 2016), correlating with infant nutrition absorption (Yatsunenko et al., 2012) and growth development (Mennella et al., 2022), with these effects persisting into adulthood. In terms of disease, *Ruminococcus gnavus* is closely associated with gastrointestinal diseases and immune regulation. Research revealed that the relative abundance of *Ruminococcus gnavus* in normal humans is usually below 1%, while in some inflammatory bowel disease patients, it can reach around 70% (Zhang et al., 2023). However, some researchers found that after transferring *Ruminococcus gnavus* and other microbes into colorectal cancer mice, *Ruminococcus gnavus* could inhibit tumor growth and activate the immune surveillance function of $CD8^+$ T cells (Zhang et al., 2023). Therefore, the role of *Ruminococcus gnavus* in the human body is complex, and its effects on disease are influenced by multiple factors. In this study, the genus *Ruminococcus gnavus* group was identified as a beneficial bacterium for NHL, which can reduce the risk of its occurrence. Lachnospiraceae and *Ruminococcus gnavus* belong to the phylum Firmicutes. Lachnospiraceae is a family of gut bacteria that is widely present in the gastrointestinal tract of fauna (Gosalbes et al., 2011; Meehan and Beiko, 2014). It is an important member of the human GM, accounting for approximately 10 to 45% of the total bacterial population (Liu et al., 2021). Lachnospiraceae can be divided into different genera, such as Lachnospira, Oribacterium, and Dorea (Vacca et al., 2020), which are the primary contributors to short-chain fatty acids that are beneficial to human health (Vital et al., 2014; Chambers et al., 2015; Bui et al., 2021). Meloxicam, a nonsteroidal anti-inflammatory drug, is associated with reducing the risk of cancer, while Lachnospiraceae can produce meloxicam by altering the heterocyclic structure of flavonoids (Sugiyama et al., 2013; Braune and Blaut, 2016). Although there is limited research on the association between Lachnospiraceae and NHL, and it is not commonly found in other hematological tumors (Guevara-Ramírez et al., 2023), the viewpoint of Lachnospiraceae being considered beneficial bacteria in previous literature is similar to the results of this study. Therefore, more attention should be paid to the study of the association between the phylum Firmicutes and NHL as well as blood tumors, to clearly elucidate the specific mechanisms by which Lachnospiraceae may contribute to the treatment of NHL, thereby providing new insights into the prevention and treatment of NHL.

Bifidobacterium is a well-recognized beneficial microorganism for human health (Hidalgo-Cantabrana et al., 2017; Leser and Baker, 2023), with functions such as inhibiting intestinal pathogens (Moreno Muñoz et al., 2011), preventing gastrointestinal infections (Weizman et al., 2005), improving gastrointestinal symptoms (Waller et al., 2011), and regulating the immune system (Roller et al., 2007), thus it is widely used in the food and pharmaceutical industries. Studies have shown that GM such as Bifidobacterium can influence the therapeutic effects of immunotherapy on tumors (Matson et al., 2018). Bifidobacterium can also enhance the efficacy of ICIs in cancer mice by producing adenosine (Mager et al., 2020). Chimeric antigen receptor T-cell immunotherapy (CAR-T) is a novel precision-targeted therapy for treating malignant tumors of the hematopoietic system. Studies have found that GM such as Bifidobacterium are associated with the efficacy of Chimeric antigen receptor T-cell therapy in BCL and can influence the progression of BCL (Stein-Thoeringer et al., 2023). In addition, researchers have observed that the diversity of Bifidobacterium in multiple myeloma people after receiving CAR-T therapy vary depending on the efficacy of the treatment (Hu et al., 2022). Therefore, the differences in the diversity and abundance of Bifidobacterium are important indicators for predicting the therapeutic effects of lymphoma and other malignant tumors of the hematopoietic system. This study found that Bifidobacterium can effectively reduce the risk of NHL, while previous literature has not addressed this aspect of research. Therefore, we hope that this study can provide valuable reference for future exploration. Moreover, existing studies indicate an association between Bifidobacterium and the immunotherapeutic effects on tumors such as BCL and multiple myeloma, yet they do not directly establish a connection between Bifidobacterium and BCL. Therefore, subsequent research can use this as a starting point.

In this study, we found that genus *Faecalibacterium* and genus *Sellimonas* are the only two intestinal microbiota that can increase the risk of NHL. However, it is worth noting that genus

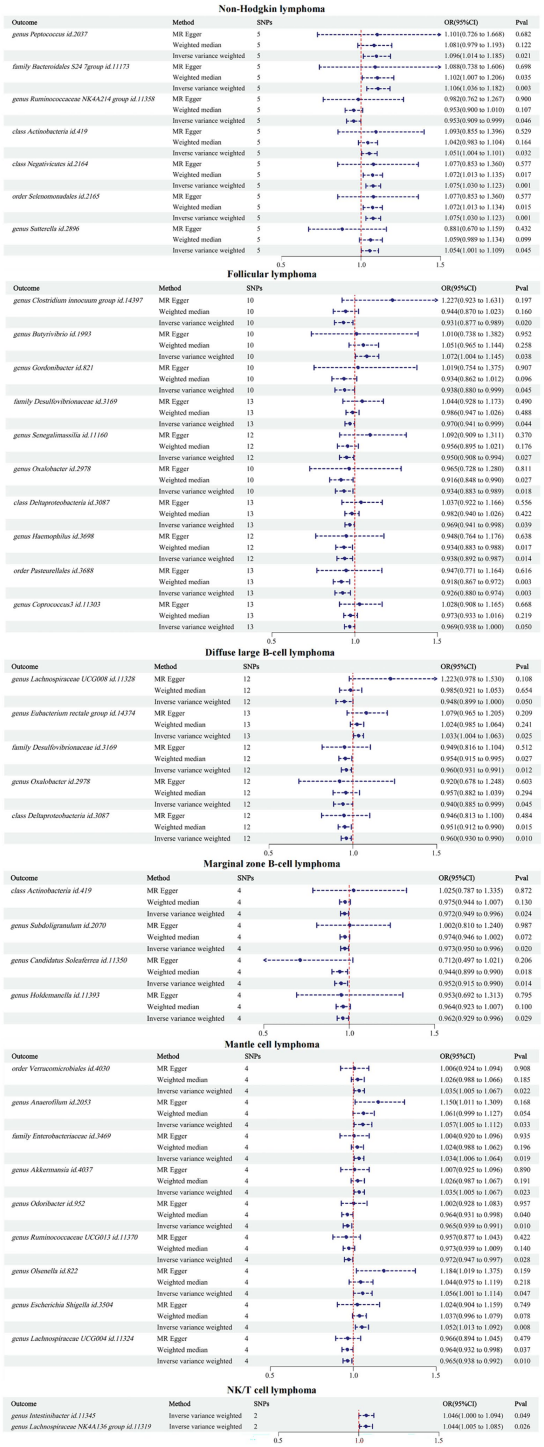

FIGURE 4
Inverse MR results between GMs and NHL.

Faecalibacterium is commonly found in the population and is generally considered beneficial to health, with the potential to become the next generation of probiotics (Langella et al., 2019). For example, *Faecalibacterium prausnitzii*, an important member of the genus *Faecalibacterium*, constitutes more than 5 percent of the overall fecal microbiome of healthy individuals. It can maintain the stability of the healthy gut environment (Miquel et al., 2013) and also act as a probiotic to regulate the intestinal environment of Crohn's disease patients (Sokol et al., 2008). Additionally, some species within the genus *Faecalibacterium* can produce significant amounts of fructose, providing energy for human colonic epithelial cells and supporting epithelial cell growth (Fagundes et al., 2021; Park J.-H. et al., 2022). Therefore, the results regarding genus *Faecalibacterium* in this study differ somewhat from previous related research. However, some researchers suggest that the interaction between *Faecalibacterium* and its host is not always constant (Martín et al., 2023). Since the discovery of *Faecalibacterium*, with the continuous advancement of techniques such as 16S rRNA gene sequence as well as whole-genome sequencing, the taxonomy of this genus has been evolving. In 2021, two new species were added: *Faecalibacterium butyricigenerans* and *Faecalibacterium longum* (Zou et al., 2021); and in 2022, three more new species were discovered, namely: *Faecalibacterium duncaniae*, *Faecalibacterium hattorii*, and *Faecalibacterium gallinarum* (Sakamoto et al., 2022). Therefore, the interactions between the genus *Faecalibacterium* and the host are continually being updated. Further research is needed to explore the impact of *Faecalibacterium* on NHL.

The causal relationship between GM and NHL is influenced not only by internal factors but also by external factors such as diet, medication, and delivery type. Dietary fiber is an important nutrient that is difficult for the human body to digest and absorb. However, there is a significant association between a high consumption of fruits, soy, and green vegetables and a reduced risk of NHL (Chiu, 1996; Wei et al., 2016). It is worth noting that certain GM, such as Lachnospiraceae, can ferment dietary fiber and produce substances like short-chain fatty acids, increasing the content of butyrate in the body, thereby promoting apoptosis of lymphoma cells (Wei et al., 2016; Zaplana et al., 2024). Therefore, increasing the intake of dietary fiber in the body appropriately can promote the growth of GM such as Lachnospiraceae. Additionally, certain living biotherapeutic products (LBPs) associated with Lachnospiraceae have been attempted to be developed as probiotics to improve conditions such as metabolic syndrome (Gilijamse et al., 2020). Probiotics are a type of beneficial active microorganisms for the human body. Bifidobacterium, as a crucial member of probiotics, plays an important role in the prevention and treatment of cancers such as colon cancer (Bahmani et al., 2019), gastric cancer (Devi et al., 2021), breast cancer (Shimizu et al., 2020), and lung cancer (An et al., 2020). This study identified a significant number of GM, including Bifidobacterium and *Ruminococcus gnavus*, that may potentially reduce the risk of NHL. Whether these GM can participate in the prevention and treatment of NHL as probiotics or other forms such as LBPs in the future is worth exploring.

The research has a few restrictions. Firstly, since the data on GM and NHL and its subtypes are all from European populations, we cannot guarantee whether the results are applicable to other populations. The GM dataset included in this study is currently the largest GWAS dataset of GM, but it predominantly focuses on the European population, hence there are limitations in generalizing to other populations. As GWAS databases of GM in various populations continue to be updated, we will continue to monitor research on the causal relationship between GM and NHL in other populations.

TABLE 3 Sensitivity analysis results for 3 GMs and NHL inverse MR results.

Exposure	Outcome	Q	Q_pval	MR-Egger intercept test		MR-PRESSO global test	
				Egger_ intercept	pval	RSS obs	*p*-value
Follicular lymphoma	*order Pasteurellales*	21.424	0.045	−0.006	0.828	25.277	0.058
	genus Haemophilus	18.885	0.063	−0.003	0.925	22.189	0.087
Diffuse large B-cell lymphoma	*family Desulfovibrionaceae*	2.775	0.993	0.003	0.876	111.769	0.468

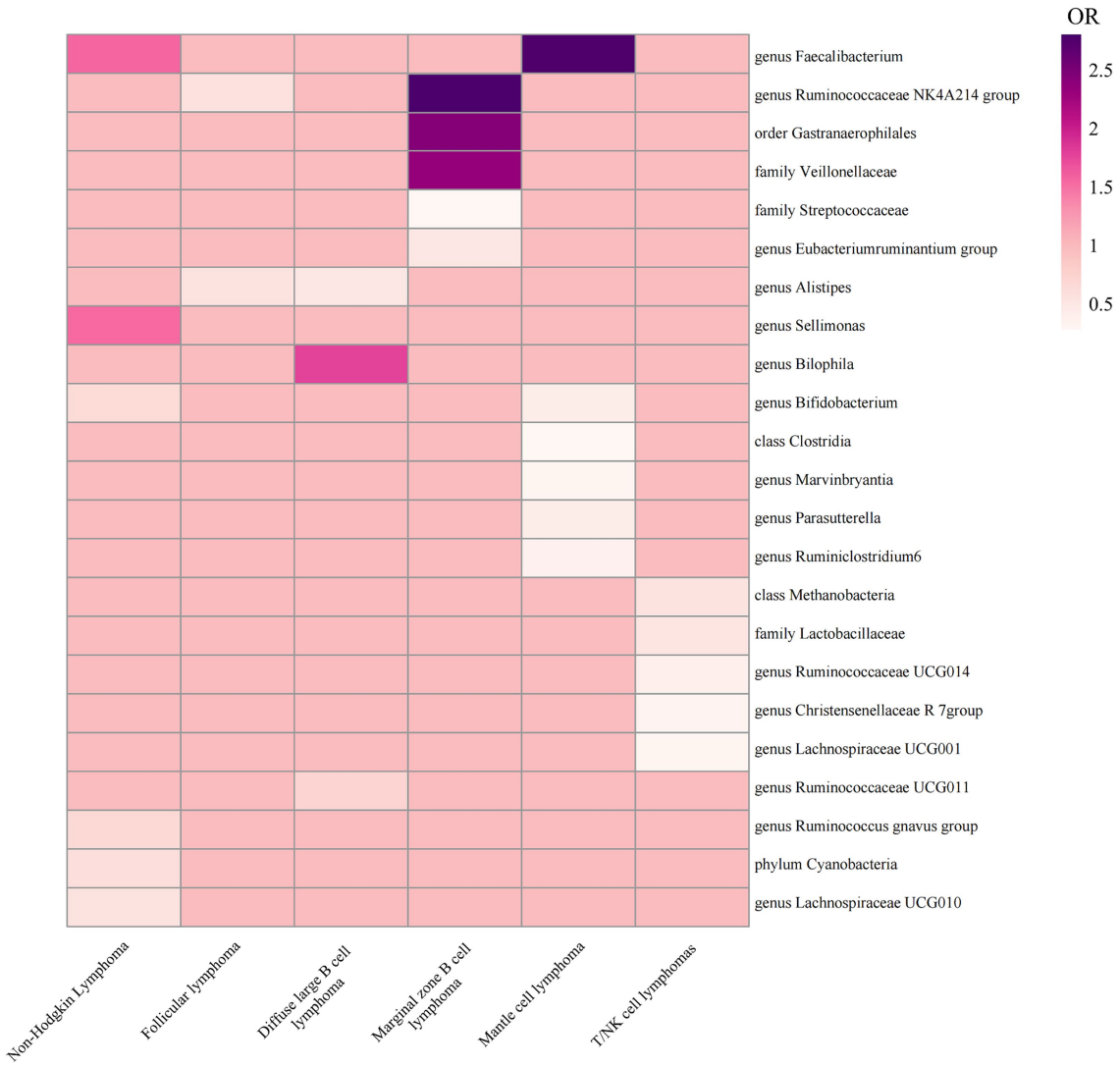

FIGURE 5
Heatmap of ORs in MR results for 27 GMs and NHL.

Secondly, there are fewer cases in certain subtypes of NHL, such as MZBL, MCL, and T/NK cell lymphoma, which limits the scope of the study. We will continue to monitor this aspect of the research as the FinnGen database is continually updated. Lastly, this study only elucidates the causality between GM and NHL, and the underlying mechanisms driving this association are not yet clear, requiring further research for support.

5 Conclusion

Through this study, we have identified the causality between GM and NHL, and determined the beneficial and harmful microbiota for NHL. In the future, it may be considered to selectively alter these GM through measures such as diet, probiotics, and prebiotics to influence NHL. Additionally, the

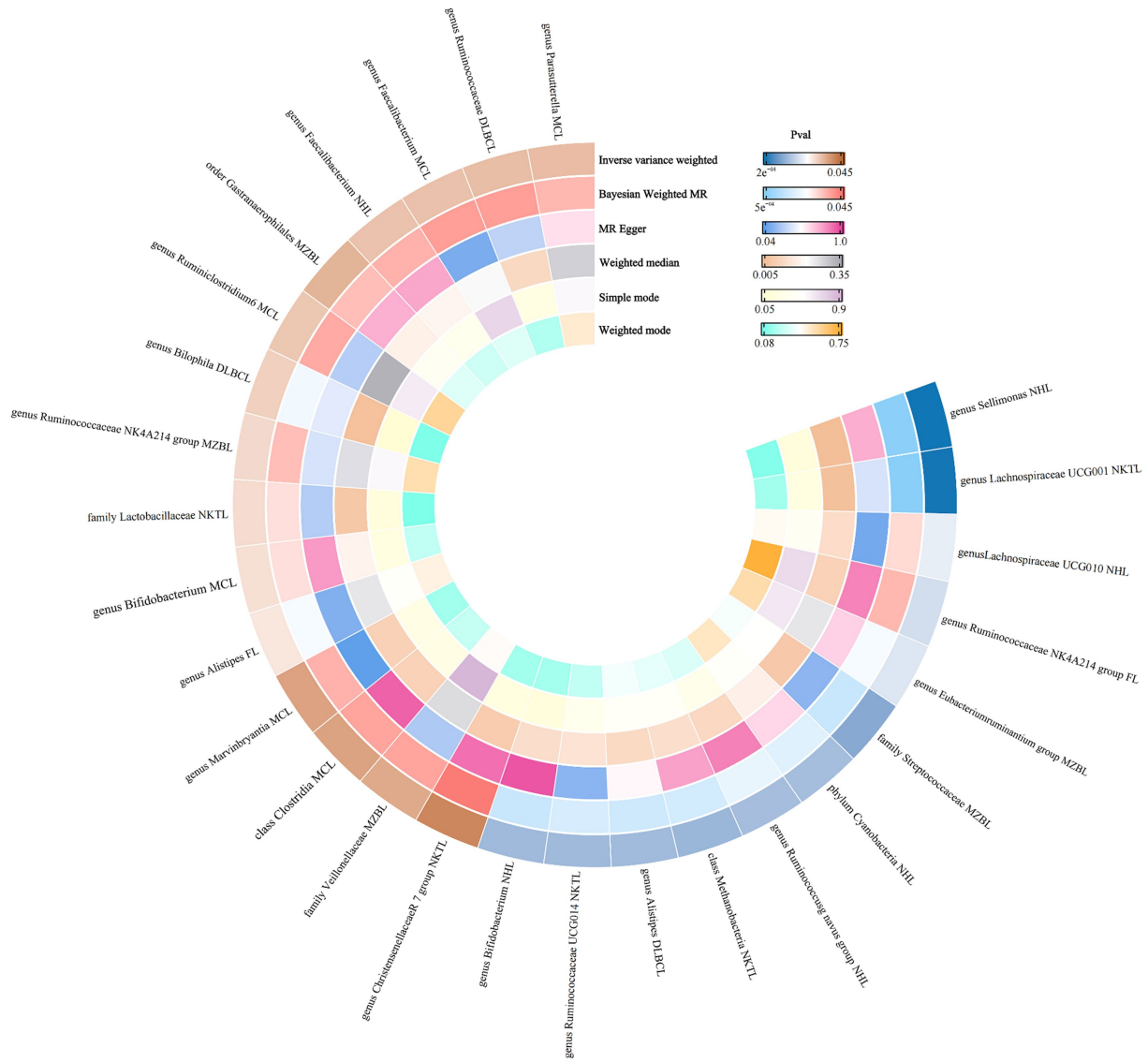

FIGURE 6
Ring thermograms of different MR results for 27 GMs and NHL.

development of targeted and effective GM in clinical settings holds certain reference significance as novel therapeutic modalities and monitoring indicators for NHL. Therefore, this research offers novel ideas to prevent, monitor, and cure NHL later.

Data availability statement

The original contributions presented in the study are included in the article/Supplementary material, further inquiries can be directed to the corresponding author.

Author contributions

JF: Data curation, Writing – original draft, Writing – review & editing, Software. ZH: Funding acquisition, Project administration, Resources, Supervision, Validation, Writing – review & editing.

Funding

The author(s) declare financial support was received for the research, authorship, and/or publication of this article. This study was supported by the scientific research project of the State Administration of Traditional Chinese Medicine (GZY-KJS-2020-037).

Acknowledgments

We express our sincere gratitude to the FinnGen and GWAS Catalog personnel and volunteers, as well as the MiBioGen consortium, for their invaluable contribution in supplying gut microbiology data.

Conflict of interest

The authors declare that the research was conducted in the absence of any commercial or financial relationships that could be construed as a potential conflict of interest.

Publisher's note

All claims expressed in this article are solely those of the authors and do not necessarily represent those of their affiliated organizations, or those of the publisher, the editors and the reviewers. Any product that may be evaluated in this article, or claim that may be made by its manufacturer, is not guaranteed or endorsed by the publisher.

Supplementary material

The Supplementary material for this article can be found online at: https://www.frontiersin.org/articles/10.3389/fmicb.2024.1403825/full#supplementary-material

References

Abou Dalle, I., Dulery, R., Moukalled, N., Ricard, L., Stocker, N., El-Cheikh, J., et al. (2024). Bi- and tri-specific antibodies in non-Hodgkin lymphoma: current data and perspectives. *Blood Cancer J.* 14:23. doi: 10.1038/s41408-024-00989-w

An, J., Kim, H., and Yang, K. M. (2020). An aqueous extract of a Bifidobacterium species induces apoptosis and inhibits invasiveness of non-small cell lung cancer cells. *J. Microbiol. Biotechnol.* 30, 885–893. doi: 10.4014/jmb.1912.12054

Ansell, S. M. (2015). Non-Hodgkin lymphoma: diagnosis and treatment. *Mayo Clin. Proc.* 90, 1152–1163. doi: 10.1016/j.mayocp.2015.04.025

Armitage, J. O., Gascoyne, R. D., Lunning, M. A., and Cavalli, F. (2017). Non-Hodgkin lymphoma. *Lancet* 390, 298–310. doi: 10.1016/S0140-6736(16)32407-2

Arpaia, N., Campbell, C., Fan, X., Dikiy, S., Van Der Veeken, J., deRoos, P., et al. (2013). Metabolites produced by commensal bacteria promote peripheral regulatory T-cell generation. *Nature* 504, 451–455. doi: 10.1038/nature12726

Bahmani, S., Azarpira, N., and Moazamian, E. (2019). Anti-colon cancer activity of Bifidobacterium metabolites on colon cancer cell line SW742. *Turk. J. Gastroenterol.* 30, 835–842. doi: 10.5152/tjg.2019.18451

Blokhin, A. V., Yoo, H. D., Geralds, R. S., Nagle, D. G., Gerwick, W. H., and Hamel, E. (1995). Characterization of the interaction of the marine cyanobacterial natural product curacin a with the colchicine site of tubulin and initial structure-activity studies with analogues. *Mol. Pharmacol.* 48, 523–531

Bock, A. M., Nowakowski, G. S., and Wang, Y. (2022). Bispecific antibodies for non-Hodgkin lymphoma treatment. *Curr. Treat. Options Oncol.* 23, 155–170. doi: 10.1007/s11864-021-00925-1

Bohlin, L., Göransson, U., Alsmark, C., Wedén, C., and Backlund, A. (2010). Natural products in modern life science. *Phytochem. Rev.* 9, 279–301. doi: 10.1007/s11101-009-9160-6

Bowden, J., Davey Smith, G., and Burgess, S. (2015). Mendelian randomization with invalid instruments: effect estimation and bias detection through egger regression. *Int. J. Epidemiol.* 44, 512–525. doi: 10.1093/ije/dyv080

Bowden, J., Davey Smith, G., Haycock, P. C., and Burgess, S. (2016). Consistent estimation in Mendelian randomization with some invalid instruments using a weighted median estimator. *Genet. Epidemiol.* 40, 304–314. doi: 10.1002/gepi.21965

Braune, A., and Blaut, M. (2016). Bacterial species involved in the conversion of dietary flavonoids in the human gut. *Gut Microbes* 7, 216–234. doi: 10.1080/19490976.2016.1158395

Bui, T. P. N., Mannerås-Holm, L., Puschmann, R., Wu, H., Troise, A. D., Nijsse, B., et al. (2021). Conversion of dietary inositol into propionate and acetate by commensal anaerostipes associates with host health. *Nat. Commun.* 12:4798. doi: 10.1038/s41467-021-25081-w

Burgess, S., Davey Smith, G., Davies, N. M., Dudbridge, F., Gill, D., Glymour, M. M., et al. (2020). Guidelines for performing Mendelian randomization investigations. *Wellcome Open Res.* 4:186. doi: 10.12688/wellcomeopenres.15555.2

Catassi, A., Cesario, A., Arzani, D., Menichini, P., Alama, A., Bruzzo, C., et al. (2006). Characterization of apoptosis induced by marine natural products in non small cell lung cancer A549 cells. *Cell. Mol. Life Sci.* 63, 2377–2386. doi: 10.1007/s00018-006-6264-7

Chambers, E. S., Viardot, A., Psichas, A., Morrison, D. J., Murphy, K. G., Zac-Varghese, S. E. K., et al. (2015). Effects of targeted delivery of propionate to the human colon on appetite regulation, body weight maintenance and adiposity in overweight adults. *Gut* 64, 1744–1754. doi: 10.1136/gutjnl-2014-307913

Chaudhari, K., Rizvi, S., and Syed, B. A. (2019). Non-Hodgkin lymphoma therapy landscape. *Nat. Rev. Drug Discov.* 18, 663–664. doi: 10.1038/d41573-019-00051-6

Chiu, B. C.-H. (1996). Diet and risk of non-Hodgkin lymphoma in older women. *JAMA* 275, 1315–1321. doi: 10.1001/jama.1996.03530410029029

Chu, Y., Liu, Y., Fang, X., Jiang, Y., Ding, M., Ge, X., et al. (2023). The epidemiological patterns of non-Hodgkin lymphoma: global estimates of disease burden, risk factors, and temporal trends. *Front. Oncol.* 13:1059914. doi: 10.3389/fonc.2023.1059914

Costea, P. I., Coelho, L. P., Sunagawa, S., Munch, R., Huerta-Cepas, J., Forslund, K., et al. (2017). Subspecies in the global human gut microbiome. *Mol. Syst. Biol.* 13:960. doi: 10.15252/msb.20177589

Davey Smith, G., and Hemani, G. (2014). Mendelian randomization: genetic anchors for causal inference in epidemiological studies. *Hum. Mol. Genet.* 23, R89–R98. doi: 10.1093/hmg/ddu328

Davies, N. M., Holmes, M. V., and Davey Smith, G. (2018). Reading Mendelian randomisation studies: a guide, glossary, and checklist for clinicians. *BMJ* 362:k601. doi: 10.1136/bmj.k601

De Morais, M. G., Vaz, B. D. S., De Morais, E. G., and Costa, J. A. V. (2015). Biologically active metabolites synthesized by microalgae. *Biomed. Res. Int.* 2015, 1–15. doi: 10.1155/2015/835761

Devi, T. B., Devadas, K., George, M., Gandhimathi, A., Chouhan, D., Retnakumar, R. J., et al. (2021). Low Bifidobacterium abundance in the lower gut microbiota is associated with *Helicobacter pylori*-related gastric ulcer and gastric cancer. *Front. Microbiol.* 12:631140. doi: 10.3389/fmicb.2021.631140

Fagundes, R. R., Bourgonje, A. R., Saeed, A., Vich Vila, A., Plomp, N., Blokzijl, T., et al. (2021). Inulin-grown *Faecalibacterium prausnitzii* cross-feeds fructose to the human intestinal epithelium. *Gut Microbes* 13:1993582. doi: 10.1080/19490976.2021.1993582

Gilijamse, P. W., Hartstra, A. V., Levin, E., Wortelboer, K., Serlie, M. J., Ackermans, M. T., et al. (2020). Treatment with Anaerobutyricum soehngenii: a pilot study of safety and dose–response effects on glucose metabolism in human subjects with metabolic syndrome. *NPJ Biofilms Microbiomes* 6:16. doi: 10.1038/s41522-020-0127-0

Gopalakrishnan, V., Spencer, C. N., Nezi, L., Reuben, A., Andrews, M. C., Karpinets, T. V., et al. (2018). Gut microbiome modulates response to anti–PD-1 immunotherapy in melanoma patients. *Science* 359, 97–103. doi: 10.1126/science.aan4236

Gosalbes, M. J., Durbán, A., Pignatelli, M., Abellan, J. J., Jiménez-Hernández, N., Pérez-Cobas, A. E., et al. (2011). Metatranscriptomic approach to analyze the functional human gut microbiota. *PLoS One* 6:e17447. doi: 10.1371/journal.pone.0017447

Greco, M. F. D., Minelli, C., Sheehan, N. A., and Thompson, J. R. (2015). Detecting pleiotropy in Mendelian randomisation studies with summary data and a continuous outcome. *Stat. Med.* 34, 2926–2940. doi: 10.1002/sim.6522

Guevara-Ramírez, P., Cadena-Ullauri, S., Paz-Cruz, E., Tamayo-Trujillo, R., Ruiz-Pozo, V. A., and Zambrano, A. K. (2023). Role of the gut microbiota in hematologic cancer. *Front. Microbiol.* 14:1185787. doi: 10.3389/fmicb.2023.1185787

Hanafy, A. K., Morani, A. C., Menias, C. O., Pickhardt, P. J., Shaaban, A. M., Mujtaba, B., et al. (2020). Hematologic malignancies of the gastrointestinal luminal tract. *Abdom Radiol* 45, 3007–3027. doi: 10.1007/s00261-019-02278-8

Hemani, G., Zheng, J., Elsworth, B., Wade, K. H., Haberland, V., Baird, D., et al. (2018). The MR-base platform supports systematic causal inference across the human phenome. *eLife* 7:e34408. doi: 10.7554/eLife.34408

Hidalgo-Cantabrana, C., Delgado, S., Ruiz, L., Ruas-Madiedo, P., Sánchez, B., and Margolles, A. (2017). Bifidobacteria and their health-promoting effects. *Microbiol. Spectr.* 5:5.3.21. doi: 10.1128/microbiolspec.BAD-0010-2016

Hu, Y., Li, J., Ni, F., Yang, Z., Gui, X., Bao, Z., et al. (2022). CAR-T cell therapy-related cytokine release syndrome and therapeutic response is modulated by the gut microbiome in hematologic malignancies. *Nat. Commun.* 13:5313. doi: 10.1038/s41467-022-32960-3

Keefe, D. M., Schubert, M. M., Elting, L. S., Sonis, S. T., Epstein, J. B., Raber-Durlacher, J. E., et al. (2007). Updated clinical practice guidelines for the prevention and treatment of mucositis. *Cancer* 109, 820–831. doi: 10.1002/cncr.22484

Kleinstern, G., Camp, N. J., Berndt, S. I., Birmann, B. M., Nieters, A., Bracci, P. M., et al. (2020). Lipid trait variants and the risk of non-Hodgkin lymphoma subtypes: a Mendelian randomization study. *Cancer Epidemiol. Biomarkers Prev.* 29, 1074–1078. doi: 10.1158/1055-9965.EPI-19-0803

Kuo, S.-H., Wu, M.-S., Yeh, K.-H., Lin, C.-W., Hsu, P.-N., Chen, L.-T., et al. (2019). Novel insights of lymphomagenesis of *Helicobacter pylori*-dependent gastric mucosa-associated lymphoid tissue lymphoma. *Cancers* 11:547. doi: 10.3390/cancers11040547

Kurilshikov, A., Medina-Gomez, C., Bacigalupe, R., Radjabzadeh, D., Wang, J., Demirkan, A., et al. (2021). Large-scale association analyses identify host factors influencing human gut microbiome composition. *Nat. Genet.* 53, 156–165. doi: 10.1038/s41588-020-00763-1

Kurki, M. I., Karjalainen, J., Palta, P., Sipilä, T. P., Kristiansson, K., Donner, K. M., et al. (2023). FinnGen provides genetic insights from a well-phenotyped isolated population. *Nature* 613, 508–518. doi: 10.1038/s41586-022-05473-8

Langella, P., Guarner, F., and Martín, R. (2019). Editorial: next-generation probiotics: from commensal Bacteria to novel drugs and food supplements. *Front. Microbiol.* 10:1973. doi: 10.3389/fmicb.2019.01973

Legason, I. D., Pfeiffer, R. M., Udquim, K.-I., Bergen, A. W., Gouveia, M. H., Kirimunda, S., et al. (2017). Evaluating the causal link between malaria infection and endemic Burkitt lymphoma in northern Uganda: a Mendelian randomization study. *EBioMedicine* 25, 58–65. doi: 10.1016/j.ebiom.2017.09.037

Leser, T., and Baker, A. (2023). *Bifidobacterium adolescentis* – a beneficial microbe. *Benef. Microbes* 14, 525–551. doi: 10.1163/18762891-20230030

Li, Z., Wang, Q., Huang, X., Wu, Y., Fu, R., Wen, X., et al. (2024). A Mendelian randomisation analysis reveals no relationship between periodontitis and coronary atherosclerosis. *Int. Dent. J.*:S0020653924000534. doi: 10.1016/j.identj.2024.01.027

Liu, C., Du, M.-X., Abuduaini, R., Yu, H.-Y., Li, D.-H., Wang, Y.-J., et al. (2021). Enlightening the taxonomy darkness of human gut microbiomes with a cultured biobank. *Microbiome* 9:119. doi: 10.1186/s40168-021-01064-3

Lu, C., Chen, Q., Tao, H., Xu, L., Li, J., Wang, C., et al. (2023). The causal effect of inflammatory bowel disease on diffuse large B-cell lymphoma: two-sample Mendelian randomization study. *Front. Immunol.* 14:1171446. doi: 10.3389/fimmu.2023.1171446

Mafra, A., Laversanne, M., Gospodarowicz, M., Klinger, P., De Paula Silva, N., Piñeros, M., et al. (2022). Global patterns of non-Hodgkin lymphoma in 2020. *Int. J. Cancer* 151, 1474–1481. doi: 10.1002/ijc.34163

Mager, L. F., Burkhard, R., Pett, N., Cooke, N. C. A., Brown, K., Ramay, H., et al. (2020). Microbiome-derived inosine modulates response to checkpoint inhibitor immunotherapy. *Science* 369, 1481–1489. doi: 10.1126/science.abc3421

Martín, R., Rios-Covian, D., Huillet, E., Auger, S., Khazaal, S., Bermúdez-Humarán, L. G., et al. (2023). *Faecalibacterium*: a bacterial genus with promising human health applications. *FEMS Microbiol. Rev.* 47:fuad039. doi: 10.1093/femsre/fuad039

Martín-Masot, R., Herrador-López, M., Navas-López, V. M., Carmona, F. D., Nestares, T., and Bossini-Castillo, L. (2023). Celiac disease is a risk factor for mature T and NK cell lymphoma: a Mendelian randomization study. *IJMS* 24:7216. doi: 10.3390/ijms24087216

Matson, V., Fessler, J., Bao, R., Chongsuwat, T., Zha, Y., Alegre, M.-L., et al. (2018). The commensal microbiome is associated with anti–PD-1 efficacy in metastatic melanoma patients. *Science* 359, 104–108. doi: 10.1126/science.aao3290

Meehan, C. J., and Beiko, R. G. (2014). A phylogenomic view of ecological specialization in the Lachnospiraceae, a family of digestive tract-associated Bacteria. *Genome Biol. Evol.* 6, 703–713. doi: 10.1093/gbe/evu050

Mennella, J. A., Li, Y., Bittinger, K., Friedman, E. S., Zhao, C., Li, H., et al. (2022). The macronutrient composition of infant formula produces differences in gut microbiota maturation that associate with weight gain velocity and weight status. *Nutrients* 14:1241. doi: 10.3390/nu14061241

Miller, R. A., Maloney, D. G., Warnke, R., and Levy, R. (1982). Treatment of B-cell lymphoma with monoclonal anti-idiotype antibody. *N. Engl. J. Med.* 306, 517–522. doi: 10.1056/NEJM198203043060906

Miquel, S., Martín, R., Rossi, O., Bermúdez-Humarán, L., Chatel, J., Sokol, H., et al. (2013). Faecalibacterium prausnitzii and human intestinal health. *Curr. Opin. Microbiol.* 16, 255–261. doi: 10.1016/j.mib.2013.06.003

Mondal, A., Bose, S., Banerjee, S., Patra, J. K., Malik, J., Mandal, S. K., et al. (2020). Marine cyanobacteria and microalgae metabolites—a rich source of potential anticancer drugs. *Mar. Drugs* 18:476. doi: 10.3390/md18090476

Montassier, E., Al-Ghalith, G. A., Ward, T., Corvec, S., Gastinne, T., Potel, G., et al. (2016). Pretreatment gut microbiome predicts chemotherapy-related bloodstream infection. *Genome Med.* 8:49. doi: 10.1186/s13073-016-0301-4

Moreno Muñoz, J. A., Chenoll, E., Casinos, B., Bataller, E., Ramón, D., Genovés, S., et al. (2011). Novel probiotic *Bifidobacterium longum* subsp. infantis CECT 7210 strain active against rotavirus infections. *Appl. Environ. Microbiol.* 77, 8775–8783. doi: 10.1128/AEM.05548-11

Nagarajan, M., Maruthanayagam, V., and Sundararaman, M. (2012). A review of pharmacological and toxicological potentials of marine cyanobacterial metabolites. *J. Appl. Toxicol.* 32, 153–185. doi: 10.1002/jat.1717

Park, E. M., Chelvanambi, M., Bhutiani, N., Kroemer, G., Zitvogel, L., and Wargo, J. A. (2022). Targeting the gut and tumor microbiota in cancer. *Nat. Med.* 28, 690–703. doi: 10.1038/s41591-022-01779-2

Park, J.-H., Song, W.-S., Lee, J., Jo, S.-H., Lee, J.-S., Jeon, H.-J., et al. (2022). An integrative multiomics approach to characterize prebiotic inulin effects on *Faecalibacterium prausnitzii*. *Front. Bioeng. Biotechnol.* 10:825399. doi: 10.3389/fbioe.2022.825399

Qin, J., Li, R., Raes, J., Arumugam, M., Burgdorf, K. S., Manichanh, C., et al. (2010). A human gut microbial gene catalogue established by metagenomic sequencing. *Nature* 464, 59–65. doi: 10.1038/nature08821

Roller, M., Clune, Y., Collins, K., Rechkemmer, G., and Watzl, B. (2007). Consumption of prebiotic inulin enriched with oligofructose in combination with the probiotics *lactobacillus rhamnosus* and *Bifidobacterium lactis* has minor effects on selected immune parameters in polypectomised and colon cancer patients. *Br. J. Nutr.* 97, 676–684. doi: 10.1017/S0007114507450292

Routy, B., Le Chatelier, E., Derosa, L., Duong, C. P. M., Alou, M. T., Daillère, R., et al. (2018). Gut microbiome influences efficacy of PD-1–based immunotherapy against epithelial tumors. *Science* 359, 91–97. doi: 10.1126/science.aan3706

Ruan, X., Huang, D., Zhan, Y., Huang, J., Huang, J., Ng, A. T.-L., et al. (2023). Risk of second primary cancers after a diagnosis of first primary cancer: a pan-cancer analysis and Mendelian randomization study. *eLife* 12:e86379. doi: 10.7554/eLife.86379

Sagheddu, V., Patrone, V., Miragoli, F., Puglisi, E., and Morelli, L. (2016). Infant early gut colonization by Lachnospiraceae: high frequency of *Ruminococcus gnavus*. *Front. Pediatr.* 4. doi: 10.3389/fped.2016.00057

Sakamoto, M., Sakurai, N., Tanno, H., Iino, T., Ohkuma, M., and Endo, A. (2022). Genome-based, phenotypic and chemotaxonomic classification of Faecalibacterium strains: proposal of three novel species Faecalibacterium duncaniae sp. nov., Faecalibacterium hattorii sp. nov. and Faecalibacterium gallinarum sp. nov. *Int. J. Syst. Evol. Microbiol.* 72. doi: 10.1099/ijsem.0.005379

Sanna, S., van Zuydam, N. R., Mahajan, A., Kurilshikov, A., Vich Vila, A., Võsa, U., et al. (2019). Causal relationships among the gut microbiome, short-chain fatty acids and metabolic diseases. *Nat. Genet.* 51, 600–605. doi: 10.1038/s41588-019-0350-x

Sathasivam, R., Radhakrishnan, R., Hashem, A., and Abd_Allah, E. F. (2019). Microalgae metabolites: a rich source for food and medicine. *Saudi J. Biol. Sci.* 26, 709–722. doi: 10.1016/j.sjbs.2017.11.003

Schirrmeister, B. E., Antonelli, A., and Bagheri, H. C. (2011). The origin of multicellularity in cyanobacteria. *BMC Evol. Biol.* 11:45. doi: 10.1186/1471-2148-11-45

Senousy, H. H., Abd Ellatif, S., and Ali, S. (2020). Assessment of the antioxidant and anticancer potential of different isolated strains of cyanobacteria and microalgae from soil and agriculture drain water. *Environ. Sci. Pollut. Res.* 27, 18463–18474. doi: 10.1007/s11356-020-08332-z

Shankland, K. R., Armitage, J. O., and Hancock, B. W. (2012). Non-Hodgkin lymphoma. *Lancet* 380, 848–857. doi: 10.1016/S0140-6736(12)60605-9

Shi, Z., Hu, G., Li, M. W., Zhang, L., Li, X., Li, L., et al. (2023). Gut microbiota as non-invasive diagnostic and prognostic biomarkers for natural killer/T-cell lymphoma. *Gut* 72, 1999–2002. doi: 10.1136/gutjnl-2022-328256

Shi, X., Wallach, J. D., Ma, X., and Rogne, T. (2024). Autoimmune diseases and risk of non-Hodgkin lymphoma: a Mendelian randomisation study. *medRxiv*. doi: 10.1101/2024.01.20.24301459

Shimizu, Y., Isoda, K., Taira, Y., Taira, I., Kondoh, M., and Ishida, I. (2020). Anti-tumor effect of a recombinant Bifidobacterium strain secreting a claudin-targeting molecule in a mouse breast cancer model. *Eur. J. Pharmacol.* 887:173596. doi: 10.1016/j.ejphar.2020.173596

Sieber, S. A., and Marahiel, M. A. (2005). Molecular mechanisms underlying nonribosomal peptide synthesis: approaches to new antibiotics. *Chem. Rev.* 105, 715–738. doi: 10.1021/cr0301191

Sithranga Boopathy, N., and Kathiresan, K. (2010). Anticancer drugs from marine flora: an overview. *J. Oncol.* 2010, 1–18. doi: 10.1155/2010/214186

Smith, P. M., Howitt, M. R., Panikov, N., Michaud, M., Gallini, C. A., Bohlooly-Y, M., et al. (2013). The microbial metabolites, short-chain fatty acids, regulate colonic T reg cell homeostasis. *Science* 341, 569–573. doi: 10.1126/science.1241165

Sokol, H., Pigneur, B., Watterlot, L., Lakhdari, O., Bermúdez-Humarán, L. G., Gratadoux, J.-J., et al. (2008). *Faecalibacterium prausnitzii* is an anti-inflammatory commensal bacterium identified by gut microbiota analysis of Crohn disease patients. *Proc. Natl. Acad. Sci. USA* 105, 16731–16736. doi: 10.1073/pnas.0804812105

Stein-Thoeringer, C. K., Saini, N. Y., Zamir, E., Blumenberg, V., Schubert, M.-L., Mor, U., et al. (2023). A non-antibiotic-disrupted gut microbiome is associated with clinical responses to CD19-CAR-T cell cancer immunotherapy. *Nat. Med.* 29, 906–916. doi: 10.1038/s41591-023-02234-6

Sugiyama, Y., Masumori, N., Fukuta, F., Yoneta, A., Hida, T., Yamashita, T., et al. (2013). Influence of isoflavone intake and equol-producing intestinal Flora on prostate cancer risk. *Asian Pac. J. Cancer Prev.* 14, 1–4. doi: 10.7314/APJCP.2013.14.1.1

Sung, H., Ferlay, J., Siegel, R. L., Laversanne, M., Soerjomataram, I., Jemal, A., et al. (2021). Global Cancer Statistics 2020: GLOBOCAN estimates of incidence and mortality worldwide for 36 cancers in 185 countries. *CA Cancer J Clin.* 71, 209–249. doi: 10.3322/caac.21660

Tanaka, T., Matsuno, Y., Torisu, T., Shibata, H., Hirano, A., Umeno, J., et al. (2021). Gastric microbiota in patients with *Helicobacter pylori*-negative gastric MALT lymphoma. *Medicine* 100:e27287. doi: 10.1097/MD.0000000000027287

Taur, Y., Jenq, R. R., Perales, M.-A., Littmann, E. R., Morjaria, S., Ling, L., et al. (2014). The effects of intestinal tract bacterial diversity on mortality following allogeneic hematopoietic stem cell transplantation. *Blood* 124, 1174–1182. doi: 10.1182/blood-2014-02-554725

Upadhyay Banskota, S., Skupa, S. A., El-Gamal, D., and D'Angelo, C. R. (2023). Defining the role of the gut microbiome in the pathogenesis and treatment of lymphoid malignancies. *IJMS* 24:2309. doi: 10.3390/ijms24032309

Vacca, M., Celano, G., Calabrese, F. M., Portincasa, P., Gobbetti, M., and De Angelis, M. (2020). The controversial role of human gut Lachnospiraceae. *Microorganisms* 8:573. doi: 10.3390/microorganisms8040573

Vital, M., Howe, A. C., and Tiedje, J. M. (2014). Revealing the bacterial butyrate synthesis pathways by analyzing (meta)genomic data. *MBio* 5, e00889–e00814. doi: 10.1128/mBio.00889-14

Waller, P. A., Gopal, P. K., Leyer, G. J., Ouwehand, A. C., Reifer, C., Stewart, M. E., et al. (2011). Dose-response effect of *Bifidobacterium lactis* HN019 on whole gut transit time and functional gastrointestinal symptoms in adults. *Scand. J. Gastroenterol.* 46, 1057–1064. doi: 10.3109/00365521.2011.584895

Walter, J. M., Coutinho, F. H., Dutilh, B. E., Swings, J., Thompson, F. L., and Thompson, C. C. (2017). Ecogenomics and taxonomy of Cyanobacteria phylum. *Front. Microbiol.* 8:2132. doi: 10.3389/fmicb.2017.02132

Wei, W., Sun, W., Yu, S., Yang, Y., and Ai, L. (2016). Butyrate production from high-fiber diet protects against lymphoma tumor. *Leuk. Lymphoma* 57, 2401–2408. doi: 10.3109/10428194.2016.1144879

Weizman, Z., Asli, G., and Alsheikh, A. (2005). Effect of a probiotic infant formula on infections in child care centers: comparison of two probiotic agents. *Pediatrics* 115, 5–9. doi: 10.1542/peds.2004-1815

Wrasidlo, W., Mielgo, A., Torres, V. A., Barbero, S., Stoletov, K., Suyama, T. L., et al. (2008). The marine lipopeptide somocystinamide a triggers apoptosis via caspase 8. *Proc. Natl. Acad. Sci. USA* 105, 2313–2318. doi: 10.1073/pnas.0712198105

Yatsunenko, T., Rey, F. E., Manary, M. J., Trehan, I., Dominguez-Bello, M. G., Contreras, M., et al. (2012). Human gut microbiome viewed across age and geography. *Nature* 486, 222–227. doi: 10.1038/nature11053

Yuan, L., Wang, W., Zhang, W., Zhang, Y., Wei, C., Li, J., et al. (2021). Gut microbiota in untreated diffuse large B cell lymphoma patients. *Front. Microbiol.* 12:646361. doi: 10.3389/fmicb.2021.646361

Zaplana, T., Miele, S., and Tolonen, A. C. (2024). Lachnospiraceae are emerging industrial biocatalysts and biotherapeutics. *Front. Bioeng. Biotechnol.* 11:1324396. doi: 10.3389/fbioe.2023.1324396

Zhang, X., Yu, D., Wu, D., Gao, X., Shao, F., Zhao, M., et al. (2023). Tissue-resident Lachnospiraceae family bacteria protect against colorectal carcinogenesis by promoting tumor immune surveillance. *Cell Host Microbe* 31, 418–432.e8. doi: 10.1016/j.chom.2023.01.013

Zhao, J., Ming, J., Hu, X., Chen, G., Liu, J., and Yang, C. (2020). Bayesian weighted Mendelian randomization for causal inference based on summary statistics. *Bioinformatics* 36, 1501–1508. doi: 10.1093/bioinformatics/btz749

Zheng, T., Liu, C., Wang, Y., Zhou, H., Zhou, R., Zhu, X., et al. (2024). Inflammatory cytokines mediating the effect of oral lichen planus on oral cavity cancer risk: a univariable and multivariable Mendelian randomization study. *BMC Oral Health* 24:375. doi: 10.1186/s12903-024-04104-0

Zhou, M., Xia, J., Chen, X., Wu, T., Xu, K., Zou, Y., et al. (2024). Assessing the causal association between dietary vitamin intake and lymphoma risk: a Mendelian randomisation study. *Int. J. Food Sci. Nutr.* 75, 92–101. doi: 10.1080/09637486.2023.2278420

Zou, Y., Lin, X., Xue, W., Tuo, L., Chen, M.-S., Chen, X.-H., et al. (2021). Characterization and description of Faecalibacterium butyricigenerans sp. nov. and F. Longum sp. nov., isolated from human faeces. *Sci. Rep.* 11:11340. doi: 10.1038/s41598-021-90786-3

frontiers | Frontiers in Microbiology

TYPE Original Research
PUBLISHED 12 June 2024
DOI 10.3389/fmicb.2024.1367877

OPEN ACCESS

EDITED BY
Congying Chen,
Jiangxi Agricultural University, China

REVIEWED BY
Jun Chen,
Jiangxi Agricultural University, China
Yang Li,
Shandong Agricultural University, China

*CORRESPONDENCE
Zhiyong Fan
✉ fzyong04@163.com
Bi'e Tan
✉ bietan@hunau.edu.cn

†These authors have contributed equally to this work and share first authorship

RECEIVED 09 January 2024
ACCEPTED 21 May 2024
PUBLISHED 12 June 2024

CITATION
Yu J, Wang J, Cao C, Gong J, Cao J, Yin J, Wu S, Huang P, Tan B and Fan Z (2024) Maternal intervention with a combination of galacto-oligosaccharides and hyocholic acids during late gestation and lactation increased the reproductive performance, colostrum composition, antioxidant and altered intestinal microflora in sows. *Front. Microbiol.* 15:1367877. doi: 10.3389/fmicb.2024.1367877

Maternal intervention with a combination of galacto-oligosaccharides and hyocholic acids during late gestation and lactation increased the reproductive performance, colostrum composition, antioxidant and altered intestinal microflora in sows

Jian Yu†, Jie Wang†, Chang Cao, Jiani Gong, Jiaqi Cao, Jie Yin, Shusong Wu, Peng Huang, Bi'e Tan* and Zhiyong Fan*

College of Animal Science and Technology, Hunan Agricultural University, Changsha, China

Introduction: This study was conducted to evaluate the effects of dietary galacto-oligosaccharides (GOS) and hyocholic acids (HCA) during late gestation and lactation on reproductive performance, colostrum quality, antioxidant capacity and gut microbiota in multiparous sows.

Methods: A total of 60 healthy multiparous cross-bred sows (Landrace × Yorkshire) were randomly fed 4 groups diets as follows: the basal diets (CTRL group), or the basal diets containing only 600 mg/kg GOS (GOS group), 600 mg/kg GOS + 100 mg/kg HCA (GOS + Low HCA group), and 600 mg/kg + 200 mg/kg HCA (GOS + High HCA group) from d 85 of gestation to weaning. Multiple parameters of sows were determined.

Results: There was a trend of shortening the labor process of sows ($p = 0.07$) in the GOS group and GOS + Low/High HCA group. Compared with the CTRL group, the GOS + Low/High HCA group increased the average piglets weight at birth ($p < 0.05$), and increased the IgA concentration of colostrum ($p < 0.05$). In addition, serum triglyceride (TG) concentration was lower ($p < 0.05$), and serum total antioxidant capacity (T-AOC) was higher ($p < 0.05$) in the GOS and GOS + Low/High HCA groups than in the CTRL group at farrowing. Serum catalase (CAT) activities was higher in the GOS and GOS + High HCA groups than in the CTRL group at farrowing. The 16S rRNA analysis showed that GOS combination with high-dose HCA shaped the composition of gut microbiota in different reproductive stages (d 107 of gestation, G107; d 0 of lactation, L0; d 7 of lactation, L7). At the phylum level, the relative abundance of *Bacteroidota* and *Desulfobacterota* in G107, *Bacteroidota*, and *Proteobacteria* in L0, and *Planctomycetota* in L7 was increased in GOS + High HCA group ($p < 0.05$). Spearman correlation analysis showed that *Streptococcus* was positively correlated with the serum TG but negatively correlated with the average piglets weight at birth ($p < 0.05$).

Conclusion: This investigation demonstrated that the administration of galacto-oligosaccharides (GOS) in conjunction with hyocholic acids (HCA), to sows with nutrient restrictions during late gestation and lactation, further improved their antioxidant capacity and milk quality. The observed beneficial effects of GOS + HCA supplementation could potentially be linked to an improvement in gut microbiota disorders of the sows.

KEYWORDS

sow, galacto-oligosaccharides, hyocholic acids, reproductive performance, gut microbiota

1 Introduction

The pivotal role of breeding sows in the pig industry is well known, particularly in terms of their health and reproductive performance. However, sows are vulnerable to major immune system and physiological metabolism changes during pregnancy, including heightened oxidative stress and inflammatory response, which can result in blood levels of pro-inflammatory factors like interleukin-6, tumor necrosis factor, and reactive oxygen species being elevated (Berchieri et al., 2011). Constipation, miscarriages, and intrauterine development retardation are among the reproductive disorders that are intimately linked to an imbalance in the inflammatory response. Therefore, in order to improve sows' reproductive success, it is crucial to boost their immunity throughout the late gestation phase.

As a natural functional oligosaccharide, galacto-oligosaccharides (GOS) are not easily digested and hydrolyzed but are fermented by microflora in hindgut to produce short-chain fatty acids (Vos et al., 2007). Furthermore, supplementation with GOS has been indicated to stimulate the proliferation and/or activity of beneficial bacteria, especially *Bifidobacteria* and *Lactobacillus* (Gopal et al., 2001; Monteagudo et al., 2016). In fact, research data have demonstrated that dietary supplementation of GOS in pregnancy sows can elevate the plasma immunoglobulin A to enhance the immune status (Wu et al., 2021; Lee et al., 2023).

It has recently been established that bile acids (BAs), which are amphipathic chemicals produced by the liver's catabolism of cholesterol, are important signaling molecules in the body. They play a role in several physiological processes, such as immunological regulation, hepatic insulin resistance, energy balance, lipid and glucose metabolism, and bile acid metabolism (Zong et al., 2019; Cao et al., 2021). This recognition primarily stems from their ability to activate specific bile acids receptors, as evidenced in recent studies (Molinaro et al., 2018; Ahmad and Haeusler, 2019). A great deal of study has been done on feeding BAs to weaned pigs. These investigations have shown that taking such supplements might enhance humoral immune responses and raise blood antioxidant capacity.

However, there is a paucity of research exploring the potential benefits of dietary mixtures of GOS and bile acids (BAs) on the health of suckling piglets via maternal nutrition. Given the complementary and synergistic biological functions of GOS and BAs, it is hypothesized that incorporating a combination of these substances into the diets of perinatal sows could markedly enhance reproductive performance, bolster antioxidant capacity, and improve colostrum quality through modulation of the gut microbiota.

2 Materials and methods

2.1 Ethics approval

All animal care procedures in our study were approved by the Institution of Animal Care and Use Committee of the College of Animal Science and Technology, at Hunan Agricultural University (Changsha, China), and were conducted in accordance with the National Institutes of Health (Changsha, China) guidelines for the care and use of experimental animals.

2.2 Galacto-oligosaccharides (GOS) and bile acids (BAs)

The GOS (product name: Kang Liwei, purity ≥88%, moisture ≤2%, light yellow, fine sand) was provided by the Chengdu Associated Bio-Technology Co., Ltd. (Chengdu, China). The BAs were hyocholic acids (product name: glycinocholic acid sodium salt, total acidity ≥85%, moisture ≤2%, white, powder) and were provided by the Wuhan Huaxiang Kejie Bio-Technology Co., Ltd. (Wuhan, China).

2.3 Animals and experimental design

Third to fifth parity late pregnancy sow ($n = 60$; d 85 of gestation, Landrace × Yorkshire) with similar backfat thickness and an average body weight of 302 ± 13 kg were randomly assigned to one of 4 treatments: the basal diets (diets without GOS and HCA, $n = 15$, CTRL group), basal diets containing only 600 mg/kg GOS ($n = 15$, GOS group), basal diets containing 600 mg/kg GOS + 100 mg/kg HCA ($n = 15$, GOS+ Low HCA group), and basal diets containing 600 mg/kg GOS + 200 mg/kg HCA ($n = 15$, GOS + High HCA group). The basal diets (Table 1) were divided into a pregnancy and a lactation diet and nutritional requirements were formulated on the basis of the recommendations by the National Research Council (National Research Council, 2012). Sows were raised individually in stalls (2.0 m × 0.6 m) with concrete-floored from d 85 to 107 and fed a total of 3 kg diet daily (8:30 and 15:30). Then, the sows were shifted to farrowing stalls (2.13 m × 0.66 m) with concrete-floored and offered

TABLE 1 Composition and nutrient contents of basal diets (as-fed basis, %).

Ingredients	Content	
	Late gestation	Lactation
Corn	5.40	20.00
Red Sorghum	15.00	10.00
Wheat	–	29.20
Hulled barley	54.60	13.20
Wheat bran	15.00	–
Soybean meal (43% crude protein)	5.55	20.30
Soybean oil		2.50
L-Lys-HCI (98%)	0.28	0.38
Limestone	1.81	1.70
Dicalcium phosphate	0.65	1.2
Salt	0.40	0.40
Vitamin-mineral premix[a]	1.31	1.12
Total	100	100
Nutrient composition[b]		
Digestible energy, kcal/kg	3,022	3,471
Crude protein, %	12.06	17.15
Crude fiber, %	3.18	2.63
Calcium, %	0.85	0.76
Total phosphorus, %	0.55	0.61
Available phosphorus, %	0.33	0.43
Total lys, %	0.79	1.26

[a]The premix provided the following per kilogram of complete diets: Zn, 80.0 mg; Cu, 6.0 mg; Fe, 80.0 mg; Mn, 20.0 mg; I, 0.15 mg; Se, 0.15 mg; vitamin A, 10,000 IU; vitamin D_3, 2,100 IU; vitamin E, 45 IU; vitamin K_3, 4 mg; vitamin B_1, 2.0 mg; vitamin B_2, 8.0 mg; vitamin B_6, 4.0 mg; vitamin B_{12}, 0.025 mg; nicotinic acid, 25.0 mg; pantothenic acid, 20.0 mg; folic acid, 1.0 mg; biotin 0.5 mg.
[b]The nutrient levels of crude protein, crude fiber, calcium and total phosphorus were measured values; other values were calculated.

2 kg of daily diet (8:30 and 15:30) during d 108 of gestation to delivery. After farrowing, all sows were switched to lactation diets and had free access to the diets until weaning. In the whole experiment procedure, sows and piglets were allowed to drink water freely. During the entire experiment, laboratory animals and pigsty were provided by Chenfeng farm of Hunan Yangxiang Agriculture and Animal Husbandry Co., Ltd., and feeding management and immunization procedures of sows and piglets were carried out according to the company's standards.

2.4 Sample collection and processing

Basal diets were ground to pass through a 0.5 mm screen using a mill grinder. Crude protein, crude fiber, calcium and total phosphorus contents of the diets were determined according to AOAC (2007).

Fresh feces of the sows ($n = 6$ per group) were collected individually by massaging the rectum at d 107 of gestation (d 7 before delivery), and d 0 and d 7 of lactation (before each sampling, the buttocks of the sows were washed with 1/1000 potassium permanganate, the anus was disinfected with alcohol cotton balls). Next, 24 fecal samples were transported to the laboratory and stored at −80°C until later analysis.

Six sows per group were randomly selected for blood samples. A 10 mL blood was collected into centrifuge tubes from the sows' ear veins on the farrowing day (within 2 h of delivery). The serum samples were obtained by centrifuging blood samples at 3000 r/min for 15 min. Whereafter they were stored at −20°C for the analysis.

On the farrowing day (within 2 h of delivery), the mixed colostrum samples ($n = 6$) were collected from the anterior, middle and posterior three milk areas of the sows. Approximately 10 mL of colostrum per sow was collected into a centrifuge tube. The samples were rapidly stored at −20°C for the analysis.

2.5 Determination of redox status of serum

Total antioxidant capability (T-AOC), the activities of superoxide dismutase (SOD), catalase (CAT), total glutathione (T-GSH) and malonaldehyde (MDA) in serum were estimated using commercial kits (Nanjing Jiancheng Bioengineering Institute, Nanjing, China), according to the manufacturer's protocols with a V1600 Split Beam Visible Spectrophotometer (Meipuda Co., Shanghai, China). The results were expressed as units per milliliter of serum.

2.6 Determination of milk composition and immunoglobulin

Colostrum samples were analyzed for total cholesterol (TC) and triglyceride (TG) using a fully automated biochemical analyzer. Whey samples were obtained by centrifuging colostrum samples at 4000 r/min for 10 min, and the concentration of immunoglobulin A (IgA) was analyzed by using commercial kits (Cusabio Biotech Co., Ltd., Wuhan, China), according to the manufacturer's protocols.

2.7 Determination of serum metabolites

Glucose (GLU), triglyceride (TG), total cholesterol (TC), high-density lipoprotein cholesterol (HDL-C) and low-density lipoprotein cholesterol (LDL-C) were determined using reagent kits (Nanjing Jiancheng Bioengineering Institute, Nanjing, China). All of the procedures were carried out in accordance with the manufacturer's protocols.

2.8 DNA extraction, PCR amplification, and bacterial 16S ribosomal RNA (rRNA) gene sequencing

The total genomic DNA was extracted from fecal samples of sows (at d 107 of gestation, at farrowing and at d 7 of lactation) using a DNA kit (LC-Bio Technology Co., Ltd., Hangzhou, China). The quality of isolated DNA was determined by agarose gel electrophoresis. Subsequently, the V3-V4 hypervariable region of the bacterial 16S rRNA gene was used as a template for PCR amplification. The V3-V4 gene region of 16S rRNA was amplified by using the forward primer

338F: 5'-ACTCCTACGGGAGGCAGCAG-3′ and 806R: 5'-GGACTACHVGGGTWTCTAAT-3′. For each sample, a 8-digit barcode sequence was added to the 5′ end of the forward and reverse primers (provided by Allwegene Company, Beijing). The volume of the PCR was 25 μL and included 12.5 μL 2 × Taq PCR MasterMix (Vazyme Biotech Co., Ltd., China), 3 μL BSA (2 ng/μL), 1 μL Forward Primer (5 μM), 1 μL Reverse Primer (5 μM), 2 μL template DNA, and 5.5 μL double distilled H_2O. Cycling parameters were 95°C for 5 min, followed by 28 cycles of 95°C for 45 s, 55°C for 50 s and 72°C for 45 s with a final extension at 72°C for 10 min. The PCR products were purified using a Agencourt AMPure XP Kit (Beckman Coulter, Inc., United States). Sequencing libraries were generated using NEB Next Ultra II DNA Library Prep Kit (New England Biolabs, Inc., United States) following the manufacturer's recommendations. The sequences were clustered into operational taxonomic units (OTU) at a similarity level of 97% to generate rarefaction curves and to calculate the richness and diversity indices.

2.9 Statistical analysis

The sows were treated as an experimental unit in all of the statistical analyses. First tests for normal distribution and homogeneity of variance were performed on the data. Subsequently, the data between different groups were analyzed by a one-way ANOVA and Duncan's multiple range test using SPSS 26.0 software (SPSS Inc., Chicago, IL, United States). GraphPad Prism 8 (San Diego, CA, United States) was used to plot Figures. The correlation between gut microbiota and the detection indexes of sows was analyzed with R software (version. 3. 5. 1). Results were shown as means ± standard error. Probability values <0.05 and < 0.01 were considered statistically significant and highly significant, respectively.

3 Results

3.1 Effect of GOS and HCA supplementation on reproductive performance of the sows

The results of reproductive performance are shown in Table 2. There were no differences ($p > 0.05$) in Total pigs born, pigs born alive, pigs born robust, stillbirth number, mummy number, and coefficient variation of piglet litter among the four groups. Similarly, treatment differences in pig number at weaned, litter weight at weaned, and coefficient of variation at weaned were small and not important ($p > 0.10$). However, compared with the basal diets, there was a trend for the labor process from sows fed GOS and GOS + Low/High HCA diets to be shorter ($0.05 < p < 0.10$). Sows fed the GOS + Low/High HCA diets increased the average piglets weight at birth compared with sows fed the basal diets ($p < 0.05$).

3.2 Effect of GOS and HCA supplementation on concentrations of serum and colostrum metabolites

As reported in Table 3, GOS and GOS + Low/High HCA supplementation decreased the serum TG concentration of sows at delivery ($p < 0.05$), and the concentration of GLU increased slightly ($0.05 < p < 0.10$). However, the sows were not observed distinct differences in serum LDL-C, HDL-C, TC and TBA concentrations between the CTRL group and GOS or GOS + Low/High HCA groups at delivery ($p > 0.10$).

As shown in Table 4, it was found that the concentrations of TG on colostrum increased slightly in the GOS and GOS + Low/High HCA supplementation groups compared with the CTRL group at farrowing ($0.05 < p < 0.10$). In addition, the IgA concentration of colostrum was significantly increased by dietary GOS + Low/High HCA supplementation ($p < 0.05$).

3.3 Effect of GOS and HCA supplementation on serum antioxidant capacity of sows

The results of serum antioxidant indexes are reported in Table 5. Compared with the control sows, GOS and GOS + Low/High HCA supplementation increased serum T-AOC ($p < 0.05$). At the same time, sows in the GOS and GOS + High HCA groups had higher activities of CAT ($p < 0.05$) than sows in the CTRL group. There was no evident difference in the activities of serum MDA between the four groups ($0.05 < p < 0.10$).

3.4 Effect of GOS and HCA supplementation on community composition of microbiota at phyla or genera level and alpha-diversity

According to the differences in reproductive performance, serum metabolite concentration, and serum antioxidant indexes of sows among the four groups, 16S rRNA sequencing was performed on fecal microflora of sows (at d 107 of gestation, at farrowing and at d 7 of lactation) in the CTRL group, GOS group, and GOS+ High HCA group to determine their diversity and composition. GOS combined with high-dose HCA changed the gut microbiota diversity of sows at d 107 of gestation, at farrowing and at d 7 of lactation, but the trend was different for these 3 time points. All 54 fecal samples were subjected to 16S rRNA gene sequencing (Supplementary Table S1). 1,534,842 raw_tages, 1,510,440 raw_tages and 1,510,290 raw_tages were filtered to obtain 1,350,659, 1,336,069 and 1,347,266 valid_tages at d 107 of gestation, at farrowing and at d 7 of lactation. On the basis of 97% sequence similarity, 870, 1,004 and 969 OTUs were obtained at d 107 of gestation, at farrowing and at d 7 of lactation, respectively. Next, variations in the microbial composition of all groups were explored. Linear discriminant analysis effect size (LEfSe) analysis of the bacterial community was used to filter the significantly different OTUs among groups, and the results demonstrate that there were dramatic differences in microbial composition between the treatment groups and the CTRL group (Figure 1).

In the present study, the bacterial diversity (Shannon and Simpson) and richness estimators (Chao 1 and Observed) were higher for sows in the GOS and GOS + High HCA groups ($p < 0.05$) compared with sows in the CTRL group at d 107 of gestation (Figure 2A). However, there was no difference between any of the groups regards to the Chao 1 values, number of observed species, and Shannon and Simpson indices ($p > 0.05$) at farrowing (Figure 2B). The sows fed diets

TABLE 2 Effects of galacto-oligosaccharides (GOS) and hyocholic acids (HCA) on the reproductive performance of sows.

Items	Maternal treatment[1]				*p*-value
	CTRL	GOS	GOS + Low HCA	GOS + High HCA	
Parturition					
Labor process, h	3.80 ± 0.31	2.48 ± 0.64	1.62 ± 0.47	2.34 ± 1.27	0.07
Number of piglets born per litter	14.93 ± 1.00	16.20 ± 1.27	14.00 ± 0.86	15.47 ± 0.94	0.50
Number of piglets born alive per litter	13.31 ± 0.90	15.40 ± 1.05	13.08 ± 0.38	14.73 ± 0.86	0.35
Number of piglets born robust per litter	12.92 ± 0.90	15.27 ± 1.02	12.85 ± 0.39	14.27 ± 0.85	0.11
Number of stillbirths per litter	0.53 ± 0.17	0.47 ± 0.19	0.36 ± 0.17	0.50 ± 0.17	0.90
Average piglets weight at birth, kg	1.13 ± 0.10^{b}	1.34 ± 1.17^{ab}	1.45 ± 0.06^{a}	1.49 ± 0.06^{a}	0.02
Intralitter coefficient of variation of piglets at birth, %	0.21 ± 0.01	0.15 ± 0.02	0.17 ± 0.01	0.16 ± 0.01	0.24
Weaning (21 d of age)					
Number of piglets weaned per litter	11.18 ± 0.54	12.14 ± 0.57	12.02 ± 0.26	12.00 ± 0.40	0.29
Average piglets weight at weaning, kg	7.32 ± 0.15	7.40 ± 0.18	7.31 ± 0.22	7.57 ± 0.24	0.11
Average litter weight at weaning, kg	81.97 ± 3.75	89.85 ± 4.48	88.06 ± 4.41	90.74 ± 4.20	0.64
Average litter weight gain, kg	65.36 ± 3.16	69.40 ± 3.97	69.43 ± 3.55	70.05 ± 4.45	0.47
Intralitter coefficient of variation of piglets at weaning, %	0.13 ± 0.02	0.12 ± 0.01	0.10 ± 0.01	0.13 ± 0.01	0.43

[1] CTRL = basal diets; GOS = basal diets +600 mg/kg GOS; GOS + Low HCA = basal diets +600 mg/kg GOS + 100 mg/kg HCA; GOS + High HCA = basal diets +600 mg/kg GOS + 200 mg/kg HCA. Values are expressed as means ± standard error, $n = 15$ for each group. [a, b] Mean values within a row with different letter superscripts are significantly different ($p < 0.05$).

TABLE 3 Effect of galacto-oligosaccharides (GOS) and hyocholic acids (HCA) on serum metabolites levels of sows at farrowing.

Items[2]	Maternal treatment[1]				*p*-value
	CTRL	GOS	GOS + Low HCA	GOS + High HCA	
LDL-C, mmol/L	0.42 ± 0.02	0.48 ± 0.04	0.46 ± 0.04	0.46 ± 0.04	0.83
HDL-C, mmol/L	0.66 ± 0.03	0.60 ± 0.04	0.58 ± 0.04	0.62 ± 0.03	0.34
TC, mmol/L	1.61 ± 0.08	1.56 ± 0.08	1.52 ± 0.06	1.57 ± 0.08	0.85
TG, mmol/L	0.55 ± 0.02^{a}	0.30 ± 0.02^{b}	0.31 ± 0.03^{b}	0.34 ± 0.05^{b}	<0.01
TBA, mmol/L	74.37 ± 3.59	56.77 ± 11.22	54.83 ± 4.55	59.99 ± 12.84	0.38
GLU, mmol/L	4.02 ± 0.15	4.58 ± 0.55	5.18 ± 0.22	5.24 ± 0.35	0.08

[1] CTRL = basal diets; GOS = basal diets +600 mg/kg GOS; GOS + Low HCA = basal diets +600 mg/kg GOS + 100 mg/kg HCA; GOS + High HCA = basal diets +600 mg/kg GOS + 200 mg/kg HCA. Values are expressed as means ± standard error, $n = 15$ for each group. [2] LDL-C = low density lipoprotein cholesterol; HDL-C = high density lipoprotein cholesterol; TC = total cholesterol; TG = triglyceride; TBA = total bile acids; GLU = glucose. [a, b] Mean values within a row with different letter superscripts are significantly different ($p < 0.05$).

containing GOS + High HCA had higher Shannon and Simpson diversity indices ($p < 0.05$) compared with the sows fed basal diets (Figure 2C). Using principal component analysis (PCA) based on OTUs, it was found that the gut microbiota of sows in the GOS and combined GOS and high-dose HCA supplementation groups were distinctly segregated from those in the CTRL group at d 107 of gestation, at farrowing and d 7 of lactation (Figures 2D–F).

The effect of dietary supplementation of GOS and HCA on gut microbiota composition of sows at d 107 of gestation in Figure 3. At the phylum level, the abundance of *Bacteroidota* and *Desulfobacterota*

TABLE 4 Effect of galacto-oligosaccharides (GOS) and hyocholic acids (HCA) on colostrum metabolites and immunoglobulin a levels of sows at farrowing.

Items[2]	Maternal treatment[1]				*p*-value
	CTRL	GOS	GOS + Low HCA	GOS + High HCA	
TC, mmol/L	3.24 ± 0.18	3.51 ± 0.26	3.76 ± 0.31	3.29 ± 0.18	0.41
TG, mmol/L	30.90 ± 3.29	36.00 ± 1.70	37.16 ± 0.95	37.17 ± 1.10	0.08
IgA, mg/mL	375878.67 ± 54654.21[b]	314293.33 ± 24431.04[b]	556164.00 ± 67100.28[a]	599001.33 ± 28031.05[a]	0.01

[1] CTRL = basal diets; GOS = basal diets +600 mg/kg GOS; GOS + Low HCA = basal diets +600 mg/kg GOS + 100 mg/kg HCA; GOS + High HCA = basal diets +600 mg/kg GOS + 200 mg/kg HCA. Values are expressed as means ± standard error, $n = 15$ for each group. [2] TC = total cholesterol; TG = triglyceride; IgA = immunoglobulin A. [a,b] Mean values within a row with different letter superscripts are significantly different ($p < 0.05$).

TABLE 5 Effects of galacto-oligosaccharides (GOS) and hyocholic acids (HCA) on serum antioxidant index of sows at farrowing.

Items[2]	Maternal treatment[1]				*p*-value
	CTRL	GOS	GOS + Low HCA	GOS + High HCA	
T-AOC, U/mL	0.75 ± 0.02[b]	0.78 ± 0.01[a]	0.80 ± 0.01[a]	0.79 ± 0.01[a]	0.03
T-GSH, μmol/L	3.30 ± 0.85	4.26 ± 0.47	3.39 ± 0.39	5.39 ± 0.65	0.11
CAT, U/mL	1.33 ± 0.17[c]	4.87 ± 0.63[a]	2.92 ± 0.72[bc]	3.34 ± 0.46[ab]	<0.01
SOD, U/mL	22.79 ± 1.69	26.32 ± 0.84	25.85 ± 1.55	26.91 ± 1.11	0.17
MDA, nmol/mL	3.17 ± 0.57	1.90 ± 0.28	3.07 ± 0.34	2.39 ± 0.22	0.09

[1] CTRL = basal diets; GOS = basal diets +600 mg/kg GOS; GOS + Low HCA = basal diets +600 mg/kg GOS + 100 mg/kg HCA; GOS + High HCA = basal diets +600 mg/kg GOS + 200 mg/kg HCA. Values are expressed as means ± standard error, $n = 15$ for each group. [2] T-AOC = total antioxidant capacity; T-GSH = total glutathione; CAT = catalase; SOD = superoxide dismutase; MDA = malondialdehyde. [a,b] Mean values within a row with different letter superscripts are significantly different ($p < 0.05$).

was higher in the GOS+ HCA group sows, compared with sows in the CTRL group (Figure 3A). At the genus level, the abundance of *g_Ruminococcaceae_UCG005* ($p < 0.05$) and *g_Lachnospiraceae_XPB1014* ($p < 0.05$) was greater in the treatment groups than in the CTRL group (Figure 3D). Besides this, the abundance of *g_Ruminococcaceae_UCG002* and *g_Muribaculaceae_unclassified*, in the GOS + HCA group increased significantly ($p < 0.05$), but *Streptococcus* reduced significantly ($p < 0.05$).

The effect of dietary supplementation of GOS and HCA on gut microbiota composition of sows at farrowing in Figure 4. At the phylum level (Figure 4C), the abundances of *Bacteroidota* and *Proteobacteria* were higher ($p < 0.05$), and the abundance of *Firmicutes* was lower ($p < 0.05$) in sows in the GOS+ HCA group, compared with sows in the CTRL group at farrowing. At the genus level (Figure 4D), the abundance of *g_Escherichia-Shigella* was higher ($p < 0.05$) in sows in the GOS + HCA group compared with the CTRL group. The abundances of *g_Eubacterium_coprostanoligenes_group_unclassified* and *g_Ruminococcaceae_ unclassified* were higher ($p < 0.05$), but the abundance of *g_Streptococcus* was lower ($p < 0.05$) in sows in the GOS group, compared with the CTRL group.

The relative abundance of bacteria at the phylum and genus level of sows at d 7 of lactation are presented in Figure 5. As shown, at the phylum level (Figure 5C), the abundance of *Planctomycetota* was higher ($p < 0.05$) in sows in the GOS + HCA group compared with sows in the CTRL group, but the abundance of *Cyanobacteria* was lower ($p < 0.05$) in sows in the GOS group compared with sows in the CTRL group. At the genus level (Figure 5D), compared with the CTRL group, the abundance of *g_Clostridia_UCG-014_unclassified* was increased ($p < 0.05$) by GOS+ HCA supplementation, whereas the abundance of *g_Clostridiales_unclassified* was increased ($p < 0.05$) by GOS alone supplementation.

3.5 Correlation between gut microbiota at genera level and the sows' reproductive performance, concentrations of serum and colostrum metabolites and serum antioxidant index

As shown in Figure 6, the Spearman correlation matrix illustrated that the relative abundance of *g_Streptococcus* was positively correlated with serum TG of sows ($p < 0.05$), but negatively correlated with the average piglets weight at birth ($p < 0.05$). In contrast, *g_Eggerthellaceae_unclassified* and *g_Escherichia-Shigella* were positively correlated with the average piglet birth weight ($p < 0.05$). In addition, *g_Eggerthellaceae_unclassified* was negatively correlated with serum TG and the labor process of sows ($p < 0.05$). *g_Escherichia-Shigella* was negatively correlated with serum HDL-C, LDL-C and TC of sows ($p < 0.05$). *g_Eubacterium_coprostanoligenes_group_unclassified* was positively correlated with serum CAT of sows ($p < 0.05$), but was negatively correlated with intralitter coefficient of variation of piglets at birth ($p < 0.01$).

4 Discussion

Litter size and birth weight are pivotal traits in porcine production. This study examined the impact of dietary supplementation with galacto-oligosaccharides (GOS), both alone and in combination with hyocholic acids (HCA), on these traits in sows. Results indicated that such supplementation did not significantly alter the total number of piglets born. Prior research suggests that litter size is influenced primarily by fertilization rates and prenatal mortality in early gestation (Edwards et al., 2012). Moreover, the variation in birth weight within

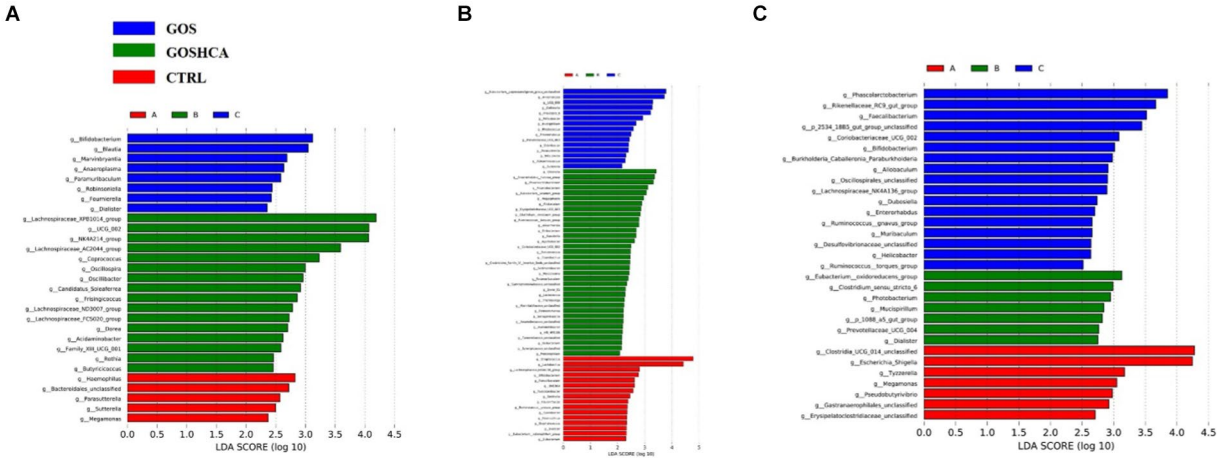

FIGURE 1
LEfSe analysis of the gut microbiota composition of sows at d 107 of gestation, at farrowing, and at d 7 of lactation. At d 107 of gestation, histogram of the Linear Discriminant Analysis (LDA) scores reveals the most differentially abundant taxa among different dietary treatment **(A)**. At farrowing, histogram of the LDA scores reveals the most differentially abundant taxa among different dietary treatment **(B)**. At d 7 of lactation, histogram of the LDA scores reveals the most differentially abundant taxa among different dietary treatment **(C)**. CTRL = basal diets; GOS = basal diets +600 mg/kg GOS; GOS + HCA = basal diets +600 mg/kg GOS + 200 mg/kg HCA.

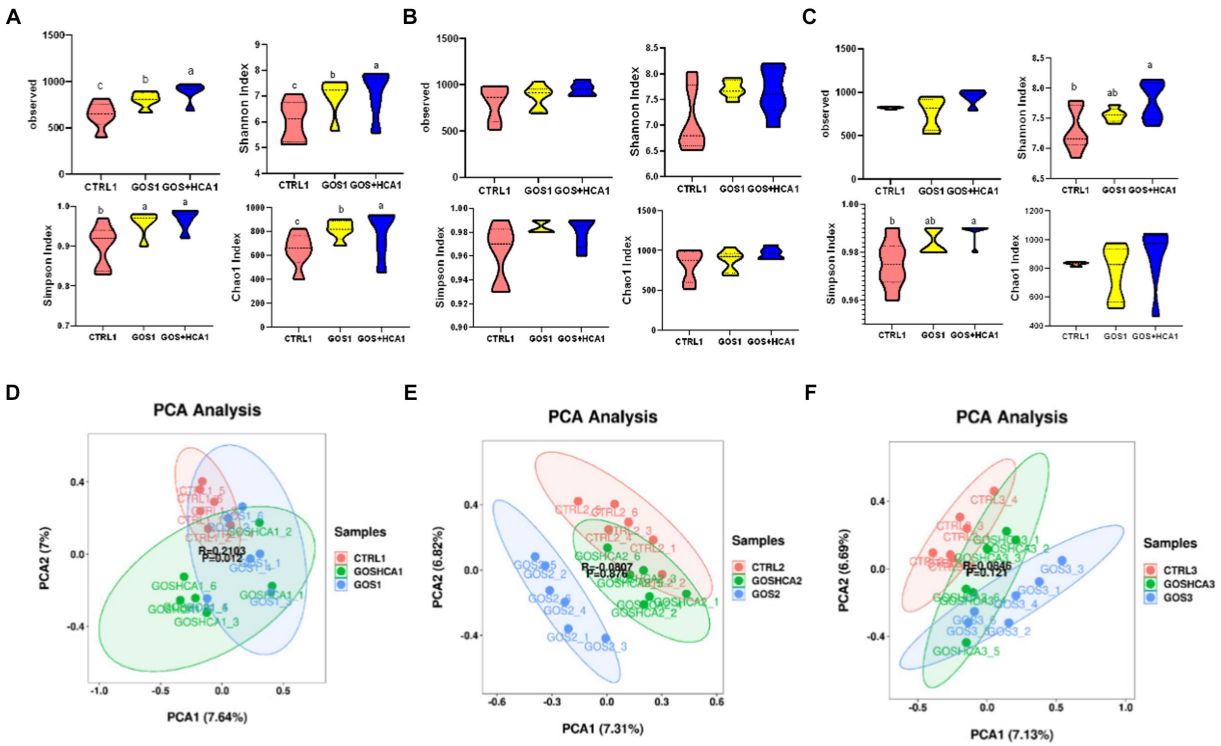

FIGURE 2
Effect of galacto-oligosaccharides (GOS) and hyocholic acids (HCA) on fecal diversity of sows. at d 107 of gestation **(A)**, at farrowing **(B)** and at d 7 of lactation **(C)**, comparison of the number of gut microbiota α-diversity containing bias-corrected Chao richness estimator (Chao 1), observed species, Shannon diversity indices and Simpson diversity indices among sows subjected to different dietary treatments. CTRL = basal diets; GOS = basal diets +600 mg/kg GOS; GOS + HCA = basal diets +600 mg/kg GOS + 200 mg/kg HCA. At d 107 of gestation **(D)**, at farrowing **(E)** and at d 7 of lactation **(F)**, principal component analysis (PCA) based on operational taxonomic units (OTU) among samples of different groups. Each point represents 1 sample.

a litter is a key factor influencing piglet survival during lactation (Škorput et al., 2018). In this study, supplementation with GOS and GOS + Low/High HCA was observed to increase the average birth weight of piglets. This is comparable to earlier reports. Previous work has shown that supplementation with GOS for sows significantly decreased the number of stillborn piglets and increased the body

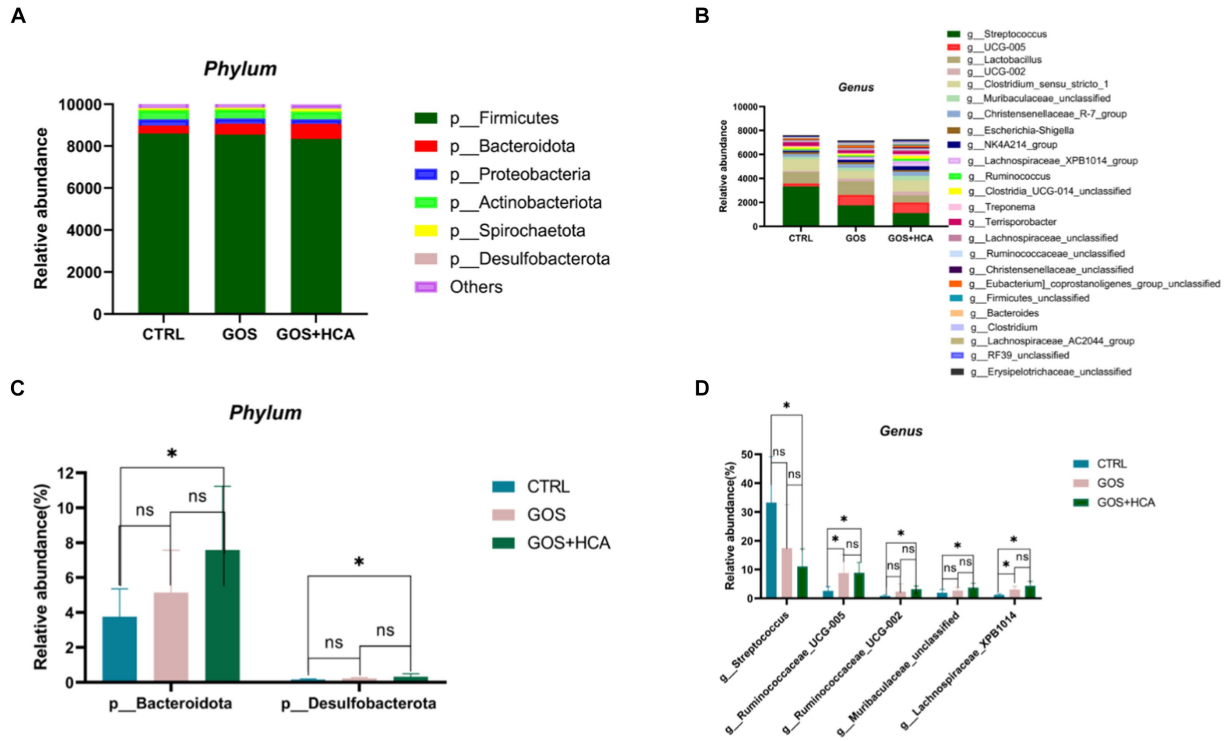

FIGURE 3
Effects of galacto-oligosaccharides (GOS) and hyocholic acids (HCA) on gut microbiota composition of sows at d 107 of gestation. Relative abundance at the phylum level of sows **(A)**, Relative abundance at the genus level of sows **(B)**. Significance test at the phylum level of sows **(C)**, significance test at the genus level of sows **(D)**. CTRL = basal diets; GOS = basal diets +600 mg/kg GOS; GOS + HCA = basal diets +600 mg/kg GOS + 200 mg/kg HCA, $n = 6$ for each group. * is significantly different ($p < 0.05$), whereas ns is not different ($p > 0.05$).

weight and average daily weight gain of the offspring during the neonatal period (Wu et al., 2021). However, in this study, the impact of GOS and HCA supplementation on litter weight at weaning was minimal, potentially due to the specific dosages and environmental conditions affecting the sows (Quiniou and Noblet, 1999). Shorter farrowing durations, associated with improved piglet survival, were noted (Langendijk and Plush, 2019). Interestingly, while increased birth weight can typically extend the farrowing process due to increased mechanical resistance in the birth canal, the combination of GOS and high-dose HCA both increased average birth weight and shortened the farrowing duration. This could be attributed to the potential of GOS and HCA to modulate gut microbial communities, thereby alleviating compression from fecal matter in the birth canal and facilitating quicker delivery (Feyera et al., 2017; Lai et al., 2023). GOS has been reported to enhance the prevalence of beneficial gut bacteria, particularly *Bifidobacteria*, over pathogenic strains (Vulevi et al., 2008). Similarly, HCA has been shown to inhibit *Helicobacter pylori* growth (Itoh et al., 1999), suggesting that these supplements may alleviate constipation by restoring gut microbiota balance.

LDL-C, HDL-C, TG and TC are useful biomarkers for monitoring the absorption and transport of lipids, and the serum level of GLU can reflect energy and glucose metabolism (Shang et al., 2021). However, fat metabolism in serum could be regulated by oligosaccharide intake. It was found that supplementation of xylo-oligosaccharide reduced the serum concentration of triglyceride in nursery piglets (Hou et al., 2020). Similarly, it was found that supplementary feeding of GOS or combined with GOS and Low/High HCA in the perinatal period of sows could also significantly reduce serum TG. Bile acids have a beneficial effect in maintaining TG homeostasis. Research has indicated that bile acids, being the natural ligand of farnesoid X receptor (FXR), has the ability to activate FXR, modify the expression of genes related to triglyceride metabolism, and lower the level of triglycerides in plasma (Watanabe et al., 2004). This study also discovered that supplementing sows' diets with GOS or a combination of GOS and Low/High HCA caused serum TG levels to drop and GLU levels to slightly rise. It is speculated that in order to fulfill the energy requirements of the sow's delivery, this causes TG to be converted into GLU. Therefore, our experiment showed that the addition of the combination with GOS and Low/High HCA in sows' diets could improve the efficiency of fat utilization, supplying more energy for the farrowing process. This is one of the explanations for the control group's higher labor process than that of the GOS and HCA combined.

As the only energy and immune source for suckling piglets, the composition of colostrum and milk is critical for improving growth performance, especially immunoglobulin (Li et al., 2023). A previous study has shown that isomaltooligosaccharide could significantly improve the concentrations of colostrum IgA, IgG and IgM (Zhang et al., 2021). Paradoxically, another study reported that the sows fed mannan oligosaccharides did not affect IgA, IgG and IgM contents in colostrum (Duan et al., 2016). In our study, we found that only GOS supplementation did not affect the concentration of IgA in colostrum. The aforementioned circumstance might be linked to the quantity of oligosaccharides that were added, as well as to the structural units of oligosaccharides and the various ways in which they are connected.

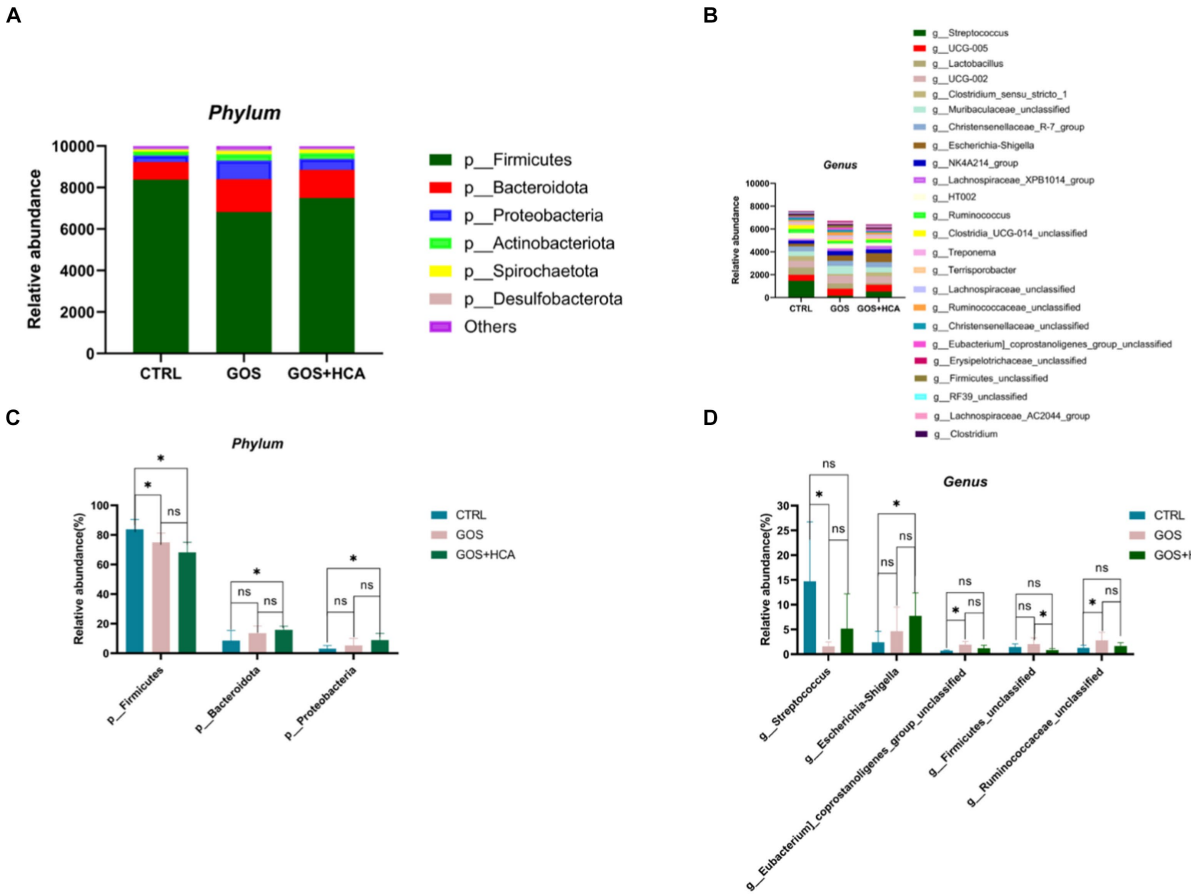

FIGURE 4
Effects of galacto-oligosaccharides (GOS) and hyocholic acids (HCA) on gut microbiota composition of sows at farrowing. Relative abundance at the phylum level of sows **(A)**, relative abundance at the genus level of sows **(B)**. Significance test at the phylum level of sows **(C)**, significance test at the genus level of sows **(D)**. CTRL = basal diets; GOS = basal diets +600 mg/kg GOS; GOS + HCA = basal diets +600 mg/kg GOS + 200 mg/kg HCA, $n = 6$ for each group. * is significantly different ($p < 0.05$), whereas ns is not different ($p > 0.05$).

However, this study has demonstrated that adding Low/High HCA on the basics of the GOS supplement great boosted the amount of IgA in milk. This might have to do with the fact that bile acids have the ability to stimulate the growth of intestinal epithelial cells, which improves the absorption of amino acids and other nutrients while also increasing the amounts of raw materials available for the production of milk components, particularly milk proteins (Dossa et al., 2015). At the same times, it partly explains why average litter gain weight of the GOS + Low/High HCA groups was slightly heavier than that of the CTRL group.

The pregnant animals appear particularly vulnerable to reactive oxygen species because of the placenta's extensive cell division and high metabolic activity (Sultana et al., 2023). Wang et al. (2022) has reported that the combination of GOS and *L. plantarum* supplementation in mice's diets inhibited d-gal-induced oxidative stress. A recent study showed that early-life GOS supplements in suckling piglets' diets alleviated the LPS-induced reactive oxygen species secretion, and inhibited the LPS-induced decrease of GSH-Px, T-AOC and SOD activities in serum (Tian et al., 2022). Consistent with these studies, the results of our experiment showed that activities of T-AOC and CAT in serum were significantly increased after GOS or GOS + High HCA treatment at farrowing. For the development of advantageous bacteria like *Lactobacilli* and *Bifidobacteria*, GOS is a high-quality nutritional source and an influential growth factor, which modulates the composition and amount of intestinal microbiota, restores the integrity of the intestinal barrier, and reduces oxygen free radicals (Schwab and Ganzle, 2011). Furthermore, GOS may be digested in the large intestine by bifidobacteria to create short-chain fatty acids, which lower intestinal pH values and prevent pathogenic bacteria from colonizing and growing (Fanaro et al., 2009). Simultaneously, the process by which exogenous bile acids can boost antioxidant activity in the body might be associated with the activation of nuclear factor erythroid-2-related factor 2 (Nrf2), which boosts the activity of enzymes like glutathione peroxidase, superoxide dismutase, and catalase in cells, and consequently lowers the levels of reactive oxygen species and malondialdehyde in cells (Li et al., 2020). Considering this observation, our research provides evidence of improvements in immunity and antioxidant ability in response to GOS or GOS + HCA supplementation for sows during the perinatal period.

The mammalian gastrointestinal tract is inhabited by trillions of microbes, which play a vital role in physiology, metabolism, immunity and so on. However, the composition of gut microbiota is implicated in various factors, including gut environment, nutrition and

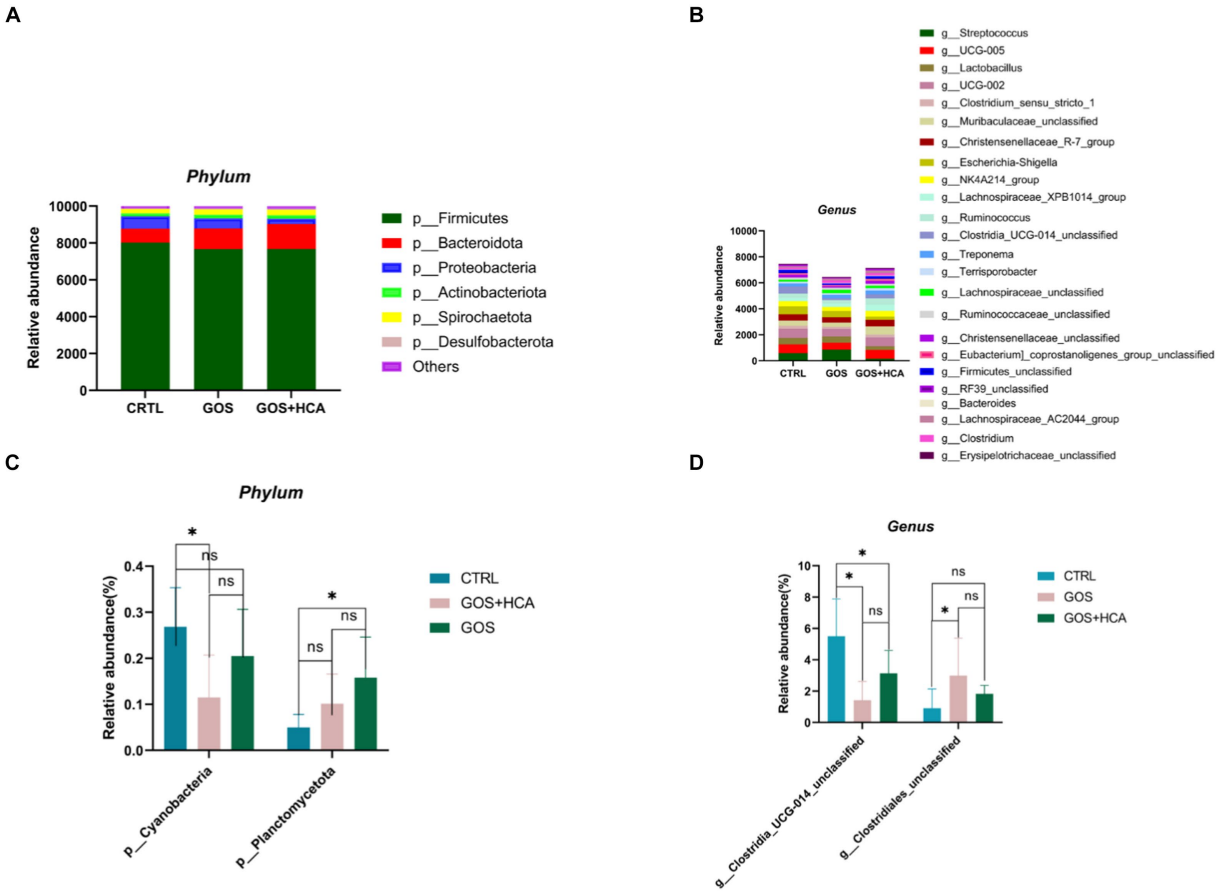

FIGURE 5
Effects of galacto-oligosaccharides (GOS) and hyocholic acids (HCA) on gut microbiota composition of sows at d 7 of lactation. Relative abundance at the phylum level of sows **(A)**, relative abundance at the genus level of sows **(B)**. Significance test at the phylum level of sows **(C)**, significance test at the genus level of sows **(D)**. CTRL = basal diets; GOS = basal diets +600 mg/kg GOS; GOS + HCA = basal diets +600 mg/kg GOS + 200 mg/kg HCA, $n = 6$ for each group. * is significantly different ($p < 0.05$), whereas ns is not different ($p > 0.05$).

development stage. It is a remarkable fact that maternal gut microbiota can be passed to the developing fetus or newborn via the placenta, breast milk, or other routes (Koren et al., 2012). Nevertheless, the maternal will undergo metabolic syndrome during normal pregnancy, especially in late gestation, which decreases dramatically gut microbiota diversity and richness (Collado et al., 2010; Cheng et al., 2018). Recent studies showed that GOS had the promising potential to alleviate metabolic diseases by regulating the intestinal flora (Silk et al., 2009; Roselli et al., 2022). The dominating prebiotic functions of GOS are to selectively stimulate probiotic proliferation (*Bifidobacteria*, *Bacteroides*) and to produce short-chain fatty acids by fermenting (Li et al., 2015; Vulevic et al., 2015; Grimaldi et al., 2016). Similarly, bile acids, the compounds prevailingly regulating glucose and lipid metabolism, possess also potent antibacterial functions and play a pivotal role in shaping the microbial ecology of the gut by promoting the growth of bile acid-metabolizing bacteria and controlling the growth of bile acid-sensitive bacteria (Tian et al., 2020). Based on the above studies, we investigated the effects of GOS and combined GOS and HCA on the intestinal microbiome of sows during the perinatal period. Our results showed a profound alteration of the gut microbiota to be associated with different treatments and periods. At d 107 of gestation and at d 7 of lactation, sows fed GOS or combined GOS and HCA showed significantly higher gut microbial richness and α-diversity values than without them. Interestingly, at farrowing, the difference in the gut microbial richness and α-diversity values of sows among all groups was not found. The reason for this result may be an increased degree of metabolic disorder in sows at delivery, counteracting the positive effects of our current dose of added GOS and HCA (Cheng et al., 2018).

In the context of porcine pregnancy and lactation, *Firmicutes* and *Bacteroidetes* constitute the predominant bacterial phyla, a finding corroborated by our experimental data (Wang et al., 2021). Our research further revealed that dietary inclusion of galacto-oligosaccharides (GOS) and hyocholic acids (HCA) in sow diets resulted in a notable shift in gut microbiota composition. Specifically, there was a reduction in the relative abundance of the *Firmicutes* phylum and a corresponding increase in the *Bacteroidetes* phylum at farrowing, thereby lowering the *Firmicutes* to *Bacteroidetes* ratio, which is beneficial for improving intestinal microbiota disorders (Jiang et al., 2021). Meanwhile, *Bacteroides*, a dominant gut bacterium,

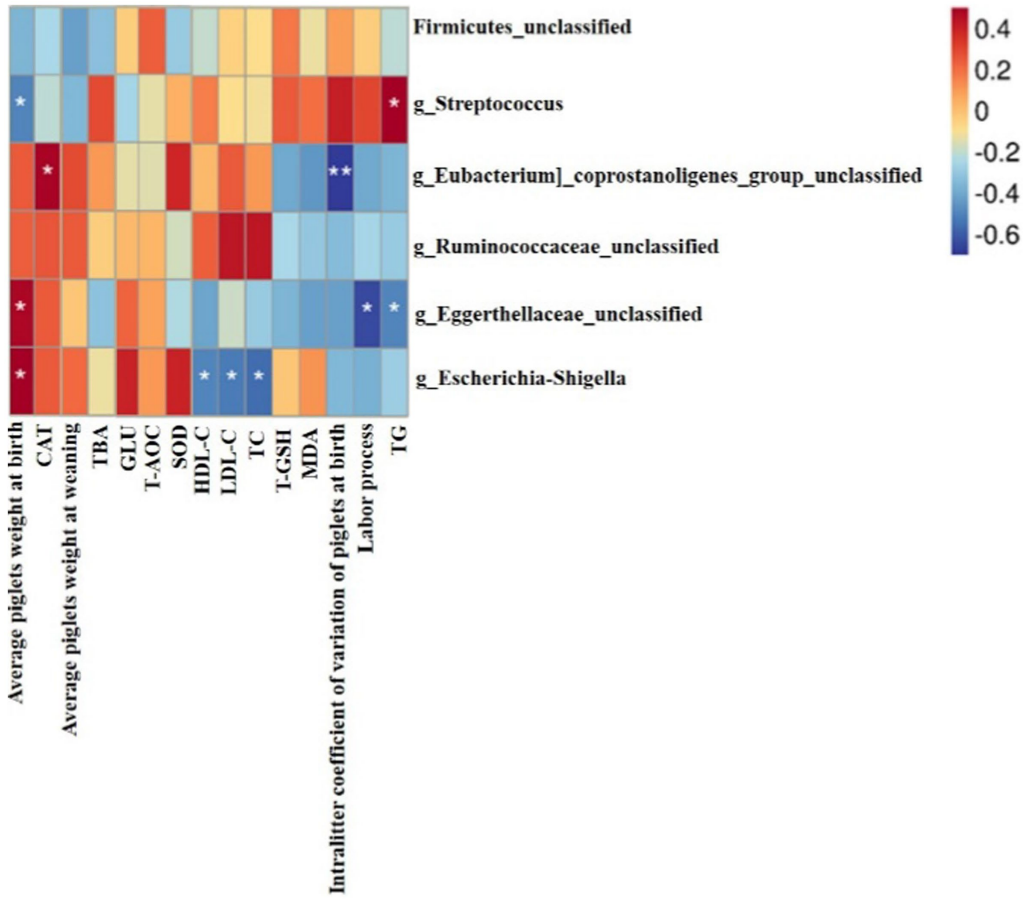

FIGURE 6
Heatmap of the spearman correlations between the gut microbiota significantly modified by different diets treatment and the detection indexes of sows at farrowing, $n = 6$ for each group. * $p < 0.05$; ** $p < 0.01$.

plays a critical role in degrading polysaccharides and starches. This process not only supplies energy to the host but also maintains intestinal ecological balance through the fermentation of polysaccharides, leading to the production of short-chain fatty acids (Wang et al., 2017; Dejean et al., 2020). In our study, enrichment of *Ruminococcus* in sows after GOS and HCA supplementation might contribute to enhance nutritional metabolism, immune statues, and health outcomes (Blanton et al., 2016). These findings may elucidate the observed reduction in the duration of the labor process in sows fed with GOS or GOS + HCA supplemented diets. However, unexpectedly, the relative abundance of the *g_Escherichia_Shigella* increased significantly at farrowing when GOS + HCA was added to sows' diet. As far as we are aware, intestinal inflammation can be brought on by a rise in the quantity of the *g_Escherichia*_Shigella (Sousa et al., 2010). During transit to the large intestine, bile acids undergo modifications to the steroid nucleus by some members of the gut microbiota, yielding deoxycholic acid (DCA) that the most typical secondary bile acids (Islam et al., 2011). Cao et al. (2017) has investigated that DCA-induced dysbiosis can increase the relative abundance of *g_Escheerichia-Shigella*, and disrupt intestinal barrier function. Our speculation is that this could be associated with the quantity of bile acids that have been introduced.

The intestinal microbiota plays a leading part in regulating mammalian lipid absorption, metabolism and storage (Wang et al., 2023). In our study, the relative abundance of *Streptococcus* was positively correlated with the content of serum TG. Meanwhile, the relative abundance of *Streptococcus* and the content of serum TG were significantly reduced, when sows were fed GOS diets. To some degree, it can be concluded from our research that GOS can ameliorate lipid metabolism disorder by modulating the composition of the gut microbiota.

5 Conclusion

In summary, this investigation demonstrated that the administration of galacto-oligosaccharides (GOS) in conjunction with hyocholic acids (HCA), to sows with nutrient restrictions during late gestation and lactation, further improved their antioxidant capacity and milk quality. However, further studies are warranted to elucidate the dose-dependent effects and causal relationships between the supplementation of GOS and HCA, the modulation of gut microbiota, and the reproductive performance of sows, including the underlying biological mechanisms.

Data availability statement

The data presented in the study are deposited in the NCBI repository, accession number PRJNA1117460.

Ethics statement

The animal studies were approved by animal care and use committee certificate of approval this is to certify that project no: 20230423 project title: study on the mediating mechanism of gut microbiota in the regulation of liver lipid metabolism in periparturient sows by dietary fiber. Principal researchers: ZF and BT the project proposal submitted on 1-January-2021 was reviewed by three members of the animal care and use committee, and was approved on 9-March-2021. It is the Principal researcher's responsibility to ensure that all researchers associated with this project are aware of the conditions of approval and which documents have been approved. The principal researcher is required to notify the secretary of the animal care and use committee, via amendment or progress report, of any significant change to the project and the reason for that change, including an indication of ethical implications (if any); any other unforeseen events or unexpected developments that merit notification; the inability of the principal researcher to continue in that role, or any other change in research personnel involved in the project; Signed by: Dr. He Xi. the studies were conducted in accordance with the local legislation and institutional requirements. Written informed consent was obtained from the owners for the participation of their animals in this study.

Author contributions

JYu: Conceptualization, Data curation, Investigation, Methodology, Software, Writing – original draft, Writing – review & editing. JW: Conceptualization, Data curation, Investigation, Methodology, Software, Writing – original draft, Writing – review & editing. CC: Investigation, Supervision, Writing – review & editing. JG: Supervision, Writing – review & editing. JC: Investigation, Supervision, Writing – review & editing. JYi: Conceptualization, Supervision, Writing – review & editing. SW: Conceptualization, Supervision, Writing – review & editing. PH: Conceptualization, Supervision, Writing – review & editing. BT: Conceptualization, Methodology, Supervision, Writing – review & editing. ZF: Conceptualization, Data curation, Methodology, Supervision, Writing – review & editing.

Funding

The author(s) declare financial support was received for the research, authorship, and/or publication of this article. This work was supported by the National Key R&D Program of China (2021YFD1300202).

Acknowledgments

The authors are grateful to the staff at the Department of Animal Nutrition and Feed Science of Hunan Agricultural University for their assistance in conducting the experiment. The authors would like to thank the workers at Chenfeng farm of Hunan Yangxiang Agriculture and Animal Husbandry Co., Ltd.

Conflict of interest

The authors declare that the research was conducted in the absence of any commercial or financial relationships that could be construed as a potential conflict of interest.

Publisher's note

Supplementary material

The Supplementary material for this article can be found online at: https://www.frontiersin.org/articles/10.3389/fmicb.2024.1367877/full#supplementary-material

References

Ahmad, T. R., and Haeusler, R. A. (2019). Bile acids in glucose metabolism and insulin signalling—mechanisms and research needs. *Nat. Rev. Endocrinol.* 15, 701–712. doi: 10.1038/s41574-019-0266-7

AOAC (2007). *Official methods of analysis. 18th* Edn. Gaithersburg: Association of Official Analytical Chemists.

Berchieri, C. B., Kim, S. W., Zhao, Y., Correa, C. R., Yeum, K. J., and Ferreira, L. A. (2011). Oxidative stress status of highly prolific sows during gestation and lactation. *Animal* 5, 1774–1779. doi: 10.1017/S1751731111000772

Blanton, L. V., Charbonneau, M. R., Salih, T., Barratt, M. J., Venkatesh, S., Ilkaveya, O., et al. (2016). Gut bacteria that prevent growth impairments transmitted by microbiota from malnourished children. *Science* 351, 1–9. doi: 10.1126/science.aad3311

Cao, A. Z., Lai, W. Q., Zhang, W. W., Dong, B., Lou, Q. Q., Han, M. M., et al. (2021). Effects of porcine bile acids on growth performance, antioxidant capacity, blood metabolites and nutrient digestibility of weaned pigs. *Anim. Feed Sci. Technol.* 276, 114931–114940. doi: 10.1016/j.anifeedsci.2021.114931

Cao, H. L., Xu, M. Q., Dong, W. X., Deng, B. R., Wang, S. N., Zhang, Y. J., et al. (2017). Secondary bile acid-induced dysbiosis promotes intestinal carcinogenesis. *Tumor Immunol. Microenviron.* 140, 2545–2556. doi: 10.1002/ijc.30643

Cheng, C. S., Wei, H. K., Yu, H. C., Xu, C. H., Jiang, S. W., and Peng, J. (2018). Metabolic syndrome during perinatal period in sows and the link with gut microbiota and metabolites. *Front. Microbiol.* 9, 1989–2004. doi: 10.3389/fmicb.2018.01989

Collado, M. C., Isolauri, E., Laitinen, K., and Salminen, S. (2010). Effect of mother's weight on infant's microbiota acquisition, composition, and activity during early infancy: a prospective follow-up study initiated in early pregnancy. *Am. J. Clin. Nutr.* 92, 1023–1030. doi: 10.3945/ajcn.2010.29877

Dejean, G., Tamura, K., Cabrera, A., Jain, N., Pudlo, N. A., Pereira, G., et al. (2020). Synergy between cell surface glycosidases and glycan-binding proteins dictates the

utilization of specific beta(1,3)-glucans by human gut bacteroides. *MBio* 11, 95–115. doi: 10.1128/mBio.00095-20

Dossa, A. Y., Escobar, O., Golden, J., Frey, M. R., Ford, H. R., and Gayer, C. P. (2015). Bile acids regulate intestinal cell proliferation by modulating EGFR and FXR signaling. *Am. J. Physiol. Gastrointest. Liver Physiol.* 310, G81–G92. doi: 10.1152/ajpgi.00065.2015

Duan, X. D., Chen, D. W., Zheng, P., Tian, G., Wang, J. P., Mao, X. B., et al. (2016). Effects of dietary mannan oligosaccharide supplementation on performance and immune response of sows and their offspring. *Anim. Feed Sci. Technol.* 218, 17–25. doi: 10.1016/j.anifeedsci.2016.05.002

Edwards, A. K., Wessels, J. M., Kerr, A., and Tayade, C. (2012). An overview of molecular and cellular mechanisms associated with porcine pregnancy success or failure. *Reprod. Domest. Anim.* 47, 394–401. doi: 10.1111/j.1439-0531.2012.02103.x

Fanaro, S., Marten, B., Bagna, R., Vigi, V., Fabris, C., and Arguelles, F. (2009). Galacto-oligosaccharides are bifidogenic and safe at weaning:a double -blind randomized multicenter study. *J. Pediatr. Gastroenterol. Nutr.* 48, 82–888. doi: 10.1097/MPG.0b013e31817b6dd2

Feyera, T., Højgaard, C. K., Vinther, J., Bruun, T. S., and Theil, P. K. (2017). Dietary supplement rich in fiber fed to late gestating sows during transition reduces rate of stillborn piglets. *J. Anim. Sci.* 95, 5430–5438. doi: 10.2527/jas2017.2110

Gopal, P. K., Sullivan, P. A., and Smart, J. B. (2001). Utilisation of galacto-oligosaccharides as selective substrates for growth by lactic acid bacteria including *Bifidobacterium lactis* DR10 and *Lactobacillus rhamnosus* DR20. *Int. Dairy J.* 11, 19–25. doi: 10.1016/S0958-6946(01)00026-7

Grimaldi, R., Cela, D., Swann, J. R., Vulevic, J., Gibson, G. R., Tzortzis, G., et al. (2016). In vitro fermentation of B-GOS: impact on faecal bacterial populations and metabolic activity in autistic and non-autistic children. *FEMS Microbiol. Ecol.* 93, 233–248. doi: 10.1093/femsec/fiw233

Hou, Z. P., Wu, D. Q., and Dai, Q. Z. (2020). Effects of dietary xylo-oligosaccharide on growth performance, serum biochemical parameters, antioxidant function, and immunological function of nursery piglets. *Brazilian J. Anim. Sci.* 18, 100519–100557. doi: 10.1016/j.aqrep.2020.100519

Islam, K. B., Fukiya, S., Hagio, M., Fujii, N., Ishizuka, S., Ooka, T., et al. (2011). Bile acid is a host factor that regulates the composition of the cecal microbiota in rats. *Gastroenterology* 141, 1773–1781. doi: 10.1053/j.gastro.2011.07.046

Itoh, M., Wada, K., Tan, S., Kitano, Y., Kai, J., and Makino, I. (1999). Antibacterial action of bile acids against helicobacter pylori and changes in its ultrastructural morphology: effect of unconjugated dihydroxy bile acid. *J. Gastroenterol.* 34, 571–576. doi: 10.1007/s005350050374

Jiang, P. R., Zheng, W. Y., Sun, X. N., Jiang, G. P., Wu, S., Xu, Y. X., et al. (2021). Sulfated polysaccharides from Undaria pinnatifida improved high fat diet-induced metabolic syndrome, gut microbiota dysbiosis and inflammation in BALB/c mice. *Int. J. Biol. Macromol.* 167, 1587–1597. doi: 10.1016/j.ijbiomac.2020.11.116

Koren, O., Goodrich, J. K., Cullender, T. C., Spor, A., Laitinen, K., Backhed, H. K., et al. (2012). Host remodeling of the gut microbiome and metabolic changes during pregnancy. *Cell* 150, 470–480. doi: 10.1016/j.cell.2012.07.008

Lai, H., Li, Y. F., He, Y. F., Chen, F. Y., Mi, B. B., Li, J. Q., et al. (2023). Effects of dietary fibers or probiotics on functional constipation symptoms and roles of gut microbiota: a double-blinded randomized placebo trial. *Gut Microbes* 15, 2197837–2197852. doi: 10.1080/19490976.2023.2197837

Langendijk, P., and Plush, K. (2019). Parturition and its relationship with stillbirths and asphyxiated piglets. *Animals* 9, 885–897. doi: 10.3390/ani9110885

Lee, A., Liang, L., Connerton, P. L., Connerton, L. F., and Mellits, K. H. (2023). Galacto-oligosaccharides fed during gestation increase rotavirus a specific antibodies in sow colostrum, modulate the microbiome, and reduce infectivity in neonatal piglets in a commercial farm setting. *Front. Vet. Sci.* 10, 302–315. doi: 10.3389/fvets.2023.1118302

Li, L. X., Wang, H. K., Dong, S., and Ma, Y. X. (2023). Supplementation with alpha-glycerol monolaurate during late gestation and lactation enhances sow performance, ameliorates milk composition, and improves growth of suckling piglets. *J. Anim. Sci. Biotechnol.* 14, 848–860. doi: 10.1186/s40104-023-00848-x

Li, W., Wang, K. Q., Sun, Y., Ye, H., Hu, B., and Zeng, X. X. (2015). Influences of structures of galactooligosaccharides and fructooligosaccharides on the fermentation in vitro by human intestinal microbiota. *J. Funct. Foods* 13, 158–168. doi: 10.1016/j.jff.2014.12.044

Li, C., Zhang, S., Li, L. M., Hu, Q., and Ji, S. (2020). Ursodeoxycholic acid protects against arsenic induced hepatotoxicity by the Nrf2 signaling pathway. *Front. Pharmacol.* 11, 594496–594520. doi: 10.3389/fphar.2020.594496

Molinaro, A., Wahlström, A., and Marschall, H. U. (2018). Role of bile acids in metabolic control. *Trends Endocrinol. Metabol.* 29, 31–41. doi: 10.1016/j.tem.2017.11.002

Monteagudo, A., Arthur, J. C., Jobin, C., Keku, T., Bruno, J. M., and Azcarate, M. A. (2016). High purity galacto-oligosaccharides enhance specific Bifidobacterium species and their metabolic activity in the mouse gut microbiome. *Benefic. Microbes* 7, 247–264. doi: 10.3920/BM2015.0114

National Research Council. (2012). Nutrient Requirements of Swine: Eleventh Revised Edition. Washington. DC: The National Academies Press.

Quiniou, N., and Noblet, J. (1999). Influence of high ambient temperatures on performance of multiparous lactating sows. *J. Anim. Sci.* 77, 2124–2134. doi: 10.2527/1999.7782124x

Roselli, M., Maruszak, A., Grimaldi, R., Harthoorn, L., and Finamore, A. (2022). Galactooligosaccharide treatment alleviates DSS-induced colonic inflammation in Caco-2 cell model. *Front. Nutr.* 9, 2974–2989. doi: 10.3389/fnut.2022.862974

Schwab, C., and Ganzle, M. (2011). Lactic acid bacteria fermentation of human milk oligosaccharide components, human milk oligosaccharides and galactooligosaccharide. *FEMS Microbiol. Lett.* 2, 141–148. doi: 10.1111/j.1574-6968.2010.02185.x

Shang, Q. H., Liu, S. J., Liu, H. S., Mahfuz, S., and Piao, X. S. (2021). Impact of sugar beet pulp and wheat bran on serum biochemical profile, inflammatory responses and gut microbiota in sows during late gestation and lactation. *J. Anim. Sci. Biotechnol.* 12, 54–68. doi: 10.1186/s40104-021-00573-3

Silk, D. A., Davis, A., Vulevic, J., Tzortzis, G., and Gibson, G. R. (2009). Clinical trial: the effects of a trans-galactooligosaccharide prebiotic on faecal microbiota and symptoms in irritable bowel syndrome. *Aliment. Pharmacol. Ther.* 29, 508–518. doi: 10.1111/j.1365-2036.2008.03911.x

Škorput, D., Dujmović, Z., Karolyi, D., and Luković, Z. (2018). Variability of birth weight and growth of piglets in highly prolific sows. *J. Cent. Eur. Agric.* 19, 823–828. doi: 10.5513/JCEA01/19.4.2355

Sousa, M. A. B., Mendes, E. N., Apolonio, A. C. M., Farias, L. D. M., and Magalhaes, P. P. (2010). Bacteriocin production by *Shigella sonnei* isolated from faeces of children with acute diarrhoea. *J. Pathol. Microbiol. Immunol.* 118, 125–135. doi: 10.1111/j.1600-0463.2009.02570.x

Sultana, Z., Qiao, Y. X., Maiti, K., and Smith, R. (2023). Involvement of oxidative stress in placental dysfunction, the pathophysiology of fetal death and pregnancy disorders. *Reproduction* 166, R25–R38. doi: 10.1530/REP-22-0278

Tian, Y., Gui, W., Koo, I., Smith, P. B., Allman, E. L., Nichols, R. G., et al. (2020). The microbiome modulating activity of bile acids. *Gut Microbes* 11, 979–996. doi: 10.1080/19490976.2020.1732268

Tian, S. Y., Wang, J., Gao, R., Wang, J., and Zhu, W. Y. (2022). Early-life galacto-oligosaccharides supplementation alleviates the small intestinal oxidative stress and dysfunction of lipopolysaccharide-challenged suckling piglets. *J. Anim. Sci. Biotechnol.* 13, 70–726. doi: 10.1186/s40104-022-00711-5

Vos, A. P., M'Rabet, L., Stahl, B., Boehm, G., and Garssen, J. (2007). Immune-modulatory effects and potential working mechanisms of orally applied nondigestible carbohydrates. *Crit. Rev. Immunol.* 27, 97–140. doi: 10.1615/critrevimmunol.v27.i2.10

Vulevi, C. J., Drakoularakou, A., Yaqoob, P., Tzortzis, G., and Gibson, G. R. (2008). Modulation of the fecal microflora profile and immune function by a novel trans-galactooligosaccharide mixture (B-GOS) in healthy elderly volunteers. *Am. J. Clin. Nutr.* 88, 1438–1446. doi: 10.3945/ajcn.2008.26242

Vulevic, J., Juric, A., Walton, G. E., Claus, S. P., Tzortzis, G., Toward, R. E., et al. (2015). Influence of galacto-oligosaccharide mixture (B-GOS) on gut microbiota, immune parameters and metabonomics in elderly persons. *Br. J. Nutr.* 114, 586–595. doi: 10.1017/S0007114515001889

Wang, L. L., Hu, L. J., Yan, S., Jiang, T., Fang, S. G., Wang, G., et al. (2017). Effects of different oligosaccharides at various dosages on the composition of gut microbiota and short-chain fatty acids in mice with constipation. *Food Funct.* 8, 1966–1978. doi: 10.1039/c7fo00031f

Wang, R. J., Liu, N., Yang, Y. C., Lei, Y., Lyu, J. R., Dai, Z. L., et al. (2021). Flavor supplementation during late gestation and lactation periods increases the reproductive performance and alters fecal microbiota of the sows. *Anim. Nutr.* 7, 679–687. doi: 10.1016/j.aninu.2021.01.007

Wang, Y. H., Wang, M., Chen, J. X., Li, Y., Kuang, Z., Dende, C., et al. (2023). The gut microbiota reprograms intestinal lipid metabolism through long noncoding RNA Snhg9. *Science* 381, 851–857. doi: 10.1126/science.ade0522

Wang, W., Xu, C., Zhou, X., Zhang, L., Gu, L. Y., Liu, Z. J., et al. (2022). *Lactobacillus plantarum* combined with galactooligosaccharides supplement: a neuroprotective regimen against neurodegeneration and memory impairment by regulating short-chain fatty acids and the c-Jun N-terminal kinase signaling pathway in mice. *J. Agric. Food Chem.* 70, 8619–8630. doi: 10.1021/acs.jafc.2c01950

Watanabe, M., Houten, S. M., Wang, L., Moschetta, A., Mangelsdorf, D. J., Heyman, R. A., et al. (2004). Bile acids lower triglyceride levels via a pathway involving FXR, SHP, and SREBP-1c. *J. Clin. Invest.* 113, 1408–1418. doi: 10.1172/JCI21025

Wu, Y. J., Zhang, X. Y., Pi, Y., Han, D. D., Feng, C. P., Zhao, J. Y., et al. (2021). Maternal galactooligosaccharides supplementation programmed immune defense, microbial colonization and intestinal development in piglets. *Food Funct.* 12, 7260–7270. doi: 10.1039/d1fo00084e

Zhang, L. L., Gu, X. L., Wang, J., Liao, S., Duan, Y. H., Li, H., et al. (2021). Effects of dietary isomaltooligosaccharide levels on the gut microbiota, immune function of sows, and the diarrhea rate of their offspring. *Front. Microbiol.* 11, 588986–588998. doi: 10.3389/fmicb.2020.588986

Zong, E. Y., Yan, S. L., Wang, M. W., Yin, L. M., Wang, Q. Y., Yin, J., et al. (2019). The effects of dietary supplementation with hyodeoxycholic acid on the differentiation and function of enteroendocrine cells and the serum biochemical indices in weaned piglets. *J. Anim. Sci.* 97, 1796–1805. doi: 10.1093/jas/skz059

frontiers | Frontiers in Microbiology

TYPE Original Research
PUBLISHED 14 June 2024
DOI 10.3389/fmicb.2024.1394332

OPEN ACCESS

EDITED BY
François J. M. A. Meurens,
University of Montreal, Canada

REVIEWED BY
Jie Yin,
Hunan Agricultural University, China
Shenglan Hu,
Guangdong Academy of Agricultural Sciences, China

*CORRESPONDENCE
Zuohua Liu
✉ liuzuohua66@163.com
Renli Qi
✉ qirenli1982@163.com

RECEIVED 18 March 2024
ACCEPTED 21 May 2024
PUBLISHED 14 June 2024

CITATION
Liu X, Qiu X, Yang Y, Wang J, Wang Q, Liu J, Huang J, Yang F, Liu Z and Qi R (2024) Uncovering the mechanism of *Clostridium butyricum* CBX 2021 to improve pig health based on *in vivo* and *in vitro* studies. *Front. Microbiol.* 15:1394332. doi: 10.3389/fmicb.2024.1394332

Uncovering the mechanism of *Clostridium butyricum* CBX 2021 to improve pig health based on *in vivo* and *in vitro* studies

Xin Liu[1], Xiaoyu Qiu[1,2], Yong Yang[2,3], Jing Wang[1,2], Qi Wang[1,2], Jingbo Liu[3], Jinxiu Huang[1,2], Feiyun Yang[1,2], Zuohua Liu[1,2]* and Renli Qi[1,2]*

[1]National Center of Technology Innovation for Pigs, Chongqing, China, [2]Chongqing Academy of Animal Science, Chongqing, China, [3]College of Life Sciences, Southwest University of Science and Technology, Mianyang, Sichuan, China

Introduction: As a symbiotic probiotic for the host, *Clostridium butyricum* (CB) has the potential to strengthen the body's immune system and improve intestinal health. However, the probiotic mechanism of CB is not completely understood. The *Clostridium butyricum* CBX 2021 strain isolated by our team from a health pig independently exhibits strong butyric acid production ability and stress resistance. Therefore, this study comprehensively investigated the efficacy of CBX 2021 in pigs and its mechanism of improving pig health.

Methods: In this study, we systematically revealed the probiotic effect and potential mechanism of the strain by using various methods such as microbiome, metabolites and transcriptome through animal experiments *in vivo* and cell experiments *in vitro*.

Results: Our *in vivo* study showed that CBX 2021 improved growth indicators such as daily weight gain in weaned piglets and also reduced diarrhea rates. Meanwhile, CBX 2021 significantly increased immunoglobulin levels in piglets, reduced contents of inflammatory factors and improved the intestinal barrier. Subsequently, 16S rRNA sequencing showed that CBX 2021 treatment implanted more butyric acid-producing bacteria (such as *Faecalibacterium*) in piglets and reduced the number of potentially pathogenic bacteria (like *Rikenellaceae RC9_gut_group*). With significant changes in the microbial community, CBX 2021 improved tryptophan metabolism and several alkaloids synthesis in piglets. Further *in vitro* experiments showed that CBX 2021 adhesion directly promoted the proliferation of a porcine intestinal epithelial cell line (IPEC-J2). Moreover, transcriptome analysis revealed that bacterial adhesion increased the expression of intracellular G protein-coupled receptors, inhibited the Notch signaling pathway, and led to a decrease in intracellular pro-inflammatory molecules.

Discussion: These results suggest that CBX 2021 may accelerate piglet growth by optimizing the intestinal microbiota, improving metabolic function and enhancing intestinal health.

KEYWORDS

***Clostridium butyricum* CBX 2021, intestinal microbiota, intestinal health, weaned piglets, IPEC-J2 cells**

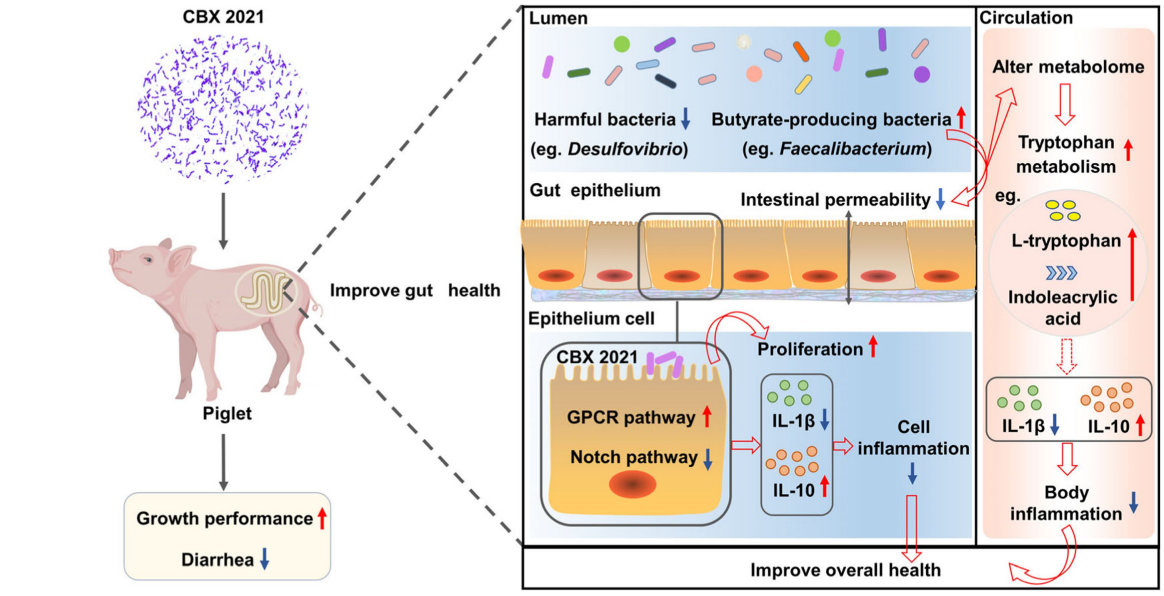

GRAPHICAL ABSTRACT

Introduction

A healthy gastrointestinal tract is the cornerstone for improving animal growth performance and overall health. However, in modern intensive livestock production, weaned piglets experience drastic changes in diet, environment, and management that can disrupt normal GI function, resulting in delayed growth and compromised health (Tang X. P. et al., 2022). Multiple evidence suggests that probiotics can improve intestinal health in weaned piglets, thereby promoting body growth and overall health (Mun et al., 2021; Tang et al., 2021).

Clostridium butyricum (CB) serves as an effective probiotic for restoring the disrupted intestinal microbiota in livestock due to weaning stress. Additionally, CB has been proven to alleviate diarrhea and enhance growth performance (Lu et al., 2020; Ye et al., 2022). Extensive evidence shows that butyric acid, the major functional metabolite produced by CB bacteria, repairs intestinal mucosa damage, maintains intestinal immune homeostasis, and alleviates inflammation in the body (Abdelqader and Al-Fataftah, 2016; Chen G. X. et al., 2018). In recent years, CB has become popular in animal husbandry production as a probiotic preparation for its beneficial characteristics. Despite ongoing research, there is still much to uncover about the specific mechanisms through which CB regulates intestinal health and promotes growth.

Screening and confirming a suitable bacterial strain is crucial for the development of microbial ecological preparations due to the significant differences in physiological characteristics among the different strains from different sources. Our team isolated the *Clostridium butyricum* CBX 2021 strain from a healthy adult pig, which has shown a high capability for producing butyric acid. The strain was found to produce endospores and have a butyric acid production of 2.15 mg/mL during the exponential growth phase. Additionally, it is non-pathogenic to animals and can effectively restore antibiotic-induced intestinal dysbiosis and damage in mice by rebuilding the gut microbiota and optimizing metabolic function (Liu et al., 2023). Thus, it appears that CBX 2021 shows promise for application in the field of feed probiotics. However, the impact and mechanism of this strain on pig health, especially intestinal health, are currently unclear.

This study examines the impacts of the CBX 2021 strain on the growth and overall health of piglets. Various methods, including microbiome, metabolomics, and transcriptome analysis, were used in both *in vivo* and *in vitro* experiments to systematically reveal the potential mechanisms of its probiotic effects. The study provides guidance for developing and using new micro-ecological products.

Materials and methods

Bacteria and its preparation

Clostridium butyricum CBX 2021 strain was isolated and screened from the intestines of a healthy 6-month-old boar in our laboratory, and is currently stored at the *Guangdong Microbial Culture Collection Center* (GDMCC No.62503).

The CBX 2021 strain was incubated under anaerobic environment at 37°C for 12 h in reinforced *Clostridium* medium. For animal administration, the harvested bacterial solution (3×10^8 CFU/mL) obtained at this time point was orally administered to weaned piglets. For cell culture assays, the bacterial solution was centrifuged at 5,000 × *g* at 4°C for 10 min to collect the bacteria. Then, the bacteria were resuspended in DMEM/F12 cell culture medium without penicillin/streptomycin (1.5×10^8 CFU/mL) for cell experiments.

Animal experiment design and sample collection

The experiment included forty-eight 28-day-old healthy piglets (8.16 ± 0.77 kg) split evenly into 2 groups, with 6 replicates per group

and 4 piglets per replicate. The control (CON) group piglets were administered a 5 mL sterile saline orally, while the CB group piglets were given a 5 mL CBX 2021 bacterial solution (with an effective bacterial count of 3×10^8 CFU/mL) orally once daily. The experiment lasted for 28 days and utilized a commercially available, standard-formulated feed. The composition and nutritional levels of it are displayed in Supplementary Table S1.

After the experiment concluded, one piglet from each replicate was chosen at random to gather fresh fecal samples for 16S rRNA sequencing analysis. Meanwhile, the venous blood of piglets was collected. After the blood samples stood overnight, the serum was collected by centrifugation at 3,000 × *g* at 4°C for a duration of 15 min and stored at −80°C for subsequent analysis of immune, growth-related hormones, and intestinal permeability.

Growth performance

All piglets were weighed on an empty stomach on d 0 and 28, and the daily feed intake for each replicate was noted daily. These values are utilized in the computation of the average daily gain (ADG), average daily feed intake (ADFI), and feed-to-gain ratio (F/G).

Monitor the fecal consistency of each piglet during the trial, and document the number of piglets with diarrhea. Assess the piglet feces according to the following scoring standards reported in previous studies and calculate the frequency and index of diarrhea (Hung et al., 2019).

$$\text{Diarrhea frequency}(\%) = [\sum(\text{number of piglets with diarrhea} \times \text{number of days with diarrhea}) / (\text{total number of piglets} \times \text{test days})] \times 100.$$

$$\text{Diarrhea index} = \text{sum of diarrhea scores} / (\text{total number of piglets} \times \text{test days}).$$

Blood biochemical indicators

As per the manufacturer's guidelines, the ELISA kit (Enzyme-linked Biotechnology Co., Ltd., Shanghai, China) was utilized to measure serum immune indicators: immunoglobulin A (IgA), IgG, and IgM, as well as interleukin-1β (IL-1β), IL-10, and tumor necrosis factor-α (TNF-α); growth-related hormone indicators: growth hormone (GH), gastrin (GAS), ghrelin (GHRL), peptide YY (PYY), and glucagon-like peptide-1 (GLP-1); intestinal permeability indicators: D-lactic acid (DLA) and diamine oxidase (DAO).

Fecal microbiome analysis

As previously mentioned, we extracted and purified total genomic DNA from piglet fecal samples (Wang J. L. et al., 2016). The quantitative PCR products were then examined through the Illumina NovaSeq platform for sequencing at Beijing Biocloud Biotechnology Co., Ltd. (Beijing, China[1]) via paired-end sequencing. The raw data can be found in the NCBI Sequence Read Archive (SRA) database and accessed using the login number PRJNA947735.

Sequencing reads were denoised using the DADA2 method and clustered into amplicon sequence variants (ASVs). The SILVA 138 database was used as a reference for classifying and annotating each representative sequence of the ASVs using a naive Bayes classifier, with a 70% confidence threshold. The unweighted unifrac distance algorithm was used for principal coordinate analysis (PCoA) at the bacterial genus level. ANOSIM function was used for statistical analysis. Student's *t*-test or Mann–Whitney *U* test was used to analyze the differences in microbial distribution at phylum and genus level. Additionally, Linear discriminant analysis (LDA) effect size (LEfSe) was employed to identify biomarkers (from family to genus level), with a significance threshold set at an LDA value of ≥3.0.

Serum metabolomics analysis

The serum samples from the piglets were sent to Beijing Biocloud Biotechnology Co., Ltd. (Beijing, China) for metabolite extraction, detection and analysis. The Progenesis QI software was utilized to process the raw data, including peak detection, calibration, and other essential operations for data processing. Upon peak area normalization, the processed data were exported for further analysis. The orthogonal partial least squares discriminant analysis (OPLS-DA) was utilized to compare and identify the overall metabolic variations in the CON and CB groups. Differential metabolites were chosen based on VIP values >1 in the OPLS-DA model and *p*-value <0.01. The pathway enrichment analysis of the differential metabolites was then conducted using the Kyoto Encyclopedia of Genes and Genomes (KEGG) database. The Spearman correlation algorithm was applied to analyze the relationships among the top 20 bacterial genera, differential metabolites, and serum biochemical indicators, generating correlation matrices to assess their associations.

Cell and cell culture

IPEC-J2 cells were graciously provided by Dr. Yongjiang Wu (Chongqing University of Arts and Sciences, Chongqing, China). The cells were grown in DMEM/F12 medium supplemented with 10% fetal bovine serum (Gibco, Paisley, USA), 1% penicillin/streptomycin (Solarbio, Beijing, China), and 1% insulin-transferrin-selenium (Sigma-Aldrich, MO, USA). And they were incubated in biochemical incubators (5% CO_2, 37°C).

Determination of the adhesion ability of the CBX 2021 strain to IPEC-J2 cells

IPEC-J2 cells were inoculated in a 6-well plate (5×10^5 cells/ well), and divided into 2 groups after the confluence reached 70–80%. CB

1 https://www.biocloud.net

group was exposed to CBX 2021 bacterial suspension (1.5×10^8 CFU/mL, 2 ml/well), and CON group was treated with an equivalent volume of DMEM/F12 medium, with three replicates in each group. After incubation at 37°C for 4, 6, and 8 h, the cells were treated according to the standard procedure. Subsequently, they underwent fixation with 4% neutral formaldehyde for 15 min before being subjected to gram staining. The samples were examined under inverted fluorescence microscope with magnification of ×40 for analysis. Lastly, 25 cells were randomly selected, and the average number of CBX 2021 bacterial adhesion on visible cell surfaces was calculated and documented through photography.

IPEC-J2 cell proliferation assay

IPEC-J2 cells were inoculated in a 96-well plate (1×10^4 cells/ well) and grew to the above degree. The cells were classified into 3 distinct groups: the blank group (without cells), CON group, and CB group. Each group had 3 replicate wells (100 μl/ well). After the cells were incubated for 2, 4, 6, 8, and 12 h, the old medium was aspirated and DMEM/F12 medium with 10% CCK-8 was added (100 μl/ well) within the specified culture time, followed by 2 h of additional incubation. Then, OD values at 450 nm were determined using plate reader, and the cell proliferation activity was calculated at each culture time point to ascertain the optimal time for coculture of the bacterial strain and cells.

$$\text{Cell proliferation activity}(\%) = \left[\text{OD}(\text{CB group}) - \text{OD}(\text{blank group})\right] / \left[\text{OD}(\text{CON group}) - \text{OD}(\text{blank group})\right] \times 100$$

Determination of inflammatory factor secretion in IPEC-J2 cells

Cell processing and grouping were as described in the above adhesion experiment. After incubation for 6 h, the coculture supernatant was gathered to measure the secretion levels of IL-1β and IL-10 using porcine ELISA kits as per the manufacturer's guidelines.

RNA-seq and gene expression analysis

Cell processing and grouping were as described in the above adhesion experiment, and each group had 5 replicates. After incubation for 6 h, cell digestion and collection were performed using 0.25% pancreatase-EDTA (Sigma-Aldrich, MO, USA). The cell samples were then sent to Hangzhou Lianchuan Biotechnology Co., Ltd. (Hangzhou, China) for total RNA isolation, quality control, cDNA library construction, and transcriptome sequencing. The raw data can be found in the NCBI SRA database and accessed using the login number PRJNA948058.

The raw sequencing data underwent quality control, which involved removing reads that had low-quality bases and adapter contamination. Fragment per kilobase per million mapped reads were used to determine gene expression levels. DESeq2 was applied for the differential expression analysis, with the false discovery rate (FDR) controlled through the Benjamini-Hochberg procedure. The screening condition of differentially expressed genes (DEGs) was FDR < 0.05 and |log2(Fold change)| > 1. Additionally, the enrichment analyses were conducted using the OmicStudio cloud platform, including gene ontology (GO) term, KEGG pathway, and gene set enrichment analysis (GSEA). GSEA analysis relied on the GO database and involved calculating a normalized enrichment score (NES) for each gene set through 1,000 permutations of the genome. Gene sets with |NES| > 1 and FDR < 0.05 were considered significantly enriched in the GSEA analysis.

Quantitative real-time PCR

The previously mentioned RNA samples underwent reverse transcription to generate cDNA, utilizing a commercially available reverse transcription kit (Yeasen, Shanghai, China) in a two-step reaction. Then, we followed the instructions provided by the manufacturer of the fluorescent quantitative PCR assay kit (Yeasen, Shanghai, China) in order to conduct our experiments. The 10 μl reaction mixture was prepared containing 1 μl of cDNA, 0.2 μl of upstream and downstream primer, 3.6 μl of RNA-free water, and 5 μl of SYBR fluorescent dye. The mixture underwent cDNA amplification and fluorescence signal collection using a real-time fluorescence quantitative PCR instrument (Thermo Scientific, Wilmington, DE, USA). The amplification program was performed as instructed. In this study, the PCR amplification efficiency was always between 95 and 100%, so the $2^{-\Delta\Delta CT}$ method was used to analyze the relative mRNA expression levels of the target genes mRNA (Livak and Schmittgen, 2001). A single internal reference gene GAPDH was selected for normalization based on previous studies (Wang H. et al., 2019; Wu et al., 2021; Li et al., 2023). Primers utilized in this research were synthesized by Shanghai Sangon Biotech Co., Ltd. (Shanghai, China) (Supplementary Table S2).

Statistical analysis

After the data were preliminarily organization in Excel 2021, SPSS 26.0 software was used for statistical analysis. The Shapiro–Wilk test is used to evaluate whether the data obeys normality. Student's *t*-test was conducted for the data that followed normal distribution and showed homogeneity of variance, while Mann–Whitney *U* test was used for non-parametric analysis when variance was unequal. The results are expressed as means ± SEM. Statistical significance was defined as $p < 0.05$ (*), $p < 0.01$ (**), and $p < 0.001$ (***). A significant trend was noted when $0.05 \geq p > 0.10$. Data visualization was carried out using GraphPad Prism 9.0 software.

Results

Supplementation with CBX 2021 improved the growth performance in weaned piglets

Table 1 presents the growth performance results of piglets. The CB piglets showed a 10.10% increase in body weight after 28 days

compared to the CON piglets ($p = 0.06$). The ADG of CB treated pigs significantly increased by 24.95%, and F/G obviously reduced by 15.82% ($p < 0.05$). However, no difference in ADFI was witnessed between CON and CB piglets ($p > 0.05$). Compared to the CON group, CB piglets experienced a significant reduction in diarrhea frequency and diarrhea index by 36.15 and 40.74%, respectively ($p < 0.05$). The findings indicate that CBX 2021 improves the growth performance of piglets and helps manage post-weaning diarrhea.

Research suggests that there is a strong correlation between peripheral hormone secretion and improved growth performance (Li et al., 2021). Thus, we analyzed the serum levels of growth- and appetite-related hormones in piglets (Table 2). Compared with CON piglets, the of GH and GAS levels in the CB piglets increased by 6.33 and 7.74%, respectively ($p < 0.05$). The level of GHRL, a key appetite-stimulating hormone, showed a trend of increase by 3.90% ($p = 0.06$). Elevated levels of GAS and GHRL expression play a significant role in stimulating digestive fluid secretion, which is vital for increasing feed intake and conversion (Mazzoni et al., 2022; Rodríguez-Viera et al., 2022). However, there were no notable variations in the concentrations of the anorectic hormones PYY and GLP-1 between the piglets in the two groups ($p > 0.05$). The results indicate that CBX 2021 may positively impact the growth and development of piglets by enhancing endocrine hormone levels.

TABLE 1 Effect of *Clostridium butyricum* CBX 2021 on growth performance in weaned piglets.

Items	CON group	CB group	*P*-value
Initial body weight (kg)	8.18 ± 0.22	8.14 ± 0.27	0.920
Body weight at d28 (kg)	17.62 ± 0.72	19.40 ± 0.54	0.064
ADG (g/d)	334.53 ± 26.53	418.00 ± 16.94	0.028
ADFI (g/d)	519.84 ± 29.47	553.69 ± 17.15	0.344
F/G	1.58 ± 0.09	1.33 ± 0.05	0.030
Diarrhea frequency (%)	37.48 ± 2.28	23.93 ± 3.14	0.006
Diarrhea index	0.81 ± 0.05	0.48 ± 0.08	0.005

$N = 6$.

Supplementation with CBX2021 enhanced the immunity and intestinal barrier function in weaned piglets

The serum immunoglobulin levels in Table 2 reflect the humoral immune response level. The CB group piglets showed a significant increase of 5.90, 11.02, and 7.31% in IgA, IgG, and IgM levels, respectively, compared with CON piglets ($p < 0.05$).

Furthermore, we assessed serum levels of inflammatory mediators as indicators of weaning stress-induced inflammation within the body. The study revealed that compared with CON piglets, IL-10 content of CB piglets increased by 13.05%, and IL-1β content decreased by 15.53% ($p < 0.05$). However, there was no significant difference in TNF-α level between the two groups ($p > 0.05$).

The impact of CBX 2021 on piglet' intestinal permeability was studied by measuring serum DLA levels and DAO activity. Elevated levels of DLA and DAO are typically indicative of heightened intestinal permeability (Cai et al., 2019). The findings indicated that the DLA level and DAO activity in the CB piglets were significantly reduced by 15.27 and 9.98%, respectively ($p < 0.05$) compared with CON piglets.

To sum up, the results indicate that CBX 2021 effectively enhanced immune response, strengthened intestinal barrier, and alleviated inflammatory stress in weaned piglets. This may lead to an overall improvement in the animals' health status.

Supplementation with CBX 2021 optimized the fecal microbiota in weaned piglets

A balanced microbial community structure contributes to immune system development and intestinal health (Wang et al., 2018; Wu et al., 2023). Here, we conducted an analysis on the diversity and structure of fecal microbiota by 16S rDNA sequencing to evaluate the gut bacterial community of piglets. The PCoA scatter plot, which illustrates the β diversity of microbiota, showing that the microbial distribution of the two groups of piglets is obviously different ($R = 0.670$, $p = 0.002$, Figure 1A). This result indicated that

TABLE 2 Effect of *Clostridium butyricum* CBX 2021 on blood biochemical indicators in weaned piglets.

Items	CON group	CB group	*P*-value
Growth hormone (GH, ng/mL)	17.69 ± 0.32	18.81 ± 0.41	0.047
Gastrin (GAS, pg./mL)	628.07 ± 15.86	676.67 ± 13.98	0.037
Ghrelin (GHRL, pg./mL)	7083.87 ± 83.48	7360.06 ± 108.52	0.063
Peptide YY (PYY, pmol/mL)	15.91 ± 0.33	15.46 ± 0.38	0.384
Glucagon-like peptide-1 (GLP-1, pmol/mL)	12.11 ± 0.19	11.40 ± 0.38	0.119
Immunoglobulin A (IgA, μg/mL)	767.25 ± 11.41	812.55 ± 6.83	0.004
IgG (mg/mL)	24.68 ± 0.41	27.40 ± 0.59	0.002
IgM (mg/mL)	17.38 ± 0.47	18.65 ± 0.24	0.029
Interleukin-1β (IL-1β, pg./mL)	462.49 ± 14.96	390.66 ± 16.18	0.006
IL-10 (pg/mL)	121.55 ± 4.35	137.41 ± 5.06	0.032
TNF-α (pg/mL)	162.44 ± 3.16	165.97 ± 2.49	0.394
D-lactic acid (DLA, μmol/L)	347.52 ± 19.81	294.45 ± 7.71	0.034
Diamine oxidase (DAO, ng/mL)	227.45 ± 5.88	204.74 ± 5.56	0.014

$N = 6$.

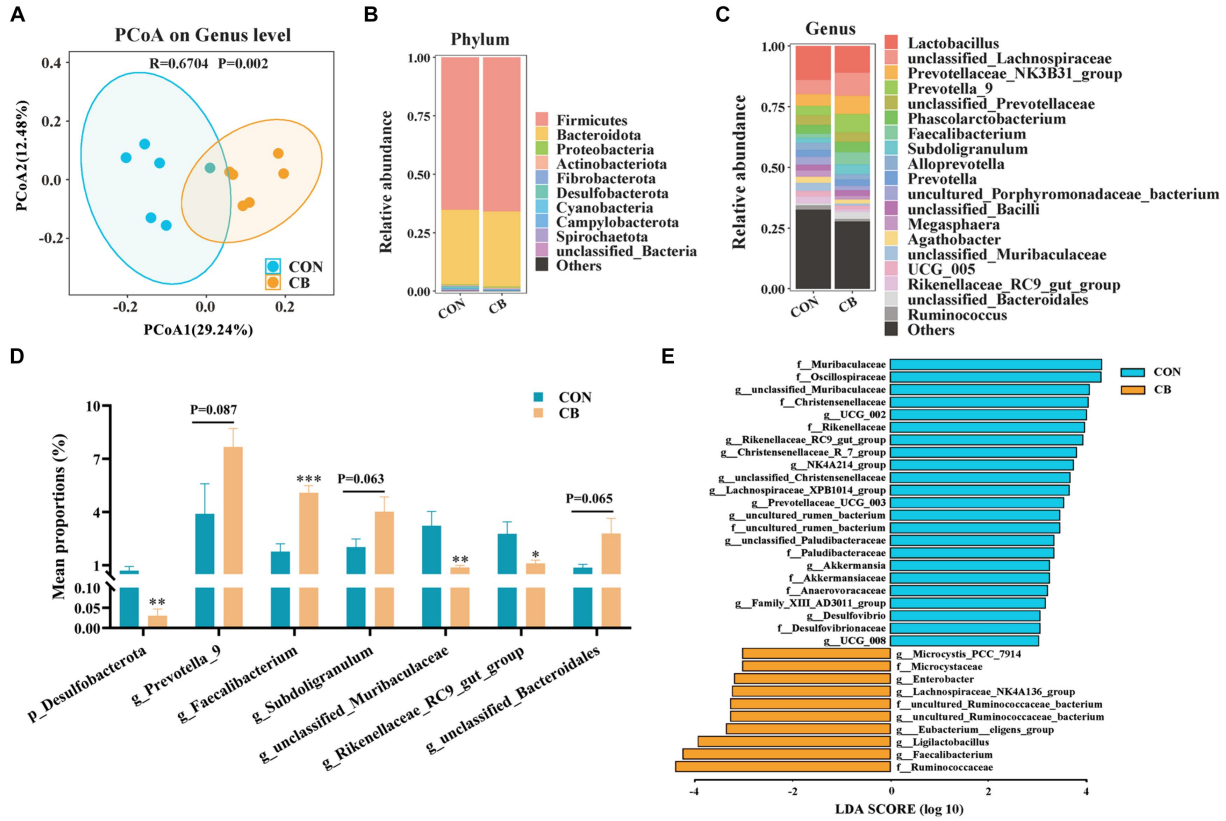

FIGURE 1
Effects of *Clostridium butyricum* CBX 2021 on fecal microbiota in weaned piglets ($n = 6$). **(A)** Principal coordinate analysis (PCoA) scatter diagram based on genus level. Column chart of species composition at the phylum **(B)** and genus **(C)** level. **(D)** Histogram of bacterial differences at the phylum and genus level. **(E)** Linear discriminant analysis (LDA) histogram of differential microbial community in the CON and CB group. Data are displayed as the mean ± SEM. *** Indicates $p < 0.001$, ** indicates $p < 0.01$, * indicates $p < 0.05$, and $0.05 \geq p > 0.10$ indicates a significant trend in comparison with the CON piglets.

supplementation with CBX 2021 obviously altered the composition of microbial community in piglet feces.

Subsequently, an analysis of the bacterial population structure was conducted, focusing specifically on phylum and genus levels (Figures 1B,C). A combined total of 12 bacterial phyla were recognized in both groups of piglets. *Firmicutes* and *Bacteroidota* were the main phyla among them, comprising over 97% of the total abundance (Figure 1B). Notably, the abundance of *Desulfobacterota* was significantly decreased by CBX 2021 treatment ($p < 0.05$, Figure 1D). Figure 1C illustrates the relative abundance of the top 20 genera. *Faecalibacterium*, a butyrate producer, had a higher relative abundance in piglets receiving CBX 2021 intervention than CON piglets ($p < 0.05$). Additionally, there was an increasing trend in the number of helpful bacteria, particularly *Prevotella_9* ($p = 0.087$), *Subdoligranulum* ($p = 0.063$), and *unclassified_Bacteroidales* ($p = 0.055$), with their numbers 1.97-, 1.99-, and 4.65-fold higher than those of the CON piglets, respectively (Figure 1D). Furthermore, the addition of CBX 2021 caused a substantial drop in the number of proinflammatory bacteria, including *unclassified_Muribaculaceae* and *Rikenellaceae_RC9_gut_group* ($p < 0.05$, Figure 1D). The findings suggest that exogenous administration of CBX2021 had a positive impact on the gut microbiota as a whole.

LEfSe analysis was used to study the key bacterial species that drive variations within the microbial population. As shown in Figure 1E, a total of 33 different taxa were found in both groups (LDA score ≥ 3.0). In the CB piglets, seven genera, including *Faecalibacterium*, *Ligilactobacillus*, *Eubacterium_eligens_group*, and *Lachnospiraceae_NK4A136_group*, were significantly enriched and could serve as biomarker genera. Furthermore, CON piglets exhibited 14 characteristic genera, such as *unclassified_Muribaculaceae*, *Rikenellaceae_RC9_gut_group*, *Desulfovibrio*, and *Family_XIII_AD3011_group*.

Supplementation with CBX 2021 altered the serum metabolome in weaned piglets

LC-Q/TOF-MS technology was employed to examine the serum metabolome changes in weaned piglets treated with CBX 2021.The OPLS-DA score plots clearly showed clear separation between the two groups, suggesting that CBX 2021 significantly influenced the serum metabolite composition in piglets (Figures 2A,B). The high statistical values of R^2Y (explanatory ability parameter) and Q^2 (predictive ability parameter) in the score plots demonstrated that the models had good applicability and predictability. Furthermore, in the permutation tests of both ion modes, the intercepts of the Q^2Y fitted regression lines with the vertical axis were below 0, confirming the reliability of the OPLS-DA model and its suitability for identifying differential metabolites between groups (Figures 2C,D).

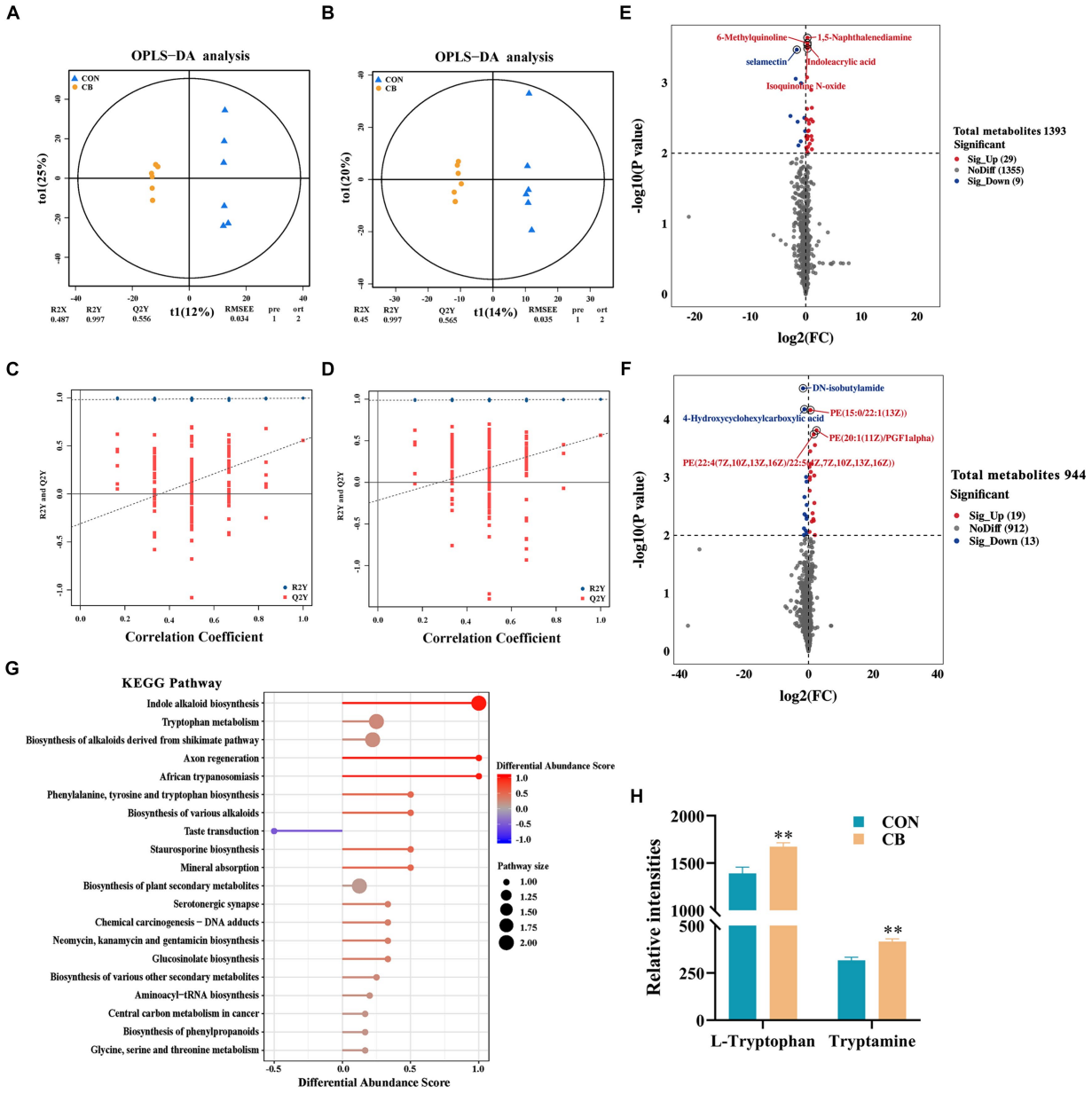

FIGURE 2
Effects of *Clostridium butyricum* CBX 2021 on serum metabolome in weaned piglets ($n = 6$). Orthogonal partial least squares discriminant analysis (OPLS-DA) score chart under positive **(A)** and negative **(B)** ion modes. Permutation test chart under positive **(C)** and negative **(D)** ion modes. Difference statistics volcano plot under positive **(E)** and negative **(F)** ion modes. **(G)** KEGG enrichment pathway diagram of different metabolites in two groups of piglets. **(H)** Histogram of the differential metabolites (L-tryptophan and tryptamine) that cause KEGG enrichment. Data are displayed as the mean ± SEM. ** Indicates $p < 0.01$ in comparison with the CON piglets.

A total of 70 differential metabolites were screened between the two groups of piglets, with 38 being positive ions and 32 being negative ions (Figures 2E,F and Supplementary Table S3). In the positive ion mode, the contents of 29 metabolites, such as 1,5-naphthalenediamine, 6-methylquinoline, indoleacrylic acid, and isoquinoline N-oxide, were significantly higher in the CB piglets than CON piglets, while the contents of 9 metabolites, such as selamectin, were significantly lower ($p < 0.01$). In the negative ion mode, the contents of 19 metabolites, such as PE(22:4(7Z,10Z,13Z,16Z)/22:5(4Z,7Z,10Z,13Z,16Z)), PE(20:1(11Z)/PGF1alpha), and PE(15:0/22:1(13Z)), showed a significant increase, while the contents of 13 metabolites, such as DN-isobutylamide and 4-hydroxycyclohexylcarboxylic acid, exhibited a significant decrease ($p < 0.01$).

Subsequently, an analysis of KEGG pathway enrichment was conducted on all differential metabolites found in the piglets from both groups. As shown in Figure 2G, CBX 2021 highly affected 5 pathways, including indole alkaloid biosynthesis, and tryptophan metabolism ($p < 0.05$). The significant increase in L-tryptophan and tryptamine mediated by CBX 2021 mainly contributed to the enrichment of these pathways ($p < 0.05$, Figure 2H). These outcomes show that CBX 2021 modulated tryptophan metabolism and biosynthesis of various alkaloids by altering the levels of

metabolites, thus affecting the metabolic function of weaned piglets.

Correlation analysis of microbiota, differential metabolites and blood biochemical indicators

Metabolomics is considered an important tool for elucidating potential interactions between the microbiota and host phenotypes. Therefore, this study investigated the correlations between the top 20 bacterial genera and serum differential metabolites, along with the relationships between these metabolites and blood indicators. Figure 3A shows that in the CB piglets, upregulated genera (*Faecalibacterium*, *unclassified_Bacteroidales*, and *Subdoligranulum*) and downregulated genera (*unclassified_Muribaculaceae* and *Rikenellaceae_RC9_gut_group*) were highly correlated with differential metabolites. Specifically, *Faecalibacterium* showed positive correlations with upregulated metabolites in the CB piglets; these metabolites included 6-methylquinoline, indoleacrylic acid, isoquinoline N-oxide, L-tryptophan, and tryptamine ($p < 0.05$). *Faecalibacterium* exhibited negative correlations with downregulated metabolites in the CB piglets; these metabolites included selamectin, 4-hydroxycyclohexylcarboxylic acid, and DN-isobutylamide ($p < 0.05$). Interestingly, *unclassified_Bacteroidales* and *Subdoligranulum* showed similar trends to that of *Faecalibacterium*, while *unclassified_Muribaculaceae* and *Rikenellaceae_RC9_gut_group* showed opposite trends.

The correlation analysis results between differential metabolites and blood indicators are shown in Figure 3B. Serum immunoglobulins showed positive correlations with a majority of the upregulated metabolites in the CB piglets ($p < 0.05$), while they showed negative correlations with downregulated metabolites, especially 4-hydroxycyclohexylcarboxylic acid ($p < 0.05$). Regarding inflammatory factors, IL-1β was negatively correlated with tryptamine, and IL-10 was negatively correlated with selamectin, 4-hydroxycyclohexylcarboxylic acid, and DN-isobutylamide ($p < 0.05$). Notably, growth-related hormones, including GH, GHRL, and GAS, were consistent with the trend of immunoglobulin. Furthermore, in terms of indicators reflecting intestinal permeability, serum DAO activity showed positive correlations with the content of DN-isobutylamide and selamectin ($p < 0.05$), and it showed negative correlations with the content of PE(22:4(7Z,10Z,13Z,16Z)/22:5(4Z,7Z,10Z,13Z,16Z)), PE(20:1(11Z)/PGF1alpha), and PE(15:0/22:1(13Z)) ($p < 0.05$).

The aforementioned findings indicate that alteration in gut microbiota composition mediated by CBX 2021 intervention may positively influence hormone levels, immune responses and gut barrier function by regulating metabolic function, ultimately improving growth, development and overall health of piglets.

Adhesion of CBX 2021 promoted the proliferation and reduced the inflammatory response in IPEC-J2 cells

Adhesion of strains to the surface of intestinal epithelial cells (IEC) is crucial for achieving their maximum probiotic effect (Kainulainen et al., 2015). Therefore, we assessed the ability of the CBX 2021 strain to adhere to IPEC-J2 cells in this study. The results,

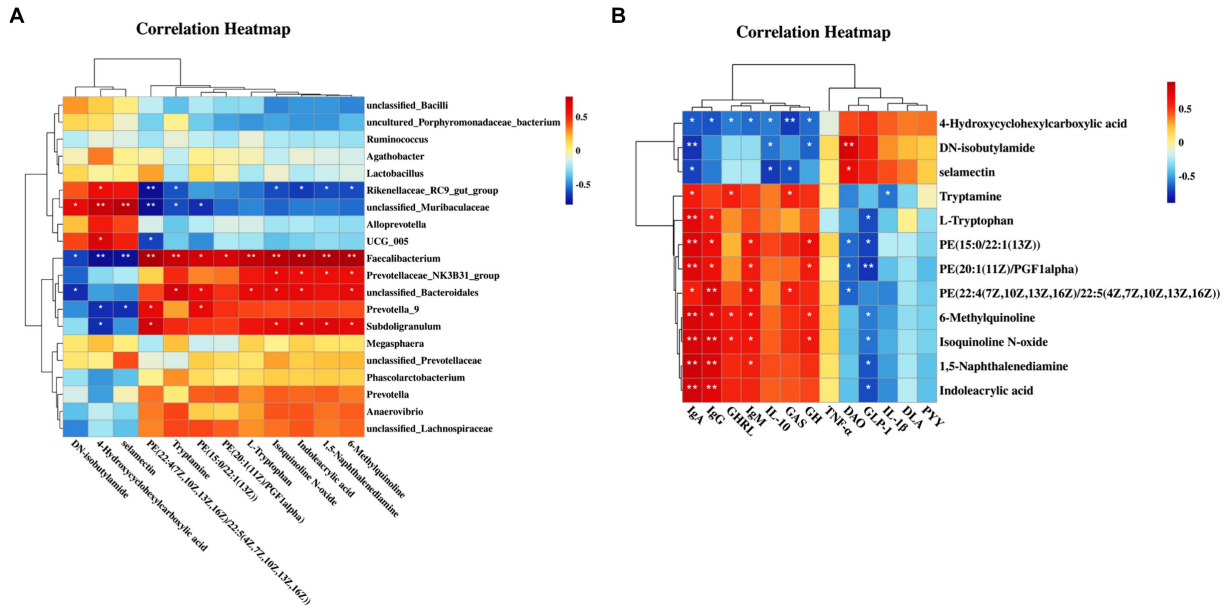

FIGURE 3
Correlation of microbiota, metabolites, and blood biochemical indicators ($n = 6$). **(A)** Heatmap of correlations between the top 20 bacterial genera and serum differential metabolites; The abscissa is the fecal bacteria with relative abundance of top 20; The ordinate is 12 serum differential metabolites. **(B)** Heatmap of correlations between serum differential metabolites and blood indicators; The abscissa is 12 serum differential metabolites; The ordinate is the blood biochemical indicators (immunoglobulin A/G/M, ghrelin, interleukin-10, growth hormone, gastrin, tumor necrosis factor-α, Glucagon-like peptide-1, diamine oxidase, interleukin-1β, peptide YY, D-lactic acid).

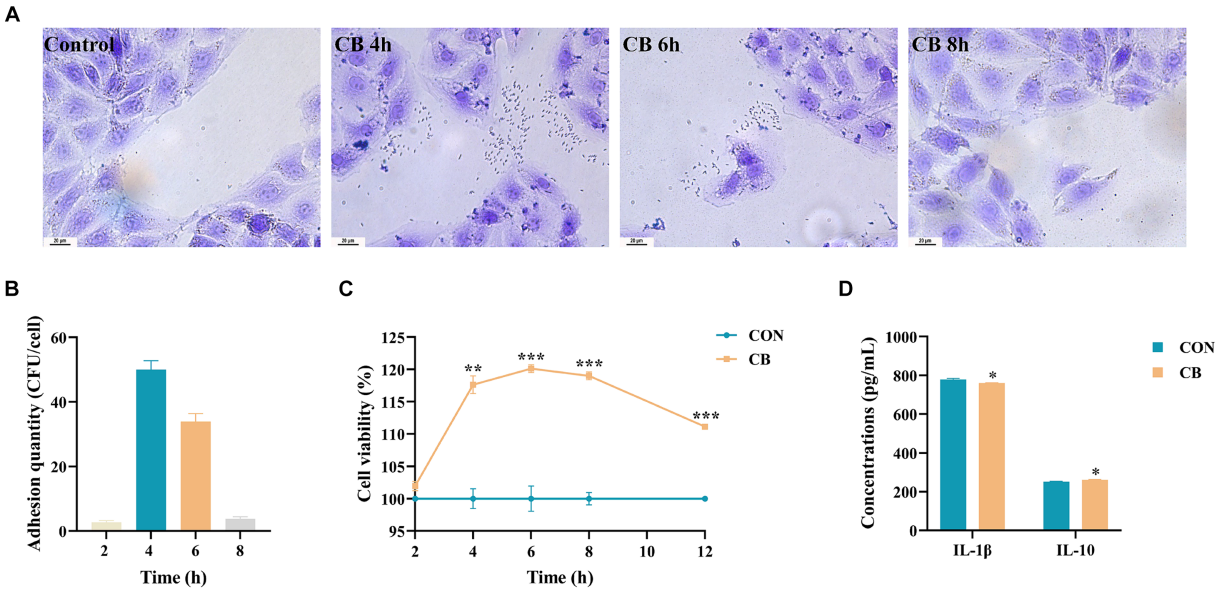

FIGURE 4
Effects of *Clostridium butyricum* CBX 2021 adhesion on the proliferation and inflammatory factors in IPEC-J2 cells ($n = 25$ or 3). **(A)** Gram staining microscopy of IPEC-J2 cells (scale bar = 20 μm). **(B)** Adhesion quantity of the CBX 2021 strain cocultured with IPEC-J2 cells at different time. **(C)** Line chart of cell proliferation activity. **(D)** Histogram showing the difference in inflammatory cytokine levels in the cell supernatant between two groups. Data are displayed as the mean ± SEM. *** Indicates $p < 0.001$, ** indicates $p < 0.01$, and * indicates $p < 0.05$ in comparison with the CON group.

shown in Figures 4A,B, indicate that after 2 h of co-culture, there was almost no bacterial adhesion. After 4 h of co-culture, the average bacteria amount of adhesion was 50.04 ± 2.74 CFU/cell. After 6 h of co-culture, the average bacterial adhesion decreased to 33.92 ± 2.48 CFU/cell. When co-cultured for 8 h, there was almost no detectable bacterial adhesion. These findings indicate that the adhesion capability of CBX 2021 to IPEC-J2 cells is time-dependent, reaching its peak at approximately 4 h of co-culture.

The integrity of the intestinal barrier is dependent on the proliferation of IEC (Xie et al., 2019). Therefore, we investigated the impact of CBX 2021 adhesion on the proliferation activity of IPEC-J2 cells. The results in Figure 4C indicate that the strain adhesion did not significantly affect cell viability through 2 h of co-culture ($p > 0.05$). However, between 4 to 12 h of co-culture, CBX 2021 demonstrated a significant proliferative effect on IPEC-J2 cells ($p < 0.01$). As the co-culture time increased, cell viability gradually increased and reached its peak at 6 h, with a value of 120.14%. Subsequently, with a further increase in time, cell viability slightly declined, reaching 111.15% at 12 h. However, the CB group cells still demonstrated a significant proliferative effect on the cells at this time point ($p < 0.001$) compared to the CON group cells. The outcomes suggest that CBX 2021 significantly promoted IPEC-J2 cells proliferation, reaching peak activity after a 6-h co-culture. Therefore, a 6-h co-culture time was chosen for subsequent experiments.

To assess the potential anti-inflammatory properties of CBX 2021 in the intestine, we also analyzed the levels of inflammatory mediators in the cell supernatant. The data shows that CBX 2021 effectively decreased IL-1β levels, while enhancing IL-10 secretion in IPEC-J2 cells following 6 h of stimulation, ($p < 0.05$, Figure 4D). These findings are consistent with the *in vivo* experimental results, and thus suggesting that CBX 2021 can reduce the inflammatory response of IEC.

Adhesion of CBX 2021 altered inflammation and immune regulatory genes in IPEC-J2 cells

To delve deeper into the molecular mechanisms responsible for reducing inflammation in IPEC-J2 cells through CBX 2021 adhesion, RNA-seq analysis was conducted to confirm changes in the relative gene expression. The PCA scatter plot indicates that the two groups of cells formed distinct clusters, suggesting significant differences in gene expression profiles (Figure 5A). A total of 1892 DEGs were distinguished between the CON and CB groups. Among them, 1,387 genes, including TCIM, ZC3H12A, NFKBIE, and GPR20, showed a marked increase in the CB group compared to the CON group, while 505 genes, including KEAP1, PANK1, and CDCA7, were significantly downregulated (Figure 5B). The heatmap was generated using the top 100 genes with the smallest adjust *p*-value (Supplementary Figure S1). It is obvious that cell samples within the same group have high repeatability in gene expression. Notably, the TCIM and ZC3H12A genes were mapped to GO database and involved in various immune-related pathways. For instance, the TCIM gene was implicated in negative regulation of the Notch signaling pathway. The ZC3H12A gene is involved in activating immune response signals and negatively regulating the production of IL-1β, IL-6, and TNF. The GPR20 gene is involved in the G protein-coupled receptor (GPCR) signaling pathway (Supplementary Table S4).

Subsequently, enrichment analyses were carried out for all DEGs using GO and KEGG databases. The findings showed that numerous DEGs were significantly enriched in GPCR signaling pathway, inflammatory and immune response, which are related to cellular health and stress adaptation (Figure 5C). The KEGG pathway analysis revealed multiple immune and inflammatory pathways, including cytokine-cytokine receptor interaction (52 DEGs), PI3K-Akt signaling

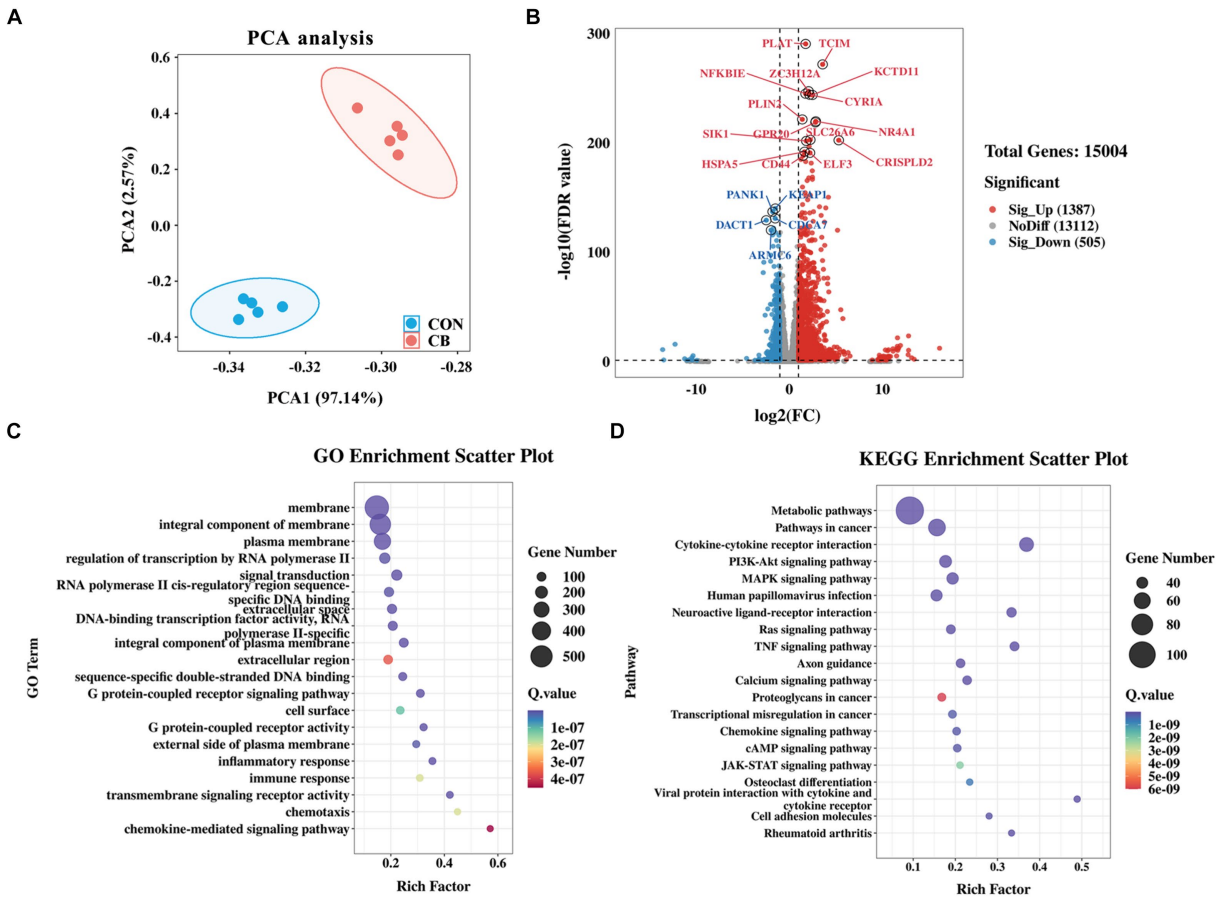

FIGURE 5
Effects of *Clostridium butyricum* CBX 2021 adhesion on the transcriptomics in IPEC-J2 cells ($n = 5$). **(A)** Principal component analysis (PCA) plot between the CON and CB RNA-seq samples. **(B)** The volcano plot displays differentially expressed genes (DEGs) from CON vs. CB. Bubble diagram of GO **(C)** and KEGG **(D)** enrichment analysis of differentially expressed genes.

pathway (44 DEGs), JAK–STAT signaling pathway (23 DEGs), were altered by the adhesion of CBX 2021 (Figure 5D). By screening for these DEGs, we found that IL10RA and IL22RA1, which are anti-inflammatory cytokine receptors, were significantly upregulated in the CB-treated cells. In contrast, the pro-inflammatory gene IL17D was significantly downregulated in the cells.

To further reveal the details of changes in cellular immunity and inflammatory response, GESA was conducted using the Go database on all gene sets of the CON and CB groups. As shown in Figures 6A–F, adhesion of CBX 2021 significantly enhanced immune response (ES = 0.58, NES = 2.26), GPCR activity (ES = 0.55, NES = 2.17), and GPCR signaling pathway (ES = 0.55, NES = 2.27) in the cells. In addition, CBX 2021 was able to improve the negative regulation for the Notch signaling pathway (ES = 0.66, NES = 1.85), the negative regulation of the production of IL-6 (ES = 0.67, NES = 1.94) and the negative regulation of tumor necrosis factor (ES = 0.60, NES = 1.80). The changes in these gene sets supported the fact that CBX 2021 decreased pro-inflammatory cytokines like IL-1β in IPEC-J2 cells. It is obvious that this result interprets the molecular pathway for CBX adhesion to reduce cellular inflammation at the gene level.

Next, the transcriptomic result was validated by using qRT-PCR method. Twelve genes (*PLAT*, *TCIM*, *ZC3H12A*, *GPR20*, *IL10RA*, *IL22RA1*, *TLR2*, *KEAP1*, *PANK1*, *DACT1*, *ARMC6*, and *LMNB1*) were subjected to qRT-PCR analysis. The findings indicated a high degree of concordance between the qRT-PCR data and transcriptomics results and thus confirming the reliability of the RNA sequencing (Figure 6G).

Discussion

Weaning is often associated with impaired immune and metabolic function, compromised small intestinal structure, and dysbacteriosis, leading to postweaning diarrhea and growth retardation. In the context of feed antibiotic bans, CB, an important member of the animal gut symbiotic bacteria, helps to alleviate weaning stress and improve overall health (Chen L. et al., 2018). In this study, we demonstrated that porcine-derived CBX 2021, which has independent intellectual property rights, had the ability to enhance growth rate and lower diarrhea frequency in piglets. This is achieved by modulating gut microbiota structure, optimizing metabolic functions, reducing intestinal permeability, enhancing intestinal and serum immune functions, and promoting IPEC-J2 cell proliferation.

In our study, the experiment demonstrated that supplementing CBX 2021 improved piglets' growth performance. This aligns with earlier studies suggesting that CB can improve the well-being of

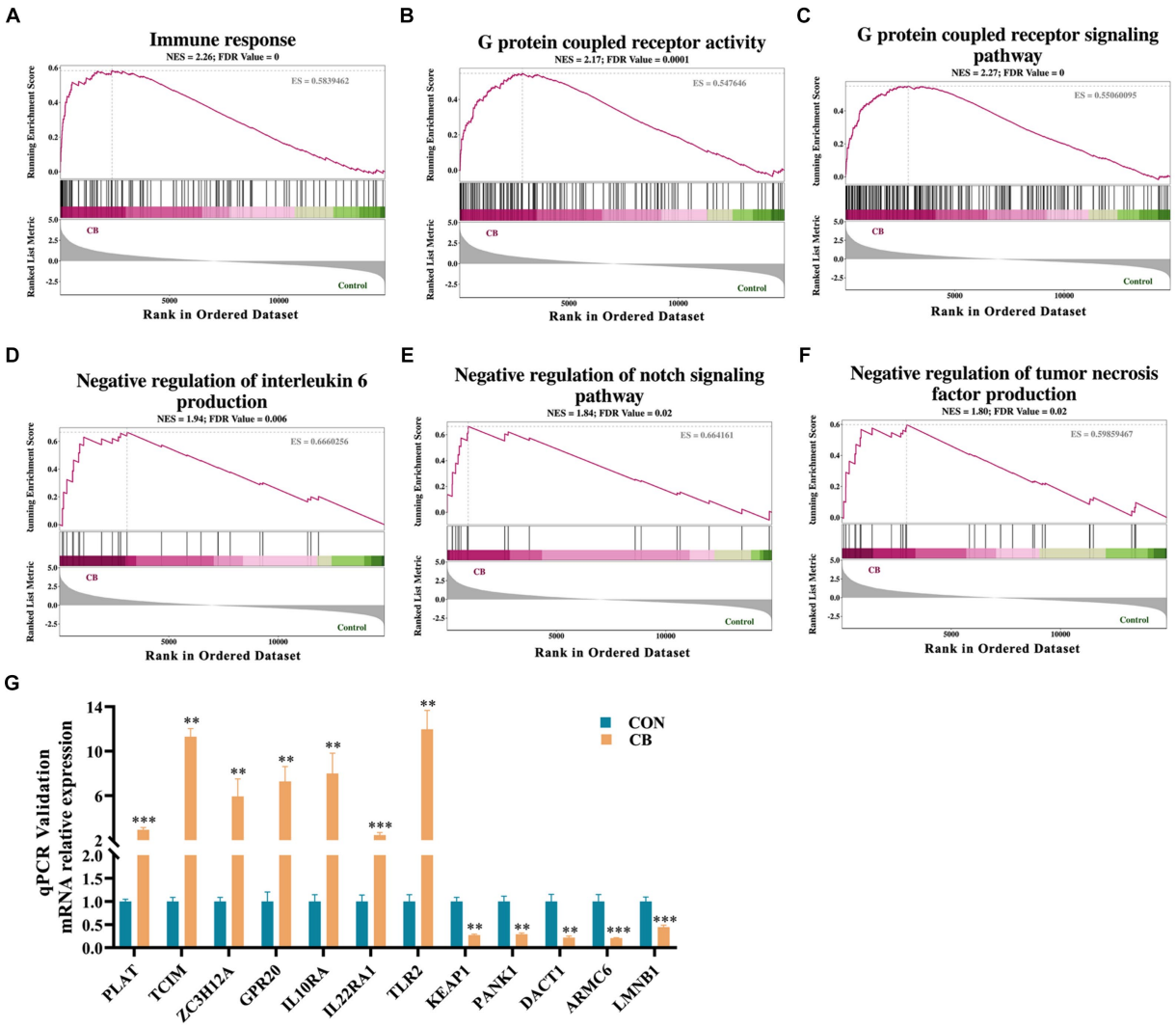

FIGURE 6
Gene set enrichment analysis (GSEA) pathway analysis and qRT-PCR validation **(A–F)** GSEA signal pathway analysis. **(G)** Histograms of target gene expression levels showed by qRT-PCR. Data are displayed as the mean ± SEM. *** Indicates $p < 0.001$ and ** indicates $p < 0.01$ in comparison with the CON group.

weaned piglets, Ira rabbits and calves (Li et al., 2019; Ye et al., 2022; Wu et al., 2023). Clearly, these reports also reflect that improving intestinal health is effective in alleviating the growth stress in animals caused by weaning. In addition, the enhancement in growth performance may be attributed not solely to the amelioration in peripheral hormone levels, but also to the reduction in intestinal permeability, which contributes to improved digestion and absorption of nutrients within the intestine (Guilloteau et al., 2006; Goes et al., 2022; Lee et al., 2022). Post-weaning diarrhea, primarily resulting from an imbalance in intestinal microbiota and the rapid proliferation of pathogens, is the chief contributor to growth retardation in animals (Rhouma et al., 2017). Research findings have indicated a strong correlation between reduction of diarrhea and the subsequent improvement in growth performance, and factors such as immune, intestinal barrier integrity, gut microbiota, and bacterial metabolism (Lu et al., 2020; Zhang R. Q. et al., 2021; Yu et al., 2022; Chen et al., 2023). In this research, CBX 2021 administration effectively reduced postweaning diarrhea in piglets, confirming the efficacy of *Clostridium butyricum* in improving the gut microbiota and restoring gut health. Thus, the overall health and development of the CB piglets was better than that of the CON piglets.

CBX 2021 effectively enhanced immunity and reduced inflammation in piglets. Specifically, on the one hand, the increased serum immunoglobulin concentration of CB piglets suggests that the ability to resist pathogen infection may be stronger. This observation aligns with previous research (Zhang et al., 2014; Han et al., 2020; Wang et al., 2021). A previous study showed that CB can promote IgA secretion by inducing an increase in IL-17-producing CD4+ T cells (Hagihara et al., 2021). However, we found that the improvement in immunity may be related to the upregulated metabolites mediated by CBX 2021, including phosphatidylethanolamine (PE), L-tryptophan, and bacterial tryptophan metabolites. PE supplementation has been reported to effectively restore impaired humoral immune function (Fu et al., 2021). L-tryptophan and its derivatives have demonstrated roles in modulating host immunity and maintaining intestinal balance (Gao et al., 2018). Therefore, CBX 2021 may promote immunoglobulin

secretion by positively regulating the metabolite profile. On the other hand, CBX 2021 significantly reduced IL-1β levels and promoted IL-10 production in piglets mirroring the results reported by Li et al. (2018). IL-1β is a typical inflammatory mediator, and its overexpression can damage the animal intestine (Kruse et al., 2008). Conversely, IL-10 serves as an anti-inflammatory regulator that not only inhibits the overexpression of proinflammatory factors, but also regulates intestinal homeostasis during immune defense processes (Gao et al., 2012; Zigmond et al., 2014; Xu S. Q. et al., 2020). Generally speaking, CB primarily regulates the secretion of inflammatory cytokines through Toll-like receptor (TLR) pathways, such as TLR4/NF-κB pathway and TLR2/MyD88-independent pathway (Hayashi et al., 2013; Wang et al., 2022).Then, we further uncovered the potential molecular pathways that contribute to anti-inflammatory properties of CBX 2021 through transcriptomics analysis. Interestingly, GSEA intuitively showed that CBX 2021 enhanced GPCR activity and its signaling pathway, while downregulating the Notch signaling pathway and the production of proinflammatory factors (IL-6 and TNF-α).

Research indicates that elevated levels of Notch signaling within the intestine can suppress goblet cell differentiation, causing a rise in intestinal permeability and invasion of exogenous harmful substances, thereby inducing inflammation (Xie et al., 2020). Probiotics, such as *Bacillus subtilis* RZ001 and *Lactobacillus acidophilus* LA85, can repair the intestinal barrier and alleviate inflammation through inhibiting the Notch signaling pathway (Li et al., 2020; Xue et al., 2022). These studies were strongly supported in the current research. Notably, GPCRs have the potential to regulate immune activity and anti-inflammatory properties. For example, the researcher discovered that activation of GPR39 led to an increase in IL-10 release, which ultimately reduced inflammation in macrophages (Muneoka et al., 2018). Furthermore, activation of GPR109A has been shown to inhibit downstream Akt and NF-κB p65 phosphorylation in macrophages, thereby maintaining the barrier integrity and suppressing colonic inflammation (Chen G. X. et al., 2018). Therefore, it is speculated that CBX 2021 may reduce inflammation by activating the GPCR pathway and downregulating the Notch signaling pathway, thereby effectively reducing intestinal diseases such as diarrhea. Moreover, we hypothesized that after CBX 2021 adheres to cells, it may induce changes in cellular inflammation levels and gene expression profiles through its cell wall component, lipoteichoic acid (LTA). Research has found that *Clostridium butyricum* LTA can affect intracellular inflammatory responses by mediating NF-κB and ERK pathways (Wang H. et al., 2016). However, this is merely a preliminary guess, and we plan to further explore this mechanism through additional experiments in future research.

Weaning-induced inflammation often disrupts intestinal barrier function, leading to negative impacts on growth, development and general well-being (Stewart et al., 2017). In the present research, CBX 2021 reduced intestinal permeability and ameliorated weaning-induced intestinal barrier damage by reducing DLA and DAO levels. This is similar to reports in broiler chickens afflicted with *Escherichia coli* K88 and rats experiencing pancreatitis (Zhang et al., 2016; Zhao et al., 2020). Reducing intestinal permeability has proven to enhance piglet growth performance and reduce the incidence of diarrhea (Huang et al., 2015). And the recovery of intestinal barrier function is related to the cytokine levels and the GPCR pathway activated by CB (Lee, 2015; Ariyoshi et al., 2021). With respect to cytokines, proinflammatory cytokines can impair intestinal tight junctions and increase permeability, whereas anti-inflammatory cytokines protect and maintain intestinal barrier integrity (Lee, 2015). CBX 2021 did indeed induce positive changes in cytokine levels. In addition, we found that the improvement in intestinal permeability may be related to CBX 2021-mediated increases in a number of PE metabolites. PE is a vital constituent of cell membranes and has been demonstrated to play a significant role in repairing damaged intestinal cells damaged intestinal cells (Sawai et al., 2001).

Based on this, we further explained the potential mechanism of CBX2021 at the cellular level. The outcomes indicated that the adhesion of the CBX 2021 strain significantly promoted the proliferation of IPEC-J2 cells. Intestinal cell proliferation is a major driving force for intestinal growth and development, which is beneficial for repairing damaged intestinal barriers and preventing intestinal infections (Wang J. L. et al., 2019). Previous research has shown that stimulating PI3K/Akt and GPR84 pathway can induce the multiplication of mammary epithelial cells and promote mammary gland development (Meng et al., 2017). In our study, CBX 2021 significantly enhanced GPCR activity and its signaling pathway, as well as regulated the PI3K/Akt signaling pathway. Therefore, CBX 2021 might promote intestinal cell proliferation by modulating the GPCR and PI3K/Akt signaling pathways, thereby exerting probiotic effects on piglet intestinal structure.

Undoubtedly, CBX2021 has a regulatory effect on piglets by inducing changes in their gut microbiota. In our research, CBX2021 optimized the composition and structure of the fecal microorganism in weaned piglets. Notably, CBX 2021 significantly decreased the number of proinflammatory bacteria, including *unclassified_Muribaculaceae*, *Rikenellaceae_RC9_gut_group*, and *Family_XIII_AD3011_group*. Studies have indicated that the lower the abundance of these bacteria, the less the content of pro-inflammatory factors including IL-1β, IL-5 and IL-6 (Cai et al., 2021; Zhang L. et al., 2021; Zhang et al., 2022). The decrease in IL-1β content observed in this study is consistent with these findings. Additionally, CBX 2021 markedly decreased the abundance of *Desulfovibrio*. The bacterium secretes toxic metabolites that harm IEC and immune function (Verstreken et al., 2012; Kushkevych et al., 2018). It is speculated that the decrease in these bacteria may be one of the reasons for the decrease in the incidence of diarrhea in piglets.

In addition, CBX 2021 enriched many functional bacteria that produce butyric acid, including *Faecalibacterium*, *[Eubacterium]_eligens_group*, and *Lachnospiraceae_NK4A136_group*. These bacteria serve as anti-inflammatory regulators and enhance intestinal barrier function (Dou et al., 2020; Xu J. H. et al., 2020; Tang S. S. et al., 2022). For instance, *Faecalibacterium* exerts anti-inflammatory actions by suppressing histone deacetylase activity through producing butyric acid (Zhou et al., 2018). The *Lachnospiraceae_NK4A136_group* has been shown to promote the expression of the tight junction protein claudin-1, which is negatively correlated with intestinal permeability and serum LPS levels (Ma et al., 2020). Additionally, CBX 2021 promoted the growth of helpful bacteria, including *Prevotella_9* and *Ligilactobacillus*. Notably, *Prevotella_9* has demonstrated a positive relationship with weight, ADG, and ADFI, and a negative relationship with diarrhea incidence (Hung et al., 2019; Yang et al., 2021). Therefore, CBX 2021 may have beneficial effects on weaned piglets by modulating the gut microbiota.

Alterations in the gut microbiome undoubtedly result in changes in metabolic function and levels of metabolites (Ariyoshi et al., 2021). These metabolites act as messengers of the intestinal microbiota, directly regulating various physiological processes in the host. CBX 2021 significantly enhanced the biosynthesis of various alkaloids, including indole alkaloids, and tryptophan metabolism. Studies have demonstrated that indole alkaloids exhibit a range of advantageous effects, such as anti-inflammatory, anti-pathogenic bacteria, and antioxidant properties (Song et al., 2018; Hu et al., 2021). Therefore, it is reasonable to believe that the reduction in proinflammatory mediators and harmful bacteria in the intestines of weaned piglets may be partly associated with these effects. Tryptophan and its derivatives, including kynurenine, indole, indoleacrylic acid, and tryptamine, play important roles in inflammatory responses (Kim et al., 2010; Bhattarai et al., 2020; Liu et al., 2022; Duan et al., 2023). Indoleacrylic acid, for example, can promote IL-10 production and enhance intestinal epithelial barrier function, resulting in anti-inflammatory effects (Wlodarska et al., 2017). In addition to regulating inflammation, tryptophan metabolism is also important for maintaining immune homeostasis, protecting intestinal integrity, and promoting animal growth (Yao et al., 2011; Liang et al., 2018; Seo and Kwon, 2023). It is worth noting that we found that the levels of L-tryptophan and tryptamine were positively correlated with the abundance of *Faecalibacterium* and *unclassified_Bacteroidales*. Therefore, CBX 2021 may boost tryptophan metabolism through the increased proliferation of these bacteria. This can positively regulate inflammation, immune function, and intestinal barrier function, ultimately promoting healthy growth of piglets.

Conclusion

In conclusion, exogenous administration of CBX 2021 effectively reduced postweaning diarrhea and accelerated growth of piglets through enhancing immune function and intestinal barrier integrity. The mechanism is mainly related to the improvement of intestinal health by CBX 2021. CBX 2021 not only optimized gut microbiota structure and improved bacterial metabolic functions in piglets, and also directly promoted epithelial cell proliferation and reduced inflammation by altering cellular gene expression. Thus, the current research reveals the probiotic mechanism of *Clostridium butyricum* and establishes a theoretical foundation for the potential application of CBX 2021.

Data availability statement

The raw 16S rRNA sequencing data and transcriptome sequencing data presented in the study are deposited in the NCBI Sequence Read Archive (SRA), accession number PRJNA947735 and PRJNA948058.

Ethics statement

The animal study was approved by Ethics Committee of National Center of Technology Innovation for Pigs. The study was conducted in accordance with the local legislation and institutional requirements.

Author contributions

XL: Writing – review & editing, Writing – original draft, Visualization, Validation, Supervision, Methodology, Investigation, Formal analysis, Data curation, Conceptualization. XQ: Writing – review & editing, Validation, Methodology, Investigation, Funding acquisition, Formal analysis, Data curation. YY: Writing – review & editing, Validation, Methodology, Investigation, Formal analysis, Data curation. JW: Writing – review & editing, Validation, Methodology, Investigation, Formal analysis, Data curation. QW: Writing – review & editing, Validation, Methodology, Investigation, Funding acquisition. JL: Writing – review & editing, Validation, Methodology, Investigation. JH: Writing – review & editing, Validation, Investigation, Conceptualization. FY: Writing – review & editing, Validation, Investigation, Conceptualization. ZL: Writing – review & editing, Writing – original draft, Validation, Supervision, Investigation, Funding acquisition, Conceptualization. RQ: Writing – review & editing, Writing – original draft, Validation, Supervision, Resources, Project administration, Methodology, Investigation, Funding acquisition, Conceptualization.

Funding

The author(s) declare that financial support was received for the research, authorship, and/or publication of this article. This work was jointly supported by the National Natural Science Foundation of China (U21A20245 and 32272830), the Strategic Priority Research Program of the National Center of Technology Innovation for Pigs (NCTIP-XD/B04), and the Financial Resourced Program of Chongqing (23509J).

Conflict of interest

The authors declare that the research was conducted in the absence of any commercial or financial relationships that could be construed as a potential conflict of interest.

Publisher's note

Supplementary material

The Supplementary material for this article can be found online at: https://www.frontiersin.org/articles/10.3389/fmicb.2024.1394332/full#supplementary-material

SUPPLEMENTARY FIGURE S1
Cluster analysis of the top 100 DEGs with the smallest *P*-value.

References

Abdelqader, A., and Al-Fataftah, A.-R. (2016). Effect of dietary butyric acid on performance, intestinal morphology, microflora composition and intestinal recovery of heat-stressed broilers. *Livest. Sci.* 183, 78–83. doi: 10.1016/j.livsci.2015.11.026

Ariyoshi, T., Hagihara, M., Tomono, S., Eguchi, S., Minemura, A., Miura, D., et al. (2021). *Clostridium butyricum* MIYAIRI 588 modifies bacterial composition under antibiotic-induced dysbiosis for the activation of interactions via lipid metabolism between the gut microbiome and the host. *Biomedicines* 9, 1065–1083. doi: 10.3390/biomedicines9081065

Bhattarai, Y., Jie, S., Linden, D. R., Ghatak, S., Mars, R. A. T., Williams, B. B., et al. (2020). Bacterially derived tryptamine increases mucus release by activating a host receptor in a mouse model of inflammatory bowel disease. *iScience* 23, 101798–101823. doi: 10.1016/j.isci.2020.101798

Cai, J. R., Chen, H., Weng, M. L., Jiang, S. Y., and Gao, J. (2019). Diagnostic and clinical significance of serum levels of D-lactate and diamine oxidase in patients with Crohn's disease. *Gastroent. Res. Pract.* 2019, 8536952–8536959. doi: 10.1155/2019/8536952

Cai, B. N., Pan, J. Y., Chen, H., Chen, X., Ye, Z. Q., Yuan, H. B., et al. (2021). Oyster polysaccharides ameliorate intestinal mucositis and improve metabolism in 5-fluorouracil-treated S180 tumour-bearing mice. *Carbohyd. Polym.* 256, 117545–117554. doi: 10.1016/j.carbpol.2020.117545

Chen, L., Li, S., Zheng, J., Li, W. T., Jiang, X. M., Zhao, X. L., et al. (2018). Effects of dietary *Clostridium butyricum* supplementation on growth performance, intestinal development, and immune response of weaned piglets challenged with lipopolysaccharide. *J. Anim. Sci. Biotechnol* 9, 62–75. doi: 10.1186/s40104-018-0275-8

Chen, G. X., Ran, X., Li, B., Li, Y. H., He, D. W., Huang, B. X., et al. (2018). Sodium butyrate inhibits inflammation and maintains epithelium barrier integrity in a TNBS-induced inflammatory bowel disease mice model. *EBioMedicine* 30, 317–325. doi: 10.1016/j.ebiom.2018.03.030

Chen, J., Xu, X. W., Kang, J. X., Zhao, B. C., Xu, Y. R., and Li, J. L. (2023). Metasilicate-based alkaline mineral water confers diarrhea resistance in maternally separated piglets via the microbiota-gut interaction. *Pharmacol. Res.* 187, 106580–106593. doi: 10.1016/j.phrs.2022.106580

Dou, X. J., Gao, N., Yan, D., and Shan, A. S. (2020). Sodium butyrate alleviates mouse colitis by regulating gut microbiota dysbiosis. *Animals (Basel)* 10, 1154–1164. doi: 10.3390/ani10071154

Duan, X. Y., Luan, Y. M., Wang, Y. C., Wang, X. L., Su, P., Li, Q. W., et al. (2023). Tryptophan metabolism can modulate immunologic tolerance in primitive vertebrate lamprey via IDO-kynurenine-AHR pathway. *Fish Shellfish Immun.* 132, 108485–108492. doi: 10.1016/j.fsi.2022.108485

Fu, G. T., Guy, C. S., Chapman, N. M., Palacios, G., Wei, J., Zhou, P. P., et al. (2021). Metabolic control of T_{FH} cells and humoral immunity by phosphatidylethanolamine. *Nature* 595, 724–729. doi: 10.1038/s41586-021-03692-z

Gao, Q. X., Qi, L. L., Wu, T. X., and Wang, J. B. (2012). An important role of interleukin-10 in counteracting excessive immune response in HT-29 cells exposed to *Clostridium butyricum*. *BMC Microbiol.* 12, 100–107. doi: 10.1186/1471-2180-12-100

Gao, J., Xu, K., Liu, H. N., Liu, G., Bai, M. M., Peng, C., et al. (2018). Impact of the gut microbiota on intestinal immunity mediated by tryptophan metabolism. *Front. Cell Infect. Mi* 8, 13–34. doi: 10.3389/fcimb.2018.00013

Goes, E. C., Dal Pont, G. C., Maiorka, A., Bittencourt, L. C., Bortoluzzi, C., Fascina, V. B., et al. (2022). Effects of a microbial muramidase on the growth performance, intestinal permeability, nutrient digestibility, and welfare of broiler chickens. *Poultry Sci.* 101, 102232–102240. doi: 10.1016/j.psj.2022.102232

Guilloteau, P., Le Meuth-Metzinger, V., Morisset, J., and Zabielski, R. (2006). Gastrin, cholecystokinin and gastrointestinal tract functions in mammals. *Nutr. Res. Rev.* 19, 254–283. doi: 10.1017/s0954422407334082

Hagihara, M., Ariyoshi, T., Kuroki, Y., Eguchi, S., Higashi, S., Mori, T., et al. (2021). *Clostridium butyricum* enhances colonization resistance against *Clostridioides difficile* by metabolic and immune modulation. *Sci. Rep.* 11, 15007–15021. doi: 10.1038/s41598-021-94572-z

Han, Y. S., Tang, C. H., Li, Y., Yu, Y., Zhan, T. F., Zhao, Q. Y., et al. (2020). Effects of dietary supplementation with *Clostridium butyricum* on growth performance, serum immunity, intestinal morphology, and microbiota as an antibiotic alternative in weaned piglets. *Animals (Basel)* 10, 2287–2303. doi: 10.3390/ani10122287

Hayashi, A., Sato, T., Kamada, N., Mikami, Y., Matsuoka, K., Hisamatsu, T., et al. (2013). A single strain of *Clostridium butyricum* induces intestinal IL-10-producing macrophages to suppress acute experimental colitis in mice. *Cell Host Microbe* 13, 711–722. doi: 10.1016/j.chom.2013.05.013

Hu, Y., Chen, S. L., Yang, F., and Dong, S. (2021). Marine indole alkaloids-isolation, structure and bioactivities. *Mar. Drugs* 19, 658–708. doi: 10.3390/md19120658

Huang, C., Song, P. X., Fan, P. X., Hou, C. L., Thacker, P., and Ma, X. (2015). Dietary sodium butyrate decreases postweaning diarrhea by modulating intestinal permeability and changing the bacterial communities in weaned piglets. *J. Nutr.* 145, 2774–2780. doi: 10.3945/jn.115.217406

Hung, D. Y., Cheng, Y. H., Chen, W. J., Hua, K. F., Pietruszka, A., Dybus, A., et al. (2019). *Bacillus licheniformis*-fermented products reduce diarrhea incidence and alter the fecal microbiota community in weaning piglets. *Animals (Basel)* 9, 1145–1159. doi: 10.3390/ani9121145

Kainulainen, V., Tang, Y., Spillmann, T., Kilpinen, S., Reunanen, J., Saris, P. E., et al. (2015). The canine isolate *Lactobacillus acidophilus* LAB20 adheres to intestinal epithelium and attenuates LPS-induced IL-8 secretion of enterocytes in vitro. *BMC Microbiol.* 15, 4–11. doi: 10.1186/s12866-014-0337-9

Kim, C. J., Kovacs-Nolan, J. A., Yang, C., Archbold, T., Fan, M. Z., and Mine, Y. (2010). L-tryptophan exhibits therapeutic function in a porcine model of dextran sodium sulfate (DSS)-induced colitis. *J. Nutr. Biochem.* 21, 468–475. doi: 10.1016/j.jnutbio.2009.01.019

Kruse, R., Essen-Gustavsson, B., Fossum, C., and Jensen-Waern, M. (2008). Blood concentrations of the cytokines IL-1beta, IL-6, IL-10, TNF-alpha and IFN-gamma during experimentally induced swine dysentery. *Acta Vet. Scand.* 50, 32–38. doi: 10.1186/1751-0147-50-32

Kushkevych, I., Dordević, D., Vítězová, M., and Kollár, P. (2018). Cross-correlation analysis of the *Desulfovibrio* growth parameters of intestinal species isolated from people with colitis. *Biologia* 73, 1137–1143. doi: 10.2478/s11756-018-0118-2

Lee, S. H. (2015). Intestinal permeability regulation by tight junction: implication on inflammatory bowel diseases. *Intest. Res.* 13, 11–18. doi: 10.5217/ir.2015.13.1.11

Lee, L. R., Holman, A. E., Li, X., Vasiljevski, E. R., O'Donohue, A. K., Cheng, T. L., et al. (2022). Combination treatment with growth hormone and zoledronic acid in a mouse model of *Osteogenesis imperfecta*. *Bone* 159, 116378–116389. doi: 10.1016/j.bone.2022.116378

Li, H. H., Jiang, X. R., and Qiao, J. Y. (2021). Effect of dietary *Bacillus subtilis* on growth performance and serum biochemical and immune indexes in weaned piglets. *J. Appl. Anim. Res.* 49, 83–88. doi: 10.1080/09712119.2021.1877717

Li, H. H., Li, Y. P., Zhu, Q., Qiao, J. Y., and Wang, W. J. (2018). Dietary supplementation with *Clostridium butyricum* helps to improve the intestinal barrier function of weaned piglets challenged with enterotoxigenic *Escherichia coli* K88. *J. Appl. Microbiol.* 125, 964–975. doi: 10.1111/jam.13936

Li, J., Xie, K., Yang, J., Zhang, J., Yang, Q., Wang, P., et al. (2023). S100A9 plays a key role in *Clostridium perfringens* beta2 toxin-induced inflammatory damage in porcine IPEC-J2 intestinal epithelial cells. *BMC Genomics* 24:16. doi: 10.1186/s12864-023-09118-6

Li, Y. R., Zhang, T. X., Guo, C. C., Geng, M., Gai, S. L., Qi, W., et al. (2020). *Bacillus subtilis* RZ001 improves intestinal integrity and alleviates colitis by inhibiting the notch signalling pathway and activating ATOH-1. *Pathog. Dis.* 78:ftaa016. doi: 10.1093/femspd/ftaa016

Li, W. X., Zhou, S., Zhang, L. Y., Wang, N., Sun, Y. K., and Yonggen, Z. (2019). Effects of *Clostridium butyricum* on growth performance, serum biochemical indices, antioxidant capacity and immune function of weaning calves. *Chin. J. Anim. Nutr.* 31, 369–377. doi: 10.3969/j.issn.1006-267x.2019.01.044

Liang, H. W., Dai, Z. L., Kou, J., Sun, K. J., Chen, J. Q., Yang, Y., et al. (2018). Dietary L-tryptophan supplementation enhances the intestinal mucosal barrier function in weaned piglets: implication of tryptophan-metabolizing microbiota. *Int. J. Mol. Sci.* 20, 20–32. doi: 10.3390/ijms20010020

Liu, X., Qiu, X. Y., Yang, Y., Wang, J., Wang, Q., Liu, J. B., et al. (2023). Alteration of gut microbiome and metabolome by *Clostridium butyricum* can repair the intestinal dysbiosis caused by antibiotics in mice. *iScience* 26, 106190–106208. doi: 10.1016/j.isci.2023.106190

Liu, G. M., Tao, J. Y., Lu, J. J., Jia, G., Zhao, H., Chen, X. L., et al. (2022). Dietary tryptophan supplementation improves antioxidant status and alleviates inflammation, endoplasmic reticulum stress, apoptosis, and pyroptosis in the intestine of piglets after lipopolysaccharide challenge. *Antioxidants (Basel)* 11, 872–883. doi: 10.3390/antiox11050872

Livak, K. J., and Schmittgen, T. D. (2001). Analysis of relative gene expression data using real-time quantitative PCR and the $2^{-\Delta\Delta CT}$ method. *Methods* 25, 402–408. doi: 10.1006/meth.2001.1262

Lu, J. J., Yao, J. Y., Xu, Q. Q., Zheng, Y. X., and Dong, X. Y. (2020). *Clostridium butyricum* relieves diarrhea by enhancing digestive function, maintaining intestinal barrier integrity, and relieving intestinal inflammation in weaned piglets. *Livest. Sci.* 239, 104112–104119. doi: 10.1016/j.livsci.2020.104112

Ma, L. Y., Ni, Y. H., Wang, Z., Tu, W. Q., Ni, L. Y., Zhuge, F., et al. (2020). Spermidine improves gut barrier integrity and gut microbiota function in diet-induced obese mice. *Gut Microbes* 12, 1832857–1832819. doi: 10.1080/19490976.2020.1832857

Mazzoni, M., Zampiga, M., Clavenzani, P., Lattanzio, G., Tagliavia, C., and Sirri, F. (2022). Effect of chronic heat stress on gastrointestinal histology and expression of feed intake-regulatory hormones in broiler chickens. *Animal* 16, 100600–100609. doi: 10.1016/j.animal.2022.100600

Meng, Y. Y., Zhang, J., Zhang, F. L., Ai, W., Zhu, X. T., Shu, G., et al. (2017). Lauric acid stimulates mammary gland development of pubertal mice through activation of GPR84 and PI3K/Akt signaling pathway. *J. Agric. Food Chem.* 65, 95–103. doi: 10.1021/acs.jafc.6b04878

Mun, D., Kyoung, H., Kong, M., Ryu, S., Jang, K. B., Baek, J., et al. (2021). Effects of *Bacillus*-based probiotics on growth performance, nutrient digestibility, and intestinal health of weaned pigs. *J. Anim. Sci. Technol.* 63, 1314–1327. doi: 10.5187/jast.2021.e109

Muneoka, S., Goto, M., Kadoshima-Yamaoka, K., Kamei, R., Terakawa, M., and Tomimori, Y. (2018). G protein-coupled receptor 39 plays an anti-inflammatory role by enhancing IL-10 production from macrophages under inflammatory conditions. *Eur. J. Pharmacol.* 834, 240–245. doi: 10.1016/j.ejphar.2018.07.045

Rhouma, M., Fairbrother, J. M., Beaudry, F., and Letellier, A. (2017). Post weaning diarrhea in pigs: risk factors and non-colistin-based control strategies. *Acta Vet. Scand.* 59, 31–49. doi: 10.1186/s13028-017-0299-7

Rodríguez-Viera, L., Martí, I., Martínez, R., Perera, E., Estrada, M. P., Mancera, J. M., et al. (2022). Feed supplementation with the GHRP-6 peptide, a ghrelin analog, improves feed intake, growth performance and aerobic metabolism in the gilthead sea bream *Sparus aurata*. *Fishes (Basel)* 7, 31–43. doi: 10.3390/fishes7010031

Sawai, T., Drongowski, R. A., Lampman, R. W., Coran, A. G., and Harmon, C. M. (2001). The effect of phospholipids and fatty acids on tight-junction permeability and bacterial translocation. *Pediatr. Surg. Int.* 17, 269–274. doi: 10.1007/s003830100592

Seo, S. K., and Kwon, B. (2023). Immune regulation through tryptophan metabolism. *Exp. Mol. Med.* 55, 1371–1379. doi: 10.1038/s12276-023-01028-7

Song, L. L., Mu, Y. L., Zhang, H. C., Wu, G. Y., and Sun, J. Y. (2018). A new indole alkaloid with anti-inflammatory from the branches of *Nauclea officinalis*. *Nat. Prod. Res.* 34, 2283–2288. doi: 10.1080/14786419.2018.1536130

Stewart, A. S., Pratt-Phillips, S., and Gonzalez, L. M. (2017). Alterations in intestinal permeability: the role of the leaky gut in health and disease. *J. Equine Vet.* 52, 10–22. doi: 10.1016/j.jevs.2017.02.009

Tang, S. S., Liang, C. H., Liu, Y. L., Wei, W., Deng, X. R., Shi, X. Y., et al. (2022). Intermittent hypoxia is involved in gut microbial dysbiosis in type 2 diabetes mellitus and obstructive sleep apnea-hypopnea syndrome. *World J. Gastroenterol.* 28, 2320–2333. doi: 10.3748/wjg.v28.i21.2320

Tang, X. P., Xiong, K. N., Fang, R. J., and Li, M. J. (2022). Weaning stress and intestinal health of piglets: a review. *Front. Immunol.* 13, 1042778–1042791. doi: 10.3389/fimmu.2022.1042778

Tang, Q. S., Yi, H. B., Hong, W. B., Wu, Q. W., Yang, X. F., Hu, S. L., et al. (2021). Comparative effects of *L. plantarum* CGMCC 1258 and *L. reuteri* LR1 on growth performance, antioxidant function, and intestinal immunity in weaned pigs. *Front. Vet. Sci.* 8, 728849–728858. doi: 10.3389/fvets.2021.728849

Verstreken, I., Laleman, W., Wauters, G., and Verhaegen, J. (2012). *Desulfovibrio desulfuricans* bacteremia in an immunocompromised host with a liver graft and ulcerative colitis. *J. Clin. Microbiol.* 50, 199–201. doi: 10.1128/JCM.00987-11

Wang, T. H., Fu, J., Xiao, X., Lu, Z. Q., Wang, F. Q., Jin, M. L., et al. (2021). CBP22, a novel bacteriocin isolated from *Clostridium butyricum* ZJU-F1, protects against LPS-induced intestinal injury through maintaining the tight junction complex. *Mediat. Inflamm.* 2021, 8032125–8032136. doi: 10.1155/2021/8032125

Wang, J., Ji, H. F., Wang, S. X., Liu, H., Zhang, W., Zhang, D. Y., et al. (2018). Probiotic *Lactobacillus plantarum* promotes intestinal barrier function by strengthening the epithelium and modulating gut microbiota. *Front. Microbiol.* 9, 1953–1966. doi: 10.3389/fmicb.2018.01953

Wang, J., Qi, L., Mei, L., Wu, Z., and Wang, H. (2016). *C. butyricum* lipoteichoic acid inhibits the inflammatory response and apoptosis in HT-29 cells induced by *S. aureus* lipoteichoic acid. *Int. J. Biol. Macromol.* 88, 81–87. doi: 10.1016/j.ijbiomac.2016.03.054

Wang, K. X., Wang, K., Wang, J. R., Yu, F., and Ye, C. (2022). Protective effect of *Clostridium butyricum* on *Escherichia coli*-induced endometritis in mice via ameliorating endometrial barrier and inhibiting inflammatory response. *Microbiol. Spectr.* 10, 1–12. doi: 10.1128/spectrum.03286-22

Wang, L. X., Yan, S. L., Li, J. Z., Li, Y. L., Ding, X. Q., Yin, J., et al. (2019). Rapid communication: the relationship of enterocyte proliferation with intestinal morphology and nutrient digestibility in weaning piglets. *J. Anim. Sci.* 97, 353–358. doi: 10.1093/jas/sky388

Wang, J. L., Zhang, T., Shen, X. T., Liu, J., Zhao, D. L., Sun, Y. W., et al. (2016). Serum metabolomics for early diagnosis of esophageal squamous cell carcinoma by UHPLC-QTOF/MS. *Metabolomics* 12, 116–125. doi: 10.1007/s11306-016-1050-5

Wang, H., Zong, Q., Wang, S., Zhao, C., Wu, S., and Bao, W. (2019). Genome-wide DNA methylome and transcriptome analysis of porcine intestinal epithelial cells upon deoxynivalenol exposure. *J. Agric. Food Chem.* 67, 6423–6431. doi: 10.1021/acs.jafc.9b00613

Wlodarska, M., Luo, C., Kolde, R., d'Hennezel, E., Annand, J. W., Heim, C. E., et al. (2017). Indoleacrylic acid produced by commensal Peptostreptococcus species suppresses inflammation. *Cell Host Microbe* 22, 25–37.e6. doi: 10.1016/j.chom.2017.06.007

Wu, Q., Cui, D., Chao, X., Chen, P., Liu, J., Wang, Y., et al. (2021). Transcriptome analysis identifies strategies targeting immune response-related pathways to control Enterotoxigenic *Escherichia coli* infection in porcine intestinal epithelial cells. *Front. Veter. Sci.* 8, 677897–677912. doi: 10.3389/fvets.2021.677897

Wu, J. M., Wang, J. P., Lin, Z. S., Liu, C. C., Zhang, Y. C., Zhang, S. M., et al. (2023). *Clostridium butyricum* alleviates weaned stress of piglets by improving intestinal immune function and gut microbiota. *Food Chem.* 405, 135014–135026. doi: 10.1016/j.foodchem.2022.135014

Xie, S., Jiang, L., Wang, M. J., Sun, W. J., Yu, S. Y., Turner, J. R., et al. (2020). Cadmium ingestion exacerbates Salmonella infection, with a loss of goblet cells through activation of notch signaling pathways by ROS in the intestine. *J. Hazard. Mater.* 391, 122262–122273. doi: 10.1016/j.jhazmat.2020.122262

Xie, S., Zhao, S. Y., Jiang, L., Lu, L. H., Yang, Q., and Yu, Q. H. (2019). *Lactobacillus reuteri* stimulates intestinal epithelial proliferation and induces differentiation into goblet cells in young chickens. *J. Agr. Food Chem.* 67, 13758–13766. doi: 10.1021/acs.jafc.9b06256

Xu, S. Q., Bao, W. J., Men, X. L., Liu, Y., Sun, J., Li, J., et al. (2020). Interleukin-10 protects schwann cells against advanced glycation end products-induced apoptosis via NF-κB suppression. *Exp. Clin. Endocrinol. Diabetes* 128, 89–96. doi: 10.1055/a-0826-4374

Xu, J. H., Liang, R. R., Zhang, W., Tian, K. Y., Li, J. Y., Chen, X. M., et al. (2020). *Faecalibacterium prausnitzii*-derived microbial anti-inflammatory molecule regulates intestinal integrity in diabetes mellitus mice via modulating tight junction protein expression. *J. Diabetes* 12, 224–236. doi: 10.1111/1753-0407.12986

Xue, L. Y., Li, Z. Q., Xue, J. B., Wang, H. T., Wu, T., Liu, R., et al. (2022). *Lactobacillus acidophilus* LA85 ameliorates cyclophosphamide-induced immunosuppression by modulating notch and TLR4/NF-κB signal pathways and remodeling the gut microbiota. *Food Funct.* 13, 8107–8118. doi: 10.1039/d1fo04331e

Yang, Y., Liu, Y. D., Liu, J., Wang, H. Z., Guo, Y. L., Du, M., et al. (2021). Composition of the fecal microbiota of piglets at various growth stages. *Front. Vet. Sci.* 8, 661671–661681. doi: 10.3389/fvets.2021.661671

Yao, K., Fang, J., Yin, Y. L., Feng, Z. M., Tang, Z. R., and Wu, G. Y. (2011). Tryptophan metabolism in animals: important roles in nutrition and health. *Front. Biosci.* 3, 286–297. doi: 10.2741/s152

Ye, X. X., Li, K. Y., Li, Y. F., Lu, J. N., Guo, P. T., Liu, H. Y., et al. (2022). The effects of *Clostridium butyricum* on Ira rabbit growth performance, cecal microbiota and plasma metabolome. *Front. Microbiol.* 13, 974337–974351. doi: 10.3389/fmicb.2022.974337

Yu, X. R., Cui, Z. C., Qin, S. K., Zhang, R. Q., Wu, Y. P., Liu, J. S., et al. (2022). Effects of *Bacillus licheniformis* on growth performance, diarrhea incidence, antioxidant capacity, immune function, and fecal microflora in weaned piglets. *Animals (Basel)* 12, 1609–1621. doi: 10.3390/ani12131609

Zhang, L., Cao, G. T., Zeng, X. F., Zhou, L., Ferket, P. R., Xiao, Y. P., et al. (2014). Effects of *Clostridium butyricum* on growth performance, immune function, and cecal microflora in broiler chickens challenged with *Escherichia coli* K88. *Poult. Sci.* 93, 46–53. doi: 10.3382/ps.2013-03412

Zhang, L., Jing, J. R., Han, L., Wang, J. Y., Zhang, W., Liu, Z. Y., et al. (2021). Characterization of gut microbiota, metabolism and cytokines in benzene-induced hematopoietic damage. *Ecotoxicol. Environ. Saf.* 228, 112956–112967. doi: 10.1016/j.ecoenv.2021.112956

Zhang, R. Q., Zhang, H. R., Liu, J. S., Zeng, X. F., Wu, Y. P., and Yang, C. M. (2021). Rhamnolipids enhance growth performance by improving the immunity, intestinal barrier function, and metabolome composition in broilers. *J. Sci. Food Agr.* 102, 908–919. doi: 10.1002/jsfa.11423

Zhang, L., Zhang, L. L., Zhan, X. A., Zeng, X. F., Zhou, L., Cao, G. T., et al. (2016). Effects of dietary supplementation of probiotic, *Clostridium butyricum*, on growth performance, immune response, intestinal barrier function, and digestive enzyme activity in broiler chickens challenged with *Escherichia coli* K88. *J. Anim. Sci. Biotechnol.* 7, 3–11. doi: 10.1186/s40104-016-0061-4

Zhang, H. Q., Zuo, Y. W., Zhao, H. C., Zhao, H., Wang, Y. T., Zhang, X. Y., et al. (2022). Folic acid ameliorates alcohol-induced liver injury via gut–liver axis homeostasis. *Front. Nutr.* 9, 989311–989326. doi: 10.3389/fnut.2022.989311

Zhao, H. B., Jia, L., Yan, Q. Q., Deng, Q., and Wei, B. (2020). Effect of *Clostridium butyricum* and butyrate on intestinal barrier functions: study of a rat model of severe acute pancreatitis with intra-abdominal hypertension. *Front. Physiol.* 11, 561061–561073. doi: 10.3389/fphys.2020.561061

Zhou, L. X., Zhang, M. M., Wang, Y. M., Dorfman, R. G., Liu, H., Yu, T., et al. (2018). *Faecalibacterium prausnitzii* produces butyrate to maintain Th17/Treg balance and to ameliorate colorectal colitis by inhibiting histone deacetylase 1. *Inflamm. Bowel Dis.* 24, 1926–1940. doi: 10.1093/ibd/izy182

Zigmond, E., Bernshtein, B., Friedlander, G., Walker, C. R., Yona, S., Kim, K. W., et al. (2014). Macrophage-restricted interleukin-10 receptor deficiency, but not IL-10 deficiency, causes severe spontaneous colitis. *Immunity* 40, 720–733. doi: 10.1016/j.immuni.2014.03.012

Frontiers in Microbiology

Explores the habitable world and the potential of microbial life

The largest and most cited microbiology journal which advances our understanding of the role microbes play in addressing global challenges such as healthcare, food security, and climate change.

Discover the latest Research Topics

See more →

Frontiers

Avenue du Tribunal-Fédéral 34
1005 Lausanne, Switzerland
frontiersin.org

Contact us

+41 (0)21 510 17 00
frontiersin.org/about/contact